ЖУРНАЛ
ЭКСПЕРИМЕНТАЛЬНОЙ И ТЕОРЕТИЧЕСКОЙ
ФИЗИКИ
АКАДЕМИЯ НАУК СССР

SOVIET PHYSICS

JETP

VOLUME 1 NUMBER 3

A Translation

of the

Journal of Experimental and Theoretical Physics

of the

Academy of Sciences of the USSR

NOVEMBER, 1955

Published by the

AMERICAN INSTITUTE OF PHYSICS
INCORPORATED

SOVIET PHYSICS
JETP

A translation of the Journal of Experimental and Theoretical Physics of the USSR.

A publication of the

AMERICAN INSTITUTE OF PHYSICS

Governing Board

FREDERICK SEITZ, *Chairman*
ALLEN V. ASTIN
ROBERT F. BACHER
H. A. BETHE
J. W. BUCHTA
S. A. GOUDSMIT
DEANE B. JUDD
HUGH S. KNOWLES
W. H. MARKWOOD, JR.
WILLIAM F. MEGGERS
PHILIP M. MORSE
BRIAN O'BRIEN
HARRY F. OLSON
R. F. PATON
ERIC RODGERS
RALPH A. SAWYER
WILLIAM SHOCKLEY
H. D. SMYTH
J. H. VAN VLECK
MARK W. ZEMANSKY

Administrative Staff

HENRY A. BARTON,
Director
GEORGE B. PEGRAM,
Treasurer
WALLACE WATERFALL,
Executive Secretary
THEODORE VORBURGER,
Advertising Manager
RUTH F. BRYANS,
Publication Manager
EDITH I. NEFTEL,
Circulation Manager
KATHRYN SETZE,
Assistant Treasurer
MELVIN LOOS,
Consultant on Printing

American Institute of Physics Advisory Board on Russian Translations

ELMER HUTCHISSON, *Chairman*
DWIGHT GRAY, MORTON HAMERMESH, VLADIMIR ROJANSKY, VICTOR WEISSKOPF

Editor of SOVIET PHYSICS

ROBERT T. BEYER, DEPARTMENT OF PHYSICS, BROWN UNIVERSITY, Providence, R.I.

SOVIET PHYSICS is a bi-monthly journal published by the American Institute of Physics for the purpose of making available in English reports of current Soviet research in physics as contained in the Journal of Experimental and Theoretical Physics of the Academy of Sciences of USSR. The page size of SOVIET PHYSICS will be 7⅞" x 10½", the same as other Institute journals.

Transliteration of the names of Russian authors follows the system employed by the Library of Congress.

This translating and publishing project was undertaken by the Institute in the conviction that dissemination of the results of researchs everywhere in the world is invaluable to the advancement of science. The National Science Foundation of the United States encouraged the project initially and is supporting it in large part by a grant.

The American Institute of Physics and its translators propose to translate faithfully all the material in the Journal of EXPERIMENTAL & THEORETICAL PHYSICS OF THE USSR appearing after January 1, 1955. The views expressed in the translated material, therefore, are intended to be those expressed by the original authors, and not those of the translators nor of the American Institute of Physics.

One volume is published annually. Volume 1 (1955) contains three issues. Subsequent volumes, beginning with January 1956, will contain six issues.

Subscription Prices:

Per year (6 issues)	
United States and Canada	$30.00
Elsewhere	32.00
1st Volume (3 issues)	
United States and Canada	$15.00
Elsewhere	16.00
Back Numbers	
Single copies	$ 6.00

Subscriptions should be addressed to the American Institute of Physics, 57 East 55 Street, New York 22, New York.

SOVIET PHYSICS

JETP

7

SOVIET PHYSICS JETP VOLUME 1, NUMBER 3 NOVEMBER, 1955

Albert Einstein

(1879 - 1955)

J. Exper. Theoret. Phys. USSR **28**, 637-638 (May, 1955)

ON April 18, 1955, Albert Einstein died at the age of 76. All the world honored in him the great scientist, the "great regenerator of natural science" (Lenin), but it is easier for a physicist than for anyone else to realize, concretely and in detail, the significance of the scientific revolution due to Einstein.

Einstein was born on March 14, 1879, at Ulm, and spent his childhood in Germany, but at 14 he moved to Switzerland, where he received his higher education, and where he lived during the first period of his scientific career -- up to 1914 (with the exception of the two years, 1911-1912, during which time he was Professor at the University at Prague). His life in this period was an unusual one. Upon finishing at the Zürich Polytechnic Institute (1900), he busied himself with the activities of a teacher, but in 1902 he began work as an expert in the patent office in Bern. He worked there until 1909, and this period coincided with the beginning of his brilliant scientific work. During this time he produced the special theory of relativity, the quantum concept of radiation, works on the theory of diffusion and Brownian motion. In 1909, the scientific services of Einstein received official recognition. He was appointed Professor, first at the University of Zürich, then (in 1911) at the University in Prague, and subsequently at the Zürich Technical Institute. In 1913 Einstein was chosen a member of the Prussian Academy of Sciences, and in 1914 he went to Berlin.

In the Berlin period of his life, Einstein created the general theory of relativity, and also developed the quantum theory of the emission and absorption of radiation, and quantum statistics (the so-called Bose-Einstein statistics). After the Nazis came into power, Einstein left Germany and settled in Princeton, U.S.A., where he lived to the end of his life, continuing the development of various problems in the general theory of relativity.

Einstein was a member of many Academies of Sciences. In 1926 the Academy of Sciences of the USSR named him an honorary foreign member.

Both branches of theoretical physics of the twentieth-century -- relativity and quantum theory - owed their development to Einstein, although in unequal measure.

The theory of relativity appeared as a brilliant creation of Einstein. Its concrete physical content forms a necessary and basic element of contemporary physics. Phenomena in which the failure of the classical theory appeared in the eighth decimal place served as the starting experimental material for its construction; subsequently, the same theory of relativity explained phenomena in which the difference (change in mass) was measured by a factor of 100 (in the case of an accelerator) or even by $10^3 - 10^{10}$ (in cosmic rays). Contemporary nuclear physics and the physics of elementary particles would be unthinkable without the theory of relativity.

Moreover, the theory of relativity also has enormous significance as the theory which essentially changed the previous, oversimplified representations of space and time extension , as the theory which permits us in every phenomenon to distinguish quantities objectively inherent to it, which do not depend on the particular choice of the "frame of reference".

No less important is the general historical significance of the theory of relativity. After centuries of domination of the Newtonian concept, during which time the idea of universal applicability of the laws of classical mechanics became accepted in the minds of physicists, the concept telescopes increases so much that it becomes comparable with its assumed radius of curvature, an appeal to the general theory of relativity will be inevitable.

(natural enough for us of the present day) developed that the study of a new range of phenomena, in a new scale of velocities, lengths, etc., could lead to a significant change in physical concepts and physical laws, since the previous laws and concepts possessed only limited applicability in the framework of the phenomena investigated in their development. This concept was clearly expressed by Engels and Lenin, but in the world of physics it marked a genuine revolution.

The general theory of relativity, containing in itself the theory of gravitation, has not yet found such wide application as the special theory, although its ideas have been confirmed in three phenomena in the field of astronomy. It undoubtedly will serve as a basis for the solution of cosmological and cosmogonic problems, whose investigation is still in the initial stages. When the dimensions of the region of space accessible to

The researches of Einstein on the quantum theory of radiation also have shown a notable effect on the subsequent development of physics. The concept of the quantum structure of radiation flow which he introduced with extraordinary daring in 1905 cannot be completely justified today from a purely logical viewpoint, and in no way possesses the completeness and rigor of the theory of relativity. This was a physically heuristic concept which showed itself, however, to be exceedingly fruitful in the clarification of a large range of diverse physical phenomena. It found its full basis and confirmation only within the last quarter century, when quantum electrodynamics was developed.

It is hardly proper here to speak of the other remarkable researches of Einstein, each of which appeared as a great scientific event. They remain in the background only because they are eclipsed by the theory of relativity-gravity in which the remarkable characteristics of Einstein as a thinker and his exactness of thought and fearlessness of mind are most strikingly evident.

Einstein took an active part in public life and was warmly aroused on questions which disturbed the more advanced of mankind. He repeatedly came out against war, for international understanding and against the use of atomic weapons.

Soviet physicists deeply honor the memory of Albert Einstein.

Translated by R. T. Beyer
117

SOVIET PHYSICS JETP VOLUME 1, NUMBER 3 NOVEMBER, 1955

Description of the Electromagnetic Field by Means of Matrices

G. A. ZAITSEV
Ivanovo

(Submitted to JETP editor April 3, 1954)
J. Exper. Theoret. Phys. USSR **28**, 524-529 (May, 1955)

The characteristics of matrix-tensors are described. The equations of the electromagnetic field are given in matrix form.

IN three-dimensional space it is convenient to denote vectors by a single letter, e.g., **c**, **d**, etc. On the other hand, in the four-dimensional space of special relativity, tensors usually are given by their components, which depend on the particular coordinate system used. But it is clear that the physical system described by a tensor does not depend on the particular coordinate system used to label the components of the tensor. One should therefore work directly with the tensor as such which then would describe the system in a way valid in any coordinate system.

The tensors of four-dimensional space can be represented by matrices[1]; these are independent of the coordinate system used and therefore are well suited for this purpose. These matrix-tensors are very useful in connection with problems of relativistic invariance. Utilizing them, it is very easy, e.g., to express relations between them, to find their invariants, to determine their character with respect to the transformations of the Lorentz-group, etc.

We shall first investigate the application of matrix-tensors to the description of the classical electromagnetic field. The results thus obtained will be used in following papers[2].

1. For the investigation of four-dimensional matrix-tensors it is useful to start with the properties of matrix-tensors corresponding to vectors in three-dimensional space.

We shall use the following notation: let $\mathbf{d} = \sum_k d^k \mathbf{e}_k$; then the three-dimensional matrix-vector will be denoted by underlining: $\underline{\mathbf{d}} = d_k R^k = d^k R_k$. Furthermore, an underlined letter will denote a matrix (not necessarily a vector) which is a linear combination of R^1, R^2, R^3. So, if **E** and **H** are the electric and magnetic fields, respectively, then

$$\underline{\mathbf{E}} = \sum_{k=1}^{3} E_k R^k = E_k R^k, \quad \underline{\mathbf{H}} = H_k R^k = \underline{H} \qquad (1)$$

(H_k is a component of a pseudovector), etc.

The following relations hold for three-dimensional matrix-vectors:

$$\underline{\mathbf{c}}\underline{\mathbf{d}} = (1/2)(\underline{\mathbf{c}}\underline{\mathbf{d}} + \underline{\mathbf{d}}\underline{\mathbf{c}}) + (1/2)(\underline{\mathbf{c}}\underline{\mathbf{d}} - \underline{\mathbf{d}}\underline{\mathbf{c}}) \qquad (2)$$

$$= (\mathbf{cd}) + R\,\underline{[\mathbf{cd}]}, \quad R = R^1 R^2 R^3.$$

In particular, taking for $\underline{\mathbf{c}}$ the matrix-operator $\underline{\nabla} = R^k \; \partial/\partial x^k$ which corresponds to the operator ∇, we obtain

$$\underline{\nabla}\underline{\mathbf{d}} = \operatorname{div} \mathbf{d} + R\,\underline{\operatorname{curl} \mathbf{d}} \qquad (3)$$

$$= \frac{\partial d^k}{\partial x^k} + R R_k \varepsilon^{kjs} \frac{\partial d_s}{\partial x^j}.$$

Utilizing Eq. (2). it is easy to show that

$$\underline{\mathbf{c}}\underline{\mathbf{b}}\underline{\mathbf{d}} = (\mathbf{cb})\,\underline{\mathbf{d}} + R([\mathbf{cb}]\,\mathbf{d}) + \underline{[\mathbf{d}\,[\mathbf{cb}]]} = \qquad (4)$$

$$= (\mathbf{cb})\,\underline{\mathbf{d}} + (\mathbf{bd})\,\underline{\mathbf{c}} - (\mathbf{cd})\,\underline{\mathbf{b}} + R\,(\mathbf{b}\,[\mathbf{dc}])$$

etc.

The components of the electromagnetic field tensor are

$$(F^{\alpha\beta}) = \begin{pmatrix} 0 & H_3 & -H_2 & -E_1 \\ -H_3 & 0 & H_1 & -E_2 \\ H_2 & -H_1 & 0 & -E_3 \\ E_1 & E_2 & E_3 & 0 \end{pmatrix} \qquad (5)$$

$$(\tilde{F}^{\alpha\beta}) = \begin{pmatrix} 0 & E_3 & -E_2 & H_1 \\ -E_3 & 0 & E_1 & H_2 \\ E_2 & -E_1 & 0 & H_3 \\ -H_1 & -H_2 & -H_3 & 0 \end{pmatrix}.$$

---

[1] see, e.g., G. A. Zaitsev, J. Exper. Theoret. Phys. USSR **25**, 667 (1953). In the following we shall use the notation and the results of the first part of that paper.

[2] G. A. Zaitsev, J. Exper. Theoret. Phys. USSR **28**, 530 (1955); Soviet Phys **1**, 491 (1955)

Here $\tilde{F}^{\alpha\beta}$ are the components of the dual tensor to $F^{\alpha\beta}$ which is defined by $\tilde{F}^{\alpha\beta} = \frac{1}{2}\epsilon^{\alpha\beta\gamma\delta} F_{\gamma\delta}$. The matrix F, representing the field tensor, is given by[1]:

$$F = {}^{1}/_{2} F^{\alpha\beta} R_{\alpha} R_{\beta}, \tag{6}$$

or, using Eqs. (1) and (5),

$$F = R\underline{\mathbf{H}} + R_4 \underline{\mathbf{E}}. \tag{7}$$

Similarly,

$$F = JF = R\underline{\mathbf{E}} - R_4 \underline{\mathbf{H}}. \tag{8}$$

As an example of the application of Eq. (7), we shall obtain from it the law of transformation of $\underline{\mathbf{E}}$ and $\underline{\mathbf{H}}$ under a change of the coordinate system.

If the basis matrix-vectors R^{α} of the old system of coordinates are connected with the $\tilde{R}^{\alpha}$ of the new system by

$$\tilde{R}^{\alpha} = A^{-1} R^{\alpha} A \quad (A = \dots A_2 A_1, \quad A_i^2 = \pm 1), \tag{9}$$

then the new components $\tilde{H}_k$ and $\tilde{E}_k$ are obtained from

$$F = R R^k H_k + R_4 R^k E_k \tag{10}$$

$$= \tilde{R} \tilde{R}^k \tilde{H}_k + \tilde{R}_4 \tilde{R}^k \tilde{E}_k \quad (\tilde{R} = \tilde{R}^1 \tilde{R}^2 \tilde{R}^3)$$

or*

$$AFA^{-1} = R R^k \tilde{H}_k + R_4 R^k \tilde{E}_k = R\underline{\tilde{\mathbf{H}}} + R_4 \underline{\tilde{\mathbf{E}}}. \tag{11}$$

In particular, for the case of a single symmetry, that is, if

$$A = A_1 = a_{\alpha} R^{\alpha} \tag{12}$$

$$= \underline{\mathbf{a}} + a_4 R^4 \quad (A_1^2 = \pm 1, \quad A_1^{-1} = \pm A_1),$$

we have

$$A_1 F A_1^{-1} = \pm R (\underline{\mathbf{a}} - a_4 R^4)\, \underline{\mathbf{H}}\, (\underline{\mathbf{a}} + a_4 R^4)$$

$$\mp R_4 (\underline{\mathbf{a}} - a_4 R^4)\, \underline{\mathbf{E}}\, (\underline{\mathbf{a}} + a_4 R^4),$$

and, because of

$$(\underline{\mathbf{a}} - a_4 R^4)\, \underline{\mathbf{d}}\, (\underline{\mathbf{a}} + a_4 R^4)$$

$$= \underline{\mathbf{ada}} + a_4 R^4 (\underline{\mathbf{ad}} - \underline{\mathbf{da}}) - a_4^2 \underline{\mathbf{d}},$$

there holds

$$\pm \underline{\mathbf{H}}^{+} = \underline{\mathbf{aHa}} - a_4^2 \underline{\mathbf{H}} - 2a_4 \underline{[\mathbf{aE}]}, \tag{13}$$

$$\pm \underline{\mathbf{E}}^{+} = - \underline{\mathbf{aEa}} + a_4^2 \underline{\mathbf{E}} - 2a_4 \underline{[\mathbf{aH}]}.$$

By performing two symmetry operations consecutively, namely

$$A_1 = R^1, \; A_2 = \lambda\, [R^1 \cos(\alpha/2) + R^4 \sin(\alpha/2)], \tag{14}$$

$$\cos\alpha = 1/\lambda^2 = + \sqrt{1 - (v/c)^2},$$

which corresponds to a Lorentz transformation[1] one obtains

$$\mathbf{H}^{++} = [(1 + \cos\alpha)/2\cos\alpha]\; \underline{\mathbf{H}} \tag{15}$$

$$- [(1 - \cos\alpha)/2\cos\alpha]\, R^1 \underline{\mathbf{H}} R^1 - \operatorname{tg}\alpha\, \underline{[\mathbf{e}_1, \; \mathbf{E}]},$$

$$\mathbf{E}^{++} = [(1 + \cos\alpha)/2\cos\alpha]\, \underline{\mathbf{E}}$$

$$- [(1 - \cos\alpha)/2\cos\alpha]\, R^1 \underline{\mathbf{E}} R^1 + \operatorname{tg}\alpha\, \underline{[\mathbf{e}_1, \; \mathbf{H}]}$$

Therefore the new components are given by the old components in the following way

$$\begin{aligned} H_1^{++} &= H_1, \\ H_2^{++} &= [H_2 + (v/c)\, E_3] / \sqrt{1 - (v/c)^2}, \\ H_3^{++} &= [H_3 - (v/c)\, E_2] / \sqrt{1 - (v/c)^2}, \\ E_1^{++} &= E_1, \\ E_2^{++} &= [E_2 - (v/c)\, H_3] / \sqrt{1 - (v/c)^2}, \\ E_3^{++} &= [E_3 + (v/c)\, H_2] / \sqrt{1 - (v/c)^2}. \end{aligned} \tag{16}$$

which are the well known expressions for the components of **E** and **H** in a moving frame of reference (see for example p. 72 of reference 3 or references 4, 5, etc.).

2 We shall now find some relations pertaining to four-dimensional matrix-tensors.

The product of the two matrix-fourvectors $C = c_{\beta} R^{\beta}$ and $D = d^{\beta} R_{\beta}$ is given by

---

* One can look at the components $\tilde{H}_k$ and $\tilde{E}_k$ either as being the components of the new tensor $\tilde{F} = AFA^{-1}$ obtained from F by rotation or reflection, or as the components of the same tensor F in the new coordinate system. In the latter point of view the basis matrix-vectors of the new system of coordinates are obtained by a four-dimensional rotation or reflection characterized by the matrix A^{-1}.

[3] L. D. Landau, E. M. Lifshitz, *Theory of Fields*, 1948

[4] Ia. I. Frenkel, *Electrodynamics*, 1934, part 1

[5] I. E. Tamm, *Principles of Electricity*, 1949

$$CD = (\underline{\mathbf{c}} + c_4 R^4)(\underline{\mathbf{d}} + d^4 R_4) \tag{17}$$
$$= (\mathbf{cd}) + c_4 d^4 + R\,\underline{[\mathbf{cd}]} + R_4(-c_4\,\underline{\mathbf{d}} - \underline{\mathbf{c}}d^4)$$

or

$$CD = c_\alpha d^\alpha + \frac{1}{2} R^\alpha R^\beta (c_\alpha d_\beta - c_\beta d_\alpha) \tag{18}$$
$$= c_\alpha d^\alpha - \frac{1}{2} J R_\gamma R_\delta\, \varepsilon^{\gamma\delta\alpha\beta} c_\alpha d_\beta.$$

Equations (17) and (18) hold also for the case that the components of the fourvectors are operators.

A particularly important matrix-operator is

$$\nabla = R^\alpha \frac{\partial}{\partial x^\alpha} = \underline{\nabla} + \frac{1}{c} R^4 \frac{\partial}{\partial t}. \tag{19}$$

Application of Eq. (18) yields

$$\nabla^2 = \Box = \Delta - \frac{1}{c^2}\frac{\partial^2}{\partial t^2} \tag{20}$$

Using Eq. (2) we further obtain

$$DF = -\underline{[\mathbf{dH}]} + d_4\,\underline{\mathbf{E}} + R^4(\mathbf{dE}) \tag{21}$$
$$- J(\underline{[\mathbf{dE}]} + d_4\,\underline{\mathbf{H}} + R^4(\mathbf{dH})),$$

or

$$DF = - R_\alpha d_\beta F^{\alpha\beta} - J R_\alpha d_\beta \tilde{F}^{\alpha\beta} \tag{22}$$

Similarly,

$$FD = -\underline{[\mathbf{Hd}]} + \underline{\mathbf{E}}\, d^4 - R^4(\mathbf{Ed}) \tag{23}$$
$$+ J(\underline{[\mathbf{Ed}]} + \underline{\mathbf{H}}\, d^4 - R^4(\mathbf{Hd}))$$

or

$$FD = R_\alpha F^{\alpha\beta} d_\beta - J R_\alpha \tilde{F}^{\alpha\beta} d_\beta. \tag{24}$$

Finally, the product of two second rank matrix tensors is given by

$$F_{(1)} F_{(2)} = (R\,\underline{\mathbf{H}}_{(1)} + R_4\,\underline{\mathbf{E}}_{(1)})(R\,\underline{\mathbf{H}}_{(2)} \tag{25}$$
$$+ R_4\,\underline{\mathbf{E}}_{(2)}) = (\mathbf{E}_{(1)}\mathbf{E}_{(2)}) - (\mathbf{H}_{(1)}\mathbf{H}_{(2)})$$
$$+ J((\mathbf{H}_{(1)}\mathbf{E}_{(2)}) + (\mathbf{E}_{(1)}\mathbf{H}_{(2)}))$$
$$+ R(\underline{[\mathbf{E}_{(1)}\mathbf{E}_{(2)}]} - \underline{[\mathbf{H}_{(1)}\mathbf{H}_{(2)}]})$$
$$+ R^4(\underline{[\mathbf{H}_{(1)}\mathbf{E}_{(2)}]} + \underline{[\mathbf{E}_{(1)}\mathbf{H}_{(2)}]})$$

or

$$F_{(1)} F_{(2)} = -\frac{1}{2} F^{\alpha\beta}_{(1)} F^{(2)}_{\alpha\beta} + \frac{1}{2} J (F^{\alpha\beta}_{(1)} \tilde{F}^{(2)}_{\alpha\beta}) \tag{26}$$
$$+ \frac{1}{2} R_\beta R_\gamma (F^{\beta\alpha}_{(1)} F_{\alpha(1)}^{\ \ \gamma} - F^{\beta\alpha}_{(2)} F_{\alpha(1)}^{\ \ \gamma}).$$

In particular.

$$F^2 = C_1 + C_2 J, \tag{27}$$

where $C_1 = -\frac{1}{2} F^{\alpha\beta} F_{\alpha\beta}$ is an invariant, and $C_2 = \frac{1}{2} F^{\alpha\beta} \tilde{F}_{\alpha\beta}$ is a pseudoinvariant which changes sign by reflection (i.e., after an odd number of inversions); they are invariant under four-dimensional rotations. $F^2 = 0$ means $C_1 = C_2 = 0$.

3. We shall now write down the equations of electrodynamics using the above formulas.

Let $J_{el} = \underline{\mathbf{j}}_{el} + c\rho_{el} R_4$ be the current matrix-fourvector. The equations

$$\operatorname{div}\mathbf{E} = 4\pi\rho_{el}, \quad \operatorname{div}\mathbf{H} = 0; \tag{28}$$

$$\operatorname{curl}\mathbf{H} - \frac{1}{c}\frac{d\mathbf{E}}{\partial t} = \frac{4\pi}{c}\mathbf{j}_{el}, \quad \operatorname{curl}\mathbf{E} + \frac{1}{c}\frac{\partial\mathbf{H}}{\partial t} = 0,$$

can be written, putting in Eq. (22) $D = \nabla$,

$$\nabla F = -\frac{4\pi}{c} J_{el} \left(\text{or}\ , \frac{\partial}{\partial x^\alpha} F R^\alpha = \frac{4\pi}{c} J_{el} \right). \tag{29}$$

Maxwell's equations, Eqs. (28), when written in the matrix notation, appear as the single equation (29), where the relativistic invariance is already obvious from the form of the equations.

Maxwell's equations for free space, i.e., if $J_{el} = 0$, are given by $\nabla F = 0$. This is very similar in form to the special case of Maxwell's equations for the electromagnetic field given in reference 6*: $\nabla\psi = 0$. However, this similarity is superficial because here F denotes a matrix-tensor, while ψ is a column composed of the components of spinor .

Let the matrix-fourvector of the potentials be denoted by

$$A = A_\alpha R^\alpha = \underline{\mathbf{A}} + A_4 R^4, \quad A^4 = -A_4 = \varphi. \tag{30}$$

---

[6] G. A. Zaitsev, J. Exper. Theoret. Phys. USSR **25**, 675 (1953)

* We shall use this occasion to remark that in the references given in reference 6, the quoted page numbers should be exchanged: in reference 1, the page number should be 667, in reference 2 it should be 653.

From Eq. (18) we obtain

$$\nabla A\chi = (\partial A^{\alpha}/\partial x^{\alpha})\chi + F\chi + R^{\alpha}A(\partial/\partial x^{\alpha})\chi, \tag{31}$$

where χ is an arbitrary matrix or column vector. Assuming in the usual way $\partial A^{\alpha}/\partial x^{\alpha} = 0$, we obtain

$$F = \nabla A. \tag{32}$$

It is easy to obtain in matrix form the forces exerted by the fields on the charges. From Eqs. (21) and (23) we have

$$(1/2)(FJ_{el} - J_{el}F) = c(\rho_{el}\underline{\mathbf{E}} + (1/c)\underline{[\mathbf{j}_{el}\mathbf{H}]}) + R_4(\mathbf{j}_{el}\mathbf{E}) = cf_{el}, \tag{33}$$

where f_{el} is the matrix-fourvector of the force. The components of the energy-momentum tensor $T^{\alpha\beta}$ must yield $-\partial T^{\alpha\beta}/\partial x^{\beta} = f^{\alpha}_{el}$. From Eqs. (29) and (33) we obtain

$$-\frac{\partial}{\partial x^{\beta}}(R_{\alpha}T^{\alpha\beta}) = f_{el} = \frac{1}{8\pi}\left(-\frac{\partial(FR^{\alpha})}{\partial x^{\alpha}} - F\nabla F\right) = -\frac{1}{8\pi}\frac{\partial(FR^{\alpha}F)}{\partial x^{\alpha}}, \tag{34}$$

and we therefore can put

$$8\pi R_{\alpha}T^{\alpha\beta} = FR^{\beta}F. \tag{35}$$

It is immediately possible to show that $T^{\alpha\beta}$ really are the components of the energy-momentum tensor. Indeed, putting $\underline{\mathbf{b}} = R^k$ in Eq. (4), and with Eq. (7), we obtain for Eq. (35) the expressions

$$8\pi T^{ik} = -2H_iH_k - 2E_iE_k + \delta_{ik}(\mathbf{E}^2 + \mathbf{H}^2), \quad 8\pi T^{44} = \mathbf{E}^2 + \mathbf{H}^2, \tag{36}$$

$$8\pi T^{4k} = 8\pi T^{k4} = 2\varepsilon^{kjs}E_jH_s,$$

as it should be.

Up to now, we limited ourselves to the case of electromagnetic fields *in vacuo*. However, the notation of matrix-fourtensors can be used also in the case of the presence of a medium, especially if questions of relativistic invariance are involved. Here one has to introduce to antisymmetric matrix-fourtensors of second rank

$$F = R\underline{\mathbf{B}} + R_4\underline{\mathbf{E}}, \quad \Phi = R\underline{\mathbf{H}} + R_4\underline{\mathbf{D}}, \tag{37}$$

Here $\mathbf{B}$ is the magnetic induction, etc. Instead of Eq. (35) we now have

$$\frac{1}{8\pi}FR^{\alpha}\Phi = \underset{(c)}{T^{\alpha\beta}}R_{\beta} + J(P^{\alpha\beta}R_{\beta}),$$

where

$$8\pi \underset{(c)}{T^{ik}} = -B_iH_k - H_iB_k - E_iD_k - D_iE_k + \delta_{ik}((\mathbf{BH}) + (\mathbf{ED})),$$

$$8\pi \underset{(c)}{T^{44}} = (\mathbf{ED}) + (\mathbf{BH}),$$

$$8\pi \underset{(c)}{T^{4k}} = 8\pi \underset{(c)}{T^{k4}} = \varepsilon^{kjs}(E_jH_s + D_jB_s).$$

The $\underset{(c)}{T^{\alpha\beta}}$ are the components of Minkowski's symmetrized energy-momentum tensor in an arbitrary medium. In order to obtain the components of the general energy-momentum tensor[5] $T^{\alpha\beta}$, i.e., if $T^{\alpha\beta} \neq T^{\beta\alpha}$ one has to use the antisymmetric tensor of second rank $\frac{1}{2}(F\Phi - \Phi F)$.

Finally, we shall give the tensor of the moment of momentum of the field. Putting $X = x^{\alpha}R_{\alpha}$ we obtain, according to Eq. (18),

$$\frac{1}{2}(XR_{\alpha}T^{\alpha\gamma} - R_{\alpha}T^{\alpha\gamma}X) = \frac{c}{2}R_{\alpha}R_{\beta}M^{\alpha\beta\gamma}, \tag{38}$$

where

$$M^{\alpha\beta\gamma} = \frac{1}{c}(x^{\alpha}T^{\beta\gamma} - x^{\beta}T^{\alpha\gamma}) \tag{39}$$

are the components of the angular momentum density of the field.

Translated by M.Danos

SOVIET PHYSICS JETP VOLUME 1, NUMBER 3 NOVEMBER, 1955

Capture of Electrons and Ionization by Protons in Hydrogen

IA. M. FOGEL', L. I. KRUPNIK AND B. G. SAFRONOV
Physico-Technical Institute, Academy of Sciences, Ukrainian SSR

(Submitted to JETP editor April 3, 1954)
J. Exper. Theoret. Phys. USSR **28**, 589-602 (May, 1955)

The effective cross section of single electron capture and ionization in hydrogen by means of protons of energy in the region of 12.3 to 36.7 kev was measured by means of an improved method of collecting slow particles on the electrode of a plane parallel condenser. The results obtained are compared with data obtained by other workers as well as with theoretical calculations. When protons pass through hydrogen, negative hydrogen ions are found in the proton beam. It is shown that at low gas pressures the appearance of negative hydrogen ions is connected with the process of double electron capture from hydrogen by the protons. Preliminary measurements of the effective cross section for this process with protons of energy 13, 21 and 31.4 kev show that this phenomenon cannot distort the measurements on the effective cross section of single electron capture as we have measured it.

INTRODUCTION

A considerable amount of work has been devoted to the study of elemental processes that take place during the collision of positive ions with gas particles. This work is reviewed in a monograph by Massey and Burhop[1]. Among other inelastic processes, there were studied single electron capture and ionization by positive ions passing through a gas. Several researches are devoted to the study of these processes in the passage of protons through hydrogen[2-5]. An acquaintance with these works shows that the effective cross section of single electron capture varies markedly from author to author; as to the effective cross section for ionization, it was measured only by one author[4].

The differences in the results of the various authors is connected with certain errors in their experimental methods that distort their results.

When fast, singly charged ions pass through a gas, the following elemental processes are possible:

$$A^+ + B \to A + B^+ \quad \text{(capture of a single electron);} \qquad (1)$$

$$A^+ + B \to A^- + B^{++} \quad \text{(capture of two electrons);} \qquad (2)^*$$

$$A^+ + B \to A^{k+} + (k-1)e + B \quad (2 < k < Z_A) \quad \text{(loss of electrons);} \qquad (3)$$

$$A^+ + B \to A^+ + B^{k+} + ke \quad (1 < k < Z_B) \quad \text{(ionization).} \qquad (4)$$

As a result of these processes in the beam, some of the singly charged ions are converted to multiple charged ions, neutral atoms or negative ions. In addition, there appear in the gas through which the beam passes a variety of slow particles, such as positive ions and electrons.

Upon the passage of protons through hydrogen one gets specifically the following reactions:

$$H_1^+ + H_2 \to H_1 + H_2^+ \quad \text{(capture of one electron);} \qquad (5)$$

$$H_1^+ + H_2 \to H_1^- + H_1^+ + H_1^+ \quad \text{(capture of two electrons);} \qquad (6)$$

$$H_1^+ + H_2 \to H_1^+ + H_2^+ + e \quad \text{(single ionization);} \qquad (7)$$

$$H_1^+ + H_2 \to H_1^+ + H_1^+ + H_1^+ + 2e \quad \text{(double ionization).} \qquad (8)$$

The effective cross sections of the above reactions can be studied either by analyzing the nature of the fast particles in the beam that passes through the gas, or by analyzing the slow ions and electrons that appear in the gas upon passage through it of a beam of fast ions.

Realizing the importance of these measurements, we undertook to repeat the experiments with the aim of removing, as far as possible, the errors peculiar to the method of slow particle collection.

---

* Process (2) can take place only when atom A has a positive electron affinity.

[1] H. S. W. Massey and E. H. S. Burhop, *Electronic and Ionic Impact Phenomena*, Ch. VIII, Oxford University Press, 1952

[2] H. Bartels, Ann. Physik **13**, 373 (1932)

[3] H. Meyer, Ann. Physik **30**, 635 (1937)

[4] J. P. Keen, Phil. Mag. **40**, 369 (1949)

[5] W. Sherwin, Phys. Rev. **57**, 814 (1940)

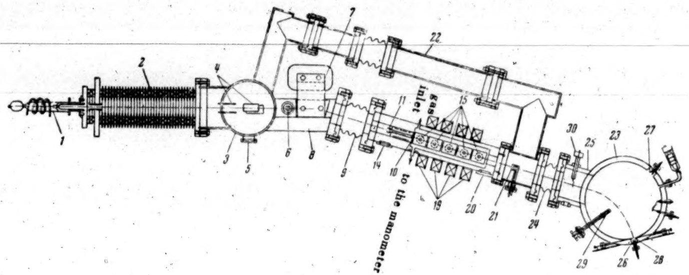

FIG. 1

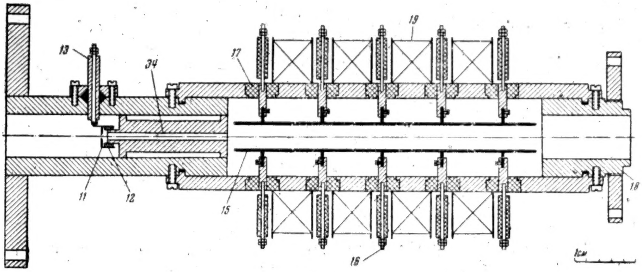

FIG. 2

The method of our measurements is similar to the experiments of Bredov and Fedorenko with some additions that yield somewhat better precision.

During the course of our experiments on single electron capture and ionization with protons in hydrogen, we were the first to observe the phenomenon of double electron capture by protons in a single collision with a hydrogen molecule, and to obtain a tentative value for the effective cross section of this process.

DESCRIPTION OF THE APPARATUS

Figure 1 is a schematic drawing of our experimental equipment.

As a proton source we used a high frequency ion source *1* of the type employed by Tonemann[7]. Having passed through the focusing and accelerating electrodes *2*, the beam of hydrogen ions entered the chamber that connected the equipment to the vacuum system. In this chamber *3* were found a pair of crossed plane condensers *4* that constituted the electrostatic corrector for the beam direction. The focusing of the beam was observed through the window *5*. In order to measure the ionic beam current we used a Faraday cylinder so mounted that it could be removed from the path of the beam.

In order to remove protons from the ion beam, we used a mass monochromator *7* with a beam rotation of 15°. The magnetic field of the mass monochromator was enough to give a 60 kev proton beam. The mass monochromator was connected to the collision chamber *10* by means of a flexible connection *9*. This allowed the proper orientation of the collision chamber with the beam.

A cross sectional drawing of the collision chamber is shown in Fig. 2. The proton beam enters the collision chamber through the diaphragm *11* which is insulated from the body of the instrument by means of ring *12*. Input *13* was used to

---

[6] M. M. Bredov and N. V. Fedorenko, Zh. Tekhn. Fiz. **20**, 1464 (1950)

[7] P. S. Tonemann, J. Moffatt, D. Roaf and J. H. Sanders, Proc. Phys. Soc. (London) **61**, 483 (1948)

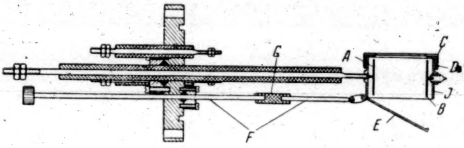

FIG. 3

apply voltage to the diaphragm. The beam then entered the measuring space of the chamber through a tube *34* which was 5 mm in diameter and 100 mm long. The passage of the beam through the entrance diaphragm could be observed through window *14*. The measuring space consisted of five plane condensers *15* with electrodes 50 by 50 mm^2 in area and a separation of 20 mm. Voltage to the condensers was applied through electrodes *16* that were insulated from the body of the chamber by means of polystyrene washers. The main body of the chamber consisted of a copper block *18* of rectangular cross section. A space for the various electrodes was milled out inside this block.

Four coils *19*, wound around the chamber, were used to introduce a longitudinal magnetic field. By means of these coils a magnetic field of the order of 300 oersteds could be introduced into the chamber. The proton beam emerged from the measuring chamber through a canal 35 mm in diameter and 74 mm long. A viewing window *20* was used to observe the beam as it emerged from the collision chamber. Hydrogen was allowed into the chamber through a palladium filter from a steel tank that held the gas at a pressure of 5 atmospheres. The pressure inside the chamber was measured with a McLeod gauge. A mercury vapor trap was installed between the McLeod gauge and the chamber.

The proton beam current was measured with a Faraday cylinder *21* shown in Fig. 3. Two electrodes *A* and *B* inside the Faraday cylinder *J* served to introduce a transverse electric field that prevented secondary electron emission from the cylinder. The entrance to the cylinder was covered with a circular diaphragm *C* that had an opening of diameter 17 mm, and that was insulated from the body of the cylinder with a polystyrene ring *D*. This diaphragm was intended to limit the degree of dispersion of the proton beam. The cylinder had a movable bottom *E*, connected to rod *F* that was insulated from the ground with a polystyrene connector *G*. The collision chamber was connected to the vacuum system by means of a brass tube *22*, 140 mm in diameter. After the collision chamber, the proton beam entered the space of the magnetic analyzer *23* that was between the poles of an electromagnet. The magnetic analyzer was oriented in the direction of the beam by means of the flexible connection *24*.

The analyzing chamber was a brass ring of outer diameter 290 mm, inner diameter 220 mm and height 20 mm. The covers consisted of iron discs 290 mm in diameter and 30 mm thick. An iron pipe *25* connected the analyzer to the rest of the equipment. This pipe was made of iron in order to minimize the spreading of the beam as it enters the chamber. Inside the analyzer were two Faraday chambers *26* and *27*, so arranged as to intercept protons and negative hydrogen ions that were deflected through an angle of 60°. A regulating slit *28* was placed in front of cylinder *26* that served to measure the proton component of the beam. No special precautions were taken to avoid secondary emission from the Faraday cylinders in the analyzer since they were in the presence of a magnetic field.

A ballistic coil *29* was used to measure the magnetic field inside the analyzing chamber. After its assembly, the analyzing chamber was placed between the poles of an electromagnet. The diameter of the poles was 290 mm. The distance between the pole faces was 80 mm, leaving ample room for the analyzer. The field inside the analyzer could be as high as 6000 oersteds.

The current in the measuring electrode was measured with a mirror galvanometer of sensitivity 1.8×10^{-10} amperes per division. The beam current was measured with a shadow galvanometer of sensitivity 6.9×10^{-9} amperes per division. The current in the Faraday cylinders inside the analyzing chamber was measured with a constant deflection string electrometer. By switching in different values of resistances, the sensitivity of the electrometer could be changed. We used resistances with values of 1.4×10^{11} and 3.1×10^{9} ohms.

The energy of the protons was determined by the various potentials applied to them. These included the emission potential, the focusing potential and the accelerating potential. The first two were measured with an electrostatic voltmeter, while the last was measured with a system of graded resistors.

EXPERIMENTAL METHOD

Although in principle it should be easy to measure the cross section of single electron capture and ionization by the method of slow particle analysis, in practice, reliable results are to be expected only when the following conditions are satisfied:

a) The probability of all processes that occur during the collisions of protons with hydrogen molecules and that result in the appearance of slow charged particles must be small compared to the probability of single electron capture and ionization.

b) One must prevent the appearance in the measuring chamber of secondary electrons originating in the various parts of the instrument.

c) One must prevent the exchange of slow particles between the measuring space and the Faraday cylinders. This can be accomplished with a longitudinal electric field.

d) The spreading of the proton beam in the measuring chamber must be negligible.

e) One must prevent the emission of electrons from the measuring electrodes due to the impact of positive ions (cold emission) and photons (photoeffect).

f) The slow particles in the measuring chamber should be the result of a single stage process.

g) In measuring the proton beam current, one must account for the neutralization of some of the protons in the measuring chamber.

Preliminary experiments were performed in order to determine to what extent the above conditions were satisfied. As was mentioned in the introduction, in the interaction of protons with hydrogen molecules, double electron capture and double ionization may result, in addition to single electron capture and single ionization.[as a result of which there arise slow molecular ions of hydrogen and slow electrons {see Eqs. (5) and (7)}].

As a result of two-electron capture slow protons appear in the measuring chamber while fast negative hydrogen ions appear in the beam. Two stage ionization gives rise to both slow electrons and slow protons in the measuring chamber [see Eqs. (6) and (8)].

With the aid of a mass spectroscopic analysis of the slow particles that appear in hydrogen when a proton beam passes through it, one can estimate the probability of the process of single electron capture and single ionization relative to the probability of the process of double electron capture and double ionization.

Such a mass spectroscopic analysis was performed by Keen[4]. The mass spectrum showed one peak of mass 2(H_2^+ ions) and another smaller peak at mass 1(protons). The intensity of the proton peak was only a few percent of the mass 2 peak. When fast He^+ ions were passed through hydrogen the mass spectrum showed a peak only at mass 2.

The results of mass spectroscopic analysis of the slow particles show that the probability of processes (6) and (8), that are related to the presence of slow protons, is small compared to the probability of processes (5) and (7).

Since the process of double electron capture by protons is connected with the appearance of fast negative hydrogen ions in the proton beam, it is possible to estimate the probability of this process by analyzing the beam after it passed through the collision chamber. Since our equipment included a magnetic analyzer after the collision chamber, it was possible for us to make this analysis. The results of this analysis confirm the conclusion, based on mass spectroscopic data, that the probability of double electron capture by protons is low.

A potential of 70 volts was applied between the inlet diaphragm and the body of the collision chamber in order to remove the possibility of the appearance of secondary electrons in the measuring space. This voltage on the diaphragm does not introduce an electric field into the measuring space because the two are separated by a long tube. This was confirmed by special measurements that showed that the positive voltage applied to the entrance diaphragm does not change the current even in the measuring electrode that is nearest to the diaphragm.

If the protons are allowed to strike the walls of the entrance canal then the secondary electrons may enter the measuring space and distort the results. That this is possible is shown in Fig. 4 which shows the ratio of the positive or negative current in the measuring electrode I_{eff} to the proton beam current I_0 as a function of the diameter of the entrance diaphragm.

The unequal distribution of negative current in the different measuring electrodes (the number of the electrode goes up as its distance from the entrance canal increases), as was observed for the case of entrance diameter of 3 mm and gas pressure of 8×10^{-6} mm Hg, shows that secondary electrons from the walls of the entrance canal do not penetrate into the measuring chamber. As the diameter of the diaphragm is decreased to 1 mm the

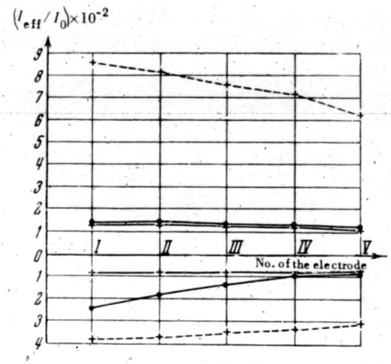

FIG. 4. Gas pressure in the chamber: solid line curves 8×10^{-6} mm Hg (background), dashed curves 6.5×10^{-4} mm Hg. Diameter of the diaphragm: ● = 3 mm, × = 1 mm.

phenomenon disappears. We therefore used a diaphragm of 1 mm diameter in our experiments. The slight decrease in the positive and negative currents that occurred at the pressure of 6.5×10^{-4} mm Hg as one passed from electrode one to five was due to the decrease in the number of protons in the beam because of neutralization.

We took measures to prevent the entrance of secondary electrons from the Faraday cylinder into the measuring space. To suppress secondary electron emission from the walls of the Faraday cylinder a transverse electric field was applied between electrodes *A* and *B* in Fig. 3. It was shown that when the potential difference between electrodes *A* and *B* is 150 volts, secondary electron emission from the Faraday cylinder is completely suppressed.

In order to suppress secondary electron emission from the diaphragm of the Faraday cylinder a positive potential was applied to it. To determine the magnitude of the potential necessary to suppress the secondary emission from the diaphragm of the Faraday cylinder, we measured the effect of positive voltage (on the diaphragm) on the negative current in the measuring electrodes. Figure 5 shows this effect on the fifth electrode, the one nearest to the Faraday cylinder. Similar curves were obtained for the other electrodes. The transverse electric field during these measurements was 160 volts. As Fig. 5 shows, complete suppression of secondary emission from the diaphragm of the Faraday cylinder obtains when the voltage applied to it is plus ten volts.

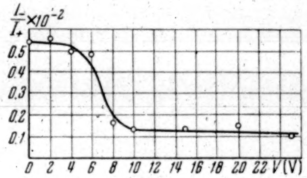

FIG. 5

The presence of a transverse potential difference in the Faraday cylinder can result in a longitudinal field that will encourage the exchange of slow particles between the Faraday cylinder and the measuring space.

The measurements shown in Fig. 6 show that the effect does not take place. Figure 6 shows the dependence of the positive current in the fifth electrode on the transverse potential difference in the Faraday chamber. The measurements show that the current in the electrode nearest to the Faraday cylinder does not depend on the transverse potential difference up to a voltage of 400 volts. During these measurements, the voltage on the diaphragm of the Faraday chamber was plus 10 volts. It is quite certain that there is no exchange of particles between the Faraday cylinder and the measuring space, since the two are separated by a long canal.

Figure 7 shows the current through the diaphragm of the Faraday cylinder as a function of the transverse potential across electrodes *A* and *B* (see Fig. 3) and plus ten volts applied to the diaphragm. The negative current through the diaphragm is due to the incidence upon it of part of the secondary electrons from the walls of the Faraday cylinder. When the transverse potential difference is of the order of 400 volts the current through the diaphragm becomes positive, because it collects some of the protons from the spreading proton beam. The small value of this current indicates the slight spreading of the proton beam in our experiments.

Control experiments on the spreading of the proton beam in the presence of positive current in the circular diaphragm of the Faraday cylinder indicate that the effect is so small that it may be neglected.

To avoid the possibility of secondary electron emission from the walls of the measuring electrodes we used a longitudinal magnetic field obtained from coils around the collision chamber. The magnetic field was made strong enough to return all secondary electrons back to the electrodes and yet not so strong as to prevent

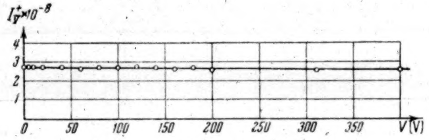

FIG. 6

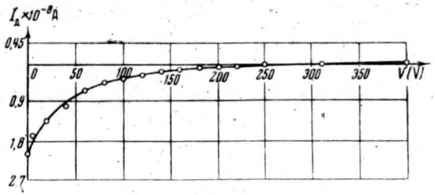

FIG. 7

positive ions from reaching the electrodes. The magnitudes of the positive and negative currents in the measuring electrodes in the presence of magnetic field can be expressed as follows:

$$i_+ = i_1 + i_2 + i_3, \tag{9a}$$

$$i_- = i_2 + i_3, \tag{9b}$$

where i_1 is the ionic current that results when the protons capture electrons from gas molecules, i_2 is the ionic or electronic current that results from the ionization of gas molecules by protons and i_3 is the current of secondary emission from the measuring condenser.

In the presence of a magnetic field, the positive and negative currents are given by:

$$i_+^H = i_1 + i_2, \tag{10a}$$

$$i_-^H = 0. \tag{10b}$$

From Eqs. (9a), (9b) and (10a) we obtain the following relations for i_1 and i_2:

$$i_1 = i_+ - i_- \tag{11a}$$

$$i_2 = i_+^H - (i_+ - i_-). \tag{11b}$$

By measuring the positive and negative current in the absence of a magnetic field and the positive current in the presence of a magnetic field, we can determine the ionic and electronic currents that arise from electron capture and ionization, without the distortion due to secondary emission.

The current-voltage characteristics of the measuring electrodes, with and without a longitudinal magnetic field of 70 oersteds, show that in both cases the current is saturated at a voltage of ±25 v.

Figures 8 and 9 show the dependence of the positive and negative currents in the measuring electrodes upon the pressure of hydrogen in the collision chamber and upon the strength of the beam current. As is seen from the graphs, the dependence is linear up to pressures of 3.5×10^{-4} mm Hg and beam currents of 0.5 micro-amperes. This indicates that the slow particles found in the gas are the result of single stage processes.

Having convinced ourselves that it is possible to eliminate the sources of systematic error, we began the measurements of the effective cross section.

The actual measurements of the positive and negative currents were made on electrode *IV*. Electrodes *III* and *V* were included as checks. Electrodes *I* and *II* were grounded.

The following potentials were used during our measurements: on the entrance diaphragm, + 70 v; on the diaphragm of the Faraday cylinder, + 10v; between the electrodes *A* and *B* of the Faraday cylinder, 400 v; and on electrodes *III*, *IV* and *V*, ± 25 v.

Keeping the energy of the proton beam constant, we first measured the positive and negative currents with the gas in the collision chamber at the terminal pressure of 6 to 8×10^{-6} mm Hg. Then the palladium filter was warmed until the hydrogen current was such that the pressure in the chamber was in the vicinity of 3 to 4×10^{-4} mm Hg. At this

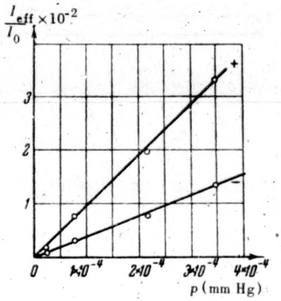

FIG. 8

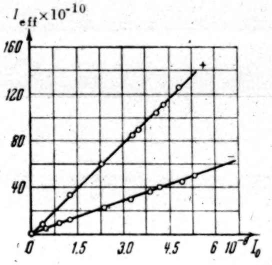

FIG. 9

pressure we again measured the positive and negative currents. During this measurement the pressure was measured at least twice The hydrogen stream was then shut off and again we measured positive and negative current at the residual pressure in the chamber. The values of the positive and negative currents, obtained at the residual pressures before and after hydrogen was introduced, were averaged, and this average value (the background) was subtracted from the corresponding values obtained while hydrogen was present.

The magnitudes of the positive and negative currents were taken as the average of ten readings. The proton beam current was constantly monitored in order to eliminate the effects of proton beam fluctuations on the results of our measurements.

The current measurements were made both with and without a magnetic field in the measuring chamber. The effective cross section of single electron capture and ionization, σ_{10} and σ_i, were calculated from the values of i_1 and i_2, which in turn were calculated [with the help of Eq. (11)] from the measured values of positive and negative current.

In calculating the values of σ_{10} and σ_i, we introduced a correction to account for the decrease of the proton beam due to neutralization of protons as the beam passes from the measuring condensers to the Faraday cylinder.

The calculations of σ_{10} and σ_i, including the correction, were made from the following equations:

$$\sigma_{10} = \left(\frac{i_+}{I_0} - \frac{i_-}{I_0}\right) T \left[9.65 \cdot 10^{18} pL \right. \tag{12a}$$

$$\left. \times \left\{1 + \frac{l_{\text{эфф}}}{L}\left(\frac{i_+}{I_0} - \frac{i_-}{I_0}\right)\right\}\right]^{-1};$$

$$\sigma_{\lambda} = \left\{\frac{i_+^H}{I_0} - \left(\frac{i_+}{I_0} - \frac{i_-}{I_0}\right)\right\} T \left[9.65 \cdot 10^{18} pL \right. \tag{12b}$$

$$\left. \times \left\{1 + \frac{l_{\mathrm{eff}}}{L}\left(\frac{i_+}{I_0} - \frac{i_-}{I_0}\right)\right\}\right]^{-1},$$

where l_{eff} is the effective length of the collision chamber, L the length of the measuring electrode, p is in mm Hg, T is in absolute degrees and I_0 is the initial value of the beam current.

The errors of a single determination of σ_{10} and σ_i are 12 and 18% respectively. A considerable part of the error (8%) is due to the inaccuracy of the pressure determination with the McLeod gauge. Errors in the energy determination of the protons account for another 3%.

We did not make a great effort to reduce the random error in these measurements since our aim was to develop a method that eliminated the systematic errors that at times may distort the results two or three fold (see the discussion of Sherwin's measurements[5] in the paper by Bredov and Fedorenko[6]).

TABLE I

Energy of Protons in kev	$\sigma_{10} \times 10^{16}$ in cm^2	$\sigma_i \times 10^{16}$ in cm^2
12.3	8.1	1.4
16.6	6.5	1.5
20.8	5.2	1.6
25.4	4.5	1.7
29.7	3.6	1.8
33.0	3.1	2.0
36.7	2.6	2.2

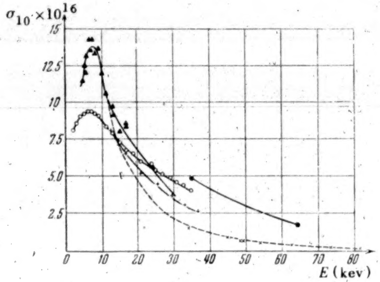

FIG. 10. σ_{10} as a function at proton energy according to: ▲-Bartels[2]; ○-Keen[4]; ●-Meyer[3]; +-Our results; × -Ribe[8]; Dashed curve = theoretical results of Jackson and Shiff[9].

RESULTS OF THE MEASUREMENTS

Using the method described above we measured the effective cross section of single electron capture and ionization by protons in hydrogen. The energy of the protons varied from 12.3 to 36.7 kev.

The results of our measurements are shown in Table I.

In Fig. 10 we plot the effective cross section σ_{10} as a function of proton energy from our data, and also similar curves as obtained by Bartels[2], Meyer[3], Keen[4] and Ribe[8].

As is seen from the graphs, the results obtained by different authors are in very poor agreement. Even those results obtained by the same method differ considerably. Thus the points obtained by Meyer do not lie on the extension of Bartel's curve into the high energy region even though the two used the same experimental method. Bartels and Keen established the maximum value of the cross section σ_{10} at 7 kev, but the magnitude of σ_{10} as measured by Bartels is always greater than that obtained by Keen for all the measured values of proton energies. The magnitude of σ_{10} in reference 8 is considerably less than in all the other works. This may be explained by the distorting influence of double collisions of protons with hydrogen molecules.

Our results agree best with those of Keen, whose experiments were also based on the method of slow particle collection. Our values of σ_{10} are almost invariably lower than those of Keen in all regions of proton energies that were used.

Theoretical calculations of the effective cross section of electron capture by protons in hydrogen* were made in references 9 and 10.

Both calculations considered the capture of electrons in the principal state 1*s* as well as the excited states 2*s*, 2*p*, etc. The results obtained by the two authors were similar. In view of the fact that the Born approximation was used in the above calculations, the results can be correct only for energies above 25 kev (when the energy is 25 kev the proton velocity is the same as the velocity of the electrons in hydrogen). Nevertheless, the authors in reference 9 compare their theoretical results with the experimental values in reference 8 and conclude that there is good agreement between theory and experiment up to 33 kev (the lowest proton energy used in reference 8). A glance at Fig. 10, that plots the theoretical results alongside the experimental shows that, with the exception of the work by Ribe, the agreement between theory an experiment is very poor. Considering the fact that the theoretical calculations neglected the effect of the hydrogen bond and also that the Born approximation is not good in the vicinity of 25 kev, we believe that the divergence of our data and Keen's from the theoretically predicted values is a better representation of the true state than the agreement found between the theory and the results of Ribe[8].

---

[8] F. L. Ribe, Phys. Rev. **83**, 1217 (1951)

* These authors calculated the effective cross section of electron capture by collision of protons with atomic hydrogen.

[9] J. D. Jackson and H. Shiff, Phys. Rev. **89**, 359 (1953)

[10] D. R. Bates and A. Dalgarno, Proc. Phys. Soc. (London) **A65**, 919 (1952); **A66**, 972 (1953)

Our results on the effective cross section of ionization of hydrogen by protons can be compared only with the results of Keen, since no other work in this energy region is known to us.

Figure 11 shows the magnitude of σ_i as a function of energy obtained by us and by Keen[4]. The graphs show a constant difference between the two results, those obtained by the present authors always higher at all proton energies. This can be explained by the fact that in Keen's set up there was always a longitudinal field between the Faraday cylinder and the measuring space. This field produced a force that tended to pull electrons from the measuring space. This effect decreased the value of the measured cross section of ionization. If our interpretation is right, then the values of σ_{10} obtained by us and by Keen must differ, and the difference should increase with increase in proton energy. This is indeed so, as may be seen in Fig. 10.

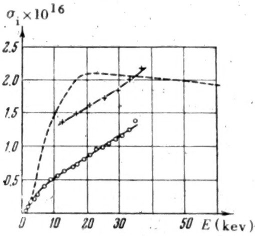

FIG. 11. σ_i as a function of proton energy according to: ○ Keen[4]; + Our results; Dashed curve = theoretical results by Bates and Griffing[11].

A theoretical calculation of the effective cross section of the ionization of hydrogen atoms by means of protons was made by Bates and Griffing[11]. These calculations also used the Born approximation. The results of the calculations are shown in Fig. 11 as a broken line. Again there is a considerable difference between the theoretical values and the experimental results. Not only are the theoretical values almost at all energy levels higher than the experimental results, but they go through a maximum in the region of 2 to 36 kev whereas the experimental results rise monotonically throughout this energy interval. The difference between the theoretical and experimental values of σ_i can be explained in the same manner as the corresponding differences in σ_{10}.

RESULTS ON STUDIES OF THE CAPTURE OF TWO ELECTRONS BY PROTONS FROM HYDROGEN

Because of the stability of negative hydrogen ions, it is possible for a proton to capture two electrons from a molecule of hydrogen [see process (6)].

To calculate the possibility of the formation of negative hydrogen ions in a beam passing through matter, the following differential equations apply:

$$dN_+/d(nx) = -(\sigma_{10}+\sigma_{1-1})N_+ + \sigma_{01}N_0 + \sigma_{-11}N_-; \qquad (13a)$$

$$dN_0/d(nx) = \sigma_{10}N_+ - (\sigma_{01}+\sigma_{0-1})N_0 + \sigma_{-10}N_-; \qquad (13b)$$

$$dN_-/d(nx) = \sigma_{1-1}N_+ + \sigma_{0-1}N_0 - (\sigma_{-11}+\sigma_{-10})N_-, \qquad (13c)$$

where N_+, N_0 and N_- represent the number of protons, hydrogen atoms and negative hydrogen ions in the beam, respectively, and σ_{ik} the cross section for the transition from one particle to the other [for example σ_{1-1} is the cross section for process (6), σ_{10} the cross section for process (5) and so on].

To determine the cross section of the capture by protons of two electrons σ_{1-1}, we can use the differential equation (13c) which, under the initial conditions $N_+ = N_+^*$, $N_0 = 0$ and $N_- = 0$ (meaning that the initial beam consists of protons only) takes the form

$$\left[\frac{dN_-}{d(nx)}\right]_{nx=0} = \sigma_{1-1}N_+^{\bullet},$$

from which

$$\sigma_{1-1} = \frac{1}{N_+^{\bullet}}\left[\frac{dN_-}{d(nx)}\right]_{nx=0} \qquad (14)$$

If we substitute the corresponding currents in Eq. (14) for the number of particles and use the pressure p as a measure of n, we have the following relation for σ_{1-1}:

$$\sigma_{1-1} = 1.08\cdot 10^{-19}\,\frac{T}{L}\left[d\left(\frac{I_-}{I_+^{\bullet}}\right)\Big/ dp\right]_{p=0}, \qquad (15)$$

---

[11] D. R. Bates and S. Griffing, Proc. Phys. Soc. (London) **A66**, 961 (1953)

where L is the length of the gas interval, I_- is the current of negative ions and I_+^* is the current of the entering proton beam.

In principle, the determination of σ_{1-1} from Eq. (15) depends on the determination of the dependence of the ratio I_-/I_+^* on the gas pressure. The magnitude of $\frac{d}{dp}\left(\frac{I_-}{I_+^*}\right)$ is determined from the linear portion of this curve. The presence of the linear portion depends on the formation of negative ions of hydrogen by single collisions of the type described in Eq. (6).

Because ouf equipment contained magnetic analyzer after the collision chamber, we were able to analyze the beam after its passage through the gas and thus determine the cross section σ_{1-1}.

The following method was used to measure σ_{1-1}. The proton beam passed the outlet diaphragm of the collision chamber into the magnetic analyzer where it was deflected through an angle of 60°, thus entering the Faraday cylinder marked *26* in Fig. 1. The negative hydrogen ions in the beam, which arose because of capture of electrons by protons, were deflected in the magnetic field through an angle of 60° in the opposite direction and fell into Faraday cylinder *27*. In this manner we could measure the ratio of the negative ion current to the proton current I_-/I_+.

A simple calculation showed that the measured value of I_-/I_+ did not differ from $(I_-/I_+)_0$, its value before entering the analyzer, by more than 3%.

Equation (15) contains the ration I_-/I_+^*, where I_+^* is the proton beam current before it enters the gas space. Because some protons are neutralized in the passage from the entrance diaphragm to the analyzer, the magnitude I_-/I_+ is somewhat different from the magnitude I_-/I_+^*. Even at the highest pressure on the linear portion of the curve in Fig. 12, this difference is less than 10%. Since the errors in pressure measurements in this range are considerably greater, we made no corrections for this effect.

Figure 12 is a graph of the tatio I_-/I_+ as a function of hydrogen pressure for protons of energy 21 kev. In constructing the curve, we subtracted the value of the background ratio $(I_-/I_+)_{\text{background}}$ from the measured value of I_-/I_+. The background is the value I_-/I_+ measured at the residual pressure, which was of the order of 6 to 8 × 10^{-6} mm Hg.

As can be seen from Fig. 12, I_-/I_+ varies linearly with pressure at low pressures. As the pressure goes up, the curve deviates from linearity because of the increased probability of two consecutive collisions between the particles in the beam and the gas molecules.

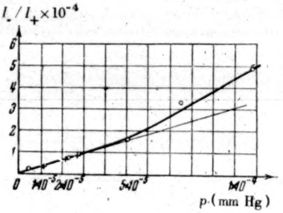

FIG. 12

The magnitude of the differential $d(I_-/I_+)/dp$ can be obtained from the linear portion of the curve, and the value of σ_{1-1} can then be determined with the help of Eq. (15).

Using this method, we determined the effective cross section with three proton energies. The results are shown in Table II.

TABLE II

Energy of Protons in kev	$\sigma_{1-1} \times 10^{18}$ in cm^2
13.0	2.7
21.0	2.3
31.4	1.1

The error of a single determination is about 50%, due largely to the inaccuracy of the pressure determination in the linear region of the graph $(I_-/I_+) = f(p)$.

The data shown in Table II indicates that the effective cross section of double electron capture by protons is much smaller than the cross section for single electron capture. From this we conclude that the effective cross section σ_{10} for single electron capture by protons as measured by us is not materially distorted by the presence of the process of double electron capture.

The observation of negative hydrogen ions arising from the process of double electron capture by protons upon collision with hydrogen molecules has not previously been observed by others. We undertook a preliminary study of this phenomenon in order to determine its effect on the determination of the cross section of single electron capture. However, the proton capture of two electrons resulting in the formation of negative hydrogen ions is in itself of interest. We intend to improve our experimental method and continue the study of double electron capture by protons and the resulting negative ions, using a variety of positive ions with positive electron affinities.

In conclusion we wish to thank Prof. A. K. Valter for his help and interest.

Translated by M. M. Kessler
101

SOVIET PHYSICS JETP VOLUME 1, NUMBER 3 NOVEMBER, 1955

Entropy in Quantum Statistics

R. L. STRATONOVICH
Moscow State University

(Submitted to JETP editor January 19, 1954; resubmitted February 4, 1955)
J. Exper. Theoret. Phys. USSR **28**, 547-558 (May, 1955)

The state and entropy of quantum mechanical systems are considered for non-orthogonal representations of the wave function. It is shown that there follow from the general formulas, on the one hand, the expressions of classical statistics, and, on the other, the well-known results of quantum statistics.

WHEN one speaks of quantum theory, the word "statistics" must be understood in two different senses. Quantum theory is statistical in itself; the wave function, in particular, has a statistical meaning. The statistical aggregates which correspond to these can, in the terminology of D. I. Blokhintsev, be called "pure" ensembles. But side by side with these "pure" statistics, there exist statistics of another type, which come into force whenever the wave function itself is random. Under the term "quantum statistics", we shall denote the latter, i.e., statistics which are concerned with the study of "mixed" ensembles. At the same time we shall associate with quantum statistics not only statistical physics of equilibrium processes, i.e., statistical thermodynamics, but also the quantum statistics of non-equilibrium states, although the latter has not yet been developed at the present time.

Contemporary quantum statistics, which is confined to statistical thermodynamics, operates with a statistical collection of wave functions, such that the separate representations of the wave function, which are the eigenfunctions of the energy, are mutually orthogonal. For such a collection there are formulas which determine the entropy.

It is natural to raise the question as to what is the entropy of an arbitrary statistical aggregate of wave functions, in other words, an arbitrary system on which a complete determination has not been fully carried out, i.e., an arbitrary mixed ensemble. The desired formula must undergo transition to the formula of classical statistics under appropriate conditions, and must also become the known formula in quantum statistical thermodynamics for orthogonal representations of the wave function.

1. Consider a sequence of possible representations of the wave function: $\psi_1(x), \psi_2(x), \ldots$ (x denotes the totality of arguments $x_1, \ldots, x_r$, which can also be discrete). Furthermore, let w_1 be the known probability associated with $\psi_1(x)$, w_2 that associated with $\psi_2(x)$, etc., i.e., we have the probabilities

$$w_i = \mathrm{P}\{\psi(x) = \psi_i(x)\}, \quad i = 1, 2, \ldots .$$

In such a case we shall say that the scheme

$$\begin{pmatrix} \psi_1(x) & \psi_2(x) & \ldots \\ w_1 & w_2 & \ldots \end{pmatrix} \tag{1}$$

is given.

The wave function $\psi(x)$ can sometimes be represented as a function of some continuous set of functions. In the arbitrary case, $\psi(x)$ is a random function, and as such can be completely described by the known statistical characteristics of random functions, e.g., by an infinite sequence of moment functions:

$$\begin{gathered} \mathrm{M}\,\psi(x), \quad \mathrm{M}\,\psi(x_1)\psi(x_2), \quad \mathrm{M}\,\psi(x_1)\psi^*(x_2), \\ \mathrm{M}\,\psi(x_1)\psi(x_2)\psi(x_3), \quad \mathrm{M}\,\psi(x_1)\psi(x_2)\psi^*(x_3), \ldots \end{gathered} \tag{2}$$

(here M is the mathematical expectation).

From the very beginning, there arises the question of the role played by these or other moment functions, and whether they are all important in the description of the physical object (the mixed quantum ensemble). In this connection, the following postulate is far from trivial: there is no moment function of the set (2) except $\mathrm{M}\,\psi(x)\psi^*(x') = \rho(x, x')$, that has absolutely no significance.

If we fix $\rho(x, x')$ and vary the other moment functions, then the random wave function will invariably describe the same physical object. There is an analogous situation in electrodynamics, where the different four component vector potentials $\mathbf{A}_1$ and $\mathbf{A}_2$ describe the same field, if the difference $\mathbf{A}_1 - \mathbf{A}_2$ is the gradient of some function, or, in quantum mechanics, if it is given by the multiplication of the wave function by a number of unit absolute value. The reason for this circumstance must be sought in what follows. "The state matrix" $\psi(x)\psi^*(x')$ plays, in quantum mechanics, the role of the probability density distribution (thus, for $x = x'$, we have an exact probability density distribution, but in reduced space). If the distribution density is random, then in all probable problems only the mathematical expectation of the distribution density has significance --- which is equivalent to the linearity of the mathematical apparatus of quantum mechanics. Thus, both the postulate which has been stated, and the linearity of the mathematical apparatus have as their fundamental basis the ("pure") statistics of quantum theory.

Instead of the system (1) we could also have chosen any other scheme

$$\begin{pmatrix} \psi'_1(x) & \psi'_2(x) & \ldots \\ w'_1 & w'_2 & \ldots \end{pmatrix}, \tag{3}$$

for which

$$\sum_i w'_i \psi'_i(x) \psi'^*_i(x') = \sum_i w_i \psi_i(x) \psi^*_i(x').$$

Such schemes, which equally describe the same physical object, we shall call equivalent.

To each quantum-statistical system, and to the density matrix describing it, there corresponds an infinite set of equivalent schemes which represent the given physical object. Among these, the basic role is played by those schemes with orthogonal representations, i.e., the schemes

$$\begin{pmatrix} \varphi_1(x) & \varphi_2(x) & \ldots \\ p_1 & p_2 & \ldots \end{pmatrix}, \tag{4}$$

for which

$$\int \varphi_i(x) \varphi_j^*(x)\, dx = \delta_{ij}. \tag{5}$$

Let an arbitrary non-orthogonal scheme be given. We attempt to find an equivalent scheme with orthogonal representations. This problem is equivalent to the problem of reducing the Hermitian matrix

$$\rho(x, x') = \sum_i w_i \psi_i(x) \psi_i^*(x') \tag{6}$$

to diagonal form by a unitary transformation. The latter can be found for an arbitrary matrix (6), as long as this matrix is Hermitian. As usual, this transformation is found by the solution of the equation

$$\rho\varphi = \lambda\varphi, \tag{7}$$

or, for a continuous coordinate x,

$$\int \rho(x, x') \varphi_m(x')\, dx' = \lambda_m \varphi_m(x). \tag{7a}$$

For a discrete spacing x, the integrals in Eqs. (5), (7a) and also in many of the following equations, must be replaced by summations.

The matrix $\phi_m(x)$ will also be the matrix of the desired unitary transformation. In the new representation, the density matrix will have the diagonal form

$$\rho_{mn} = \iint \varphi_m^*(x) \rho(x, x') \varphi_n(x')\, dx\, dx' = \lambda_m \delta_{mn}.$$

The inverse transformation is written in the form

$$\rho(x, x') = \sum \varphi_m(x) \rho_{mn} \varphi_n^*(x') \tag{8}$$

$$= \sum \lambda_m \varphi_m(x) \varphi_m^*(x'),$$

whence it is evident that $\rho(x, x')$ is the density matrix of the scheme

$$\begin{pmatrix} \varphi_1(x) & \varphi_2(x) & \ldots \\ \lambda_1 & \lambda_2 & \ldots \end{pmatrix}, \tag{9}$$

which, by virtue of Eqs. (6) and (8) is equivalent to the scheme (1). The orthogonality of this scheme, i.e., Eq. (5), follows from the unitary property of the matrix $\phi_m(x)$.

As a consequence of the invariance of the trace of a matrix for a unitary transformation, we have

$$\sum \lambda_m = \mathrm{Tr}\,\rho = \int \rho(x, x)\, dx = 1. \tag{10}$$

It remains only to prove the non-negative character of the λ_m, i.e., that λ_m can actually play the role of a probability.

The density matrix is always positive definite, since, for an arbitrary function $f(x)$,

$$\iint \rho(x, x') f(x) f^*(x')\, dx\, dx' \tag{11}$$

$$= \sum_i w_i \left| \int \psi(x) f(x)\, dx \right|^2 \geqslant 0.$$

It then follows that all the λ_m are non-negative; this can easily be established by setting $f(x) = \phi_m^*(x)$ in Eq. (11) (in this case the left hand side of Eq. (11) reduces to λ_m).

We now discuss the problem of the uniqueness of the scheme of orthogonal representations. Linear algebra furnishes the information that the decomposition of the density matrix into orthogonal representations can have a unique form if, and only if, there are no duplicates among the eigenvalues λ_1, λ_2, ... On the other hand, suppose that there is degeneracy. Let $\Lambda_1, \Lambda_2, \ldots$ be the collection of different values which occur among the $\lambda_1, \lambda_2, \ldots$, and let $l_1, l_2, \ldots$ be the corresponding multiplicity (Λ_j occurs among the λ_j just l_j times). In such notation, Eq. (10) can be written

$$\sum_j l_j \Lambda_j = 1.$$

To each Λ_j there will correspond l_j orthogonal functions

$$\varphi_{j1}, \ldots, \varphi_{jl_j} \left(\int \varphi_{jm}(x) \overset{*}{\varphi}_{jn}(x)\, dx = \delta_{mn}\right). \tag{12}$$

However, the set of functions (12) is not uniquely determined; it is possible to replace it by any other set obtained from Eq. (12) by means of the application of a unitary transformation. Only the linear manifold remains invariant in all these transformations:

$$[\varphi_{j1}, \ldots, \varphi_{jl_j}] \equiv \mu_1\varphi_{j1} + \ldots + \mu_{l_j}\varphi_{jl_j} \tag{13}$$

($\mu_1, \ldots, \mu_{l_j}$ arbitrary numbers), and also the sphere $|\mu_1|^2 + \ldots + |\mu_{l_j}|^2 = 1$ is invariant.

In the case of degeneracy ($l_j > 1$), the selection of any preferred system of representations has no meaning, and even the requirement of orthogonality cannot lead to such a system. Avoiding unjustified multivaluedness, and not wanting to redefine the object (i.e., to speak of it somewhat unnecessarily) we shall here characterize the object by a designation which describes its linear manifold (or sphere)

$$[\psi_1(x), \ldots, \psi_s(x)]. \tag{14}$$

The quantum statistical state that is described by Eq. (14) is a generalization of the state which is described by the individual wave function $\psi(x)$. Choosing a state of type (14) as a possible representation, we get the equivalent scheme

$$\begin{pmatrix} [\varphi_{11}(x), \ldots, \varphi_{1l_1}(x)] & [\varphi_{21}(x), \ldots, \varphi_{2l_2}(x)] & \cdots \\ P_1 & P_2 & \cdots \end{pmatrix} \quad (P_j = l_j\Lambda_j). \tag{15}$$

This scheme is fundamental in this sense, that each quantum-statistical state (each scheme) reduces to it single-valuedly, and conversely, to the different states (density matrices) there correspond different fundamental schemes, i.e., there exists a one-to-one correspondence. The different representations of Eq. (15) (for example, $[\phi_{j1}, \ldots, \phi_{jl_j}]$ and $[\phi_{k1}, \ldots, \phi_{kl_k}]$, $j \neq k$) are mutually orthogonal. The linear manifolds are orthogonal if their elements are orthogonal :

$$\int \varphi_{j\alpha} \overset{*}{\varphi}_{k\beta} = 0, \quad \alpha = 1, \ldots, l_j,$$

$$\beta = 1, \ldots, l_k \quad (j \neq k).$$

If there is no degeneracy, the form of Eq. (15) can also be used formally, since, in the case of a single function, $[\phi(x)]$ coincides with $\phi(x)$.

2. We proceed to a consideration of the entropy, by which we understand, in keeping with references 1 and 2, a quantity which characterizes the indefiniteness (neginformation), or statistical dispersion, of a given state. Following the custom established in information theory, we shall denote dimensionless entropy by H. Then the ordinary entropy, which has the dimensions of energy/degree, will be given by

$$S = kH,$$

where k is the Boltzmann constant.

We shall denote by A_i an event which consists of the identification of $\phi_i(x)$ with one of the scheme (1), $i = 1, 2, \ldots$. If the events A_1, A_2, . . . are mutually exclusive, then, by the

---

[1] *The Theory of the Transmission of Electrical Signals in the Presence of Interference*, Collected Translations under the editorship of N. A. Zheleznov, Moscow, 1953

[2] R. L. Stratonovich, J. Exper. Theoret. Phys. USSR **28**, 409 (1955); Soviet Phys **1**, 254 (1955)

general formula which appears in reference 2, the entropy of the system is equal to

$$H = -\sum_i P(A_i)\ln\frac{P(A_i)}{Q(A_i)}, \tag{16}$$

where $P(A_i)$ and $Q(A_i)$ are the probability and abstract "volume" of the event A_i.

Making use of the independence of the "volumes" of the events of the probability distribution, we determine $Q(A_i)$. We recall that the entropy of a "determined" (in the sense of the absence of "mixed statistics") quantum state, which is described by the wave function $\psi_i(x)$, is equal to zero. Substituting $w_i = 1$, $w_j = 0$ ($j \neq 1$) in Eq. (16) and equating this expression to zero, we obtain $Q(A_i) = 1$. We can carry out such a procedure for different i, so that

$$H = -\sum_i w_i \ln w_i. \tag{17}$$

This well-known formula is correct when the events $A_1, A_2, \ldots$ are mutually exclusive.

It is a characteristic feature of quantum theory that a system described by the wave function ψ_i will be found in the state of ψ_j with the probability

$$P_{ij} = \left|\int \psi_i\psi_j^* dx\right|^2. \tag{18}$$

Therefore, if $P_{ij} \neq 0$, a duality exists in regard to the incompatibility of the events A_i and A_j ($i \neq j$): on the one hand, they appear to be incompatible since the function ψ_j is not obtained if the function $\psi_i \neq \psi_s$ is obtained (and conversely); on the other hand, the probability of locating (by measurement) in the state ψ_j the system, which is described by the function ψ_i, is different from zero. If by A_i we understand the appearance of the system in the physical state ψ_i, then in the well-known sense the probability of the joint event A_iA_j is equal to P_{ij}. According to quantum theory, knowing the wave function, it is impossible (without measurement of this function) to carry further the precise identification of the state of the system. This prevents the separation of each event A_i into arbitrary elementary sub-events (for example, into A_iA_j and $A_i - A_iA_j$) for the purpose of defining the entropy analogous to Eq. (16) by summing over the elementary events.

If, to one physical state, one can refer different wave functions, (of course, with different probabilities), then, consequently, in the description of the state by wave functions there takes place a certain redefinition (over describing). In the introduction of mixed statistics, which describe the one mathematical object (the density matrix of the fundamental scheme) by many different equivalent schemes, we frequently remove this redefinition and in this sense the quantum description approximates the classical. Therefore, the solution of the difficulty in the definition of the entropy of a non-orthogonal scheme, arising as a consequence of the redefinition, must be sought in the idea equivalence set forth in Sec. 1.

We substitute for the original scheme (1) the equivalent orthogonal scheme (9). For orthogonal representations, the events $A_1, A_2, \ldots$ are mutually exclusive in both senses, and therefore Eq. (17) is applicable. Equivalent schemes which describe one and the same object must have identical entropy; therefore, the entropy of the nonorthogonal scheme (1) is equal to

$$H = -\sum_m \lambda_m \ln \lambda_m, \tag{19}$$

where λ_m are the eigenvalues of the density matrix (8).

For example, we consider the scheme

$$\begin{pmatrix}\psi_1(x) & \psi_2(x)\\ w_1 & w_2\end{pmatrix},$$

which consists of two nonorthogonal representations. When $\psi_1 \neq \psi_2$, $w_1 \neq 0, 1$, there is an additional indefiniteness in the system; consequently,

$$H > 0.$$

But since, as a consequence of the nonorthogonality , the states ψ_1 and ψ_2 represent in known degree one and the same object, but the entropy will be less than for the completely different states, i.e.,

$$H < -w_1 \ln w_1 - w_2 \ln w_2.$$

Actually, interpolation according to Eq. (19) in the intermediate case, when $0 < P_{12} < 1$, gives

$$H = -\lambda_1 \ln \lambda_1 - \lambda_2 \ln \lambda_2,$$

where

$$\lambda_{1,2} = \frac{w_1 + w_2}{2} \pm \sqrt{\left(\frac{w_1 - w_2}{2}\right)^2 - P_{12} w_1 w_2}.$$

When degeneracy of the eigenvalues occurs, Eq. (19) can be written in the form

$$H = -\sum_j l_j \Lambda_j \ln \Lambda_j.$$

The quantity $l_j \Lambda_j = P_j$ is nothing else than the probability of obtaining the jth linear manifold [state of type (14)]. Therefore, in complete correspondence with Eq. (16), we have

$$H = -\sum_j P_j \ln (P_j/Q_j), \qquad (20)$$

where Q_j is the abstract "volume" of the event which consists of the obtaining of the jth linear manifold, and is equal to the weight l_j of the latter.

Eqs. (19) and (20) can be written in matrix form:

$$H = -\mathrm{Tr}\,\lambda \ln \lambda \quad (\lambda = \|\lambda_{mn}\| = \|\lambda_m \delta_{mn}\|),$$

or in the arbitrary representation

$$H = -\mathrm{Tr}\,\rho \ln \rho. \qquad (21)$$

From such a form of description, and especially from the form $H = -\ln \rho$, it is evident that the entropy of a quantum-statistical system is a direct generalization of the classical entropy.

3. We have shown that the formulas introduced for corresponding conditions lead to formulas for the entropy of "classical" statistics.

If the quantum system (which does not consist of identical particles) does not have a cyclic or spin degree of freedom, and the coordinates x are continuous, then its density matrix can be written in the form

$$\rho(x, x') = \int w\left(\frac{x + x'}{2}, p\right) \times \exp\{ip(x - x')/\hbar\}\, dp, \qquad (22)$$

where $w(q, p)$ is the normalized "probability density" in phase space:

$$\int w(q, p)\, dq\, dp = 1.$$

However, each function $w(q, p)$, being transformed according to Eq. (22), yields the function $\rho(x, x')$ which becomes a sort of density matrix, since the condition of positive definiteness of the matrix $\rho(x, x')$ can be violated. The quantum "probability density" $w(q, p)$ satisfies the condition

$$\iiint w\left(\frac{x + x'}{2}, p\right) e^{ipx/\hbar} f(x) \times [e^{ipx'/\hbar} f(x')]^* \, dx\, dx'\, dp \geqslant 0 \qquad (23)$$

for an arbitrary function $f(x)$. The inequality in Eq. (23) is a precise, although not clear, mathematical formulation of the Heisenberg uncertainty principle.

From the quantum formula (19) we derive an expression for the entropy under the condition of the applicability of the classical approximation, when

$$p_{0i} q_{0i} \gg h, \qquad \frac{1}{p_{0i}} \sim \frac{1}{w} \frac{\partial w}{\partial p_i}; \quad \frac{1}{q_{0i}} \sim \frac{1}{w} \frac{\partial w}{\partial q_i} \quad (i = 1, \ldots, r). \qquad (24)$$

For this purpose, we consider Eq. (7a), where we represented the density matrix in the form (22). We choose the interval

$$\tilde{\lambda}_j < \lambda_m < \tilde{\lambda}_j + \Delta\lambda, \qquad (25)$$

in which l_j coincides with the eigenvalues ($m = m_j + 1, \ldots, m_j + l_j$). When $\Delta\lambda$ is sufficiently small, all the eigenvalues entering into Eq. (25) can be replaced by $\tilde{\lambda}_j$. Therefore, for the eigenfunctions which correspond to the λ_m, we have

$$\int \rho(x, x') \varphi_m(x')\, dx' \approx \tilde{\lambda}_j \varphi_m(x). \qquad (26)$$

An arbitrary linear combination of eigenfunctions satisfies the same equation. In particular,

$$\int \rho(x, x') \tilde{\varphi}_s(x')\, dx' \approx \tilde{\lambda}_j \tilde{\varphi}_s(x); \qquad (27)$$

$$\tilde{\varphi}_s(x) = \sum_{k=1}^{l_j} c_{sk} \varphi_{m_j + k}(x) \quad (s = 1, \ldots, l_j).$$

The transformation from Eq. (7a) to (27) is a transformation to an approximately equivalent scheme. We choose $\| c_{sk} \|$ in such a fashion that each function $\phi_s(x)$ maintains a harmonic factor which rapidly decreases relative to the other (amplitude) factor:

$$\tilde{\varphi}_s(x) = \varphi_s^0(x) \exp\{ik_s x\}; \tag{28}$$

$$k_s \gg \frac{1}{\varphi_s^0} \frac{\partial}{\partial x} \varphi_s^0; \tag{29}$$

and that $\phi_s^0(x)$, nonetheless, be appreciably different from zero only in a small (in comparison with q_{oi}) region near some point q_s. The existence of such a selection, together with the condition for the smallness of $\Delta\lambda$ is valid only for the actual fulfilling of the inequality (24).

Substituting Eq. (28) into Eq. (27) and writing $p_s = k_s \hbar$, we find

$$\int w\left(\frac{x+x'}{2}, p\right) \exp\{i(p - p_s) \tag{30}$$

$$\times (x - x')/\hbar\} \varphi_s^0(x')\, dp\, dx' \approx \lambda_j \varphi_s^0(x).$$

We make valid use of the equation

$$\int F(x', y') \exp\{i(y - y') \tag{31}$$

$$\times (x - x')/\hbar\}\, dx' dy' \approx h^r F(x, y),$$

as can easily be seen from

$$\int F(x', y') \exp\{i(y - y')(x - x')/\hbar\}\, dy'$$

$$= F(x', y) \int \exp\{i\eta(x' - x)/\hbar\}\, \mu(\eta)\, d\eta$$

$$= F(x', y)(2\pi\hbar)^r \delta_\varepsilon(x' - x),$$

under the condition

$$\left(F \Big/ \frac{\partial F}{\partial x_i}\right)\left(F \Big/ \frac{\partial F}{\partial y_i}\right) \gg h. \tag{32}$$

Here $\eta = y' - y$, $\mu(\eta) = F(x', y + \eta)/F(x', y)$ [i.e., $\mu(\eta) \sim 1$ for $\eta \lesssim F/[\partial F/\partial y]$):

$$\delta_\varepsilon(x' - x) = \prod_{i=1}^{r} \delta_{\varepsilon_i}(x'_i - x_i);$$

$\delta_{\epsilon i}(x'_i - x_i)$ is a function which approximates the δ function, and which has the equivalent width

$$\varepsilon_i \sim \hbar \frac{1}{F} \frac{\partial F}{\partial y_i}.$$

For $F = w\phi_s^0$, Eq. (32) is satisfied as a consequence of Eqs. (24) and (29) (since $p_{oi} \sim k_s \hbar = p_s$); therefore, Eq. (31) can be applied for the calculation of the left hand side of Eq. (30). As a result, we obtain from Eq. (30)

$$\tilde{\lambda}_j \varphi_s^0(x) \approx h^r w(x, p_s) \varphi_s^0(x)$$

$$\approx h^r w(q_s, p_s) \varphi_s^0(x)$$

or

$$\tilde{\lambda}_j \approx h^r w(q_s, p_s). \tag{33}$$

In replacing x by q_s, use is made of the fact that $\phi_s^0(x)$ differs significantly from zero only in the region close to q_s.

In taking various s, we shall get different points q_s, p_s ($s = 1, \ldots, l_j$), but for all these points,

$$h^r w(q_1, p_1) \approx \ldots \approx h^r w(q_{l_j}, p_{l_j}) \approx \tilde{\lambda}_j.$$

Considering this, we have

$$H = -\sum \lambda_m \ln \lambda_m \tag{34}$$

$$\approx -\sum_j \tilde{\lambda}_j \sum_{s=1}^{l_j} \ln h^r w(q_s, p_s).$$

Let $L(q, p)$ be an arbitrary function and let L be the corresponding operator *. According to the correspondence principle, when the classical approximation is applied,

$$\bar{L} = \mathrm{Tr}(\rho \mathrm{L}) \approx \int L(q, p)\, w(q, p)\, dq\, dp, \tag{35}$$

But

$$\mathrm{Tr}(\rho \mathrm{L}) = \sum \lambda_m (\varphi_m^* \mathrm{L} \varphi_m) \tag{35a}$$

$$\approx \sum_j \tilde{\lambda}_j \sum_{s=1}^{l_j} (\tilde{\varphi}_s^* \mathrm{L} \tilde{\varphi}_s).$$

We then have

---

* We note, without proof, that the following relation holds:

$$\mathrm{L} = \frac{1}{h^r} \int L\left(\frac{x+x'}{2}, p\right) \exp\{ip(x - x')/\hbar\}\, dp.$$

$$\sum_j \lambda_j \sum_{s=1}^{l_j} L(q_s, p_s) \tag{36}$$

$$\approx \int w(q, p) L(q, p)\, dq\, dp.$$

If we put $L(q, p) = \ln h^r w$ then, from Eqs. (34) and (36), we get

$$H \approx -\int w(q, p) \ln [h^r w(q, p)]\, dq\, dp \tag{37}$$

(r = number of degrees of freedom). This formula, which differs from the usual formula

$$H = -\int w \ln w\, dq\, dp$$

(in which an additive constant is undetermined), by a constant $r \ln h$, is identical with the exact formula given in reference 2. The considerations of this latter work, which lead to formulas containing Planck's constant, are verified in the same way.

One can arrive at Eq. (37) by a different sort of demonstration, namely, that the density matrix is the operator for the "physical quantity" $h^r w(q, p)$ with subsequent use of Eq. (35) for $L = \ln \rho$. From the considerations set forth above, it is evident that we can take as one of the possible schemes in the classical approximation, the scheme which consists of functions localized in the neighborhood of the point in phase space. The latter scheme is far more graphic from the point of view of the calssical representation.

When the system consists of identical particles, i.e., particles which obey the Bose or Fermi statistics, specific differences appear from the case considered earlier. For M identical particles, each of which has n degrees of freedom ($r = nM$) the denisty matrix, instead of (22), has the form

$$\rho(x_1, \ldots, x_M; x'_1, \ldots, x'_M)$$

$$= C \sum_\alpha \varkappa_\alpha r(x_1, \ldots, x_M; x'_{\alpha_1}, \ldots, x'_{\alpha_M}), \tag{38}$$

where

$$r(x_1, \ldots, x_M; x'_1, \ldots, x'_M)$$

$$= \int \cdots \int w\left(\frac{x_1 + x'_1}{2}, \ldots, \frac{x_M + x'_M}{2}; p_1, \ldots, p_M\right)$$

$$\times \exp\left\{\frac{i}{\hbar}[p_1(x_1 - x'_1)\right.$$

$$\left. + \ldots + p_M(x_M - x'_M)]\right\} dp_1, \ldots, dp_M.$$

The $\alpha_1, \ldots, \alpha_M$ are some permutation of the numbers 1, 2, . . . , M; $\sum_\alpha$ is the sum over all $M!$ such permutations, $\kappa_\alpha = 1$ for bosons and $\kappa_\alpha = (-1)^{p_\alpha}$ for fermions (p_α is the number of transpositions of the permutation $\alpha_1, \ldots, \alpha_M$); C is a normalizing constant. The density of distribution w for identical particles we shall of course assume to be symmetric.

Under the condition of applicability of the classical approximation (24), the functions $r(x_1, \ldots; x'_1, \ldots)$ are significantly different from zero only for nearly identical values of the primed and unprimed arguments:

$$r(x_1, \ldots; x'_1, \ldots) = \tilde{r}(x_1, \ldots, x_M) \delta_{\varepsilon_1}(x_1 - x'_1)$$

$$\ldots \delta_{\varepsilon_M}(x_M - x'_M), \quad (\varepsilon \sim \hbar/p_0).$$

From this it follows that for $x_1 = x'_1, \ldots, x_M = x'_M$, $x_\alpha - x_\beta \gg \epsilon$ ($\alpha \neq \beta$) we can take into consideration only one of the terms of the sum (38), for which

$$\rho(x_1, \ldots, x_M; x_1, \ldots, x_M)$$

$$\approx C r(x_1, \ldots, x_M; x_1, \ldots, x_M).$$

Neglecting the integral over volumes where the arguments reduce to distances of the order of ϵ ($\epsilon \ll q_0$) and where this equality is invalid, we have

$$\int \rho(x_1, \ldots, x_M; x_1, \ldots, x_M)\, dx_1 \ldots dx_M$$

$$\approx C \int r(x_1, \ldots, x_M;$$

$$x_1, \ldots, x_M)\, dx_1 \ldots dx_M = C,$$

from which

$$C \approx 1. \tag{39}$$

We shall take the local wave function $\tilde{\psi}_{q_1 \ldots q_M p_1 \ldots p_M}(x_1, \ldots, x_M)$ which corresponds to this case, when one particle is close to the point (q_1, p_1), another close to (q_2, p_2) and so forth:

$$\tilde{\psi}_{q_1 \ldots q_M p_1 \ldots p_M}(x_1, \ldots, x_M) \tag{40}$$

$$= C' \sum_\beta \varkappa_\beta \psi^0_{q_1 \ldots q_M}(x_{\beta_1}, \ldots, x_{\beta_M})$$

$$\times \exp\left\{\frac{i}{\hbar}(p_1 x_{\beta_1} + \ldots + p_M x_{\beta_M})\right\}.$$

Here C' is the normalizing constant, $\psi^0_{q_1 \ldots q_M}(x_1, \ldots, x_M)$ is a slowly changing function (in comparison with the harmonic factor) which differs appreciably from zero only for $x_1 \sim q_1, \ldots, x_M \sim q_M$.

We apply the operator ρ to Eq. (40). Taking into account Eq. (38), and changing the signs of the transformed integrations, we get

$$\rho\tilde{\psi} = M!C'C \sum_{\gamma} \varkappa_{\gamma} \int w\left(\frac{x_1 + x_1'}{2}, \ldots, \frac{x_M + x_M'}{2}; p_1', \ldots, p_M'\right) \psi^0 (x_{\gamma_1}', \ldots)$$

$$\times \exp\left\{\frac{i}{h}[p_1'(x_1 - x_1') + p_1 x_{\gamma_1}' + \ldots]\right\} dx_1' \ldots dp_1' \ldots$$

$$= M!C'C \sum_{\gamma} \varkappa_{\gamma} \exp\left\{\frac{i}{h}(p_1 x_{\gamma_1} + \ldots)\right\} \int w\left(\frac{x_1 + x_1'}{2}, \ldots; p_1', \ldots\right) \psi^0 (x_{\gamma_1}', \ldots)$$

$$\times \exp\left\{\frac{i}{h}[(p_1' - p_{\sigma_1})(x_1 - x_1') + \ldots]\right\} dx_1' \ldots dp_1' \ldots,$$

where $\sigma_1, \ldots, \sigma_M$ are permutations inverse to $\gamma_1, \ldots, \gamma_M$ ($\gamma_{\sigma i} = i$). Applying Eq. (31) we then obtain

$$\rho\tilde{\psi} \approx M!C'h^r \sum_{\gamma} \varkappa_{\gamma} \exp\left\{\frac{i}{h}(p_1 x_{\gamma_1} + \ldots)\right\}$$

$$\times w(x_1, \ldots; p_{\sigma_1}, \ldots) \psi^0_{q_1 \ldots}(x_{\gamma_1}, \ldots)$$

$$\approx M!\, h^r C' \sum_{\gamma} \varkappa_{\gamma} \exp\left\{\frac{i}{h}\, p_1 x_{\gamma_1} + \ldots)\right\}$$

$$\times w(q_{\sigma_1}, \ldots; p_{\sigma_1}, \ldots) \psi^0_{q_1 \ldots}(x_{\gamma_1}, \ldots)$$

or, considering the symmetry of the density function,

$$\rho\tilde{\psi}_{q_1 \ldots p_1 \ldots}(x_1, \ldots) \tag{41}$$

$$\approx M!\, h^r w(q_1, \ldots; p_1 \ldots) \tilde{\psi}_{q_1 \ldots p_1 \ldots}(x_1, \ldots).$$

Taking into account the equality thus obtained or the relation stemming from it

$$(\tilde{\psi}^*_{q_1 \ldots p_1 \ldots} \rho\tilde{\psi}_{q_1 \ldots p_1 \ldots}) \tag{42}$$

$$\approx M!\, h^r w(q_1, \ldots; p_1, \ldots),$$

we conclude that the denisty matrix is the operator of the "physical quantity" $M!\,h^r w(q_1, \ldots; p_1, \ldots)$. Furthermore, the functions $\ln \times [M!\,h^r w(q_1, \ldots; p_1, \ldots)]$ correspond to the operator $\ln \rho$ and, as a consequence of Eqs. (21), (35), and (35a), we have

$$H \approx -\int w(q, p) \ln [M!\, h^r w(q, p)]\, dq\, dp, \tag{43}$$

$$[q = (q_1, \ldots, q_r);$$

$$p = (p_1, \ldots, p_r); \quad r = nM].$$

A similar formula was obtained in reference 2 as the formula which determines the configurational neginformation, which coincides with the actual neginformation for essentially indistinguishable particles. Thus the quantum consideration verifies the conclusions of the previous work.

4. In those cases in which a scheme of type (1) is not assigned, but some information Γ of another kind is available concerning the quantum-statistical system, the density matrix can be determined by use of the following principal of maximum neginformation: since nothing is known about the system except Γ, then the desired density matrix must have the maximum neginformation (entropy) of all density matrices consisting with Γ.

The choice of another density matrix which has a smaller neginformation would have implied a fixing of some additional information in addition to Γ. Thus the problem of the search for an unknown density matrix reduces to the conventional extremal problem for expressions which determine the entropy. We note that the principle just demonstrated does not appear as a consequence of the second law of thermodynamics, since it is far wider than the latter and is suitable for investigation of density matrices for nonequilibrium states, i.e., it emerges from the framework of statistical thermodynamics. If we choose the condition $E \leqq H \leqq E + \Delta E$ for Γ (H is the Hamiltonian of the system), then the solution of the extremal problem leads to the quantum microcanonical distribution. However, in physical problems, there cannot be complete certainty that the energy for any other physical quantity does not exceed the limits of some interval. It is more accurate to use for the condition on Γ the fixing of the phenomenological parameters: $\mathcal{L}_1, \ldots, \mathcal{L}_m$. But in the transition from the phenomenological picture to dynamic, there corresponds a statistical mean to the phenomenological parameters. From this point of view it is more accurate to put the conditions Γ in the form: $\overline{L}_1 = \mathcal{L}_1, \ldots, \overline{L}_m = \mathcal{L}_m$. Then the variational problem will have the form

$$\delta \operatorname{Tr}(\rho \ln \rho) = 0 \tag{44}$$

for the conditions

$$\operatorname{Tr} \rho = 1; \ \operatorname{Tr}(\rho L_1) = \mathcal{L}_1; \ldots; \tag{45}$$
$$\operatorname{Tr}(\rho L_m) = \mathcal{L}_m.$$

To these conditions, generally speaking, one would have to add the condition of positive definiteness and Hermitian character of the function ρ. However, functions which are not positive definite, have less (and even negative) entropy; therefore, their inclusion in the class of functions of comparison cannot change the result. Since we do not introduce the Hermitian condition, we also broaden the class of the functions of comparison. If the extremal of this expanded class is Hermitian (which is fulfilled, as is easy to prove), then it will be simultaneously an extremal for the much narrower class of Hermitian functions of comparison.

Solving Eqs. (44) and (45) with the help of Lagrangian multipliers and bearing in mind that, in general,

$$\delta \operatorname{Tr}(\rho^k) = \operatorname{Tr}(k\rho^{k-1}\delta\rho),$$

we find

$$\operatorname{Tr}[(\ln \rho + \gamma_0 + \gamma_1 L_1 + \ldots + \gamma_m L_m + 1)\delta\rho] = 0,$$

whence

$$\rho = \exp\{\gamma - \gamma_1 L_1 - \ldots - \gamma_m L_m\}, \tag{46}$$

where $\gamma_1, \ldots, \gamma_m$ and $\gamma = -\gamma_0 - 1$ are defined by Eq. (45).

When $m = 1$, $L_1 = H$, the density matrix (46) coincides with the quantum canonical distribution, which is usually hypothesized[3] or derived from the (hypothesized in its turn) microcanonical distribution[4].

Starting out from the framework of statistical thermodynamics, it is possible to put for $L_1, \ldots, L_m$ non-equilibrium distribution of energy, density, current, etc., and to obtain the density matrices which describe such systems. Thus, furnishing a basis for the analytic use of the principal of maximum neginformation, the formula of quantum entropy is shown to be useful in the quantum statistical theroy of nonequilibrium processes.

Translated by R. T. Beyer
96

[3] M. A. Leontovich, Statistical Physics GITTL, Moscow-Leningrad, 1944

[4] A. Ia. Khinchin, *Mathematical Foundations of Quantum Statistics*, Dover, New York, 1949

SOVIET PHYSICS JETP VOLUME 1, NUMBER 3 NOVEMBER, 1955

Ranges of Protons in Medium and Heavy Elements

B. V. RYBAKOV
Academy of Science, USSR

(Submitted to JETP editor March 9, 1955)
(J. Exper. Theoret. Phys. USSR **28**, 651-654 (June, 1955)

We have measured the aluminum equivalents of the ranges of protons with energies 1-7 Mev in Fe, Cu, Mo, Cd, Sn, Ta and Pb. A method is presented for constructing an empirical range-energy curve on the basis of available data for all medium and heavy elements in the indicated range of energies.

INTRODUCTION

IN the work of Vlasov and others [1] on the interaction of protons with tritons, protons are slowed to various energies by means of lead filters. There it is necessary, knowing the initial energy of the protons, to determine their energy after passing through a given thickness of lead. Up to this time there is lacking in the literature a sufficiently exact range-energy curve for Pb and other heavy and medium elements in the energy range 1-7 Mev. Reliable calculation of these curves on the basis of existing data on mean excitation potentials of atoms appears difficult, since the Bethe-Bloch formula, to which current theories of the passage of charged particles through matter lead, is correct only under the condition $E_p \gg (M/m) E_{el}$, which is poorly satisfied for heavy elements with protons whose energy is not large. (For Pb with protons of 1 Mev energy, it is not satisified for K-, L-, M- and N-electrons.) In connection with this we carried out measurements of the aluminum equivalents of the ranges of protons in Fe, Cu, Mo, Cd, Sn, Ta and Pb and constructed range-energy curves for these elements on the basis of the existing curve for Al[2].

APPARATUS AND METHOD OF MEASUREMENT

The work was performed with a beam of protons of energy 7.3 Mev, brought out of a cyclotron into a vacuum channel and focused by a special magnet. At the focus of the magnet in the vacuum chamber was located a remote-control arrangement for placing in the path of the beam filters of the substances to be studied and measuring the proton current which passes through the filter and the proton current which is stopped by it. The schematic arrangement is shown in Fig. 1. A beam of protons is collimated by diaphragms 1 and 2. Diaphragm 2 serves as trimmer for tuning the cyclotron. The diaphragms are kept at a potential of + 200 V, preventing secondary emission electrons from them from falling onto other parts of the equipment. The filters are placed in two disc-shaped plate-holders 6 and 7, with 12 in each. The discs are mounted on the axis of telephone searchers 5 and 8 and can be turned independently of one another into any of 12 positions. The permanent magnet 3 is intended to catch the secondary emission electrons from the filters. Under the action of the magnetic field it sets up, the electrons are either turned into the disc or fall on the magnet.

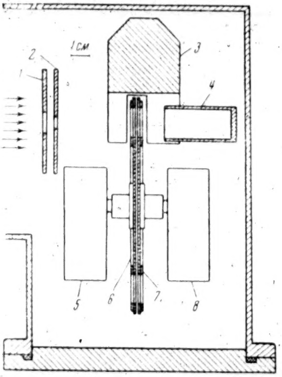

FIG. 1. Diagram of apparatus for measuring the aluminum equivalent of the range of protons in various substances. *1* and *2*- diaphragms; *3* - permanent magnet; the field is perpendicular to the plane of the figure; *4* - Faraday cylinder; *5* and *8* - remote controlled rotating mechanism; *6* and *7* - disc-shaped plate-holder with filters.

---

[1] N. A. Vlasov, C. P. Kalinin, A. A. Ogloblin, L. N. Samoilov, V. A. Sidorov, V. I. Chuev, J. Exper. Theoret. Phys. USSR **28**, 639 (1955)

Both the magnet and the discs are insulated from the body and connected together by sliding contacts. The charge collecting on this system determines the number of protons stopping in the filters. After passing through the filters the beam is completely stopped in a Faraday cylinder, the fore edge of which enters the gap between the poles of the magnet. The magnetic field does not permit secondary emission electrons to leave the cylinder.

The currents I_1 (from the Faraday cylinder) and I_2 (from the disc-magnet system) are measured by string electrometers by a constant deflection method in which readings of the two electrometers are taken simultaneously. The quantity $I_1/(I_1+I_2)$ plotted in its dependence on the thickness of the filter is the usual absorption curve. The aluminum equivalents of the proton ranges are measured as follows. The absorption curve in aluminum is taken. Then, without turning off the beam, part of the aluminum in the end of the range is replaced by a specimen of the investigated substance and again an absorption curve is taken, in which the thickness of aluminum before the specimen is varied. The difference in the thickness of aluminum corresponding to the points of half absorption on these curves gives the aluminum equivalent of the specimen.

In Fig. 2 is shown one of the absorption curves of protons in Al. The mean range of the protons in Al, found from it as the thickness of aluminum absorbing half the protons, is 97.0 ± 0.3 mg/cm^2. Using the range-energy curve of protons in Al[2] we find that the mean energy of the protons in the beam is 7.3 Mev. From the absorption curve it is also possible to estimate the energy spread of the beam. The differentiated curve, shown in the same figure, has a half-width consisting of 2% of the range. Subtracting from this the half-width due to straggling, the magnitude of which for Al is 1.3% for protons of 7.3 Mev energy[3], we find that the spread in proton energies about the mean value is ± 0.07 Mev.

The mean energy of the protons fluctuated somewhat during the measurement. The error introduced by this in the magnitude of the aluminum equivalent does not exceed 0.4 mg/cm^2. (This figure also takes into account accidental errors in measuring the currents, as determined by the scatter of the point on the absorption curve.) It was observed that as a result of the cyclotron shutdown, during which the insulators of the deflection plates and the filament of the ion source were changed, etc., the change in the mean energy of the protons in the beam could amount to 0.1 Mev. In the present case this is not significant since the measurement of the aluminum equivalent is carried out without turning off the beam.

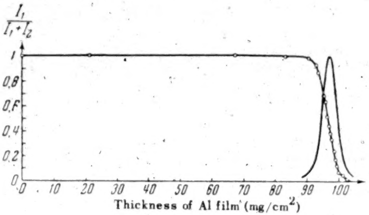

FIG. 2. Absorption curve of proton beam in Al.

The thickness of the filter in mg/cm^2 is determined from its area and weight. The following method was used to measure the area of the filters. A disc cut from the foil stock was clamped between two cylinders on the lathe and turned to a diameter of 25 mm which was measured by a micrometer to an accuracy of 0.01 mm, giving an error of less than 0.1% in the value of the area. The filter was weighed on an analytical balance with a precision of 0.1 mg. Thus the error in the mean thickness of the filter does not exceed 0.1 mg/cm^2. All the filters but molybdenum and tantalum were sufficiently uniform in thickness. The purities of the materials employed are as follows: Al – not less than 99.7%; Fe, Cu, Cd, Sn and Pb – not less than 99.8%; Mo and Ta – about 99.5%.

RESULTS OF MEASUREMENT

In the Table is presented the range of protons in the investigated substance (R) and the equivalent of this range in aluminum (R_{Al}). The uncertainty in the determination of R_{Al} is about ± 0.5 mg/cm^2. For Mo and Ta it is somewhat more, since in these cases errors are introduced by nonuniformity of the foil. Determining the proton energies corresponding to the ranges R from the range-energy curve for Al[1], it is possible to construct the range-energy curve for the investigated substances. This is presented in Fig. 3 (except for Cd, whose curve lies very close to that for Sn).

---

[2] J. H. Smith, Phys. Rev. **71**, 32 (1947)

[3] D. O. Caldwell, Phys. Rev. **88**, 131 (1952)

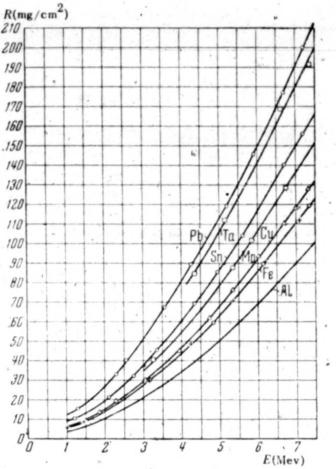

FIG. 3. Range energy curve for protons in various elements.

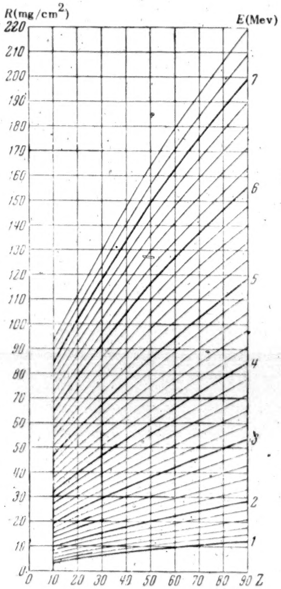

FIG. 4. Nomogram for the determination of the path R of protons with energies E in an element of atomic number Z.

TABLE

Element	Z	R (mg/cm^2)	R_{Al}(mg/cm^2)
Fe	26	5,3	3,5*
		8,8	6,5*
		29,5	23,0*
		30,1	23,3
		48,1	38,2*
		59,7	47,9
		70,5	57,5*
		89,3	72,6
		90,5	73,2*
		112,0	92,0*
		118,8	98,1
Cu	29	13,4	9,8
		19,4	13,6
		30,1	21,7
		44,8	33,5
		62,0	45,8
		75,8	65,8
		93,5	70,6
		110,2	83,4
		117,8	90,0
		127,8	97,3
Mo	42	40,6	24,4
		87,8	65,4
		101,8	66,0
		128,5	84,0
Cd	48	8,9	4,3
		19.7	10,5
		31.2	17.4
Cd	48	48,2	28,3
		64,2	37,6
		86,4	52,2
		105,2	63,0
		130,2	79,6
Sn	50	10,2	4,7
		21,3	11,9
		32,2	18,1
		45,6	25,8
		69,0	39,9
		85,4	49,8
		104,1	61,8
		140,2	84,2
		155.7	94,0
Ta	73	84,7	40,0
		112,0	53,0
		169,0	82,1
		191,5	98,5
Pb	82	15,3	5,4
		32,9	13,5
		40,2	16,1
		67,4	28.5
		89,6	38,4
		118,8	53,9
		145,6	67,6
		177,1	84,0
		200,0	94,8

Having the experimental data for the proton ranges in several elements with atomic numbers Z from 13 to 82 makes it possible to construct empirical range-energy curves for all intermediate elements. As was to be expected, the curve of range versus atomic number at given proton energy is rather smooth for many-electron atoms. Because of this it is possible by graphing the ranges we obtained in their dependence on Z for given proton energies, to find by graphical interpolation the ranges in the intermediate elements. A nomogram constructed in this way is presented in Fig. 4. This nomogram is used to determine the ranges of protons with energies from 1 to 7.4 Mev in any element with $Z > 10$. For all values of the range, the uncertainty connected with the precision of the measurements performed by us is about 0.5 mg/cm^2. To this uncertainty must be added an error of about 1% connected with the precision of the range-energy curve for Al^2, and an error of 1-2% caused by irregularities in the dependence of $R(Z)$ (decreasing with increasing Z).

In conclusion we tender our deep thanks to N. A. Vlasov and S. P. Kalinin for guidance and constant help in this work, and to V. I. Vernashevskii for taking part in the construction of the apparatus.

Translated by D. Finkelstein
119

---

* In these cases measurements were carried out on beams of deuterons with energies 14.7 mev. The paths for the protons were computed with the aid of the well-known relation: $R_p(E) = ½ R_d(2E)$.

SOVIET PHYSICS JETP VOLUME 1, NUMBER 3 NOVEMBER, 1955

The Yield of Fission and Star Formation Processes in the Capture of π^--mesons by Nuclei of U, Bi and W[1]

N. A. Perfilov, O. V. Lozhkin *and* V. P. Shamov
Radium Institute, Academy of Sciences of the USSR

(Submitted to JETP editor, March 19, 1955)
J. Exper. Theoret. Phys. USSR **28**, 655-663 (1955)

The interaction of slow π^--mesons with the nuclei of U, Bi and W has been studied by the method of thick photographic emulsions in which the element to be investigated is placed in the middle layer of the emulsion in a form which is insoluble during development and fixing. The ratio between the yield for fission and for star formation in these elements as a result of their capture of π^--mesons is obtained. The probability of nuclear fission as a result of the capture of π^--mesons strongly decreases with decreasing Z: for uranium the probability for fission is ~ 0.3, for bismuth ~ 0.02 and for wolfram, perhaps less than 0.002. The other processes of interaction of π^--mesons with heavy nuclei lead primarily to the formation of "no-prong" and "one-prong" stars. A possible mechanism for the fission of nuclei resulting from the capture of π^--mesons is discussed.

1. INTRODUCTION

It was shown[2] by Perfilov and Ivanov in 1952 that the nuclei of U, Pb and W can undergo fission as the result of π^--capture. The yield of the fission process in π^--meson capture was estimated very approximately, because of the small number of observed events.

In this work[2], the following method of investigation was used. Samples of U, Pb and W were introduced in a thick photographic emulsion, sensitive to mesons, by soaking the plates in water solutions of the salts of these elements. The plates were irradiated by π^--mesons, were developed and then, during scanning, were searched for events where tracks of mesons ended, and tracks of two strongly ionizing particles, emitted in opposite directions, appeared.

However, when using such a method of investigation, it is not possible to draw any conclusion about the ratio of the yields of the two processes of fission and star formation resulting from the capture of mesons by nuclei. This is due to the fact that star formation in photographic emulsions can take place in a number of elements which make up the emulsion (Ag, Br, C,N,O,S). The problem of the determination of this ratio, which holds great interest for the understanding of the interaction mechanism between π^--mesons with a nucleus, can be solved by observing the process of meson capture in particular nuclei.

In this present work an attempt is made to come closer to the solution of this problem by the method of introducing into the photographic emulsion finely powdered materials which do not dissolve during its processing.

2. METHOD OF INVESTIGATION

Three-layered photographic plates, the method of preparation of which was developed earlier in this laboratory, were used in this investigation.

The elements U, Bi and W were introduced in the form of finely ground oxides U_3O_8, Bi_2O_3 and WO_3 in the middle layer, whose thickness after development and fixing was less than the depth of focus of the 90x objective of the microscope. Therefore, the layer can be scanned solely through the horizontal displacement of the plate. This shortens appreciably the scanning time in comparison with the case when the loaded material is dispersed throughout the whole volume of the photographic emulsion. Moreover, the location of the element being investigated in the middle of the photographic emulsion always ensures an appreciable path length in the emulsion for the nuclear fission products. The necessary dimensions of the grains of the material introduced are obtained by means of successive elutriation of oxide powders shaken in water. In our investigation, the dimensions of the crystals were about 3μ. By means of special experiments it was shown that during the development and fixing of the photographic emulsion, the dimensions of the crystals do not change, i.e., the chosen materials do not dissolve observably under the conditions of the experiment.

The material loaded in the middle layer of the emulsion, which does not dissolve during the processing of the photographic plate, does to some extent impede the diffusion of the developer to the lower layer. Because of this effect, a three-layered plate requires some modification of the development procedure, designed to develop the lower layer sufficiently without overdeveloping the upper layer. Satisfactory results are given by the method of temperature development.

---

[1] N. A. Perfilov, O. V. Lozhkin and V. P. Shamov, Report RIAN (1952)

[2] N. A. Perfilov and N. S. Ivanova, Report RIAN (1950)

When a metal oxide is introduced in a photographic emulsion, there are two elements with which interactions may take place. However, on the basis of existing experimental data[3] and theoretical calculations[4], one expects that meson capture will occur chiefly for nuclei of high Z, if the elements are in a bound state. In our experiments oxygen was bound as an oxide of a heavy element having a Z 9 to 11 times greater than that of oxygen. Therefore, one could expect that the effect due to oxygen would be negligibly small. Our experimental data are in agreement with this conclusion.

Three-layered plates irradiated by negative π mesons slowed down by aluminum layers of suitable thickness were developed and then scanned through a microscope. Only the middle layer was examined for events in which a meson stopped in the region occupied by a crystal of the loading substance.

3. SCANNING RESULTS

In the Table below all the cases in which a π^- - meson stopped in the region occupied by a crystal are divided into "stars" and fission events. Fission events are identified by the appearance of two short, thick tracks, issuing in opposite directions from the places where the π^--meson stopped. "Star" events refer not only to those cases when a meson is captured and several ionizing charged particles, leaving tracks in the emulsion, are emitted, but also to those events when the capture of a meson does not result in the emission of charged particles (the so-called "no-prong stars"). The emulsion used (prepared by ourselves) was capable of registering π^--mesons with energies up to 5 mev.

TABLE I

Loaded material	No. of stars observed	No. of fission events
U_3O_8	210	10
Bi_2O_3	250	2
WO_3	600	1
Unloaded emulsion (AgBr + gelatin)	10 000	Not found

Table 1 shows the results of the scanning of plates (with the middle layer loaded with U_3O_8, Bi_2O_3 and WO_3) irradiated with slow negative π^--mesons.

Table 2 shows the prong distribution of the stars as a function of the loaded material, and also the prong distribution of stars caused by π^--mesons in an unloaded emulsion.

TABLE II

No. of prongs in star	No. of stars (%) for given material			
	Crystal WO_3	Crystal Bi_2O_3	Crystal U_3O_8	Unloaded emulsion
0	47	57	34	32
1	24	20	22	26
2	12	10	19	20
3	9	9	18	14
4	8	4	6	7
5	—	—	1	1

4. ANALYSIS OF THE OBTAINED DATA

The elements investigated were introduced into the photographic emulsion in the form of an oxide. Therefore, when a meson stopped in the crystal of the introduced substance, the interaction could take place either with the heavy nucleus or with the oxygen. Since the interaction of a π^- - meson with oxygen cannot result in ionizing particles similar to the fragments due to the fission of heavy nuclei, the observation of events in which two fragments issue from the crystal can be assigned with complete assurance to the fission of the nucleus being investigated as a result of its capture of a π^--meson. A decision can be made on the number of interactions between the π^--mesons and the nuclei being investigated which result in the emission of only light particles (star formation) if one can separate the following effects in the stars observed to originate in crystals:

1) The capture of mesons by oxygen resulting in stars in the oxides U_3O_8, Bi_2O_3 and WO_3, from the capture by the nuclei U, Bi and W.

2) The capture of mesons resulting in stars in the region of the emulsion near the crystals, from stars originating in the crystals.

Let us clarify the importance of the second effect in determining the true number of cases of the stopping of a meson in the crystal of the loaded substance. Let us assume that we have the case of a star formed in the photographic emulsion in a region a few grains above the loaded substance or else below it, also within a short distance. During the fixing and drying of the photographic emulsion the emulsion will shrink as a result of the removal of the silver bromide, and therefore the thickness will decrease by a factor k (k is the deformation factor. For the emulsions we used $k = 2.5$). The center of the star therefore comes nearer to the crystal of the loaded substance, and sufficiently so that during the study of such a star it will be counted as originating in the crystal.

---

[3] W. K. H. Panofsky, Phys. Rev. 78, 825 (1950)

[4] E. Fermi and E. Teller, Phys. Rev. 72, 399 (1947)

Since the deformation of the emulsion is only in one direction, during the scanning all stars (approximately) within an ellipsoid of revolution will be counted as originating in the crystals of the loaded substance.

If one assumes that if there is no deformation, stars formed in the emulsion and in the crystal could be distinguished if the distance is the size of a developed grain of silver, then the axis of the ellipsoid would have the values:

$$a = R + d, \quad b = R + kd.$$

Here a is the semi-axis parallel to the surface of the plate; R is the crystal radius, d the diameter of the developed grain in the emulsion. Obviously, the smaller the crystals, the greater will be the number of stars which will appear to be originating in the crystals (when in reality they are due to mesons stopping in the photographic layer in the vicinity of the crystal).

Let us call the neighboring layer bounded in this way the "undistinguishable zone". We will then find the true number of stars originating in the crystals by multiplying the total number of stars observed at crystal locations by the probability, W_c, that a meson will stop in the crystal, or, since $W_c + W_{uz} = 1$ (where W_{uz} is the probability that it will stop in the neighboring layer), we will have the following expression for the true number of events of mesons stopping in the crystals:

$$N_{\text{true}} = N_{\text{obs}} \frac{W_c}{W_c + W_{\text{u.z.}}}$$

$$= N_{\text{obs}} \frac{S_c V_c}{S_c V_c + S_{\text{em}} V_{\text{em}}}.$$

Here V_{em} and V_c are the volumes of the undistinguishable zone and of the crystal, S_{em} and S_c are the stopping power for mesons in the photographic emulsion and in the crystal.

If the total number of stars in the whole layer containing the loaded substance is counted, then the true number of stars in crystals is obtained by substituting in the denominator of the expression the full volume of the scanned emulsion.

One can estimate the true number of stars in crystals of the loaded substance in yet another way. Using the method of the potential barrier[5], one can distinguish between stars resulting from the interaction with light and with heavy nuclei. Then, from the obtained total number of stars, under given assumptions one can deduce the number of stars due to the elements being investigated.

The calculation of the undistinguishable zone and the estimate of the effect on the element being investigated are discussed in the Appendix to this paper. The results of the analysis of the experimental data shown in Table 1 are given in Table 3.

In this way, even from these first results one could estimate approximately the probability of fission of the nuclei of U, Bi and W after absorption of negative π mesons. For uranium this probability lies in the interval from 1.0 to 0.30, for bismuth it is ~ 0.02 and for wolfram ~ 0.007.

Later, in order to improve the data on the fission probability (as the result of π^--meson capture) of the nuclei of U and W, supplementary experiments were performed in which A. V. Pyrkin took an appreciable part. It was shown as a result that the probability for fission of the uranium nucleus for π^- meson capture was 0.3 ± 0.1[6], and that the fission probability for wolfram nuclei is approximately 0.002[7].

In addition to clearing up the question of the probability of the fission of the nuclei of U, Bi and W after π^--meson capture, the character of the stars originating as a result of the capture of mesons by heavy nuclei was also determined. The analysis of the data in Table 2 has shown that for elements with $Z \geqslant 74$, most of the π^--meson captures by nuclei result in the formation of no-prong and one-prong stars. The results of the analysis are shown in Table 4.

5. DISCUSSION OF THE RESULTS

From the experimental data on the prong distribution stars in wolfram and bismuth, one can obtain analogous information for elements with a high Z.

The direct determination of the prong distribution of stars formed through π^--meson capture by uranium nuclei was made difficult in our experiment

---

[5] M. G. K. Menon et al, Phil Mag. **41**, 583 (1950)

[6] O. V. Lozhkin and V. P. Shamov, Report RIAN, (January, 1955)

[7] N. A. Perfilov and A. V. Pyrkin, Report RIAN (1953)

TABLE III

Substance	Average size of crystal (μ)	True number of stars in crystals N_{true}	Number of stars in heavy element	Number of stars for each fission event
U_3O_8 . .	1.6	$0 \div 30$	$0 \div 24$	$0 \div 2.4$
Bi_2O_3 . .	5	130	114	57
WO_3 . .	3	176	133	133

TABLE IV

Number of charged particles in the star	No. of stars (%) as a function of the number of prongs		
	Bi	W	AgBr
0	86.2	85.5	42
1	13.8	14.5	29

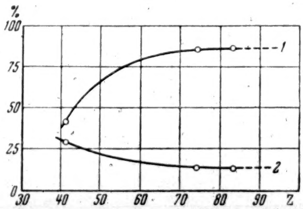

FIG. 1. Dependence of the relative number: *1* - of no-prong and *2* - of one-prong, stars on the charge of the nucleus which has a slow π^--meson.

because of the fact that, due to the small dimensions of the U_3O_8 crystals (approximately 1.6 μ), the number of events which had to be assigned to the emulsion in the undistinguishable zone accounted for 85 - 90% of the total number of stars observed on crystals. In addition, U_3O_8 crystals often cluster, which renders more difficult the measurement of the undistinguishable zone.

Figure 1 shows the dependence of the number of no-prong and one-prong stars on the Z of the nucleus capturing the π^--meson. If the curves are extrapolated to $Z = 92$, it is possible to estimate the average number of charged particles originating in the capture of one π^--meson by a uranium nucleus. We get an approximate value of 0.12. Thus 12% of the interactions of π^--mesons with uranium nuclei lead to the emission of one charged particle. In the other cases the uranium nuclei emit neutrons only, and together with this can undergo fission.

The number of stars corresponding to one fission of a uranium nucleus having captured a π^--meson are given in Table 3. In the Table the limits are indicated to lie between 0 and 24; these were obtained from the following considerations. The stars observed on the U_3O_8 crystals, separated by the method of the potential barrier, show that of the 122 stars which were analyzed, 46 must be assigned to light nuclei. Knowing the relative number of stars formed by π^--meson capture by the AgBr, and the C, N and O nuclei in the emulsion, it is possible to determine the number of stars originating in uranium nuclei (neglecting a difference in star formation by oxygen in an oxide) from the expression:

$$Z = N_{\text{H}} - qN_{\text{L}},$$

where N_{H} is the number of stars formed by π^--mesons in heavy nuclei (U,Ag,Br), N_{L} is the number of stars in light nuceli (C,N,O), and q is the relative number of stars in AgBr and stars in C,N and O in the emulsion.

Taking the ratio $q = 2$ from the work of Menon et al[5], one can come to the conclusion that, when uranium nuclei capture π^--mesons, stars are not produced[*], i.e., only fission occurs (the lower limit to the number of stars corresponding to one fission is given in Table 3).

---

[*] If one uses the more reasonable value $q = 1.4$ in this calculation (this value was obtained by us after the completion of this work) the lower value of the number of stars corresponding to one fission will be 1.7.

The upper limit to the number of stars for each fission of the uranium nucleus, equal to 2.4, was obtained from the calculation described in the Appendix. Later work by us[6] on the determination of the probability of fission of the uranium nuclei from π^--meson capture led to the value 0.3 ±0.1 for the probability of fission. This corresponds to 2.3 stars for each uranium fission.

In such a way the following conclusions can be made on the basis of the results of the experiments described:

1. Fission of nuclei may occur when π^--mesons are captured by nuclei with $Z < 74$. The probability of fission decreases from 0.3 for U to perhaps less than 0.002 for W.
2. The other cases of interaction of π^--mesons with heavy nuclei lead mostly to the formation of one-prong and no-prong stars.

The data presented permit certain conclusions on the mechanism of the fission process. As the result of the interaction of a slow π^--meson with the nucleons of a heavy nucleus, this nucleus is excited to an energy of ~ 100 mev[5,8].

There are at least three ways in which an excited nucleus can go to a state of minimum energy: (a) by particle emission from the nucleus, (b) by emitting γ- quanta, and (c) by fission.

The similarity in the average number of charged particles emitted in the capture of one π^--meson by a uranium nucleus (0.12) and in the number of complex fissions of a uranium nucleus as a result of the capture of a π^--meson (0.1) permits one to think that for such an excitation energy the process of particle emission (chiefly neutrons) from the nucleus will take place with the greatest probability**.

If the excitation energy is decreased, the relative probability of two other processes increases in the neutron emission process. At the same time the absolute magnitude of the probability of fission increases because of the increase in Z^2/A. For uranium capturing a π^--meson, after emission of 8 or 9 neutrons, the probability of fission appears to be predominant.

For nuclei with smaller Z, when the excitation energy is decreased, by the process of particle emission, to the value of activation energy (which determines the threshold for fission, for a given Z^2/A). The sum of the probability of particle emission and of γ- quanta emission will always be greater than the probability of fission. This difference will increase with decreasing Z. As a result, for nuclei in the neighborhood of Bi, the first two processes will predominate: particle emission for high excitation energies and γ- quanta emission for low excitation energies.

The fission of uranium with the emission of light, charged particles as the result of slow π^--meson capture can be explained in a natural way as fission arising after the emission of one charged particle and several neutrons. The fission of bismuth as the result of π^--meson capture is not in disagreement with the emission hypothesis: After the emission of 7 or 8 neutrons, the threshold for fission decreases to a value ~ 7 mev, beyond which the nucleus has an ascertainable fission probability.

The calculation for wolfram shows that for a decrease in the fission threshold to a value of the order of the binding energy of a neutron in the nucleus, the preliminary emission of 15 to 16 neutrons is necessary, which requires an excitation energy ~ 280 mev. This value is two times greater than the maximum possible excitation energy of the nucleus as the result of π^--meson capture. If one assumes that the fission of wolfram as the result of the capture of slow π^--mesons is established, it follows, from the statements above, that wolfram in this case is in an excited state which lies appreciably higher than the state corresponding to fission according to the emission hypothesis.

The basic results of this work were obtained in December, 1951. At this time, the authors of two other works[10,11] have estimated the probability for fission of the uranium nucleus as the result of slow π^--meson capture. In the work by S. G. Al-Salam[10] the probability for fission is given as ~ 1 and in the work by John and Fry[11] it is given as 0.18 ±0.06.

In conclusion the authors express their appreciation to M. G. Meshcheriakov and his collaborators for their assistance in this work.

The authors recall with profound gratitude the now deceased Acad. P. I. Lukirskii who showed a constant interest in this work and who participated in the discussion of the results.

** From the data of Perfilov and Ivanova[9], 10% of the fissions of uranium nuclei (as the result of π^--meson capture) are accompanied by the emission of light charged particles (usually protons).

[8] D. H. Perkins, Phil. Mag. **40**, 601 (1949)

[9] N. A. Perfilov and N. S. Ivanova, Report RIAN (1951)

[10] S. G. Al-Salam, Phys. Rev. **84**, 254 (1951)

[11] W. John and W. Fry, Phys. Rev. **91**, 1234 (1953)

APPENDIX

1. THE SEPARATION OF THE PROCESS OF STAR FORMATION IN THE EMULSION LAYER ADJACENT TO THE CRYSTALS LOADED IN THE EMULSION

Estimate of the undistinguishable zone. When the method of loading the emulsion with finely ground substances is used, because of the appreciable deformation of the emulsion after processing, and because of the appreciable dimensions of the Ag grains, there exists (within the emulsion) a region around the loaded crystals which influences the results of the observations. The calculation of this region (the so-called undistinguishable zone) carried out for WO_3 crystals, of average dimensions 3μ, assumed that they have a spherical shape. The average size of the developed Ag grains was $\sim 0.5\mu$ in the emulsion used in this work, and the deformation coefficient of the emulsion $k = 2.5$.

In this work, using a microscope with a 90 x objective, it was decided that the event takes place in the crystal if the center of the star is located inside the crystal or on its surface. In this way, if the event takes place within the emulsion volume bounded by the surface of the ellipsoid of revolution (approximately), then, after processing, the center of the star falls into in a spherical layer of $0.5\ \mu$ thickness, and it will be recorded by us as an event occurring within the WO_3 crystal. This is because of the juxtaposition of the Ag grain (which was the center of the star) and the surface of the crystal. Besides the deformation of the emulsion in the calculation of the undistinguishable zone, it is necessary to consider the region under the crystal, which is not investigated because of the opaqueness of the crystal. Figure 2 shows schematically the dimensions of the undistinguishable zone.

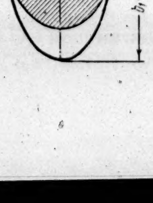

FIG. 2. Schematic representation of the undistinguishable zone. R is the radius of the crystal loaded in the emulsion; d is the diameter of the developed Ag grains. The shaded part shows the dimensions of the undistinguishable zone in the developed emulsion.

If one takes: R – the radius of the crystal ($1.5\ \mu$), d – the average size of developed Ag grains ($0.5\ \mu$), b, b_1 – the upper and lower semi-axis of the ellipsoid of revolution, then the volume of the undistinguishable zone will be

$$V_{\text{u.z.}} = {}^2/_3\,\pi(R+d)^2(b+b_1) - {}^4/_3\,\pi R^3 = 42.4\,\mu^3,$$

which is a value three times greater than the volume of the crystal having a radius of $1.5\,\mu$.

2. SEPARATION OF THE EFFECT ON WOLFRAM FROM THE TOTAL NUMBER OF STARS RELATED TO WO_3 CRYSTALS

One can assume the ratio of the probability of capture of the meson in the undistinguishable zone of the emulsion and in the crystal is equal to

$$\frac{W_{\text{em}}}{W_{WO_3}} = \frac{V_{\text{em}}}{V_{WO_3}} \frac{S_{\text{em}}}{S_{WO_3}},$$

where V_{em}, V_{WO_3} are the volumes of the emulsion in the undistinguishable zone and of the crystal, S_{em}, S_{WO_3} are the stopping powers of the meson in the emulsion and in the WO_3 oxide. The stopping power for the meson can be written analogously to the stopping cross section for heavy charged particles:

$$S = \frac{4\pi NZe^4}{mv^2} \ln \frac{2mv^2}{\overline{I}}.$$

From this,

$$\frac{W_{\text{em}}}{W_{WO_3}} = \frac{V_{\text{em}}}{V_{WO_3}} \frac{N_{\text{em}}\overline{Z}_{\text{em}}}{N_{WO_3}\overline{Z}_{WO_3}} \left(\ln \frac{2mv^2}{\overline{I}_{\text{em}}} \Big/ \ln \frac{2mv^2}{\overline{I}_{WO_3}} \right).$$

The velocity of the π^- meson for the calculation is chosen to be such that, encountering a crystal having a dimension of $\sim 3\mu$, it will stop in it; i.e., a meson having such an energy will have a path in the WO_3 oxide not greater than the diameter of the crystal. This condition will be observed for meson energies less than 100 kev, i.e., for velocities less than 1.13×10^9 cm/sec.

Substituting in the formula $\overline{Z}_{\text{em}} = 13.5$, $\overline{Z}_{WO_3} = 24.5$, $N_{\text{em}} = 8.2 \times 10^{22}\text{cm}^3$, $N_{WO_3} = 7.5 \times 10^{22}\text{cm}^3$, we obtain***

$$W_{\text{em}}/W_{WO_3} = 2.49.$$

*** The average ionization potential of atoms with stopping power I is taken, from Bloch's formula, to be:

$$\overline{I} = 11.5 \cdot \overline{Z}\text{ev}$$

Since the number of stars originating in the WO_3 oxide is determined from the formula

$$N_{\text{true}} = N_{\text{obs}} \cdot \frac{W_{WO_3}}{W_{WO_3} + W_{\text{em}}},$$

of the 600 stars observed on crystals, only 172 could be counted as originating at the WO_3 oxide, the others being due to the emulsion in the undistinguishable zone. From this it is possible to estimate the number of interaction events with wolfram nuclei, assuming that the probability of capture of the π^--meson in the oxide is proportional to the Z of the nucleus.

In this way we find that approximately 130 stars of the 172 originating at the WO_3 are due to interactions with wolfram nuclei.

An approximate expression for the number of π^--meson capture events by wolfram nuclei is obtained, by using the potential barrier method for separating the stars into stars originating in the heavy nuclei, N_H, and stars originating in the light nuclei, N_L. Then, from the expression

$$N_W = \frac{N_H - qN_L}{1 - qp}$$

one can determine the number of stars originating in the nuclei W. Here p is the probability of π^--meson capture by oxygen nuclei in the oxide, q is the ratio of the number of stars originating in AgBr and the number of stars originating in the C, N, and O of the emulsion.

Analogous calculations were carried out for bismuth and uranium.

Translated by F. Ajzenberg
120

SOVIET PHYSICS JETP VOLUME 1, NUMBER 3 NOVEMBER, 1955

Absorption and Emission of Light by a Gray Substance

B. I. STEPANOV

Institute of Physics and Mathematics of the Academy of Sciences of the Belorussian SSR, Minsk

(Submitted to JETP editor April 13, 1954)

J. Exper. Theoret. Phys. USSR **28**, 559-566 (May, 1955)

A phenomenological theory of the spectroscopic properties of a gray substance is constructed. The Einstein coefficients for absorption and for forced and spontaneous radiation are determined. An expression is obtained for the energy level distribution function. It is shown that a gray substance possesses properties closely resembling those of a classical electrodynamic system. A solution of the problem considered is essential for the explanation of the laws of absorption and emission of light by complex molecules.

1. From the point of view of the absorption and emission of light, complex molecules such as the molecules of dyes form an intermediate link between simple diatomic molecules and complex condensed systems, the radiation of which approximates in character that of a black body. The spectra of diatomic molecules are basically discrete and, what is especially important, strictly individual. The spectra of complex molecules also possess a certain individuality: the positions of the absorption and fluorescence bands are different for the various molecules. However, this individuality is extremely limited, since the intensity distribution in the long wave length absorption bands and in the fluorescence bands is the same in many molecules. Complex molecules also possess other important special characteristics. In them the laws of mirror symmetry of the absorption and emission bands are followed, the positions and forms of the emission bands are independent of the wave length of the existing light, and so forth[1,2].

The absence of specificity in the spectra of complex molecules is connected with the presence in such molecules of a very large number of oscillational degrees of freedom and with the very intimate interaction between them and the transfer of oscillational energy within the molecule. Nevertheless, there is conserved in them the basic division of the energy into electronic and oscillational, and also the specificity of the discrete electronic levels which is manifested in the existence of definite bands in the absorption and emission spectra.

The class of compounds to be treated here is different in principle, and consists of highly condensed systems, so-called gray bodies. In their absorption and thermal emission spectra there is no selectivity whatsoever; all wave lengths of incident radiation are absorbed equally, and the spectral composition of the radiation is just that of the equilibrium radiation, differing from it only in rate[3]. Fluorescence is absent in such bodies, since absorbed energy is quickly transformed into thermal energy. These features are connected with the very strong interaction between the electrons and the nucleus, as a consequence of which a division of the energy of the system into electronic and oscillational is completely inadmissible. We may speak only of the total energy of the system as a whole. In the present work we treat of the spectroscopic characteristics of a gray body --- the distribution function for the energy levels and the transition probabilities between them for absorption and emission of light. The solution of this problem will make possible the determination of these quantities in processes of emission and absorption of light by complex molecules.

2. We first consider a condensed substance (not necessarily gray) with a complex spectrum of allowed energy values and in thermal equilibrium. In view of the strong interaction of the various elements, it is impossible to distinguish in it isolated centers of absorption and emission --- it appears uniform. The Einstein coefficients must be related not to the atoms or molecules, but to a certain small volume v_0 of the substance under investigation. Let there be n such volumes in $1\,\text{cm}^3$. If the density of radiant energy within the substance

---

[1] B. S. Neporent, J. Exper. Theoret. Phys. USSR **21**, 172 (1951); Izv. Akad. Nauk SSSR, Ser. Fiz. **15**, 533 (1951)

[2] B. S. Neporent and B. I. Stepanov, Usp. Fiz. Nauk **43**, 380 (1951)

[3] Sh. Fabri, *Obshchee Vvedenie v Fotometriiu* (*General Introduction to Photometry*), ONTI, 1934

under investigation is equal to $u(\nu)$, then the number of quanta $h\nu$ in the frequency interval $d\nu$ that are absorbed in one second in the volume $d\tau$, with transitions from the levels E (in the interval dE) to the levels $E + h\nu$, is equal to

$$n\rho(E, T)\,dE\,B_{\mathrm{abs}}(E, \nu)\,u(\nu)\,d\nu\,d\tau.$$

Here $B_{\mathrm{abs}}(E, \nu)$ is the Einstein coefficient of the volume v_0 for the pair of levels E and $E + h\nu$, and $n\rho(E, T)\,dE$ is the number of volumes with energies in the interval from E to $E + dE$. The distribution function $\rho(E)$ has the usual form

$$\rho(E, T) = C(T)\,g(E)\,e^{-E/kT}, \tag{1}$$

where $g(E)$ is the statistical weight and $C(T)$ is a normalized constant. The total number of quanta absorbed during transitions from all levels E is equal to

$$nu(\nu)\,d\nu\,d\tau\int_0^\infty \rho(E, T)\,B_{\mathrm{abs}}(E, \nu)\,dE.$$

The corresponding energy absorbed is

$$dE_{\mathrm{abs}} = nu(\nu)\,h\nu\,d\nu\,d\tau\int_0^\infty \rho(E, T)\,B_{\mathrm{abs}}(E, \nu)\,dE. \tag{2}$$

If the substance is being acted on by radiant energy, then besides absorption there will always be forced emission. The energy of the forced emission is equal to

$$dE_{\mathrm{em}}^{\mathrm{forced}} = nu(\nu)\,h\nu\,d\nu\,d\tau\int_0^\infty \rho(E + h\nu, T) \tag{3}$$

$$\times\, B_{\mathrm{em}}(E, \nu)\,dE.$$

Here $B_{\mathrm{em}}(E, \nu)$ is the Einstein coefficient for forced emission for transitions from the level $E + h\nu$ to the level E (the magnitude E referring always to the lower level). Since

$$B_{\mathrm{em}}(E, \nu) = B_{\mathrm{abs}}\,g(E)/g(E + h\nu), \tag{4}$$
$$\rho(E + h\nu, T) = C(T)\,g(E + h\nu)\,e^{-(E+h\nu)/kT},$$

then Eq. (3) is equal to

$$dE_{\mathrm{em}}^{\mathrm{forced}} = e^{-h\nu/kT}\,dE_{\mathrm{abs}}. \tag{5}$$

For large values of $h\nu/kT$ the role of forced emission is insignificant, whereas for small values of $h\nu/kT$ it is very essential. During forced radiation the corresponding quantum is emitted in the direction of propagation of the incident quantum. As Frish[4] has emphasized, this circumstance allows one to consider forced emission as a special kind of "negative absorption". Experimentally, one measures not the magnitude dE_{abs} but the magnitude

$$dE'_{\mathrm{abs}} = dE_{\mathrm{abs}} - dE_{\mathrm{em}}^{\mathrm{forced}} \tag{6}$$

$$= (1 - e^{h\nu/kT})\,nu(\nu)\,h\nu\,d\nu\,d\tau\int_0^\infty C$$

$$\times\,(T)\,g(E)\,e^{-E/kT}B_{\mathrm{abs}}(E, \nu)\,dE.$$

The coefficient of proportionality a between the quantity of absorbed energy and the quantity of light energy $u(\nu)\,d\nu\,d\tau$ in the volume $d\tau$ is called, in accordance with the terminology of Frish, the absorption capacity. Thus

$$a(\nu, T) = \frac{dE'_{\mathrm{abs}}}{u(\nu)\,d\nu\,d\tau} = n(1 - e^{-h\nu/kT}) \tag{7}$$

$$\times\, h\nu\int_0^\infty C(T)g(E)e^{-E/kT}B_{\mathrm{abs}}(E, \nu)\,dE.$$

Analogously to Eqs. (2) and (5) we can write an expression for the energy of spontaneous emission per second

$$dE_{\mathrm{em}}^{\mathrm{spont}} = nh\nu\,d\nu\,d\tau\int_0^\infty \rho(E + h\nu, T)\,A(E, \nu)\,dE \tag{8}$$

$$= w(\nu, T)\,d\nu\,d\tau.$$

Here $w(\nu, T)$ is the (spontaneous) emissive power of the substance under investigation. Since

$$A = B_{\mathrm{abs}}\,\frac{8\pi h\nu^3}{v^3}\,\frac{g(E)}{g(E + h\nu)},$$

then

$$w(\nu, T) = nh\nu\int_0^\infty \rho(E + h\nu, T)\,A(E, \nu)\,dE \tag{9}$$

$$= a(\nu, T)\,\frac{8\pi h\nu^3}{v^3}\,\frac{1}{e^{h\nu/kT} - 1}.$$

---

[4] S. E. Frish, Usp. Fiz. Nauk **43**, 512 (1951); Vestn. Leningrad State Univ. **8**, 130 (1953)

3. We now consider a gray substance. We shall call a gray substance any substance whose absorption capacity is the same for all frequencies and whose radiation power is proportional to the radiation power of a black body *. From this it follows that

$$a(\nu, T) = n\,(1 - e^{-h\nu/kT}) \tag{10}$$

$$h\nu \int_0^\infty C(T)\,g(E)\,e^{-E/kT} B_{\text{abs}}(E, \nu)\,dE = P,$$

where P is a certain constant. This equation, together with the normalization condition

$$\int_0^\infty C(T)\,g(E)\,e^{-E/kT}\,dE = 1 \tag{11}$$

can serve for the determination of the unknown function $B_{\text{abs}}(E, \nu)$. Making the substitution

$$B_{\text{abs}}(E, \nu) = P\frac{1}{nh\nu}B'(E) \tag{12}$$

in Eq. (10), we obtain

$$(1 - e^{-h\nu/kT})\int_0^\infty C(T)\,g(E)\,e^{-E/kT}B'(E) = 1. \tag{13}$$

Equation (13) in conjunction with Eq. (11) has a solution only for high frequencies ($h\nu \gg kT$). In this case the factor ($1 - e^{-h\nu/kT}$) is equal to unity. An exact calculation shows that the solution is perfectly well defined:

$$B' = 1. \tag{14}$$

This same result may be obtained from simple qualitative concepts. Actually it follows from Eq. (12) that B' is independent of the temperature. If, taking account of this fact, we attempt to solve Eq. (13) in conjunction with Eq. (11) by way of the function $B'(E)$, then any function $B'(E)$ chosen so as to satisfy Eq. (13) for one temperature will not satisfy Eq. (13) for any other temperature.

Thus the solution of Eq. (10) for $h\nu \gg kT$ has the form

$$B_{\text{abs}}(\nu) = P/nh\nu. \tag{15}$$

The dependence of B_{abs} on ν has a simple significance. Actually in the equation

$$nB_{\text{abs}}(\nu)\,u(\nu)\,d\nu = P\frac{u(\nu)\,d\nu}{h\nu} \tag{16}$$

the left side is the number of quanta absorbed per unit volume per second. In the right member $u(\nu)\,d\nu/h\nu$ is equal to the number of quanta of the given frequency per unit volume. Hence for a gray substance with $h\nu \gg kT$ the number of quanta absorbed is proportional to the total number of quanta --- the probability of absorption being equal for quanta of any frequency. Since B_{abs} is independent of E, the probability of absorption of a quantum is also independent of the state of the body (its energy) at the instant of its interaction with the photon. Thus, for a gray substance, the probability of absorption of a quantum depends neither on the properties of the substance (E), nor on the properties of the quantum. The conceptual limit of the complete absence of selectivity in the processes of interaction between light and matter is realized in the gray substance.

4. The solution of Eq. (10) has been obtained for $h\nu \gg kT$. It is not applicable for $h\nu \sim kT$ nor for $h\nu < kT$. Moreover, it may be shown that in general a solution of Eq. (10) valid for all temperatures does not exist. This means that Eq. (10) itself must be invalid, that is, that the absorption capacity $a(\nu, T)$ cannot be constant for all ranges of frequency. If $a(\nu, T)$ is constant for $h\nu \gg kT$, then for $h\nu < kT$ it depends in one degree or another on ν, and this in turn means that a gray substance, in the sense in which we have defined it, does not exist in nature. This last assertion is not contradicted by the known experimental facts. Actually the usual definition of a gray substance is based on the study of absorption capacity in a wide range of wavelengths --- the ultraviolet, visible and near infra-red regions. In all these regions a is constant. Only by going over into the region of the far infra-red and the region of radio waves can we observe first a small, and then a more notable, deviation from this law.

The deviation from the law a = const on going over into the region $h\nu \sim kT$ is connected with the appearance of forced emission, the energy of which depends on the frequency and the temperature even for gray substances. If we assume that the coefficient B_{abs} retains the value of Eq. (15) even for small ν, then the absorption capacity of a gray body with account being taken of forced emission is equal to

$$a(\nu, T) = (1 - e^{-h\nu/kT})\,P. \tag{17}$$

---

* In what follows we shall speak of a gray substance rather than of gray bodies, since we are not interested in the dimensions nor in conditions on their boundaries.

In the limiting cases of very small ν ($\nu \to 0$) and very high temperatures ($T \to \infty$), the absorption capacity is negligibly small, and, consequently, a gray substance, as, indeed, any other, loses its ability to absorb incident radiation. The absorption that does occur is completely balanced by forced emission.

5. Knowing the Einstein coefficient (15) characterizing the probability of absorption of incident radiation, and using the general relation (4), we can readily write the expression for the Einstein coefficient for forced emission

$$B_{\mathrm{em}} = \frac{P}{nh\nu} \frac{g(E)}{g(E+h\nu)}. \tag{18}$$

Expressions (18) and (15) contradict each other; the coefficient B_{abs} is independent of the energy of the initial level, while the coefficient B_{em} depends on it. Selectivity is not among the properties of absorption by a gray substance. At the same time, according to Eq. (18), selectivity is a very characteristic property of forced emission. This contradiction may be eliminated only if we make a supplementary specification regarding the properties of the function $g(E)$ and require that the ratio $g(E)/g(E+h\nu)$ be independent of E. Differentiating the relation

$$g(E+h\nu) = f(h\nu)\, g(E)$$

first with respect to E and then with respect to $h\nu$, and comparing the results obtained, one can readily show that the function $g(E)$ must have the form

$$g(E) = Ae^{-\alpha E}. \tag{19}$$

There now arises the further question of the significance of the parameter α. At first sight we might suppose that it is arbitrary (positive) and that different gray substances have different values of α. However, this supposition also meets with a contradiction. Actually, according to Eq. (16), the probability of absorption of a quantum by a gray substance is independent of the frequency of the incident light. At the same time the probability of forced emission of a quantum, which is equal to

$$\frac{nB_{\mathrm{em}}\, u(\nu)\, d\nu}{u(\nu)\, d\nu / h\nu} = P\frac{g(E)}{g(E+h\nu)} = Pe^{\alpha h\nu}, \tag{20}$$

will depend on ν. Consequently, for $\alpha \neq 0$ the well-known selectivity of the process of interaction between light and matter is still observed. This cannot be allowed for a gray body, and hence $\alpha = 0$, $g(E) = 1$ for arbitrary E, and the distribution function has the form

$$\rho(E) = Ce^{-E/kT}. \tag{21}$$

6. The result obtained is, at first sight, somewhat paradoxical. In considering questions of chemical kinetics it is customary to suppose that in complex molecules the statistical weight $g(E)$ is equal to E^{L-1}, where L is the number of oscillational degrees of freedom. The corresponding distribution function then takes the usual form

$$\rho(E) = CE^{L-1}e^{-E/kT}. \tag{22}$$

In the application of this equation it is often forgotten that it is a rough approximation. Actually the expression (22) can be obtained if we assume that the energy of a molecule can be represented as the sum of $2L$ quadratic terms, that is, if we completely disregard the anharmonicity of the potential function, which includes also the interaction of the separate degrees of freedom. In actual complex molecules, and even more so in gray substances, these conditions are never realized. We recall that a characteristic property of the objects we are here considering is a strong interaction of the separate degrees of freedom and an interchange of energy among them. The degree of complexity of a molecule is characterized not only by the number of oscillational degrees of freedom L, but also, and primarily, by the magnitude of the interaction between them. From our point of view, a gray substance represents a case of extreme complexity. Hence a function $\rho(E)$ of the type of Eq. (22) is absolutely inapplicable. Calculations based on the optical properties of a gray substance (absence of selectivity) show that the form of the distribution function is given by Eq. (21), that is, that the simple distribution function for a gray substance is very simple --- it coincides with the distribution function for a classical harmonic oscillator with one degree of freedom. Consequently, in the presence of a very strong interaction between the separate degrees of freedom the form of the distribution function ceases to depend on their number. The whole object --- the gray substance --- acts as a single system. In such systems the entire energy of the whole system cannot in principle be represented in the form of a sum of energies localized in the separate degrees of freedom. In the given case the statistical weight, which for weakly interacting degrees of freedom is determined by the number of possible means of distribution of the energy is equal to unity*.

We could also have arrived at just this result in another manner. Let us suppose that, on solving the problem in the zeroth approximation and neglecting certain forms of interactions, we determine that the energy levels are completely degenerate. It is well-known that taking account of interactions always leads to a removal of degeneracy, to a splitting of levels. If this interaction is very great, then the degeneracy will always be removed, even in the case of a complex spectrum of energy values.

7. The Einstein coefficients for a gray substance are equal to

$$B_{\mathrm{abs}}(\nu) = B_{\mathrm{em}}(\nu) = \frac{P}{nh\nu}, \quad A(\nu) = \frac{8\pi\nu^2}{v^3}\frac{P}{n}. \quad (23)$$

From Eq. (23) it follows that the probability of spontaneous radiation of a gray substance, A_{em}, depends only on the frequency and, further, that the dependence itself is very simple ($A \sim \nu^2$). An analogous dependence does not exist in simple quantum mechanical systems (A depends on the properties of both of the combining levels of energy). At the same time it occurs in classical electrodynamics even for the simple dipole. The oscillational energy of the dipole is proportional to ν^2, the energy radiated per second by the dipole is proportional to ν^4, and the ratio of the radiated energy to the self energy is ν^2. An exact calculation shows (see, for example, reference 5) that this ratio is equal to

$$\gamma = \frac{8\pi^2 e^2}{3m}\frac{\nu^2}{c^3}.$$

The magnitude of γ determines the rate at which the radiation intensity falls off, and corresponds to the transition probability in quantum theory. Thus from the point of view of the laws of light emission a gray substance is notably closer to a classical object than to a quantum mechanical one. The quantum properties of an object are washed out in proportion to its complexity, to the increase in its number of degrees of freedom and to the growth of the interaction between them: a discrete spectrum of allowed energy values is converted into a continuous one, and the transition probabilities between all levels spaced at equal intervals from each other become equal.

It is evident that a gray substance cannot be compared to a single classical dipole. A classical dipole radiates only one frequency (within the limits of the natural line width), whereas a gray body radiates all frequencies. A gray body can be compared only with an infinite assembly of dipoles of all frequencies, that is a system of charges moving according to some aperiodic laws. In this last case a solution in a Fourier series will contain all frequencies.

We note that the magnitude

$$\frac{nA(\nu)\,d\nu}{P} = \frac{8\pi\nu^2}{v^3}\,d\nu \quad (24)$$

has a very simple physical interpretation. The right side coincides with the number of independent natural oscillations of the equilibrium radiation in the frequency interval $d\nu$ and in unit volume. The numerator of the left side represents the number of quanta $h\nu$ in the interval $d\nu$ emitted (spontaneously) by unit volume of the substance. Thus the number of quanta emitted by a gray substance is proportional to the number of frequencies which the equilibrium radiation must contain. This again shows that the probabilities are determined to a significant extent by purely classical considerations.

8. It must be emphasized that the definition of a gray substance is different in principle from the definition of a black body. A body which absorbs all the energy incident on it, that is, transmits none and reflects none, is called a black body. A body which is not black in small volumes (thicknesses) may become practically black in large volume. A black body need not necessarily be made up of gray material. Different frequencies may be absorbed differently. It is only necessary that the thickness of the body be large and that the energy of all frequencies be absorbed completely. Moreover, the definition of a black body is connected in principle with the properties of the medium. A body which is black with respect

---

[5] F. A. Korolev, *Spectroscopy of High Resolving Power*, GITTL, 1953, Eq. (4)

* An analogous result is obtained in the quantum mechanical treatment of the electrons of complex atoms. The energy of the entire atom cannot be represented in the form of a sum of energies of the separate electrons. In just this way only the orbital moment of the entire atom has a definite significance, whereas the orbital moments of the separate electrons do not. If by introduction of an external field we eliminate the degeneracy connected with the various orientations of the vector **L** in space, then the statistical weights of all the energy levels will equal unity.

to one medium may cease to be black in another medium. In the former case both the body and the medium must have the same index of refraction. A change in the index of refraction of the medium leads to the appearance of reflected waves. We have defined the nature of a gray substance differently. Its properties are not connected with the medium nor, moreover, with the dimensions of a body, but are determined exclusively by the properties of its own structure, by the large interaction of atoms and molecules. At the same time a black body may be very simple in composition but very large in volume.

It must be kept in mind that the absorption capacity (7) cannot be set equal to unity, although this mistake has sometimes occurred in the literature. Actually the absorption capacity (7) is the absorption of light per unit volume per unit time and consequently involves the dimension of time. The emissive power $w(\nu, T)$ involves the dimension of time in the same way, and only their ratio is independent of time. It is impossible to define the concept of a black body from Eq. (9).

9. The results obtained above for the laws of absorption and emission of light by a gray substance should aid in the clarification of the laws of absorption and emission of light by complex molecules. From the point of view of the structure of the oscillational energy levels and the transitions between them, these objects are clearly quite close to a gray substance. From the point of view of the structure of the electronic energy levels and the transitions between them, they are near to simple molecules. They retain, at least approximately, the division of the total energy of the system into electronic energy and energy of nuclear motion. On analyzing the experimental material, Neporent[1,2] came to the conclusion that the probabilities of transitions between oscillational levels of higher and lower electronic states are almost independent of the magnitude of the oscillational energy in the initial state. In the opinion of Neporent they depend only on the frequency. These experimental facts indicate that many properties characteristic of a gray substance are present also in complex molecules. Of course, for the complete explanation of the spectroscopic properties of complex molecules it is necessary to take into account specifically the interactions of the electronic and oscillational energies. This question is open to further development.

Translated by Brother Simon Peter, F.S.C.
97

SOVIET PHYSICS JETP VOLUME 1, NUMBER 3 NOVEMBER, 1955

The Spectrum of Positronium in External Fields

T. N. Tsytovich
Moscow State University

(Submitted to JETP editor March 13, 1954)
J. Exper. Theoret. Phys. USSR **28**, 664-678 (June, 1955)

The energy of interaction of the positronium atom with external electric and magnetic fields is calculated up to terms of order v^2/c^2. The splitting of the spectral lines of the positronium atom in weak and strong electric and magnetic fields is investigated.

1. INTRODUCTION

In the passage of positrons through matter, the formation of a metastable compound of an atomic type is possible, in addition to the processes of scattering and annihilation[1-5]. The simplest such atomic system is positronium. Recently, positronium has been observed experimentally[6,7], while the fine structure of the lowest energy level has also been investigated in some detail[8,9].

As was shown in references 1 and 10, a number of effects can be investigated for the positronium atom within the framework of the Pauli approximation for the wave functions, with inclusion of terms of the order of v^2/c^2. The present work is concerned with the study of some properties of the positronium atom in constant external magnetic and electric fields (both strong and weak), with the same order of accuracy (to v^2/c^2). To these limits of accuracy, the results obtained with the aid of the equation for coupled states[11], agree with the results obtained by the much simpler methods used below (in this connection, see also reference 12).

The positronium atom is a metastable system. It can decay either into three gamma rays (orthopositronium), or into two gamma rays (parapositronium)[2-5]. Investigation of the annihilation radiation (annihilation spectrum), along with a study of the spontaneous radiation (optical spectrum), can play an additional role in the study of the distribution of the energy levels of the system. As will be shown below, the external field changes the spectrum of the decay times which are related to the individual energy levels.

We begin by finding the interaction energy of the positronium atom with an external electromagnetic field. Then we shall consider the energy spectrum of the positronium atom in weak and strong external fields (magnetic and electric).

2. THE INTERACTION ENERGY OF POSITRONIUM WITH AN EXTERNAL FIELD

In calculating the interaction energy in the presence of an external electromagnetic field, it is necessary to divide the scalar and vector potentials into the internal potentials Φ_i, $\vec{\Phi}_i$ which describe the interaction processes of the electron and positron, and the potentials Φ_e, $\vec{\Phi}_e$ which arise from the external electric and magnetic fields. Then the total potentials will be given by

$$\Phi = \Phi_i + \Phi_e, \tag{1}$$

$$\vec{\Phi} = \vec{\Phi}_i + \vec{\Phi}_e. \tag{2}$$

In a similar way, the energy of the system can be written in the form

---

[1] A. A. Sokolov and V. N. Tsytovich, J. Exper. Theoret. Phys. USSR **24**, 253 (1953)

[2] I. Ia. Pomeranchuk, Dokl. Akad. Nauk SSSR **60**, 213 (1948)

[3] E. M. Lifshitz, Dokl. Akad. Nauk SSSR **60**, 21 (1948)

[4] D. D. Ivanenko and A. A. Sokolov, Dokl. Akad. Nauk SSSR **61**, 51 (1948)

[5] A. I. Mukhtarov, Dissertation, Moscow State Univ., 1950

[6] M. Deutsch, Phys. Rev. **82**, 455 (1951)

[7] M. Deutsch, Phys. Rev. **83**, 866 (1951)

[8] M. Deutsch and E. Dulit, Phys. Rev. **84**, 601 (1951)

[9] M. Deutsch and Brown, Phys. Rev. **85**, 1047 (1952)

[10] V. B. Berestetskii, J. Exper. Theoret. Phys. USSR **19**, 1130 (1949)

[11] E. E. Salpeter and H. A. Bethe, Phys. Rev. **84**, 1232 (1951)

[12] V. N. Tsytovich, J. Exper. Theoret. Phys. USSR **28**, 113 (1955); Soviet Phys. **1**, 163 (1955)

$$V = V_{\text{kin}} + V_i + V_e, \tag{3}$$

where

$$V_e = -e\int \psi^+ (\Phi_e - \vec{\alpha}\vec{\Phi}_e)\, \psi d^3x, \tag{4}$$

$$V_{\text{kin}} = \int \psi^+ (c\mathbf{p}\vec{\alpha} + \rho_3 mc^2)\, \psi d^3x, \tag{5}$$

$$\psi = \sum_n C_n e^{-icK_n t}\, \psi_n. \tag{6}$$

The interaction energy V_i for positronium is given, for example, by Sokolov and Tsytovich[1]. From the permutation relations for C_n, it follows that

$$V_e = -e\sum_n C_n^+ C_n V^e_{n,\,n}, \tag{7}$$

where

$$V^e_{n_1,\,n_2} = \int \psi^+_{n_1} (\Phi_e - \vec{\alpha}\vec{\Phi}_e)\, \psi_{n_2} d^3x \tag{8}$$

with analogous relations for V_{kin}. We obtain the energy of interaction with the external field by subtracting the energy of the vacuum in the external field from the energy V_e possessed by the electron and positron.

Quantities pertaining to the electron and the positron will be denoted by the indices 1 and 2, respectively. Wave functions which describe the motion of the electron correspond to positive energy, and those describing the motion of the positron to negative energy. Instead of taking electronic functions of negative energy for describing the motion of the positron, we make the transition to positron functions of positive energy by the scheme discussed in reference 1. In this case we have

$$\psi^+_{-e,\,-E}\,\vec{\alpha}\,\psi_{-e,\,-E} \rightarrow \psi^+_{+e,\,E}\,\vec{\alpha}_2\,\psi_{+e,\,E}, \tag{9}$$

$$\psi^+_{-e,\,E}\,\vec{\alpha}\,\psi_{-e,\,E} \rightarrow \psi^+_{-e,\,E}\,\vec{\alpha}_1\,\psi_{-e,\,E}, \tag{10}$$

$$\psi^+_{-e,\,-E}\,\rho_3\,\psi_{-e,\,-E} \rightarrow -\psi^+_{+e,\,E}\,\rho_{32}\,\psi_{+e,\,E}, \tag{11}$$

$$\psi^+_{-e,\,E}\,\rho_3\,\psi_{-e,\,E} \rightarrow \psi^+_{-e,\,E}\,\rho_{31}\,\psi_{-e,\,E}. \tag{12}$$

Finally, the following equation is obtained:

$$\Big\{E - c\mathbf{p}_1\vec{\alpha}_1 - \rho_{31}mc^2 - c\mathbf{p}_2\vec{\alpha}_2 - \rho_{32}mc^2 + \frac{e^2}{r} - U^{\text{B}} - U^0 + e(\Phi_1 - \vec{\alpha}_1\vec{\Phi}_1) - e(\Phi_2 - \vec{\alpha}_2\vec{\Phi}_2)\Big\}\,\psi = 0, \tag{13}$$

which is valid only for computation of effects of the order v^2/c^2 inclusively. In this approximation, we can make the transition from the 16 component wave function

$$\psi = \begin{pmatrix} \varphi_{11} & \varphi_{12} \\ \varphi_{21} & \varphi_{22} \end{pmatrix}, \tag{14}$$

where

$$\varphi_{11} = \begin{pmatrix} \psi_{11} & \psi_{12} \\ \psi_{21} & \psi_{22} \end{pmatrix};\quad \varphi_{12} = \begin{pmatrix} \psi_{13} & \psi_{14} \\ \psi_{23} & \psi_{24} \end{pmatrix};$$

$$\varphi_{21} = \begin{pmatrix} \psi_{31}, & \psi_{32} \\ \psi_{41}, & \psi_{42} \end{pmatrix};\quad \varphi_{22} = \begin{pmatrix} \psi_{33}, & \psi_{34} \\ \psi_{43}, & \psi_{44} \end{pmatrix},$$

to a four component one by expressing the small components ϕ_{12}, ϕ_{21}, ϕ_{22} in terms of the larger ϕ_{11}. We note that in Eq. (13), we put the Breit part of the interaction U^{B} in a form employed by Araki[13]. This form can also be written as

$$U^{\text{B}} = \frac{e^2}{2}[\vec{\alpha}_1\vec{\nabla}]\left[\frac{\mathbf{p}_2}{mc} - \frac{\hbar}{2mc}[\vec{\sigma}_2\vec{\nabla}],\ \vec{\nabla}\right]\frac{r}{2} + \frac{e^2}{2}\left[\frac{\mathbf{p}_1}{mc} + \frac{\hbar}{2mc}[\vec{\sigma}_1\vec{\nabla}],\ \vec{\nabla}\right][\vec{\alpha}_2\vec{\nabla}]\,\frac{r}{2}, \tag{15}$$

and we obtain the exchange interaction U^0 as[14]

$$U^0 = \pi\frac{e^2\hbar^2}{m^2c^2}\,\frac{3 + \vec{\sigma}_1\vec{\sigma}_2}{2}\,\delta(\mathbf{r}). \tag{16}$$

Here

$$\mathbf{r} = \mathbf{r}_1 - \mathbf{r}_2, \qquad r = |\mathbf{r}|.$$

Moreover, the normalizing condition must be satisfied:

$$\int(\varphi_{11}^+\varphi_{11} + \varphi_{12}^+\varphi_{12} + \varphi_{21}^+\varphi_{21} + \varphi_{22}^+\varphi_{22})\, d^3x_1 d^3x_2 = 1. \tag{17}$$

---

[13] Araki, Progr. Theor. Phys. 6, 379 (1951)

[14] V. B. Berestetskii and L. D. Landau, J. Exper. Theoret. Phys. USSR 19, 673 (1949)

We therefore introduce the normalized four component function χ, related to ϕ_{11} by the equation

$$\varphi_{11}=\left(1-\frac{p_1^2}{8m^2c^2}-\frac{p_2^2}{8m^2c^2}\right)\chi. \tag{18}$$

Bearing in mind that

$$V_{nn'}=\int \mathrm{Spur}\, \psi_{n'}^{+} U \psi_n \, d^3x_1 d^3x_2, \tag{19}$$

we obtain the following formulas for the transition to the four component wave function χ:

$$\psi^{+}(c\,\mathbf{p}_k\vec{\alpha}_k+\rho_{3k}mc^2-mc^2)\,\psi \tag{20}$$

$$\rightarrow \chi^{+}\left(\frac{p_k^2}{2m}-\frac{p_k^4}{8m^3c^2}-\frac{e^2}{2mc^2}\vec{\Phi}_k^2\right)\chi;$$

$$\psi^{+}(\vec{\alpha}_k\vec{\Phi}_k)\psi \tag{21}$$

$$\rightarrow \chi^{+}\left\{\left(\mathbf{p}_k+\frac{e_k}{c}\vec{\Phi}_k+\frac{\hbar}{2i}\vec{\nabla}_k+\frac{\hbar}{2}[\vec{\sigma}_k\vec{\nabla}_k]\right)\frac{\vec{\Phi}_k}{mc}\right\}\chi;$$

$$\psi^{+}\Phi_k\psi \rightarrow \chi^{+}\left\{\Phi_k+\frac{\hbar^2\nabla_k^2\,\Phi_k}{8m^2c^2}\right. \tag{22}$$

$$\left.-\frac{\hbar}{4m^2c^2}\vec{\sigma}_k[\mathbf{p}_k\vec{\nabla}_k]\,\Phi_k\right\}\chi.$$

Here

$$k=1,\ 2; \qquad e_1=-e_2=e.$$

$\mathbf{p}_1$ and $\mathbf{p}_2$ operate only on the wave function χ, and $\vec{\nabla}_1$ and $\vec{\nabla}_2$ only on the potentials Φ_1, Φ_2, $\vec{\Phi}_1$, $\vec{\Phi}_2$.

From Eqs. (20), (21) and (22), we obtain the energy of interaction (and also the kinetic energy) of the electron and positron in the presence of an external field, with accuracy to terms of order v^2/c^2:

$$U=\frac{\left(\mathbf{p}_1+\frac{e}{c}\vec{\Phi}_1\right)^2}{2m}+\frac{\left(\mathbf{p}_2-\frac{e}{c}\vec{\Phi}_2\right)^2}{2m} \tag{23}$$

$$-\frac{p_1^4}{8m^3c^2}-\frac{p_2^4}{8m^3c^2}-e\Phi_1+e\Phi_2$$

$$+\frac{e\hbar}{2mc}\{\vec{\sigma}_1\mathbf{H}_1-\vec{\sigma}_2\mathbf{H}_2\}+\frac{e\hbar}{4m^2c^2}\vec{\nabla}_1\Phi_1[\vec{\sigma}_1\mathbf{p}_1]$$

$$-\frac{e\hbar}{4m^2c^2}\vec{\nabla}_2\Phi_2[\vec{\sigma}_2\mathbf{p}_2]-\frac{e\hbar^2}{8m^2c^2}\nabla_1^2\Phi_1$$

$$+\frac{\hbar^2 e}{8m^2c^2}\nabla_2^2\Phi_2+V^{\mathrm{B}}+V^0-\frac{e^2}{r}.$$

The Breit part of the energy V^{B}, and the exchange energy V^0 which determines the fine structure in the absence of field, were found earlier by Berestetskii and Landau[14]:

$$V^{\mathrm{B}}=4\pi\mu_0^2\delta(\mathbf{r})+\frac{e}{2mc}\mu_0\frac{1}{r^3}\{\vec{\sigma}_1[\mathbf{r}\mathbf{p}_1]-\vec{\sigma}_2[\mathbf{r}\mathbf{p}_2]\} \tag{24}$$

$$+\frac{e^2}{2m^2c^2}\left\{\frac{1}{r}\mathbf{p}_1\mathbf{p}_2+\frac{x_n x_{n'} p_{1n} p_{2n'}}{r^3}\right\}$$

$$-\frac{e}{mc}\mu_0\frac{1}{r^3}\{\vec{\sigma}_2[\mathbf{r}\mathbf{p}_1]-\vec{\sigma}_1[\mathbf{r}\mathbf{p}_2]\}$$

$$+\mu_0^2\left\{\frac{8\pi}{3}(\vec{\sigma}_1\vec{\sigma}_2)\,\delta(\mathbf{r})+\frac{3(\vec{\sigma}_1\mathbf{r})(\vec{\sigma}_2\mathbf{r})-\vec{\sigma}_1\vec{\sigma}_2 r^2}{r^5}\right\};$$

$$V^0=4\pi\mu_0^2\frac{3+\vec{\sigma}_1\vec{\sigma}_2}{2}\,\delta(\mathbf{r}). \tag{25}$$

Here $\mu_0=e\hbar/2mc$ and $\vec{\sigma}_1$ and $\vec{\sigma}_2$ are the double row matrices of Pauli; in Eqs. (23), (24) and (25), p_i act both on the wave function χ, and on the potential Φ.

3. THE ENERGY SPECTRUM OF POSITRONIUM IN A WEAK MAGNETIC FIELD

In the presence of a constant external magnetic field $H=H_z=\mathrm{const}$, the energy of interaction of positronium with the external magnetic field can be obtained for Eq. (23)

$$U^H=\frac{e\hbar H}{2mc}(\sigma_{1z}-\sigma_{2z})+\frac{e^2H^2}{16mc^2}(x^2+y^2). \tag{26}$$

In a weak magnetic field ($\mu_0 H<\alpha^2e^2/r_0$) the second term of Eq. (26) is negligibly small ($<\alpha^4e^2/r_0$) in comparison with the first. Therefore, it is sufficient in computing the energy spectrum in this case to find the various matrix elements of the energy:

$$U_1^H=\frac{e\hbar H}{2mc}(\sigma_{1z}-\sigma_{2z}). \tag{27}$$

With the help of the wave functions found in the absence of field, for example, in reference 1, we have *

$$V_{\mathrm{a}}^{\mathrm{a}}=V_{\mathrm{b}}^{\mathrm{b}}=V_{\mathrm{c}}^{\mathrm{c}}=V_{\mathrm{d}}^{\mathrm{d}}=V_{\mathrm{b}}^{\mathrm{c}}$$

$$=V_{\mathrm{b}}^{\mathrm{d}}=V_{\mathrm{c}}^{\mathrm{d}}=0, \tag{28}$$

---

* Here and below, indices are used (see reference 1, A. A. Sokolov and V. N. Tsytovich, J. Exper. Theoret. Phys. USSR **24**, 253 (1953)].

$$V_{\mathrm{a}}^{\mathrm{b}}=2\mu_0 H\sqrt{\frac{l^2-m^2}{l(2l+1)}}\,(1-\delta_{l0}), \tag{29}$$

$$V_{\mathrm{a}}^{\mathrm{c}}=2\mu_0 H\frac{m}{\sqrt{l(l+1)}}\,(1-\delta_{l0}), \tag{30}$$

$$V_{\mathrm{a}}^{\mathrm{d}}=2\mu_0 H\sqrt{\frac{(l+1)^2-m^2}{(l+1)(2l+1)}}. \tag{31}$$

The matrix elements (29), (30) and (31) are taken for identical values of the quantum numbers m, n, l in the initial and final states.

The matrix elements of the fine structure (energy $U^{\mathrm{B}}+U^0$) are determined by the formula (see reference 1):

$$E=-\frac{Rh}{2n^2}+\Delta E; \tag{32}$$

$$\Delta E=\frac{Rh}{2n^2}\left\{\frac{11\alpha^2}{16n^2}+\frac{4\alpha^2}{n}\varepsilon\right\},$$

$$\varepsilon^0=-\frac{1}{4(l+{}^1\!/_2)} \quad \text{for state a} \tag{33}$$

$$\varepsilon^1=\varepsilon^0+\frac{7}{12}\delta l_0+\frac{(1-\delta_{l0})}{8(l+{}^1\!/_2)}\begin{cases}-\dfrac{1}{l(l+1)} & \text{for state b}\\ -\dfrac{3l-1}{l(2l-1)} & \text{for state c}\\ \dfrac{3l+4}{(l+1)(2l+3)} & \text{for state d}\end{cases}$$

where ϵ^0 pertains to the para-state and ϵ^1 to the ortho-state *. Here

$$Rh=me^4/2\hbar^2,\quad \alpha=e^2/\hbar c. \tag{34}$$

Solving the corresponding secular equations with the aid of the matrix elements of Eqs. (29) - (33), we can find the energy spectrum:

1. $l=0$. Here the wave functions of the ortho-state with $m=\pm 1$ are not distorted (for $l=0$, we have only solutions of the form d), while the wave functions of the ortho-state with $m=0$ are distorted, whence (see also reference 10):

$$\varepsilon^H=-\frac{5}{24}\pm\sqrt{\left(\frac{7}{24}\right)^2+\left(\frac{\mu_0 Hn^3}{Rh\alpha^2}\right)^2}, \tag{35}$$

and the energy is found with the help of Eq. (32).

In weak fields we have the quadratic effect:

$$\varepsilon^{0H}=\varepsilon^0-\frac{12}{7}\left(\frac{\mu_0 Hn^3}{Rh\alpha^2}\right)^2, \tag{36}$$

$$\varepsilon^{1H}=\varepsilon^1+\frac{12}{7}\left(\frac{\mu_0 Hn^3}{Rh\alpha^2}\right)^2. \tag{37}$$

2. $l\neq 0$. The Matrix elements (29), (30) and (31) distort the wave functions of the ortho- and para-states. The allowed vlaues of m for a given l for the para-state are $m=0, \pm 1, \ldots, \pm l$. Therefore, the ortho-states with m which do not fall into this interval in a weak magnetic field are not distorted ($\epsilon^{1H}=\epsilon^1$). For the states with m falling in this interval, we have

$$\varepsilon^{0H}=\varepsilon^0-\left(\frac{2\mu_0 Hn^3}{Rh\alpha^2}\right)^2 \tag{38}$$

$$\times\ \frac{(2l+1)\{(7l^2+7l-3)-m^2(9l^2+9l-3)\}}{(3l+4)(3l-1)};$$

$$\varepsilon_{\mathrm{b}}^{1H}=\varepsilon_{\mathrm{b}}^1-\left(\frac{2\mu_0 Hn^3}{Rh\alpha^2}\right)^2\times\frac{2l-1}{3l-1}(l^2-m^2); \tag{39}$$

$$\varepsilon_{\mathrm{c}}^{1H}=\varepsilon_{\mathrm{c}}^1-\left(\frac{2\mu_0 Hn^3}{Rh\alpha^2}\right)^2(2l+1)m^2; \tag{40}$$

$$\varepsilon_{\mathrm{d}}^{1H}=\varepsilon_{\mathrm{d}}^1+\left(\frac{2\mu_0 Hn^3}{Rh\alpha^2}\right)^2\frac{2l+3}{3l+4}\{(l+1)^2-m^2\}, \tag{41}$$

where $\epsilon_{\mathrm{b}}^{1H}$ (as also ϵ_{b}^1) does not exist for $|m|=l$.

4. THE ENERGY SPECTRUM OF POSITRONIUM IN A STRONG MAGNETIC FIELD

We can now consider the case of strong fields, for which $\mu_0 H>\alpha^2e^2/r_0$ and also $\mu_0 H<e^2/r_0$. In this case, it is necessary to consider the energy U_1^H exactly, while the energy

---

* It was noted by Berestetskii [e.g., see reference 10, V. B. Berestetskii, J. Exper. Theoret. Phys. USSR 19, 1130 (1949)] that for $n>3$, it is necessary to consider the nondiagonal matrix elements of the form $V_{j-1}^{j+1}=\text{const}\,(r^{-3})_{j-1}^{j+1}$. As calculation shows, $(r^{-3})_{n,\,j-1}^{n,\,j+1}\equiv 0$, and therefore the validity of Eq. (33) is not limited by the condition $n<4$.

$$U_2^H = \frac{e^2}{16m^2c^2} H^2 (x^2 + y^2) \tag{42}$$

can be regarded as a perturbation.

First, we consider the field for which the energy of Eq. (42) is small in comparison with the fine structure. We find the wave functions of positronium, considering the energy U_1^H.

The eigenfunctions of the commuting operators

$$\hat{H}\psi \equiv \left(\frac{p^2}{m} - \frac{e^2}{r} + \mu_0 H (\sigma_{1z} - \sigma_{2z})\right)\psi = E\psi, \tag{43}$$

$$J_z\psi \equiv \left([\mathbf{rp}]_z + \frac{\hbar}{2}\sigma_{1z} + \frac{\hbar}{2}\sigma_{2z}\right)\psi = \hbar m\psi, \tag{44}$$

$$M^2\psi \equiv ([\mathbf{rp}]^2)\psi = \hbar^2 l(l+1)\psi, \tag{45}$$

$$s_{1z} = \frac{\hbar}{2}\sigma_{1z}; \qquad s_{2z} = \frac{\hbar}{2}\sigma_{2z}, \tag{46}$$

have the form

$$\psi^{\mathrm{I}} = N_{l,\,m-1}\begin{pmatrix} Y_l^{m-1} & 0 \\ 0 & 0 \end{pmatrix} R_{n,\,l}, \tag{47}$$

$$\psi^{\mathrm{II}} = N_{l,\,m}\begin{pmatrix} 0 & Y_l^m \\ 0 & 0 \end{pmatrix} R_{n,\,l}, \tag{48}$$

$$\psi^{\mathrm{III}} = N_{l,\,m}\begin{pmatrix} 0 & 0 \\ Y_l^m & 0 \end{pmatrix} R_{n,\,l}, \tag{49}$$

$$\psi^{\mathrm{IV}} = N_{l,\,m+1}\begin{pmatrix} 0 & 0 \\ 0 & Y_l^{m+1} \end{pmatrix} R_{n,\,l}. \tag{50}$$

Here $N_{l,\,m} = \sqrt{\frac{2l+1}{4\pi}\frac{1}{(l+m)!\,(l-m)!}}$, and Y_l^m and $R_{n,\,l}$ are written in the notation of reference 1. The corresponding energy values are

$$E_n^{\mathrm{I}0} = -\frac{Rh}{2n^2}, \tag{51}$$

$$E_n^{\mathrm{II}0} = -\frac{Rh}{2n^2} + 2\mu_0 H, \tag{52}$$

$$E_n^{\mathrm{III}0} = -\frac{Rh}{2n^2} - 2\mu_0 H, \tag{53}$$

$$E_n^{\mathrm{IV}0} = -\frac{Rh}{2n^2}. \tag{54}$$

States I, IV correspond to spin projections directed along the z axis. The magnetic moments in these states are oppositely directed, and hence these states do not interact with the magnetic field. In states II and III, on the other hand, the magnetic moments are parallel (spins anti-parallel), and, corresponding to this case, the coefficient 2 appears in Eqs. (52) and (53).

It is easy to see that, in spite of the fact that the expressions for the energy (52), (53) depend linearly on the field, linear splittings will not be observed in the optical spectra. From Eqs. (47)-(50), it follows that the optical transitions between levels (51), (52), (53) and (54) are forbidden. Thus, in a strong magnetic field the linear Zeeman effect will not be observed in the optical spectra. The role of the magnetic field in the approximation under consideration reduces to a shifting of the levels which do not appear in the optical spectrum.

The spectrum of positronium in a strong magnetic field is, if we do not consider the fine structure, the usual spectrum of the hydrogenlike atom ($r_0 = 2\hbar^2/me^2$). However, the fine structure of the spectrum will be different than in the absence of the field, since the magnetic field changes the eigenfunctions of the stationary states [Eqs. (47)-(50)]. These functions are classified according to the values of the projection of the electron and positron spins in the direction of the magnetic field. In the computation of the matrix elements of the energy of the fine structure [Eqs. (24) and (25)] with the aid of the wave functions I, II, III and IV, it should be recalled that the states I and IV are degenerate.

We obtain the same values of the matrix elements for the energy which contains the correction for the dependence of mass on velocity (see references 1 and 14), and the energy which describes the Breit correction, as in the absence of the field (see references 1 and 10). The matrix elements of the energy of spin-orbit interaction

$$V_3 = \frac{3\mu_0^2}{\hbar r^3}[\mathbf{rp}](\vec{\sigma}_1 + \vec{\sigma}_2) \tag{55}$$

have the form

$$E_3 = \frac{Rh}{2n^2}\frac{3\alpha^2}{4n}\frac{1-\delta_{l0}}{l(l+1)(l+1/2)}s(m-s), \tag{56}$$

where s characterizes the magnitude of the projection of the total spin in the direction of the magnetic field, and is given by

$$s = \begin{cases} 1 \text{ for state I,} \\ 0 \text{ for states II and III} \\ -1 \text{ for state IV} \end{cases} \qquad (57)$$

The diagonal matrix elements of the energy of spin-spin interaction

$$V_4 = \mu_0^2 \left\{ \frac{8\pi}{3} \delta(\mathbf{r}) (\vec{\sigma}_1 \vec{\sigma}_2) + \frac{3(\vec{\sigma}_1 \mathbf{r})(\vec{\sigma}_2 \mathbf{r}) - (\vec{\sigma}_1 \vec{\sigma}_2) r^2}{r^5} \right\} \qquad (58)$$

have the form

$$E_4 = \frac{Rh}{2n^2} \left\{ \frac{\alpha^2}{3n} (2s^2 - 1) \delta_{l0} \right. \qquad (59)$$

$$\left. - \frac{\alpha^2 (2s^2 - 1)(1 - \delta_{l0})}{8n (l+1)(l + {}^1/_2)(l + {}^3/_2)} \left[1 - \frac{3}{2} \frac{l^2 - (m-s)^2}{l(l - {}^1/_2)} \right] \right\}.$$

Moreover, for $l > 0$, it is necessary to consider the nondiagonal elements (58) (for the degenerate states I, IV)

$$\left(V_4 \right)_{\mathrm{I}}^{\mathrm{IV}} = - \frac{Rh}{2n^2} \frac{3\alpha^2}{16n} \qquad (60)$$

$$\times \frac{\sqrt{(l^2 - m^2)((l+1)^2 - m^2)}}{l(l+1)(l + {}^1/_2)(l - {}^1/_2)(l + {}^3/_2)},$$

which express the superposition of states I and IV for values of m common to states I and IV, i.e., for

$$m = -(l-1) \ldots 0 \ldots (l-1). \qquad (61)$$

For the remaining values of m, states I and IV are unmixed:

$$m = \pm l, \pm (l+1). \qquad (62)$$

It is evident that from the matrix elements (56)-(60) that the fine structure in the case under consideration depends on the magnetic quantum number m which characterizes the magnitude of the projection of the total momentum along the direction of the magnetic field.

Finally, we get for the matrix elements of the specific exchange energy (25)

$$E_5 = \frac{Rh}{2n^2} \frac{\alpha^2}{2n} (s^2 + 1) \delta_{l0}. \qquad (63)$$

Thus the exchange energy in the states with identical directions of spin projections is twice as great as the exchange energy in the states with opposed projection directions. We note for comparison that in the absence of a magnetic field, the exchange energy of the para-state is zero, while that of the ortho-state is equal to

$$E_5 = \frac{Rh}{2n^2} \frac{\alpha^2}{n}. \qquad (64)$$

General formulas for the fine structure can also be obtained. From the invariance of the energy (24), (25) relative to changes of sign of the charge (electron changed to positron and vice versa) it follows that the fine structure of the two states of opposite directions of the projections is the same. We obtain the formula for the fine structure in the form

$$E = E^0 + \Delta E. \qquad (65)$$

Here E^0 is defined by Eqs. (51)-(54), and

$$\Delta E = \frac{Rh}{2n^2} \left\{ \frac{11\alpha^2}{16n^2} + \frac{\alpha^2}{n} \varepsilon \right\}, \qquad (66)$$

where

$$\varepsilon_0 = \delta_{l0} - \frac{1}{l + {}^1/_2} + \frac{1}{8(l+1)(l + {}^1/_2)(l + {}^3/_2)} \qquad (67)$$

$$\times \left(1 - \frac{3}{2} \frac{(l^2 - m^2)(1 - \delta_{l0})}{l(l - {}^1/_2)} \right),$$

$$\varepsilon_{1,-1} = \frac{7}{3} \delta_{l0} - \frac{1}{l + {}^1/_2} - \frac{(7l + 9)(1 - \delta_{l0})}{8l(l+1)(l + {}^1/_2)(l + {}^3/_2)} \qquad (68)$$

$$+ \frac{3}{16} \frac{(1 - \delta_{l0})}{l(l+1)(l - {}^1/_2)(l + {}^1/_2)(l + {}^3/_2)}$$

$$\times \left[l^2 - m^2 - 1 \right.$$

$$\left. \pm \sqrt{m^2 (4l^2 + 4l - 1)^2 + (l^2 - m^2)((l+1)^2 - m^2)} \right].$$

The quantity ϵ_0 corresponds to opposite directions of the projections of the electron and positron spins along the magnetic field, and $\epsilon_{1,-1}$ to identical directions of the projections; the two possible signs in Eq. (68) correspond to two possible superpositions of the states with identical projection directions $[-(l-1) \leqq m \leqq l-1]$: for $m = l, l-1$, one takes the upper sign; for $m = -l, -(l+1)$, the lower sign (superposition is absent in the last two cases).

For the remaining states ($n = 1$, $l = 0$) we obtain

$$\varepsilon_{1,-1} = {}^1/_3, \quad \varepsilon_0 = -{}^5/_6. \qquad (69)$$

The coincidence of the fine structure of the fundamental state ($n = 1$) in a strong magnetic field with the fine structure of the lowest ortho-state in the absence of a magnetic field is connected with the parity of the mean values of the energy of spin-spin interaction and the exchange energy (splitting at $n = 0$ is brought about only by the presence of just this interaction).

The difference ϵ_0 [see Eq. (69)] from the fine structure of the para-system for $H = 0$ ($\epsilon^0 = -2$) is connected with the appearance of a non-vanishing exchange energy ($\epsilon = \frac{1}{2}$) in strong fields and with a decrease in the amount of spin-spin interaction ($\epsilon = -1/3$ instead of $\epsilon = -1$).

With the help of the wave functions obtained as a result of superposition [see Eq. (60)], the correct selection for optical spectra can easily be found:

$$\Delta l = \pm 1; \quad \Delta m = 0, \pm 1. \tag{70}$$

Furthermore, transitions from states of oppositely directed projections to states of parallel projections, and also between two different states with anti-parallel projections, are forbidden.

Transitions between two states of similarly directed projections are permitted, with the exception of the forbidden transiton $m' = 0 \rightarrow m = 0$.

Finally, we consider the quadratic Zeeman effect in strong fields specified by the energy

$$U_2^H = \frac{e^2H^2}{16mc^2}(x^2 + y^2). \tag{71}$$

For the matrix elements U_2^H, which are computed with the aid of the wave functions (47) and (50), we obtain:

for diagonal elements

$$E_2^H = \frac{Rh}{2n^2}\left(\frac{2\mu_0Hn^2}{Rh}\right)^2 \frac{5n^2 + 1 - 3l(l+1)}{16(l - {}^1/_2)(l + {}^3/_2)} \times (l^2 + (m-s)^2 + l - 1); \tag{72}$$

for non-diagonal elements

$$(V_2^H)_{s,\,l}^{s,\,l-2} = -\frac{e^2H^2}{64mc^2} \times \frac{\sqrt{(l^2 - (m-s)^2)((l-1)^2 - (m-s)^2)}}{(l - {}^1/_2)\sqrt{(l + {}^1/_2)(l - {}^3/_2)}}(r^2)_l^{l-2}. \tag{73}$$

We note that tne quadratic effect of the energy (71) does not produce a splitting of the fine structure levels, since, even without taking Eq. (71) into account, the fine structure depends on the value of the magnetic quantum number *m*. According to Eqs. (72) and (73), the energy levels are shifted proportional to the square of the field ($\sim H^2$).

In particular, for the fundamental level ($n = 1$), the shift of all terms is identical. Starting out from this shift [Eq. (72)], we can calculate the diamagnetic susceptibility of the gas of positronium atoms (per mole):

$$\chi = -\frac{N}{\alpha}\left(\frac{\hbar}{mc}\right)^3 = -4.67\times10^{-6}\ \text{см}^3. \tag{74}$$

5. STARK EFFECT IN WEAK ELECTRIC FIELDS

We obtain the energy of interaction of positronium with a constant external electric field $\mathcal{E}$ from Eq. (23) in the form

$$U^{\mathcal{E}} = e\mathcal{E}z + \frac{e\hbar}{4m^2c^2}(\vec{\sigma}_1 + \vec{\sigma}_2)[\vec{\mathcal{E}}\mathbf{p}], \tag{75}$$

$$z = z_1 - z_2; \quad |\mathcal{E}| = \vec{\mathcal{E}}_z = \text{const.} \tag{76}$$

As a system of unperturbed wave functions we take the wave functions of positronium in the absence of external fields. These are found, for example, in reference 1. In weak fields it is sufficient to calculate the matrix elements of the first term of Eq. (75). The matrix element of transition between states corresponding to the values of quantum numbers $s, n, m, l, j \rightarrow s', n', m', l', j'$ we denote by $V_{s,\,n,\,m,\,l,\,j}^{s',\,n',\,m',\,l',\,j'}$, in which the index *s* pertains to the states a, b, c, d (notation in reference 1). We get

$$V_{\mathrm{a},\,n,\,m,\,l,\,l}^{\mathrm{b},\,n,\,m,\,l+1,\,l} = -\frac{3}{2}mne\mathcal{E}r_0\frac{(1-\delta_{l0})}{\sqrt{l(2l+1)}}\sqrt{\left(\frac{n}{l+1}\right)^2 - 1}; \tag{77}$$

$$V_{\mathrm{c},\,n,\,m,\,l,\,l}^{\mathrm{b},\,n,\,m,\,l-1,\,l-2} = V_{\mathrm{c},\,n,\,m,\,l,\,l}^{\mathrm{d},\,n,\,m,\,l+1,\,l+2} = 0; \tag{78}$$

$$V_{\mathrm{c},\,n,\,m,\,l,\,l}^{\mathrm{d},\,n,\,m,\,l-1,\,l} = \frac{3}{2}mne\mathcal{E}r_0\frac{(1-\delta_{l0})}{\sqrt{(l+1)(2l+1)}}\sqrt{\frac{n^2}{l^2} - 1}; \tag{79}$$

$$V_{\mathrm{b},\,n,\,m,\,l,\,l-1}^{\mathrm{d},\,n,\,m,\,l+1,\,l+2} = 0; \tag{80}$$

$$V_{\mathrm{b},\,n,\,m,\,l,\,l-1}^{\mathrm{d},\,n,\,m,\,l-1,\,l} = -\frac{3}{2}ne\mathcal{E}r_0\frac{(1-\delta_{l0})\sqrt{l^2 - m^2}}{(2l+1)(2l-1)}\sqrt{\frac{n^2}{l^2} - 1}; \tag{81}$$

$$V_{\mathrm{a},\,n,\,m,\,l,\,l}^{\mathrm{a},\,n,\,m,\,l+1,\,l+1} = -\frac{3}{2}\,ne\mathscr{E}r_0\,\frac{\sqrt{[(l+1)^2-m^2]\,[n^2-(l+1)^2]}}{\sqrt{(2l+1)\,(2l+3)}}\,; \tag{82}$$

$$V_{\mathrm{b},\,n,\,m,\,l,\,l-1}^{\mathrm{b},\,n,\,m,\,l+1,\,l} = -\frac{3}{2}\,ner_0\mathscr{E}\sqrt{\frac{l+1}{l}}\,\frac{(1-\delta_{l0})}{2l+1}\sqrt{(l^2-m^2)}\sqrt{n^2-(l+1)^2}\,; \tag{83}$$

$$V_{\mathrm{c},\,n,\,m,\,l,\,l}^{\mathrm{c},\,n,\,m,\,l+1,\,l+1} = -\frac{3}{2}\,ner_0\mathscr{E}\,\frac{\sqrt{(l+1)^2-m^2}\,\sqrt{n^2-(l+1)^2}\,\sqrt{l\,(l+2)}}{(l+1)\sqrt{(2l+1)\,(2l+3)}}\,; \tag{84}$$

$$V_{\mathrm{d},\,n,\,m,\,l,\,l+1}^{\mathrm{d},\,n,\,m,\,l+1,\,l+2} = -\frac{3}{2}\,ner_0\mathscr{E}\sqrt{\frac{l+1}{l+2}}\,\frac{\sqrt{(l+2)^2-m^2}}{2l+3}\sqrt{n^2-(l+1)^2}\,, \tag{85}$$

where

$$r_0 = 2\hbar^2/me^2.$$

Inasmuch as the projection of the total momentum along the z axis is preserved in an electric field, the matrix elements for different m vanish.

In addition to the matrix elements (77)-(85), we must also consider the matrix elements of the fine structure (33). This permits us to examine the Stark effect in weak and strong fields.

We consider a weak electric field ($er_0\mathcal{E}n^3/2Rh\alpha^2 \ll 1$). Inasmuch as there is no l degeneracy in positronium, in contrast to hydrogen-like atoms, the linear Stark effect will not be observed in weak fields, except for the multiple levels n^3P_2 and n^3D_2, which are split, proportional to the field, into five equally spaced levels.

In the calculation of the Stark effect in weak fields, we shall obtain an approximate solution of the cumbersome secular equation by expanding ΔE in powers of $\mathcal{E}$ (the electric field):

$$\Delta E_\sigma^m = E_\sigma + \lambda_\sigma^m\mathscr{E} + \mu_\sigma^m\mathscr{E}^2, \tag{86}$$

where E_σ is the fine structure energy (the index denotes the term of the fine structure); furthermore, the amount of splitting depends on the characteristic values m of the projection of the total momentum in the direction of the field. The quantities λ_σ^m, with the exception of those for the states n^3P_2 and n^3D_2, are equal to zero. We obtain the following formulas for splitting:

1. For $n = 1$, splitting is absent;
2. For $n > 1$, we have

$$\Delta E_\sigma^m = E_\sigma + \varepsilon_\sigma^m\,\frac{2Rh\alpha^2}{n^3}\left(\frac{e\mathscr{E}r_0n^3}{2Rh\alpha^2}\right)^2, \tag{87}$$

where ϵ_σ^m is given by Table I.

TABLE I

σ \ m	0	± 1	± 2	± 3
2^1S_0	—27	×	×	×
2^3P_0	—36 : 5	×	×	×
2^3P_1	0	—108 : 7	×	×
2^1P_1	27	0	×	×
2^3P_2	—720 : 23	—540 : 23	0	×
2^3S_1	4428 : 115	6264 : 161	×	×
3^3S_0	—162	×	×	×
3^3P_0	—18468 : 115	×	×	×
3^3P_1	—405 ; 2	—41553 : 112	×	×
3^1P_1	—243	—1215 : 4	×	×
3^3D_1	4779 : 46	1863 : 16	×	×
3^3P^2	—42795 : 46	7485 : 23	—210	×
3^3D_2	405 : 2	7485 : 23	—210	×
3^1D_2	405	1215 : 4	0	×
3^3D_3	756	672	420	0
3^3S_1	26568 : 115	37584 : 161	×	×

Equation (87) does not take into account the linear Stark effect for the multiple levels n^3P_2 and n^3D_2, for which there is an additional energy, besides that of Eq. (87):

$$\Delta E = \frac{\sqrt{3}}{4}\, me\, \mathcal{E} r_0 \sqrt{\frac{n^2-4}{5}}, \tag{88}$$

where $m = 0, \pm 1, \pm 2$, while the wave functions of the states n^3P_2 and n^3D_2 are mixed for $m = \pm 1, \pm 2$. For the case $m = 0$, the wave functions are not mixed, and the level is not shifted. However, in the following approximation (the effect proportional to $\mathcal{E}^2$) this multiple level divides into two, corresponding to the states n^3P_2 and n^3D_2.

6. THE STARK EFFECT IN STRONG ELECTRIC FIELDS

Neglecting the fine structure, we can write

$$\left(E + \frac{e^2}{r} - \frac{p^2}{m} - e\mathcal{E}z\right)\psi = 0. \tag{89}$$

Then, in the first approximation of excitation theory, we have

$$E = -\frac{Rh}{2n^2} + 3\frac{\hbar^2}{me^2} e\mathcal{E} n (n_1 - n_2). \tag{90}$$

Here $n_1 - n_2$ is the electric quantum number. Thus, in strong electric fields (as also in hydrogen-like atoms) the linear Stark effect must be considered. By virtue of Eq. (90), this effect is four times larger, in relative units, in positronium than in hydrogen (correspondingly, the quadratic Stark effect is 16 times larger, and the third order effect 64 times larger).

To find the fine structure of the Stark effect in strong fields, we solve the secular equation with the matrix elements (77)-(85) and (33), (34) in an approximation distinct from Eq. (86), expanding the desired difference in a power series inverse in the field:

$$\Delta E_k^m = \Delta E_k + \frac{Rh}{2n^2}\left\{\frac{11\,\alpha^2}{16\,n^2} - \frac{4\alpha^2}{n}\varepsilon_k^m\right\} \tag{91}$$

$$+ \lambda_k^m \left(\frac{2Rh\alpha^2}{n^3 e r_0 \mathcal{E}}\right)^2 \frac{2Rh\alpha^2}{n^3} + \ldots$$

Here ΔE_k is determined by Eq. (90). The third and subsequent terms of Eq. (91) describe the field-dependent fine structure. In the approximation under discussion ($2Rh\alpha^2/n^3 e r_0 \mathcal{E} \ll 1$) this represents a very small correction to the field-independent fine structure which is described by the second term of Eq. (91).

We shall write out here only the quantities ϵ_k^m for the field-independent part of the fine structure. For ϵ_k^m we have Table II ($n = 1, 2, 3$)*.

For certain levels 2^3P_2, 2^1P_1, 2^3P_1, 3^3D_3, 3^1D_2) there exist such states ($m = \pm 2, \pm 1, 0, \pm 3, \pm 2$, correspondingly) which do not interact with the electric field. They therefore pertain to fixed Stark components for the levels of the fine structure. The fine structure of these levels, in contrast to the rest, do not depend on the field at all. For the remaining Stark components ($\Delta E_k = \pm 3 e r_0 \mathcal{E}, \pm 9/2\, e r_0 \mathcal{E}, \pm 9 e r_0 \mathcal{E}, \ldots$), the coincidence of the fine structure for components of different sign takes place only if we do not consider the field-dependent part of the fine structure. For $n = 2$, the central component is split into 5 sublevels, and the edge component into 3. For $n = 3$, the central component splits into 7 levels, the next into 5, and the edge into 3, etc.

7. PROBABILITIES OF ANNIHILATION OF POSITRONIUM IN EXTERNAL ELECTRIC AND MAGNETIC FIELDS

We first consider the probability of annihilation in an electric field. It is easy to see that the matrix elements of the energy U of interaction of the positronium atom with external electric field [see Eq. (75)] are diagonal relative to the spin variable. Therefore, the electric field does not produce transitions between the ortho- and para-states (does not mix them). The para-states are annihilated into two photons, the ortho-states into three (see references 2 and 5). The change in the annihilation probability for the presence of an electric field is connected with the fact that the electric field changes the value of the quantum number l, whereas the annihilation is possible only for $l = 0$. The mixing can be found from the secular equations which are solved above. We note that for $n = 1$ the linear Stark effect is absent, and the probability of annihilation of these levels does not change upon the inclusion of the electric field. For much higher levels ($n > 1$), we have

$$\psi_\sigma^m = \sum_{\sigma'} C_{\sigma\sigma'}^m \psi_{\sigma'}. \tag{92}$$

---

* The value of ϵ for 3^3D_3 is not included in the Table and is determined by Eq. (33).

TABLE II

n	ΔEk \ m	0	± 1	± 2
2	0	$\frac{31}{120}$; $\frac{5}{24}$	$\frac{19}{120}$; $\frac{1}{6}$	$\frac{13}{120}$
2	$\pm 3er_0\mathcal{E}$	$\frac{1}{20}$; $\frac{1}{3}$	$\frac{3}{80}$	×
3	0	$\frac{17}{420}$; $\frac{7}{30}$	$\frac{69 \pm \sqrt{1373}}{840}$	$\frac{41}{420}$; $\frac{1}{10}$
3	$\pm \frac{9}{2} er_0\mathcal{E}$	$\frac{19}{120}$; $\frac{157}{840}$	$\frac{737}{7560}$; $\frac{2}{15}$	$\frac{41}{420}$
3	$\pm 9er_0\mathcal{E}$	$\frac{17}{210}$; $\frac{4}{15}$	$\frac{287}{3780}$	×

TABLE III

σ \ m	±2	±1	0
2^3S_1	×	$-\frac{4546368}{25921} w_3$	$-\frac{2388528}{13225} w_3$
2^3P_2	0	$\frac{64800}{529} w_3$	$\frac{86400}{529} w_3$
2^1P_1	×	0	$81 w_2$
2^3P_1	×	$\frac{2592}{49} w_3$	0
2^3P_0	×	×	$\frac{432}{25} w_3$
2^1S_0	×	×	$-81 w_2$

Here m is the magnetic quantum number and the index σ denotes the state a, b, c, d (see reference 1). The coefficients $C^{m}_{\sigma\sigma'}$ can be found in the two cases under consideration: weak and strong fields.

By way of an example, we take the case $n = 2$. In computing the annihilation probability, it is sufficient to know $|C_{S,\ 2S_{1/2}}|^2$. In weak fields, we will classify the state with the aid of symbols in the absence of the field. The changes in annihilation probability can be found by means of the formula

$$\Delta w^m_\sigma = \alpha^m_\sigma \left(\frac{4\, er_0 \mathcal{E}}{Rh\alpha^2}\right)^2, \tag{93}$$

where the α^m_σ are given in Table III.

Here w_3 and w_2 are the probabilities of three photon and two photon annihilation for $n = 2$. The change in the annihilation probability, compared with the case $\mathcal{E} = 0$, is proportional to the square of the electric field, and depends on the position of the level of the fine structure [the numerical coefficients in Table III correspond to Eq. (33)].

As was shown in reference 1, the states 2^3S_1 and 2^1S_0 are metastable in relation to the optical transitions. Annihilation is much more probable for them, since their lifetimes are $8\tau_3$ and $8\tau_2$, respectively, whereas τ_3 and τ_2 are the lifetimes of the fundamental state of positronium ($n = 1$), relative to three photon (ortho-positronium) and two photon (para-positronium) annihilation.

With the inclusion of the electric field the levels 2^2S_1 and 2^1S_0 cease to be metastable relative to optical transitions. An estimate, made with the aid of Eq. (92), shows that the metastability is removed for relatively weak fields, when the energy in the external electric field is approximately an order of magnitude smaller than the splitting of the fine structure. In strong electric fields, we find that, for $n = 2$, the annihilation probability of the central Stark component (states of five levels in the fine structure) is zero. The edge Stark components consist of three sublevels, one of which corresponds to para-state, the other two to ortho-state. For the annihilation probability of the para-level ($\mathring{E} \sim \pm 3er_0 \mathcal{E}$) we get $\frac{1}{2}w_2$, and for the ortho-level $\frac{1}{2}w_3$, where w_2 and w_3 are the two and three photon annihilation probabilities in the absence of the field. Thus, in a strong electric field the lifetime, relative to annihilation is the same for para-positronium as for ortho-positronium ($n = 2$).

We now consider the case of a magnetic field. The effect of a weak magnetic field on the annihilation probability was investigated in reference 1. In a strong magnetic field, the spin states of positronium are characterized by the magnitudes of the projections of the electron and positron spins in the direction of the magnetic field. It is easy to see[5] that the lifetime of the fundamental state, with oppositely directed spin projections on the magnetic field, relative to two photon annihilation, is twice as large as for $H = 0$:

$$\tau_2^H = 2.5 \times 10^{-10} \text{ sec.} \tag{94}$$

Moreover, the states of opposing projection directions can annihilate into three photons, whence the lifetime of the fundamental state ($n = 1$) relative to three photon annihilation is twice as great as the lifetime of ortho-state for $H = 0$:

$$\tau_3^H = 2.8 \times 10^{-7} \text{ sec.} \tag{95}$$

One out of about 1120 atoms with states having uniform directions of projections decays into three photons. From the selection rule (70), it is easy to see that the S states for $n = 2$ are metastable relative to the optical transitions. Because of this, their annihilation is much more probable. The lifetimes, relative to the two and three photon annihilations, of the metastable ($n = 2$) state with opposing directions of spin projections are equal to

$$\tau_2^{1H} = 2 \times 10^{-9} \text{ sec and } \tau_3^{1H} = 2.24 \times 10^{-6} \text{ sec.} \tag{96}$$

For states with uniform directions of projections, two photon annihilations are forbidden. The lifetime relative to three photon annihilation for the fundamental state ($n = 1$) is

$$\tau_3 = 1.4 \times 10^{-7} \text{ sec} \tag{97}$$

and for the metastable state ($n = 2$)

$$\tau_3^1 = 1.12 \times 10^{-6} \text{ sec} \tag{98}$$

are equal to the corresponding times for $H = 0$.

I express my deep gratitude to Prof. A. A. Sokolov for his discussion of the results of the present work.

Translated by R. T. Beyer
121

SOVIET PHYSICS - JETP VOLUME 1, NUMBER 3 NOVEMBER, 1955

Measurement of the Coefficients of Internal Conversion of γ-Rays of Sr^{87*}, In^{113*}, In^{115*} and V^{51*} on the Electrons of the Atoms

I. V. ESTULIN AND E. M. MOISEEVA
Moscow State University

(Submitted to JETP editor April 24, 1954)
J. Exper. Theoret. Phys. USSR **28**, 541-546 (May, 1955)

The total coefficients of internal conversion of γ-rays of Sr^{87*}, In^{113*}, In^{115*} and V^{51*} on the electrons of the atoms are determined by the method of direct measurement of the number of electrons and γ-quanta which are emitted by the source.

The corresponding values, which have been found, i.e., 0.26 ± 0.03, 0.39 ± 0.04, 0.9 ± 0.6 and $(3.1 \pm 0.2) \times 10^{-3}$ give basis for the conclusion that the isotopes Sr^{87*}, In^{113*} and In^{115*} have electric 2^5 pole radiation transition and that V^{51*} has electric quadrupole radiation transition.

1. INTRODUCTION

In the case of the nuclear radiation transition, the magnitude of the internal conversion coefficient of γ-rays depends on the character of the transition and the multiplicity of the radiation[1].

The coefficients of internal conversion corresponding to the electric or magnetic character of radiation in the most cases differ by no more than 20-50% in the neighboring multiplicities. Therefore, precise conclusions about the multiplicity as well as about the character of the nuclear radiant transition which may be obtained by means of comparing theoretical and experimental values of coefficients of internal conversion of γ-rays, can be made only after precise experimental works. In the experimental determination of those coefficients, it is advisable to use various methods to avoid errors which are inherent in any one method.

In this work, the coefficients α of internal conversion of γ-rays which are emitted by isomeric transitions of Sr^{87*}, In^{113*} and In^{115*}, have been determined by the means of direct measurements of the number of the γ-quanta N_γ and electrons N_e emitted by the isomer, i.e., $\alpha = N_e/N_\gamma$.

Ionization methods were used in measuring N_e and N_γ. In those particular cases which are the subject of this work, the measurement of electron and γ-monochromatic emission can also be made by the application of other methods. In this work, the emissions have been detected by means of gas-discharging counters. After the application of corrections, it was possible to determine the absolute number of electrons and γ-quanta which were emitted by sources with monochromatic spectra of γ-emission. Our investigations were performed with the purpose of verifying the data[2] which are in contradiction with the conclusions about the character of isomeric transitions Sr^{87*}, In^{113*} and In^{115*} obtained in other researches which were related to the classification of nuclear isomers[3].

2. METHODS OF EXPERIMENT

For the investigation of γ-rays in this work, the gas-discharging cylindrical counter was 10 cm long and 2 cm in diameter. The inner glass part of the counter was coated with a thin layer of copper. The efficiency ϵ of this counter, in the region of γ-ray energy with which we are concerned, was measured by means of radioactive isotopes Hg^{203}, Sr^{87*} and A^{198} with the simple γ-ray spectrum[4] which has intense monochromatic lines and energies 279, 390 and 411 kev, respectively. The number of γ-quanta emitted by the above mentioned source had been measured with an ionization chamber (provided with slit). The efficiency of this chamber with relation to the γ-quanta was known[5]. the relation between ϵ and the energy of γ-quanta was determined; it is presented by Fig. 1.

As the gas-discharging counter has a low efficiency relating to the γ-quanta, the sources of the

---

[1] L. V. Groshev and I. S. Shapiro, *The Spectroscopy of the Atomic Nuclei*, Moscow, 1952

[2] I. A. Antonova and I. V. Estulin, Izv. Akad. Nauk SSSR, Ser. Fiz. **4**, 71 (1952)

[3] M. Goldhaber and A. Suniar, The Problems of Modern Physics, **4**, 71, Foreign Literature Publishing House, Moscow, 1952; M. Goldhaber and R. D. Hill, Rev. Mod. Phys. **24**, 179 (1952)

[4] J. M. Hollander, L. Perlman and G. T. Seaborg, Rev. Mod. Phys. **25**, 469 (1953)

[5] I. V. Estulin, J. Exper. Theoret. Phys. USSR **24**, 221 (1953)

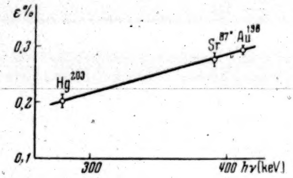

Fig. 1. The dependence of the efficiency of the gas discharging counter of the γ-quanta energy.

order of 0.1 mCu were kept at the distance 3-8 cm from the counter.

The geometrical conditions of these experiments were calibrated beforehand using the sources of higher intensity and various distances, even higher than 3-8 cm. The calculation of a solid angle of the source relative to the counter was easily done for distances of 20-50 cm.

The source was deposited on a mica plate of thickness 13.5 mg/cm^2 which in its turn was attached to a cup-shaped aluminum piece.

When electrons, emitted by the source, have been measured, the aluminum cup (*1*) with the source was placed in the inner part of a glass vacuum tube (2) with inside diameter 30-35 mm (Fig. 2).

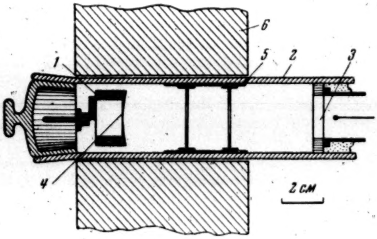

Fig. 2. Device for measuring the intensity of electrons. *1.* Aluminum cup; *2.* Vacuum tube; *3.* Gas-discharging counter; *4.* Source; *5.* Aluminum diaphragm; *6.* Electromagnet.

On the opposite end of the vacuum tube, the gas-discharging counter (*3*) with a mica window 3-4 mg/cm^2 thickness, and diameter 20 mm, was placed between the source (*4*) and counter. The aluminum diaphragm was mounted to shield the scattered electrons. Thus, the region of the tube close to the counter was free from the action of scattered electrons. The distance between a source and counter was 6-9 cm. The size of source was 4-8 mm, so that it could be considered as a point. The vacuum tube was between the magnetic poles, but the counter was placed outside of the magnetic field. During the experiments, the tube was evacuated.

The action of x-rays and γ-emission on the counter was taken into account when experiments with magnetic field of intensity 1600 gauss were performed. In order to determine the absolute intensity of electrons, the corrections were applied for absorption of electrons by the mica window of the counter as well as for back scattering of electrons.

By means of the change of pressure in the tube, the absorption of electrons was measured under the arrangements of these experiments. The measured parts of the absorption curves were approximated by exponentials having absorption coefficients $\mu = 24$ cm^2/g for the electrons emitted by In^{113*}, $\mu = 44$ cm^2/g for electrons emitted by Cr^{51} and $\mu = 46$ cm^2/g for electrons of In^{115*} The absorption of electrons in the counter window and in the preparation was calculated using these experimentally found coefficients of absorption. The correction connected with the absorption of electrons by the mica window was of the order 10-15%. The correction connected with the absorption by the specimen was dependent on the thickness of the specimen.

In the preliminary experiments, the source Cr^{51} was deposited on a mica plate 2.6 mg/cm^2 thick. Later on, an additional layer of mica was attached to the back part of the plate. The registered counts increased by 4-5% with the thickness 13.5 mg/cm^2, and up to 10-12% with thickness 2 mm. Disregarding the reflection of electrons from the thin plate, we obtained the correction with the back-scattering of electrons for measuring the number of electrons emitted by the source. The preliminary tests also proved that it is reasonable to disregard reflection by the aluminum cup. The purity of sources was controlled with the help of disintegration curves of β- and γ-emission. The energy of registered electrons was evaluated by the paths traversed in the aluminum. The values found served as proof that the measurement was concerned only with electrons of internal conversion. The distances traversed by these electrons in our cases were of the order 100 mg/cm^2.

3. THE MEASUREMENTS OF In^{113*}, In^{115*} AND Sr^{87*}

Isomer In^{113*} as a product of a disintegration of the isotope Sn^{113*} was produced in its pure chemical state from the radioactive tin. The source deposited on the mica plate was practically weight-

TABLE I

The characteristic of the isomeric transitions of In^{113*}, In^{115*} and Sr^{87*}

Name of the Isomer	The half-life in hours	The energy of an excitation in kev	The total coefficient of an internal conversion of γ-rays on the electrons of an atom $\propto$		The coefficient of an internal conversion of γ-rays on the K-shell of an atom $\propto_K$		
			According to the work (2)	According to this work	The experimental value	The Theoretical Value	
						The electric 2^5 pole transition	The magnetic 2^4 pole transition
In^{113*}	1.75	392	0.44 ±0.03	0.39 ±0.04	0.32	0.33	0.46
In^{115*}	4.5	334	0.82 ±0.13	0.9 ±0.06	0.70	0.69	0.92
Sr^{87*}	2.8	390	0.28 ±0.03	0.26 ±0.03	0.22	0.23	0.19

less. The measurements of the number of γ-quanta were first carried out.

Afterwards, the source was placed in the vacuum tube, already described. The measuring of electrons emitted by the source was performed with application of the corrections for the absorption of electrons by the window of a counter (11%) and for the electron's back scattering at the plate (4%). Altogether, four different series of experiments were performed. The pure isomer In^{115*}, which is the result of disintegration of an isomer Cd^{115} with $T = 54$ h, was produced by chemical method from the radioactive cadmium. The weight of deposited source on the mica was less than 1 mg. Therefore, the absorption in the specimen was disregarded. During the determination of the number of electrons which are liberated from an atom in the internal conversion of γ-rays, it was taken into account that In^{115*} may by the β-disintegration be transformed into Sn^{115} (the branch of β spectrum, 5.5%)[4].

The average value of the total coefficient of internal conversion of γ-rays in In^{115*}, obtained from four experimental series, is given by the Table I. When Sr^{87*} was investigated the chemically pure source of this isomer was not available. Strontium nitrite, containing the isomer in which we have been interested was deposited in the form of fine powder on the mica plate in order to avoid a dispersion in a vacuum tube. The specimen with a thickness 8-16 mg/cm^2 was covered by the organic film with a thickness ~ 0.1 mg/cm^2. The correction for the absorption of electrons by the source was of the order 10-20%. The absorption of the monochromatic electrons with an energy close to those electrons which are emitted by Sr^{87*}, was pretty well studied earlier with the weightless specimen of In^{113*} Five experimental series were carried out and the average values of results are given in the Table I. The fact that the thickness of the source had no effect is an indication that the calculation of the electron's absorption by the source was correct.

In Table I, the principle characteristics of isomeric transitions In^{113*}, In^{115*} and Sr^{87*} are presented. In the first columns of the Table, the half-lives and the energies of the corresponding transitions are shown. In the subsequent columns, the coefficients of internal conversion of γ-rays on the electrons of an atom $\propto$, which have been determined by Antonova and Estulin previously[2], as well as $\propto$ obtained by the present work, are presented.

The experimental errors estimated from the various experiments are given as the arithmetic mean.

In the work with In^{115*}, the discrepancies of separate experiments were negligible. In this particular case, half of the maximum error of the apparatus was taken as experimental error.

In the limits of the experimental error, the results of this work are in agreement with results in reference 2. It should be noted that in this work the method of absolute measurements of the number of electrons and γ-quanta was different from that used in reference 2. Thus the possibility of a systematic error of measurement in the total coefficients of internal conversion on the γ-rays is apparently diminished. On the basis of the values of $\propto$ determined in this work the experimental values of the coefficients of internal conversion of γ-rays on the electrons of K-shell $\propto_K$ have been found (column 6, Table I).

The ratio of the coefficients of internal conversion on K and $L + M + \ldots$ shells of an atom $\propto_K / \propto_{L+M+\ldots}$ is taken from the experimental works of other authors and is the same as in reference 2. The theoretical values of $\propto_K$ obtained by the method of an extrapolation* in reference 6 are shown in the last columns of the Table.

The values of α_K found by experiment are in an agreement with the theoretical values of α_K for the 2^5-fold electrical transition. Thus, if the theoretical values α_K in reference 6 are correct, the isomeric transitions In^{113*}, In^{115*} and Sr^{87*} should be considered as types of 2^5 electrical transitions. These conclusions are in agreement with results of reference 2 and do not contradict the predictions of the theory of the nuclear shells.

MULTIPLICITY OF γ-RADIATION OF V^{51*}

The radioactive isotope Cr^{51} which has a half-life of 26.5 days, decays by capture of the orbital electron and subsequently forms V^{51} partially in the excited state[4]. In reference 7 is shown the possibility of two excited states of V^{51}. However, later it was proved that when Cr^{51} decays, only one excited state of V^{51} takes part, with the energy of excitation 320 kev. In the same reference 7 the coefficient of the internal conversion of γ-radiation, which is connected with the transition $V^{51*} \rightarrow V^{51}$ is taken as $\alpha \sim 0.02$. Later on, in reference 8, the value of α is given as $\alpha = 1.5 \times 10^{-3}$.

Thus, the radioactive isotope Cr^{51} emits the intensive characteristic x-radiation and has not any other electron radiation except of those electrons which are torn out from the atom by means of the internal conversion of γ-rays of V^{51*} with the energy of excitation 320 kev.

As the continuous β-spectrum is absent, the measurement of the internal conversion coefficient of γ-rays V^{51*} by the magnetic spectrometer with the method of comparison of the areas is inapplicable. In this particular case, although α is very small, it turns out to be possible to measure its value by means of the absolute measurements of the intensity of electrons and γ-quanta by the method shown in Sec. 2 of this work.

Using the same method as in the case with measurements of In^{113*}, In^{115} and Sr^{87*}, we deposited a source containing radioactive isotope Cr^{51} on the mica plate, and after measurement of γ-rays it was placed in the vacuum tube (Fig. 2). The thickness of the source was 5.5 mg/cm^2. The correction connected with the absorption of the electrons by a source was 10%.

Since a gas-discharging counter with the thin window was effective for the characteristic x-radiation of V^{51}, the precise measurement of the counts of a counter with and without a magnetic field was possible. Altogether, five series of measurements were carried out. A value of the total coefficient of internal conversion $\alpha = (3.1 \pm 0.2) \times 10^{-3}$ was obtained.

We now come to the coefficient of conversion of γ-rays on the K-shell of an atom α_K. Its theoretical value is known[6]. For this purpose, it is reasonable to make use of the ratio of the internal conversion coefficients on the K and L shells of an atom α_K/α_L.

In the case under discussion, when there is either dipole or quadrupole emission and the parameter $Z^2/E = 1.65$ (Z = atomic number, E = the energy of the radiative transition in kev) which determines the ratio α_K/α_L [3] is small, the value of α_K/α_L is of an order 11 for a magnetic type of emission and of the order 12 for emission of an electrical type[10]

TABLE II

The coefficient of internal conversion of γ-rays V^{51*} on the K-shell of an atom α_K

Experimental value	Theoretical value	
	Dipole Magnetic Transition	Quadrupole Electric Transition
$(2.9 \pm 0.2) \times 10^{-3}$	0.95×10^{-3}	3.8×10^{-3}

These values of the ratio α_K/α_L are taken from the theoretical works and very likely can be applied in the present case. The experimental value of α_K (Table II) is obtained from α by taking into consideration the value of a ratio α_K/α_L. In Table II, there are also shown the theoretical values of α_K for the dipole magnetic and quadrupole electric transitions, which have been found with the use of extrapolation in reference 6 for $Z = 23$.

---

* This problem was considered in more detail in reference 2.

[6] M. Rose, G. Goertzel, B. Spinard, J. Harr and A. P. Strong, Phys. Rev. **83**, 79 (1951)

[7] H. Bradt, M. C. Gugelot, O. Huber, H. Medicus, P. Preiswerk and A. Strineman, Helv. Phys. Acta **25**, 461 (1952)

[8] D. Maeder, P. Preiswerk and A. Strineman, Helv. Phys. Acta **25**, 461 (1952)

[9] W. S. Lyon, Phys. Rev. **87**, 1126 (1952)

[10] M. H. Hebb and E. N. Nelson, Phys. Rev. **58**, 486 (1940); N. Tralli and J. S. Lowen, Phys. Rev. **76**, 1541 (1949)

The comparison of the experimental and theoretical values of α_K leads to the conclusion that electric quadrupole character of transition should be ascribed to $V^{51*} \rightarrow V^{51}$. It is possible that magnetic dipole emission is available in a very small quantity. In accordance with the theory of nuclear shells with a strong spin-orbital bond, the state $f_{7/2}$ corresponds to the principal state of V^{51}. In the case when the nuclear shells are successively filled up, the first excited level will have state $f_{5/2}$, hole-level will have the state $S_{1/2}$ or $d_{3/2}$.

The conclusion about the quadrupole character of an emission may find its confirmation in the fact that the nucleus of V^{51}, after getting into an excited state, fills up its nuclear levels successively, which is in agreement with an inference of reference 11. The transition $V^{51*} \rightarrow V^{51}$ belongs to the type $f_{5/2} \rightarrow f_{7/2}$.

The correlation of the decay probabilities of Cr^{51} into ground or excited state of V^{51} [8,9] is in agreement with the state $f_{7/2}$ of a nucleus of Cr^{51}, which was predicted by the theory of nuclear shells.

Translated by M. Hadsinskyj
95

[11] L. K. Peker, L. A. Sliv and L. V. Zolotavin, Doklady Akad. Nauk SSSR **88**, 781 (1953); L. K. Peker and L. A. Sliv, Izv. Akad. Nauk SSSR, Ser. Fiz. **17**, 411 (1953)

SOVIET PHYSICS - JETP VOLUME 1, NUMBER 3 NOVEMBER, 1955

Some Observations on Possible Formulations of the Theory of Extended Particles

V. S. BARASHENKOV

(Submitted to JETP editor May 8, 1954)
J. Exper. Theoret. Phys. USSR **28**, 579-583 (May, 1955)

Some of the features of possible formulations of a theory of non-localized fields are considered. In particular, it is shown that if the operators of the non-localized fields are considered to be non-diagonal matrices in coordinate space, then non-interacting non-localized fields cannot be equivalent to an aggregate of fields of local type. Finally some considerations are presented concerning the comparison of results of a theory of extended particles with experiment.

1. The search for a possibility of eliminating the fundamental difficulties of field theory, associated with the presence of divergent expressions in the apparatus of the present theory, constitutes one of the central parts of contemporary physical literature, devoted to the study of the properties and interaction of elementary particles. The importance of the problem is due to the close connection of these difficulties with the most profound problems of the structure of matter: the mass and structure of elementary particles, the coupling of these particles, nuclear forces, etc.

One may feel[1] that the elimination of many of the difficulties of present physical theory, among which are the difficulties with divergences connected with the incorrect application, for the description of phenomena taking place in small space-time regions, of concepts and principles which are in accord with experiment only over large regions of space-time*. From this point of view, some ideas which have been recently thoroughly discussed are of great interest; these are the hypothesis of non-local fields[2-4], in which the errors in determination of field, ΔA, and coordinate, Δx, are connected by the relation $\Delta A\ \Delta x \sim \lambda_0 A$, and the closely connected hypothesis of non-local interaction[5], i.e., the hypothesis that the interaction is "smeared" over a small space-time domain. Mathematically these ideas are formulated by the introduction into the theory of cut-off form factors, which can be interpreted as an attempt to introduce into the theory a space-time extension of the particles.

---

[1] D. I. Blokhintsev, Uch. Zap., Moscow State University, Phys. **3**, 77, 101 (1945); M. A. Markov, J. Exper. Theoret. Phys. USSR **8**, 124 (1938)

* On the other hand, it is hard to deny that a definite part of our difficulties is due to incorrect application in various cases of one or another mathematical method. In particular, it may be that taking account of higher approximations of perturbation theory will bring the essential corrective measure.

[2] M. A. Markov, J. Exper. Theoret. Phys. USSR **10**, 1311 (1940); **21**, 11 (1951)

[3] H. Yukawa, Phys. Rev. **77**, 219 (1950); **80**, 1047 (1950)

[4] H. Yukawa, Phys. Rev. **91**, 415, 416 (1953)

[5] C. Bloch, Kgl. Danske Videnskab. Selskab., Mat.-Fys. Medd. **27**, No. 8 (1952)

The hypotheses of non-local field and non-local interaction have no specific quantum character, and are applicable to the classical theory of fields[6].

It is essential to point out that all schemes of this sort so far proposed lead to serious difficulties connected with the breakdown of relativistic invariance[7,8]. One can try[8] to eliminate these difficulties by introducing into the theory "dynamically deformable" form factors, which correspond to the consideration of "soft" particles in the sense that the velocity of propagation of a signal for such a particle does not exceed the velocity of light. However, in our opinion, it appears extremely reasonable to investigate, within the realm of a theory with "rigid" particles, the possibility of constructing a theory in which the deviations from relativistic invariance are localized within small space-time domains. It was shown earlier[9] that such a "small space-time region" ($\lesssim \lambda_0$), in which the signal velocity can exceed that of light, remains small ($\lesssim \lambda_0$) in any coordinate system. In this sense we may say that the theory is relativistically invariant, and consider it to be the limiting case of a theory with dynamically deformable form factor.

It is also essential that the apparatus of the theory automatically guarantee the limitation of measurement in small regions ($\sim \lambda_0$); the physically observable quantities in such a theory must be quantities corresponding to a large ($> \lambda_0$) space-time interval. In this respect, the theory of non-localized fields, in which field and coordinate satisfy the relation $\Delta A\, \Delta x \sim \lambda_0 A$, has an advantage over the theory of non-local interaction.

2. An interesting variant of the theory of non-localized fields was presented and discussed in detail by Yukawa[3]. In contrast to the theory of localized fields, in which the field is regarded as a local point function $A = A(x)$, the field in Yukawa's non-localized field theory is considered to be a non-diagonal matrix in coordinate space:

$$A = (x'|A|x'') \qquad \text{with} \qquad [A, x] \neq 0.$$

The complete system of equations describing the non-interacting, non-localized field $(x'|A|x'')$, in the form in which it was given in reference 3 is:

$$\begin{gathered} [p[p, A]] + m_0^2 A = 0, \\ [x[x, A]] - \lambda_0^2 A = 0, \\ [p[x, A]] = 0. \end{gathered} \tag{1}$$

Here p is the momentum operator: $(x'|p|x'') = -i \frac{\partial}{\partial x'} \partial(x' - x'')$; x is the coordinate operator: $(x'|x|x'') = x'\delta(x' - x'')$.

Thus this variant of the theory differs from the theory of localized fields because of the change in the laws of motion for the free fields; the second quantization is carried out in accordance with the altered equations of motion[3].

Subsequently, several authors[10,11] have come to the conclusion that the theory of a free non-localized field is merely one of the possible ways of describing an aggregate of localized fields each describing particles with mass m_0 and different spins. In the light of the original idea concerning the essentially non-diagonal character of the field operator $(x'|A|x'')$, such a conclusion seems very surprising and merits more careful scrutiny.

It is easy to see that the matrix elements of the commutator of the coordinate operator and an arbitrary matrix quantity $(x'|T|x'')$ can, in accordance with the rules for matrix multiplication, be written in the form:

$$\begin{aligned} (x'|[x, T]|x'') &= \int x'\delta(x' - t)(t|T|x'')\,dt \\ &- \int (x'|T|t)\, t\,\delta(t - x'')\,dt = (x' - x'')(x'|T|x''). \end{aligned} \tag{2}$$

Similarly, we obtain for the matrix elements of the commutator of the momentum operator and a matrix T the expression:

$$\begin{aligned} &(x'|[p, T]|x'') \\ &= i \int (x'|T|t) \frac{\partial}{\partial t} \delta(t - x'')\,dt \\ &- i \int \frac{\partial}{\partial x'} \delta(x' - t)(t|T|x'')\,dt \\ &= -i \left(\frac{\partial}{\partial x'} + \frac{\partial}{\partial x''}\right)(x'|T|x''). \end{aligned} \tag{3}$$

---

[6] D. I. Blokhintsev, J. Exper. Theoret. Phys. USSR **16**, 480 (1946); **18**, 566 (1948); H. Yukawa, Progr. Theor. Phys. **2**, 209 (1947)

[7] M. A. Markov, J. Exper. Theoret. Phys. USSR **16**, 790 (1946)

[8] M. A. Markov, J. Exper. Theoret. Phys. USSR **25**, 527 (1953)

[9] D. I. Blokhintsev, J. Phys. USSR **10**, 167 (1946); J. Exper. Theoret. Phys. USSR **22**, 254 (1952)

[10] O. Hara and H. Shimazu, Progr. Theor. Phys. **7**, 255 (1952)

[11] M. Fierz, Phys. Rev. **78**, 184 (1950); Helv. Phys. Acta **23**, 412 (1950)

If we choose the matrix T in the form $(x'|T|x'') = (x'|[x, A]|x'')$ or $(x'|T|x'') = (x'|[p, A]|x'')$, then the system of equations (1) can be rewritten in the form:

$$(x'|F_1|x'') \equiv \left(\frac{\partial}{\partial x'} + \frac{\partial}{\partial x''}\right)_\mu \left(\frac{\partial}{\partial x'} + \frac{\partial}{\partial x''}\right)^\mu (x'|A|x'') - m_0^2 (x'|A|x'') = 0, \tag{4}$$

$$(x'|F_2|x'') \equiv (x' - x'')_\mu (x' - x'')^\mu (x'|A|x'') - \lambda_0^2 (x'|A|x'') = 0,$$

$$(x'|F_3|x'') \equiv (x' - x'')_\mu \left(\frac{\partial}{\partial x'} + \frac{\partial}{\partial x''}\right)^\mu (x'|A|x'') = 0.$$

In addition we introduce, in place of the matrix operators F_1, F_2, F_3, new operators E_1, E_2, E_3, whose matrix elements we define as follows:

$$(X'|E_i|X'') = (X' + X''|F|X' - X'') = (x'|F_i|x''). \tag{5}$$

If the matrix elements of the operators F_i and E_i are regarded as functions of the variables x', x'' and X', X'', then Eq. (5) corresponds to a change from the variables x', x'' to new variables $X' = \frac{1}{2}(x' + x'')$ and $X'' = \frac{1}{2}(x' - x'')$. Each matrix element of E_i coincides with one of the matrix elements of F_i; in other words, the matrix E_i is obtained from the matrix F_i by rearranging elements in accordance with the rule (5).

Thus,

$$(X'|E_1|X'') \equiv \left(\frac{\partial}{\partial X'_\mu}\frac{\partial}{\partial X'^\mu} - m_0^2\right)(X'|\bar{A}|X'') = 0, \tag{6}$$

$$(X'|E_2|X'') \equiv (X''_\mu X''^\mu - \lambda_0^2)(X'|\bar{A}|X'') = 0,$$

$$(X'|E_3|X'') \equiv X''_\mu \frac{\partial}{\partial X'_\mu}(X'|\bar{A}|X'') = 0,$$

where the operator $(X'|\bar{A}|X'')$ is defined in accordance with Eq. (5).

It is essential to remark that X', X'', just as x', x'', are completely equivalent eigenvalues of the coordinate operator.

The matrix operators E_i can be represented in the form:

$$E_1 \equiv (K - m_0^2)\bar{A} = 0, \tag{7}$$

$$E_2 \equiv \bar{A}(L - \lambda_0^2) = 0,$$

$$E_3 \equiv M\bar{A}N = 0,$$

where

$$(X'|K|X'') = \frac{\partial}{\partial X'_\mu}\frac{\partial}{\partial X'^\mu}\delta(X' - X''), \tag{8}$$

$$(X'|L|X'') = X'_\mu X'^\mu \delta(X' - X''),$$

$$(X'|M|X'') = \frac{\partial}{\partial X'}\delta(X' - X''),$$

$$(X'|N|X'') = X'\delta(X' - X'').$$

The construction, by means of a canonical transformation, of relations describing a non-localized, non-interacting field from the corresponding relations describing a local field ($\lambda_0 = 0$), is based on the possibility of presenting the system of equations (6) in the form:

$$(K - m_0^2)\bar{A} = (L - \lambda_0^2)\bar{A} = MN\bar{A} = 0,$$

where the operators K, L, M, N commute with one another[10]. However, such a form for the equation system (6) is possible only if X' and X'' are considered to be independent variables and, in accord with this, the field operator is taken as a function $\bar{A} = \bar{A}(X', X'')$ in the space of X' and X''.

The analysis of Yukawa's theory presented in reference 11 is also based, to a significant extent, on a consideration of the field operator $\bar{A}$ as a function $A(X', X'')$ in the space of X' and X''. But such a formulation of the problem differs essentially from the initially proposed idea of regarding the field A as a non-diagonal operator in the space of the coordinate x.

If we regard the operators of the non-localized field as non-diagonal matrices in the coordinate space, $A = (x'|A|x'')$, a different physical interpretation of the quantities X' and X'', which are completely equivalent in the matrix sense, is in our opinion incorrect. This last remark applies in particular to a new, recently proposed[4] variant of the theory, where the operators of the non-localized field in the equations of motion are regarded from two essentially different points of view: first, as matrices in coordinate space, $A = (x'|A|x'')$, where x' and x'' are equivalent sets of eigenvalues of the coordinate operator x; second, as functions $A = A(X', X'')$, where the independent variables X' and X'' have different physical meanings ascribed to them.

It is also very important to remark that in Yukawa's theory[3] the deviations from relativistic invariance are not localized within small space-time regions[12].

---

[12] Y. Ono and M. Sugawara, Progr. Theor. Phys. **6**, 182 (1951)

3. Recently completed experiments on the scattering of π-mesons by protons[13] show that the total cross sections in the energy range studied ($\leq$ 1.45 bev) have two well-defined maxima. One might attempt to explain such an energy dependence of the cross section in terms of the presence of isobaric states (in analogy with the classical Franck-Hertz experiments on scattering of electrons by atoms), or in terms of phenomena analogous to the Ramsauer effect[14].

Both cases require us to take account of the structure of the particles taking part in the reaction. The presence of cut-off form factors in the expressions describing the reaction can lead[8] to a rapid decrease in the magnitude of the cross section with increasing energy of the particles taking part in the reaction. But this is the case only for form factors which decrease rapidly with increasing energy, e.g., for form factors of the type $e^{-\lambda k_0 p}$[♁]. Apparently, to describe the structure of the particles it is necessary to introduce form factors which oscillate for energies $E < E^* \times (\lambda_0)$ and drop rapidly for $E > E^*(\lambda_0)$[♀].

To explain the difference in energy dependence of the cross section for scattering of π^+- and π^--mesons, it may turn out to be necessary to make such additional assumptions.

All of these questions require further study. We should remark that at present the fundamental obstacle to the study of the effect of possible extension of particles is not so much the insufficient amount of experimental data as our inexact knowledge of the limits of applicability of the various methods used in the present theory of fields. In particular, it remains unclarified how the value of a total cross section, in a theory with form-factor, is affected by the inclusion of higher approximations of the perturbation theory.

In addition, so long as the magnitude of the constant λ_0 in such a theory is not understood, one will always be able to choose it to be so small that, within the energy range reached in experiments, the dimenisons of the particle either do not as yet show themselves, or have an insignificant effect***.

In conclusion, it is a pleasant duty to express my thanks to Prof. D. I. Blokhintsev for guidance, valuable advice and interesting discussions, and also to Prof. M. A. Markov for interesting discussions concerning general questions of form-factor theories.

Note added in proof: In a recently published paper [Progr. Theor. Phys. 10, 533 (1953)], Hayashi calls attention to the fact that in a theory with form-function, combinations of the familiar $\theta^{\mp}(x_i - x_j)$ functions which link the vertices in closed parts of the Feynman diagram have no well-defined value [e.g., Eqs. (42) and (47) of Hayashi's paper]. Consequently, the singular functions Δ, $\Delta_{\pm}$ etc., in the expression for the S-matrix cannot be combined into a product of causal Δ^c-functions, which leads to a breakdown of causality in macroscopic ($\gg \lambda$) domains. The relative contribution of causal effects is proportional to a power of λ and goes to zero for $\lambda \to 0$.

Translated by M. Hamermesh
99

[♁] It is interesting to observe that the rapid decrease in cross section with increasing energy does not occur in a theory with non-local interaction, described by a form function $F(x', x'')$; but in such a theory the divergence difficulty is still not eliminated.

[♀] Other interesting possibilities in this respect are the "sign-variable form-factors", i.e., form factors like the cosine factor considered earlier (or sin kx/kx, etc.). However, in this case the expressions for the interaction energy become non-Hermitian.

[13] R. L. Cool, L. Madansky and O. Piccioni, Bull. Am. Phys. Soc. 28, No. 6, 14 (1953)

[14] N. Mott and H. Massey, *Theory of Atomic Collisions*, 2nd Ed., Oxford, 1949, chapt. X

*** The arbitrariness which exists at present in the choice of type of form factor and in the magnitude of the constant λ_0 is one of the basic defects of the theory of non-localized fields and non-localized interaction.

SOVIET PHYSICS JETP VOLUME 1, NUMBER 3 NOVEMBER, 1955

Determination of the Transverse Relaxation Time of Nuclear Magnetic Moments

S. D. GVOZDOVER, N. M. POMERANTSOV AND A. P. POLIAKOVA
Moscow State University

(Submitted to JETP editor May 8, 1954)
J. Exper. Theoret. Phys. USSR 28, 584-588 (1955)

We propose a new method of determining the transverse relaxation time from the shape of the magnetic resonance signals from atomic nuclei. In applying this method we can simultaneously measure the inhomogeneity of the magnetic field over the volume of the sample. The experiments indicated the usefulness of this method and agreed with the results of other authors, which were obtained by other methods.

1 THE shapes of the nuclear magnetic resonance signals depend to a high degree on the relaxation times T_1 and T_2, which are called, respectively, longitudinal and transverse[1]. Furthermore, the shape of the signals depends on the amplitude of the radio frequency magnetic field, and also on the amplitude and frequency of modulation of the longitudinal magnetic field[1-3]. (These latter parameters are at the disposal of the experimenter.)

In the present work, in order to determine the relaxation time T_2, we used the signals generated by a self-excited oscillating system. A description of the use of this apparatus is given in reference 4. It is shown there that when the resonance condition $\omega = |\gamma| H_0$ is realized, where ω is the angular frequency of the radio frequency field, H_0 is the longitudinal component of the vector magnetic field intensity and γ is the gyromagnetic ratio, the amplitude of the oscillation is modulated by the signal

$$v(t) = -\int_{-\infty}^{t} e^{(\xi-t)/T_2} \cos[f(t) - f(\xi)]\, d\xi, \quad (1)$$

and the frequency is modulated by the signal

$$u(t) = \int_{-\infty}^{t} e^{(\xi-t)/T_2} \sin[f(t) - f(\xi)]\, d\xi. \quad (2)$$

In these formulas, T_2 is the relaxation time, $f(t) - f(\xi)$ is a function having the form

$$f(t) - f(\xi) = \int_{\xi}^{t} [|\gamma| H_z - \omega]\, d\eta,$$

H_z is the longitudinal component of the magnetic field.

The amplitude of self-excited oscillations was maintained at a low level. The signals had the form of a damped oscillating function (Fig. 1).

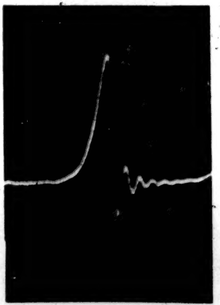

FIG. 1. Oscillogram of the signal $v(t)$ obtained from protons in 0.7 cm^3 of a one molar solution of CuSO$_4$.

2. The method of measuring the relaxation time, used in our work, is based on the fact that the ratio Z of the amplitudes $v(t)$ of the first and second extreme signals depends on T_2. The functions obtained determined the form of the signal, and one can derive the relation

$$T_2 = T_2(Z), \quad (3)$$

as that which determines T_2.

The form of the signal is also influenced by the inhomogeneity of the fixed magnetic field. In the presence of inhomogeneities, the shape of the signal $v(t)$ is of the form[5]

---

[1] S. D. Gvozdover and A. A. Magazanik, J. Exper. Theoret. Phys. USSR 20, 705 (1950)

[2] S. D. Gvozdover and N. M. Pomerantsov, Vestn. MGU 6, 85 (1953)

[3] S. D. Gvozdover and N. M. Pomerantsov, Vestn. MGU 9, 79 (1953)

[4] N. M. Pomerantsov, Vestn. MGU 2, 47 (1955)

$$v^*(t) = \int_{-\infty}^{\infty} v(\Delta H, t) f(\Delta H)\, d(\Delta H), \tag{4}$$

where ΔH is the deviation of the magnetic field intensity from resonance at a given point of the sample; $f(\Delta H)$ is the distribution function of the inhomogeneities of the field, satisfying the normalization condition

$$\int_{-\infty}^{\infty} f(\Delta H)\, d(\Delta H) = 1. \tag{5}$$

Various distribution functions were applied to the calculation; these are but idealizations of the actual distribution function of the inhomogeneities of the field. The most convenient one for calculations is the Lorentz form of the distribution function

$$f(\Delta H) = \frac{1}{\pi} \frac{\Delta H^*}{(\Delta H^*)^2 + (\Delta H)^2}, \tag{6}$$

where ΔH^* is the mean value of the inhomgeneity. The effect of the inhomogeneous field with the above-mentioned distribution function is a decrease in the relaxation time T_2 as is shown in reference 5.

For the majority of liquids at room temperature we have the equality[5,6]

$$T_1 = T_2. \tag{7}$$

Hence the relaxation time T_2 is found experimentally by the presence of inhomogeneities in the fixed magnetic field, and in this case can be written in the form[5]

$$\frac{1}{T_2} = \frac{1}{T_1} + |\gamma| \Delta H^*. \tag{8}$$

3. The construction of the functional relation (3) for experimentally determining T_2 from the ratio Z of the amplitudes $v(t)$ of the first and second extreme signals is carried out in the following manner. We use the function derived in reference 1 [Formulas (33), (33a)],

$$Z = \frac{v(t_1)}{v(t_2)} = \int_{-\infty}^{r_1} e^{\alpha(\xi - r_1)} \times \cos(r_1^2 - \xi^2)\, d\xi \Big/ \int_{-\infty}^{r_2} e^{\alpha(\xi - r_2)} \cos(r_2^2 - \xi^2)\, d\xi, \tag{9}$$

where

$$r = \sqrt{\frac{a}{2}}\, t, \quad \alpha = \frac{1}{T_2}\sqrt{\frac{2}{a}}, \quad a = |\gamma| \frac{dH_z}{di}, \tag{10}$$

t_1 and t_2, and correspondingly, r_1 and r_2 are the moments of time at which the function $v(t)$ is an extremum.

The integral in Eq. (9) can be reduced to tabulated functions in the following manner. We combine Eqs. (1) and (2) and obtain, with the substitution of Eq. (10),

$$w(r) = -v + iu = \sqrt{\frac{2}{a}}\, e^{-\alpha r + i r^2} \int_{-\infty}^{r} e^{\alpha\xi - i\xi^2}\, d\xi. \tag{11}$$

After substituting

$$\xi = -i\left(\frac{\alpha}{2} - \eta\right) \tag{12}$$

the expression for $w(r)$ takes the form

$$w(r) = i\sqrt{\frac{2}{a}} \exp\left\{-\alpha r + i \times \left(r^2 - \frac{\alpha^2}{4}\right)\right\} \int_{(\alpha/2) + i\infty}^{(\alpha/2) - ir} e^{i\eta^2}\, d\eta. \tag{13}$$

We use the residue theorem and carry out the shift in the path of integration (Fig. 2), so that

$$\lim_{R \to \infty} \int_{(\alpha/2) + iR}^{(\alpha/2) - ir} e^{i\eta^2}\, d\eta = \int_{0}^{(\alpha/2) - ir} e^{i\eta^2}\, d\eta - \int_{0}^{\infty} e^{i\eta^2}\, d\eta. \tag{14}$$

In the latter integral the right hand side of Eq. (14) is equal to $\sqrt{\pi/2}\,(1+i)/2$.

We change the variable

$$\eta = (i-1)\, t / \sqrt{2} \tag{15}$$

and assume

---

[5] B. A. Jacobson and R. K. Wangsness, Phys. Rev. **73**, 942 (1948)

[6] V. N. Faddeeva and N. M. Terente'v, *Tables of Values of the Probability Integral for Complex Argument*, GITTL, 1954

$$z' = \frac{1}{\sqrt{2}}\left(\frac{\alpha}{2} + r\right) \tag{16}$$

$$+ i\frac{1}{\sqrt{2}}\left(\frac{\alpha}{2} - r\right) = x + iy,$$

and reduce the expression for $w(r)$ to the form

$$w(r) = i\sqrt{\frac{2}{a}}\exp\left\{-\alpha r + i\left(r^2 - \frac{\alpha^2}{4}\right)\right\} \tag{17}$$

$$\times \left\{\frac{i-1}{\sqrt{2}}\int_0^{z'} e^{t^2}\,dt - \frac{\sqrt{\pi}}{2}\frac{1+i}{\sqrt{2}}\right\}.$$

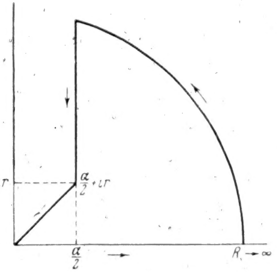

FIG. 2. Shift of path of integration for the integral of Eq. (13).

The integral in Eq. (17) can be expressed by means of the tabulated functions of a complex variable[6]:

$$W(z') = U(x, y) + iV(x, y) \tag{18}$$

$$= e^{-z'^2}\left(1 + \frac{2i}{\sqrt{\pi}}\int_0^{z'} e^{t^2}\,dt\right).$$

We finally have

$$w(r) = -v + iu = \sqrt{\frac{\pi}{a}}\left\{-\frac{1}{2}(V + U)\right. \tag{19}$$

$$+ e^{-\alpha r}\left[\cos\left(r^2 - \frac{\alpha^2}{4}\right) + \sin\left(r^2 - \frac{\alpha^2}{4}\right)\right]$$

$$+ i\left[\frac{1}{2}(U - V) + e^{-\alpha r}\sin\left(r^2 - \frac{\alpha^2}{4}\right)\right.$$

$$\left.\left. - e^{-\alpha r}\cos\left(r^2 - \frac{\alpha^2}{4}\right)\right]\right\}.$$

4. The formula given above permits calculation of Eq. (9), but for this it is necessary to know the moments of time t_1 and t_2 at which the function $v(t)$ takes on its extreme values. The values of t_1 and t_2 are found as solutions of the transcendental equation for the extremes of the function $v(r)$

$$r = \frac{\sqrt{\frac{2}{\pi}} - \frac{\alpha}{2}\left\{U + V - 2e^{-\alpha r}\left[\sin\left(r^2 - \frac{\alpha^2}{4}\right) + \cos\left(r^2 - \frac{\alpha^2}{4}\right)\right]\right\}}{U - V + 2e^{-\alpha r}\left[\sin\left(r^2 - \frac{\alpha^2}{4}\right) - \cos\left(r^2 - \frac{\alpha^2}{4}\right)\right]}, \tag{20}$$

which can be derived by differentiating Eq. (1). The solution of this equation is obtained by the method of successive approximation. The values of t_1 and t_2 (obtained approximately) are made more precise by substituting these values into Eq. (20)

The functional dependence of

$$\alpha = \sqrt{\frac{2}{a}}\frac{1}{T_2}$$

on Z obtained by the method described above is presented in Table I and is shown graphically in Fig. 3.

5. This method was used in some experiments. According to existing theory[7], for the presence in solution of paramagnetic ions, the relaxation time is inversely proportional to the concentration of the latter

$$1/T_1 = CN, \tag{21}$$

where N is the number of ions per unit volume, and C is the proportionality coefficient. From Eqs. (8) and (21) we deduce

---

[7] N. Bloembergen, *Nuclear Magnetic Relaxation*, Leiden, 1948

TABLE I. Dependence of the parameter $\alpha = \frac{1}{T_2}\left(\frac{1}{2}\left|\gamma\right|\frac{dH_z}{dt}\right)^{-1/2}$ on the ratio Z of the first and second extrema of the absorption signal.

α	0.000	0.283	0.707	0.990	1.412
Z	0.907	1.280	2.227	3.712	15.300

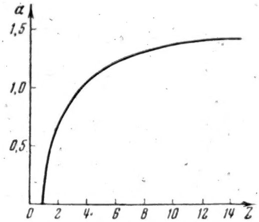

FIG. 3. Functional relation of the parameter $\alpha = \frac{1}{T_2}\left(\frac{1}{2}\left|\gamma\right|\frac{dH_z}{dt}\right)^{-1/2}$ to the ratio Z of the amplitudes of the first and second extreme signals.

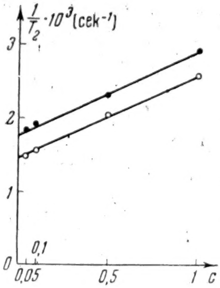

FIG. 4. Dependence of the measured experimental relaxation time T_2 on the concentration c of paramagnetic ions in a solution of $CuSO_4$ [see Eq. (22)] for two values of the inhomogeneous magnetic field; c is measured in moles.

$$1/T_2 = CN + |\gamma|\Delta H^*, \tag{22}$$

i.e., a linear equation.

In Fig. 4 is presented the experimentally determined dependence of $1/T_2$ on the concentration of ions in a solution of $CuSo_4$ for different values of the inhomogeneous magnetic field. The graph confirms the relation (21) and enables one to determine the average inhomogeneity of the magnetic field over the volume of the specimen (from the value of the intercept with the axis of ordinates). We find good agreement with the experiments of other authors[7].

Furthermore, with the method described above, we measured the relaxation time of the nucleus F^{19} in the compound $BF_3 \cdot 2H_2O$. We obtained the value $T_2 = 0.9 \times 10^{-3}$ sec.

Translated by B. Hamermesh
100

SOVIET PHYSICS JETP VOLUME 1, NUMBER 3 NOVEMBER, 1955

The Conditions for Self-Excitation of a Singing Flame

IU. I. NEIMARK AND G. V. ARONOVICH
Gorki State University

(Submitted to JETP editor May 10, 1954)
J. Exper. Theoret. Phys. 28, 567-578 (May, 1955)

The problem of the stability of a singing flame is considered, beginning with the considerations of Rayleigh, and taking into account the phenomenological delay in burning.

THE phenomenon of the singing flame was observed as early as the second half of the eighteenth century and since that time it has frequently served as the subject of an effective lecture demonstration. If a gas burner is placed inside a tube, as is shown in Fig. 1, then, under a number of conditions, intense vibrations of the flame and of the surrounding air are set up, and the tube begins to resound, or, as is said, the flame begins to sing.

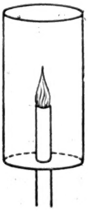

FIG. 1

This phenomenon has been observed by a number of authors [1]. Different simple hypotheses as to the reasons for the onset of vibrations have been given. The first correct, qualitative explanation of the mechanism for maintaining the vibrations was given by Rayleigh[2], who showed how the vibrating flame could maintain sound vibrations in the tube. The flame maintains the vibrations of the air column if it is located near an anti-node of pressure and vibrates so that, at the moment of compression, a larger amount of heat is evolved than at the moment of rarefaction. In subsequent researches, this qualitative picture has not been changed in any essential way, in spite of the large amount of research on the problem*.

In the present work, which is based on the considerations of Rayleigh[2], and which takes into account the phenomenological delay in burning, a detailed study is carried out on the conditions for the self-excitation of the singing flame. The results which are obtained are in excellent qualitative agreement with the known experimental facts, but they do not provide a quantitative check.

1. DISCRETE MODEL OF A SINGING FLAME (MODEL No. 1)

A study of the conditions for self-excitation of a singing flame requires the consideration of small vibrations which are superimposed on the established gas flow in the system. In the discrete model, if we idealize the sounding (air) and supplying (gas) tubes in the form of resonators, we obtain the arrangement shown in Fig. 2. Each of these resonators, for vibration frequencies $\omega < a/l$, where l is a linear dimension of the resonator, a the sound velocity, is itself an oscillator, the mass in which is the mass of the air vibrating in the neck of the resonator, and the elasticity is that of the air trapped within the resonator and compressed by the air, vibrating like a piston in the neck.

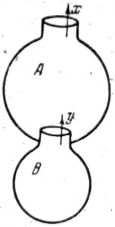

FIG. 2

Let x be a small displacement of the air in the neck of the resonator A (for graphic purposes, this displacement can be represented as a change in position of a piston in the neck of the resonator), and let y be the displacement of the gas in the neck of resonator B. Also, let m_1 and m_2 be the "masses" of vibrating gas in the necks of resonators A and B, and p, p_1 and p_2 be the external pressure, and the pressures in resonators A and B, respectively. Then the equation of motion of the masses of air in the necks can be written, for small vibrations (for those characteristic frequencies which satisfy the boundary conditions given above), as

---

* This work was complete in 1952 (see the report of GIFTI for 1952). In 1953 B. V. Raushenbakh[3] considered the problem of the excitation of vibrations in the case of slow propagation down the tube.

[1] A. T. Jones, J. Acoust. Soc. Am. 16, 254 (1945)

[2] Rayleigh, *Theory of Sound*, v. II, pp 222-228

[3] B. V. Raushenbakh, Zh. Tekhn. Fiz. 23, 358 (1953)

$$m_1\ddot{x} + \delta_1\dot{x} = S_1\Delta p_1; \qquad (1.1)$$
$$m_1\ddot{y} + \delta_2\dot{y} = S_2(\Delta p_2 - \Delta p_1),$$

where S_1 and S_2 are the cross sectional areas of the resonator necks. In the absence of flame, a mutual elastic coupling takes place between the two oscillators x and y. Actually, a change in x produces a change in p_1 proportional to S_1x, and a change in y produces changes in p_1 and p_2 proportional to S_2y, i.e.,

$$\Delta p_1 = -k_1S_1x + k_1S_2y, \quad \Delta p_2 = -k_2S_2y,$$

which, upon substitution into Eq. (1.1), yields

$$m_1\ddot{x} + \delta_1\dot{x} = -k_1S_1^2x + k_1S_1S_2y; \qquad (1.2)$$
$$m_2\ddot{y} + \delta_2\dot{y} = -(k_1 + k_2)S_2^2y + k_1S_1S_2x.$$

The second terms in the right hand sides of Eqs. (1.2) indicate the elastic coupling between the oscillators x and y. It is easy to prove that small vibrations, described by the differential equations of Eq. (1.2), die out with the passage of time, i.e., the initial system is stable.

With the appearance of the flame, the character of the coupling between the oscillators is considerably changed, and in this change lies the reason for the possible self-excitation of vibrations. Jumping ahead somewhat, we can say that the system under study consists of two dissipative parts— the sounding tube and the tube supplying the gas — between which there exists nonconservative coupling which transfers its energy into the singing flame. The problem of the investigation of the excitation condition of the singing flame is primarily the problem of the investigation of this coupling.

We assume that the rate of heat production of the flame (i.e., the rate of the chemical reaction of combustion) is proportional to the rate of flow of the gas, and takes place with a certain phenomenological delay of burning, τ (if a liquid fuel had been used, then τ would have been a quantity of the order of the time during which burning of the droplet takes place after its emission from the jet). We shall also assume that the heat loss in the burning, due to conduction and convection to the outside, remains constant. Then, in the presence of the flame, just as earlier, a change in y produces a large change in the pressure p_1, since the gas emerging from the tube, in burning, produces a positive pressure amplification.

In accordance with our assumptions, we now have

$$\Delta p_1 = -k_1S_1x + k_1S_2y + \alpha k_1S_2y_\tau$$

(α is a constant of proportionality, y_τ is the value of y at the time $t - \tau$), which, after substitution in Eq. (1.1), yields

$$m_1\ddot{x} + \delta_1\dot{x} = -k_1S_1^2x + k_1S_1S_2y + \alpha k_1S_1S_2y_\tau; \qquad (1.3)$$
$$m_2\ddot{y} + \delta_2\dot{y} = -(k_1 + k_2)S_2^2y + k_1S_1S_2x.$$

If we denote the characteristic frequencies of the resonators A and B by ω_1 and ω_2, and neglect the term $k_1S_1S_2y$ in comparison with $\alpha k_1S_1S_2y_\tau$, then we get the following linearized equations for small vibrations:

$$\ddot{x} + h_1\dot{x} + \omega_1^2x = \mu y_\tau; \qquad (1.4)$$
$$\ddot{y} + h_2\dot{y} + \omega_2^2y = \nu x.$$

Here

$$h_1 \equiv \frac{\delta_1}{m_1}, \quad \omega_1^2 \equiv \frac{k_1S_1^2}{m_1}, \quad \mu \equiv \frac{\alpha k_1S_1S_2}{m_1},$$

$$h_2 \equiv \frac{\delta_2}{m_2}, \quad \omega_2^2 \equiv \frac{(k_1 + k_2)S_2^2}{m_2}, \quad \nu = \frac{k_1S_1S_2}{m_2}.$$

The characteristic equation of this system, obtained by the usual methods, is

$$(z^2 + h_1z + \omega_1^2)(z^2 + h_2z + \omega_2^2) - \nu\mu e^{-\tau z} = 0. \qquad (1.5)$$

Solution for the parameter $\mu\nu$ is easily accomplished. Setting $z = i\omega$ in Eq. (1.5), we get

$$\nu\mu = (\omega_1^2 - \omega^2 + ih_1\omega)(\omega_2^2 - \omega^2 + ih_2\omega)e^{i\tau\omega}. \qquad (1.6)$$

For $\tau = 0$

$$(\nu\mu)_0 = (\omega_1^2 - \omega^2 + ih_1\omega)(\omega_2^2 - \omega^2 + ih_2\omega).$$

The curve $(\nu\mu)_0$ is plotted in Fig. 3a. The abscissa of point b, the intersection of the curve with the real axis, is given by

$$-\frac{h_1h_2}{h_1 + h_2}\left[(\omega_1^2 - \omega_2^2) + h_1\omega_2^2 + h_2\omega_1^2\right],$$

and decreases in value as ω_1 approaches ω_2.

With a delay τ, the curve of Fig. 3a becomes "twisted" and takes on the form shown in Fig. 3b. The region of stability is denoted by the thick line. The system will be stable for an arbitrary delay if $|\nu\mu| < r_{\min}$, where $r_{\min}$ is the minimum distance from the points of the curve of Fig. 3a to the

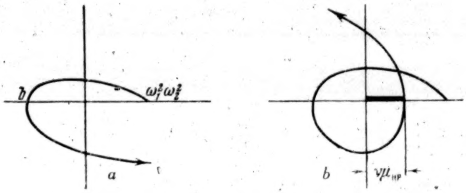

FIG. 3. $a - (\nu\mu)_0$, $b - (\nu\mu)$

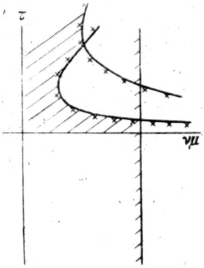

FIG. 4

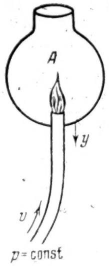

FIG. 5

origin. The plot in the plane of the parameters $\nu\mu$ and τ is represented in Fig. 4, where the region of stability is indicated by shading[4].

It follows from Figs. 3*a*, 3*b* and 4 that (a) there is no instability for small values of $\nu\mu$ without delay τ; (b) excitation of the vibrations is due to increase in $\nu\mu$, to the closeness of the frequencies ω_1 and ω_2, and also to a decrease in the damping coefficients h_1 and h_2.

2. SEMIDISTRIBUTED MODEL OF THE PHENOMENON (MODEL No. 2)

Gas is fed into the resonator A by a long narrow tube B (with cross sectional area σ) from the resonator C (Fig. 5). It is required to find the conditions for self-excitation of vibrations of the flame, assuming that, just as before, the resonator A is a discrete section, but account is now taken of wave phenomena in the delivery tube B.

The equations for small vibrations of the gas in the neck of the resonator have the form

$$m\ddot{x} + \delta\dot{x} = S\Delta p, \qquad (2.1)$$

and the equations for small vibrations of the gas which are superimposed on the flow existing in the supply tube are now described by equations with partial derivatives:

$$\frac{\partial v}{\partial t} = -\frac{1}{\rho}\frac{\partial p}{\partial y}, \quad \frac{\partial v}{\partial y} = -\frac{1}{\rho a^2}\frac{\partial p}{\partial t}, \qquad (2.2)$$

where v is the change in the velocity of the gas in the tube, p is the change in pressure, ρ is the gas density, and a is the velocity of sound in the gas.

To Eq. (2.2) we add the following boundary conditions at $y = L$ and $y = 0$: we assume the pressure to be constant in the reservoir C, or

$$p_{y=L} = 0; \qquad (2.2')$$

For $y = 0$, an efflux condition exists which, after linearization, can be put in the form

$$v = \nu(p - \Delta p), \qquad (2.2'')$$

where $\nu = \alpha_1^2 v_0/\rho$ (α_1 = coefficient of delivery, v_0 = velocity of steady gas flow).

As in the previous model,

$$\Delta p = \alpha\int v_\tau dt + \beta\int v dt - \gamma x, \qquad (2.3)$$

where v is the change in the discharge velocity of the gas in the supply tube from its stationary value at the time t, and v_τ is the corresponding value at the time $t - \tau$; α, β and γ are constants, equal, respectively, to

---

[4] Iu. I. Neimark, *Stability of Linear Systems*, Moscow, (1949)

$$\alpha = \frac{\rho\sigma nRq}{c_v M_1 V}, \quad \beta = \frac{\sigma p_0}{V}, \quad \gamma = \frac{Sp_0}{V}.$$

Here M_1 is the mass of the mixture of gaseous combustion products and air in the resonator, q the heat capacity of the gas, n the number of gram molecules, R the gas constant, ρ the density of the gas, p_0 the stationary pressure in the resonator, and V the volume of the resonator. Actually, by virtue of the linearization, the overall change in pressure Δp in the resonator is composed of changes produced by

a) the influx of gas through the tube B, equal to $\frac{\sigma p_0}{V}\int v dt$;

b) the discharge through the neck of the resonator A, equal to

$$\frac{Sp_0}{V}\int \dot{x} dt = \frac{Sp_0}{V} x;$$

c) the generation of excess heat from the burning gas, equal to**

$$\frac{\sigma\rho nRq}{c_v M_1 V}\int v_\tau dt;$$

d) a change Δp_{chem} as a result of the chemical reaction. We can neglect this latter term since, for hydrogen,

$$\left|\frac{\Delta p_{\text{chem}}}{\Delta p_T}\right| \approx \frac{1}{80}.$$

Therefore the complete system of linearized equations for the semidistributed model will be

$$m\ddot{x} + \delta\dot{x} = S\Delta p_{y=0} \tag{2.4}$$

$$= S\left[\alpha\int v_\tau dt + \beta\int v dt - \gamma x\right]_{y=0};$$

$$\frac{\partial v}{\partial t} = -\frac{1}{\rho}\frac{\partial p}{\partial y}, \quad \frac{\partial v}{\partial y} = \frac{1}{\rho a^2}\frac{\partial p}{\partial t};$$

$$p_{y=L} = 0, \ v_{y=0} = \nu(p - \Delta p).$$

In order to find the characteristic equation of the system of equations (2.4), we follow reference 5 and write

$$p(y, t) = (Ae^{-zy/a} + Be^{zy/a})e^{zt},$$

$$v(y, t) = \frac{1}{a\rho}[-Ae^{-zy/a} + Be^{zy/a}]e^{zt},$$

$$x = Ce^{zt},$$

which, after substitution into the first, third and fourth members of Eq. (2.4) reduces to the system of equations

$$C(mz^2 + \delta z) = S\left\{[\alpha(-A + B)e^{-z\tau}\right.$$

$$\left. + \beta(-A + B)]\frac{1}{a\rho z} - \gamma C\right\},$$

$$Ae^{-zL/a} + Be^{zL/a} = 0,$$

$$\frac{1}{a\rho}(-A + B) = \nu\left\{A + B\right.$$

$$\left. - \left[\frac{\alpha}{a\rho z}e^{-z\tau}(-A + B) + \frac{\beta}{a\rho z}(-A + B) - \gamma C\right]\right\}.$$

We eliminate the constants A, B and C from this system, and obtain the characteristic equation

$$(z^2 + hz + k^2)\left(1 + D\,\text{th}\frac{z\tau_1}{2}\right) \tag{2.5}$$

$$+ (z + h)E(1 + \mu e^{-\tau z}) = 0.$$

Here

$$h = \frac{\delta}{m}; \quad k^2 = \frac{\gamma S}{m}; \quad D = \nu a\rho;$$

$$E = \nu\beta; \quad \mu = \frac{\alpha}{\beta}; \quad \tau_1 = \frac{2L}{a}.$$

The system under consideration will be stable if all the roots of the characteristic equation (2.5) lie to the left of the imaginary axis. On the plane of the parameters D and τ, we find regions where this condition is satisfied, and regions where it is not. From Eq. (2.5) it follows that

$$D = -\left[\frac{P_1}{P_2}(1 + \mu e^{-\tau z}) + 1\right]\text{cth}\frac{z\tau_1}{2}, \tag{2.6}$$

$$P_1 \equiv E(z + h), \ P_2 \equiv z^2 + hz + k^2.$$

In Eq. (2.6) we set $z = i\omega$. Then (2.7)

$$D = i\left[\frac{P_1(i\omega)}{P_2(i\omega)}(1 + \mu e^{-i\tau\omega}) + 1\right]\text{ctg}\frac{\omega\tau_1}{2} \equiv Q\,\text{ctg}\frac{\omega\tau_1}{2}.$$

The boundary of the region of instability consists of points which satisfy Eq. (2.7), at least for one

---

** In burning for a time t, the mass $M = \sigma\rho\int v_\tau dt$ of combustible gas which reacts with the mass ϵM of air (ϵ is a coefficient defined by the chemical equation of the combustion process). As a result of the burning, we obtain $(1 + \epsilon)M$ products of combustion plus the heat qM. Because of the rise in temperature, the pressure in the resonator will be increased by an amount given by:

$$\Delta p_T = \frac{nR}{V}\Delta T = \frac{nR}{V}\frac{qM}{c_v M_1} = \frac{\sigma\rho nRq\int v_\tau dt}{Vc_v M_1}$$

[5] Iu. I. Neimark, Uch. Zap. Gorki State Univ. 14, 191 (1950)

real ω. Such ω must either be a root of the equation

$$\operatorname{ctg}(\omega\tau_1/2) = 0,$$

or a value which converts the expression

$$Q \equiv i\left[\frac{P_1(i\omega)}{P_2(i\omega)}(1 + \mu e^{-i\tau\omega}) + 1\right] \tag{2.8}$$

into a purely real number (because D is real). For each of the roots of the equation, cotan $(\omega\tau_1/2) = 0$, i.e.,

$$\omega = (2n+1)\pi/\tau_1 \tag{2.9}$$

so that $D = 0$.

We construct the curve $Q(i\omega)$ to find the value of ω for which Q is a real number. For $\tau = 0$, the shape of this curve is shown in Fig. 6*a* (only the part of this curve corresponding to $\omega > 0$ is shown; the second half of the curve, for $\omega < 0$, is located symmetrically with respect to the imaginary axis). Its projection, which increases with increase in the damping h, corresponds approximately to the characteristic frequency of the resonator for small h. The projection also increases for an increase in μ, since $\mu \gg 1$, with the center of symmetry at the point $(0, i)$. The presence of τ produces a rotation of the points of this curve through an angle $-\omega\tau$ about the point $(0, i)$. As a result, the points on it can intersect with the real axis (Fig. 6*b*).

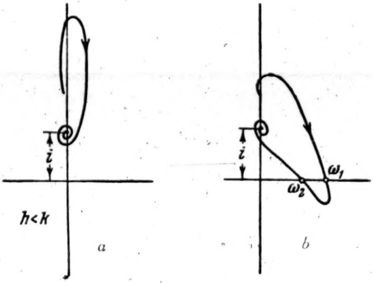

FIG. 6. $a - (Q)_0$, $b - (Q)$

The equation for the determination of the corresponding points of intersection $\omega = \omega_j$ is obtained by setting the imaginary part of $Q(i\omega)$ equal to zero. The condition $\operatorname{Im}Q(i\omega) = 0$ gives

$$(k^2 - \omega^2)^2 + h^2\omega^2 + E\,[(1 + \mu\cos\omega\tau)\,hk^2 + \mu\,\omega\sin\omega\tau\,(k^2 - \omega^2 - h^2)] = 0. \tag{2.10}$$

After the ω_j are established, the equation of the boundary of the stable region in the plane of D, τ_1 is written in the form

$$D = Q(\omega_j)\operatorname{ctg}(\omega_j\tau_1/2).$$

After drawing in the shaded lines, in accordance with the rules set forth in reference 4, we obtain the plot shown in Fig. 7. The region of stability is shaded on them. The form of the auxiliary curve is obtained from these drawings:

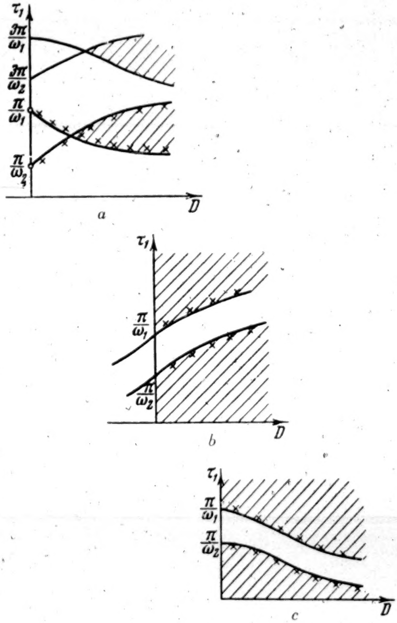

FIG. 7.

a) self-excitation is not possible without delay in burning;

b) an alternation of stability and instability takes place initially upon an increase in the length of the supply tube, but for a sufficiently long tube, instability is approached (we note that instability is possible even in the absence of the supply tube, i.e., for $\tau_1 = 0$);

c) for small damping and not very large μ, the frequency of the vibration that is excited is close to the resonant frequency of vibration of the resonator;

d) a decrease in h and an increase in E or μ favor the establishment of instability.

3. DISTRIBUTED MODEL OF THE SINGING FLAME WITHOUT CONSIDERATION OF CONVECTION (MODEL No. 3)*

We shall now consider the supply tube and the sounding tube as one-dimensional distributed links, and the flame as a distributed, linear heat source. We break up the system under consideration into four parts: the burning zone 2, the zones 1 and 3, in which we neglect the changes in temperature brought about by the vibrations of the flame, and the supply tube 4 (Fig. 8).

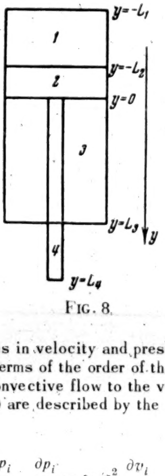

FIG. 8.

The changes in velocity and pressure in regions 1,3 and 4 (if terms of the order of the ratio of the velocity of convective flow to the velocity of sound are neglected) are described by the linearized equations

$$\frac{\partial v_i}{\partial t} = \frac{1}{\rho_{i0}}\frac{\partial p_i}{\partial y}, \quad \frac{\partial p_i}{\partial t} = \rho_{i0}a_{i0}^2\frac{\partial v_i}{\partial y} \quad (i = 1,\ 3,\ 4). \tag{3.1}$$

In the burning zone, we have the linearized Euler equation

$$\frac{\partial v_2}{\partial t} = \frac{1}{\rho_{20}}\frac{\partial p_2}{\partial y} \tag{3.2}$$

and the equation of continuity in the form

$$\frac{\partial \rho_2}{\partial t} = \rho_{20}\frac{\partial v_2}{\partial y}, \tag{3.3}$$

to which we must also add a relation between the changes in pressure and density, taken from the equation of state of the medium and the first law of thermodynamics:

$$dp_2 = \frac{p_{20}}{Ic_vT_0}\,dQ + a_{20}^2 d\rho_2 \tag{3.4}$$

where c_v is the heat capacity at constant volume.

Neglecting terms in dQ which are connected with the heat exchange between different layers of the gas, we assume that

$$dQ = bv_4(t-\tau)_{y=0}\,dt \tag{3.5}$$

(τ is the phenomenological delay in burning).

Replacing the material derivatives in Eq. (3.4) by

$$\left(\frac{\partial p_2}{\partial t} - v_{20}\frac{\partial p_2}{\partial y}\right)dt \text{ and } \left(\frac{\partial \rho_2}{\partial t} - v_{20}\frac{\partial \rho_2}{\partial y}\right)dt,$$

respectively, and neglecting the convection terms, we obtain

$$\frac{\partial p_2}{\partial t} = \frac{p_{20}}{Ic_vT_0}\,bv_4(t-\tau)_{y=0} + a_{20}^2\frac{\partial \rho_2}{\partial t}. \tag{3.6}$$

Eliminating the density ρ_2 from Eqs. (3.3) and (3.6), we finally obtain

$$\frac{\partial p_2}{\partial t} - a_{20}^2\rho_{20}\frac{\partial v_2}{\partial y} = Nv_4(t-\tau)_{y=0}, \tag{3.7}$$
$$N \equiv (p_{20}/Ic_vT_0)\,b.$$

We now write the boundary conditions for Eqs. (3.1), (3.2) and (3.7), and the conditions for connecting the solutions in regions 1,2 and 3:

$$\begin{aligned}
&\text{for}\quad y=-L_1:\ v_1=\nu_1 p_1;\\
&\text{for}\quad y=0:\ v_4=\nu_4(p_4-p_2);\\
&\text{for}\quad y=-L_2:\ v_1=v_2;\\
&\text{for}\quad y=0:\ v_2=v_3;\\
&\text{for}\quad y=L_3:\ v_3=-\nu_3 p_3;\\
&\text{for}\quad y=L_4:\ p_4=0;\\
&\text{for}\quad y=-L_2:\ p_1=p_2;\\
&\text{for}\quad y=0:\ p_2=p_3;
\end{aligned} \tag{3.8}$$

$$\nu_1 = \frac{\alpha_1^2}{v_{10}\rho_{10}},\quad \nu_3 = \frac{\alpha_3^2}{v_{30}\rho_{30}},\quad \nu_4 = \frac{\alpha_4^2}{v_{40}\rho_{40}}.$$

We can now go on to the basic problem of the investigation of the conditions for self-excitation of the vibration. Following reference 5, we must first of all establish the characteristic quasi-polynomial of of the system of equations (3.1), (3.2), (3.7) with the boundary conditions (3.8). That is, we seek solutions of Eqs. (3.1), (3.2), and (3.7) in the form

---

* The singing flame has also been observed experimentally in a horizontal pipe without a convective air flow[6]

[6] Z. Carrière, Revue d'Acoustique 4, 149 (1953)

$$p_i(y,t)=P_i(y)e^{zt}, \tag{3.9}$$

$$v_i(y,t)=V_i(y)e^{zt} \quad (i=1,2,3,4).$$

After substitution in the corresponding equation for $i = 1$, 3 and 4, we find that

$$P_i(y)=A_ie^{-zy/a_i}+B_ie^{zy/a_i}; \tag{3.10}$$

$$V_i(y)=\frac{1}{a_i\rho_i}\left[-A_ie^{-zy/a_i}+B_ie^{zy/a_i}\right],$$

where A_i and B_i are arbitrary constants.

From Eqs. (3.2) and (3.7), we get, after similar substitutions (employing the expression just now obtained for v_4),

$$zV_2=\frac{1}{\rho_{20}}P_2', \tag{3.11}$$

$$zP_2-a_{20}^2\rho_{20}V_2'=\frac{N}{a_4\rho_4}\left[-A_4+B_4\right]e^{-\tau z},$$

whose general solution is

$$P_2(y)=A_2e^{-zy/a_2}+B_2e^{zy/a_2} \tag{3.12}$$

$$+\frac{N}{a_4\rho_4z}(B_4-A_4)e^{-\tau z},$$

$$V_2(y)=\frac{1}{a_2\rho_2}\{-A_2e^{-zy/a_2}+B_2e^{zy/a_2}\}.$$

Now, substituting these solutions in the boundary conditions (3.8), we get a system of eight equations in the arbitrary constants A_i, B_i, and the frequency z. For the sake of simplicity, we shall consider a_{i0} and ρ_{i0} to be single-valued in zones 1, 2 and 3, equal, respectively, to a and ρ:

$$\begin{aligned}
&-A_1e^{zL_1/a}+B_1e^{-zL_1/a}\\
&\qquad=\nu_1a\rho\,(A_1e^{zL_1/a}+B_1e^{-zL_1/a}),\\
&-A_3e^{-zL_3/a}+B_3e^{zL_3/a}\\
&\qquad=-\nu_3a\rho\,(A_3e^{-zL_3/a}+B_3e^{zL_3/a}),\\
&-A_4+B_4=a_4\rho_4\nu_4(A_4+B_4-A_3-B_3),\\
&\quad A_4e^{-zL_4/a_4}+B_4e^{zL_4/a_4}=0,\\
&-A_1e^{zL_2/a}+B_1e^{-zL_2/a}=-A_2e^{zL_2/a}+B_2e^{-zL_2/a},\\
&\quad A_1e^{zL_2/a}+B_1e^{-zL_2/a}=A_2e^{zL_2/a}\\
&\qquad+B_2e^{-zL_2/a}+\frac{N(B_4-A_4)}{a_4\rho_4z}e^{-\tau z},\\
&-A_2+B_2=-A_3+B_3,\\
&\quad A_2+B_2+\frac{N(B_4-A_4)}{a_4\rho_4z}e^{-\tau z}=A_3+B_3.
\end{aligned} \tag{3.13}$$

We introduce the notation

$$2\frac{L_1-L_2}{a}=\tau_1,\ 2\frac{L_2}{a}=\tau_2,\ 2\frac{L_3}{a}=\tau_3,\ 2\frac{L_4}{a}=\tau_4,$$

$$N\nu_4=2\mu,\ \nu_1a\rho=\mu_1,\ \nu_3a\rho=\mu_2,\ \nu_4a_4\rho_4=\mu_3.$$

Then the characteristic equation of the problem, obtained from Eq. (3.13) by elimination of the constants A_i, B_i, can be expressed in the following form:

$$\mu_3\,\mathrm{th}\frac{z\tau_4}{2}=1 \tag{3.14}$$

$$-\frac{\mu}{z}e^{-\tau z}\frac{(1+D_2e^{z\tau_3})(1+D_1e^{z(\tau_1+{}^1\!/_2\tau_2)})(e^{z\tau_2/2}-1)}{1-D_1D_2e^{z(\tau_1+\tau_2+\tau_3)}}.$$

Here

$$D_1=(1+\mu_1)/(1-\mu_1),\ D_2=(1+\mu_2)/(1-\mu_2).$$

We consider a D-partition in the parameters μ_3 and τ_4. The boundary of the octant $\mu_3>0$, $\tau_4>0$ for these parameters consists of the series of curves

$$\mu_3=-iF(i\omega_j)\,\mathrm{ctg}\,(\omega_j\tau_4/2),$$

where ω_j are the roots of the equation $\mathrm{Re}F(i\omega_j)=0$ and $F(z)$ denotes the right hand side of Eq. (3.14). To find the roots of this equation,

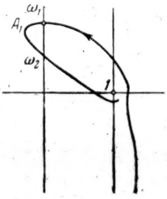

FIG. 9: (F)

we construct the auxiliary curve $F(i\omega)$. Its approximate form is shown in Fig. 9. The projections A_1, A_2,... correspond to values of ω for which the value

$$1-D_1D_2\exp\{i\omega(\tau_1+\tau_2+\tau_3)\}$$

is close to zero, which takes place (approximately) for frequencies close to the eigenfrequencies of the resonator. The magnitudes of these projections decreases in general, because of the presence of z in the denominator of $F(z)$. Furthermore, some of these can decrease or even disappear:

a) if $1+D_2e^{z\tau_3}\approx 0$, i.e., if the top of the tube which supplies the gas lies at a pressure node;

b) if $1 + D_1 \exp\{z[\tau_1 + (\tau_2/2)]\} \approx 0$, i.e., if the center of the burning zone is at a pressure node;

c) if at these frequencies $\exp[i\omega(\tau_2/2)] \approx 1$, i.e., if an integral number of waves is contained in the burning zone.

A diagram of the regions of stability and instability in terms of the parameters μ_3 and τ_4 is shown in Fig. 10*. To each projection of the auxiliary curve which intersects with the imaginary axis, there corresponds a series of regions of instability. The parameters μ_3 and τ_4 correspond to the parameters D and τ_1 of the previous model, and the difference between the plots of Fig. 7 and Fig. 10 lies only in the values and number of roots ω_j and the values of the quantities $-iF(i\omega j)$ and $Q(i\omega j)$ corresponding.

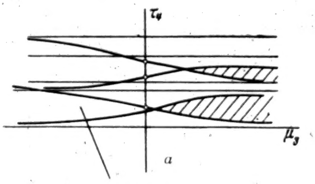

FIG. 10

The new result, on the basis of which we have developed this model, consists of the possibility of exciting not only the base frequency of the resonant tube, but also its higher harmonics, and of the discovery of the dependence of such excitation on the position of the flame, its dimensions and intensity, and the delay in burning. We note that the role of the parameters μ and τ for the auxiliary equation in this model and in the preceding one are exactly the same.

The product D_1D_2 plays a role here analogous to the damping h in the preceding model; the projections will be increased as D_1D_2 approaches unity.

4. DISCUSSION OF THE RESULTS

Let us compare the facts observed experimentally by the different authors with the conclusions which follow from the theory presented above. It is natural that the discrete model explains the smallest number of facts, and, conversely, that the distributed model describes the phenomenon most completely.

1. Experiment shows that the vibrations of the singing flame are excited periodically, independent of the length of the supply tube. Model No. 1 does not explain this fact. For models No. 2 and No. 3, this conclusion follows directly from Fig. 7 and Fig. 10. If, for fixed $D(\mu_3)$, τ_1 (τ_4) increases, then the region of stability will be changed to a region of instability, and vice versa. In this case, the excitation conditions can be shown to be quantitatively different from the conditions pointed out by Rayleigh (the flame sounds when the length of the gas tube is somewhat less than ¼λ, ¾λ,..., and is silent when its length is approximately ½λ, λ, 3/2λ,.., where λ is the wavelength in the gas). This deviation of the excitation conditions from the conditions of Rayleigh has been observed by several experimenters. The action of progressive waves was made clear in reference 1. These waves apparently arise in a gas tube along with standing waves. As can be seen from the behavior of the curves in Figs. 7 and 10, at sufficiently large τ_1 (τ_4), the system will always be unstable.

2. Experiment shows that the frequency of the singing flame is close to the fundamental eigenfrequency of the sounding tube. However, higher harmonics are sometimes excited. In the latter case, the frequency that is excited depends on the position of the flame in the sounding tube: a short flame is better for the excitation of the higher harmonics. Models No. 1 and No. 2 cannot explain these factors. Model No. 3 does explain them (in model No. 3, the dimensions of the flame are taken into consideration, directly, through the parameter τ_2, and indirectly, by the parameter μ, in which the density of the burning source appears.

3. The system is stable in the absence of flame, when the gas simply blows through the resonator. In this case, the parameter $\mu = 0$. The stability of the system for Model No. 1 can be seen directly from Fig. 4. For models No. 2 and No. 3, the stability results from the fact that the curve $Q(i\omega)$ in Fig. 6 [($-iF(i\omega)$ in Fig. 9)] does not intersect the real axis. The region of stability here occupies the first quadrant ($D > 0$, $\tau_1 > 0$) of Fig. 7 (or, correspondingly, $\mu_3 > 0$, $\tau_4 > 0$, Fig. 10). Experiment indicates that non-hydrogen flames can also sing, for example, the flame of illuminating gas[1,2], but they sing less satisfactorily than the hydrogen flame. This is accounted for by the fact that the parameter μ is less for the non-hydrogen flame.

4. Experiment shows that if the supply tube is plugged with cotton, so that the gas can still leak through the plug, then the flame will not sing. The effect of the cotton is to increase the damping of the system. For model No. 1, this means an increase in the coefficient h_2. The stability of the system increases with rise in h_2, as follows from

---

* The drawings for cases *b* and *c* of Fig. 10 are the same as for Figs. 7 *b* and 7 *c*.

Figs. 3 and 4. For model No. 2, the presence of the cotton means a decrease in the coefficient of consumption α_1, i.e., a decrease in the parameters D and E. For small E the curve $Q(i\omega)$ does not intersect the real axis, and consequently the system is stable. Similarly for model No. 2, the equation $\mathrm{Im}\,[-iF(i\omega)] = 0$ does not have real roots for small α_4.

5. Experiment shows that the flame does not sing if the opening of the supply tube is very small. For model No. 1, small S_2 corresponds to small $\mu\nu$. For small $\mu\nu$, as follows from Fig. 4, the system is stable. For model No. 2, a small area of the aperture σ is equivalent to small E, and, for model No. 3, to small μ [the area of the cross section of the gas tube is included in the coefficient b of Eq. (3.5)]. As has already been shown above, the system is stable for small E (μ).

6. Experiment shows that the frequency of the singing flame is close to the eigenfrequency of the resonator, but it can be somewhat different from it (in the case of a large aperture of the supply tube). The proposed theory explains this circumstance by the fact that the frequency ω from Eq. (1.6), and the values $\omega = \omega_j$, for which $Q(i\omega)$ and $-iF(i\omega)$ intersect the real axis, depend on the parameters of the gas tube and the parameters of burning, as well as on the parameters of the resonator.

7. Since the effect of convection was not considered in the proposed theory, none of the models explain the experimental fact that the flame, when placed in the upper part of the tube, excites vibrations more strongly than when it lies in the lower part of the tube.

Translated by R. T. Beyer
98

SOVIET PHYSICS JETP VOLUME 1, NUMBER 3 NOVEMBER, 1955

Rectangular Wilson Chamber with Bilateral Expansion

V. G. KIRILLOV-UGRIUMOV, V.M. FEDEROV AND B. N. DERIAGIN
P. N. Lebedev Institute of Physics,
Academy of Sciences, USSR

(Submitted to JETP editor April 27, 1954)
J. Exper. Theoret. Phys. USSR 28, 603-607 (May, 1955)

Description of a rectangular Wilson Chamber with bilateral expansion, suitable for use with a mass spectrometer.

RECTANGULAR Wilson chambers are now being used more and more to study the composition of cosmic rays. We constructed and prepared a rectangular Wilson chamber with bilateral expansion, intended to investigate the stopping of cosmic radiation particles that pass through the magnetic field of the large mass spectrometer of the Cosmic Ray Laboratory on the Alagez mountain[1].

Rectangular chambers are more suitable for use with a magnetic spectrometer than cylindrical chambers of equal volume, for they permit increasing the light output of the installation. Increasing the light output of the instrument is particularly essential when recording rare phenomena associated, for example, with high-energy nuclear interactions.

To brake and stop the particles, plates made of different substances were fastened horizontally inside the chamber. Since a "shining-through" illumination system was chosen, the only possible expansion was along the longest side of the chamber, i.e., sideways. Locating the expansion apparatus on the side is also advantageous because the cross section of the segment between plates is constant along the expansion direction, even when the plates are tilted relative to the center line of the objectives. A constant cross section prevents gas eddies from forming during expansion.

To prevent eddies from forming inside the chamber when the diaphragm travel is large, we used simultaneous expansion from two opposite sides. Bilateral expansion cuts diaphragm travel in two. In addition, sideways placement of the valves makes them easy to regulate and shields them from the effect of the external magnetic field.

A section through the chamber is shown schematically in Fig. 1. The volume of the chamber is approximately 10,000 cc. The dimensions of the forward window are 230× 380 mm, and the depth is 120 mm. The case is a duraluminum parallelopiped with two transverse apertures for fastening the glasses and the expansion apparatus; the parallelopiped is made of a solid piece to insure more dependable hermeticity. The case is coated on the inside with a thin layer of bakelite to prevent corrosion. The glasses, which are 35 mm thick, are clamped against the case with frames. The joint is made hermetic with rubber gaskets of 4×6 mm cross section placed between the glass and the metal.

Two grids, one movable *8* and one stationary *10*, limit the displacement of the diaphragm *9*, made of rubber sheet 2 mm thick and clamped between the case of the chamber and the case of the expansion apparatus. The moving-grid position, which determines the degree of expansion, is regulated by rotating the supporting bushings *17*; the grids are made to occupy symmetrical positions with the aid of a rigid coupling through shaft *20* and gear trains *2*. The thickness of the diaphragm is so chosen that its inertia does not affect the expansion time noticeably. The openings in the grids are of such diameter , that the degree of expansion is not affected noticeably when the rubber is deflected into the opening by fluctuations in the relative pressure in the expansion apparatus. Expansion was effected by two electromagnetic valves releasing compressed air from the expansion reservoirs. A mixture of 65% ethyl alcohol and 35% water (by volume) was fed to the chamber. The non-condensing gas used was argon, pumped into the chamber to a relative pressure of two atmospheres.

Because of the limited space available under the electromagnet poles, the inside of the chamber had to be photographed from a close distance. Consequently, it was necessary to employ only small apertures to insure depth of focus over the entire volume. The usual techniques for photography at right angles to the direction of illumination at small apertures call for illumination sources of increased power. In the chamber described here, illumination was by "shining through", so that the optical axis of the objective made an angle of approximately 50° with the

---

[1] A. A. Alikhanian, V. G. Kirillov-Ugriumov, N. V. Shostakovich, and V. M. Fedorov, Dokl. Akad. Nauk SSSR **92**, 255 (1953)

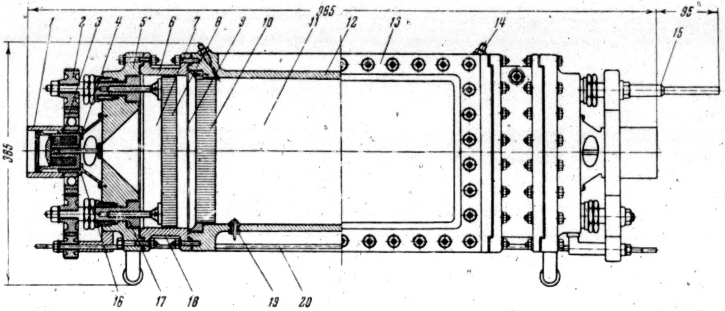

FIG. 1. Diagram of Chamber. *1*- magnetic shield, *2* - gears, *3* - brass cylinder, *4* - valve, *5* - cover of expansion head, *6* — case of expansion head, *7* - expansion apparatus, *8* - movable grid, *9* - rubber diaphragm, *10* - stationary grid, *11* - glass, *12* - case of chamber, *13* - flange, *14* - fitting for filling the working volume, *15* - vernier, *16* - bushing for fastening valve, *17* - mechanism for displacing movable grid, *18* - water jacket, *19* - input point for "clearing" field, *20* - rod connecting the gear trains.

incident light. According to Webb[2], the intensity of the light scattered from the droplet increases considerably as the angle decreases, and is 3-4 times greater at the angle chosen here than at a 90° scattering angle. The photographs were taken at a distance of 650 mm with a stereo camera having a 135 mm base and "Jupiter 12" objectives with $f = 35$ mm. The diaphragm f stop was 11, and the angle between the objective axes was 6.5°. The chamber was illuminated with two IP K-400 flash bulbs. Each bulb was fed by a 48 microfarad capacitor charged to 3.5 kilovolts. The lens system suggested in reference 3 was used to focus the light. The focused beam was so directed to the chamber, that no direct light was incident on the photographic camera lenses (Fig. 2).

Great attention has been paid to temperature stabilization. Water from a TS-15 thermostatic bath is circulated through metallic jackets soldered onto each expansion apparatus. In addition, air of the same temperature is blown through the light-tight boxes. The diagram of the thermostatic regulation (with accuracy to 1°) is shown in Fig. 3. A ratio meter is used for monitoring. The use of several transmitters permits easy monitoring of the temperature in various parts of the chamber.

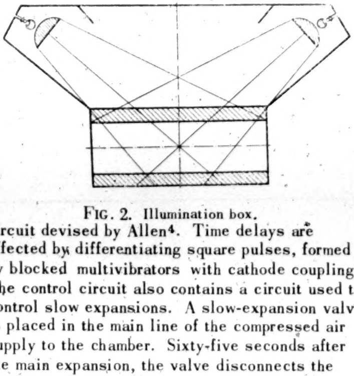

FIG. 2. Illumination box.

The chamber is controlled with an electronic circuit devised by Allen[4]. Time delays are effected by differentiating square pulses, formed by blocked multivibrators with cathode coupling. The control circuit also contains a circuit used to control slow expansions. A slow-expansion valve is placed in the main line of the compressed air supply to the chamber. Sixty-five seconds after the main expansion, the valve disconnects the compressed-air supply and connects the expansion volume to the atmosphere. The compressed air escapes through a small-diameter aperture for five seconds, permitting the diaphragm to move away toward the rear, stationary grid. The slow expansion causes the droplets that have not been evaporated by the working expansion to increase in size and to settle on the bottom. This process reduces considerably the lateral fog background during the next working expansion.

---

[2] C. Webb, Phil. Mag. 19, 927 (1935)

[3] E. Lofgren, E. Ney and F. Oppenheimer, Rev. Sci. Inst. 19, 271 (1948)

[4] F. Allen, Rev. Sci. Inst. 19, 918 (1948)

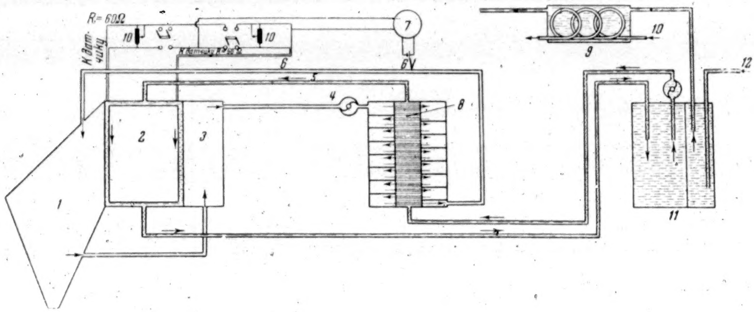

FIG. 3. Diagram of thermostatic regulation. *1* — photographic camera body, *2* - head of chamber, 3 - illumination box, *4* - air blower, *5* - thermostatically-controlled water, *6* - thermostatically-controlled air, *7* - ratio meter, *8* - radiator, *9* - refrigerator, *10* - compressed air for the expansion apparatus, *11* - thermostatic bath, *12* - tap water. The resistances are given in kilohms.

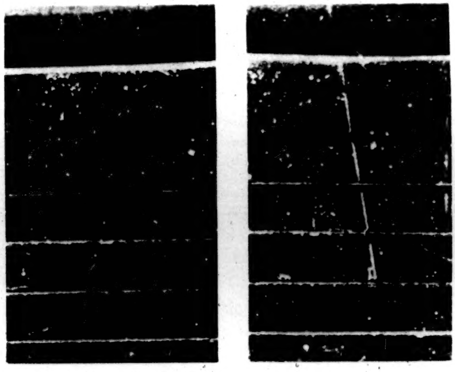

FIG. 4. Photograph of tracks of cosmic particles, recorded in a chamber with bilateral expansion.

Study of the photographs has shown that tracks of the penetrating particles are obtained over the entire volume of the chamber without noticeable distortion. As can be seen from Fig. 3, the illumination is worse in the region adjacent to the grids than in the center of the chamber on the photographs, and the density of tracks of penetrating particles is therefore different in various parts of the chamber. This is easily taken into account when the data are processed. Photographs obtained with the valves operating with a time difference up to 4-6 milliseconds do not differ from photographs obtained with a smaller time difference; this agrees with the results of measurements on the degree of supersaturation as a function of expansion time, reported by Hazen[5].

To increase the intensity of the observed cases of particle stoppage, it is desirable that as many plates as possible be placed in the chamber. However, a large number of plates reduces the brightness of the tracks. The best performance was obtained with this chamber when nine plates were used. The sensitive time of the chamber, determined from the number of cosmic particles, recorded at no-field expansion and constant illumination, is 0.2 second. To eliminate the ions produced by extraneous particles passing through the chamber up to the time of the working expansion, an electrostatic field of 30 volts/cm intensity is applied between the plates. The control circuit is capable of removing this field within 10^{-5} second.

---

[5] W. Hazen, Rev. Sci. Inst. **13**, 247 (1942)

The clearest photographs in which both thin and thick tracks are produced without noticeable fog are obtained with type 10-100 or higher-sensitivity "Panchrom" film developed in amidol.

By way of an example, Fig. 4 shows the photographs of the trajectories of a relativistic particle and a proton that is stopped by ionization in the sixth plate.

This work was performed under the leadership of Prof. A. I. Alikhanian, to whom we feel it our duty to express our deepest gratitude. We are also grateful for the help by M. M. Vermeev, V. A. Nikolaiev, G. D. Davimus, S. G. Riumin, and N. A. Golubchikov.

Translated by J. G. Adashko
102

SOVIET PHYSICS JETP VOLUME 1, NUMBER 3 NOVEMBER, 1955

The Dynamical Theory of Electron Scattering in Crystals

I. A. OVSIANNIKOVA AND M. IA. SHIROBOKOV
Gor'kii State University

(Submitted to JETP editor May 10, 1954)
J. Exper. Theoret. Phys. USSR **28**, 695-698 (June, 1955)

On the basis of the dynamical theory of scattering of electrons in crystals when two intense beams are present, a formula is obtained for the intensity of symmetrically scattered beams of fast electrons. The scattering of convergent beams is considered.

THE kinematical theory of electron scattering in crystals enables us, in most cases, to calculate the directions and intensities of the diffracted beams sufficiently accurately, while neglecting the energy loss of the initial beam which is associated with the formation of the scattered waves. However, for scattering blocks whose linear dimensions are of order 10^{-5}cm[1], a more thorough consideration of the processes connected with the motion of electrons in the periodic crystalline field becomes necessary.

The dynamical theory, which is the next approximation to the solution of the problem, leads to an infinite system of linear equations for the Fourier coefficients of the wave function describing the electron state. The simplest solution, which is also the one most suitable for comparison with experiment, is obtained for the case when two waves – the incident and one of the scattered waves – have high intensity. It has been shown[2] to be possible in principle to use this solution in the case of symmetrical scattering for a problem with a greater number of beams. This solution was not used in later work, although symmetrical scattering was observed in experiment [3].

1. In reference 2 it was shown that crystal symmetry shows itself in the equality of corresponding coefficients in the Fourier expansion of the internal crystalline potential: $v_{\mathbf{g}} = v_{\mathbf{g}'}$, where **g** and **g**′ are reciprocal lattice vectors related by a symmetry transformation. This results in the equality of the dynamical potentials for symmetrically scattered beams, and this in turn results in the equality of all the amplitudes of symmetrically scattered waves, if the initial ray is directed along the crystal symmetry axis. Starting from this, one obtains a system of equations completely similar in form to the equations for the case of two scattered beams

$$\begin{gathered}\psi_0(\varkappa^2 - k_0^2 - V_{11}) - V_{12}\psi_h = 0,\\ -\psi_0 V_{12} + (\varkappa^2 - k_h^2 - V_{22})\psi_h = 0;\end{gathered} \tag{1}$$

except that here the dynamical potentials V_{ik} and the amplitude ψ_h have different meanings:

$$V_{12} = \sqrt{n}V_{12}^i, \quad \psi_h = \psi_h^i\sqrt{n}, \tag{2}$$

$$V_{22} = \sum_{j=1}^{n} V_{22}^{ij},$$

where the indices i and j designate the numbering of the symmetrically scattered beams.

The total intensity I_h of all the scattered beams is expressed in the same way as the intensity of the single scattered beam in the problem with two beams. The intensity of each of the symmetrically scattered beams is I_h/n.

Using the solution for two beams[1], with the appropriate values of the dynamical potentials, we have from Eq. (2)

$$\psi_{hi} = \psi_h \frac{V_{12}^j}{\varkappa\cos\vartheta_h}\frac{\sin(\frac{1}{2}H\sqrt{p})}{\sqrt{p}}, \tag{3}$$

where

$$p = \left(\frac{V_{11}}{2\varkappa\cos\vartheta_{hi}} + \frac{\zeta_i}{\cos\vartheta_{hi}} - \frac{\sum_{j=1}^{n} V_{22}^{ij}}{2\varkappa\cos\vartheta_{hi}}\right)^2 + \frac{nV_{12}^{j2}}{\varkappa^2\cos\vartheta\cos\vartheta_{hi}}. \tag{4}$$

We give the pendulum solution for fast electrons. In this case the ζ_i can be expressed as follows:

$$\zeta = \varkappa(\vartheta_i - \vartheta_0)\sin 2\vartheta_0, \tag{5}$$

where $_0$ is the angle corresponding to the center of the region of selective reflection.

Evaluation of the maximum value of the dynamical potential

$$V_{11} = \sum_g \frac{v_g v_{-g}}{\varkappa^2 - k_g^2} \qquad (\varkappa^2 = K^2 + v_0) \tag{6}$$

---

[1] Z. G. Pinsker, *Electron Diffraction*, Pub. House, Acad. Sci. USSR, 1949

[2] H. Bethe, Ann. Physik **87**, 55 (1928)

[3] Z. G. Pinsker, B. K. Vainshtein, Izv. Akad. Nauk SSSR **14**, 212 (1950)

for an accelerating voltage $E = 40\,\mathrm{kV}$, using the Fourier coefficients v_g for nickel which were calculated in reference 2, gives

$$V_{11\,\max} = 0.08\ \mathrm{\mathring{A}}^{-2}.$$

In the dynamical potentials V_{ik} $(i \neq k)$, the most important terms are the v_{h_j}, whose maximum value can be $\sim 4\,\mathrm{\mathring{A}}^{-2}$. Thus we can neglect the quantity V_{11} and the second term in V_{ik} compared to v_{h_j}. In this approximation,

$$V_{12} = \sqrt{n}\, V_{12}^{j} \tag{7}$$

$$= \sqrt{n}\left(-v_{-h_j} + \sum_g \frac{v_{-g}v_{g-h_j}}{\varkappa^2 - k_g^2}\right) = -\sqrt{n}\,v_{-h_j},$$

$$V_{22} = \sum_j V_{22}^{ij} \tag{8}$$

$$= \sum_j \sum_g \frac{v_{g-h_j}v_{h_i-g}}{\varkappa^2 - k_g^2} - \sum_j v_{h_i-h_j} = -\sum_j v_{h_i-h_j}.$$

Taking into account the smallness of the angle ϑ in electron diffraction, we obtain

$$p = \left[\varkappa(\vartheta_i - \vartheta_0)\sin 2\vartheta_0 + \frac{1}{2\varkappa}\sum v_{h_i-h_j}\right]^2 + \frac{nv_{-h_j}}{\varkappa^2}. \tag{9}$$

The intensity of a single scattered beam, for symmetrical scattering in the approximation for fast electrons, is the pendulum solution

$$I_h = I_0\,\frac{v_{-h_j}}{\varkappa^4}\,\frac{\sin^2\left\{{}^1\!/_2 H\varkappa\sqrt{\left[(\vartheta - \vartheta_0)\sin 2\vartheta_0 + \left(\sum_j v_{h_i-h_j}\right)/2\varkappa^2\right]^2 + \frac{nv^2_{-h_j}}{\varkappa^4}}\right\}}{\left[(\vartheta - \vartheta_0)\sin 2\vartheta_0 + \left(\sum_j v_{h_i-h_j}\right)/2\varkappa^2\right]^2 + nv^2_{-h_j}/\varkappa^4}, \tag{10}$$

We apply the result to a calculation of the integral reflections of the scattered beams for dynamical scattering from a mosaic layer. It was shown in reference 3 that the integral reflections are proportional to the intensities. Noting that there is a symmetric wave field in each block of the mosaic, we can estimate the value of the angle integral using the interference conditions, which are much simpler than the dynamical theory[3]. The calculation shows that approximately half of the blocks take part in the formation of each interference maximum.

To calculate the integral reflection, we must average I_h over the thickness H of the crystal

$$\bar{I}_h \tag{11}$$

$$= I_0\,\frac{v^2_{-h_j}}{2\left\{\left[\varkappa^2(\vartheta - \vartheta_0)\sin 2\vartheta_0 + {}^1\!/_2\sum_j v^2_{h_i-h_j}\right]^2 + v_h^2 n\right\}},$$

$$I_{\text{int.}} = I_0\,\frac{1}{\omega}\int_{-\infty}^{\infty}\frac{I}{I_0}\,d\alpha, \quad \alpha = \vartheta - \vartheta_0, \tag{12}$$

$$\bar{I}_{\text{int.}} = \frac{I_0}{2n\omega}\,\frac{v_h\sqrt{n}}{2\vartheta_0\varkappa^2}\int_{-\infty}^{\infty}\frac{dW}{1+W^2} = \frac{I_0}{\omega}\,\frac{\pi v_{hkl}}{4\varkappa^2\vartheta_0\sqrt{n}}, \tag{13}$$

where

$$W = \frac{\varkappa^2(\vartheta - \vartheta_0)\sin 2\vartheta_0 + {}^1\!/_2\sum v_{h_i-h_j}}{v_{h_j}\sqrt{n}}. \tag{14}$$

Here, as compared with the formula for integral reflection in the problem with two beams, there appears the factor $1/\sqrt{n}$, where n is the order of the symmetry axis.

2. The solution (10) which we have obtained can be extended to the case of a convergent beam, as was done in reference 4. The axis of the beam must coincide with the direction of the axis of symmetry of the crystal.

Minimum intensity will occur for

$$\sin\left({}^1\!/_2 H\sqrt{p}\right) = 0. \tag{15}$$

From this we obtain, after transformation,

$$\vartheta_{\min} - \vartheta_0$$

$$= d_{hkl}\left[\frac{\sum_j v_{h_i-h_j}}{4\pi\varkappa} \pm \sqrt{\frac{m^2}{H^2} - \frac{nv^2_{-h_j}}{4\pi^2\varkappa^2}}\right]. \tag{16}$$

Equation (16) is applicable for $m > Hv_{h_j}\sqrt{n}/2\pi\kappa$. The width of the interference band turns out to be

$$\vartheta^{\min}_{m+1} - \vartheta^{\min}_{m} = \pm d_{hkl}\left[\sqrt{\frac{(m+1)^2}{H^2} - \frac{nv^2_{-h_j}}{4\pi^2\varkappa^2}} - \sqrt{\frac{m^2}{H^2} - \frac{nv^2_{-h_j}}{4\pi^2\varkappa^2}}\right].$$

---

[4] C. H. Mac Gillavry, Physica 7, 329 (1940)

different from the case of two beams. This is caused by the interaction of several beams. Our calculation was made for symmetrical scattering, but it can serve as the basis for the qualitative conclusion that in asymmetrical scattering, if the wave field contains several strong beams, the width of the interference band will differ from its value in the case of two beams because of the interaction of the electron beams. In this way we can explain the disagreement of Ackerman's results[5] with the theoretical values; in these experiments on scattering from PbI_2 and mica, there was a very complicated wave field while the theoretical calculations were made with the formula for two beams.

The case of symmetrical scattering can easily be realized experimentally, so our solution can be used practically for the calculation of the structure factor from the geometry of electron diffraction patterns by the method proposed by Mac Gillavry[4], and also for other calculations.

In conclusion, we express our gratitude to Prof. Z. G. Pinsker for discussion of the problem and valuable advice.

Translated by M. Hamermesh
123

---

[5] I. Ackerman, Ann. Physik 2, 19,41 (1948)

SOVIET PHYSICS JETP VOLUME 1, NUMBER 3 NOVEMBER, 1955

Relativistically Invariant Equations for the Electron which Take the Place of Dirac's System of Equations

G. A. ZAITSEV
Ivanovo

(Submitted to JETP editor April 3, 1954)
J. Exper. Theoret. Phys. USSR **28**, 530-540 (1955)

Making use of the properties of real spinors, additional terms are found which make the equations for the electron used in non-relativistic quantum mechanics relativistically invariant. The second order differential equations found in this way, which connect the components of one real spinor, are simpler than those which are obtained through Dirac's theory. The relativistically invariant equations introduced are solved for the hydrogen atom in the absence of external fields. It turns out that in that case the usual fine structure formula is obtained, just as in the Dirac theory. It is shown that the considered second order differential equations can be obtained from a system of relativistically invariant equations of first order which, however, no longer contain one, but two, real spinors.

1. INTRODUCTION

A descriptive interpretation of the ideas and concepts used in non-relativistic quantum mechanics for study of the behavior of particles with spin 1/2 was given in reference 1. The problem of finding relativistically invariant equations for the electron must also be reexamined from this point of view.

Currently, as is well known, Dirac's system of equations[2] is considered as the system of relativistically invariant equations which characterize the behavior of an electron in various external fields (see also references 3-6 etc.). This choice was based on the possibility of getting the ordinary non-relativistic equations from them in a special case and also on their ability to explain more exactly the available experimental facts. Most important of such facts is the existence of fine structure in the spectrum of the hydrogen atom, and its explanation by the use of Dirac's equations is accordingly the chief argument in favor of the validity of the Dirac theory. It is obvious that any relativistically invariant equations for the electron which claim to replace Dirac's system of equations must also reduce to the equations of nonrelativistic quantum mechanics in a special case and at the same time explain experimental facts not explained by the latter. Above all, moreover, they must lead to a formula for the fine structure experimentally confirmed.

Relativistically invariant equations for the electron, which satisfy the formulated requirements and which at the same time are simpler than the Dirac equations, will be obtained in the present paper. During the derivation of these equations we will make any hypotheses but will not be guided only by the fact that the equations of non-relativistic quantum mechanics for the electron interpreted with the aid of the graphical concepts developed in reference 1 must be generalized in such a way that they become relativistically invariant, i.e., that they don't change under arbitrary transformations of the general Lorentz group. We will need the mathematical apparatus developed in references 7 and 8.

2. DERIVATION OF THE RELATIVISTICALLY INVARIANT EQUATIONS TO REPLACE DIRAC'S SYSTEM OF EQUATIONS

As is known, the components of the momentum operator and the energy operator which are used in

---

[1] G. A. Zaitsev, J. Exper. Theoret. Phys. USSR **25**, 653 (1953)

[2] P. A. M. Dirac, Proc. Roy. Soc. London 117, 610; 118, 351 (1928)

[3] V. A. Fock, *Principles of Quantum Mechanics*, Kubuch, 1932

[4] Louis De Broglie, *The Magnetic Electron*, Paris, 1934

[5] W. Pauli, *General Principles of Wave Mechanics*, (Ann Arbor, Mich) Edwards 1946

[6] P. A. M. Dirac, *Quantum Mechanics*, (1935) 2nd Ed. (Oxford)

[7] G. A. Zaitsev, J. Exper. Theoret. Phys. USSR **25**, 667 (1953)

[8] G. A. Zaitsev, J. Exper. Theoret. Phys. USSR **28**, 524; Soviet Phys. **1**, 411 (1955)

non-relativistic quantum mechanics, from the point of view of graphical representations of the states of particles with spin 1/2, must be written in the form:

$$\hat{p}_k = -\hbar I \frac{\partial}{\partial x^k}, \quad \hat{E} = \hbar I \frac{\partial}{\partial t} \tag{1}$$

(see reference 1). Therefore, on going over to four-dimensional pseudo-Euclidian space, we shall have the following relations for a real spinor which is a "proper" spinor of these operators:

$$-\hbar I \frac{\partial \psi}{\partial x^\alpha} = p_\alpha \psi \tag{2}$$

$$(x^4 = ct,\ p_4 = -E/c,\ \alpha = 1, 2, 3, 4).$$

The p_α must transform as components of a four-vector, since they are components of four-dimensional momentum. Furthermore, we know the transformation rule for a rela spinor ψ under transformations of the Lorentz group.

Taking into account that, under arbitrary rotations and reflections of four-dimensional space, both sides of Eq. (2) must transform in like manner, we can determine to which of the fourth order real matrices considered in reference 7 the matrix I correspo[illegible] It is easy to see that here there are only two po[illegible]lities: The matrix I must compare with J or $-J$. Here, however, $\hbar$ must be considered not as a scalar (as has usually been assumed) but as a pseudoscalar, which changes sign upon four dimensional reflections but remains invariant for four-dimensional rotations. More exactly, this is the sole component of the matrix-pseudoscalar $T_4 = \hbar J$, and one must regard the numerical value of Planck's constant as the absolute value of the corresponding pseudoscalar.

The fact that the matrix J should agree with I rorrect as to sign leads to the imposition of a restriction on the choice of the remaining basic matrices considered in reference 7. Namely, they must correspond to the ones which were presented in the first or the second line of Table I from reference 7. For definitness,we shall assume that $J = I$ (the choice of sign has no significance), so that

$$R^k = BS_k,\ R^4 = B,\ R = BI,\ J = I. \tag{3}$$

Thus, from the postulate of relativistic invariance, it follows that Eqs. (1) and (2) can be written in the form

$$-\hbar J\,(\partial\psi/\partial x^\alpha) = p_\alpha \psi, \tag{4}$$

where $\hbar$ is the component of a pseudoscalar. We note that the replacement of $\hbar$ by $-\hbar$ corresponds to a change of sign of $I = J$. It is well known that the results of non-relativistic quantum mechanics do not change if i is everywhere changed to $-i$. Therefore they do not change if $\hbar$ is changed to $-\hbar$ in the basic formulas.

As the initial non-relativistic equation for the electron, to which we shall have to add the terms which make it relativistically invariant, we can take Pauli's equation, writing it in the form

$$\left[-i\hbar\frac{\partial}{\partial t} + \frac{1}{2m_0}\sum_{k=1}^{3}\left(-\hbar i\frac{\partial}{\partial x^k} + \frac{e}{c}A_k\right)^2 - e\varphi\right]\xi_0 + \frac{e\hbar}{2m_0 c}\sum_{k=1}^{3} H_k \sigma_k \xi_0 = 0, \tag{5}$$

where e is the electronic charge and A_k are the components of the vector potential. (See, for example, reference 9 etc.).

From this equation (more exactly, two equations) it is necessary to go over to a real relation[1], since, on consideration of arbitrary transformations of the Lorentz group, the original entity, for which the law of transformation is defined, is a real spinor, and a spinor of first rank is not suitable for this purpose. Substituting for all the complex quantities in Eq. (5) the real quantities corresponding to them, we get

$$\left[-\hbar J\frac{\partial}{\partial t} + \frac{1}{2m_0}\sum_{k=1}^{3}\left(-\hbar J\frac{\partial}{\partial x^k} + \frac{e}{c}A_k\right)^2 - e\varphi\right]\psi_0 + \frac{e\hbar}{2m_0 c}\sum_{k=1}^{3} R_4 R^k H_k \psi_0 = 0. \tag{6}$$

In order to make Eq. (6) relativistically invariant, it is necessary to replace the operator

$$-\hbar J\frac{\partial}{\partial t} + eA_4 + \frac{1}{2m_0}\sum_k\left(-\hbar J\frac{\partial}{\partial x^k} + \frac{e}{c}A_k\right)^2,\quad A_4 = -\varphi$$

by

$$\frac{1}{2m_0}\left[-\left(-\hbar J\frac{\partial}{\partial x^4} + \frac{e}{c}A_4\right)^2 + \sum_k\left(-\hbar J\frac{\partial}{\partial x^k} + \frac{e}{c}A_k\right)^2 + m_0^2 c^2\right],$$

and $R_4 R^k H_k$ by $-J\,(RR^k H_k + R_4 R^k E_k) = -JF$. Thereby Eq. (6) goes over to

$$\left[-\left(-\hbar J\frac{\partial}{\partial x^4} + \frac{e}{c}A_4\right)^2 + \sum_k\left(-\hbar J\frac{\partial}{\partial x^k} + \frac{e}{c}A_k\right)^2 + m_0^2 c^2 - \frac{e\hbar}{c}JF\right]\psi = 0, \tag{7}$$

---

[9] D. I. Blokhintsev, *Principles of Quantum Mechanics*, GITTL, 1949

where ψ is a real spinor. The Pauli equation (5) or (6) is obtained from Eq.(7) if we take $\Psi = [\exp(-J\frac{m_0 c^2 t}{\hbar})]\psi_0$, disregard the quantities $\frac{m_0\hbar^2}{c^2}\frac{\partial^2\psi_0}{\partial t^2}$, $\frac{m_0 e^2\phi^2}{c^2}\psi_0$, $\frac{m_0 e\hbar}{c^2}\left(J\times\frac{\partial}{\partial t}\phi + J\phi\frac{\partial}{\partial t}\right)\psi_0$ and also discard the term $-\frac{e\hbar}{c}JR_4\underline{E}$.

The relativistic invariance of Eq. (7) comes out of the following : If one denotes the expression in the square brackets by the symbol G, then upon a similarity transformation characterized by the matrix A_1 , G goes over to $A_1 GA_1^{-1}$. Therefore the the equation $G\psi = 0$ goes over to $A_1\ GA_1^{-1}\ (A_1\psi) = A_1\ G\psi = 0$, whence it follows that it is actually relativistically invariant.

We rewrite Eq. (7) in the form

$$\left(\hat{E}^2 - c^2\sum_k \hat{P}_k^2 - m_0^2c^4 + e\hbar cJF\right)\psi = 0, \qquad (8)$$

$$\hat{E} = \hbar J\frac{\partial}{\partial t} + e\varphi,$$

$$\hat{P}_k = -\hbar J\frac{\partial}{\partial x^k} + \frac{e}{c}A_k.$$

and this is the desired relativistically invariant equation which replaces the Dirac system of equations. (Strictly speaking, Eq. (8) is a system of four linear differential equations with real elements).

Already at first sight it is evident that the system of equations (8) is simpler than that which is obtained from Dirac's equations as a result of squaring. Actually,there are there four complex or eight feal functions, whereas our problem is reduced to the finding of four real functions-the components of a real spinor. Also, Pauli's equation is obtained from Eq. (8) considerably more easily than from Dirac's equations. The sense of Dirac's equations in the usual understanding is also different from that of Eq. (8). Inasmuch as the components of a real spinor are parameters which characterize a four-dimensional vector and an antisymmetrical tensor, Eq. (8) is, strictly speaking, a system of equations for the determination of four dimensional tensors. However, in the present article we shall not discuss in more detail the similarity and differences between Eq. (8) andDirac's equations. We also postpone the general analysis to later articles. In the current work, we restrict ourselves to the discussion of the electron in a hydrogen atom and to the calculation of the fine structure.

Before going over to the solution of this problem, we shall write Eq. (8) in a somewhat different form. Using Eq. (3) and reverting from real to complex quantities (assuming $JR_4R^k \leftrightarrow i\sigma_k$, $\psi \leftrightarrow \xi$, etc.). we find that the fundamental relativistically invariant equation (8) for the electron can be written in the form

$$\Big[\left(\hbar i\frac{\partial}{\partial t} + e\varphi\right)^2 - c^2\sum_k\left(-\hbar i\frac{\partial}{\partial x^k} + \frac{e}{c}A_k\right)^2 \qquad (9)$$

$$- m_0^2c^4 + e\hbar c\,(i\sigma_k E_k - \sigma_k H_k)\Big]\xi = 0.$$

In such a form it has a particularly simple appearance and is convenient to use for solving concrete physical problems. However, for the consideration of questions connected with relativistic invariance, it is expedient to use a form of the type of Eqs. (7) or (8). The point is that under arbitrary transformations of the Lorentz group ξ no longer is multiplied from the left by some matrix, in the way this occurred for three-dimensional rotations, but is transformed in a more complicated manner. Moreover, if we admit complex quantities, then we can no longer use the very simple transformation matrices (four dimensional tensors), and as a result, a demonetration of relativistic invariance becomes considerably complicated, etc.

3. EQUATIONS FOR THE ELECTRON IN A HYDROGEN ATOM IN THE ABSENCE OF EXTERNAL FIELDS

For the electron in a hydrogen atom, we can assume

$$A_k = 0, \quad \varphi = e/r. \qquad (10)$$

We will consider that the electron is in a stationary state, such that

$$\hbar i\frac{\partial}{\partial t}\xi = E\xi, \quad \xi = [\exp(-iEt/\hbar)]\xi_0, \qquad (11)$$

where ξ_0 does not depend on time. Therefore Eq. (9) takes the form

$$\left[\nabla^2 + \frac{1}{\hbar^2c^2}\left[\left(E + \frac{e^2}{r}\right)^2 - m_0^2c^4\right]\right. \qquad (12)$$

$$\left. + \frac{e^2}{\hbar c}i\left(\frac{x^k}{r^3}\right)\sigma_k\right]\xi = 0,$$

whereupon in the following we will use the abbreviated notations:

$$\alpha = \frac{e^2}{\hbar c}, \quad \sigma_{(r)} = \frac{x^k\sigma_k}{r},$$

$$\nabla^2_{\vartheta\varphi} = \frac{1}{\sin\vartheta}\frac{\partial}{\partial\vartheta}\left(\sin\vartheta\frac{\partial}{\partial\vartheta}\right) + \frac{1}{\sin^2\vartheta}\frac{\partial^2}{\partial\varphi^2}.$$

Our problem consists of finding the energy levels $\mathcal{E} = E - m_0 c^2$ and the corresponding characteristic functions of Eq. (12). For its solution it is necessary to find a system of operators which commute with the operator

$$\nabla^2 + \frac{1}{\hbar^2 c^2}\left[\left(E + \frac{e^2}{r}\right)^2 - m_0^2 c^4\right] \tag{13}$$

$$+ \frac{i\alpha\sigma_{(r)}}{r^2} = \frac{1}{r^2}\left(\frac{\partial}{\partial r} r^2 \frac{\partial}{\partial r}\right)$$

$$+ \frac{1}{\hbar^2 c^2}\left[\left(E + \frac{e^2}{r}\right)^2 - m_0^2 c^4\right] + \frac{\nabla^2_{\vartheta\varphi} + i\alpha\sigma_{(r)}}{r^2}$$

and with one another. Then the "proper" functions ξ of equation (12) can be chosen in such a way that they will also be characteristic functions of all of these operators at the same time.

We can attain a separation of variables if we assume $\xi_0 = f(r)\begin{pmatrix} y_1(\vartheta,\varphi) \\ y_2(\vartheta,\varphi)\end{pmatrix}$ whence

$$-(\nabla^2_{\vartheta\varphi} + i\alpha\sigma_{(r)})\begin{pmatrix} y_1 \\ y_2 \end{pmatrix} = \hat{L}y = \lambda y. \tag{14}$$

Then the energy levels of the electron in a hydrogen atom will be determined from the equation

$$\left[\frac{\partial^2}{\partial r^2} + \frac{2}{r}\frac{\partial}{\partial r} + \frac{1}{\hbar^2 c^2}\left[\left(E + \frac{e^2}{r}\right)^2 - m_0^2 c^4\right] - \frac{\lambda}{r^2}\right] f(r) = 0. \tag{15}$$

It is not difficult to verify that the operators (16) commute with (13) and $\hat{L}$.

$$\hat{M}_k = \hbar\left(-i\varepsilon^{kjs} x_j \frac{\partial}{\partial x^s} + \frac{1}{2}\sigma_k\right). \tag{16}$$

This can be seen from the following: if we set $[\hat{A},\hat{B}] = \hat{A}\hat{B} - \hat{B}\hat{A}$, then

$$\left[\varepsilon^{kjs} x_j \frac{\partial}{\partial x^s},\ \frac{x^t\sigma_t}{r}\right] = \frac{1}{r}\varepsilon^{kjs} x_j \sigma_s,$$

$$\left[\sigma_k,\ \frac{x^t\sigma_t}{r}\right] = \frac{2i}{r}\varepsilon^{kjs} x_j \sigma_s.$$

Furthermore, the operators $\hat{L}$, $\hat{M}_k$ and $\hat{M}^2 = \hat{M}_1^2 + \hat{M}_2^2 + \hat{M}_3^2$ commute with one another. Therefore we can choose y_1 and y_2 such that y, and consequently also ξ_0, will be a characteristic function of the operators $\hat{L}$, $\hat{M}_3$ and $\hat{M}^2$, simultaneously, i.e.,

$$M_3 y = \hbar m y, \tag{17}$$

$$\hat{M}^2 y = \hbar^2 j(j+1) y, \tag{18}$$

and the state of the electron in a hydrogen atom will be characterized by the quantum numbers m, j, λ and the radial quantum number which we introduce below.

From the commutation relations between the $\hat{M}_k$, as is well known, it follows that for a given j, m can take the values $m = -j, -j+1, \ldots, j-1, j$ (see references 6, 10, 11, etc.). It is possible to show, that from the stipulations (17) and (18) it follows that y has the form:

$$y = \begin{pmatrix} y_1 \\ y_2 \end{pmatrix} = \begin{pmatrix} (C_{j'}P_{j',m'} + C_{j'+1}P_{j'+1,m'})e^{im'\varphi} \\ \left(-\sqrt{\frac{j'-m'}{j'+m'+1}}C_{j'}P_{j',m'+1} + \sqrt{\frac{j'+m'+2}{j'-m'+1}}C_{j'+1}P_{j'+1,m'+1}\right)e^{i(m'+1)\varphi} \end{pmatrix}; \tag{19}$$

where $C_{j'}$, $C_{j'+1}$ are arbitrary constants, $j' = j - ½$ and $m' = m - ½$ are integers,

$$P_{j',m'} = \sqrt{\frac{(2j'+1)}{2}\frac{(j'-m')!}{(j'+m')!}} \tag{20}$$

$$\times\ (1-x^2)^{m'/2}\frac{1}{2^{j'}j'!}\frac{d^{j'+m'}}{dx^{j'+m'}}(x^2-1)^{j'},$$

$$x = \cos\vartheta.$$

We shall develop the proof of these assertions.

The functions y_1 and y_2 can be expanded into a Laplace series, i.e., presented in the form

$$y_1 = \sum_{k,n} C_{kn}P_{n,k}e^{ik\varphi} = \sum_{k=-\infty}^{\infty} A_k e^{ik\varphi},$$

---

[10] L. D. Landau and E. M. Lifshitz, *Quantum Mechanics*, GITTL, 1948

[11] E. U. Condon and G. H. Shortley, *Theory of Atomic Spectra*, Cambridge, 1935

$$y_2 = \sum_{k,\, n} D_{kn} P_{n,k}\, e^{ik\varphi} = \sum_{k=-\infty}^{\infty} B_k e^{ik\varphi}.$$

Substituting these expansions in Eq. (17), we get

$$y_1 = A_{m'} e^{im'\varphi}, \quad y_2 = B_{m'+1} e^{i(m'+1)\varphi}, \tag{21}$$

$$m' = m - {}^1/_2$$

(m' is an integer). Here we can assume

$$A_{m'} = \sum_l C_l P_{l,m'}, \quad B_{m'+1} = \sum_l D_l P_{l,\, m'+1} \tag{22}$$

(C_l and D_l are constants). Further, using the the fact that

$$\sigma_1 \mp i\sigma_2 = \begin{pmatrix} 0 & 1\mp 1 \\ 1\pm 1 & 0 \end{pmatrix},$$

we obtain

$$\frac{1}{h^2}\hat{M}^2 y = \left(-\nabla^2_{\vartheta,\varphi} + \frac{3}{4} + \begin{pmatrix} -i\dfrac{\partial}{\partial\varphi} & -i(\hat{l}_1 - i\hat{l}_2) \\ -i(\hat{l}_1 + i\hat{l}_2) & i\dfrac{\partial}{\partial\varphi} \end{pmatrix} \right) \begin{pmatrix} y_1 \\ y_2 \end{pmatrix} \tag{23}$$

$$= j(j+1)y, \quad \hat{l}_k = \varepsilon^{kjs} x_j \frac{\partial}{\partial x^s}.$$

Now use is made of the fact that

$$(l_1 \pm i\hat{l}_2) P_{l,\, m\mp {}^1/_2} e^{i(m\mp {}^1/_2)\varphi} \tag{24}$$

$$= -i\sqrt{(l+m'+1)(l-m')}\, P_{l,}$$

$$_{m\pm {}^1/_2} e^{i(m\pm {}^1/_2)\varphi}, \quad m' = m - {}^1/_2$$

(See references 6, 10-12, etc. In this series of works, functions are used which are different from the $P_{l,m}$, we use by the factor $(-1)^m$. On using them, the sign before the right-hand side of (24) must be changed).

Substituting the expression (21) and (22) in (23) and taking (24) into account, we get

$$[l(l+1) + {}^3/_4 + m' - j(j+1)]\, C_l \tag{25}$$

$$-\sqrt{(l+m'+1)(l-m')}\, D_l = 0$$

$$(l \geqslant m'),$$

$$-\sqrt{(l+m'+1)(l-m')}\, C_l \tag{26}$$

$$+ [l(l+1) - {}^1/_4 - m' - j(j+1)]\, D_l = 0$$

$$(l \geqslant m'+1).$$

In order that Eqs. (25) and (26) have a non-zero solution, it is necessary that for $l \geq m'+1$,

$$\begin{vmatrix} l(l+1) + {}^3/_4 + m' - j(j+1) & -\sqrt{(l+m'+1)(l-m')} \\ -\sqrt{(l+m'+1)(l-m')} & l(l+1) - {}^1/_4 - m' - j(j+1) \end{vmatrix} = 0 \tag{27}$$

or

$$[l(l+1) - j(j+1) + {}^1/_4]^2 = (l + {}^1/_2)^2, \quad l = j \pm {}^1/_2. \tag{28}$$

Thus, there are possible two solutions of Eqs. (25), (26), corresponding to the two possible choices of sign in Eq. (28), and the general solution will be a linear combination of these. We shall find it. If $l = j - ½ = j'$, then

$$D_{j'} = -\sqrt{\frac{j-m'}{j+m'+1}}\, C_{j'}, \tag{29}$$

and if $l = j + ½ = j' + 1$, then

$$D_{j'+1} = \sqrt{\frac{j+m'+2}{j'-m'+1}}\, C_{j'+1}, \tag{30}$$

so that as the general solution, we actually get Eq. (19).

Now we can go over to the analysis of Eq. (14), from which must be found the third quantum number λ and the ratio of $C_{j'+1}$ to $C_{j'}$.

Making use of the fact that $x_3 = r\cos\theta$, $x_1 \pm ix_2 = r\sin\theta\, e^{\pm i\phi}$, for the matrix $\sigma_{(r)} = \sum_k x^k \sigma_k / r$ we can write the expression

---

[12] H. A. Bethe, *Quantum Mechanics of the Simplest Systems*, ONTI, 1935

$$\sigma_{(r)} = \cos\vartheta\sigma_3 + \frac{1}{2}\sin\vartheta e^{i\varphi}(\sigma_1 - i\sigma_2) \quad (31)$$

$$+ \frac{1}{2}\sin\vartheta e^{-i\varphi}(\sigma_1 + i\sigma_2) = \begin{pmatrix} \cos\vartheta & \sin\vartheta e^{-i\varphi} \\ \sin\vartheta e^{i\varphi} & -\cos\vartheta \end{pmatrix}.$$

Therefore, taking Eq. (19) into account, we can rewrite Eq. (14) in the form of a system of two equations:

$$[j'(j'+1) - \lambda]\, C_{j'} P_{j', m'} \quad (32)$$

$$+ [(j'+1)(j'+2) - \lambda]\, C_{j'+1} P_{j'+1, m'}$$

$$- i\alpha \cos\vartheta C_{j'} P_{j', m'} - i\alpha \cos\vartheta C_{j'+1} P_{j'+1, m'}$$

$$+ i\alpha \sqrt{\frac{j'-m'}{j'+m'+1}} \sin\vartheta C_{j'+1} P_{j', m'+1}$$

$$- i\alpha \sqrt{\frac{j'+m'+2}{j'-m'+1}} \sin\vartheta\, C_{j'+1} P_{j'+1, m'+1} = 0;$$

$$- \sqrt{\frac{j'-m'}{j'+m'+1}} [j'(j'+1) - \lambda]\, C_{j'} P_{j', m'+1} \quad (33)$$

$$+ \sqrt{\frac{j'+m'+2}{j'-m'+1}} [(j'+1)(j'+2) - \lambda]$$

$$C_{j'+1} P_{j'+1, m'+1} - i\alpha \Big[\sin\vartheta P_{j', m'}$$

$$+ \sqrt{\frac{j'-m'}{j+m'+1}} \cos\vartheta P_{j', m'+1}\Big] C_{j'}$$

$$- i\alpha \Big[\sin\vartheta P_{j'+1, m'}$$

$$- \sqrt{\frac{j'+m'+2}{j'-m'+1}} \cos\vartheta P_{j'+1, m'+1}\Big] C_{j'+1} = 0.$$

Further, we use the fact that from the properties of $P_{j', m'}$ (reference 12, pp. 383-4) it is possible to derive the following relations:

$$- \cos\vartheta P_{j', m'} + \left(\sqrt{j'-m'} \,/\, \sqrt{j'+m'+1}\right) \sin\vartheta P_{j', m'+1} \quad (34)$$

$$= - \left(\sqrt{(j'-m'+1)(2j'+1)} \,/\, \sqrt{(j'+m'+1)(2j'+3)}\right) P_{j'+1, m'};$$

$$- \cos\vartheta P_{j'+1, m'} - \left(\sqrt{j'+m'+2} \,/\, \sqrt{j'-m'+1}\right) \sin\vartheta P_{j'+1, m'+1} \quad (35)$$

$$= - \left(\sqrt{(j'+m'+1)(2j'+3)} \,/\, \sqrt{(j'-m'+1)(2j'+1)}\right) P_{j', m'};$$

$$- \sin\vartheta P_{j', m'} - \left(\sqrt{j'-m'} \,/\, \sqrt{j'+m'+1}\right) \cos\vartheta P_{j', m'+1} \quad (36)$$

$$= - \left(\sqrt{(j'+m'+2)(2j'+1)} \,/\, \sqrt{(j'+m'+1)(2j'+3}\right) P_{j'+1, m'+1};$$

$$- \sin\vartheta P_{j'+1, m'} + \left(\sqrt{j'+m'+2} \,/\, \sqrt{j'-m'+1}\right) \cos\vartheta P_{j'+1, m'+1} \quad (37)$$

$$= \left(\sqrt{(j'-m')(2j'+3)} \,/\, \sqrt{(j'-m'+1)(2j'+1)}\right) P_{j', m'+1}.$$

Taking into account these formulas and comparing the coefficients which occur with the $P_{j',m'}$, $P_{j'+1,m'}$ in Eq. (32), we obtain from Eq. (14)

$$[j'(j'+1) - \lambda]\, C_{j'} \quad (38)$$

$$= i\alpha \left(\frac{\sqrt{(j'+m'+1)(2j'+3)}}{\sqrt{(j'-m'+1)(2j'+1)}}\right) C_{j'+1},$$

$$[(j'+1)(j'+2) - \lambda]\, C_{j'+1} \quad (39)$$

$$= i\alpha \left(\frac{\sqrt{(j'-m'+1)(2j'+1)}}{\sqrt{(j'+m'+1)(2j'+3)}}\right) C_{j'}.$$

Equation (33) leads to the same relations.

From Eqs. (38) and (39) we obtain

$$C_{j'+1} / C_{j'} = \frac{[j'(j'+1) - \lambda]}{i\alpha \sqrt{\dfrac{(j+m'+1)(2j'+3)}{(j'-m'+1)(2j'+1)}}} \quad (40)$$

$$= \frac{i\alpha \sqrt{\dfrac{(j'-m'+1)(2j'+1)}{(j'+m'+1)(2j'+3)}}}{[(j'+1)(j'+2) - \lambda]},$$

whence

$$\lambda = (j'+1)^2 \mp \sqrt{(j'+1)^2 - \alpha^2}. \quad (41)$$

We see that the quantum number λ for given j and m can take only two values, corresponding to the two possible choices of sign in Eq. (41). If one neglects the quantity α^2 and in Eq. (41) considers $\alpha^2 = 0$, then for this limiting case, instead of the quantum number λ we can introduce another quantum number l, defined according to

$$\lambda = l(l+1), \quad l \geqslant 0. \tag{42}$$

This quantum number, for a given j and m can take the following two values:

$$l_1 = j' = j - {}^1/_2, \quad l_2 = j' + 1 = j + {}^1/_2. \tag{43}$$

Conditionally, we can consider that even in that case where we do not neglect the quantity α^2, the state of the electron in a hydrogen atom is still characterized (aside from j and m) by the quantum number l (instead of λ), which can take the two values $l_1 = j - ½$ and $l_2 = j + ½$ (corresponding to the two possible values of λ : λ_1 and λ_2).

For given λ (or correspondingly, l), Eq. (40) permits one to find the ratio of $C_{j'+1}$ to $C_{j'}$.

Now we can go over to the solution of the equation for the radial function (15), which we write down in the form:

$$\left(\frac{\partial^2}{\partial r^2} + \frac{2}{r}\frac{\partial}{\partial r} - A + \frac{2B}{r} - \frac{C}{r^2}\right) f(r) = 0, \tag{44}$$

where

$$A = (m_0^2 c^2 / \hbar^2)[1 - (1 + \mathscr{E} / m_0 c^2)^2] \quad (\mathscr{E} = E - m_0 c^2). \tag{45}$$

$$B = (m_0 e^2 / \hbar^2)(1 + \mathscr{E} / m_0 c^2), \tag{46}$$

$$C = \lambda - \alpha^2 = (j'+1)^2 \mp \sqrt{(j'+1)^2 - \alpha^2} - \alpha^2 = l'(l'+1), \quad l' > 0. \tag{47}$$

The solution of such an equation is very well known (see e.g. reference 13, pg. 438).
In particular, in order to obtain the energy levels $\mathscr{E}$, it is necessary to introduce the radial quantum number k according to the formula *

$$B / \sqrt{A} = l' + k + 1 \tag{48}$$

(We are interested only in the discrete spectrum). The radial quantum number can take the values $k = 0, 1, 2, \ldots$. The energy levels are determined from the formula

$$\begin{aligned} 1 + \mathscr{E} / m_0 c^2 &= [1 + \alpha^2 / (l' + k + 1)^2]^{-1/2} \qquad (49) \\ &= [1 + \alpha^2 / (k + {}^1/_2 + \sqrt{{}^1/_4 + \lambda - \alpha^2})^2]^{-1/2}. \end{aligned}$$

Expanding the right side of Eq. (49) into a power series in α^2 and limiting ourselves to terms of the order of α^4, we shall have

$$\mathscr{E} / h = -\frac{R}{n^2}\left(1 + \frac{\alpha^2}{n^2}\left(\frac{n}{j + {}^1/_2} - \frac{3}{4}\right)\right), \tag{50}$$

$$n = j + 1 \mp \frac{1}{2} + k, \quad R = \frac{m_0 e^4}{4\pi h^3} = \frac{\alpha^2 m_0 c^2}{2h}.$$

We have derived precisely the fine structure formula, which corresponds to that obtained upon solution of Dirac's system of equations.

Thus, both the relativistically invariant equation of Dirac and the relativistically invariant Eq. (8) introduced in the present work, similarly lead to the fine structure formula (50). The shift in the energy levels, which is corroborated by recently obtained experimental data[14], is not predicted in either case. But the approach to this question from the viewpoint of the validity of the (approximate) equation (8) must understandably be out of the ordinary. The question about which of the relativistically invariant equations, Eq. (8) or the Dirac equation, better reveals the characteristics of phenomena in the micro-world, remains open.

4. CONVERSION TO A SYSTEM OF DIFFERENTIAL EQUATIONS OF FIRST ORDER

The relativistically invariant Eq. (8) which we used is a differential equation (more exactly, a system of equations) of second order. Dirac's equations, however, are first order differential equations. The natural question arises as to whether it is possible also to derive Eq. (8) from a system of first order differential equations which are themselves relativistically invariant. We shall show this is actually possible.

Let us consider the system of first order differential equations which relate the components of the two real spinors $\psi_{(1)}$ and $\psi_{(2)}$:

---

* If we take the value of l' negative, then the series for the radial function diverges.

[13] A. A. Sokolov and D. D. Ivanenko, *Quantum Field Theory*, GITTL, 1952

[14] Collection of Papers:*On Shift of the Levels of Atomic Electrons*", IIL, 1950

$$\nabla\psi_{(1)} - \frac{e}{\hbar c} JA\psi_{(1)} \tag{51}$$

$$= \frac{m_0 c}{\hbar}\psi_{(2)} \quad \left(A = A_\beta R^\beta, \nabla = R^\beta \frac{\partial}{\partial x^\beta}\right),$$

$$\nabla\psi_{(2)} + \frac{e}{\hbar c} JA\psi_{(2)} = \frac{m_0 c}{\hbar}\psi_{(1)}. \tag{52}$$

These equations are relativistically invariant. In fact, since $e/\hbar c$ and $m_0 c/\hbar$ are pseudoscalars, then as a result of the symmetry transformation characterized by the matrix-four dimensional vector A_1, the first equation goes over to

$$-A_1 \nabla A_1^{-1} A_1\psi_{(1)}$$

$$-\left(-\frac{e}{hc}\right) J(-A_1 A A_1^{-1}) A_1\psi_{(1)} = \left(-\frac{m_0 c}{\hbar}\right) A_1\psi_{(2)},$$

which corresponds to Eq. (51). Consequently, Eq. (51) is invariant with respect to transformations of the Lorentz group. Analogously, we convince ourselves of the relativistic invariance of Eq. (52).

A characteristic feature of Eqs. (51) and (52), as well as of Eq. (8), is that they do not change upon substitution of

$$\psi_{(1)} \text{ by } e^{Jf}\psi_{(1)}, \quad \psi_{(2)} \text{ by } e^{-Jf}\psi_{(2)}, \tag{53}$$

$$A_\alpha \text{ by } A_\alpha - \frac{\hbar c}{e}\frac{\partial f}{\partial x^\alpha}.$$

The conversion of all the quantities according to Eq. (53) can be considered as a gauge transformation. It is important only to note that the determination of the gauge transformation in accordance with Eq. (53) differs from the usual, in particular in that here f must be considered as an arbitrary function multiplied by a pseudoscalar, which accordingly changes sign under four-dimensional reflections.

Let us multiply both sides of Eq. (51) from the left by the operator $\nabla + \frac{e}{\hbar c} JA$. Using formula Eq. (31) of reference 8, we obtain

$$\left[\nabla^2 + \frac{e}{\hbar c} JF + \frac{e}{hc} JR^\alpha R^\beta A_\beta \frac{\partial}{\partial x^\alpha}\right.$$

$$\left. + \frac{e}{hc} JR^\beta A_\beta R^\alpha \frac{\partial}{\partial x^\alpha} - \left(\frac{e}{hc}\right)^2 A^2\right]\psi_{(1)} = \frac{m_0^2 c^2}{h^2}\psi_{(1)}$$

or, considering that $R^\alpha A + AR^\alpha = 2\,\delta^\alpha_\beta\, 2A^\alpha$, we find

$$\left[\Box - \left(\frac{e}{\hbar c}\right)^2 A^2\right.$$

$$\left. + \frac{e}{\hbar c} J\left(F + A^\alpha \frac{\partial}{\partial x^\alpha} + \frac{\partial}{\partial x^\alpha} A^\alpha\right)\right]\psi_{(1)} = \frac{m_0^2 c^2}{h^2}\psi_{(1)}.$$

Having assumed $\hat{E} = \hbar J \frac{\delta}{\delta t} + e\phi$, $\hat{P}_k = -\hbar J \frac{\delta}{\delta x^k} + \frac{e}{c} A_k$, we shall have

$$\left(\hat{E}^2 - c^2 \sum_k \hat{P}_k^2 - m_0^2 c^4 + e\hbar c JF\right)\psi_{(1)} = 0, \tag{54}$$

which agrees with Eq. (8).

Analogously, multiplying Eq. (52) from the left by the operator $\nabla - \frac{e}{\hbar c} JA$, we obtain

$$\left[\left(-\hbar J \frac{\partial}{\partial t} + e\varphi\right)^2 - c^2 \sum_k \left(\hbar J \frac{\partial}{\partial x^k} + \frac{e}{c} A_k\right)^2\right.$$

$$\left. - m_0^2 c^4 - e\hbar c JF\right]\psi_{(2)} = 0. \tag{55}$$

This equation differs from Eq. (8) only in that J is replaced by $-J$, which corresponds to replacing i by $-i$ in Eq. (9), but this can not change the physical results, so that Eq. (55) is equivalent to Eq. (54).

In this way, the relativistically invariant differential equation of second order which we studied, and which becomes directly a simple generalization of Pauli's equation (5), is obtained as a result of the system of first order Eqs. (51) and (52).

We note that for the consideration of discrete problems, another manner of writing Eqs. (51) and (52) may prove useful. Namely, we consider

$$\psi_{(1)} \leftrightarrow \xi = \begin{pmatrix}\xi_1\\ \xi_2\end{pmatrix} = \begin{pmatrix}\psi_{(1)1} + i\psi_{(1)3}\\ \psi_{(1)2} + i\psi_{(1)4}\end{pmatrix}, \tag{56}$$

$$\psi_{(2)} \leftrightarrow \eta = \begin{pmatrix}\psi_{(2)1} + i\psi_{(2)3}\\ \psi_{(2)2} + i\psi_{(2)4}\end{pmatrix}.$$

We use the fact that, according to reference 1,

$$-B\psi_{(1)} \leftrightarrow \begin{pmatrix} 0 & -e^{-iu}\\ e^{-iu} & 0\end{pmatrix}\begin{pmatrix}\bar{\xi}_1\\ \bar{\xi}_2\end{pmatrix} \tag{57}$$

$$= e^{-i(u+\pi/2)}\sigma_2\bar{\xi}.$$

For definiteness, we can assume, as in reference 1 (pg. 662), that $u + \pi/2 = 0$, since the parameter u can be chosen arbitrarily. Therefore, from Eqs. (51) and (52), using Eq. (57), we get

$$\left[\sigma_k\left(\frac{\partial}{\partial x^k} + i\frac{e}{hc}A_k\right) + \frac{1}{c}\left(\frac{\partial}{\partial t} - i\frac{e}{h}\varphi\right)\right]\xi \tag{58}$$

$$= \frac{m_0 c}{h}\sigma_2\bar{\eta},$$

$$\left[\sigma_h\left(\frac{\partial}{\partial x^h} - i\frac{e}{hc}A_h\right) + \frac{1}{c}\left(\frac{\partial}{\partial t} + i\frac{e}{h}\varphi\right)\right]\eta \quad (59)$$

$$= \frac{m_0 c}{h}\sigma_2\bar{\xi}.$$

In order to be able to study the system of equations (51), (52) in more detail, it is necessary to find out for which system of tensors the two real spinors $\psi_{(1)}$ and $\psi_{(2)}$ are parameters, and how the primary tensors are related among themselves. This question will be considered in the following paper.

Translated by R. L. Eisner
94

SOVIET PHYSICS JETP VOLUME 1, NUMBER 3 NOVEMBER, 1955

Interaction of Protons with Tritium and the Excited State of He^4

N. A. VLASOV, S. P. KALININ, A. A. OGLOBLIN, L. N. SAMOILOV, V. A. SIDOROV AND V. I. CHUEV
Academy of Sciences of the USSR

(Submitted to JETP editor March 9, 1955)
J. Exper. Theoret. Phys. USSR **28**, 639-650 (June, 1955)

Experiments are described in which the reactions $T(pn)He^3$ and $T(p\gamma)He^4$ were investigated in the proton energy range up to 7 Mev. The energy of the protons in the beam emerging from the cyclotron chamber was varied by means of lead filters. An "all-wave" counter and a uranium chamber served as neutron detectors, while a scintillation counter with a crystal of NaI(Tl) was used as a γ-ray detector. The curve of $\sigma(E_p)$ for the first reaction has a maximum at $E_p = 3$ Mev. The cross section for the second reaction increases monotonically in the entire energy interval. Angular distributions of the neutrons and the γ-rays were also investigated. The characteristics of the excited state of He^4 are discussed.

THE first indications of the existence of an excited state of He^4 were obtained in the work of Taschek and collaborators[1,2] in which it was found that the cross section for the reaction $T(pn)He^3$ increases monotonically in the proton energy range E_p from the threshold (1.019 Mev) to 2.8 Mev, and in which γ-rays with energy > 20 Mev, formed as a result of radiative capture of a proton by tritium, i.e., the reaction $T(p\gamma)He^4$ were observed. The absence of a horizontal portion in the curve of $\sigma(E_p)$ for the reaction $T(pn)He^3$ at energies higher than 1.5 - 2 Mev, exceeding the potential barrier, was explained by the existence of a resonance maximum of the cross section outside the energy range which was investigated, connected with an excited state of He^4. The discovery of γ-rays from the reaction $T(p\gamma)He^4$ and the increase in their yield with E_p were regarded as a confirmation of this hypothesis.

In order to observe the resonance with certainty and to decide the question as to the existence or non existence of an excited state of He^4, it was obviously necessary to investigate the cross sections for the reactions $T(pn)He^3$ and $T(p\gamma)He^4$ in a wider energy range. It was in this connection that the present investigation was undertaken. The main results were obtained early in 1953 and reported to the Academy of Sciences of the USSR in March of 1953. At this time only the short communication of Willard and Bair[3] was available, stating that the cross section for the reaction $T(pn)He^3$ increases monotonically up to $E_p = 5$ Mev. This was in contradiction to our results which indicated the existence of a cross section maximum at $E_p = 3$ Mev. Later, Willard, Bair and Kington[4] published a detailed report of their work giving results which are in satisfactory agreement with ours in the common energy interval.

The present paper contains a description of our experiments and gives the results obtained. Excitation curves of the reactions $T(pn)He^3$ and $T(p\gamma)He^4$ were investigated in the proton energy interval up to 7 Mev. For the first reaction the absolute value of the cross section was found, for the second only the lower limit of the cross section. The angular distribution of the neutrons was investigated for several values of E_p, as well as the angular distribution of the γ-rays at $E_p = 6.7$ Mev.

THE REACTION $T(pn)He^3$

For the investigation of the excitation curves a beam of protons was used which was brought out of the cyclotron and focused by means of a magnetic prism at a distance of 12 meters from the cyclotron chamber. The energy of the protons in the beam was determined by Rybakov[5] on the basis of their range in aluminum, using Smith's[6] curve and was found to be 7.3 ± .1 Mev.

Proton energy was varied by passing the beam through retarding filters of variable thickness. The filters were placed immediately in front of the target in order to minimize changes in intensity of the beam due to scattering in them. In order to minimize neutron background due to (p, n) reactions, lead, instead of aluminum, was used as

---

[1] G. A. Jarvis, A. Hemmendinger, H. V. Argo and R. E. Taschek, Phys. Rev. **79**, 929 (1950)

[2] H. V. Argo, H. T. Gittings, A. Hemmendinger, G. A. Jarvis and R. E. Taschek, Phys. Rev. **78**, 691 (1950)

[3] H. B. Willard and J. K. Bair, Phys. Rev. **86**, 629 (1952)

[4] H. B. Willard, J. K. Bair and J. D. Kington, Phys. Rev. **90**, 865 (1953)

[5] B. V. Rybakov, J. Exper. Theoret. Phys. USSR **28**, 651 (June, 1951); Soviet Phys. **1**, 435 (1955)

[6] J. H. Smith, Phys. Rev. **71**, 32 (1947)

filter material. The curve giving the dependence of proton energy on the thickness of the lead filter obtained by Rybakov[5] was used.

A zirconium foil saturated with tritium was used as target. The mean energy loss in the target for protons with energy of 7 Mev was 0.6 Mev; with decrease of mean proton energy it increased, reaching 1.1 Mev at $E_p = 3$ Mev. Because of this, the low energy end of the excitation curve was obtained under conditions of poor resolution in energy, and the maximum of neutron yield at angle of emergence $\theta = 0°$ with above-threshold proton energy was not observed. In Fig. 1 the energy spread of the proton beam passing through the target is represented by horizontal line segments about the points, Nevertheless, the width of the maximum sought was markedly greater than this instrumental width, and the shape of the curve obrained in our experiments in the region of the maximum and beyond is, apparently, not far from the true one.

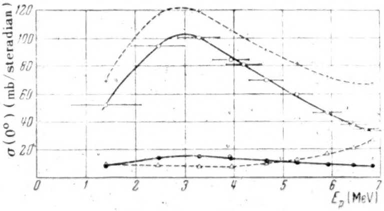

Fig. 1. Differential cross section for the reaction $T(pn)He^3$ at the angle of 0°. O = σ (0°) for the reaction $T(pn)He^3$, + = target, Δ = control, ● = background of scattered neutrons.

In order to estimate the considerable neutron background due principally to (*pn*) reactions in zirconium, the measurements were made alternately with the tritium-zirconium target and with a zirconium target (without tritium) which will be referred to in what follows, for brevity, as the control. The zirconium foil on the control was of the same thickness as on the target. Subtracting the effect of the control from the effect due to the target gave, therefore, the effect due to the tritium. Change from target to control and vice versa was made very quickly by means of remote control mechanisms. A similar mechanism was used for changing filters, hence measurements under different conditions could be repeated many times and be alternated with each other without disconnecting the cyclotron and the measuring apparatus.

As the basic neutron detector, the "all-wave" counter described in reference 7 was used. A fission chamber with a layer of natural uranium was used as a control detector. The detector was attached to the remotely-controlled turntable and could be placed so as to make any angle θ with the proton beam from 0° to 140°.

The detector counts were related to a definite proton beam current which was measured by means of a current integrator. In order to exclude the distorting influence of electron emission from the target on measurements of proton current, the target was covered with a thin sheet of mica coated on both sides with a thin layer of aluminum. The front layer of aluminum (facing the beam) was grounded, while the rear layer was in contact with the target and together with it, was electrically insulated. This construction of the target results in a slight lowering of the initial energy of the protons because of slowing down in the mica (under our conditions 200 kev at $E = 7$ Mev), but is very simple and convenient to work with.

Figure 1 gives the curve showing the dependence of the differential cross section at $\theta = 0°$ on the energy of the protons (upper solid curve); it is based on the mean of several series of measurements. Dotted curves represent, to a corresponding scale, the magnitude of neutron flux from target and control. The absolute value of the cross section was found by means of special measurements of neutron flux by comparing it with the flux from a calibrated (with accuracy of 5%) Ra + Be source in the same position as the target. The amount of tritium in the target was known from the preparer's certificate and in addition was measured by a calorimetric method with accuracy of ± 4%*. The two results coincided within the limits of experimental error. Errors in the absolute value of the differential cross section (± 10%) result from errors in calibration of the Ra + Be source given above and the determinations of the amount of tritium in the target, as well as from errors in the measurements of proton flux (± 2%). Statistical errors of all measurements did not exceed 1%.

In the adjustment of the results of measurements, it was assumed that the sensitivity of the all-wave detector was the same in the entire neutron energy range (up to 6 Mev). Control measurements with a proportional countertelescope showed that the sensitivity of the "all-wave" counter to neutrons with energy of 4.4 and 6.3 Mev differs by not more than 10%. In addition, the excitation curve of the reaction under investigation was also determined by using the uranium fission chamber. After correcting for the energy dependence of the uranium fission cross section[8], satisfactory agreement was found between this curve and the curve obtained with the "all-wave" counter in the interval $2.5 < E_p < 7$ Mev. At $E_p < 2.5$ Mev the results of the comparison are less certain because of rapid variation in the uranium fission cross section.

---

* The authors are grateful to A. I. Shal'nikov for the preparation of the target and to N. S. Shimanskaia for calorimetric measurements.

[7] A. O. Hanson and J. H. McKibben, Phys. Rev. **72**, 673 (1947)

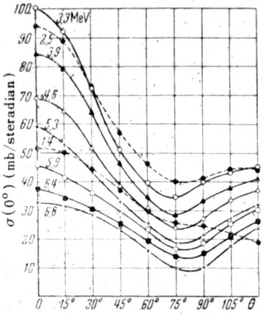

Fig. 2. Angular distribution of the neutrons in the reaction $T(pn)He^3$ in the laboratory coordinate system.

Figure 2 gives the results of the measurements of angular distribution of the neutrons for several values of proton energy. Each curve is the result of several series of measurements, the results of which were averaged. The values of the differential cross sections were found by means of a joining to the absolutized excitation curve for $\theta = 0$. In angular distribution measurements, besides the effect of the control, the background of neutrons scattered from the walls of the room was taken into account. For this prupose, a paraffin cone 40 cm long was placed between target and counter, the distance between which was 1 meter (to the front side of the counter). The direct flux of neutrons from the reaction under investigation for each value of the angle was calculated on the basis of four measurements, according to the formula

$$N(\theta) = M_0(\theta) - \Phi_0(\theta) + \Phi_к(\theta) - M_к(\theta),$$

where M_0 is the number of counts with target in the beam without the paraffin cone, Φ_0 the same with control but without the cone, M_k with target but without cone, Φ_k with control and cone. In order to give an idea of the relative values of these four quantities, Fig. 3 gives their angular distributions corresponding to $E_p = 7$ Mev. With large angles (greater than 130°) the background of scattered neutrons increases greatly; therefore, the results in this region are less depdedable than with $\theta < 130°$.

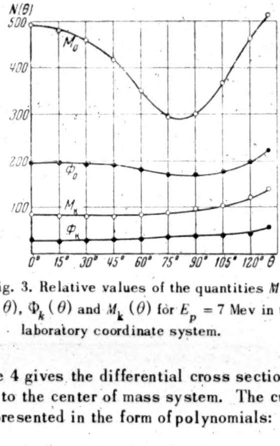

Fig. 3. Relative values of the quantities $M_0(\theta)$, $\Phi_0(\theta)$, $\Phi_k(\theta)$ and $M_k(\theta)$ for $E_p = 7$ Mev in the laboratory coordinate system.

Figure 4 gives the differential cross sections reduced to the center of mass system. The curves were represented in the form of polynomials:

$$N(\vartheta) = A + B\cos\vartheta + C\cos^2\vartheta + D\cos^3\vartheta + E\cos^4\vartheta,$$

whose coefficients were found by the method of least squares from the experimental points for θ from 0° to 120° (θ is the angle in the center of mass system). Figure 5 gives the dependence of the coefficients on the proton energy. By integrating the polynomials the total reaction cross section for the reaction $T(pn)He^3$ was obtained for each value of E_p. Figure 6 gives the dependence of the total cross section on E_p.

Measurements were also made of the spectrum of neutrons emerging from the tritium-zirconium target by means of the proportional counter telescope. The measurements were made with $\theta = 0^\circ$ at $E_p = 7.1$ and 5.2 Mev. The telescope consisted of three counters. The first two were in coincidence, while the third was in anticoincidence with respect to the first two. Recoil protons, knocked forward at a narrow angle from a paraffin radiator 10.4 mg/cm^2 thick, were slowed down in aluminum filters of variable thickness placed beyond the radiator. Simultaneously, the number of coincidences and of the anticoincidences were recorded as a function of filter thickness. Passage from filter thickness to energy of recoil proton, equal to energy of neutron, was made with the aid of Smith's[6] curve, referred to above. The number of recoil protons in the energy interval ΔE, depending on the thickness of the filter between the second and third counter, is equal to the number of anticoincidences. Under our conditions, $\Delta E = 650$ kev at $E_n = 6$ Mev. Figure 7 gives the dependence of the numbers of coincidences and anticoincidences on neutron energy, estimated from filter thickness. The curve of anticoincidences with a maximum at $E = 6$ Mev represents the spectrum of the neutrons. The width of the maximum depends not only on the scatter of neutrons in energy, but also on the resolving power of the telescope. The natural line width of the telescope calculated from geometrical conditions and the thicknesses of radiator and absorber between second and third counters was .85 Mev (at half-height), while the observed width was 1.0 Mev. The small number of anticoincidences at $E_n < 5$ Mev is due, apparently, chiefly to the geometrical imperfection of the telescope, and, to a lesser extent, to scattered neutrons.

---

[8] Canad. J. Phys. **29**, 204 (1951)

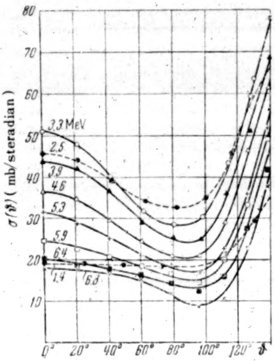

Fig. 4. Angular distribution of the neutrons in the reaction $T(pn)He^3$ in the center-of-mass system.

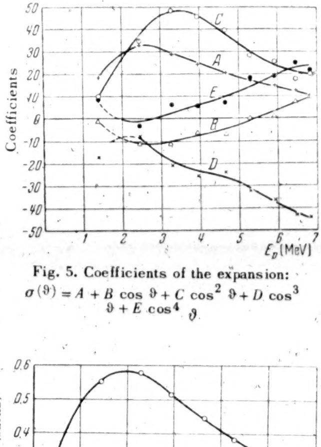

Fig. 5. Coefficients of the expansion: $\sigma(\vartheta) = A + B\cos\vartheta + C\cos^2\vartheta + D\cos^3\vartheta + E\cos^4\vartheta$.

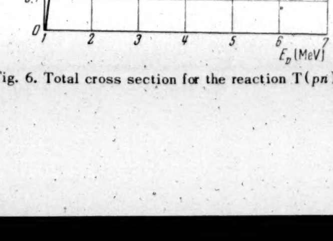

Fig. 6. Total cross section for the reaction $T(pn)He^3$.

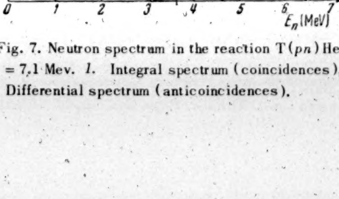

Fig. 7. Neutron spectrum in the reaction $T(pn)He^3$ at $E_p = 7.1$ Mev. *1.* Integral spectrum (coincidences), *2.* Differential spectrum (anticoincidences).

These measurements indicate that a monochromatic group of neutrons is emitted from the target with mean energy of 6 Mev, which coincides with the calculated value, if one uses proton energy of 7.1 Mev and reaction energy $Q = -.764$ Mev. If other groups of neutrons are formed in this reaction, the probability of their formation must be relatively small. When the zirconium control is placed in the beam of protons, recoil protons in the telescope are observed only with energy less than 3 Mev (dotted curve in Fig. 7). This indicates that neutrons formed in (pn) reactions in zirconium have energy less than 3 Mev.

Analogous results were obtianed also at $E_p = 5.2$ Mev. In this case the maximum of the neutron spectrum corresponds to an energy of 4 Mev.

Using the known values of scattering cross sections of neutrons on protons[9] and knowing the known geometrical parameters of the telescope, it is possible to calculate the absolute intensity of the flux of neutrons of the main group, and hence the absolute value of the differential cross section of the reaction $T(pn)He^3$ at the angle $\theta = 0$. Measurements of the proton current in this experiment were made by the same methods as in the preceding ones. The values of the cross section calculated in this way are in satisfactory agreement with values obtained by comparison of the neutron flux from the target with the flux from the Ra + Be source with the aid of the all-wave counter.

REACTION $T(p\gamma)He^4$

Studies of the reaction $T(p\gamma)He^4$ were made following the same procedure as described above, except that a scintillation counter with a NaI(Tl) crystal and FEU-19 photomultiplier was used as a γ-ray detector. It was known[2], and confirmed by our very first experiments, that the intensity of γ-rays is low, and hence to register them a highly effective detector is necessary. In addition, in our experimental conditions, an intensive background of γ-rays was present around the target, due to reactions and radioactivity produced by protons and neutrons. It is possible to eliminate this background, using the fact that the γ-rays in question have energy not less than 20 Mev, while the background γ-rays have a markedly lower energy. For this a detector-spectrometer is necessary, which can make an energy analysis of the γ-rays. It was because of these considerations that the crystal of NaI(Tl) was chosen as detector. The counter pulses were registered by an 8-channel pulse height analyzer adapted for switching the working interval into different regions of the spectrum. The crystal had the form of a rectangular prism about 4 cm high and with a 2×2 cm cross section. It was placed directly on the photomultiplier column and was coated with a layer of magnesium oxide. Optical contact between the crystal and the FEU was made by means of a layer of oil.

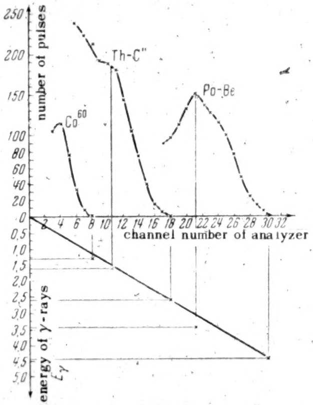

Fig. 8. Spectral characteristics of the γ-ray detector.

The spectrometric properties of our detector are represented by the curves of Fig. 8, which give the differential spectra of the pulses produced by γ-rays of Co^{60} (1.3 Mev), ThC'' (2.6 Mev) and C^{12*} (4.4 Mev, Po + Be source). The curves do not show distinct peaks corresponding to photoelectrons, Compton-electrons or pairs, formed in the crystal, but the limits of the spectra are rather sharp. If the pulse heights corresponding to them are taken as proportional to the total energy of the quanta, the dependence of the pulse height on energy turns out to be linear. This dependence is pictured in the lower part of Fig. 8. If the upper limit of the spectrum of γ-rays from the target is regarded as being due to the γ-rays of the reaction $T(p\gamma)He^4$ whose energy should be equal to 25 Mev, and the corresponding point be plotted in the lower half of Fig. 8, it is found to fall satisfactorily on the straight line through the other points. This indicates that high pulses in the counter were actually produced by γ-rays from the reaction $T(p\gamma)He^4$. It is to be remarked that in order to maintain the linear relation between spectral limit and γ-ray energy it was necessary to increase the potential difference between the last dynodes of the multiplier. With a uniform distribution of potential between dynodes, the linearity was not maintained, and this occurred the sooner, the higher the total voltage.

---

[9] C. Bailey, W. Bennett, T. Bergstralh, R. Nukkols, H. Richards and J. Williams, Phys. Rev. 70, 583 (1946)

It is clear that if one registers only the high pulses it is possible to separate out the γ-rays sought. In fact, experiments showed that with a discrimination level corresponding to γ-ray energy exceeding 15 Mev, the background from the zirconium control remained low. Hence during all measurements the analyzer was tuned for the energy interval from 14 to 25 Mev. Spectra of the pulses from target and control at $E_p = 6.8$ Mev and 5.7 Mev are given in Fig. 9.

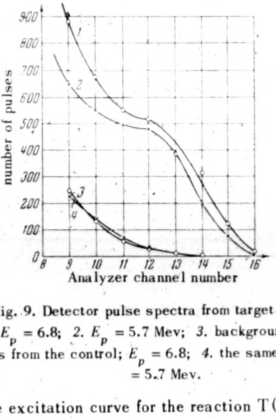

Fig. 9. Detector pulse spectra from target γ-rays. 1. $E_p = 6.8$; 2. $E_p = 5.7$ Mev; 3. background of γ-rays from the control; $E_p = 6.8$; 4. the same, $E_p = 5.7$ Mev.

The excitation curve for the reaction $T(p\gamma)He^4$ was taken as follows. The counter was placed at an angle $\theta = 90°$ to the proton beam at a distance of 50 cm from the target, and the number of counts was recorded in each of the eight channels of the analyzer, at the maximum proton energy and one of the lower energies in turn. In this way the intensities of the γ-ray flux at $\theta = 90°$ and various energies of bombarding protons were compared with the intensity at $E_p = 6.8$ Mev. This method of making the measurements was necessary in order to exclude the effect of detector instability. All counts, as in the experiments described above, were related to a definite proton current measured with an integrator.

Passage from the number of counts to γ-ray intensity is complicated by the circumstance that γ-ray energy varies with proton energy. As a result the limits of pulse spectra are displaced toward the region of smaller pulse heights with decreasing proton energy. The results of our experiments showed that the displacement of spectral limit is correlated with change of γ-ray energy calculated according to the formula

$$E_\gamma + \frac{E_\gamma^2}{2M_{He}c^2} = Q + \frac{M_t}{M_t + M_p} E_p,$$

where M_{He}, M_t and M_p are the masses of He^4, T and H^1 and $Q = 19.8$ Mev is the binding energy of the proton in He^4. Since the pulse spectra have neither a maximum nor even a clearly defined plateau, it would be incorrect to regard the intensity of the γ-rays as proportional to the number of counts in a given channel of the analyzer at any proton energy. Therefore, in order to determine the ratios of γ-ray intensity at two values of E_p, we calculated the ratios of the spectrum areas bounded on the left by ordinates proportionally distant from the upper limit. Depending on the magnitude of the portion of the proportionally cut out areas these ratios fluctuated about a mean value, which was taken as the true one. This method of reduction assumes similarity of spectra at all values of E_p. Absence of systematic variation of the ratios studied with increase of portions compared confirms this supposition.

Ratios of areas obtained in this way are not, in general, equal to the ratio of intensities of the γ-rays at corresponding E_p, since, first, the probability of absorption of the quantum in the crystal, and second, the probability of complete slowing down in the crystal of electrons produced by the quantum in the crystal, both depend on the energy of the γ-rays. But since these effects have opposite sign and, in our conditions, are small and approximately equal in magnitude, the ratios of areas were taken to be equal to the ratios of intensities.

Figure 10 gives the dependence of the intensity of γ-rays at the angle of 90° on proton energy, obtained in this way. As is shown below, the angular distribution of γ-rays varies little in the entire interval of E_p under investigation. Hence it can be assumed that the total reaction cross section for $T(p\gamma)He^4$ varies similarly.

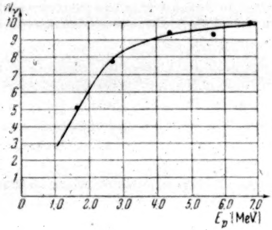

Fig. 10. Relative yield of γ-rays N_γ in the reaction $T(p\gamma)He^4$ at angle of 90° as a function of proton energy E_p.

To determine the absolute value of the effective cross section of the reaction on the basis of the available data is impossible. One can estimate only the lower bound of the cross section by the following method. The pulse spectra from the γ-rays of the target have a slight shelf not far from the limit. If one drops an ordinate from the middle of the shelf and assumes that the total number of pairs formed in the crystal is given by twice the area to the right of the ordinate, then, using this number and knowing the cross section for pair formation as well as the flux of protons to the target and the amount of tritium in it, it is possible to calculate the differential cross section of the reaction $T(p\gamma)He^4$ for the angle of 90°. It is obvious that the area of the spectrum bounded in this way does not include all pairs formed in the crystal, since pairs with nonsymmetrically distributed energy have a greater probability to carry off out of the crystal part of the energy, and give a pulse markedly lass than maximal. Hence the calculated value of the cross section is only a lower bound. For $E_p = 6.8$ Mev the value $\sigma(90°) > 0.006$ mb/steradian was obtained.

Taking the angular distribution of the γ-rays to have the form $\sigma(\theta) = \sin^2\theta + 0.05$, we obtain as the lower bound of the total cross section $\sigma_{total} > 0.04$ mbn. These results are in agreement with those of Perry and Bame[10], obtained with $E_p < 4.3$ Mev. The angular distribution of γ-quanta was not systematically investigated at all angles, since the construction of the target was such that the flux of γ-rays was diminished differently (up to 40%) in different directions due to variable thicknesses of material. It is impossible to obtain a dependable estimate of this decrease by calculation. Hence, in order to check the angular distribution, we carried out a comparison of the γ-ray intensities for several pairs of angles relative to which the target could be placed symmetrically. Thus, e.g., in order to compare the intensities at 0° and 90°, the target was placed at 45° to the proton beam; hence equal thicknesses of material were in the path of the γ-rays in both directions. The comparison was made for the following pairs of angles: 0 - 90°, 0 - 30°, 0 - 60° with maximal energy of protons.

The angular distribution of γ-rays at lower proton energies was investigated previously[2]. It was found to have the form

$$\sigma(\theta) \doteq \sin^2\theta + a,$$

where $a \doteq 0.11$ at $E_p = 1.52$ Mev and $a = 0.09$ at $E_p = 2.16$ Mev. We assumed that it has the same form also at high E_p, and compared the results of intensity measurements at each pair of angles, finding the suitable value of a from the relation

$$a = \frac{I_1 \sin^2\theta_2 - I_2 \sin^2\theta_1}{I_2 - I_1}.$$

For the various pairs of angles the following values were obtained:

$$\theta = 0 - 90°,\ a = 0.06;$$
$$\theta = 0 - 60°,\ a = 0.04;$$
$$\theta = 0 - 30°,\ a = 0.03.$$

Although the scatter of the values of a obtained is rather large, which is natural since the result depends on the difference of two quantities of the same order of magnitude, nevertheless, these results indicate that the given formula satisfactorily describes the angular distribution of the γ-quanta at $E_p = 6.8$ Mev. The value of the quantity a is most reliably found from a comparison of the intensities at 0° and 90°. The measurements for this pair of angles were made with greater care than for other angles; hence for the quantity a at $E_p = 6.8$ Mev the value $a = 0.05$ can be taken.

Measurements at 120° showed that the distribution is approximately symmetrical relative to the 90° direction. In comparing intensity at 120° with intensities at smaller angles, the absorption of γ-rays in the details of the target was taken into account. In reducing the results of angular distribution measurements, the displacement of the spectra was not taken into account, since the energy of the γ-quanta varies comparatively little with angle of emission.

---

[10] J. E. Perry and S. J. Bame, Phys. Rev. 90, 380 (1953)

DISCUSSION OF RESULTS

The curve giving the dependence of the cross section on proton energy, for the reaction $T(pn)He^3$, has a broad maximum at $E_p = 3$ Mev. (cf. Fig. 6). The width of the maximum is markedly greater than the instrumental width due to measuring apparatus. In reference 4 a similar curve was obtained in the energy range up to 5 Mev under better conditions of resolution in energy. The results of this paper (reference 4) are more accurate at low energy. In the region of the maximum and beyond they agree satisfactorily with ours in respect to both the absolute value of σ and its variation with energy.

In spite of the large width of the maximum, the shape of the curve $\sigma(E_p)$ indicates a resonance in the reaction, connected with an excited state of He^4. The position of the resonance and the energy of the level cannot be determined with high accuracy for two reasons. First, the level is very broad, and second, besides the state responsible for resonance, large but undetermined contributions to the cross section are made by nonresonant states, as follows from a consideration of the angular distribution of the neutrons (cf. below). Hence an analysis of the curve $\sigma(E_p)$ by means of the Breit-Wigner formula cannot give unique results. Using directly the value $E_p = 3$ Mev, corresponding to the maximum of the curve of $\sigma(E_p)$, it is possible to give the value of the energy of the excited state of He^4 as 22 Mev. This level exceeds by 2.2 Mev the energy of dissociation of He^4 into $T + p$ and by 1.5 Mev the energy of dissociation into $He^3 + n$. It is therefore to be expected that the level should be wide and that the lifetime of He^4 in the corresponding state is very short.

Attempts to observe the excited states of He^4 by other methods[11,12] did not give positive results. They indicate only that He^4 does not have excited states at lower energies. In reference 12 in which the scattering of protons with energy of 32 Mev on He^4 was investigated, no inelastic scattering was found. However, the proton energy corresponding to excitation of He^4 to the 22 Mev level is near the lower limit of the spectrum observed in the experiment, and the large width of the level unquestionably leads to a marked blurring of the spectrum of the inelastically scattered protons; hence, the results of reference 12 cannot be regarded as contradicting our results.

The absolute value of the cross section for the reaction $T(pn)He^3$ at maximum, equal to 0.58 bn, is rather large. According to a remark of Baz' and Smorodinskii[13], this indicates that the resonance corresponds to a 2^- state, since the maximum value of the resonance cross section cannot exceed $\frac{1}{4}\pi\lambdabar^2(2l+1)$ ($\lambdabar = \lambda/2\pi$ is the wavelength of the proton in the center of mass system). At $E_p = 3$ Mev, $\frac{1}{4}\pi\lambdabar^2 = 0.36$ bn and comparison with the experimental cross section of 0.58 bn gives $l > 1$. It is to be remarked that with a large contribution to the cross section by nonresonant states this condition does not apply too rigorously, but if one takes $l = 1$, more than half of the cross section has to be attributed to nonresonant states, which seems improbable. The supposition that the resonance corresponds to a 1^- state is also contradicted by the excitation curve of the reaction $T(p\gamma)He^4$ which does not show a resonance in the region of 3 Mev. In this reaction the intermediate state is undoubtedly the 1^- state from which an electric dipole transition to the ground state 0^+ takes place. That the radiative transition is in fact electric dipole is indicated by the angular distribution of the γ-rays which has the form $\sigma(\theta) = \sin^2\theta + a$ where $a \ll 1$. The transition from the state 2^- to the ground state 0^+ must be a magnetic quadrupole transition. The probability of such a transition is much less than for an electric dipole transition, and it is, therefore, not surprising that no resonance is visible in the reaction $T(p\gamma)He^4$.

The supposition that the resonance is connected with the 2^- state is also in accord with the predictions of nuclear shell theory, according to which, above states s_0, there should be $p_{3/2}$ and $p_{1/2}$, the first of these corresponding to lower energy as is observed in He^5 and Li^5. The 2^- state in He^4 can be formed only from the $p_{3/2}$ proton state, and the angular momenta of the proton and of the tritium must be parallel. If the 2^- state is in fact the lowest excited state of He^4, this is in agreement not only with the level order predicted by shell theory, the levels being split by spin-orbit interaction, but with the fact that

---

[11] J. C. Allred, Phys. Rev. **84**, 695 (1951)

[12] J. Benveniste and B. Cork, Phys. Rev. **89**, 422 (1953)

[13] A. I. Baz' and Ia. A. Smorodinskii, J. Exper. Theoret. Phys. USSR **27**, 382 (1954)

the lowest levels are those with the maximum value of the spin, since from the $p_{3/2}$ proton state two states of He^4 can be formed, viz., 2^- and 1^-. In the latter state the spins of proton and tritium are antiparallel.

The angular distribution of the neutrons in the reaction $T(pn)He^3$ is characterized by a strong asymmetry (cf. Fig. 4). In the first place, the ratio of intensities at 0 and 180° to intensity at 90° (in the center-of-mass system) is rather large. As was pointed out by Baz' and Smorodinskii[13], the large value of the ratio $\frac{1}{2}[\sigma(0°) + \sigma(180°)]/\sigma(90°)$ indicates a large contribution to the cross section of the 1^- state. It is to be noted that this ratio continues to increase up to $E_p = 7$ Mev. If the level 1^- exists, this indicates that it is situated at $E_p > 7$ Mev, and, therefore, the magnitude of the splitting between the levels 2^- and 1^- exceeds 3 Mev in this case. Second, the asymmetry of the angular distribution relative to the angle of 90° is very great. If one calculates the ratio $\sigma(180°)/\sigma(0°)$, using empirical formulas in which the cross section is expanded in a series of cosines, the ratio turns out to be equal to 2.3 at $E_p = 3.3$ Mev and 4.9 at $E_p = 7$ Mev. The very large probability of the neutron emerging backward is a characteristic peculiarity of the reaction $T(pn)He^3$. This peculiarity distinguishes it from many other reactions. Formally this peculiarity of the reaction can be easily explained by the interference of waves ofdifferent parity, e.g., p-wave with s-wave. With the value of the ratio $\sigma(180°)/\sigma(0°) = 4$, the amplitude of the even wave must not be less than 1/3 the amplitude of the odd (p) wave. From this it is seen that the relative contribution of the even states to the reaction cross section is rather large. This is confirmed by the following: 1) The cross section of the inverse reaction $He^3(np)T$ with thermal neutrons is very large (5000 bn) and 2) The coefficient E of the $\cos^4 \vartheta$ term (Fig. 5) whose magnitude is apparently chiefly determined by the contribution of the d-state, reaches a large value at $E_p = 7$ Mev. The angular distribution obtained in the experiments of Willard et al. is in satisfactory agreement with the one obtained by us in the common energy interval.

The excitation curve for the reaction $T(p\gamma)He^4$, as already noted above, does not show resonance behavior, hence the state 1^- is not related to resonance in the reaction $T(pn)He^3$.

The radiative capture of the proton can be explained also with the assumption of the existence of a definite 1^- state. A formula is given by Flowers and Mandle[14] which gives the variation with energy of the cross section for non-resonant radiative capture for an electric dipole transition. Comparison of this formula with the experimentally determined variation of the cross section shows that agreement can be obtained if the constant ϵ in the formula of Flowers and Mandle[14], which represents the mean binding energy per nucleon in He^4, is set equal to 5 Mev, and if the range R of nuclear forces, used in calculating the penetrability of the potential barrier, is set equal to $R = 5 \times 10^{-13}$ cm. It should be noted that the shape of the theoretical curve is very sensitive to the magnitude of R.

The angular distribution of the γ-rays at $E_p = 7$ Mev turned out to be close to the one observed earlier[2]:

$$\sigma(\theta) \approx \sin^2\theta + a.$$

For the quantity a our results lead to the value $a = 0.05 \pm 0.01$, somewhat less than at $E_p = 1.52$ and 2.16 Mev ($a = 0.11$ and 0.09 resp). Apparently, the decrease of the magnitude of a with energy is beyond the limits of experimental error, even though the precision of the determination of this quantity is not great. It is not possible to explain the fact that $a \neq 0$ by the finiteness of the angular width of the apparatus and the scattering of protons in the target. Hence, the departure of the angular distribution from $\sin^2\theta$ must be regarded as real, but as one which decreases with proton energy. From an examination of the angular distribution of the neutrons it follows that the relative role of the 1^- state in the reaction $T(pn)He^3$ increases with E_p. The same is observed in the reaction $T(p\gamma)He^4$ if one assumes that the component connected with $a \neq 0$ is due to a different intermediate state.

The demonstration of the existence of the excited state of He^4 makes it possible to make certain conclusions concerning the states of the isobaric nuclei H^4 and Li^4. Since no levels lower than 22 Mev have been found in He^4, H^4 and Li^4 cannot have bound states. If the excited state of He^4 with energy near 22 Mev has isotopic spin $T = 1$, corresponding (similar) states, shifted by the difference in Coulomb energies, can also be present in H^4 and Li^4. Although the lifetimes of these states must be very small, nevertheless it would be possible to detect them in various nuclear reactions, e.g., T(*dp*)H^4, He^3(*dn*)Li^4. If, however, the 22 Mev level of He^4 is characterized by isotopic spin $T = 0$, as is supposed by Baz' and Smorodinskii [13], then corresponding states of H^4 and Li^4 cannot exist, and the question as to the existence of H^4 and Li^4 is decided in the negative sense.

---

[14] B. H. Flowers and F. Mandle, Proc. Roy. Soc. (London) **206 A**, 131 (1951)

The authors express their gratitude to the staff of the Cyclotron Laboratory for making this work possible, and to Ia. A. Smorodinskii, A. I. Baz' and Iu. M. Popov for discussion of the results.

Translated by A. V. Bushkovitch
118

SOVIET PHYSICS JETP VOLUME 1, NUMBER 3 NOVEMBER, 1955

The Effect of Electrical Fluctuations on a Vacuum Tube Oscillator

P. I. KUZNETSOV, R. L. STRATONOVICH AND V. I. TIKHONOV
Moscow State University

(Submitted to JETP editor June 15, 1954)
J. Exper. Theoret. Phys. USSR **28**, 509-523 (May, 1955)

The effect of "slowly varying" normally distributed random fluctuations on a vacuum tube oscillator is investigated. Expressions are obtained for the one-dimensional probability density functions of amplitude and phase. An approximation method is shown for the determination of the correlation functions of amplitude and phase.

RECENTLY great interest has been shown in the behavior of a vacuum tube oscillator subjected to electrical fluctuations originating either within the oscillator itself ("internal fluctuations"), or caused by external random occurrences ("external fluctuations"). These latter are sometimes the result of irregular voltage fluctuations of the power supply and occasionally they may be caused by the modulating effect of the oscillator voltage. Frequently these external fluctuations are characterized by a correlation time which is much longer than the corresponding time constants of the oscillator, and therefore, the fluctuations can be regarded as varying slowly compared with the natural oscillations of the oscillator in the absence of these fluctuations.

In the present paper, a general method will be shown for predicting the behavior of the oscillator under the influence of slowly varying electrical fluctuations. The method is based on the generalized equation of Einstein-Fokker [1] and differs slightly from the method given in a previous paper[2-4] for the analysis of high frequency internal fluctuations, provided they are of small order of magnitude.

1. It is well known[5] that a harmonic vacuum tube oscillator can be regarded as a quasi-linear self-oscillatory conservative system with one degree of freedom. The behavior of such a system in presence of an external random disturbance $\xi(t)$ can be generally described by the following equations:

$$\frac{dx_1}{dt} = f_1(x_1, y_1, \xi), \qquad \frac{dy_1}{dt} = g_1(x_1, y_1, \xi), \tag{1}$$

wherein x_1 and y_1 are characteristic variables describing the state of the system, e.g., current and voltage.

Separating in these equations the constant and linear parts and expressing the time derivative by a dot over the variables, we can write,

$$\dot{x}_1 = a_0 + a_1 x_1 + a_2 y_1 + f(x_1, y_1, \xi), \qquad \dot{y}_1 = b_0 + b_1 x_1 + b_2 y_1 + g(x_1, y_1, \xi), \tag{1a}$$

where the constants (a_0, b_0) and the coefficients of x_1 and y_1 depend on $\xi(t)$. The nonlinear terms f and g can be of the form

$$f = a_3 x_1^2 + a_4 x_1 y_1 + a_5 y_1^2 + a_6 x_1^3 + \ldots,$$
$$g = b_3 x_1^2 + b_4 x_1 y_1 + b_5 y_1^2 + b_6 x_1^3 + \ldots$$

Introducing new variables

$$x = x_1 - \alpha, \quad y = y_1 - \beta,$$

with

$$\alpha = \frac{b_0 a_2 - a_0 b_2}{a_1 b_2 - b_1 a_2}, \quad \beta = \frac{a_0 b_1 - a_1 b_0}{a_1 b_2 - b_1 a_2},$$

Eqs. (1a) become

$$x = a_1 x + a_2 y + f(x + \alpha, y + \beta, \xi) - \dot{\alpha}, \qquad \dot{y} = b_1 x + b_2 y + g(x + \alpha, y + \beta, \xi) - \dot{\beta}. \tag{2}$$

We shall consider first a linear system described by the differential equations of the first order:

$$\dot{x} = a_1 x + a_2 y, \quad \dot{y} = b_1 x + b_2 y.$$

As known, the solution of this system is

$$x = A_0 e^{-pt}[n \sin(\omega t + \varphi_0) + m \cos(\omega t + \varphi_0)],$$
$$y = A_0 e^{-pt} \sin(\omega t + \varphi_0),$$

---

[1] P. I. Kuznetsov, R. L. Stratonovich, V. I. Tikhonov, J. Exper. Theoret. Phys. USSR **26**, 189 (1954)

[2] L. Pontriagin, A. Andronov and A. Vitt, J. Exper. Theoret. Phys. USSR **3**, 165 (1933)

[3] I.L. Bershtein, Zh. Tekhn. Fiz. **11**, 305 (1941)

[4] I. L. Bershtein, Izv. Akad. Nauk SSSR, Ser. Fiz. **14**, 1 (1950)

[5] A. A. Andronov, S. E. Khaikin, *Theory of Oscillations*, State Technical Publishing House, 1937

wherein A_0 and ϕ_0 are integration constants determined by the initial conditions, and

$$\omega = \sqrt{-a_2 b_1 - \left(\frac{a_1 - b_2}{2}\right)^2}, \quad p = -\frac{a_1 + b_2}{2}, \qquad (3)$$

$$n = \frac{a_1 - b_2}{2b_1}, \quad m = \frac{\omega}{b_1}.$$

Going back to the original Eqs. (2), we notice that, in the absence of the random disturbance $\xi(t)$, we have the ordinary case of self-oscillatory operating condition of the oscillator. The consideration of the nonlinear terms will usually cause only a slight change in the frequency ω of the oscillations and will allow the determination of its stable amplitude. The presence of the random disturbance $\xi(t)$ at the stationary operating condition will cause random fluctuations of amplitude and phase about a certain mean.

Rewriting Eq. (2) in polar-coordinates

$$y = A \sin \vartheta, \quad x = A(n \sin \vartheta + m \cos \vartheta).$$

and taking Eq. (3) into consideration, we obtain

$$\dot{A} = F(A, \vartheta, \xi) - \dot{\gamma} \cos \vartheta - \dot{\beta} \sin \vartheta, \qquad (4)$$

$$\dot{\vartheta} = -\omega + G(A, \vartheta, \xi) - (1/A)(\dot{\beta} \cos \vartheta + \dot{\gamma} \sin \vartheta),$$

wherein

$$F(A, \vartheta, \xi) = -nA + \frac{f - ng}{m} \cos \vartheta + g \sin \vartheta,$$

$$G(A, \vartheta, \xi) = \frac{1}{A}\left(g \cos \vartheta + \frac{f - ng}{m} \sin \vartheta\right),$$

$$\gamma = (\alpha - n\beta) / m.$$

According to the method of Bogoliubov[5,6] (of which the well known method of van der Pol is a special case) we can introduce into these equations the mean of all terms over θ. This is justified even when the random disturbances $\xi(t)$ are of a higher order of magnitude, under the assumption that the time correlation of the random function $\xi(t)$ is very high as compared to the period T of the oscillations in the absence of $\xi(t)$:

$$\tau_{\mathrm{corr}} \gg 2\pi / \omega = T, \qquad (5)$$

Under this condition $\xi(t)$ will not change noticebly during one period (corresponding to one passage of the descriptive point through its cycle, i.e., the change of θ by 2π), so that it can be regarded substantially as constant.

Averaging, we obtain

$$\dot{A} = \Phi(A, \xi) + M, \quad \dot{\vartheta} = -\omega + \Psi(A, \xi) + N, \qquad (6)$$

wherein

$$\Phi(A, \xi) = \frac{1}{2\pi} \int_0^{2\pi} F(A, \vartheta, \xi)\, d\vartheta, \qquad (7)$$

$$\Psi(A, \xi) = \frac{1}{2\pi} \int_0^{2\pi} G(A, \vartheta, \xi)\, d\vartheta,$$

$$M = -\frac{1}{2\pi} \int_0^{2\pi} (\dot{\gamma} \cos \vartheta + \dot{\beta} \sin \vartheta)\, d\vartheta,$$

$$N = -\frac{1}{2\pi A} \int_0^{2\pi} (\dot{\beta} \cos \vartheta + \dot{\gamma} \sin \vartheta)\, d\vartheta.$$

As β and γ are changing slowly with time, their derivatives with respect to time, which are contained in the expressions for M and N, will be of small order of magnitude, also very slowly varying with time. The quantities M and N can therefore be neglected in the expressions for $\dot{A}$ and $\dot{\theta}$; we then obtain

$$\dot{A} = \Phi(A, \xi), \quad \vartheta = -\omega + \Psi(A, \xi). \qquad (6a)$$

2. For every given case Eq. (7) allows determination of the function Φ and Ψ which appear in the Eqs. (6a). Herein the first equation determines the fluctuations of the amplitude and the second the fluctuations of the phase. As the first of these equations is independent of θ it can be solved by itself. For the solution the generalized equation of Einstein-Fokker can be applied, which, under the condition

$$\tau_{\mathrm{corr}} \ll \tau_1, \qquad (8)$$

where τ_1 is the relaxation time of the amplitude, given approximately by

$$\tau_1 \approx \left| \left(\frac{\partial \Phi}{\partial A}\right)^{-1} \right|, \qquad (9)$$

takes the form:

$$\frac{\partial w(A, t)}{\partial t} = \sum_{s=1}^{\infty} \frac{(-1)^s}{s!} \frac{\partial}{\partial A^s} [K_s(A)\, w(A, t)]. \qquad (10)$$

In this equation, $w(A, t)$ is the one-dimensional probability density and $K_s(A)$ is the system function (sometimes called the g-function) related for stationary processes to the correlation function of $s^{\underline{\text{th}}}$ order by:

$$K_s(A) \qquad (11)$$

$$= \int_{-\infty}^{\infty} \cdots \int_{-\infty}^{\infty} k_{(s)\Phi}(\tau_1, \ldots, \tau_{s-1})\, d\tau_1 \ldots d\tau_{s-1},$$

---

[6] H. Bogoliubov, *Certain Statistical Methods in Mathematical Physics*, 1945

$$K_1 = k_{\Phi}.$$

As the function Φ is known, the characteristic functions $K_s(A)$ can be determined, provided the correlation functions $k_{(s)\xi}$ for $\xi(t)$ are known. Thereby the problem is reduced to the solving of Eq. (10). If the terms of order higher than 2 can be neglected, this equation reduces to the special form of the Einstein-Fokker equation

$$\frac{\partial w(A,t)}{\partial t} = -\frac{\partial}{\partial A}[K_1(A)\,w(A,t)] + \frac{1}{2}\frac{\partial^2}{\partial A^2}[K_2(A)\,w(A,t)]. \tag{12}$$

with

$$K_1(A) = \overline{\Phi(A,\xi)}, \tag{11a}$$

$$K_2(A) = \int_{-\infty}^{\infty}\{\overline{\Phi(A,\xi)\,\Phi(A,\xi_\tau)} - [\overline{\Phi(A,\xi)}]^2\}\,d\tau.$$

where; inthe determination of the mean values, A is to be regarded as a parameter and not as a random variable.

From Eq. (12) it is not difficult to find the expression for the one-dimensional stationary probability density function directly by quadrature. Actually, the stationary probability density function must be independent of time, i.e., as t approaches infinity the system has come to statistical equilibrium; $\partial w/\partial t$ must vanish:

$$\partial w/\partial t = 0.$$

and Eq. (12) becomes

$$K_1(A)\,w(A) - {}^1/_2(d/dA)[K_2(A)\,w(A)] = \text{const}. \tag{12a}$$

The expression

$$j(A) = K_1(A)\,w(A) - {}^1/_2(d/dA)[K_2(A)\,w(A)]$$

represents the "probability current" or, with statistical interpretation of probability, the rate of flow of the descriptive points. In problems of this type, where the descriptive point does not leave the phase space (i.e., it cannot enter from one direction and leave through the other), the "probability current" should be assumed zero (since probability is conserved, i.e., it can neither disappear nor be created). Therefore, the solution of Eq. (12 a) may be written as

$$w(A) = \frac{C_0}{K_2(A)}\exp\left[2\int\frac{K_1(A)}{K_2(A)}dA\right], \tag{13}$$

where the integration constant C_0 is given by the normalizing condition:

$$\int_0^{\infty} w(A)\,dA = 1. \tag{14}$$

3. For the solution of many problems it is not enough to know only the one-dimensional distribution of the random function, but it is also necessary to determine the correlation function. For the determination of the latter, we will show a method based on the following formula:

$$\frac{d}{d\tau}\overline{F(x_0,x_\tau)} = \overline{K_1(x_\tau)\frac{\partial}{\partial x_\tau}F(x_0,x_\tau)} + \overline{\frac{1}{2}K_2(x_\tau)\frac{\partial^2}{\partial x_\tau^2}F(x_0,x_\tau)}, \tag{15}$$

wherein F is an arbitrary function, $x_0 = A(t)$, $x_\tau = A(t+\tau)$. To derive this formula let $w_0(x_0)$ be the probability density distribution function of the random variable x_0, and let $w(x_0, x_\tau, \tau)$ give the probability $w_1(x_0, x_\tau, \tau)\,dx_\tau$ of the transition of a point, originally at x_0 in the interval $[x_\tau, x_\tau + dx_\tau]$ in time τ. The distribution density function $w_1(x_0, x_\tau, \tau)$ satisfies Eq. (12):

$$\frac{\partial w_1}{\partial \tau} = -\frac{\partial}{\partial x_\tau}[K_1(x_\tau)\,w_1(x_0,x_\tau,\tau)] + \frac{1}{2}\frac{\partial^2}{\partial x_\tau^2}[K_2(x_\tau)\,w_1(x_0,x_\tau,\tau)].$$

Inserting this expression into the relation

$$\frac{d}{d\tau}\overline{F(x_0,x_\tau)} = \int\int_{-\infty}^{\infty} F(x_0,x_\tau)\,w_0(x_0)\frac{\partial w_1(x_0,x_\tau,\tau)}{d\tau}\,dx_0dx_\tau$$

and integrating the result by parts leads to Eq. (15) (considering that,by the normalizing condition, the difference of the probability currents $j(\infty) - j(-\infty)$ must vanish, and also that the probability density by itself is zero as $x_\tau \to \pm\infty$). In our special case where A is a non-negative function as the integration is carried out in the limits from 0 to ∞, Eq. (15) still holds, since

$$w_1(x_0,x_\tau,\tau) = 0 \quad \text{and} \quad x_\tau \to \infty,$$
$$K_2(0) = 0.$$

As the one-dimensional probability density distribution $w(x)$ is given by Eq. (13), we can calculate

$$\overline{F(x_0, x_\tau)}\big|_{\tau=0} = \overline{F(x_0, x_0)}. \qquad (16)$$

If we assign for the function F in Eq. (15) the value

$$F_1 = K_1(x_\tau)\frac{\partial}{\partial x_\tau} F(x_0, x_\tau), \qquad (17)$$

$$F_2 = K_2(x_\tau)\frac{\partial^2}{\partial x_\tau^2} F(x_0, x_\tau),$$

it is possible to obtain relations which will determine the time variations of $\overline{F}_1$ and $\overline{F}_2$, if their initial values, corresponding to $\tau = 0$, are also known.

Continuing this process, we will obtain a system of linear equations (generally infinite in number) which can be solved by known methods. An example with the application of this method will be considered below.

4. As an illustration, and to clarify the conditions under which the Einstein-Fokker method may be applied, we will consider the following typical example. Let stationary Gauss fluctuations be present in the grid circuit of a vacuum tube oscillator with a resonant-circuit in the anode loop. (See Fig. 1). For such a system, under the usual assumptions (no grid current, neglecting the effect of the loaded anode, and so on), and approximating the anode-grid characteristic of the tube by a polynomial of the third degree

$$i_a = \varphi(u_c) = i_0 + \alpha u_c$$
$$+ \beta u_c^2 - \gamma u_c^3 \ (\alpha > 0,\ \gamma > 0),$$

the equation system (1) becomes

$$\dot{x} = -\frac{r}{L}x_1 + \omega_0 y_1, \qquad (18)$$
$$y_1 = -\omega_0 x_1 + \frac{1}{C}\varphi\left[\frac{M}{L}(y_1 - \delta x_1) + \xi(t)\right].$$

wherein

$$x_1 = i\rho, \quad y_1 = u, \quad \omega_0 = 1/\sqrt{LC}, \qquad (19)$$
$$\delta = r/\rho, \quad \rho = \sqrt{L/C},$$

and i and u are current and voltage respectively in the resonant circuit, the meaning of the other parameters being shown in Fig. 1.

Separating the constant parts and those linear in x_1 and y_1, Eq. (18) can be rewritten as

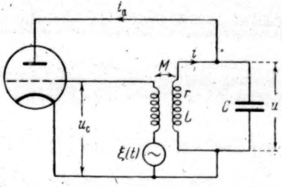

FIG. 1. Schematic diagram of the vacuum tube oscillator

$$\dot{x}_1 = -(r/L)x_1 + \omega_0 y_1, \qquad (18a)$$
$$\dot{y}_1 = (1/C)\varphi(\xi) - \omega_0(1 + \omega_0\alpha M\delta)x_1$$
$$+ \omega_0^2\alpha M y_1 + \Theta(x_1, y_1, \xi),$$

with

$$\Theta(x_1, y_1, \xi) = (\beta/C)[k^2(y_1 - \delta x_1)^2$$
$$+ 2k\xi(y_1 - \delta x_1)] - (\gamma/C)[k^3(y_1 - \delta x_1)^3$$
$$+ 3k^2\xi(y_1 - \delta x_1)^2 + 3k\xi^2(y_1 - \delta x_1)],$$
$$k = M/L.$$

Introducing new variables

$$x = x_1 - \rho\varphi(\xi), \ y = y_1 - r\varphi(\xi), \qquad (20)$$

we obtain

$$\dot{x} = -(r/L)x + \omega_0 y, \qquad (18b)$$
$$\dot{y} = -\omega_0(1 + \omega_0\alpha M\delta)x + \omega_0^2\alpha M y + \Theta(x, y, \xi).$$

Inserting the individual terms into Eq. (3), and using the condition of self-excitation of the oscillator, which is for $\xi(t) \equiv 0$ given approximately by

$$M > rC/\alpha, \qquad (21)$$

leads to

$$n \approx \delta \approx 0, \quad m \approx 1/(1 + \delta^2) \approx 1,$$

since usually $\delta \ll 1$. Therefore, the transition to polar-coordinates can be made by

$$x = A\cos\vartheta, \quad y = A\sin\vartheta. \qquad (22)$$

Before performing this transition, we notice, however, that in the neighborhood of self-excitation

$$\omega_0\alpha M\delta \approx \delta^2 \ll 1.$$

and, therefore, we can neglect the second coefficient of x in the second of equations (18b), [as is usually done in the analysis of a vacuum-tube oscillator in the absence of the random disturbances $\xi(t)$]. .

Now, changing to polar-coordinates [Eq. (22)] and introducing the mean over θ the Eqs. (6a) become

$$\dot{A} = {}^1/_2\,\omega_0^2\,[(\alpha M - rC + 2\beta M\xi - 3\gamma M\xi^2)\,A \qquad (23)$$

$$- {}^3/_4\,\gamma M(M/L)^2 A^3],$$

$$\dot{\vartheta} = -\,\omega_0 + \frac{\delta\omega_0^2 M}{2}\left[\frac{3\gamma}{4}\left(\frac{M}{L}\right)^2 A^2 + (3\gamma\xi^2 - 2\beta\xi)\right].$$

Setting $\xi(t) \equiv 0$, the first of these equations gives the condition (21) for self-excitation of the oscillator and also for the radius of the maximum stable cycle:

$$A_0 = 2\,\frac{L}{M}\sqrt{\frac{\alpha M - rC}{3\gamma M}}\,. \qquad (24)$$

It reaches its largest value

$$A_{0\,\mathrm{MAX}} \approx 0.14\,L/rC\sqrt{\gamma}$$

at

$$M = 1.5\,r\,C/\alpha.$$

5. As was shown before, the basic equation (12) is correct only if

$$T_0 \ll \tau_{\mathrm{corr}} \ll \tau_1. \qquad (25)$$

To estimate the order of magnitude of τ_{corr}, we shall assume the following numerical values for the circuit parameters of Fig. 1:

$$f_0 = 2\pi/\omega_0 = 10^7\ \mathrm{cps.}, \quad r = 10\,\Omega,$$

$$\rho = 6\cdot 10^3\,\Omega, \quad M = 1.1\,rC/\alpha, \quad A_0 = 10\ \mathrm{volts.}$$

Differentiating Eq. (23) over A gives

$$\partial\Phi/\partial A = {}^1/_2\omega_0^2\,[(M\alpha - rC + 2\beta M\xi - 3\gamma M\xi^2)$$

$$-{}^9/_4\gamma M(M/L)^2 A^2].$$

We will now evaluate $\partial\Phi/\partial A$ at $A = A_0$. Inserting the value of A_0 from Eq. (24), we find

$$\left.\frac{\partial\Phi}{\partial A}\right|_{A=A_0}$$

$$= -\frac{1}{2}\,\omega_0^2\left[0{,}2rC + \frac{0{,}33\alpha^2\rho^3}{\omega_0 r A_0^2}\left(1 - \frac{2\beta}{3\gamma\xi}\right)\xi^2\right].$$

The inequality (25) must be satisfied for all values of ξ with nonnegligible probability, and, in particular, it must also be satisfied in the case $\xi = 0$. Thereby,

$$\tau_1 = \left|\left(\frac{\partial\Phi}{\partial A}\right)^{-1}\right| \approx \frac{2}{0.2\,\omega_0^2 rC} = \frac{10\rho}{\omega_0 r} = 10^{-4}\ \mathrm{sec}$$

Thus the basic Eq. (12) will hold for all practical purposes; if the correlation time of the random function $\xi(t)$ is

$$\tau_{\mathrm{corr}} \approx (10^{-6} \div 10^{-5})\ \mathrm{sec} \qquad (25a)$$

These conditions will be fulfilled in most cases. For the transition to spectral quantities we shall assume that the correlation function for "low-frequency" fluctuations $\xi(t)$ is of the form

$$k_2(\tau) = c_0 e^{-\alpha|\tau|}$$

and, correspondingly, the spectral density of the fluctuations will be given by

$$S(f) = c_0\,\frac{\varkappa}{\varkappa^2 + (2\pi f)^2}\,.$$

In this case the correlation time is

$$\tau_{\mathrm{corr}} = 2\int_0^\infty e^{-\varkappa\tau}d\tau = \frac{2}{\varkappa}\,.$$

In order that condition (25a) is fulfilled for this specific example, it is necessary that

$$\varkappa \approx 2\,(10^6 \div 10^5)\ \mathrm{sec}^{-1}\,.$$

Let

$$\tau_{\mathrm{corr}} = 0.2\cdot 10^{-5}\ \mathrm{sec}$$

If, for practical purposes, we neglect all spectral densities at frequencies for which

$$\frac{S(f)}{S(0)} = \frac{1}{1 + (2\pi f/\alpha)^2} \leqslant 5\%,$$

then, the bandwidth of the fluctuations for which this method can be applied will be

$$f_{\mathrm{MAX}} \approx 0.7 \times 10^6\ \mathrm{cps}$$

It should be noted, however, that because of the high values of ρ/r for high frequency resonant circuit, the range of τ_{corr} for which the method of Einstein-Fokker is valid is considerably larger at high frequency oscillations.

6. We shall now evaluate the one dimensional stationary probability density function $w(A)$ for the fluctuations of the amplitude. In accordance with Eq. (11a) we can find the system functions from the first of the Eqs. (23). Indeed, they can be found very easily if $\xi(t)$ are normally distributed fluctuations with a mean of zero, i.e.,

$$w_2(\xi, \xi_\tau) = \frac{1}{2\pi\sigma^2 \sqrt{1 - R^2(\tau)}} \times \exp\left[- \frac{\xi^2 + \xi_\tau^2 - 2R(\tau)\,\xi\xi_\tau}{2\sigma^2(1 - R^2(\tau))}\right], \tag{26}$$

wherein σ^2 is the dispersion and $R(\tau)$ is the correlation coefficient.
Actually, let, for example,

$$\eta(\tau) = a + b\xi(t) + c\xi^2(t).$$

In this case, as all odd moments of $\xi(t)$ vanish, Eq. (11a) becomes

$$K_{(2)\eta} = K_{(2)b\xi+c\xi^2} = b^2 K_{(2)\xi} + c^2 K_{(2)\xi^2},$$

where

$$K_{(2)\xi} = \int\limits_{-\infty}^{\infty} k_{(2)\xi}(\tau)\,d\tau = \sigma^2 \int\limits_{-\infty}^{\infty} R(\tau)\,d\tau, \tag{27}$$

$$K_{(2)\xi^2} = \int\limits_{-\infty}^{\infty} k_{(2)\xi^2}(\tau)\,d\tau.$$

But, in case of stationary processes the correlation function $k_{(2)\xi^2}$ of $\xi^2(t)$ can be expressed either by the moments or by the correlation functions of $\xi(t)$:

$$k_{(2)\xi^2}(\tau) = m_{(2)\xi^2}(\tau) - (m_{\xi^2})^2$$
$$= m_{(4)\xi}(t,\ t,\ t + \tau,\ t + \tau) - \sigma^4.$$

Moreover, in accordance with the general relations between the moments and correlation functions, we have, if $m = 0$,

$$m_4(t_1, t_2, t_3, t_4) = k_2(t_1, t_2)\,k_2(t_3, t_4)$$
$$+ k_2(t_1, t_3)\,k_2(t_2, t_4) + k_2(t_1, t_4)\,k_2(t_2, t_3),$$

and, consequently,

$$m_{(4)\xi}(t, t, t + \tau, t + \tau) = k^2_{(2)\xi}(0)$$
$$+ 2k^2_{(2)\xi}(\tau) = \sigma^4\,[1 + 2R^2(\tau)].$$

Hence,

$$K_{(2)\xi^2} = 2\sigma^4 \int\limits_{-\infty}^{\infty} R^2(\tau)\,d\tau. \tag{28}$$

Using this relation, and performing all necessary operations, we obtain

$$K_1(A) = \mu A - \nu A^3, \quad K_2(A) = \lambda A^2, \tag{29}$$

where

$$\mu = {}^1/_2\omega_0^2(\alpha M - rC - 3\gamma M\sigma^2), \tag{30}$$

$$\nu = {}^3/_8\omega_0^2\gamma M(M/L)^2,$$

$$\lambda = (\omega_0^2 M\sigma)^2(\beta^2\tau_{\text{corr}} + {}^9/_2\gamma^2\sigma^2\tau_{k2}),$$

$$\tau_{\text{corr}} = \int\limits_{-\infty}^{\infty} R(\tau)\,d\tau, \quad \tau_{k2} = \int\limits_{-\infty}^{\infty} R^2(\tau)\,d\tau.$$

Substituting the values of the system functions into Eq. (13), we obtain

$$w(A) = \frac{C_0}{\lambda} A^{2(\mu/\lambda - 1)} \exp\left(-\frac{\nu}{\lambda} A^2\right), \tag{31}$$

This equation shows that for $\mu / \lambda < 1$ the probability density $w(A)$ becomes infinite at $A = 0$. However, it should be remembered that this result is obtained because $K_2(0) = 0$ at $A = 0$, and that this latter value of K_2 is not an exact one, due to the approximation by which Eq. (29) was obtained.

To find a more exact expression for $K_2(0)$ we will not neglect the term M in the first of Eqs. (6). Owing to the fact that the descriptive point actually moves in the phase plane, not on a circle (ellipse), but along a spiral with a variable radius

$$A(t) = A(t_0) + \dot{A}(t_0)(t - t_0)$$
$$\approx A(t_0)\left[1 + \frac{\Phi(A, 0)}{A(t_0)}(t - t_0)\right],$$

it will be more accurate to write the expression for the mean M in the form:

$$M = -\frac{1}{2\pi}\int\limits_0^{2\pi}\left[1 + \frac{\Phi(A, 0)}{A(t_0)}(t - t_0)\right]$$
$$\left[\frac{d\gamma}{d\vartheta}\cos\vartheta + \frac{d\beta}{d\vartheta}\sin\vartheta\right]\frac{d\vartheta}{dt}\,d\vartheta,$$

wherein the time function can be transformed into function of θ by the substitution

$$t - t_0 = \vartheta / \omega.$$

Substitution in this equation of the approximate expression for θ from Eq. (6a) gives

$$M = -\frac{1}{2\pi}\int\limits_0^{2\pi}\left[1 + \frac{\Phi(A, 0)}{A(t_0)}(t - t_0)\right] \times\left[\frac{d\gamma}{d\vartheta}\cos\vartheta + \frac{d\beta}{d\vartheta}\sin\vartheta\right]\times[-\omega + \Psi(A, \xi)]\,d\vartheta. \tag{32}$$

It can easily be shown that $K_2(0)$ is equal to the system function of this expression with A equal to zero. Generally $K_2(0)$ will not be zero.

If we assume

$$K_2(A) = \rho + \lambda A^2,$$

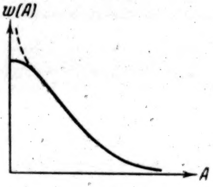

FIG. 2. Condition of not developed oscillations

where ρ is a small quantity, we will obtain a probability density function $w(A)$ which is finite and which can be integrated over all possible values of A. Furthermore, we will have

$$\frac{dw}{dA}\bigg|_{A=0} = 0,$$

which is in conformity with the stipulation of conservation of the descriptive point. However, it should be pointed out that Eq. (30) gives the correct slope of the curve $w(A)$ even for $\mu / \lambda < 1$ as long as A is not too small. Nevertheless, for the determination of the integration constant C_0 the more exact equation (32) should be used.

From the qualitative point of view, the operating condition of the oscillator can be classified as follows:

1. $\mu < \lambda$; condition of not developed oscillations. The descriptive point is located mainly in the neighborhood of the equilibrium (see Fig. 2.).

2. $\lambda < \mu < {}^3/_2\,\lambda$; condition of not fully developed oscillations. The amplitude of the oscillations is scattered on a large zone and may be close to zero (See Fig. 3).

3. $\mu > {}^3/_2\,\lambda$;the most interesting case-condition of fully developed oscillations - when the descriptive point is located mainly in the neighborhood of the critical cycle (see Fig. 4). In the Figs. 2 and 3, the dotted line in the neighborhood of $A = 0$ shows the slope of $w(A)$ according to Eq. (31), the solid line – the corrected value.

We will now determine the integration constant C_0 , and also the moments of the random variable A. It is

$$\overline{A^m} = \frac{C_0}{\lambda}\int\limits_0^\infty A^{2s+m}\exp\left(-\frac{\nu}{\lambda}A^2\right)dA$$

$$= \frac{C_0}{2\lambda}\left(\frac{\lambda}{\nu}\right)^{(2s+m+1)/2}\int\limits_0^\infty x^{(2s+m-1)/2}\,e^{-x}dx$$

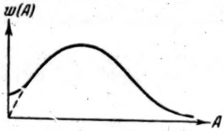

FIG. 3. Condition of not fully developed oscillations

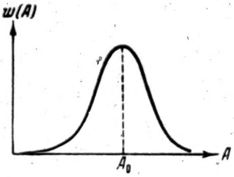

FIG. 4. Condition of fully developed oscillations.

$$= \frac{C_0}{2\lambda}\left(\frac{\lambda}{\nu}\right)^{(2s+m+1)/2}\Gamma\left(\frac{2s+m+1}{2}\right),$$

where

$$s = (\mu / \lambda) - 1.$$

Assuming here, in accordance with the normalizing condition (14), $\overline{A}_0 = 1$, we obtain

$$C_0 = \frac{2\lambda\,(\lambda/\nu)^{-s-{}^1/_2}}{\Gamma(s+{}^1/_2)}. \tag{33}$$

Consequently,

$$\overline{A^m} = \left(\frac{\lambda}{\nu}\right)^{m/2}\Gamma\left(s+\frac{m+1}{2}\right)\Big/\,\Gamma\left(s+\frac{1}{2}\right). \tag{34}$$

and, for the even moments of A, (34a)

$$\overline{A^{2k}} = (\lambda/\nu)^k\,(s+{}^1/_2)(s+{}^3/_2)\cdots(s+k-{}^1/_2).$$

7. We shall now find the correlation functions for $A(t)$. Assuming in Eq. (15)

$$F(x_0,\ x_\tau) = x_0x_\tau,$$

we will obtain

$$(d/d\tau)\,u_1 = \mu u_1 - \nu u_3, \tag{35}$$

with

$$u_1 = \overline{x_0x_\tau},\quad u_3 = \overline{x_0x_\tau^3}.$$

Similarly, for μ_3

$$(d/d\tau)\,u_3 = 3\mu u_3 - 3\nu u_5 + 3\lambda u_3. \tag{36}$$

In general for μ_n , we have

$$\frac{d}{d\tau} u_n = n\left[\mu u_n - \nu u_{n+2} + \frac{n-1}{2} \lambda u_n\right], \quad (37)$$

with

$$u_n = \overline{A(t) A^n (t+\tau)},$$

$$\tau > 0, \quad n = 1, 3, 5, \ldots,$$

and

$$u_n(0) = \overline{A^{n+1}} \quad (38)$$

$$= \left(\frac{\lambda}{\nu}\right)^{(n+1)/2} \Gamma\left(s + \frac{n}{2} + 1\right) \Big/ \Gamma\left(s + \frac{1}{2}\right).$$

An approximate solution of this system of equations can be obtained by the following method. Using Eq. (35), we will first determine the coefficients of the Taylor-expansion of $\mu_1(\tau)$:

$$u_1(\tau) = u_1(0) + u_1'(0)\tau + \frac{u_1''(0)}{2!}\tau^2 + \cdots \quad (39)$$

Setting

$$u_n^{(\alpha)}(0) = u_n(0) k_{n,\alpha}, \quad (40)$$

and differentiating Eq. (37) we find the recursion formula for the determination of $k_{n,\alpha}$:

$$k_{n,\alpha+1} = n\left[\left(\mu + \frac{n}{2}\lambda\right)(k_{n,\alpha} - k_{n+2,\alpha}) \quad (41)\right.$$

$$\left. - \frac{1}{2}\lambda k_{n,\alpha}\right],$$

with

$$k_{n,0} = 1.$$

Hence, from here

$$k_{n,1} = -(n/2)\lambda,$$

and, as

$$k_{n,1} - k_{n+2,1} = \lambda,$$

we have

$$k_{n,2} = n\left[\left(\mu + \frac{n}{2}\lambda\right)\lambda + \frac{1}{4} n\lambda^2\right] = n\mu\lambda + \frac{3}{4} n^2\lambda^2.$$

Subsequently, as

$$k_{n,2} - k_{n+2,2} = -2\mu\lambda - 3\lambda^2 (n+1),$$

we obtain

$$k_{n,3} = -2n\mu^2\lambda - n\lambda^2\left(\frac{9}{2}n + 3\right)$$

$$- \frac{n^2}{2}\lambda^3\left(\frac{15}{4}n + 3\right) \quad \text{, etc.}$$

Consequently,

$$k_{1,1} = -\lambda/2, \quad (42)$$
$$k_{1,2} = \mu\lambda + {}^3/_4\lambda^2,$$
$$k_{1,3} = -2\mu^2\lambda - {}^{15}/_2\mu\lambda^2 - {}^{27}/_8\lambda^3,$$

. . . .

Thus, using the first four terms of Eq. (39) we obtain

$$\overline{A(t) A(t+\tau)}$$

$$= \frac{1}{\nu}\left(\mu - \frac{\lambda}{2}\right)\left[1 - \frac{\lambda}{2}\tau + \left(\mu\lambda + \frac{3}{4}\lambda^2\right)\frac{\tau^2}{2}\right.$$

$$\left. - \left(2\mu^2\lambda + \frac{15}{2}\mu\lambda^2 + \frac{27}{8}\lambda^3\right)\frac{\tau^3}{6} + \ldots\right].$$

This determines the correlation coefficient

$$R_A(\tau) = \frac{\overline{AA_\tau} - \overline{A}^2}{\overline{A^2} - \overline{A}^2} = 1 - \frac{\lambda}{2}\frac{\tau}{1-B} \quad (43)$$

$$+ \left(\mu\lambda + \frac{3}{4}\lambda^2\right)\frac{\tau^2}{2(1-B)}$$

$$- \left(2\mu^2\lambda + \frac{15}{2}\mu\lambda^2 + \frac{27}{8}\lambda^3\right)\frac{\tau^3}{6(1-B)},$$

where

$$B = \Gamma\left(\frac{\mu}{\lambda}\right)^2 \Big/ \Gamma\left(\frac{\mu}{\lambda} - \frac{1}{2}\right)\Gamma\left(\frac{\mu}{\lambda} + \frac{1}{2}\right). \quad (44)$$

Using a sufficient number of terms in the expansion Eq. (39), we can attain any required accuracy.

8. We shall now consider the second of the Eqs. (23), which determines the phase change of the oscillations. Since we have assumed $\tau_{corr} \ll \tau_1$ the random processes $\xi(t)$ and $A(t)$ can be regarded as mutually uncorrelated. Therefore determining the probability characteristics of the process $A(t)$ from the first of Eqs. (23), we can basically determine the probability characteristics of the phase $\theta(t)$. The most important of these characteristics is D – the system function for the phase $\theta(t)$. The probability density distribution of the increment $\theta(t_0 + T) - \theta(t_0) = \theta_T - \theta_0$ in the time interval T, which is much longer than the correlation time τ_{corr} of the process $\theta(t)$, is approximately given by

$$w(\vartheta_T - \vartheta_0) = C_0 \exp\left\{-\frac{(\vartheta_T - \vartheta_0 - \omega T)^2}{2DT}\right\}, \quad (45)$$

where

$$\omega = \overline{\dot{\vartheta}} = -\omega_0 + \frac{\delta\omega_0^2 M}{2}\left[\frac{3\gamma}{4}\left(\frac{M}{L}\right)^2 \overline{A^2} + 3\gamma\sigma^2\right].$$

Hence, D determines (for sufficiently long T) the rate of increase of the dispersion of the difference $\theta_T - \theta_0$.

Equation (23) can be written in the form

$$\dot{\vartheta} = -\omega_0 + c_1 A^2 + c_2\xi^2 - c_3\xi = N. \quad (46)$$

As there is no correlation between A and ξ the second characteristic function will be given by

$$K_{(2)N} = c_1^2 K_{(2)A^2} + K_{(2)c_2\xi^2 - c_3\xi},$$

where, because all odd moments of ξ vanish

$$K_{(2)c_2\xi^2 - c_3\xi} = c_2^2 K_{(2)\xi^2} + c_3^2 K_{(2)\xi}.$$

and

$$K_{(2)\xi} = \sigma^2 \tau_{\text{corr}}$$

$$= \sigma^2 \int_{-\infty}^{\infty} R(\tau)\, d\tau, \quad K_{(2)\xi^2} = 2\sigma^4 \tau_{k2},$$

Consequently, for the determination of

$$D = c_1^2 K_{(2)A^2} + 2c_2^2 \sigma^4 \tau_{k2} + c_3^2 \sigma^2 \tau_{\text{corr}} \tag{47}$$

we must find $K_{(2)A^2}$. For this we will apply a method used previously.

Setting

$$v_n(\tau) = \overline{A^2(t)\, A^{2n}(t+\tau)},$$

we obtain a system of equations, similar to that of Eq. (37):

$$\frac{d}{d\tau} v_n(\tau) = n\left[\mu v_n - \nu v_{n+2} + \frac{n-1}{2} \lambda v_n\right], \tag{48}$$

but with different initial conditions

$$v_n(0) = \overline{A^{n+2}}. \tag{49}$$

Assuming, as before,

$$v_n^{(\alpha)}(\tau) = v_n(0)\, l_{n,\alpha}, \tag{50}$$

we obtain

$$l_{n,\alpha+1} = n\left[\left(\mu + \frac{n-1}{2}\lambda\right) l_{n,\alpha} - \nu l_{n+2,\alpha} \frac{\overline{A^{n+4}}}{\overline{A^{n+2}}}\right],$$

with

$$\frac{\overline{A^{n+4}}}{\overline{A^{n+2}}} = \frac{\lambda}{\nu} \frac{\Gamma\left(s + \frac{n+1}{2} + 2\right)}{\Gamma\left(s + \frac{n+1}{2} + 1\right)}$$

$$= \frac{\lambda}{\nu}\left(s + 1 + \frac{n+1}{2}\right) = \frac{1}{\nu}\left(\mu + \frac{n+1}{2}\lambda\right).$$

Consequently,

$$l_{n,\alpha+1} = n\left[\left(\mu + \frac{n+1}{2}\lambda\right)\right. \tag{51}$$

$$\left.\times (l_{n,\alpha} - l_{n+2,\alpha}) - \lambda l_{n,\alpha}\right],$$

where $l_{n,0} = 1$.

Using this relation, we find

$$l_{2,1} = -2\lambda, \tag{52}$$
$$l_{2,2} = 4\mu\lambda + 5\lambda^2,$$
$$l_{2,3} = -2(8\mu^2\lambda + 42\mu\lambda^2 + 44\lambda^3), \ \ldots$$

Therefore,

$$\overline{A^2 A_\tau^2} = \overline{A^4}\left[1 - 2\lambda\tau + (4\mu + 5\lambda)\lambda \frac{\tau^2}{2}\right. \tag{53}$$

$$\left. - (8\mu^2 + 42\mu\lambda + 44\lambda^2)\lambda \frac{\tau^3}{3} + \ldots\right].$$

Correspondingly, we obtain for the correlation coefficient

$$R_{A^2}(\tau) = \frac{\overline{A^2 A_\tau^2} - (\overline{A^2})^2}{\overline{A^4} - (\overline{A^2})^2} = 1 \tag{54}$$

$$- \frac{2\lambda}{1-c}\tau + \frac{4\mu\lambda + 5\lambda^2}{1-c}\frac{\tau^2}{2}$$

$$- \frac{8\mu^2 + 42\mu\lambda + 44\lambda^2}{1-c}\lambda \frac{\tau^3}{3} + \ldots,$$

with

$$c = \frac{(\overline{A^2})^2}{\overline{A^4}} = \frac{\Gamma\left(s + \frac{3}{2}\right)^2}{\Gamma\left(s + \frac{1}{2}\right)\Gamma\left(s + \frac{5}{2}\right)} \tag{55}$$

$$= \frac{\Gamma\left(\frac{\mu}{\lambda} + \frac{1}{2}\right)^2}{\Gamma\left(\frac{\mu}{\lambda} - \frac{1}{2}\right)\Gamma\left(\frac{\mu}{\lambda} + \frac{3}{2}\right)}.$$

It is approximately

$$K_{(2)A^2} = \overline{A^4} \int_{-\infty}^{\infty} R_{A^2}(\tau)\, d\tau \tag{56}$$

$$= \left(\frac{\lambda}{\nu}\right)^2 \left(s + \frac{1}{2}\right)\left(s + \frac{3}{2}\right) \int_{-\infty}^{\infty} R_{A^2}(\tau)\, d\tau$$

$$= 2\, \frac{\mu^2 - (\lambda^2/4)}{\nu^2} \int_0^{\infty} R_{A^2}(|\tau|)\, d\tau.$$

Confining ourselves to only three terms of the expansion Eq. (54) we can set

$$R_{A^2}(\tau) = e^{-\alpha\tau} \cos \beta\tau. \tag{57}$$

For the determination of α and β we have

$$\alpha = \frac{2\lambda}{1-c}, \quad \alpha^2 - \beta^2 = \frac{4\mu\lambda + 5\lambda^2}{1-c}. \tag{58}$$

which gives

$$\beta = \left[\left(\frac{2\lambda}{1-c}\right)^2 - \frac{4\mu\lambda + 5\lambda^2}{1-c}\right]^{1/2}.$$

Integrating

$$\int_0^{\infty} e^{-\alpha\tau} \cos \beta\tau\, d\tau = \frac{\alpha}{\alpha^2 + \beta^2},$$

and considering the Eqs. (56), (57) and (58), gives

$$K_{(2)A^2} = \frac{4\mu - \lambda^2}{\nu^2} \frac{1-c}{(3+5c)\lambda - 4\mu(1-c)}. \qquad (59)$$

Substituting this into Eq. (47) we obtain D.

We should point out, however, that the approximate expression Eq. (57) for $R_{A^2}(\tau)$ is valid if

$$4\mu + 5\lambda \leqslant \frac{4\lambda}{1-c}, \qquad (59a)$$

Otherwise we must use a different expression, e.g.,

$$R_{A^2}(\tau) = e^{-\alpha\tau}\left(1 + \frac{\beta\tau^2}{2}\right), \qquad (60)$$

where

$$\alpha = \frac{2\lambda}{1-c}, \qquad \alpha^2 + \beta^2 = \frac{4\mu\lambda + 5\lambda^2}{1-c}, \qquad (61)$$

Integrating

$$\int_0^\infty R_{A^2}(\tau)\, d\tau = \frac{1}{\alpha} + \frac{\beta}{\alpha^3},$$

and subtituting the values of a and β from Eq. (61), we find

$$K_{(2)A^2} = \frac{4\mu^2 - \lambda^2}{(4\lambda\nu)^2}(1-c)^2(4\mu + 5\lambda). \qquad (62)$$

Equation (60) can also be used in case condition (59a) is satisfied.

If a closer approximation for $K_{(2)A^2}$ is required, we can set

$$R_{A^2}(\tau) = e^{-\alpha\tau}\left(1 + \frac{\beta_2\tau^2}{2} + \frac{\beta_3\tau^3}{6} + \ldots\right). \qquad (63)$$

and we will obtain

$$\int_0^\infty R_{A^2}(\tau)\, d\tau = \frac{1}{\alpha}\left(1 + \frac{\beta_2}{\alpha^2} + \frac{\beta_3}{\alpha^3} + \ldots\right), \qquad (64)$$

where β_2 ,β_3 ,...are found from the conditions for the constants at $\tau = 0$.

In conclusion the authors wish to express their appreciation to Iu. B. Kobzarev for the interest shown in this work.

Translated by L. Bergsteinn
92

SOVIET PHYSICS JETP VOLUME 1, NUMBER 3 NOVEMBER, 1955

Statistical Problems of an Electron Multiplier

L. JANOSSY
Central Physics Research Institute, Hungarian Academy of Sciences, Budapest

(Submitted to JETP editor May 24, 1954)
J. Exper. Theoret. Phys. USSR **28**, 679-694 (June, 1955)

We give a method of determining the distribution functions of impulse amplitudes in an electron multiplier, if we know the probability that n secondary electrons are produced in one elementary act. We answer the question of how to determine the probability of this elementary event, if we know experimentally the distribution curve of the impulse amplitudes in the multiplier.

---

1. In this article we consider the following two problems:

1) Given a distribution $P(\nu)$, where $P(0)$, $P(1)$, $P(2)$, . . . are the probabilities that the collision of an electron with a multiplier electrode leads to the appearance of 0, 1, 2, . . . secondary electrons. We shall determine the probability $P_N(\nu)$ that ν electrons are ejected from the Nth electrode if a primary electron strikes the first electrode[1]. In addition, we shall consider the quantity $P^{(k)}_N(\nu)$, which denotes the probability of producing ν electrons at the Nth multiplier electrode, if there are k primary electrons.

2) Given a distribution $P_N(\nu)$ of electrons, appearing at the Nth multiplier plate. We shall determine the distribution $P(\nu)$, of the electrons emanating from one electrode, which leads in N steps to the given distribution $P_N(\nu)$.

2. We begin by considering the probability distributions $P_2(\nu)$, $P_3(\nu)$, . . . obtained from the primary distribution $P(\nu)$. Let us extend the definition given above to the cases $N = 0$ and $N = 1$ by writing

$$P_0(\nu)=\begin{cases}1, & \nu=1,\\ 0, & \nu\neq 1,\end{cases}\qquad P_1(\nu)=P(\nu). \tag{1}$$

Next we introduce the generating function $G_N(u)$ of the distribution $P_N(\nu)$:

$$G_N(u)=\sum_{\nu=0}^{\infty}u^{\nu}P_N(\nu). \tag{2}$$

In particular, we have

$$\begin{aligned}G_0(u)&=u,\\ G_1(u)&=\sum u^{\nu}P(\nu)=G(u),\end{aligned} \tag{3}$$

where $G(u)$ is the generating function of the initial distribution $P(\nu)$.

We construct a recurrence formula for $G_N(u)$ in the following way. Consider the case where not one but $k > 1$ particles impinge on the first electrode. Designate by $P^{(k)}_N(\nu)$ the probability that k primary electrons yield just ν electrons at the Nth electrode. We have

$$P_N^{(k+l)}(\nu)=\sum_{\nu_1+\nu_2=\nu}P_N^{(k)}(\nu_1)\,P_N^{(l)}(\nu_2).$$

Multiplying this equation by u^{ν} and summing with respect to ν, we obtain in the usual way the corresponding generating function

$$G_N^{(k+l)}(u)=G_N^{(k)}(u)\,G_N^{(l)}(u).$$

Bearing in mind that $G^{(1)}_N(u) = G_N(u)$ by definition, and setting $l = 1$, $k = 1, 2, 3,$ . . . , we obtain, in general,

$$G_N^{(k)}(u)=(G_N(u))^k,\quad k=0,1,2,\ldots, \tag{4}$$

where $G^0(u) = 1$ is the generating function of a distribution such that not a single electron falls on the multiplier, so that $P^{(0)}_N = 0$, $\nu \neq 0$.

To derive a recurrence formula for $G_N(u)$, we observe that ν particles will appear at the Nth stage if at some intermediate stage, say the kth, there are μ particles, and if they give rise to just $\nu - \mu$ particles at the remaining $N - k$ stages. The probability of such an event for a fixed value of μ is

$$P_k(\mu)\,P_{N-k}^{(\mu)}(\nu).$$

Summing over all possible intermediate values of μ, we obtain for the total probability

$$P_N(\nu)=\sum_{\mu=0}^{\infty}P_k(\mu)\,P_{N-k}^{(\mu)}(\nu).$$

---

[1] L. Janossy, Acta Mathematica **2**, 165 (1951)

Multiplying the last equation by u^ν and summing over $\nu = 0, 1, 2, \ldots$, we get, with the aid of Eq. (4),

$$G_N(u) = \sum_{\nu=0}^{\infty} u^\nu \sum_{\mu=0}^{\infty} P_k(\mu)\, P_{N-k}^{(\mu)}(\nu)$$

$$= \sum_{\mu=0}^{\infty} P_k(\mu)\, (G_{N-k}(u))^\mu .$$

Moreover, using Eq. (2), we have

$$G_N(u) = G_k G_{N-k}(u), \tag{5}$$

where we have written for brevity $G_k G_{N-k}(u)$ instead of $G_k[G_{N-k}(u)]$. Setting $k = 1$ in Eq. (5), we obtain in particular

$$G_N(u) = G G_{N-1}(u),$$

whence

$$G_0(u) = u, \quad G_1(u) = G(u),$$

$$G_2(u) = GG(u), \ldots,$$

$$G_N(u) = \underbrace{GG\ldots G}_{N}(u).$$

In this way we have obtained the successive generating functions $G_1(u)$, $G_2(u)$, . . . by iterating the initial function.

3. Thus, we can calculate $G_N(u)$ for a given $G(u)$; the corresponding $P_N(\nu)$ is obtained by a complex integration, namely

$$P_N(\nu) = \frac{1}{2\pi i} \oint_{u=0} u^{-\nu-1} G_N(u)\, du. \tag{6}$$

To simplify the calculations, it is convenient to introduce

$$u = e^v, \quad G_N(u) = \exp\{H_N(v)\}. \tag{7}$$

Transforming Eq. (5) with the help of Eq. (7), we obtain

$$H_N(v) = H_k H_{N-k}(v), \quad H_0(v) = v.$$

In this way, the quantities H_N, i.e., the logarithmic generating functions, can be calculated in just the same way as the usual functions G_N.

Moreover, Eq. (6) can be rewritten in the form

$$P_N(\nu) = \frac{1}{2\pi i} \int_{(v_0)} \exp\{-v\nu + H_N(v)\}\, dv, \tag{8}$$

where the integration is to be carried out on a suitable path in the complex plane, a path which intersects the real axis at $v = v_0$. The latter integral can be calculated to a good approximation by the method of steepest descents. Then, designating the first term of the well-known asymptotic expansion of the function $P_N(\nu)$ by $P_N^*(\nu)$, we obtain

$$\nu = H_N'(v),$$

$$P_N(\nu) \sim P_N^*(\nu) \tag{9}$$

$$= \exp\{-v\nu + H_N(v)\} / (2\pi H''(v))^{1/2},$$

where we have written v instead of v_0. The prime designates differentiation with respect to v; the relation (9) furnishes an approximate parametric representation of $P_N(\nu)$, where v plays the role of the independent parameter.

Thus our problem reduces to tabulating the functions $H_N(v)$, $H_N'(v)$, and $H_N''(v)$.

Calculating $H_N(v)$ by iterations, we can obtain $H_N'(v)$ and $H_N''(v)$ by numerical differentiation, and then, with the help of Eq. (9), we can calculate ν and $P_N(\nu)$ as functions of the independent parameter v. The fact that arbitrarily chosen values of v do not generally coincide with integral values of ν does not matter, since, in the cases of practical interest, ν takes on very large values.

4. Before giving a practical method of calculation, we shall introduce simple formulas for some of the moments of the distribution $P_N(\nu)$. The expressions

$$\left(\frac{d^k H_N(v)}{dv^k}\right)_{v=0} = K_k^{(N)} \tag{10}$$

are the so-called semi-invariants of the distribution. In particular

$K_1^{(N)} = \nu_N$, the mean value of ν,

$K_2^{(N)} = \overline{(\nu - \overline{\nu}_N)^2}$, the variance,

$K_3^{(N)} = \overline{(\nu - \overline{\nu}_N)^3}$, the mean cube of the deviation.

M

Setting $k = N - 1$ in Eq. (5), differentiating with respect to v, and then setting $v = 0$, we obtain (after some simple calculations) recurrence formulas for the moments $K_k^{(N)}$

$$K_1^{(N)} = p^N, \quad K_2^{(N)} = Q\,\frac{p^{2N} - p^N}{p^2 - p}\,, \tag{11}$$

$$K_3^{(N)} = \frac{p^N}{p\,(p^2 - 1)}\left\{R\left(p^{2N} - 1\right)\right.$$

$$\left. + \frac{3Q^2}{p-1}\left(p^{2N-1} - p^N - p^{N-1} + 1\right)\right\},$$

where we have set

$$K_1^{(1)} = p, \quad K_2^{(1)} = Q, \quad K_3^{(1)} = R.$$

The first of the formulas (11) shows that the mean number of electrons at the Nth stage equals the product of the mean multiplication factors p pertinent to the separate stages. The second formula shows that $K_2^{(N)}/(K_1^{(N)})^2 \sim Q/(p^2 - p)$ does not depend on N if $N \gg 1$, $p > 1$. This indicates that the spread of the distribution $P_N(\nu)$ with respect to its mean value does not change greatly as N increases, i.e., if we were to plot $P_N(\nu)$ for $\nu = 1, 2, 3, \ldots$, changing the scale so that the mean values coincide, we would get distributions with the same spread. In other words, the distributions

$$p^N P_N(\nu / p^N) \tag{12}$$

have identical mean values, and moreover, the same spread. This agreement of the distributions does not carry over for the higher moments; the third moments of these distributions will differ considerably.

5. Computing the iterations. The iteration process can be given a simple geometrical interpretation (Fig. 1). On the (u, U) plane we have drawn the curve M, corresponding to the formula $U = G(u)$, and the straight line L corresponding to the formula $U = u$. There are two intersections, one at point A, where $u = U = 1$, and the other at point B, where $u = U = u_1$. There are two and only two such intersections if

$$1)\ G'(1) = p > 1,$$

$$2)\ G(0) = P(0) > 0.$$

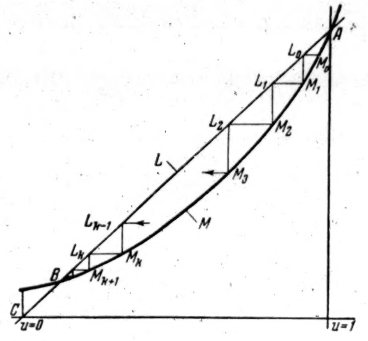

Fig. 1. Geometrical representation of the iteration process.

In fact, at the point A, M has a greater slope than L, and at the point C, where $u = 0$, $U = P(0)$, M lies above L; thus, there must be at least one intersection, say at $u = u_1$, in the interval $0 < u_1 < 1$; moreover, inasmuch as $G(u)$ has only positive derivatives and is concave downward, there can only be one such intersection.

Beginning now with a value of u, for example, $1 - \epsilon$, such that $u_1 < u < 1$, we find the corresponding point M_0 on the curve M. Drawing a horizontal through M_0, we obtain on the left an intersection L_0 with the line L; the coordinates of L_0 will be $u = U = G(1 - \epsilon)$. Now, dropping a vertical through L_0, we intersect the curve M at the point M_1, with coordinates $u = G(1 - \epsilon)$, $U = GG(1 - \epsilon)$. Repeating this procedure, we obtain a broken line. The abscissae of the points $M_0, M_1, M_2, \ldots$ (on the curve M) will be

$$1 - \varepsilon, \quad G(1 - \varepsilon), \quad GG(1 - \varepsilon), \ldots,$$

i.e., the iterations of $1 - \epsilon$.

As the point B is approached, the segments become shorter and shorter, and it can be seen that the sequence $G_n(1 - \epsilon)$, $n = 1, 2, 3, \ldots$, monotonically converges to the value u_1.

In the same way, we see that, starting with a value $0 < 1 - \epsilon < u_1$, we obtain an increasing sequence of points, which also converge to the limit u_1. Starting from the point $u = 1 + \epsilon$, we get a sequence of rapidly increasing values of u.

With a little more argument we can show that

$$\lim_{N=\infty} G_N(u) = G^*(u) = u_1, \quad 0 \leqslant u < 1.$$

Indeed, in the interval $u_1 < u < 1$, we have

$$u_1 < G(u) < u.$$

Iterating this N times, we find [since $G(u)$ is a monotone function] that

$$u_1 < G_{N+1}(u) < G_N(u).$$

Thus we see that the sequence

$$G_1(u), \quad G_2(u), \ldots \tag{13}$$

is monotonically decreasing and bounded, i.e., it must have a limit. The limit can only be u_1. Thus $G^*(u) = u_1, \quad u_1 \leqslant u < 1.$

Furthermore, starting from

$$u_1 > G(u) > u \quad \text{for} \quad u_1 > u \geqslant 0,$$

we see that the sequence (13) is monotonically increasing and bounded in the specified interval, and consequently converges to u_1. Thus

$$G^*(u) = u_1 \quad \text{for} \quad 0 \leqslant u < 1.$$

Let us extend the result obtained above to complex values of u, since complex u are of interest in calculating the integral (9).

We have

$$G_N(u) - G_N(0) = P_N(1)\,u + P_N(2)\,u^2 + \ldots;$$

The coefficients are probabilities and, consequently, non-negative. We thus have

$$|G_N(u) - G_N(0)| \leqslant |G_N(|u|) - G_N(0)|.$$

Inasmuch as the right-hand side of this expression has the limit zero for $|u| < 1$, the same must be true for the left-hand side. Thus, we obtain

$$G^*(u) = u \quad \text{for} \quad |u| < 1. \tag{14}$$

6. It is of some interest to determine the size of the steps of the iterational procedure in a very small neighborhood of the points of intersection A and B. Consider the intersection A; in its neighborhood the curve M can be replaced to a good approximation by a straight line M' with slope p. Carrying out the iteration between the two straight lines, we see that the abscissae of the steps are, to a good approximation,

$$1 - \varepsilon; \quad 1 - p\varepsilon, \quad 1 - p^2\varepsilon, \ldots$$

Thus, to a first approximation, the distances from $u = 1$ constitute an increasing geometrical progression (Fig. 2). This simple behavior changes for orders of iteration such that there is an appreciable difference between the directions of the curve M and the tangent M'. In most of the interval between A and B, the curve bends away strongly from its tangent, and the steps are given by a complicated function of their index. Near B the steps again approximate a geometrical progression, so that for a large enough number k of steps, the abscissae are given to a good approximation by an expression of the form $u_1 + p_1^k \epsilon$, where $p_1 = G'(u_1)$, so that $0 < p_1 < 1$.

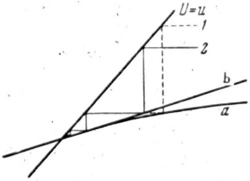

Fig. 2. *a.* curve, *b.* tangent; 1. exact steps, 2. approximate steps.

From the picture introduced above, we can derive a simple practical method of tabulating $G_N(u)$ for a given value of N. Let us draw, as was done above, a broken line $M_1, L_1; M_2, L_2, \ldots$, starting within a small neighborhood of the point A, so that the abscissa of the first point M_1 must be

$$u(0) = 1 - \varepsilon,$$

where ϵ is positive, but very small. Designating the subsequent abscissae by $u(1)$, $u(2)$, $\ldots$, we have

$$u(k) = G_k(1 - \varepsilon).$$

Comparing the kth and $(N+k)$th steps, we have

$$u(N+k) = G_{k+N}(1 - \varepsilon) = G_N(u(k)).$$

Thus, taking k as an independent parameter, we obtain a parametric representation of the function $G_N(u)$; indeed, we have

$$u = u(k), \quad G_N(u) = u(N+k).$$

Consequently, the tabulation of $G_N(u)$ consists in reading the kth abscissa as the value of the variable, and the $(k+N)$th abscissa as the corresponding value of the function, and repeating this operation for $k = 1, 2, \ldots$, etc.

Tabulation by the means just indicated has, nevertheless, the defect that the steps are comparatively large in the intermediate region between A and B. However, to get a more exact tabulation, we can construct several broken lines with mutually related steps. A more staisfactory procedure consists in interpolating between the first and second steps with a geometrical progression; in this way, we can determine a certain value u between $u(0)$ and $u(1)$, by setting

$$u(x) = 1 - p^{x}\varepsilon.$$

Starting from an iteration of the form

$$u(x+k) = G_k(u(x)) \quad \text{for} \quad x = 0;\ 0{,}2;\ 0{,}4;\ 0{,}6;\ 0{,}8;\ k = 1, 2, \ldots,$$

we determine the function

$$G^{*}_{x+k}(1-\varepsilon) = G_k(u(x))$$

for the step 0.2, so that the parametric representation of $G_N(u)$ can be written as

$$u = G^{*}_{k+x}(1-\varepsilon), \quad G_N(u) = G^{*}_{k+x+N}(1-\varepsilon). \tag{15}$$

We have tabulated $G_{10}(u)$ by the means indicated, assuming that $P(\nu)$ is a Poisson distribution. Thus, taking

$$P(\nu) = e^{-p}\frac{\nu^{p}}{\nu!} \qquad \text{and } G(u) = \exp\{p(u-1)\},$$

we found that for the indicated distribtuion, with $p = 5$,

$$u_1 = 0.006997.$$

Then, starting form $\epsilon = 2.358 \times 10^{-7}$, and dividing the first interval $u(0)$, $u(1)$ into five parts, we obtained Tables I and II. In Table I we tabulated $G^{*}_{k+x}(1 \pm \epsilon)$ according to Eq. (15); in Table II we tabulated the function $G_{10}(u)$ using Table I.

7. We must now determine the derivatives of $G_N(u)$. According to the parametric representation (15), differentiation with respect to u can be carried out as follows:

$$\frac{dG_N(u)}{du} = \frac{dG^{*}_{k+x+N}(1-\varepsilon)}{dx}\,\frac{dx}{du};$$

whence the derivatives of $G_N(u)$ are obtained in the following parametic representation

$$\frac{dG_N(u)}{du} = \frac{dG^{*}_{k+x+N}(1-\varepsilon)}{dx} \bigg/ \frac{dG^{*}_{k+x}(1-\varepsilon)}{dx}, \qquad u = G_{k+x}(1-\varepsilon). \tag{16}$$

The derivatives $dG^{*}_{k+x}(1-\epsilon)/dx$ can be obtained by numerical differentiation of $G^{*}_{k+x}(1-\epsilon)$.

Differentiating again, we find

$$\frac{d^2G(u)}{du^2} = \frac{d}{dx}\left(\frac{dG_N(u)}{du}\right) \bigg/ \frac{dG^{*}_{k+x}(1-\varepsilon)}{dx}. \tag{17}$$

In differentiating the function $dG_N(u)/du$ with respect to x, it must be understood that u itself is a function of x. Equation (17) is given in the form most useful for computation. We also tabulated these functions in Tables I and II.

The functions $G_N(u)$ for $N = 0, 1, 2, \ldots$, are shown in Fig. 3. It is clear that as N increases, the functions rapidly approach their limiting values.

With the help of the tables given, we calculated $P^{*}_{10}(\nu)$. In Fig. 4 are shown $P^{*}_{10}(\nu)$ and $P(\nu)$ in the units given by Eq. (12); it is clear that the two distributions are quite alike.

8. Below we shall investigate more rigorously the properties of the iterations $G_k(u)$, and show that the method of calculation used earlier in this paper leads to a generalization of the iterational process. Using this generalized iterational process, we shall give the solution of the inverse multiplier problem, mentioned at the beginning of the paper.

9. Iterations of negative index. We can introduce $G_{-k}(u)$ as the inverse function of $G_k(u)$. Recalling that the $G_k(u)$ are monotonically increasing functions of the argument u, we see that the inverse function is uniquely defined, at least, in the interval $u_1 \leq u \leq 1$; the function $G_{-k}(u)$ can

TABLE I

$\varepsilon = 2.35785 \cdot 10^{-7}$

$k + x$	$G^*_{k+x}\ (1-\varepsilon)$	$\frac{\partial G_{k+x}\ (1-\varepsilon)}{\partial x}$	$G^*_{k+x}\ (1+\varepsilon)$	$\frac{\partial G^*_{k\pm x}\ (1-\varepsilon)}{\partial x}$
>5	$\sim 1-\varepsilon p^{k+x}$	$\sim 1-\varepsilon \ln p\ p^{k+x}$	$\sim 1+\varepsilon p^{k+x}$	$\sim 1+\varepsilon \ln p\ p^{k+x}$
5.0	0.9993	0.0012	1.0007	0.0012
5.2	0.9990	0.0016	1.0010	0.0016
5.4	0.9986	0.0023	1.0014	0.0023
5.6	0.9981	0.0031	1.0019	0.0031
5.8	0.9973	0.0043	1.0027	0.0043
6.0	0.9963	0.0059	1.0037	0.0060
6.2	9.9949	0.0081	1.0051	0.0082
6.4	0.9930	0.0112	1.0070	0.0114
6.6	0.9904	0.0154	1.0097	0.0157
6.8	0.9868	0.0211	1.0135	0.0219
7.0	0.9818	0.0290	1.0186	0.0303
7.2	0.9750	0.0396	1.0258	0.0422
7.4	0.9657	0.0540	1.0358	0.0589
7.6	0.9531	0.0733	1.0499	0.0826
7.8	0.9359	0.0989	1.0696	0.1168
8.0	0.9130	0.1323	1.0976	0.1663
8.2	0.8824	0.1749	1.1378	0.2398
8.4	0.8424	0.2276	1.1963	0.3517
8.6	0.7908	0.2900	1.2831	0.5285
8.8	0.7259	0.3591	1.4173	0.8227
9.0	0.6472	0.4281	1.6294	1.3410
9.2	0.5555	0.4856	1.9917	2.3361
9.4	0.4547	0.5170	2.6681	4.4319
9.6	0.3513	0.5086	4.1195	8.9592
9.8	0.2540	0.4555	8.0150	
10.0	0.1713	0.3666	23.2646	
10.2	0.1083	0.2634	142.3725	
10.4	0.0654	0.1697	4190.2500	
10.6	0.0390	0.0996		
10.8	0.0240	0.0547		
11.0	0.0159	0.0290		
11.2	0.0116	0.0152		
11.4	0.0093	0.0079		
11.6	0.0082	0.0040		
11.8	0.0076	0.0021		
12.0	0.0073	0.0011		
12.2	0.0071	0.0006		
12.4	0.0071	0.0003		
12.6	0.0070	0.0001		
12.8	0.0070			
13.0	0.0070			

TABLE II

$$u = G^{*}_{k+x}(1-\varepsilon)\,, \quad v = G^{*}_{k+x}(1+\varepsilon)$$

$k+x-10$	$G_{10}(u)$	$\frac{\partial G_{10}(u)}{\partial u}\times 5^{-10}$	$\frac{\partial^2 G_{10}(u)}{\partial u^2}\times 5^{-20}$	$G_{10}(v)$	$\frac{\partial G_{10}(v)}{\partial v}\times 5^{-10}$	$\frac{\partial^2 G_{10}(v)}{\partial v^2}\times 5^{-20}$
5.0	0.9993			1.0007		
5.2	0.9990	0.9992		1.0010		
5.4	0.9986	0.9996		1.0014		
5.6	0.9981	0.9980		1.0019	1.0010	
5.8	0.9973	0.9966		1.0027	1.0030	
6.0	0.9963	0.9971		1.0037	1.0042	
6.2	0.9949	0.9936		1.0051	1.0056	
6.4	0.9930	0.9914		1.0070	1.0079	
6.6	0.9904	0.9876		1.0097	1.0109	
6.8	0.9868	0.9837		1.0135	1.0167	
7.0	0.9818	0.9770		1.0186	1.0229	
7.2	0.9750	0.9688		1.0258	1.0316	
7.4	0.9657	0.9571	0.5491	1.0358	1.0438	
7.6	0.9531	0.9415	0.5340	1.0499	1.0610	
7.8	0.9359	0.9205	0.5195	1.0696	1.0870	
8.0	0.9130	0.8924	0.5031	1.0976	1.1219	0.6455
8.2	0.8824	0.8551	0.4785	1.1378	1.1725	0.6811
8.4	0.8424	0.8067	0.4469	1.1963	1.2465	0.7270
8.6	0.7908	0.7449	0.4062	1.2831	1.3573	0.8101
8.8	0.7259	0.6685	0.3596	1.4173	1.5315	0.9209
9.0	0.6472	0.5776	0.3031	1.6294	1.8093	1.0975
9.2	0.5555	0.4749	0.2406	1.9917	2.2844	1.4230
9.4	0.4547	0.3664	0.1769	2.6681	3.1411	
9.6	0.3513	5.2613	0.1182	4.1195	4.6022	
9.8	0.2540	0.1696	0.0704	8.0150		
10.0	0.1713	0.0989	0.0366	23.2646		
10.2	0.1083	0.0515	0.0165	142.3725		
10.4	0.0654	0.0241	0.0064	4190.2500		
10.6	0.0390	0.0102	0.0022			
10.8	0.0240	0.0041	0.0007			
11.0	0.0159	0.0016				
11.2	0.0116	0.0010				
11.4	0.0093	0.0002				
11.6	0.0082	0.0001				
11.8	0.0076					
12.0	0.0073					
12.2	0.0071					
12.4	0.0071					
12.6	0.0070					
12.8						

sometimes be defined in a larger interval. From the definition introduced above, it follows that

$$G_k G_l(u) = G_{k+l}(u) \tag{18}$$

for arbitrary integers k and l.

Iterations of fractional order. We can generalize the definition of $G_k(u)$ to include fractional orders, while retaining the validity of the relation (18) for interpolating values of k. The interpolation can be done by a method like that already used in this paper. We shall show that this method can be made mathematically rigorous.

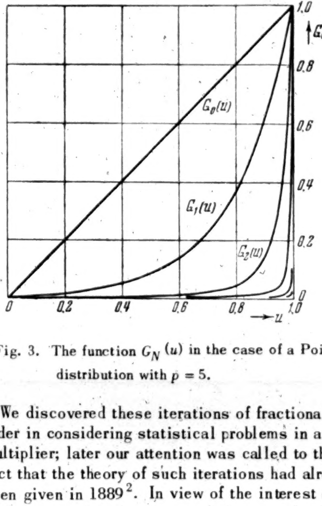

Fig. 3. The function $G_N(u)$ in the case of a Poisson distribution with $p = 5$.

We discovered these iterations of fractional order in considering statistical problems in a multiplier; later our attention was called to the fact that the theory of such iterations had already been given in 1889[2]. In view of the interest of a whole group of questions pertaining to multipliers, we repeat here the theory of such iterations; the present exposition is somewhat more detailed than the original one[2].

In close analogy to Eq. (15), we define the following function

$$\tilde{G}_{x,n}(1-\varepsilon) = G_n(1-\varepsilon p^x). \tag{19}$$

We must perform a suitable passage to the limit $n \to \infty$, $\epsilon \to 0$, and thereby hope to get a generalized iteration. Such a passage to the limit can be achieved by substituting in Eq. (19)

$$\varepsilon = 1 - G_{-n}(u), \quad n \to \infty,$$

where u is fixed

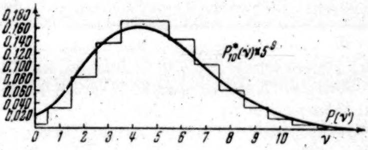

Fig. 4. The distributions $P^*_{10}(\nu)$ and $P(\nu)$(Poisson distribution), $\nu' = 5^9\nu$.

In this way, we define (first for finite values of n)

$$G_{x,n}(u) = G_n[1 - p^x(1 - G_{-n}(u))]. \tag{20}$$

The geometrical meaning of the functions $G_{x,n}(u)$ defined in this way can be shown graphically in Fig. 1 as follows. Beginning with the point $[u, U = G(u)]$ on the curve M, we make a large number n of steps to the right, and finally approach the point with abscissa $G_{-n}(u) \approx 1$ in the neighborhood of A. The abscissa of the latter point differs from unity by the small quantity

$$\varepsilon = 1 - G_{-n}(u).$$

Multiplying this distance by p^x, we arrive approximately at the point x steps back, provided that x is an integer; consequently, for integral x,

$$p^x(1 - G_{-n}(u)) \approx 1 - G_{-x-n}(u).$$

Thus, for integral x we expect that

$$G_{x,n}(u) \approx G_n G_{x-n}(u) = G_x(u).$$

Inasmuch as the approximation should improve with increasing n, we can expect that the limit

$$\lim_{n=\infty} G_{x,n}(u) = G^*_x(u) \tag{21a}$$

exists, and that

$$G^*_x(u) = G_x(u), \tag{21b}$$

if x is integral. Below we shall show that not only Eq. (21a) but also Eq. (21b) actually are valid, and moreover, that for arbitrary real x we have

---

[2] M. Lémeray, Compt. rend. **128**, 278 (1889)

$$G^{*}_{x}G^{*}_{y}(u)=G^{*}_{x+y}(u). \tag{22}$$

10. For the proof, we first investigate $G_{x,n}(u)$, defined by Eq. (20) for finite values of n.

Since $p > 1$, the argument of G_n for $x \leq 0$ in the right-hand side of Eq. (20) lies between zero and one, if $G_{-n}(u)$ is in the same interval. Thus $G_{x,n}(u)$ is completely defined for $u_1 \leq u \leq 1$ and $x < 0$. For $x > 0$, the argument of G_n in the right-hand side of Eq. (20) can be negative, and therefore we must restrict ourselves to a consideration of values of u that are not too small.

Furthermore, from Eq. (20) we have

$$G_{x,n}G_{y,n}(u)=G_{x+y,n}(u), \tag{23}$$

and also

$$G_{0,n}(u)=u. \tag{24}$$

Setting $x = -y$, we obtain

$$G_{x,n}G_{-x,n}(u)=u.$$

Thus $G_{-x,n}$ is the inverse function of $G_{x,n}$. Differentiating Eq. (20) with respect to x, we find

$$\frac{\partial G_{x,n}(u)}{\partial x}=(\ln p)\,p^{x}(1-G_{-n}(u))$$

$$G_n'\,[1-p^{x}(1-G_{-n}(u))]>0.$$

Consequently, $G_{x,n}(u)$ is a monotone increasing function of x, and therefore has a unique inverse function.

Equations (23) and (24) show that for fixed n and $x = 0, 1, 2, \ldots$, $G_{x,n}(u)$ represents a sequence of iterations, where the iterated function is $G_{1,n}(u)$. It remains to show that the limits exist as $n \to \infty$.

The passage to the limit. To prove the existence of the limits $G^{*}_{x}(u)$, it is necessary to assume that the first and second derivatives of $G(u)$ exist at $u = 1$. As before, we write

$$G'(1)=p,\ G''(1)=Q+p^{2}=q.$$

From the fact that $G'(u)$ and $G''(u)$ are nonnegative in the interval $0 \leq u \leq 1$, it is easily found that

$$1-p(1-u)\leqslant G(u) \tag{25}$$

$$\leqslant 1-p(1-u)+{}^{1}/_{2}\,q\,(1-u)^{2}.$$

Analogously, for $G_n(u)$ with $0 \leq u \leq 1$, $n = 1, 2, \ldots$, it can be shown that

$$1-p^{n}(1-n)\leqslant G_n(u) \tag{26}$$

$$\leqslant 1-p^{n}(1-u)+{}^{1}/_{2}\,\alpha p^{2n}(1-u)^{2},$$

where

$$\alpha p^{2n}=G_n''(1).$$

Thus [cf. Eq. (11)]

$$\alpha=\alpha_0(1-p^{-n}),\ \ \alpha_0=q\,/\,p(p-1).$$

We shall examine the behavior of $1 - G_{-n}(1-\epsilon)$ for small values of ϵ, and large positive values of n. At the beginning of this paper, we arrived qualitatively at the conclusion that $1 - G_{-n}(1-\epsilon)$ approaches its limiting value of zero almost like a geometrical progression. In order to make the qualitative conclusions given above more rigorous, we shall show the existence of a finite limit $A(u)$ such that, for $n > 0$

$$p^{n}(1-G_{-n}(u))<A;\quad u_1\leqslant u<1.$$

For the proof, we shall write

$$G_n(1-\varepsilon)=u \tag{27}$$

or

$$\varepsilon=1-G_{-n}(u).$$

Approximating $G_n(1-\epsilon)$ by polynomials in accordance with Eq. (26), we get from Eq. (27)

$$1-p^{n}\varepsilon<u\leqslant 1-p^{n}\varepsilon+{}^{1}/_{2}\,\alpha_0 p^{2n}\varepsilon^{2}.$$

On the left-hand side of the inequality is a monotone decreasing function of ϵ; thus, there exists an $\epsilon' \leq \epsilon$ for which the first equality becomes an equality if ϵ is replaced by ϵ'. Analogously, for not too large ϵ, there exists an $\epsilon'' \geq \epsilon$ for which the second inequality becomes an equality if ϵ is replaced by ϵ''. Thus we can write

$$\varepsilon'\leqslant\varepsilon\leqslant\varepsilon''$$

and $$1-p^{n}\varepsilon'=u=1-p^{n}\varepsilon''+{}^{1}/_{2}\,\alpha_0 p^{2n}\varepsilon''^{2}.$$

Solving these equations with respect to ϵ' and ϵ'', we obtain

$$\varepsilon' = \frac{1-u}{p^n}, \quad \varepsilon'' = \frac{\alpha_0}{p^n}\left(1-\sqrt{1-\frac{2(1-u)}{\alpha_0}}\right).$$

Bearing in mind that $1-\sqrt{1-2h} \leqslant h+2h^2$ for $h \leqslant {}^1/_2$, we can write the inequality for ϵ in the form

$$\begin{aligned} 1-u &\leqslant p^n\varepsilon \\ &\leqslant 1-u+\frac{2(1-u)^2}{\alpha_0} = A(u), \end{aligned}$$

provided that

$$1 \geqslant u \geqslant 1-\alpha_0/2, \tag{28}$$

and also

$$1 \geqslant u \geqslant u_1, \tag{29}$$

where we must use the stronger of the stipulated conditions.

Expressing ϵ in the terms of u, we get

$$p^n(1-G_{-n}(u)) \leqslant A(u), \tag{30}$$

where the boundary value $A(u)$ certainly does not depend on n, if it is assumed that u lies within both intervals (28) and (29). However, it is possible to free ourselves from condition (29). If

$$1 > 1-\alpha_0/2 > u_1,$$

and u lies in the interval

$$1-\alpha_0/2 \geqslant u \geqslant u_1,$$

i.e., if u lies outside the interval (29), then there must exist a finite k, dependent on $u > u_1$, such that $1 \geq G_{-k}(u) \geq 1-\alpha_0/2$; then $v = G_{-k}(u)$ lies inside the interval (29), although u does not lie inside this interval. Substituting $v = G_{-k}(u)$ in the inequality (30) instead of u, and multiplying by p^k, we find that

$$p^{n+k}(1-G_{-n-k}(u)) \leqslant p^k A(G_{-k}(u));$$

then, setting

$$p^k A(G_{-k}(u)) = B(u),$$

we have

$$p^n(1-G_{-n}(u)) \leqslant B(u) \tag{31}$$

$$u_1 < u \leqslant 1, \; n > k.$$

Thus we have an upper bound, even if u lies outside the interval (28), but inside the interval (29). For $u = u_1$, the upper bound does not exist, inasmuch as

$$p^n(1-G_{-n}(u_1)) = p^n(1-u_1) \to \infty$$

as

$$n \to \infty.$$

With the help of the result just obtained, we can show the existence of the limit of $G^*_x(u)$. To do this, we evaluate the difference

$$\begin{aligned} h_n &= G_{x,n}(u) - G_{x,n+1}(u) \\ &= G_n[1-p^x(1-G_{-n}(u))] \\ &\quad - G_{n+1}[1-p^x(1-G_{-n-1}(u))]. \end{aligned}$$

Setting

$$1-G_{-n-1}(u) = \varepsilon$$

or

$$u = G_{n+1}(1-\varepsilon),$$

we have

$$h_n = G_n(u') - G_n(u''), \tag{32}$$

where

$$\begin{aligned} u' &= 1-p^x(1-G(1-\varepsilon)), \\ u'' &= G(1-p^x\varepsilon). \end{aligned} \tag{33}$$

From Eq. (32) we have

$$|h_n| \leqslant |u'-u''|\, p^n. \tag{34}$$

From Eq. (33) we find, with the help of Eq. (25), that

$$\begin{aligned} 1-p^{x+1}\varepsilon &\leqslant u' \leqslant 1-p^{x+1}\varepsilon + {}^1/_2 q p^x \varepsilon^2, \\ 1-p^{x+1}\varepsilon &\leqslant u'' \leqslant 1-p^{x+1}\varepsilon + {}^1/_2 q p^{2x} \varepsilon^2. \end{aligned}$$

Thus $$|\hat{u}'-u''| \leqslant {}^1/_2 q\varepsilon^2 (p^x + p^{2x}). \tag{35}$$

It was shown above that $\epsilon < B(u)/p^n$; hence, from the inequalities (34) and (35) we have

$$|h_n| \leqslant {}^1/_2 (B(u))^2 q (p^x + p^{2x}) / p^n = C(u)/p^n,$$

so that the sequence $G_{x,n}(u)$, $n = 1, 2, \ldots$, converges for sufficiently large values of n, at least as fast as a geometrical series, and hence the limit $G_x^*(u)$ necessarily exists.

For integral x, the value $G_x^*(u)$ can easily be calculated. We shall consider only the case $x = 1$. We introduce two quantities ϵ' and ϵ'' as follows

$$1 - \varepsilon' = G(1 - \varepsilon) \text{ и } 1 - \varepsilon'' = 1 - p\varepsilon. \qquad (36)$$

In analogy with the derivation of the inequality (35), we find that ϵ' and ϵ'' satisfy the following relation

$$|\varepsilon' - \varepsilon''| < q\varepsilon^2.$$

Thus

$$|G_n(1 - \varepsilon') - G_n(1 - \varepsilon'')| \leqslant p^n q \varepsilon^2.$$

Setting

$$\varepsilon = 1 - G_{-n}(u),$$

and taking account of Eq. (36), we can write

$$|G(u) - G_{1,n}(u)| \leqslant p^n q \varepsilon^2.$$

Inasmuch as ϵ^2 is of order p^{-2n}, as shown above [cf. Eq. (31)], the expression on the right-hand side goes to zero, and we have

$$\lim_{n=\infty} G_{1,n}(u) = G(u).$$

11. We note that instead of using expression (20), we could have begun our investigation by introducing the expression

$$\widetilde{G}_{x,n}(u) = G_{-n}\{u_1 - p_1^x (u_1 - G_n(u))\}, \qquad (37)$$

where

$$p_1 = G'(u_1).$$

Expressions (20) and (37) are analogous, but nevertheless

$$\lim_{n=\infty} \widetilde{G}_{x,n}(u) = \widetilde{G}_x^{\bullet}(u)$$

and

$$\lim_{n=\infty} G_{n,x}(u) = G_x^{\bullet}(u)$$

are two completely different limiting processes. Therefore, it should by no means be considered trivial that these two processes lead to one and the same limiting function. However, more detailed examination shows that

$$G_x^{\bullet}(u) = \widetilde{G}_x(u).$$

Thus Eq. (37) can be used instead of Eq. (20) for obtaining iterations of fractional order. We note that in just the same way that we proved the relation $G_1^*(u) = G(u)$, we can show that $\widetilde{G}_1^*(u) = G(u)$; furthermore

$$\widetilde{G}_x^{\bullet} \widetilde{G}_y^{\bullet}(u) = \widetilde{G}_{x+y}^{\bullet}(u);$$

whence it follows that

$$\widetilde{G}_k^{\bullet}(u) = G_k^{\bullet}(u) = G_k(u)$$

for an arbitrary integral value of k. The proof can also be extended to non-integral values of the index. Indeed, we shall write

$$g_1(u) = G_x(u),$$

$$g_2(u) = G_{2,x}(u), \ldots, g_k(u) = G_{k,x}(u).$$

Here $g_1(u)$, $g_2(u)$, . . . are also a sequence of iterations, which for $x > 1$ can be considered as a basis; we can define

$$g_x^{\bullet}(u) = \lim_{n=\infty} g_n\{1 - p'^y (1 - g_{-n}(u))\},$$

$$p' = p^x,$$

$$\widetilde{g}_y^{\bullet}(u) = \lim_{n=\infty} g_{-n}\{u_1 - p_1'^y (u_1 - g_n(u))\},$$

$$p_1' = p_1^x.$$

As before, we have

$$g_1^{\bullet}(u) = \widetilde{g}_1^{\bullet}(u) = g_1(u).$$

Hence

$$\widetilde{G}_x^{\bullet} = G_x^{\bullet}(u).$$

We see that for $x > 1$, Eqs. (20) and (37) lead to identical results. With the help of Eq. (22), the result obtained above can be extended to arbitrary real values of x.

12. The "inverse" problem of the multiplier, mentioned in Sec. 1, can be formulated as follows.

Given $P_N(\nu) = \pi(\nu)$, the distribution arising at the Nth stage of the multiplier; we want to find $P(\nu) = P_1(\nu)$. With the help of the generating functions, we can write

$$\Gamma(u) = \sum_{\nu=0}^{\infty} u^{\nu}\pi(\nu) = G_N(u).$$

Using the generalized iterational process, we obtain

$$G(u) = \Gamma_{1/N}(u).$$

Indeed

$$G_N(u) = \underbrace{G\ldots G(u)}_{N}$$
$$= \underbrace{\Gamma_{1/N}\ldots\Gamma_{1/N}(u)}_{N} = \Gamma(u).$$

Clearly we have

$$G(u) = \lim_{n=\infty} \Gamma_n\{1 - \pi^{1/N}(1 - \Gamma_{-n}(u))\},$$

where $\pi = \Gamma'(1)$ is the mean number of electrons ejected at the last stage.

Numerical calculations are immediately effective only when the distribution $\pi(\nu)$ is known sufficiently exactly. It goes without saying that we cannot require that $\pi(\nu)$ be known for the separate integral values of ν; the most that can be hoped for is that $\pi(\nu)$ be known over a range of values of ν that is not too broad. If the distribution is given in this way, then $\Gamma(u)$ can be calculated by numerical integration:

$$\Gamma(u) = \int_{-\infty}^{+\infty} u^{\nu}\pi(\nu)\,d\nu.$$

Only those values which are near $u = 1$ are of interest. Indeed, if $|1 - u| \gg 1/p^N$, then the value of the integral is practically equal to either zero or infinity, and the calculation loses its meaning. However, there is a small interval near $u = 1$ where the calculation can be made, which permits the determination of the main part of $\Gamma(u)$, from which we can find the iteration $\Gamma_{1/N}(u)$.

The procedure described above can always be carried out mathematically, and thus the distribution $P_1(\nu)$ can be calculated. However, if we started from an arbitrary distribution $\pi(\nu)$, the calculated result would in general lead to an unacceptable distribution $P_1(\nu)$, containing negative probabilities. Thus if we start with a distribution $\pi(\nu)$ and obtain an acceptable distribution $P(\nu)$, this may be regarded as a check on the correctness of the method used.

Translated by R. Silverman
122

SOVIET PHYSICS JETP VOLUME 1, NUMBER 3 NOVEMBER, 1955

Calculation of the Ultimate Thickness of an Emulsion Layer in the Investigation of Nuclear Processes by Means of the Photographic Method, II.

A. A. BENE

(Submitted to JETP editor May, 1954)
J. Exper. Theoret. Phys. USSR **28**, 706-710 (1955)

Herein is derived the correction formula used in the determination of the total number of tracks which are formed by a nuclear reaction within a photographic emulsion when the number of tracks which are completely within the emulsion layer are known. One considers only those tracks which lie within the angles $|\alpha| < \alpha_0$ and $|\beta| < \beta_0$ where α_0 is the maximum track inclination with respect to the emulsion plane and β_0 is the maximum inclination of the projection of the track onto the emulsion plane with respect to the direction of the incident particles.

An additional assumption is made that the beam of incident particles lies parallel to the emulsion plane.

1. INTRODUCTION

BY irradiating a photographic emulsion with nuclear particles of differing energies one obtains, within the emulsion, tracks of secondary particles. In addition a primary particle of given energy can be identically referred to a track of a secondary particle, however, only in the case that the track is totally within the emulsion. In a previous paper[1] a correction formula was obtained which permits one to determine the total number of tracks that characterize primary particles of specific energy when one knows the number of tracks which are completely within the emulsion. In this case the authors considered all tracks distributed about the direction of the incident particle within a maximum angle of θ_0. In many cases, however, it appears impossible to determine with sufficient accuracy the number of long tracks which possess large inclinations relative to the emulsion plane, i.e., relative to the plane in the visual field of a microscope. In this connection, we develop, in the present communication, an analogous correction formula which estimates the total number of tracks from the number of tracks within an angle α ($\alpha \leq \alpha_0$). The second limiting condition is that the angle β formed by the projection of the track onto the plane of the emulsion and the direction of the incident particle does not exceed the value β_0 (compare Fig. 1 and Fig. 2).

In these instances when α_0 is essentially small, β_0 can be assigned a large value, since its magnitude does not influence the accuracy in the measurement of long tracks. The direction of the incident particle is assumed to be parallel to the emulsion plane.

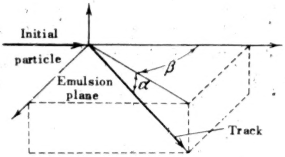

FIG. 1. Specification of the path of a track by the angles α and β.

2. DEVELOPMENT OF CORRECTION FORMULAS

Let σ represent the total number of secondary particles which are scattered within the given region of $-\alpha_0 \leq \alpha \leq \alpha_0$; $-\beta_0 \leq \beta \leq \beta_0$, and let σ' be the number of secondary tracks which terminate in the emulsion averaged relative to y over the entire emulsion thickness d. In this case y is the depth of the point of nuclear interaction beneath the surface of the emulsion. The ratio W of the number of tracks falling completely within the emulsion to the total number of tracks, has the form

$$W = \frac{N_1}{N} = 1 - \frac{\sigma'}{\sigma}. \tag{1}$$

Derivation of the expression for σ. Let us now consider the expression for σ. It is easily seen that this expression has the form

$$\sigma = \int_0^{2\pi} d\varphi \int_0^{\theta_1(\varphi)} f(\theta) \sin\theta \, d\theta, \tag{2}$$

where θ and ϕ are the usual spherical coordinates (Fig. 2) and $f(\theta)$ is the intensity of the secondary particles in the scattering angle θ which is measured in the laboratory system of coordinates.

---

[1] A. A. Bene and M. M. Agrest, J. Exper. Theoret. Phys. USSR **27**, 557 (1954)

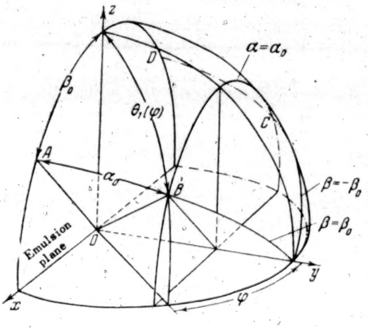

FIG. 2. The unit sphere with the region $\sigma \leq \alpha \leq \alpha_0$ and $-\beta_0 \leq \beta \leq \beta_0$ (surface *ABCD*) within which is scattered half of all the secondary particles under consideration. The figure is symmetric about plane *xz* (the emulsion plane). The direction of the incident particle is along the *z* axis. *O* is the point of the nuclear interaction.

By considering Fig. 2 one can show that

$$\cos\theta = \cos\alpha\cos\beta. \tag{3}$$

$$\operatorname{tg}\varphi = \operatorname{ctg}\alpha\sin\beta.$$

equation (2) then transforms to

$$\sigma = 4\int_0^{\beta_0} d\beta \int_0^{\alpha_0} f(\alpha,\beta)\cos\alpha\, d\alpha, \tag{4}$$

where $f(\alpha,\beta)$ is the intensity function $f(\theta)$ transformed with the aid of the first equation of (3).

To perform the integration in Eq. (4) we assume that the function $f(\theta)$ can be represented sufficiently accurately by

$$f(\theta) = a_0 + a_1\cos\theta + a_2\cos^2\theta$$

or

$$f(\alpha,\beta) = a_0 + a_1\cos\alpha\cos\beta + a_2\cos^2\alpha\cos^2\beta. \tag{5}$$

With this substitution we obtain (6)

$$\frac{1}{4}\sigma = a_0K_0\sin\alpha_0 + \frac{1}{2}a_1K_1(\alpha_0 + \sin\alpha_0\cos\alpha_0) + a_2K_2\left(\sin\alpha_0 - \frac{1}{3}\sin^3\alpha_0\right),$$

where K_i are functions of β_0 and are given below [see Eq. (10)].

Derivation of the Expression for σ′. In order to develop the expression for σ' we must consider the distribution of path lengths $S(\theta) = S(\alpha,\beta)$ of the secondary particles that are under under consideration (Fig. 3). In this figure the circles $\alpha = \alpha_0$ and $\beta = \beta_0$ were obtained by a central projection from the unit sphere (see Fig. 2) onto the surface $S = S(\theta)$, where the center of projection is the origin of coordinates. In addition, two locations of the emulsion surface which are essential for the derivation of σ' are shown in the Fig. 3.

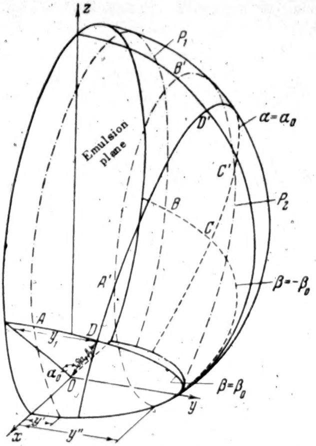

FIG. 3. The dependence of the path lengths *S* of the secondary particles on the angles of scattering is shown. The incident particle is directed along the *z* axis. The nuclear reaction occurs at the point *O*. Two positions of the surface layer of the emulsion are illustrated (circles P_1 and P_2) with $y = y' < y_1$ and $y = y'' > y_1$. Tracks which leave the emulsion lie in the regions *ABCD′DA* or *A′B′C′D′A′* for $y = y'$ or $y = y''$ respectively.

For a given value y the number of tracks $\sigma_1(y)$ which pass out through the surface of the emulsion is given by

$$\sigma_1(y) = 2\int_0^{\beta_0} d\beta \int_{\alpha_1}^{\alpha_0} f(\alpha,\beta)\cos\alpha\, d\alpha,$$

if

$$0 \leqslant y \leqslant y_1 = S(\alpha_0,\beta_0)\sin\alpha_0$$

and by

$$\sigma_1(y) = 2\int_0^{\beta_1} d\beta \int_{\alpha_1}^{\alpha_0} f(\alpha,\beta)\cos\alpha\, d\alpha,$$

if

$$y \geqslant y_1.$$

In this case α_1 is the value of α which specifies the location of the emulsion surface for a given value of y and β. The values of α_1 and β_1 are determined by the relations:

$$\sin\alpha_1 = y / S(\alpha_1, \beta);$$
$$S(\alpha_0, \beta_1) = y / \sin\alpha_0.$$

We shall evaluate $\sigma'(\sigma_1$ averaged over y) only for the case $d \geq S(\alpha_0, 0)$ (case B 1)) since, thanks to the existence of modern thick photo-emulsions, this condition is satisfied for most experiments.

If we consider that the tracks can break through on both sides of the emulsion, we obtain

$$\frac{d}{4}\sigma' = \int_0^{y_1} dy \int_0^{\beta_0} d\beta \int_{\alpha_1}^{\alpha_0} f(\alpha, \beta)\cos\alpha\, d\alpha + \int_{y_1}^{S(\alpha_0, 0)\sin\alpha_0} dy \int_0^{\beta_1} d\beta \int_{\alpha_1}^{\alpha_0} f(\alpha, \beta)\cos\alpha\, d\alpha, \tag{7}$$

where d is the emulsion thickness. Equation (7) is correct only for those cases with $\alpha_0 \leq \bar{\alpha}$, where $\bar{\alpha}$ is the value of α for which the function $\psi(\alpha) = S(\alpha, 0)\sin\alpha$ is a maximum(see reference 1,Fig. 3).

If we assume that the path length S depends upon the scattering angle in the manner of

$$S(\vartheta) = A_0 + A_1\cos\vartheta + A_2\cos^2\vartheta$$

or

$$S(\alpha, \beta) = A_0 + A_1\cos\alpha\cos\beta + A_2\cos^2\alpha\cos^2\beta,$$

we obtain

$$W = 1 - \frac{1}{d}\left\{S(\alpha_0, \beta_0)\sin\alpha_0 + \frac{4}{\sigma}I\right\}. \tag{8}$$

The quantity I has the form

$$\begin{aligned} I = {} & P_1\sin^2\alpha_0 + P_2\sin^4\alpha_0 + P_3\sin^6\alpha_0 \\ & + P_4\sin^2\alpha_0\cos\alpha_0 + P_5\sin^4\alpha_0\cos\alpha_0 \\ & + P_6\alpha_0\sin\alpha_0 + P_7\alpha_0\sin\alpha_0\cos\alpha_0 \\ & + P_8\alpha_0\sin\alpha_0\cos^2\alpha_0 - P_9\cos\alpha_0 + P_9, \end{aligned} \tag{9}$$

where the coefficients are

$$\begin{aligned} P_1 = {} & \frac{1}{8}Z_{22}K_5 + \frac{1}{2}Z_{02}K_8 + \frac{1}{2}Z_{11}[K_0 \\ & - K_2] - \frac{1}{2}Z_{00}K_0 - \frac{1}{2}Z_{20}K_2, \end{aligned}$$

$$\begin{aligned} P_2 = {} & -\frac{1}{6}Z_{22}[K_5 - K_4] - \frac{1}{2}Z_{02}\left[K_8 - \frac{1}{2}K_2\right] \\ & + \frac{1}{4}Z_{11}\,[3K_2 - 2K_0] + \frac{1}{12}Z_{20}K_2, \end{aligned}$$

$$P_3 = \frac{1}{24}Z_{22}K_5,$$

$$\begin{aligned} P_4 = {} & Z_{12}\left[K_1 - \frac{11}{10}K_3\right] + Z_{21}\left[K_6 - \frac{1}{5}K_3\right] \\ & + Z_{01}K_7 - \frac{1}{6}Z_{10}K_1, \end{aligned}$$

$$P_5 = -Z_{12}\left[K_1 - \frac{13}{10}K_3\right] - \frac{1}{3}Z_{21}K_6,$$

$$P_6 = -\frac{1}{2}Z_{10}K_1,$$

$$P_7 = \frac{1}{2}Z_{11}[K_0 - 2K_2],$$

$$P_8 = \frac{1}{2}Z_{12}[2K_1 - 3K_3],$$

$$P_9 = \frac{1}{3}K_1[Z_{10} + Z_{01}] + \frac{1}{5}K_3[Z_{12} + Z_{21}].$$

here

$$Z_{ik} = a_i A_k$$

and

$$\begin{aligned} K_0 &= \beta_0, \\ K_1 &= \sin\beta_0, \\ K_2 &= \frac{1}{2}\beta_0 + \frac{1}{4}\sin 2\beta_0, \\ K_3 &= \frac{3}{4}\sin\beta_0 + \frac{1}{12}\sin 3\beta_0, \\ K_4 &= \frac{3}{8}\beta_0 + \frac{1}{4}\sin 2\beta_0 + \frac{1}{32}\sin 4\beta_0, \\ K_5 &= -\left[\frac{1}{2}\beta_0 + 2\beta_0\cos 2\beta_0 + \frac{3}{8}\sin 4\beta_0\right], \\ K_6 &= \frac{13}{40}\sin\beta_0 - \frac{1}{2}\beta_0\cos\beta_0 - \frac{3}{40}\sin 3\beta_0, \\ K_7 &= \frac{1}{3}\sin\beta_0 - \beta_0\cos\beta_0, \\ K_8 &= K_2 - 2\beta_0\cos^2\beta_0. \end{aligned} \tag{10}$$

Regardless of the fact that in practice α_0 is small, all powers containing α are retained in Eq. (9) since the coefficients Z_{ik} can be large for different cases. In the consideration of a specific example, one can retain a smaller number of terms.

3. GENERAL REMARKS

For the particular case of proton emission, Eq. (8) reduces to the Richards formula[2] (his Case B) when one sets $\alpha_0 = \beta_0 = \theta_0$ with θ_0 being small. Further if one sets $\alpha_0 = \beta_0 = \pi/2$ Eq. (8) coincides with the formula developed in[1] for $\theta_0 = \pi/2$.

It gives me pleasure to express my thanks to Doctor Vestmeier who suggested the problem and to M. M. Agrest for many valuable discussions.

---

[2] H. T. Richards, Phys. Rev. 59, 796 (1941)

Translated by A. Skumanish
125

SOVIET PHYSICS JETP VOLUME 1, NUMBER 3 NOVEMBER, 1955

On the Theory of Crystal Growth

(Based on the article by I. V. Salli[1])

A. V. BELIUSTIN
Gorki Physico-Technical Institute

(Submitted to JETP editor October 27, 1953)
J. Exper. Theoret. Phys. USSR 28, 725-726 (June, 1955)

IN the article "On the Theory of Crystal Growth" by I. V. Salli[1], there appears a sequence of incorrect equations, which tends to invalidate the author's conclusions to a large extent.

The author's discussion is based on Eq. (5), the equation for the linear growth velocity u of a spherical nucleus of a new phase, and on the subsequent Eqs. (6), (7), (7a) and (7b), derived from it. After a necessary correction is made (the coefficient 2 is superfluous in all expressions for u, since it appeared due to an incorrect assumption in the computation of q, on p. 209[1], where the volume of a sphere was taken to be $2/3\,\pi r^3$) Eq. (5) takes on the following form:

$$u = Dv\left(\Delta - \frac{a}{r}\right)\left(\frac{1}{x} + \frac{1}{r}\right).$$

This and the subsequent equations, which are correct for an isotropic liquid, are applied to the analysis of different cases of crystal growth without any investigation of the validity of such an application. Thus, based on the fact that the coefficient of surface tension σ appears in the expression for u only through a ($a = 2\sigma MvC \sim /RT$), the author makes the following completely unwarrented conclusion regarding the role of the coefficient of surface tension in the crystal growth process: "One of the most important consequences of Eq. (6) is that surface tension affects the growth velocity only in the early stages of growth" (p. 210). As is well known from actual cases, the strong dependence of crystal growth velocity on direction remains true also for large crystals. For example, large as well as small crystals of sodium chloride have a cubic form. The cube faces are the planes having the slowest growth velocity and the smallest of all possible values of surface energy. Analogous conditions exist for other substances also.

In his attempts to confirm the correctness of his conclusions, Salli cites as an example the formation of platelets of cementite and their conversion to globules. Actually, he gives merely the appearance of agreement between the theory developed by him and actual observations. At that, he accomplished this only by a very peculiar interpretation of the coefficients σ and r: for σ he assumes surface tension in a direction normal to the crystal boundary (as if it were possible to speak of surface tension directed perpendicularly to the surface!), and for r – the linear dimension of a given part of the crystal (?) (see pp. 210, 211). Actually, r can only mean the radius of curvature at a given point on the crystal surface.

The fallacy in I. V. Salli's approach to the solution of the problems that he raises lies in his fundamental disregard of the specific properties of crystals as compared to those of isotropic bodies. In his opinion, crystallographic properties can play a role only in the very early growth stages of the crystal. In his explanation of the occurence of one or another crystal habit, he adds the following principle to the above-mentioned equations : " . . . the growing crystallization nucleus assumes the growth form which assures the most rapid development of the crystallized substance" (p. 208). This assumption appears as the only general principle determining crystal growth. It would have been possible to agree with him if, as the author assumes, the most prominent crystal faces were the most rapidly growing ones. In fact, the reverse is true; the most prominent crystal faces are the slowest growing ones[2]. For this reason, the occurrence of a many-faced habit can in no way be made to agree with the principle of fastest growth rate. Pursuant to this, he attempts to connect the many-faced crystal habits shown by the author (pp. 211, 212, case 2a) with the above stated principle and with the constitution of their interior; however, all the arguments pertaining to case 2a can be completely carried over to the formation of drops of a liquid. In this case, one reaches the conclusion that in the presence of certain fully determinable conditions a growing drop of liquid must assume a many-faced habit! It is interesting to cite the opinion of Shubnikov[3] in this connection: " . . . two tendencies, to a certain extent contradictory, appear simultaneously during crystal growth; a tendency to minimize the free energy and a tendency to most rapidly complete the process ". The explanation of one or another crystal growth property based on only one of these tendencies is possible only within narrow limits; the author of the article under discussion, however, has gone far beyond these limits.

---

[1] I. V. Salli, J. Exper. Theoret. Phys. USSR 25, 208 (1953)

Without discussing every weak point in the author's discussion, let us consider just one characteristic example where two parts of the same sentence are completely contradictory. On page 212[1] one reads: " After boundary formation, the growth velocity does not depend on the surface tension and the final habit is determined by the Curie-Wulff law ". But the Curie-Wulff principle has as its consequence that (we cite reference 2, p. 204): " the boundary growth velocity is proportional to the individual surface energies of these boundaries with regard to the mother liquor ". It is clear, that the final crystal habit can in no way be determined by the Curie-Wulff law if the growth of the crystals does not obey this law.

The disregard for the role of crystal properties becomes the more clear in the tabulation of "fundamental factors, determining the kinetics and the form of crystal growth ", placed at the end of the article under discussion.. Here, there is not one word regarding the function of the structural properties of the crystal; the discussion concerns itself only with the constitution of the crystal's environment. Such a one-sided approach to the problem of crystal growth cannot possibly yield good results.

Translated by L. V. Azaroff
128

---

[2] V. D. Kuznetsov, *Crystals and Crystallization*, GITTL, 1953, p. 101

[3] A. V. Shubnikov, *Crystal Genesis*, Academy of Science, USSR publication, 1953, p. 101

SOVIET PHYSICS JETP VOLUME 1, NUMBER 3 NOVEMBER, 1955

A Pulse Height Analyzer with an Electron Beam Tube

V. G. KHARTMAN, I. N. LEONT'EVA, A. P. SINIAVSKII AND L. V. VASIL'EV

(Submitted to JETP editor February 11, 1954)
J. Exper. Theoret. Phys. USSR 28, 699-705 (June, 1955)

A pulse height analyzer with an electron beam tube is described. The apparatus can sort into 20 channels positive pulses with amplitudes up to 100 volts, a rise time greater than 0.1 microsecond and a duration less than 30 microseconds. With a counting rate of 17,000 counts per minute, the loss is approximately 1%. The stability of the thresholds of the channels ~ 2%.

IN determining the energy spectra of elementary particles in nuclear physics, use is made of the method of measuring the heights of voltage pulses which are produced by the particles in an ionization chamber or some other detector.

If the pulses are fed into a non-linear element, for example, a diode with suitable bias, then only those pulses with amplitudes larger than this bias will pass and actuate a registering device. Changing the bias gives the curve of $n(E)$, where n is the number of pulses in a definite time whose amplitudes exceed the bias E (V). After differentiating, the differential distribution is obtained, which shows how many pulses Δn are passed within the bias interval ΔE. Since the measurement of a number n has an associated root mean square error $n^{1/2}$ because of the statistical character of the emergence of the pulses, then the error of the resultant $\Delta n = n_1 - n_2$, obtained in the time 2τ, is determined by the expression $(n_1 + n_2)^{1/2}$. If two diodes, whose biases are different by ΔE (V), are used at the same time, then pulses whose amplitudes are greater than $E(\mathrm{V}) + \Delta E(\mathrm{V})$ will be registered by both channels. The statistical fluctuations in the rate of emergence of these pulses will effect both channels identically. Because of this it is possible to eliminate the number of pulses counted by both channels by simple subtraction. After the lapse of time τ we have $\Delta n = n_1 - n_2$ with a root mean square error $(n_1 - n_2)^{1/2}$. From these considerations we see the advantage of a differential analyzer which automatically registers the number of pulses that pass through it in a channel of width ΔE.

Any analyzer has a shaping section in which incoming pulses of different forms, rise times of the leading edge, and duration, are transformed into pulses with shapes most suitable for sorting by a given analyzer. In addition, there are the sorting elements and finally the registering devices. The latter must register only the emergence of a pulse, i.e., they do or do not operate. Thus variation in the voltage supplied to the circuit and the resulting variation of the value of the pulse, within a fairly large range, does not effect the accuracy of the operation of the circuit. The shaping section passes all incoming pulses without exception, and therefore slow small variations of the parameters of the circuit with time will not have a great significance with respect to an accurate analysis of the pulses in the spectrum. But in contrast to what has just been said, the sorting elements of the analyzer have exacting requirements relative to stability and accuracy of operation. Here to a certain degree, a common change in the bias of all channels can be tolerated, but an arbitrary change of the width of an individual channel is completely inadmissible. Therefore, every effort is directed toward the selection of such sorting elements, that if they vary, will reduce this effect to a minimum. Various designs of analyzers differ from one another basically in their sorting elements.

The pulse analyzer described below uses an electron beam tube to sort pulses into 20 channels[1-4]. With its help it is possible to determine the pulse height spectrum of pulses having a rise time of less than 5 microseconds and greater than 0.1 microsecond. However, when necessary, the upper limit can be easily extended. The duration of the pulses should not be greater than 30 microseconds. The amplitudes of the pulses can vary from 0 to + 100 volts.

The incoming pulse (Fig. 1) is transformed so that the amplitude of the transformed pulse is

---

[1] W. E. Glenn, Jr., Nucleonics **4**, No. 6, 50 (1949)

[2] W. E. Glenn, Jr., Nucleonics **9**, No. 6, 24 (1951)

[3] D. A. Watkins, Rev. Sci. Instr. **20**, 495 (1949)

[4] E. W. Titterton and R. S. Wilson, J. British Inst. Radio Engr. **13**, 173 (1953)

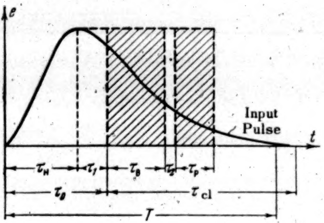

Fig. 1. The time cycle of the registration of a pulse (schematic): τ_H is the total rise time of the pulse, τ_p is the charging time of the "storage" capacitance, τ_{cl} is the time during which the input of the analyzer is clamped.

proportional to the amplitude of the incoming pulse *e*, and remains constant for a certain interval of time $\tau_1 + \tau_v + \tau_2$. After transformation, the pulse is applied to the deflecting plates of the electron beam tube. The electron beam, usually cut off by a negative bias, is intensified for the time τ_v by a pulse which is fed to the control grid of the electron beam tube at a time τ_0 after the start of the input pulse. In this way the beam, whose deflection is proportional to the amplitude of the input pulse, falls on the collector plates. The charge carried by the beam for the time τ_v is collected only by that plate whose position corresponds to the given deflection of the electron beam. An amplifier is connected to each collector plate, which amplifies and lengthens the resulting pulse so that it can actuate a mechanical register. The general arrangement of the analyzer is shown in Fig. 2 and Fig. 3.

After passing through a neutralized diode discriminator, which is supplied by a battery (Fig. 4), and the input clamping circuit (T_3, T_4), the pulses are fed to a cathode follower and charge the 200 $\mu\mu$f condenser through tube T_6 (a type 6Zh4 connected as a diode) to the amplitude of the pulse. The ungrounded side of this so-called "storage" condenser is controlled by the high resistance cathode follower T_8 (a type 6ZhZP). This tube works with its heater at low temperature (the heater voltage is 4 volts) and has a plate current ~ 50 microamperes; its grid current is 10^{-10} amp, so that in the interval of time after charging, and until the appearance of the following pulse, the capacitance discharges an insignificant amount. It is necessary to supply the heater of this tube as well as that of diode T_6 by a battery. After this, the pulse is amplified by an inverter and push-pull

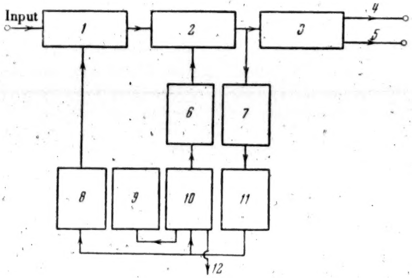

Fig. 2. Block diagram of the arrangement of the system. *1.* discriminator for reducing the noise; input clamping circuit (T_3, T_4); *2.* lengthening of pulses, charging "storage" capacitance; *3.* push-pull amplifier; *4.* and *5.* deflecting pulses to *Y* plates of the analyzer tube; *6.* delay line; *7.* amplifier, trigger generator; *8.* univibrator for clamping the input; *9.* common pulse counter; *10.* univibrator and stabilizer of the intensifying pulses; *11.* delay of 2 or 6 microseconds; *12.* intensifying pulse (to control grid of the analyzer tube).

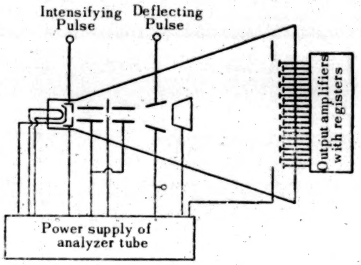
Intensifying Pulse
Deflecting Pulse
Output amplifiers with registers
Power supply of analyzer tube

Fig. 3. Block diagram of the analyzer tube.

amplifier to a voltage of ± 140 volts, when the input pulse is 100 volts. This is sufficient to deflect the electron beam along the whole collecting system (Fig. 5). Because of the large amount of negative feedback, the amplifiers are very stable and have excellent linearity (Fig. 6). In obtaining this relationship, the input pulses used were obtained from a pulse generator and had rise times varying from 0.1 microsecond to 3 microseconds, and durations from 0.5 microsecond to 30 microseconds.

For the correct operation of a complete cycle of sorting and registering, certain auxiliary pulses are required (Fig. 1). Their generation must be started by each input pulse which passes through the shaping circuit. Since the amplification of very short pulses to a value sufficient for reliable starting of the trigger is linked with known difficulties, a lengthened pulse of duration $\sim$ 13 microseconds from the cathode of tube T_9, rather than the input pulse, is fed into the input of the auxiliary circuit, which consists of an amplifier and a Schmitt trigger. After a delay time τ_0 (Fig. 1) from the beginning of the input pulse, an intensifying pulse of length τ_v must be supplied to the control grid of the electron beam tube, and a pulse of length τ_{c1} must be supplied to the clamping circuit of the input. This delay is obtained from a univibrator with a cut-off time of 2 or 6 microseconds.

For input pulses with a rise time of less than 1 microsecond, a delay of 2 microseconds is chosen, and for slower rising pulses a delay of 6 microseconds is chosen. Special care is given in obtaining the intensifying pulse, since its stability with time, and likewise stability in amplitude, determines, to a certain degree, the stability of the operation of the analyzer. A pulse of length 7 microseconds generated by a univibrator with cathode coupling, after inversion, is fed by direct coupling to the grid of the stabilizing tube T_{30}. The value of the pulse at its plate is determined by the current flowing and the value of the plate load resistor (Fig. 7 and Fig. 8). Because of the necessity of connecting the circuit to the electron beam tube by a cable of approximately 1 m in length, another cathode follower T_{31} is included. The pulse from the plate of tube T_{29} is also fed, after differentiating, through a line with a delay of 0.8 microsecond (time τ_2 in Fig. 1), and a cathode follower, to tube T_7, which discharges the "storage" condenser (Fig. 9). The pulse for the input clamping is produced by a univibrator in tube $T_{25/26}$ and has a length $\sim$ 25 microseconds (Fig. 10). Thus, a pulse applied to the input of the analyzer at a time τ_0 after the first pulse will not cause a change in the amplitude of the latter. The probability of the admission of a second pulse within the time τ_0 after first pulse is very small and is, with a counting rate $\sim$ 200 pulses per second and $\tau_0 = 2$ microseconds, $\sim$ 0.04%, and with $\tau_0 = 6$ microseconds, correspondingly, $\sim$ 0.12%. The univibrator generating the intensifying pulse also starts a common counter which is connected to the 20-fold scalers.

The electron beam tube is constructed from parts of an oscilloscope tube of domestic manufacture, type 13-L037, from which the part with the fluorescent screen is cut. The electron gun, together with the deflecting plates, is removed.

A new electron gun of the same type was constructed with the aid of a glass sleeve, since it was found that repeated activation of the oxide coated cathode formerly used did not give satisfactory results. The part of the sleeve which was cut away from the fluorescent screen was polished, and the cylinder was placed on a metallic base. The vacuum seal between the cylinder and the base was made with the aid of "pitseina". The collecting system is built up on this base. For shielding, the tube is surrounded by two iron sheaths. The collecting system consists of 21 collector plates of dimension 4 × 5 mm each. The collector plates are arranged in two rows, an upper and a lower. The effective widths of the lower collectors is determined by the distance between the upper collectors, because the lower collectors are a little wider than the upper ones. The deviation of the geometric widths of the individual collectors does not exceed 1%. The relationship between the position of the beam and the deflecting

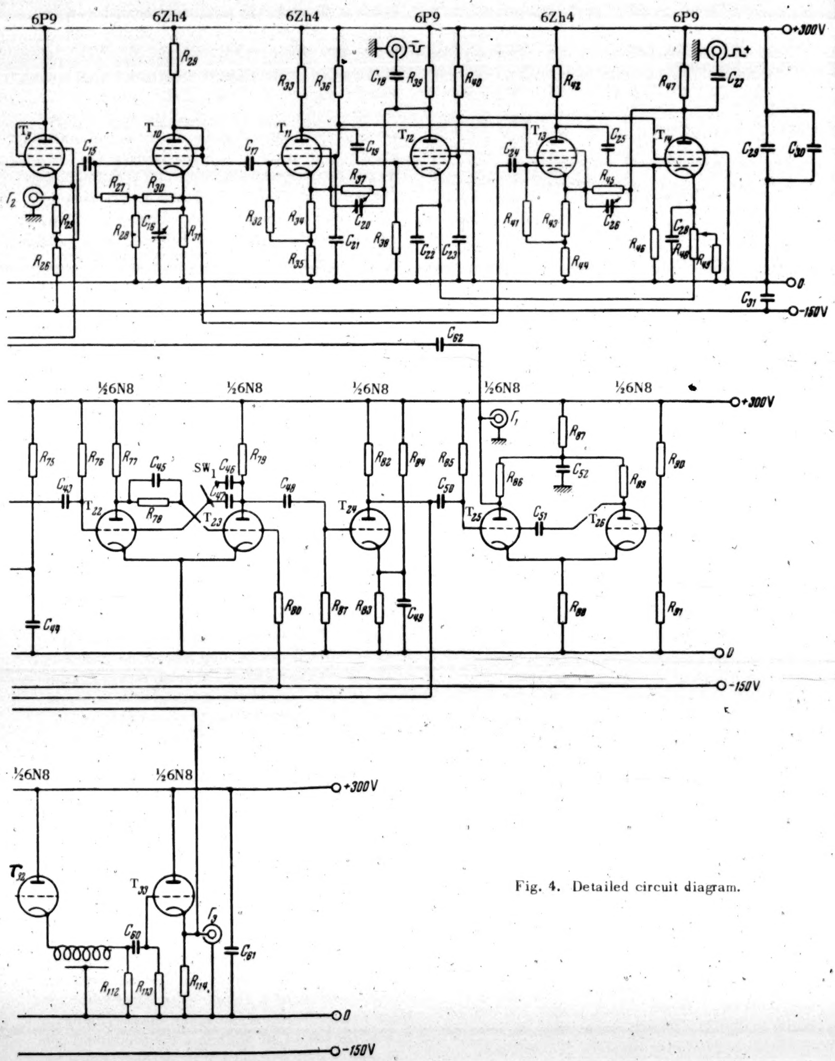
6P9
6Zh4
6Zh4
6P9
6Zh4
6P9
+300V
0
-150V
T_9
T_{10}
T_{11}
T_{12}
T_{13}
T_{14}
Γ_2
C_{15}
C_{16}
C_{17}
C_{18}
C_{19}
C_{20}
C_{21}
C_{22}
C_{23}
C_{24}
C_{25}
C_{26}
C_{27}
C_{28}
C_{29}
C_{30}
C_{31}
R_{25}
R_{26}
R_{27}
R_{28}
R_{29}
R_{30}
R_{31}
R_{32}
R_{33}
R_{34}
R_{35}
R_{36}
R_{37}
R_{38}
R_{39}
R_{40}
R_{41}
R_{42}
R_{43}
R_{44}
R_{45}
R_{46}
R_{47}
R_{48}
R_{49}
C_{62}
½6N8
½6N8
½6N8
½6N8
½6N8
+300V
0
-150V
T_{22}
T_{23}
T_{24}
T_{25}
T_{26}
Γ_1
SW$_1$
C_{43}
C_{44}
C_{45}
C_{46}
C_{47}
C_{48}
C_{49}
C_{50}
C_{51}
C_{52}
R_{75}
R_{76}
R_{77}
R_{78}
R_{79}
R_{80}
R_{81}
R_{82}
R_{83}
R_{84}
R_{85}
R_{86}
R_{87}
R_{88}
R_{89}
R_{90}
R_{91}
½6N8
½6N8
+300V
0
-150V
T_{32}
T_{33}
Γ_3
C_{60}
C_{61}
R_{112}
R_{113}
R_{114}

Fig. 4. Detailed circuit diagram.

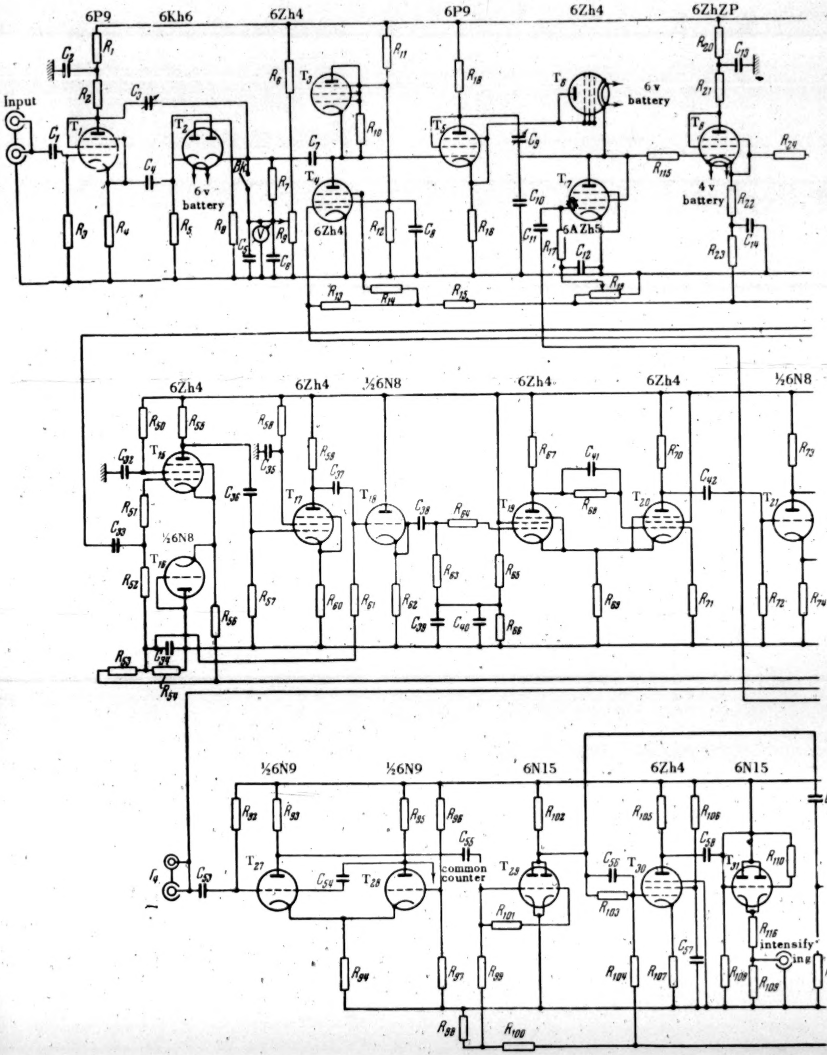
6P9
6Kh6
6Zh4
6P9
6Zh4
6ZhZP
Input
6 v battery
6 v battery
4 v battery
6Zh4
6AZh5
T1
T2
T3
T4
T5
T6
T7
T8
6Zh4
6Zh4
½6N8
6Zh4
6Zh4
½6N8
½6N8
T15
T16
T17
T18
T19
T20
T21
½6N9
½6N9
6N15
6Zh4
6N15
T27
T28
T29
T30
T31
common counter
intensifying
Г4

Resistances*

R_1	1	1**	R_{30}	50	0,25**	R_{59}	10	2**
R_2	1	1	R_{31}	5.1	2	R_{60}	150 Ω	1
R_3	100	0.25	R_{32}	800	0,25	R_{61}	510	0,25
R_4	10	2	R_{33}	15	4	R_{62}	20	2
R_5	1 MΩ	0.25	R_{34}	120 Ω	0,25	R_{63}	1 MΩ	0,25
R_6	60	4	R_{35}	5	10	R_{64}	4,5	0,25
R_7	15	0,25	R_{36}	15	2	R_{65}	120	2
R_8	51	0.5	R_{37}	20	2	R_{66}	56	2
R_9	4.5	wire wound potentiometer	R_{38}	510	0,25	R_{67}	4	2
R_{10}	1 MΩ	0.25	R_{39}	5	10	R_{68}	100	1
R_{11}	41	4	R_{40}	10	10	R_{69}	10	2
R_{12}	2.2	1	R_{41}	800	0,25	R_{70}	10	2
R_{13}	100	0.25	R_{42}	15	4	R_{71}	60	1
R_{14}	36,5	0.25	R_{43}	120 Ω	0,25	R_{72}	50	0.25
R_{15}	100	0.25	R_{44}	5	10	R_{73}	20	2
R_{16}	10	2	R_{45}	20	2	R_{74}	10	1
R_{17}	100	0,25	R_{46}	510	0.25	R_{75}	150	2
R_{18}	2.2	2	R_{47}	5	10	R_{76}	300	1
R_{19}	100	type VK 0.5	R_{48}	10 Ω	wire wound	R_{77}	20	2
R_{20}	510	0.25	R_{49}	34 Ω	2	R_{78}	240	0,25
R_{21}	200	0.25	R_{50}	60	0 5	R_{79}	20	2
R_{22}	3 MΩ	1	R_{51}	50 Ω	0.25	R_{80}	200	0,25
R_{23}	510	0,25	R_{52}	510	0.25	R_{81}	10	0,25
R_{24}	50 Ω	0.25	R_{53}	100	0,5	R_{82}	20	2
R_{25}	8	2	R_{54}	8.25	0,5	R_{83}	10	1
R_{26}	20	2	R_{55}	10	2	R_{84}	10	2
R_{27}	510	0.25	R_{56}	30	2	R_{85}	800	1
R_{28}	1 MΩ	0.25	R_{57}	200	0.25	R_{96}	4	2
R_{29}	5.1	2	R_{58}	60	0,5	R_{87}	20	2

---

* If not specifically shown, resistances are given in kilohms.

** In watts.

Capacitances***

R_{88}	2	1**	C_1	0.1		C_{32}	10	
R_{89}	20	2	C_2	10		C_{33}	5000 μμF	
R_{90}	300	1	C_3	5—30 μμF		C_{34}	1	
R_{91}	15	1	C_4	0.03		C_{35}	10	
R_{92}	390	0.5	C_5	0.015		C_{36}	5000 μμF	
R_{93}	3	1	C_6	20		C_{37}	5000 μμF	
R_{94}	2.2	2	C_7	200 μμF		C_{38}	1000 μμF	
R_{95}	20	2	C_8	40		C_{39}	10	
R_{96}	300	1	C_9	5—20 μμF		C_{40}	0,02	
R_{97}	15	0.25	C_{10}	200 μμF		C_{41}	32 μμF	
R_{98}	43	0.5	C_{11}	0,01		C_{42}	50 μμF	
R_{99}	200	0,25	C_{12}	0.5		C_{43}	50 μμF	
R_{100}	300	1	C_{13}	2		C_{44}	5000 μμF	
R_{101}	100	0.25	C_{14}	2		C_{45}	32 μμF	
R_{102}	3	2	C_{15}	0,01		C_{46}	30 μμF	
R_{103}	100	2	C_{16}	7—45 μμF		C_{47}	25 μμF	
R_{104}	53	1	C_{17}	0.01		C_{48}	50 μμF	
R_{105}	4	2	C_{18}	0.01		C_{49}	5000 μμF	
R_{106}	30	1	C_{19}	0,01		C_{50}	50 μμF	
R_{107}	150Ω	0.5	C_{20}	1—5 μμF		C_{51}	200 μμF	
R_{108}	100	0.25	C_{21}	0.1		C_{52}	10	
R_{109}	2	1	C_{22}	20		C_{53}	50 μμF	
R_{110}	100Ω	0,25	C_{23}	0.1		C_{54}	100 μμF	
R_{111}	50	0,25	C_{24}	0,01		C_{55}	5000 μμF	
R_{112}	3	2	C_{25}	0.01		C_{56}	10 μμF	
R_{113}	1 MΩ	0,25	C_{26}	1—5 μμF		C_{57}	10	
R_{114}	20	2	C_{27}	0,01		C_{58}	0 .02	
R_{115}	50Ω	0.25	C_{28}	20		C_{59}	20 μμF	
R_{116}	2	1	C_{29}	20		C_{60}	1000 μμF	
			C_{30}	0 25		C_{61}	20	
			C_{31}	0,1		C_{62}	0.1	

*** If not specifically shown, capacitances given in μF.

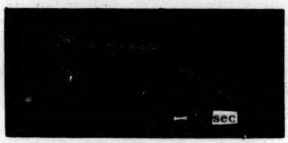

Fig. 5. Lengthened pulse of positive polarity, supplied to one deflecting plate of the electron beam tube.

voltages is linear over the whole length of the system. The collectors are surrounded by a frame-plate which simultaneously serves several purposes. It is coated with a fluorescent material which forms a convenient means of observing the focusing of the beam and its path upon deflection. On the axis of symmetry two lines are drawn which serve for checking the path of the beam along the collectors. A voltage of – 750 volts with respect to ground is applied to the frame, i.e., with respect to the potential of the collectors. Secondary electrons knocked out by the beam from the aquadag coating of the collectors pass in this way into a strong retarding field and fall back to the collectors. Use of the secondary electron emission to amplify the collector current seems very doubtful to us because of the difficulty of securing its stability, even with special treatment of the collector material. Finally, the frame does not permit the beam to fall on the insulator which serves as the holder of the collectors; i.e., in the present case, on the plate of the surrounding glass.

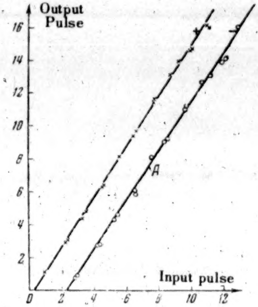

Fig. 6. Linearity of the assembled system (10 divisions = 100 volts). The input pulse is 4 microseconds, the delay is 2 microseconds, the intensifying pulse is 7 microseconds. The line *A* corresponds to negative pulses and is displaced to the right by 2 divisions for display purposes.

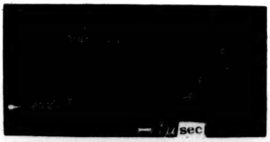

Fig. 7. Intensifying pulse.

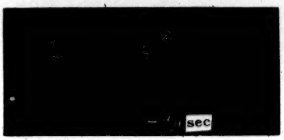

Fig. 8. That section, during which time the intensifying pulse is supplied to the control grid of the electron beam tube, is cut out on the lengthened pulse.

The experimental electron beam tube is evacuated by a mercury diffusion pump, through a liquid-air trap, during the time of operation. The tube works satisfactorily with a vacuum of the order of 10^{-6} mm of mercury. The electron current in the beam was 10 microamperes with an accelerating voltage of 2000 volts and a bias on the control grid of 65 volts.

An amplifying channel is connected to each of the collectors (Fig. 11) which actuates a mechanical register. The collector is connected to the input of a cathode follower by means of a cable which has a double shield for reducing the effective input capacitance. To shield the collector completely from large signals in the following univibrator, and to prevent coupling from one operating channel to a neighboring one, the second half of the tube is used as an amplifier with a grounded grid. A potentiometer is used in its plate circuit, and serves to vary the threshold of operation of the channel. The following univibrator generates a pulse of duration ~ 10 microseconds, which starts a second univibrator. A pulse of 3 microseconds duration is taken from the latter univibrator and fed to the grid of the last

Fig. 9. The pulse which makes tube T_{17} conduct and discharge the "storage" capacitance.

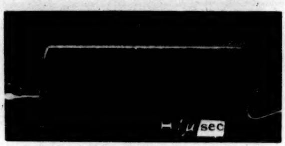

Fig. 10. The pulse which clamps the input.

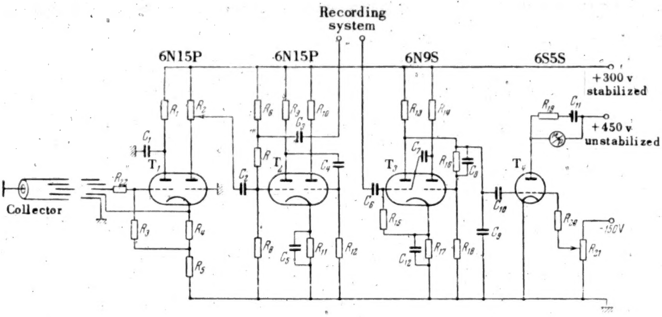
Recording system
6N15P
6N15P
6N9S
6S5S
+300 v stabilized
+450 v unstabilized
-150V
Collector
T1
T2
T3
T4
R1
R2
R3
R4
R5
R6
R7
R8
R9
R10
R11
R12
R13
R14
R15
R16
R17
R18
R19
R20
R21
R22
C1
C2
C3
C4
C5
C6
C7
C8
C9
C10
C11
C12

Fig. 11. Diagram of a collector channel

Resistances (in kilohms)

R_1	30	1*	R_{12}	50	0.25*
R_2	500 potent. type VK	0,5	R_{13}	39	1
R_3	100	0.5	R_{14}	39	1
R_4	1	1	R_{15}	1 MΩ	0.25
R_5	1	1	R_{16}	510	0.5
R_6	2,5 MΩ	0.5	R_{17}	39	1
R_7	510	0.5	R_{18}	200	0.25
R_8	100	0.5	R_{19}	2.2	1
R_9	30	1	R_{20}	200	0,25
R_{10}	15	1	R_{21}	1 MΩ potent type VK	0,5
R_{11}	7	0.5	R_{22}	300 Ω	0,25

Capacitances (in μμf)

C_1	5000	C_7	1000
C_2	5000	C_8	32
C_3	50	C_9	100
C_4	50	C_{10}	0.25 μF
C_5	100	C_{11}	0.05 μF
C_6	100	C_{12}	0.01 μF

---

* in watts

tube, in the plate circuit of which is a mechanical register of type SB - 1M. The plate of this tube is connected to an unstabilized power supply. When necessary, a scale of 16 scaler can be connected between the two univibrators. In the present system ten such circuits have been provided.

If we consider the discrimination of the system, i.e., the electron beam tube, together with the included amplifiers and univibrators in the collector channel, we obtain at the boundary of some collector plate

$$e_{\mathrm{d}} = e_1 + \frac{e_2}{K_1} = e_1 + \frac{e_3}{K_1 K_2},$$

$$[\Delta e_{\mathrm{d}}]_{\mathrm{max}} = \Delta e_1 + \frac{e_3}{K_1 K_2}\left[\frac{\Delta e_3}{e_3} + \frac{\Delta K_1}{K_1} + \frac{\Delta K_2}{K_2}\right],$$

where e_D is the overall threshold of the discriminator, e_1 is the threshold of boundary of the collector plate, for the tube considered, e_2 is the threshold of operation of the collector channel, e_3 is the threshold of operation of the univibrator in the collector channel, K_1 is the amplification coefficient of the tube from the deflecting plate to the collector and K_2 is the amplification coefficient of the input amplifier of the collector channel.

For the given instrument we have

$$K_1 \approx \Delta e_{\text{coll}} / \Delta e_{\text{plate}} = n i_0 \tau_v / C = 3$$

Here n is the number of incoming beam diameters passed over by the beam at the plane of the collectors when the deflecting voltage equals 1 volt, i_0 is the current in the beam, τ_v is the duration of the intensifying pulse and C is the input capacity of the collector channel, $K_2 \sim 25$ and e_3 is of the order of several volts. From this it follows that a variation of e_3, K_1 and K_2 will not cause much variation of the threshold, and that the greatest attention must be given to the stability of operation of the tube. It is necessary to note that the power supplied to all circuits except the counters is produced by electronically stabilized sources. After adjusting the voltage stabilizers to the operating voltages, the stability of the output voltage in time $\sim 10^{-2}$%. With unfavorable conditions:

$$\Delta e_3 / e_3 = \Delta K_1 / K_1 = \Delta K_2 / K_2 = 0.1.$$

$$\Delta E_0 / E_0 = 0.01$$

(where E_0 is the voltage accelerating the electrons in the tube) the stability of the thresholds of the channels is of the order 1 - 2 %. The condition is verified by an experiment with the analyzer. If, after 1½ hours of warming up by all of the instruments, pulses with amplitudes within the limit of a given channel are supplied from a stabilized pulse generator, then in the course of 6 hours the departure of the beam and change of the operation of the analyzer cannot be observed. With the aid of the potentiometers installed in the plate circuits of the second tubes of the collector channels, it is possible to obtain overlapping of the electrical widths of the channels or to have a gap between them. The pulses within this gap will not be counted. The width of the gap can be set equal to 2% of the width of the channel. Since the time cycle of the registrations of one pulse $\sim$ 35 microseconds, the loss of pulses equals 1% when the counting rate is 285 impulses per second, =17,000 impulses per minute. If it is necessary, the time can be decreased to $\sim$ 15 microseconds.

'Translated by F. P. Dickey

SOVIET PHYSICS VOLUME 1, NUMBER 3 NOVEMBER, 1955

Formation of Negative Hydrogen Ions in the Passage of Protons through Thin Metal Foils

IA. M. FOGEL, B. G. SAFRONOV AND L. I. KRUPNIK
Physico Technical Institute, Academy of Sciences, Ukranian SSR

(Submitted to JETP editor April 3, 1954)
J. Exper. Theoret. Phys. USSR **28**, 711-718 (June, 1955)

By means of a dual capability mass spectrometric apparatus, the ratio of negative hydrogen ions to protons has been determined for a beam of protons with energies in the interval from 11.5 to 28 kev which have passed through thin foils of Be, Al and Cu. It has been found that approximately 10 percent of the protons which fall on a thin Be foil are changed into negative hydrogen ions.

INTRODUCTION

WITH the passage of fast positive ions through matter, collisions between the ions of the beam and the atoms of matter occur which are accompanied by a capture or loss of electrons by the ions. As a result the composition of a beam which has traversed several layers of matter can be substantially different from that of the incident beam. Thus, for example, if the incident beam consists of singly charged ions, then the traversing beam can contain, in addition to the singly charged ions, multi-charged ions, neutral atoms and singly charged negative ions. Negative ions will occur in the traversing beam only in the case that the corresponding atoms pass a positive electron affinity.

In the case of protons passing through matter, the processes of electron capture or loss imply that the traversing beam will contain neutral atoms and negative hydrogen ions in addition to protons. Negative hydrogen ions will be produced in a beam as a result of protons capturing two electrons in a single collision event with the particles of the medium* , or as a result of two successive collisions with the capture of one electron in each collision.

The percentage of neutral atoms in a proton beam which was passed through thin foils of Be, Al, Ag, and Au was studied by Hall[2] for protons with energies ranging from 20 to 400 kev. In this work the presence of negative hydrogen ions in the emergent beam was ignored for small proton energies. For this reason the ratio of hydrogen atoms to protons as determined by the author for these energies must be corrected.

The first mention of the formation of negative hydrogen ions in the passage of a proton beam through a thin aluminum foil is contained in a work by Ribe[3] dedicated to the study of the neutralization of protons in hydrogen. With the idea of evaluating the influence of the presence of negative hydrogen ions on the results of his experiments, this author performed measurements for protons with energies from 35 to 90 kev. At 35 kev, the percentage of ions H_1^- reached 3 percent of the number of protons in the emergent beam, while at 90 kev, within the limits of experimental errors (of the order of 0.1 percent), the presence of negative hydrogen ions was not detected in the emergent beam.

Some data on the percentage of negative deuterium ions in a beam of deuterons which had passed through an aluminum foil of thickness 0.01 milligrams/cm^2 are presented by Alvarez[4].

One can conclude from the data that, for deuterons with energies of 10 kev, the number of negative deuterium ions formed in a beam passing through metal foils reaches as much as 26 percent of the number of deuterons incident on the foil. Finally, in a recently published short report by Phillips[5] some results are presented on investigations of the equilibrium composition of proton beams with energies from 4 to 140 kev which have passed through thin foils of Al, Al_2O_3 , SiO and Au.

It appears from the preceding short summary that the study of the concentration of negative ions in a proton beam which has passed through metal foils and its dependence upon proton energies and the nature of the foil is not sufficiently complete. In this connection we undertake to report experiments performed with the aim of studying the formation of negative hydrogen ions for proton beams which have passed through thin foils of Be, Al, and Cu.

---

* An essentially similar process was discovered by us in the passage of a proton beam through hydrogen[1].

[1] Ia. M. Fogel, L. I. Krupnik , and B. G. Safranav, J. Exper. Theoret. Phys. USSR **28**, 589 (1955); Soviet Phys. 1, 415 (1955)

[2] T. Hall, Phys. Rev. **79**, 504 (1950)

[3] F. L. Ribe, Phys. Rev. **83**, 1217 (1951)

[4] L. W. Alvarez, Rev. Sci.Instr. **22**, 705 (1951)

[5] J. A. Phillips, Phys. Rev. **91**, 455 (1953)

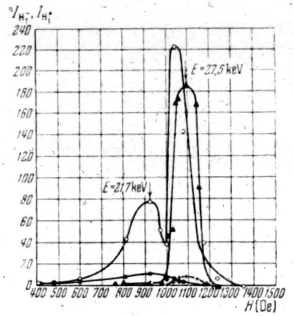

FIG. 1. ▲ – positive ion current obtained without a foil (the scale is reduced 200 times); + – negative ion current obtained without a foil; o – positive ion current, with foil in place; ● – negative ion current, with foil in place.

DESCRIPTION OF APPARATUS AND METHOD OF MEASUREMENT

The apparatus used in this experiment has been reported in an earlier paper[1] (consider Figure 1 in that report). The proton beam was defined by a diaphragm (diameter of 2 mm) which covered the entrance window of a Faraday cylinder *21*. The beam current passing through the diaphragm was measured by the Faraday cylinder. The foil holder *30* was introduced through a slide sealed within a sleeve *25*. The beam, after passing through a foil which was carried by one of the windows in the holder, is analyzed with the help of the magnetic analyzer *23*. To study the composition of the incident beam,it was allowed to pass through one of the windows in the holder which did not contain a foil.

Since we had in mind to work with protons with energies from 10 to 30 kev, it was necessary to prepare sufficiently thin foils so that the protons could penetrate through the foils, i.e., thicknesses of the order of 0.01 milligram/cm^2 . We prepared two types of foils – with and without backing. The method of preparing foils with backing was as follows: A drop of enamel lacquer thinned by amyl acetate was placed on the surface of distilled water. The lacquer spread over the surface of the water and, when it dried, formed a thin film. In the container with the water was a brass plate with a window lying on a small table in such a fashion that the plate surface was beneath the water. After the formation of the enamel film the water was let out of the container, and as the water level fell, the enamel film, settling gradually with the water, settled onto the brass mask and closed the window.

The thickness of the enamel film could be changed by varying the degree of dilution of the lacquer in the amyl acetate. The thickness of the enamel film was obtained by weighing a known area of the film on a microbalance. The backing thickness with which we worked was of the order 0.01 milligram/cm^2 . To obtain backings of smaller thickness appeared too difficult because of their instability.

After the introduction of the enamel film across the window of the brass plate, the film was exposed to air drying for several hours. The brass plate with its enamel film was then inserted in a vacuum apparatus for the deposition of a metal layer onto the enamel film. The determination of the thickness of the metal layer was accomplished by first weighing the backing and then weighing the backing together with the metal layer. For plating the backing with a metal layer, the time of deposition and the rate of heating the evaporator were fixed. In the subsequent deposition of a metal layer, we maintained a constant heating and were able to obtain one or another layer thickness by varying the evaporation time. In this fashion we obtained foils of Be, Al, and Cu with thicknesses from 0.01 to 0.03 milligram/cm^2 .

For the preparation of metal foils without backing we employed another method as follows: A carefully cleaned glass plate was dipped into a solution of cellulose nitrate varnish and acetone. After removing the plate from the varnish it was set vertical, the excess varnish running off. After a short time a film of varnish was formed on the surface of the plate. This film was then removed from the glass and fastened to a thin brass ring which was placed in a chamber where a thin metal layer was deposited on the film by an evaporation process. After this, the ring with its foil and varnish backing was placed on the surface of acetone which had been poured into a suitable container. The varnish backing dissolved in the acetone and the thin metal foil was left floating on the surface. Within the acetone container was a small table containing an inclined brass plate with a window. As the acetone was slowly let out, it was possible to set the metal foil over the window of the brass plate. It was not possible to determine the thickness of such foils (i.e. without backing), but, judging from the foil transparency, they were believed to have thickness of the same order as foils with backing.

After the foil had been set over the window in the brass plate, the plate was attached to a holder which in turn was introduced into a sleeve *25*, in the magnetic analyzer chamber (Fig. 1, reference 1).

Before we approached the study in question (i.e., the dependence on proton energies and foil material of the composition of a beam of protons which has been affected by passage through a metal foil), we had performed some preliminary measurements. In these we had studied the dependence of the proton and negative hydrogen ion currents in the Faraday analyzer on the magnetic field intensity in the analyzer cell. In Fig. 1 the characteristic curves for a beam which had passed through an uncovered window** and for a beam which had passed through a beryllium unbacked foil are represented.

The noticeable width of the curve $I = f(H)$ is due to the fact that the diameter of the aperture of the Faraday cylinder (= 15 mm) was larger than the diameter of the incident beam. Nevertheless, the sharp fall off of the curves testifies to the monoenergetic nature of the incident beam.

The curve $I = f(H)$ for protons which have passed through a Be foil possesses two maxima. The presence of two maxima is due to the fact that the observed curve is a composite of two curves: one for protons which have passed through holes in the foil (i.e., have suffered no interaction) and the other for protons which have suffered energy losses and scattering in their passage.

A first glance comparison of the nondisplaced and displaced maxima suggests that a considerable fraction of the incident beam has passed through holes in the foil. In reality this is incorrect, since one must keep in mind that only a small fraction of the protons passing through the foil enter the Faraday chamber of the analyzer because of the scattering of protons. A calculation which included this effect shows that about 3 percent of the protons pass through openings in the foil. Further observation showed that an undisplaced maximum was always found for foils without backing testifying to the presence of holes in these foils.

The proton and negative hydrogen ion currents for a backed beryllium foil is illustrated in Fig. 2 (the incident proton energies was 28.3 kev). The absence of an undisplaced maximum testifies to the absence of holes in foils with enamel backing.

This is characteristic for all foils of this type. By measuring the difference in the magnetic field intensity for the displaced and the undisplaced maximum, we determined the energy loss for passage through the foil.

After these measurements we embarked on the problem under question. One other point that had to be considered was the conditions for an equilibrium composition of the proton beam. The above experiments implied that a foil thickness of about 10^{16} atoms/cm^2 is needed (compare Phillips[5]). The aluminum foils which we used had a thickness of the order of 2×10^{17} atoms/cm^2. The thickness of the beryllium was even larger. Thus the thicknesses of our foils were sufficiently larger than the thickness needed for equilibrium for the incident proton energies in question. In this connection it must be remembered that the equilibrium composition of the emergent beam corresponds to the energy of the emergent protons. If the deviation of the maximum of the emergent energies is a significant fraction of the incident energy, then the results obtained deviate considerably from that characteristic for the incident energies. Thus it should be kept in mind that the composition of the emergent beam, for a given incident energy, may depend on the thickness of the foil.

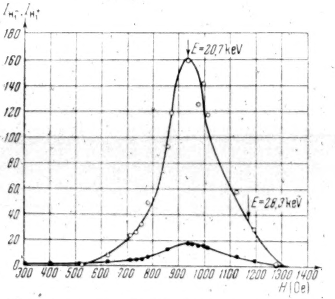

FIG. 2. O – positive current; ● – negative current

The basic measured quantity in our experiment was the ratio of the negative hydrogen ion current to the proton current in the Faraday cylinder of the magnetic analyzer. The values of these currents were obtained from the maxima of the curves $I = f(H)$. Because of the identical width of the proton curve and the negative ion curve, the ratio of the maximum currents gives the correct characteristic percentage of respective particles in the emergent beam.

** In the incident beam there were a few negative hydrogen ions which were formed by collisions between the protons and the residual gas molecules in the path to the analyzer.

The magnetic analyzer was set up in relation to the beam in such a fashion that the maximum of $I = f(H)$ for the negative ions and for the protons occurred at the same magnetic field intensity. Thanks to this arrangement, the measurements of one current could be carried out immediately after the other, thus minimizing errors introduced by variations in the incident beam during the time of a measurement.

The proton and negative ion current in the Faraday cylinder of the analyzer was measured by a string electrometer employing a constant deflection wiring scheme. Two electrometer resistances were used for measuring the two currents, viz., 3.9×10^8 ohms and 3.3×10^{11} ohms. The error in the measurement of the incident beam of protons was of the order of 3 percent and in the measurement of the ratio of currents ~ 7-10 percent.

RESULTS

The majority of our measurements were performed with unbacked foils in order that the results not be influenced by the enamel backing. For those cases when a backed foil was employed, no burning out under the influence of the proton beam was observed. On the other hand, a carbonaceous layer was observed if the backed foil was exposed to the beam for a long time. This was produced by the decomposition of the butyrous film under the action of the proton beam. Consequently, the exposure time was kept small for the measurements to be described, and no carbonaceous layer was formed.

In the process of making measurements we obtained soma data on the relative stability of foils under the continuous action of protons with energies from 10 to 30 kev. Greater foil stability was obtained by the use of small window diameters. For this reason nearly all measurements were made with foils on windows having 4-5 mm diameter. Enamel backed foils showed the greatest stability. They sustained a continuous current density of $3\,\mu A/cm^2$ for 6 hours. Unbacked foils sustained a current density of $1\,\mu A/cm^2$ for one or two hours. Foil collapse for the current densities employed (not greater than $10\,\mu A/cm^2$) occurred because of the gradual loss of material due to the particle blow-off produced by the proton beam.

Unbacked aluminum foils were the first to be studied. The results for four foils are shown in Fig. 3 where the ratio of $I_{H_1^-}/I_{H_1^+}$ is plotted against incident proton energies. The figure shows an increase in the ratio for decreasing energies, reaching ~ 20 percent for 15 kev. In this instance, foils of the same thickness (foils 18*a* and 18*b*, $\Delta E = 2.2$ kev) gave identical ratios. For foils of greater thicknesses this ratio was somewhat larger, in which case the deviation enters into the determination of measuring errors. This result is completely understood since the characteristic composition of the beam is dependent upon the energies of the emergent protons.

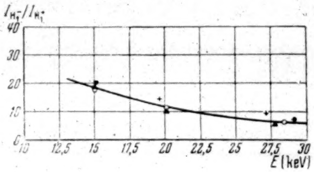

FIG. 3. Here, + = Al-foil No. 23, $\Delta E = 4.5$ kev; ● = Al-foil No. 15, $\Delta E = 5$ kev; O = Al-foil No. 18a, $\Delta E = 2.2$ kev; ▲ = Al-foil No. 18 *b*, $\Delta e = 2.2$ kev.

Beryllium and copper foils were employed next. Figure 4 shows the results for these foils along with the data for aluminum. It is evident that the ratio for the Be foil is quite different from that for Al or Cu.

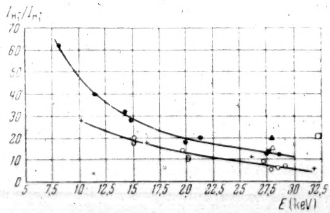

FIG. 4. Value of $I_{H_1^-}/I_{H_1^+}$ for a beam of H_1^+ passing through: O = Al-foil; ● = Be-foil; + = Cu-foil. Values for I_{D^+} for a beam of D^+, passing through: Δ = Al-foil; ▲ = Be-foil; Value of $I_{H_2^-}/I_{H_2^+}$ for H_2^+ beam passing through: □ = Al-foil .

Measurements on beryllium with and without backing are presented in Fig. 5. In the case of the backed beryllium foil, the proton beam passed through the metal layer first, i.e., the composition of the beam was characterisitc of the backing material[‡] . It is seen that a difference exists in the composition of the emergent beam for a metal layer and an enamel backing. These differences enter into the determination of measurement errors.

[‡] Measurements on an enamel film were not possible because of their rapid deterioration in the proton beam.

TABLE I

Foil Material	Proton energy in kev	$\frac{p}{p+1}$	$\frac{I_{H_1^-}}{I_{H_1^+}}\cdot 10^2$	$\frac{I_{H_1^-}}{I_{H_1^+ \text{incident}}}\cdot 10^2$
Be	27.4 21.3 14.3 11.5	0.6 0.55 0.47 0.43	13.4 20.1 32.3 40.0	7.1 9.2 11.5 12.3
Al	28.2 20.2 15.0 28.0[4]	0.6 0.55 0.47 0.47[4]	6.0 10.9 18.1 15.5[4]	3.4 5.4 7.2 6.3[4]

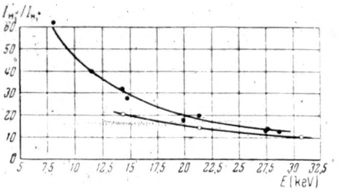

FIG. 5. ● = Be-foil without backing, ΔE = 5-9 kev; O = Be-foil with backing, ΔE = 10-12 kev.

One would expect that in a beam of deuterons passing through a metal foil the negative deuterium ion content should be larger than for a proton beam of the same energy because of the lower deuteron velocity ($v_{D_1^+} = \frac{1}{2} v_{H_1^+}$). Measurements with deuterons having an energy of 28 kev were performed for an aluminum and beryllium foil. The results, confirming our expectations, indicate a ratio I_{D^-} / I_{D^+} of 15.5 percent and 19.4 percent for Al and Be respectively, or approximately equal to the ratio $I_{H_1^-} / I_{H_1^+}$ for 14 kev protons (Fig. 4).♀

Finally, we made measurements with a beam of molecular hydrogen ions H_2^+ with an energy of 32 kev. During the beam's passage through the aluminum foil complete dissociation occured so that the beam was found to contain only protons and negative hydrogen ions with an energy of 16 kev. The ration of $I_{H_1^-} / I_{H_1^+}$ was found to be close to that for incident protons of 16 kev energy (Fig. 4).

The measurements which we made do not permit the calculation of the negative ion content of the emergent beam since the intensity of the neutral component was not measured. However, if we use our data together with those of Hall[2] we can calculate the negative ion content. Actually, Hall determined the quantity $p = (\bar{N}_1 + \bar{N}_{-1}) / N_0$, that is the ratio of the charged to the neutral component. It can be easily shown that the conversion efficiency, $I_{H_1^-} / (I_{H_1^+})_{\text{incident}}$ has the form

$$\frac{I_{H_1^-}}{I_{H_1^+ \text{incident}}} = \frac{p}{p+1} \frac{(I_{H_1^-} / I_{H_1^+})}{1 + (I_{H_1^-} / I_{H_1^+})}. \quad (1)$$

To the accuracy to which the number of incident protons equals the sum of the number of emergent protons, atoms, and negative ions, the ratio $I_{H_1^-} / (I_{H_1^+})_{\text{incident}}$ is representative of the conversion factor for a proton beam passing through metal foils.

Employing Hall's data[2] for beryllium and aluminum foils, we calculate with formula (1) the negative hydrogen ion content in the beam passing through these foils. Table 1 summarizes these results. The presented conversion coefficients can be compared with the results of others. Our conversion coefficient for 28 kev deuterons (conversion into negative deuteron ions) in aluminum foils agrees quite well with Alvarez's data[4] for 30 kev deuterons. A comparison of our results for aluminum with those of Phillips[5] shows our negative hydrogen ion content to be significantly larger. Since the method of measurement used by Phillips is not known, it is difficult to say anything about the reason for this discrepancy.

♀ *Translator's note*: Appears to be more like 17.5 to 19 kev.

In conclusion it appears from Table 1 that approximately 10 percent of the protons incident on a metal foil are transformed into negative hydrogen ions. Thus the usefulness of this method for obtaining a sufficiently intense beam of negative hydrogen ions for experimental purposes is confirmed.

In conclusion we wish to express our gratitude to Prof. A. K. Bal'teru for his continuing interest and attention.

Translated by A. Skumanich
126

SOVIET PHYSICS JETP VOLUME 1, NUMBER 3 NOVEMBER, 1955

Some Notes on the Researches of S. G. Salikhov

N. N. NEPRIMEROV
Kazan State University

(Submitted to JETP editor March 27, 1955)
J. Exper. Theoret. Phys. USSR **28**, 719-724 (1955)

SALIKHOV is known as the coauthor of several studies of considerable note, devoted to research of paramagnetic resonance absorption, initiated in 1944 at the Kazan State University. However, a number of serious inconsistencies appear in several of his papers, published over the past few years.

For example, let us examine his paper entitled "Microwave Measurements of Magnetic Permeability and Dielectric Constants of Some Ferrodielectrics"[1]. In this paper the author maintains that "in the case of a ferromagnetic substance, the electric loss, governed by the finite specific resistance of the substance, cannot be distinguished from the magnetic loss". There is no need to attempt to disprove this statement, as the author does so himself, unwittingly, in the second part of the paper, in which $\mathrm{tg}\delta_\epsilon$ and $\mathrm{tg}\delta_\mu$ are separately identified.

A second statement, presented further on, suffers a similar fate: "It is assumed that μ'' is of prime importance in this process, while the significance of μ' is negligible". However, Table 3, presented at the end of the paper, clearly shows that, without exception, μ' and μ'' have similar values and, moreover, about one half of the substances examined show a value of $\mu' > \mu''$.

A third statement, pertaining to the analysis of samples, fares no better: "Disc-shaped samples, 2 to 3 mm in diameter and 0.1 mm thick, were placed at the bottom of the resonator. The demagnetizing fields were not significant". Unperturbed by this baseless claim, the author in order to compute the g-factor for these samples, makes use of the special case formula of Landau-Lifshitz-Kittel,

$$\omega_{\max} = \gamma \{HB\}^{1/2}, \tag{1}$$

which, as is well known, is based on the assumption that two of the demagnetization factors are equal to zero, while the third is of the highest possible magnitude, equal to 4π[1-4].

Material presented at the end of the second page of the study under discussion[1] bears no relation to the subject matter at hand, but coincides with statements in the pertinent portion of a paper by Kittel (reference 2, p 22). Equation (1) makes its appearance further on in the text, identified as Eq. (2) and, just eight lines later, it is again presented, this time as Eq. (4). Moreover, the sentence contains an error which renders it meaningless: in place of the "minimum μ_R" used in Kittel's text, the author writes "maximum μ''".

Judging on the basis of its title and factual content, the study under discussion is a purely experimental one; however, it appears fruitless to search for the principal ingredient of such a paper: a description of the procedures employed in conducting the experiment, as well as formulae that would relate the characteristic of the analyzed substance to the system's parameters that are being measured. Only indirectly can one deduce, from one of the sentences quoted above, that the author, in the course of his measurements, did not take into account the displacement of the resonant frequency of the gap, which is dependent upon the magnitude of μ'; therefore, when μ' and μ'' were of equal magnitude, he obtained a strongly distorted curve for $\mu''(H)$.

Let us examine the results of the measurements. These data are presented in a series of curves and in Table 1, which summarizes some of the characteristics of the analyzed substances. It is regrettable that no analysis or discussion of these results is offered, since only a review of this nature could aid in judging the quality of the data obtained. For instance, let us examine several curves and other data in Fig. 4[1]. In the case of two samples of nickel-zinc ferrite, differing slightly in their composition, the author has located anti-resonance minima on the absorption curves. It must be remembered that, while such minima have been observed earlier, they normally become noticeable only when the effective permeability $\mu_R = (\mu'^2 + \mu''^2)^{1/2} + \mu''$ can be determined on the logarithmic scale (the so-called μ_R - effect), when their magnitude does not exceed 0.5% of $\mu_{R\max}$ and, therefore, never reaches the value $\mu_R = 0$ (reference 2, pp 1, 2 , 19). Figure 4 shows the minima on the μ'' curve. Their magnitudes are 10 and 20% of $\mu''_{\max}$, and they are all within the range of $\mu'' < 0$. What is the meaning of the negative value of the coefficient that characterizes the absorption? It would appear that not only does the substance not absorb any more energy from a high-frequency electromagnetic field, but, on the contrary, it radiates it!?

---

[1] S. G. Salikhov, Izv. Akad. Nauk SSSR, Ser. Fiz. **18**, 456 (1954)

[2] Ferromagnetic Resonance, Symposium, IIL, 1952

[3] N. N. Malov, J. Exper. Theoret. Phys. USSR **16**, 78 (1946)

[4] V. N. Lazukin, Izv. Akad. Nauk SSSR, Ser. Fiz. **16**, 510 (1952)

A second point, no less curious, is related to these minima. From the Kittel formula,

$$\omega_{\min} = \gamma B, \tag{2}$$

quoted by the author, it follows that the minimum is determined by the magnitude of induction in the substance. We know from Table 1 that, for nickel-zinc ferrite of 17-33-50 composition, the magnitude of the resonance field H = 3100 oersteds, and the induction B = 3100 gauss (curve 1 in Fig. 4). The following three conclusions are made: (1) the given ferrite is paramagnetic; (2) formulae (1) and (2) become identical; and (3) the maximum and the minimum on the absorption curve must coincide. Which, then, is to be believed, the table or the illustrations, theory or the experiment? A second sample of the ferrite, of 20-30-50 composition, produces H = 3100 oersteds and B = 3000 gauss; thus it would appear to be not a ferrite at all, but some sort of super-diamagnetic substance with a magnetic susceptibility of $\chi = 10^{-2}$.

The unexplained influence of the dispersion of susceptibility on the μ'' curve, the composition of the samples, the incorrectly applied induction values, and the unjustified use of Eq. (1) indicate that data in Table 1, pertaining to the value of the g - factors, represent magnitudes obtained by pure coincidence and, naturally, these figures differ from those obtained by other authors (for example, the author shows, for magnetite in the direction (100), that g = 2.34, while Bickford finds that g = 2.12 ± 0.04 (reference 2, p 24).

Let us now turn to the second part of this paper[1]. This portion deals with experiments utilizing the same substances; however, a different procedure has been employed, namely that of measuring on the basis of standing waves in a wave guide, developed in the work of Birks (reference 2, p 37), Malov[3] , and Lazukin[4] . The computation formulae of this method are presented in most complete form in the Lazukin paper [Eqs. (4) and (4a) in reference 4].

Without justification the author ''simplifies'' these: he eliminates terms containing area tangents; he assigns values of relative input impedances of open and closed circuits, Z_{open} and Z_{closed} , to coefficients A_1 and A_2, which were introduced by Lazukin merely to simplify the expression; the author further places each side of the equations between absolute value signs, and presents the equations in the following form:

$$|\mu| = \left|\frac{\lambda}{2\pi d}(Z_{\text{от}} Z_{\text{кз}})^{1/2}\right|; \tag{3}$$

$$|\varepsilon| = \left|\frac{\lambda}{2\pi d}\frac{1}{(Z_{\text{от}} Z_{\text{кз}})^{1/2}}\right|. \tag{4}$$

Another curious detail is the fact that an obvious error has been overlooked in Lazukin's paper[4]: The index figure 1 of coefficient K_1 has been placed after an imaginary number, i.e., the coefficient appears as Ki_1 . The author has completely done away with this index in his Z_0 [equation (10) in reference 1] and thus, in place of two, shows three K coefficients.

Furthermore, the Lazukin formulas are applicable to cylindrical coordinates and are valid only for a coaxial line. The author employs the formulas with respect to a right-angled wave guide.

Also, these equations are inconsistent as far as dimensions are concerned. In the following, only one of several possible variants of the author's method of deriving Eqs. (3) and (4) is described. But independent of the method of their derivation, it is not difficult to show that they are incorrect. To accomplish this, it is sufficient to multiply Eqs. (3) and (4) by one another and to extract the the square root. Thus:

$$(|\mu||\varepsilon|)^{1/2} = \lambda / 2\pi d. \tag{5}$$

As one can see, the refractive index has become a function of the thickness of the layer!? Table 2 serves as a graphic illustration of this relationship: the thicker the sample, the lower its dielectric and magnetic permeability.

Table 2 is followed by Table 3 in which " there are presented data concerning the dielectric constant, magnetic permeability and tangents of magnetic and dielectric losses, computed for the same substances by the method of closing and opening a circuit; these data closely correspond to results obtained by other authors". It is not clear how this table was prepared. Certainly the information presented in this table does not follow from the discussions preceding it. A great many errors can be found in this table: the effective portion of the dielectric permeability of magnetite-II, $\epsilon' = 0.23$; of nickel-zinc ferrite, $\epsilon' = 0.34$; furthermore, the effective portion of magnetic permeability of magnetite-I, $\mu' = 0.95$; of FeS, $\mu' = 0.71$; of magnetite-II, $\mu' = 0.98$, and of nickel-zinc ferrite, $\mu' = 0.97$. All this, the author claims, "closely parallels results obtained by other authors".

The paper[1], presented at the Second All-Soviet Conference on Ferrites, was subjected to severe criticism; as stated above, the values of moduli $|\epsilon|$ and $|\mu|$, computed from Table 3, did not correspond to values for identical substances presented in Table 2.

Similar errors appear in other independent studies of S. G. Salikhov, published during the same period. Let us examine his papers on the measurement of paramagnetic resonance absorption in metals[5-7]. It is difficult to determine what methods of measurement were employed by the author. For example, he states in one paper[5]: "Measurements were made on standing waves at the point of the exact amplitude minimum". However, only a few lines further down, he states that "The Q-quality of the contour was measured by a special precision method". In a later paper[7], a more detailed, but not at all more comprehensible, description of this method is given. A special paragraph listing the different steps is followed by a statement describing the well-known determination that utilizes a standing wave guide, both ends of which are closed (see reference 8, pages 200 and 201). All this is followed by several sentences bearing no relation to each other and frequently containing incorrect statements. For example: "The decrease in power given off by the generator, ΔW, had no practical effect on the magnitude of measured resonance absorption. This is so because in determining paramagnetic resonance absorption, we used samples that had been specially tested for static susceptibility"!? Another example of the author's inconsistency is contained in the following statements: "Furthermore, because of the difference in refractive indexes, determined by either right-or left-hand polarization of the waves, there occurs oblique elliptical polarization. Rotation of the polarization plane changes the sign in the range of the absorption curve and, therefore, does not affect the position of the resonance absorption maximum. Also, it does not materially effect the form of the curve, since comparatively small samples have been used"!? If this approach, which is outlined in the thesis work of Garif'ianov[9], may be assumed to hold true for measurements of paramagnetic salts, it certainly cannot be applied to the author's experiments. Indeed, no one has ever observed rotation of a polarization plane, either during the passage or during the reflection of waves from the paramagnetic metal; certainly this does not hold true for perpendicular fields and microwaves.

The author devotes only two sentences to a description of his procedure[7]: "A probe is placed at either the maximum or the minimum of the standing waves; as the constant magnetic field intensity is changed, a change, proportional to $\chi''(H)$, is obtained in the amplitude of the standing waves. If the probe is placed at a distance of $\lambda/8$ from the maximum of the standing wave, the changes in amplitude will be proportional to the displacement of the phase which is linearly bound to $\chi'(H)$". This is a new development in the science of microwaves. Hitherto, the standing wave coefficient and the displacement of the wave's minimum position had served as the parameters to be measured; χ' and χ'' can be derived from these only by the use of the complex conversion equations(4).

It is quite obvious that, at the maximum or minimum voltage of the standing waves, with the position of the probe remaining unchanged, changes in voltage will be caused by both the real and the imaginary complex component load; in other words, the changes will be proportional to some arbitrary combination of χ' and χ''. Similar results, though in slightly different proportion, will be observed at a distance of $\lambda/8$ from the maximum point. This is clearly shown in Fig. 1 of the reference 5, in which the dispersion curve of platinum simply represents an inverted absorption curve with a slightly distorted wing in the large fields. This also explains the displacement of the resonance point of this "dispersion" curve by 400 oersteds toward the large fields, a circumstance which has no significance from the physics viewpoint. Incidentally, these dispersion curves which the author "succeeded in obtaining in individual cases" seem to have been largely ignored following the Bloembergen paper[10]. Instead, the earlier absorption curves made their appearance as a two-part combination, showing both paramagnetic losses and conductivity losses[6,7].

---

[5] S. G. Salikhov, Izv. Akad. Nauk SSSR, Ser. Fiz. 16, 748 (1952)

[6] S. G. Salikhov, Dokl. Akad. Nauk. SSSR, 93, 241 (1953)

[7] S. G. Salikhov, J. Exper. Theoret. Phys. USSR 26, 447 (1954)

[8] Methods of Microwave Measurements, Soviet Radio, 1949

[9] N. S. Garif'ianov, Thesis, Kazan State University, 1952

[10] N. Bloembergen, J. Appl. Phys. 23, 1383 (1952)

Turning again to procedure, we note that the curves showing these combined losses are expressed in relative units. However, this does not prevent the author from stating in the introductions to these papers[6,7] that "in order to compare these absorptions that were determined for metals of differing conductivities and shapes, the absorption energy values obtained in the experiment were recomputed on the basis of the following formula:

$$W_{\text{eff}} = \frac{Sd\sqrt{\rho}}{M} W_0, \qquad (6)$$

that is, "an amplitude change, proportional to χ'' is to be converted to W_0, the absorption energy, which was obtained experimentally". The impossibility of obtaining W_0 by this method is only too obvious. The measuring line, the author admits, assures an accuracy no higher than 5%[1], while energy absorbed by the metal, constitutes no more than 0.01-0.001% of the energy drop. Moreover, Eq. (6) is inverted and, therefore, used in the conversion computation. As a matter of fact, the larger the area S, the larger is W_0, and the larger is W_{eff}. Nor does this appear to be a misprint, as this formula appears in each of two separate papers[6,7], published one year apart.

A further analysis indicates that the author does not even make use of Eq. (6), Captions of all illustrations in references 6,7 indicate that the magnitude W_{eff} is plotted along the ordinate axis. In reality, this is not the case at all. It is not W_{eff} that is scaled off along that axis, but some magnitude of unknown origin called "line intensity". This circumstance is easily discovered when one compares information in the Table with the curves in the illustrations. To appear more convincing, the author writes: "Figure 1 shows curves indicating combined losses, at room temperature, for potassium, sodium, and bismuth; W_{eff} is scaled along the ordinate axis, while H_0, the external static field, is plotted along the abscissa. As can be seen from the illustration, the line for potassium is 3.5 times more intensive than that for sodium, and 7 times more intensive than the bismuth line"[7]. However, the tables of this same paper indicate that the reverse is true as far as the relative magnitudes of W_{eff} for these metals are concerned. In addition, it is not at all clear what units were used in the computation of the χ' and χ'' curves.

Let us turn to the author's low temperature measurements: "A special apparatus for the measurement of paramagnetic absorption at low temperatures consists of an extension of the metal wave guide, made of a dielectric material and having a metallized inner surface" (reference 7, p 449). This sentence is followed by a reference to the Garif'ianov thesis[9]. From it we learn that this portion of the wave guide is made of plexiglass layers having tin foil on one side. Considering that the pole shoes of the electromagnet are 100 × 100 millimeters in dimension, that the wave guide is 28.5 × 12.7 millimeters in size, and the sample is located in the center of the gap, we note that more than 40 cm^2 of the tin foil is in the magnetic field. A baffling question arises: how can one detect the absorption effect on a tin sample of 2.3 cm^2 area when the sample is surrounded by a 40 cm^2 area of the same metal?

It is pointless to look for an evaluation of results in these papers. What conditions cause the effect observed by the author? The statement made above would seem to place some doubt as to the very existence of this effect, particularly since recent studies into the absorption of potassium and sodium[11], as well as researches involving gadolinium and beryllium[12] and several other metals[13], indicate that the effect of resonance absorption in metals can be determined only when exceptionally pure samples are used. Resonance lines obtained in these studies are extremely narrow (half-thickness on the order of several oersteds) and have a g-factor of a magnitude close to that of a free electron. Obviously, such results are in complete disagreement with those obtained by Salikhov. As a matter of fact, he makes no reference to them.

The limitations of a brief review make it impossible to discuss additional shortcomings in these and other studies by the author; however, it is doubtful whether that would serve any purpose since one can arrive at several specific conclusions without such.

1. A primary condition governing experimental work remains unfulfilled in the papers under review: authenticity of the results.
2. No attempt has been made to correct errors that are in contradiction with the most basic precepts of the science of physics in general, and the study of magnetic resonance in particular.

---

[11] G. A. J. Hutchison and R. C. Pastor, J. Chem. Phys. **21**, 1959 (1953)

[12] A. F. Kip, Revs. Modern Phys., **25**, 229 (1953); A. F. Kip, C. Kittel et al, Phys. Rev. **89**, 518 (1953); C. Foher and A. F. Kip, Phys. Rev., **95**, 1343 (1954)

[13] N. S. Gutovsky and H. J. Frank, Phys. Rev. **94**, 1067 (1954)

Translated by F. Haimson
127

The Effect of Lunar-Tidal Oscillation of the Atmosphere on the Intensity of the Hard Component of Cosmic Rays

A. I. KUZ'MIN AND G. V. SKRIPIN
Yakutsk Branch of the Academy of Sciences of the USSR

(Submitted to JETP editor January 19, 1954)
J. Exper. Theoret. Phys. USSR **28**, 608-609 (1955)

1. The investigation of the effect of the lunar-tidal oscillation of the atmosphere on the intensity of the hard component of cosmic rays is of interest for the study of the nature of the twelve hour variation of cosmic ray intensity[1] and of the diurnal variation of the temperature of the upper layers of the atmosphere[2]. Since the principal period of the lunar-tidal oscillation is equal to one-half a lunar day [3], one would expect it to give rise to a regular variation of the same period in the cosmic ray intensity. However, since regular variations might be masked by statistical fluctuations of the cosmic ray particle flux, the study of the lunar-tidal effect must utilize statistical methods.

Consider the observed twelve hour variation in cosmic ray intensity, δI, as the sum of two waves: one, S, with a period $T_S = 12$h; and the other M, with period $T_M = 12$h 25m 14s, half the lunar period. Also, let the phase difference of the two be $\Delta\phi_0$ degrees at time $t_0 = 0$. In a length of time T_S, the phase difference will increase by $360(T_M - T_S)/T_S$ degrees, and in $n = T_S/(T_M - T_S) = 28.6$ periods of T_S, or 14.3 solar days, the phase difference will have changed by 360°. Therefore, S and M will have the same phase differences, $\Delta\phi_i (i = 0,1,2\ldots)$, at the times $t_i, t_i + n, t_i + 2n, \ldots, t_i + kn$. Now, one can average the values of δI at these intervals of time, determining an average value corresponding to a particular phase difference, $\Delta\phi_i$. Repeating this procedure for different starting times, $t_0, t_1, t_2, \ldots$, a curve can be constructed giving the dependence of δI on the phase difference $\Delta\phi_i$. This curve would then show the effect of the lunar-tidal component, M, on the twelve hour variation, δI.

2. Experimental values of δI, obtained with an accuracy of several tenths of one percent per hour of observation, were analyzed according to this scheme. Seventy days of data were used to determine the average amplitudes for the phase differences $\Delta\phi_0$, $\Delta\phi_0 + 100°$, $\Delta\phi_0 + 175°$, and $\Delta\phi_0 + 275°$. The results are shown in the Figure.

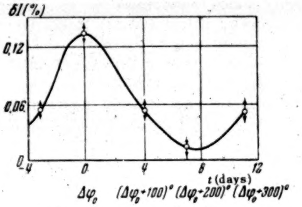

It is seen there that δI exhibits a strong dependence on the phase difference, i.e., on the choice of the time t_i, and that its variation is sinusoidal with a period of 14.3 days. This can occur only when δI contains a component of period 12h 25m 14s.

The reality of the wave, M, is substantiated by the Table, in which are listed the amplitudes of δI for two-month intervals of hourly observations. It is seen there that uncertainties in amplitude are on the average 0.008%, while it was seen that the variation of the averages obtained by summing at 14.3 day intervals reached 0.04%. Assuming that the maximum and minimum of the curve in the Figure correspond to the waves S and M being in phase and out of phase by π, and using the data in the Table, one obtains an average amplitude for M of 0.05%. Knowing the amplitudes of S and M, one can determine the phase of the resultant wave for each t_i. Calculations show that the phase of the resultant curve should fluctuate within the limits of three hours (90°). The points shown in the Figure fall within this limit, and the behavior of the curve corresponds to the premises of this calculation.

	Amplitude	Time of Maximum
1951		
March-April	0.069 ± 0.008	1 hr 40 min
May-June	0.078 ± 0.008	2 hr 40 min
July-August	0.036 ± 0.008	1 hr 30 min
September-October	0.070 ± 0.008	2 hr 40 min
November-December	0.063 ± 0.008	1 hr 16 min

The amplitude and phase of M exhibited the same characteristics when calculated from 1951-1952 data for δI by summation at intervals corresponding to the principal lunar wave of period 24h 50m 14s.

3. The lunar-tidal wave in the atmosphere[4,5] has an amplitude of surface pressure variation of about 0.08 mb. A pressure variation of this amount can cause 20% of the observed amplitude of the waves M in the intensity of cosmic rays. In order to explain the remaining 0.04% amplitude of M, it is necessary to assume that the main effect of the tidal oscillations is through the vertical redistribution of the mass of the air. Such a redistribution would necessarily be associated with a twelve hour variation in the temperature of the upper layers of the atmosphere, which variation was indeed observed by Selesneva[2] in 1945. The analysis[2] of a large amount of statistical data showed that, starting at an altitude of 3 km, the diurnal fluctuations had several maxima. The basic maximum is of 24-hour period, while the others are 12-hour, and the amplitude of the latter increases with altitude. It would seem that tidal oscillations, as well as the other factors indicated by Selezneva[2] hold an important place in the explanation of the maxima in the diurnal temperature variations of the troposphere.

In conclusion, we would like to thank Prof. E. L. Feinberg for several valuable comments.

Translated by V. A. Nedzel
103

[1] P. Nicolson and V. Sarabhai; Proc. Phys. Soc. **64**, 609 (1948)

[2] E. S. Selezneva; Izv. Akad Nauk SSSR, Ser. Geograf. **9**, 82 (1945)

[3] N. E. Kochun, *Collected Works*, 1, Moscow-Leningrad, 1949

[4] J. Bartels, *Gezeitenschwingungen der Atmosphäre, Handbuch der Experimental Physik*, **25**, part 1, page 161 (1929)

[5] S. R. Chapman, Met. Soc. **50**, 165 (1924)

Variation of the Global Intensity of the Hard Component of Cosmic Rays During the Passage of Air Mass Fronts

D. D. KRASIL'NIKOV
Yakutsk Branch of the Academy of Sciences, USSR

(Submitted to JETP editor January 19, 1954)
J. Exper. Theoret. Phys. USSR **28**, 610-613 (1955)

1 The investigation of the variation of cosmic ray intensity with typical states of the atmosphere (as regards the vertical density distribution) is of interest in the study of the variation of cosmic ray intensity outside the atmosphere in cases where adequate temperature soundings of the atmosphere are unavailable. In the latter cases (when it is impossible to determine the appropriate integral [1,2]) such study is complicated by the impossibility of determining the magnitude and sign of the meteorological effect. It is hoped that the investigations comprised in this paper may help in estimating this latter quantity, and, in addition, that they may help evaluate the possibilities of bringing about the observation of cosmic ray intensity in meteorological investigations[3] . One can consider making such observations during various meteorologically well-defined different types of fronts[4,5], a type of work of which only one example has been reported to date [6] .

In that paper the average variation of the intensity of the hard component during the passage of four types of fronts, and during periods of no frontal development, was reported. In contrast to the procedures in that study, here: 1) the measurement of cosmic ray intensity was made near sea level in a stationary apparatus, 2) all observations were made during periods of no magnetic activity, 3) the observed intensity variations were corrected for the diurnal effect, 4) the variations in the velocity of the fronts were taken into account, 5) the periods with no fronts were classified according to type of surface pressure change.

2. The average hourly global intensity of the hard component was measured to an accuracy of several tenths of one percent. In addition, surface pressure and the earth's magnetic field were measured every hour, the synoptic situation was recorded every three hours, and the cloud state was observed visually every hour.

Fronts were selected for study if the following conditions were satisfied: 1) magnetic storms did not occur and the horizontal component of the earth's field did not change by more than 100 γ-units during the period of observation; 2) the fronts could be identified by type; 3) they appeared tropospheric and dynamically significant (in the case of warm and cold fronts) and they passed through the point of observation in a direction closely perpendicular to the surface line of the front; 4) secondary passages did not occur during the period of observation; 5) the fronts remained clearly defined during the period of observation (from 1500 km prior to reaching the point of observation, to a distance of 400-500 km past it), and appeared on all synoptic charts during the intervening period.

In all, 107 cases were selected, comprising four types of fronts: 32 warm, 48 cold, 14 warm type occluded, 13 cold type occluded. Corresponding to each case of frontal passage the beginning and end of three intervals of time were recorded: the first and third in the zone of "pure" air mass (corresponding to the cold and warm in the case of warm fronts, and vice versa for cold fronts); and the second in the zone of the projection of the frontal surface (Fig. 1). For the case of occluded fronts two periods were used: 600 km before and 400 km after the passage of the front on the ground. The most reliable of these observations were the observed times of passage of the fronts on the ground, while those of the upper boundaries were determined with the help of data from the literature[4,5,7] and from cloud observations. It was assumed that on the average the upper boundary of a warm front is overhead when the surface boundary is still 800 km away, while that of a cold front is behind the surface boundary by 400 km.

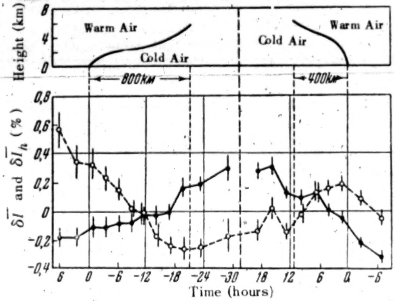

FIG. 1. At the top are shown profiles of a warm front (left) and a cold front (right). Below is shown the average observed variation in the intensity of cosmic rays, $\delta\bar{I}$ (shown by circles), and the same quantity corrected for the barometric effect, $\delta\bar{I}_h$ (shown by dots), during the passage of warm fronts (left; 32 cases) and cold fronts (right; 48 cases).

Periods of observation with no frontal development were used when: 1) the synoptic charts showed no primary or secondary fronts within 1000 km: 2) magnetic storms did not occur nor did the horizontal component of the earth's field change by more than 100 γ-units during the period. By far the largest number of cases of this type were those in the neighborhood of anticyclones. These periods could be subdivided into two groups on the basis of the type of change of the surface pressure: those in which the pressure rose (54 cases), and those in which it decreased (42 cases). The average change of pressure in the groups cited (5-6 mb) was larger than that occuring in the frontal cases. Corresponding to each of the different cases cited, average curves of the variation of the observed intensity of the hard component $\delta\bar{I}$ were determined, and also the same quantity corrected for the barometric effect, δI_h. In this connection the following points should be noted: 1) For the determination of δI_h the same barometric coefficient was used as that in the previous work[6], namely, $k_\delta = -0.14\%$ of I_0 per 1 mb change in the atmospheric pressure at the point of observation (where I_0 is the mean value of the intensity). 2) The diurnal variation, which is equal to 0.3% of I_0, was excluded from the given values of δI and δI_h; from the observed variation and from supplemental calculations there is an indication that the observed diurnal effect of the hard component near sea level does not depend on the synoptic situation. 3) The curves of δI and δI_h plotted against time for the individual cases were combined for each type of case by averaging the values of cosmic ray intensity at moments of time corresponding to similar positions of the fronts relative to the point of observation (for the cases with fronts), or corresponding to similar variations of pressure (for the cases without fronts).

The results are shown in Figs. 1-3, in which the scale of time indicated corresponds to the average intervals of observation in the individual cases. The standard deviations shown in Figs. 1 and 2 do not have quite the usual meaning, as they include the effect of the real differences between the fronts averaged. Also, in one case of the passage of a sharply defined cold front, it was possible to calculate the theoretically predicted meteorological effect[1,2] of the variation of the intensity δW (Fig. 4). The calculation was performed using a temperature distribution extending to a height of 300 mb.

3. The following can be seen from the results obtained:

1) The intensity of the hard component of cosmic rays exhibits a characteristic variation during the passage of a front. These variations differ by type corresponding to the type of front. In general, the intensity $\delta\bar{I}_h$ drops during the passage from cold to warm air mass. The minimum is observed in the zone of "pure" warm air and the maximum in cold. This effect in $\delta\bar{I}_h$ varies, on the average, between 0.4% and 0.6% of I_0.

2) The observed variations $\delta\bar{I}_h$ cannot be explained by the use of too high a value of the barometric coefficient. This can be seen by a comparison of the curves of $\delta\bar{I}_h$ in Figs. 1-3. The cause of the variation $\delta\bar{I}_h$, it seems, lies in the

corresponding changes in the temperature profiles of the atmosphere (Fig. 4) as it follows from the theory of the meteorological effect in cosmic rays[1,2]. The latter states that the meteorological effect is related to changes in the atmosphere at altitudes below the generating layers, and not merely within them, as was assumed previously[6].

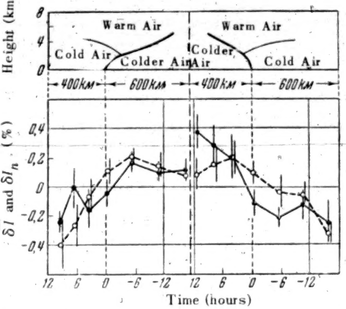

FIG. 2. Above are shown the profiles of warm- and col-type occluded fronts (left and right, respectively). Below are plotted the average variations in the observed intensity, $\delta\bar{I}$ (shown by circles), and the same quantity corrected for barometric effect, $\delta\bar{I}_h$ (shown by dots), during the passage of warm-type occluded fronts (left; 14 cases), and cold-type occluded fronts (right; 13 cases).

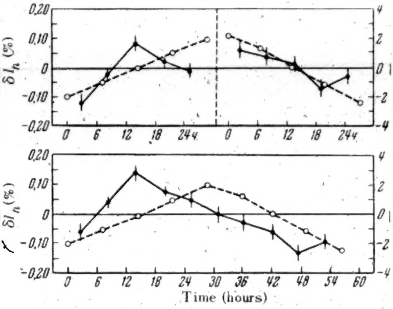

FIG. 3. Average variation of surface pressure, $\delta\bar{h}$, and the intensity of cosmic rays, $\delta\bar{I}_h$, during periods without fronts. Above: $\delta\bar{I}_h$ during increase (left; 54 cases), and during decrease (right; 42 cases), of the surface pressure $\delta\bar{h}$. Below: the variation of $\delta\bar{I}_h$ for the foregoing cases averaged together.

3) The magnitude and the variation of the cosmic ray intensity are not the same in each instance of a particular type of front, but show considerable variation (Fig. 4) which is in accordance with the differences in the strengths and profiles of the individual fronts of a given type[4,7]. The difference in trends of δW and $\delta\bar{I}_h$ apparently is due to the upper layers of the atmosphere (above $h = 300$ mb).

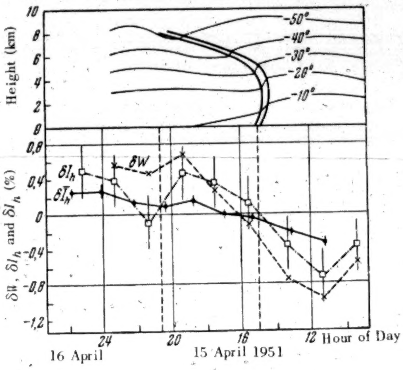

FIG. 4. Variation of the intensity of cosmic rays during the passage of the strong cold front of April 15, 1951. Below: δI_h – the observed variation of the intensity of cosmic rays, corrected for barometric effect; δW – expected variation of cosmic rays[1,2], the integral having been taken in the interval from 300 to 1000 mb; $\delta\bar{I}_h$ – average variation of the cosmic rays during the passage of the cold front (presented for comparison). Above: Temperature profile of the front (° C).

4) $\delta\bar{I}_h$ during periods without fronts is not constant, but shows definite trends (Figure 3), in contrast to previous results[6]. It also leads the surface pressure variation, δh, by about 1/4 of a wave length. The reason for this, according to theory[1,2], should be sought in the relationship of changes of pressure at the surface and at altitude, about which there exist certain meteorological views[4,8] (cf. the curves of Shedler[4]).

5) The observed variations of the intensity, $\delta\bar{I}_h$ (which were not observed in a previous study[6]), related to the upper boundaries of fronts (Fig. 1), the points of occlusion (Fig. 2), and the regions of increase and decrease of surface pressure, are of interest from the point of view of meteorology as well as from that of cosmic rays.

4. It follows from the preceding that:

1) The definite exclusion of the meteorological effect in each case when temperature profile data are unavailable requires a more detailed classification of the meteorological processes.

2) The question of the use of cosmic ray measurements in meteorological investigations requires further study. It appears to us that one can calculate $\delta \overline{W}_{\text{tropospheric}}$ given average tropospheric temperature profiles corresponding to typical meteorological situations. Assuming that the observed variations of $\delta \overline{I}_h$ are caused basically by changes in the temperature profile, i.e., $\delta \overline{I}_h \approx \delta \overline{W}$, one can calculate the contribution of the upper layers of the atmosphere, $\delta \overline{W}_{\text{upper}} \approx \delta \overline{I}_h - \delta \overline{W}_{\text{tropospheric}}$, corresponding to each typical meteorological process in the troposphere. The variation $\delta \overline{W}_{\text{upper}}$ can be considered as an indirect, though objective, factor that can be used along with other meteorological data in studying the character of the relationship of tropospheric processes with those in the layers above. As is well known, this relationship is not very well understood (References 4,5, and others).

In conclusion, I would like to express my gratitude to Prof. E. L. Feinberg, Iu. G. Shafer, and G. A. Tolstobrov for their advice and help.

Translated by V. A. Nedzei
104

[1] E. L. Feinberg, Dokl. Akad. Nauk SSSR **53**, 421 (1946)

[2] L. I. Dorman, Dokl. Akad. Nauk SSSR **94**, 433 (1954)

[3] D. D. Stranathan, *Particles in Modern Physics*, 1948

[4] C. P. Khromov, *Fundamentals of Synoptic Meteorology*, Hydro-meteorological Publishing House, Leningrad, 1948

[5] *Course in Meteorology*, edited by Prof. P. N. Tverskov, Hydrometeorological Publishing House, Leningrad, 1951

[6] D. H. Loughbridge and P. Gast, Phys. Rev. **58**, 583 (1940)

[7] A. A. Bachurin and Z. L. Turketti, *Conditions for the Formation of Atmospheric Fronts*, Hydrometeorological Publishing House, Leningrad, 1950

[8] Zh. D. Zubian, *The Formation and Development of Cyclones and Anti-Cyclones*, Hydro-Meteorological Publishing House, Leningrad, 1949

The Contribution of Meteorological Changes in the Earth's Atmosphere to the Diurnal Effect in Cosmic Rays

A. I. Kuz'min
Yakutsk Branch of the Academy of Science, USSR

(Submitted to JETP editor January 19, 1954)
J. Exper. Theoret. Phys. USSR **28**, 614-616 (1955)

1. IT is important in the investigation of the diurnal effect on the intensity of cosmic rays, as well as in the study of other regular and irregular fluctuations, to isolate those effects related to meteorological changes in the earth's atmosphere. The contribution to the diurnal effect by meteorological factors has been investigated previously (in studies 1-3 and others). In all of these investigations, however, the effect of the redistribution of the atmosphere[4] was not considered. This is as important as the effect of simple absorption of mesons, caused by variation in the mass of air overhead and the change in altitude of the meson-generating layer accompanying a change in the temperature of the atmosphere. Further, in one work[2] the so-called "temperature effect"[5] is incorrectly taken into account.

The present paper reports very accurate determinations (to a precision of several tenths of a percent per hour of observation), at a height of 100 meters, of the global intensity of the hard component of cosmic rays, δI. The analysis was based on a theoretical scheme proposed by Feinberg[4] and generalized by Dorman[5] to include μ-meson production throughout the atmosphere by the disintegration of the π-mesons produced by the primaries.

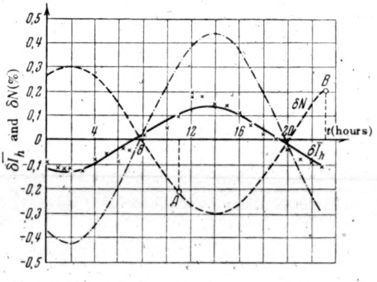

2. The Figure shows the diurnal variation of the intensity of the hard component, δI_h, corrected for the barometric pressure (barometric coefficient $k = -0.14\%$ per 1 mb), obtained by averaging the data obtained during continuous observation from July 1949 to May 1952. The solid line shows the first harmonic, with the experimental points indicated by x's. The two points A and B are values of δN (the intensity of the hard component theoretically expected from consideration of the meteorological effect) calculated from averaged meteorological data. Data were used only from those days on which radio-sonde flights extended to at least 12 km height during both the day and the night periods. This requirement avoids the danger of bias in the results due to an unequal distribution of successful flights during the year between day and night periods. In all, there were 72 paired flights, 17 in winter, 20 in summer, 14 in spring, and 21 in autumn. Table 1 presents the results for δN, the calculated meteorological effect (day-night), and δI_h, the observed variation of the intensity of the hard component of cosmic rays corrected for barometric pressure.

TABLE I

	Winter	Spring	Summer	Autumn	Average
δN in %	-0.08 ± 0.02	-0.40 ± 0.03	-0.83 ± 0.02	-0.73 ± 0.02	-0.35 ± 0.01
δI_h in %	0.34 ± 0.09	0.46 ± 0.1	0.14 ± 0.08	0.28 ± 0.08	0.21 ± 0.05

It is evident from the Figure and the Table that, first of all, the calculated effect, δN(day-night), and the observed variation of δI_h are in opposite phase, contrary to previous findings[2]; and secondly, the meteorological effect correction doubles the diurnal effect in the intensity of the hard component. The absolute values of the results in Table 1 could be in error on the high side only through systematic errors in temperature measurement resulting from the influence of solar radiation on the radio-sonde equipment[6]. This could be significant only at high latitudes in the summer, when the sun's elevation above the horizon is at a maximum. On the other hand, it is known[6] that at northern latitudes 60°– 62° this increase reaches about 2° C at a height of 13 km. It can be shown, assuming an exponential decrease of density with height, that at 6 km this error is of the order of tenths of a degree, and at the level of our meteorological observations, only hundredths of a degree. Hence, the absolute value of the expected meteorological effect, "day-night" during the summer season cannot be in error by more than 0.2%. Thus, the meteorological effect is opposite to the one observed, and has a value of about 0.4%. The correctness of this conclusion is supported by the fact that the average height at which the pressure equals 300 mb is found from three years of radio-sounding to be higher during the daytime than at night, as is shown in Table 2. It is also seen in Table 2 that the positive difference in height between day and night does not change very much from season to season. A comparison of Tables 1 and 2 suggests that a significant role is played by the redistribution of the mass of the atmosphere below the 300 mb level in the variation of the diurnal effect from season to season.

TABLE II

	Winter	Spring	Summer	Autumn
Average difference between the height of the 300 mb level during the day and at night, in meters . . .	46	38	37	30

3. In order to evaluate the full significance of the influence of meteorological changes on the diurnal effect, one would require frequent, round-the-clock sounding of the atmosphere, more frequently than is presently done by meteorologists. Nevertheless, from careful analysis by Selezneva[7] of the aerological data obtained over many years at Slutsk, it is evident that the diurnal variation of temperature above 3 km has an independent character and increases with height. The basic maximum of temperature occurs at about 1300-1400 local mean solar time. Therefore, if the maximum temperature of the entire troposphere occurs at 1400 on the average, it can be assumed that the calculations of the meteorological effect reflect about 70% of this effect, as these results apply to moments of time displaced by three hours from the experimentally observed temperatures. The value of the possible meteorological effect should be 0.6% on the average (the assumed diurnal meteorological effect, δN, is shown by the dashed line in the Figure). Then, using the observed $\delta \bar{I}_h$, one concludes that the diurnal variation of the intensity of the hard component of cosmic rays has a non-meteorological origin and amounts to about 1% (shown in the Figure by the dot-and-dash line).

4. It should be noted that the seasonal variation of the diurnal effect of cosmic rays can be explained by the seasonal change in the diurnal fluctuation of meteorological factors. It is known[7] that the largest diurnal temperature fluctuations of the troposphere occur in summer, the smallest in winter. If the diurnal variation of the intensity of cosmic rays predicted by the meteorological effect is opposite to the one observed, then one should expect that the diurnal effect observed should be smallest in summer and largest in winter. This indeed occurs, as is seen in Table 3, where are shown the amplitudes of the first harmonic, calculated from the seasonal averages of the diurnal variation of the intensity of the hard component of cosmic rays, $\delta \bar{I}_h$. It is seen that the diurnal effect in summer is only half that in winter, and this agrees with the increase in the diurnal meteorological effect in summer (Table 1).

TABLE III

	Winter	Spring	Summer	Autumn	Year-round
Amplitudes in % . . .	0.18±0.004	0.15±0.004	0.09±0.004	0.12±0.005	0.13±0.002
Time of maximum (in hours).	13.9	13.9	13.4	13.3	13.4

However, the data in Table 3 contradict the work of Duperier[1] who observed, by a coincidence method, that the total intensity of cosmic rays exhibited a larger effect during summer months than in winter. This disagreement could be explained by a considerably larger contribution of the diurnal variation of meteorological factors to those measurements than to ours, because the average particles observed there were softer. For this reason, perhaps, the seasonal changes of the diurnal effect observed there directly reflected the meteorological component of the diurnal effect of cosmic rays.

In conclusion, the author thanks Prof. E. L. Feinberg and Iu. G. Shafer for valuable suggestions and advice. The author also thanks G. V. Skripin for his help in the calculations and analysis of the data.

---

[1] A. Duperier, Nature **158**, 196 (1946)

[2] D. W. N. Dolbeara and H. Elliot, Atm. Terr. Phys. 1, 205 (1951)

[3] A. R. Hogg, Memoirs of the Commonwealth Observatory, Canberra **10**, 1 (1949)

[4] E. L. Feinberg, Dokl. Akad. Nauk SSSR **53**, 421 (1946)

[5] L. I. Dorman, Dokl. Akad. Nauk SSSR **94**, 433 (1954)

[6] A. B. Kalinovski and N. Z. Pinus, *Aerology*, Hydro-meteorological Publishing House, Leningrad (1951).

[7] E. Z. Selezneva, Izv. Akad. Nauk SSSR, Ser. Geograf. **9**, 82 (1945)

Translated by V. A. Nedzel
105

Nuclear Fissions Associated with Heavy Unstable Particles

I. M. Gramenitskii, E. A. Zamchalova
M. I. Podgoretskii, M. I. Tretiakova
and M. N. Shcherbakova
The P. N. Lebedev Institute of Physics, Academy of Sciences, USSR

(Submitted to JETP editor February 8, 1955)
J. Exper. Theoret. Phys. USSR **28**, 616-617 (May, 1955)

1. WITH the aid of thick photoemulsions there have been found to date over one hundred nuclear fissions in which there are produced hyperons (charged hyperons $Y^{\pm}$ and Λ^0 particles) and heavy mesons of mass $\sim 1000\ m_e$ (K and τ mesons). There were also detected about thirty secondary fissions produced by the nuclear capture of stopped negative heavy mesons.

This note gives a brief account of some results of the statistical analysis of these fissions. The conclusions should for the present be considered as likely hypothesis in need of additional verification and more complete proof.

TABLE

Star type	$Y^{\pm}$	Λ^0	$Y^{\pm}+\Lambda^0$	K	τ	Stars observed in the stratosphere
$\bar{N}_h$ . . .	19.3±2.5	18.8±1.9	19.0±1.7	18.0±1.8	11.2±1.9	12.3±0.9

2. The table shows the average number of gray and black rays N_h for starts containing charged hyperons, Λ^0 particles (more accurately excited fragments[1]), K mesons and τ mesons. For comparison there are also given data for ordinary cosmic ray stars observed in the strastophere[2].

In order to insure that the released energy is approximately the same in all cases only those stars were selected in which the number of relativistic particles N_s satisfied the condition $5 \leqslant n_s \leqslant 10$.

It is seen from the Table that, in regard to the value of $\bar{N}_h$, the conditions for the production of $Y\pm$ and Λ^0 particles are very similar. This agrees with the natural hypothesis that charged and neutral hyperons are particles of one type. Similarly, the concurrence of $\bar{N}_h$ for stars containing hyperons and K mesons is in agreement with the hypothesis of the pair production of particles[3,4]. On the other hand, cases are also known of hyperon and τ meson pair production[5,6]. It follows from the Table, however, that in the present case the mechanism of pair production is not the determining one. Actually, if hyperons and τ mesons originated in pairs only, then stars containing these particles would be characterized by the same $\bar{N}_h$ values.

At the present time there is an intensive consideration of a hypothesis according to which K and τ mesons are not different particles, but different types of the decay of the same particle[3,7]. If this is so, then the values of $\bar{N}_h$ for stars containing K and τ mesons must be the same. The sharp discrepancy between this conclusion and the experimental data permits one to conclude that K and τ mesons are distinct particles.

3. The value of $\bar{N}_h$ for ordinary stars agrees with that for stars containing τ mesons but differs markedly from $\bar{N}_h$ for stars containing K mesons and hyperons. This means that the probability of a τ meson production in the fission of a light nucleus of a photo emulsion is the same as in the fission of a heavy nucleus. On the contrary, K mesons and hyperons are formed mainly in the heavy emulsion nuclei. At the present time one cannot give a well-defined interpretation of this fact. It is of interest to note that qualitatively this fact agrees well with Powell's hypothesis[3,4], which assumes that hyperons and K mesons are formed in two stages during the nuclear interactions of nucleons. The first stage consists of the production of a π meson shower, the interaction of which with the nucleons in the same nucleus leads in the second stage to the pair production of hyperons and K mesons.

4. In the investigation of the stars formed as a result of the capture of stopped negative mesons with mass $\sim 1000\ m_e$, which we call conventionally K mesons, two characteristics are worthy of notice:

a) the formation of π mesons with energies $\sim 30 - 40$ Mev ;

b) the release of very small energies in a considerable number of cases.

Detailed analysis of these and certain other facts leads to the conclusion that the nuclear capture of $K-$ mesons takes place with the formation of Λ^0 particles according to the following schemes:

$$K^- + p \rightarrow \Lambda^0 + \pi^0, K^- + p \rightarrow \Lambda^0 + \gamma,$$

$$K^- + p \rightarrow \Lambda^0 + \nu.$$

Moreover, the Λ^0 particles remain, as a rule, bound within the nucleus, forming a system similar to a stationary excited fragment. Subsequent events take place as in the decay of excited fragments.

It is not excluded that during the capture of a $K-$ meson there is also formed a bound charged hyperon which is then changed inside the nucleus into an Λ^0 particle.

Translated by H. Kruglak
106

[1] C. F. Powell, Usp. Fiz. Nauk **53**, 449 (1954)

[2] C. F. Powell, U. Camerini, and others, Usp. Fiz. Nauk **40**, 76 (1950)

[3] C. F. Powell, Nuovo Cim. Suppl. **11**, 165 (1954)

[4] C. Castagnoli, G. Cortini, A. Manfredini, Nuovo Cim. **12**, 464 (1954)

[5] D. Lal, Y. Pal and B. Peters, Phys. Rev. **92**, 438 (1953)

[6] A. Debenedetti, D. M. Garelli, L. Tallone, C. M. Vigone. Nuovo Cim. **12**, 466 (1954)

[7] L. Leprince-Ringuet and A. B. Rossi, Phys. Rev. **92**, 722 (1953)

Determination of the Absolute Concentrations of Atoms in a Multi-Component Arc-Vapor

V. S. MEL'CHENKO
Siberian Physico-Technical Institute

(Submitted to JETP editor December 6, 1954)
J. Exper. Theoret. Phys. USSR **28**, 628-629 (May, 1955)

THE Prilezhaeva method[1] makes it possible to determine the absolute concentrations of atoms in the positive column of a direct-current arc[2,3]. It is generally believed that absolute concentrations can be measured by this method only in the case where the arc-vapor contains two components (a compound which is difficult to ionize --- air and carbon --- and an easily ionized one --- the vapor of the element being investigated). However, we have also applied the Prilezhaeva method in the case of a more complex arc-vapor.

Let an arc-vapor contain k elements which are to be analyzed and whose concentrations are N_1, N_2, ... N_k respectively. The general idea of the concentration of atoms is based on the fact that the degree of ionization of a mixture of different gases at a given temperature depends on the composition of the gas. By determining the fractional ionization of the gas experimentally, it is possible to determine the concentrations of the base components of the mixture.

The resultant (average) fractional ionization of the gas as a whole (i.e., the mixture), $\overline{x}$, is related to the concentrations of the components in the following way:

$$\overline{x} = \sum_{i=0}^{k} x_i N_i \Big/ \sum_{i=0}^{k} N_i, \tag{1}$$

where x_i is the fractional ionization of the ith component. Consequently, in order to determine the N_i, it is necessary to know the average fractional ionization of the gas and also the fractional ionizations of all the components. To determine these quantities, it suffices to measure experimentally the temperature of the gas and the fractional ionization of only one of the components. Then the Saha equation can be written for each component:

$$\lg \frac{x_i}{1-x_i} \frac{\overline{x}}{1+\overline{x}} = 2.5 \lg T - \frac{5040}{T} V_i - 6.5, \tag{2}$$

where T is the temperature and V_i is the ionization potential of each component in electron volts. From Eq. (2) as written for that component whose fractional ionization is measured, it is possible to determine $\overline{x}$, and then from this same equation as written for all the remaining components, it is possible to determine all the x_i. However, knowing $\overline{x}$ and the x_i is still not sufficient for finding the N_i from Eq. (1). It is necessary to have additional relations between the concentrations, N_i. Such relations can be obtained if we measure $k - 1$ ratios of the intensities of pairs of spectral lines (regardless of whether they are atomic or ionic) of the elements being investigated. For example, we take the ratio of two atomic lines of the ith and nth components to be:

$$\frac{I_i}{I_n} = \frac{N_i}{N_n} \frac{A_i g_i g_{n0}}{A_n g_{i0} g_n} e^{-(E_i - E_n)/kT} \frac{\nu_i}{\nu_n}, \tag{3}$$

where A is the transition probability, g is the statistical weight and E is the excitation potential of the line.

The ratio N_i/N_n can be determined from Eq. (3). Here, however, a complication arises from the fact that it is necessary to know the transition probabilities of the lines which are being used. In order to determine k quantities, the N_i, from $k - 1$ relations in the form of Eq. (3) and Eq. (1), it is still necessary that N_0, the last unknown quantity in Eq. (1), be eliminated. In the denominator, N_0, enters together with the N_i in the form of a sum. Since the pressure p (atmospheric) and the temperature T are known, this sum can be determined very simply from a consideration of gas kinetics by the formula:

$$N = \sum_{i=0}^{k} N_i = \frac{9.7 \cdot 10^{18}}{T} p, \tag{4}$$

where p is the pressure in mm Hg.

The numerator term containing N_0 can usually be neglected, i.e., in the majority of cases:

$$\sum_{i=1}^{k} x_i N_i \gg x_0 N_0. \tag{5}$$

This is always justified when the ionization potential, V_i, of even one of the components, which is present in not too small a concentration, is somewhat less (1-3 ev is sufficient) than the ionization potential V_0. In such a case, because of the exponential dependence of the fractional ionization on the ionization potential, x_0 is so small that the validity of the inequality in Eq. (5) is guaranteed.

As a result, Eq. (1) can now be rewritten in the form:

$$\bar{x} = \sum_{i=1}^{k} x_i N_i / N. \tag{6}$$

Using Eqs. (3) and (6), it is possible to find all the N_i, the concentrations which were to be determined. The temperature, T, and the fractional ionization of one of the components can be found in the usual manner[2].

An experiment has been carried out for the simplest case, $i = 2$, i.e., a three-component arc-vapor*. Magnesium and zinc were used as the test elements. The temperature was determined from the ratio of the intensities of the zinc atomic lines, $\lambda = 3072$ Å and $\lambda = 3076$ Å, the relative (transition) probabilities of which are known[4]. The fractional ionization of the magnesium was found experimentally from the lines Mg I, $\lambda = 2779$ Å and Mg II, $\lambda = 2795$ Å (as in reference 3). Among the Zn and Mg lines, it was possible to find lines with known transition probabilities[4,5] by which the ratio of the concentrations of Zn and Mg atoms could be determined from Eq. (3). We selected the lines Mg I, $\lambda = 2779$ Å and Zn I, $\lambda = 2741$ Å.

All measurements were made by the photographic-photometric method. Zinc was introduced in the test sample in the form of a solution of $ZnSO_4$, magnesium in the form of a solution of $MgCO_3$ and the base element of the test sample was carbon powder. The percentages by weight of the materials in the test sample were: $ZnSO_4$ – 10%; $MgCO_3$ – 3%; C – 87%.

The temperature of the arc-vapor was found to be 6300° K. The measurements of the fractional ionization of the magnesium atoms showed that $x_{\mathrm{Mg}} = 0.43$. A calculation using these values of T and x_{Mg} in the Saha formula gives $x_{\mathrm{Zn}} = 3.6 \times 10^{-2}$ and $\bar{x} = 4 \times 10^{-3}$. Correspondingly, the computed concentrations of magnesium and zinc were found to be $N_{\mathrm{Mg}} = 7.2 \times 10^{15}$ cm^{-3}; $N_{\mathrm{Zn}} = 4.3 \times 10^{16}$ cm^{-3}.

Thus, in the test sample, the number of zinc atoms is greater than the number of magnesium atoms by a factor of 1.5; in the discharge-gap, however, it is 6 times greater. It follows that the rate at which zinc atoms from the test sample enter the discharge is 4 times greater than the rate at which magnesium atoms enter. This is in agreement with Rusanov's data on volatile elements[6].

---

* The experiment was carried out by the student A. E. Kontorovich.

[1] N. A. Prilizhaeva, Trans. Siberian Phys. Tech. Inst. **28**, 83 (1949)

[2] V. N. Goriachev, Trans. Siberian Phys. Tech. Inst. **30**, 61 (1950)

[3] M. A. Alekseev, Trans. Siberian Phys. Tech. Inst. **32**, 21 (1953)

[4] J. W. Schuttevaer and J. A. Smit, Physica **10**, 502 (1943)

[5] J. A. H. Kersten and L. S. Ornstein, Physica **8**, 1124 (1941)

[6] A. K. Rusanov, *Spectral Analysis of Ores and Minerals*, State Geological Press, 1948

Translated by H. Lashinsky
112

The Relativistic Mechanics of a Material Point of Variable Mass

N. S. KALITSIN
State University of Bulgaria

(Submitted to JETP editor July 29, 1954)
J. Exper. Theoret. Phys. USSR **28**, 631-632 (May, 1955)

THE work of I. V. Meshcherskov laid the foundations for the non-relativistic mechanics of bodies of variable mass. Meshcherskov's equations are used to determine the motion of rockets, heavenly bodies of variable mass and for the solution of a range of other mechanical problems. These equations, however, which are developed on the basis of Newtonian mechanics, are valid only in the range of velocities small with respect to the velocity of light c.

It is entirely possible that in the future, velocities approaching that of light will be of interest. There exist also radioactive particles which move with velocities close to c. These particles have variable mass.

For these cases it is necessary to apply relativistic mechanics to a material point of variable mass.

For the investigation of a single particle of variable mass we will use four dimensional Minkowski space. Let x_1, x_2, x_3 be the usual space coordinates. The fourth coordinate is $x_4 = ict$, where c is the velocity of light in vacuum and t is time. The Minkowski space x_i will be denoted by R_4 and the space (x_1, x_2, x_3) by R_3.

Every material particle describes a world line in R_4. The distance between two infinitesimally close events along any world line is given by

$$ds^2 = -dx_i\,dx_i. \tag{1}$$

The four-dimensional velocity of a particle is given by the vector

$$u_i = dx_i/ds. \tag{2}$$

To find its component, we note that according to Eq. (1),

$$ds = c\,dt\sqrt{1-(v^2/c^2)}, \tag{3}$$

where v is the ordinary three-dimensional velocity of the particle in R_3. In this way

$$u_\alpha = v_\alpha \sqrt{1-(v^2/c^2)}, \qquad \alpha = 1, 2, 3,$$
$$u_4 = i/\sqrt{1-(v^2/c^2)}.$$

The components of the four-velocity are not independent. We note that for $dx_i^2 = -ds^2$, we have

$$u_i^2 = -1. \tag{4}$$

In a certain coordinate system, which we shall consider at rest, at a given time t, we investigate two material points, one with mass m having velocity u_i with respect to the given system, the other with mass dm having celocity a_i. At the time $t + dt$ these two points form one point (combination of mass) of mass $m + dm$, whose velocity is $u_i + du_i$. Instead of the time t as parameter, we introduce the arc length s, described by the point of mass m.

We now apply the momentum theorem of relativistic mechanics. At the instant s, the momentum of the system is

$$cmu_i + cdma_i,$$

whereas at the instant $s + ds$ it is

$$c\,(m + dm)\,(u_i + du_i).$$

The increase in momentum is

$$dp_i = cm\,du_i + cdm\,(u_i - a_i). \tag{5}$$

We introduce the force four-vector, determined by the derivative

$$f_i = \frac{dp_i}{ds} = cm\frac{du_i}{ds} + c\frac{dm}{ds}(u_i - a_i). \tag{6}$$

We shall now write Eq. (6) in R_3. The force vector in R_3 we define by the equation

$$\mathbf{F} = c\,(f_1, f_2, f_3)\sqrt{1-(v^2/c^2)}.$$

The first components of Eq. (6) give

$$\frac{d}{dt}\frac{m\mathbf{v}}{\sqrt{1-(v^2/c^2)}} - \frac{\mathbf{a}}{\sqrt{1-(a^2/c^2)}}\frac{dm}{dt} = \mathbf{F}. \tag{7}$$

For velocities v and a small with respect to c, Eq. (7) reduces to Mershcherkov's nonrelativistic equation

$$m\frac{d\mathbf{v}}{dt} + \frac{dm}{dt}(\mathbf{v} - \mathbf{a}) = \mathbf{F}. \tag{8}$$

Equation (6) or (7) represents the relativistic generalization of Mershcherkov's basic Eq. (8) for a material point of variable mass.

If the velocity of the added mass is relativistic, but that of mass m is nonrelativistic, then Eq. (7) assumes the form

$$\frac{d}{dt}(m\mathbf{v}) - \frac{\mathbf{a}}{\sqrt{1-(a^2/c^2)}}\frac{dm}{dt} = \mathbf{F}. \tag{9}$$

If the velocity of the added mass vanishes $(a = 0)$, then Eq. (7) assumes the form

$$\frac{d}{dt}\frac{m\mathbf{v}}{\sqrt{1-(v^2/c^2)}} = \mathbf{F}. \tag{10}$$

For $a = v$ (the relative velocity of the combining masses is zero), Eq. (7) takes the form

$$m\frac{d}{dt}\frac{\mathbf{v}}{\sqrt{1-(v^2/c^2)}} = \mathbf{F}. \tag{11}$$

Let us form the scalar product

$$f_iu_i = cm\frac{du_i}{ds}u_i + c\frac{dm}{ds}(u_iu_i - a_iu_i).$$

Since $u_iu_i = -1$, and therefore $(du_i/ds)u_i = 0$, then

$$f_iu_i = -c\frac{dm}{ds}(1 + a_iu_i). \tag{12}$$

In R_3, Eq. (12) has the following form

$$\mathbf{F}\mathbf{v} = \frac{d}{dt}\frac{mc^2}{\sqrt{1-(v^2/c^2)}} \tag{13}$$
$$-\frac{dm}{dt}\left(c^2\sqrt{1-(v^2/c^2)} + \frac{\mathbf{a}\mathbf{v}}{\sqrt{1-(a^2/c^2)}}\right),$$

One must bear in mind that in all these equations m depends on time. It can depend on time either explicitly, or implicitly by means of quantities determining the position or motion of the point. If, for example, $m = f(x_\alpha, \dot{x}_\alpha, t)$, then

$$\frac{dm}{dt} = \frac{\partial m}{\partial x_\alpha}\dot{x}_\alpha + \frac{\partial m}{\partial \dot{x}_\alpha}\ddot{x}_\alpha + \frac{\partial m}{\partial t} \quad (\alpha = 1, 2, 3).$$

The author expresses his gratitude to Professor Kh. Khristov for valuable criticism given in the examination of this work.

---

[1] L. D. Landau and E. Lifshitz, *Theory of Fields*, 1948

[2] L. Loitsianskii and A. Lur'e, *A Course in Theoretical Mechanics*, II, Moscow, Leningrad, 1948

Translated by E. L. Saletan
114

Hyperfine Structure of Paramagnetic Resonance in Copper Tutton Salts at Intermediate Fields

N. S. GARIF'IANOV AND M. M. ZARIPOV *
Physico-Technical Institute of the Kazan Branch of the Academy of Sciences USSR, Kazan State University

(Submitted to JETP editor November 30, 1954)
J. Exper. Theoret. Phys. USSR **28**, 629-630 (May, 1955)

UP to the present time the hyperfine structure of paramagnetic resonance in compounds of elements of the iron group has been studied at high frequencies, usually of the order of 10^{10} cps. In this frequency region, strong magnetic fields are required to satisfy the conditions for resonance in elements of the iron group. Such fields give rise to splittings at least an order of magnitude greater than the splittings which result from the interactions of electrons with the moments of the nucleus.

At much lower frequencies, say in the decimeter or meter region, conditions obtain which correspond to the intermediate- or weak-field Zeeman effect[1-3]. Low-frequency studies can be useful not only in checking the general theory of paramagnetic resonance absorption in crystals at low and intermediate fields[4], but also in obtaining more precise determinations of the hyperfine structure constant inasmuch as under these conditions the energy splittings produced by the nuclear moments become equal to or greater than the splitting produced by the dc magnetic field.

We have examined the paramagnetic resonance in a $CuK_2(SO_4)_2 \times 6H_2O$ single-crystal diluted in an isomorphous zinc salt in the ratio 1:200 at a frequency of 526.74×10^6 cps at liquid air temperature. The paramagnetic resonance was observed using the grid-current method[5] in conjunction with modulation of the dc magnetic field. The free radical α, α-diphenyl β-picryl hydrazyl was used to calibrate the magnetic field. The accuracy in the determination of the resonance values of the field was limited by the width of the absorption line and consequently was not better than 2%.

It is known that the unit cell of a Tutton-salt cyrstal contains two copper ions[6] and that the tetragonal symmetry axes of the electric fields around these ions form an angle of 96°.

We investigated the paramagnetic resonance spectrum in the case for which the dc magnetic field was oriented along one of the tetragonal symmetry axes of the electric field. Six absorption lines were found. The resonance values in oersteds of the dc magnetic field are shown in the Table.

An interpretation of the paramagnetic resonance spectrum at strong fields of the salt which is the subject of this paper was carried out in reference 7 with the use of the following "spin" Hamiltonian:

$$\begin{aligned}\mathscr{H} = {} & g_\parallel \beta H_z S_z + g_\perp \beta (H_x S_x \\ & + H_y S_y) + A S_z I_z + B(S_x I_x + S_y I_y) \\ & + Q\left[I_z^2 - \frac{1}{3} I(I+1)\right],\end{aligned} \qquad (1)$$

where $g_\parallel$ and $g_\perp$ are, respectively, the spectroscopic splitting factors parallel and perpendicular to the tetragonal symmetry axis of the electric field; A, B and Q are hyperfine structure constants of which the first two depend on the magnetic moment of the nucleus and the last depends on the nuclear electric quadrupole moment.

For the frequency which we used, the applied field corresponds to that of the intermediate field

Resonance values of the dc magnetic field in oersteds

Experimental	36	96	143	168	216	250
Calculated	36.11	95.85	140	168.5	221	252.5

case. Thus the calculation of the observed spectrum involves the solution of two algebraic equations of the eighth degree (for Cu^{++}, $S = \frac{1}{2}$, $I = {}^{3}/{}_{2}$) which derive from the two ions in the unit cell of the crystal. The solution of the equation in the case for which the dc magnetic field is oriented along the tetragonal axis of the electric field is found easily[3]. The probability for magnetic dipole transitions was also calculated for this case. The solutions of the equation for the second ion were found by an approximation method. The dc magnetic field resonance values were obtained using the following values of the constants which appear in Eq. (1): $A = -8.3 \times 10^{-3}$ cm^{-1}, $B = 4.5 \times 10^{-3}$ cm^{-1}, $Q = 1 \times 10^{-3}$ cm^{-1}, $g_{\parallel} = 2.47$ and $g_{\perp} = 2.08$.

Our values for these constants differ from those given in reference 8, viz. $A = -10.3 \times 10^{-3}$ cm^{-1}, $B = 3.5 \times 10^{-3}$ cm^{-1}, $Q = 1 \times 10^{-3}$ cm^{-1}, $g_{\parallel} = 2.45$ and $g_{\perp} = 2.12$. This is probably explained by the fact that in the work mentioned above, the experiments were performed at $T = 20°$ K. If one assumes that the size of the tetragonal component of the electric field should become larger with an increase of temperature, it is possible to explain qualitatively a corresponding change of these constants.

---

* The experimental work was carried out by N. S. Garif'ianov.

[1] S. A. Al'tshuler, B. M. Kozyrev and S. G. Salikhov, Dokl. Akad. Nauk SSSR **71**, 885 (1950)

[2] B. M. Kozyrev, Izv. Akad. Nauk SSSR, Ser. Fiz. **16**, 533 (1952)

[3] B. Bleaney, H. E. D. Scovil and R. S. Trenam, Proc. Roy. Soc. (London) **A 223**, 15 (1954)

[4] A. Abragam and M. H. L. Pryce, Proc. Roy. Soc. (London) **A205**, 135 (1951)

[5] E. K. Zavoiskii, *Dissertation*, Moscow, Phys. Inst. Academy of Sciences, 1944

[6] B. Bleaney, R. P. Penrose and B. I. Plumpton, Proc. Roy. Soc. (London) **A 198**, 406 (1949)

[7] A. Abragam and M. H. L. Pryce, Proc. Roy. Soc. (London) **A 206**, 164 (1951)

[8] B. Bleaney, K. D. Bowers and D. J. E. Ingram, Proc. Roy. Soc. (London) **A 64**, 758 (1951)

Translated by H. Lashinsky
113

The Representation of Green's Function in Quantum Electrodynamics in the Form of Continual Integrals

I. M. KHALATNIKOV
Institute of Physical Problems,
Academy of Sciences, USSR

(Submitted to JETP editor December 25, 1954)
J. Exper. Theoret. Phys. USSR **28**, 633-635 (May, 1955)

In quantum electrodynamics, Green's functions for various problems can be written in the form of the matrix elements of various chronologically T-ordered products of the operators for the electron and photon fields, taken between states of the unperturbed vacuum. Thus, for instance, Green's function for the single electron problem has the following form

$$G_{\alpha\beta}(x, x') = \langle T(\psi_\alpha(x)\bar{\psi}_\beta(x') S / S_{\text{vac}}\rangle. \qquad (1)$$

Here S_{vac} is the vacuum expectation value of the S-matrix

$$S = \exp\{-i \int H(x)\, dx\}. \qquad (2)$$

The symbol T denotes the operation of relativistic invariant time ordering, introduced by Wick[1]. In the case of electrodynamics, the Hamiltonian density $H(x)$ is given by

$$H(x) = -i\bar{\psi}(x)\gamma_\mu A_\mu(x)\psi(x). \qquad (3)$$

Analogously, one can write Green's function for other problems.

The aim of the present note is to present an expression for Green's function in the form of continuous integrals in the space of the ψ and A functions*.

According to Hori[3] (see also Anderson[4]), the operation of T-ordering multiplying an expression of the indicated form reduces to multiplication of these expressions by ordering operators for the electric field,

$$e^{\Sigma}, \quad \Sigma = \frac{1}{4}\int_{-\infty}^{\infty} dx \int_{-\infty}^{\infty} dx' S_{F_{\alpha\beta}} \times (x - x') \frac{\delta^2}{\delta\psi_\alpha(x)\,\delta\psi_\beta(x')} \qquad (4)$$

and for the photon field

$$e^{\Delta}, \quad \Delta = \frac{1}{4} \int_{-\infty}^{\infty} dx \int_{-\infty}^{\infty} dx' D_{F_{\mu\nu}} \times (x-x') \frac{\delta^2}{\delta A_\mu (x)\, \delta A_\nu (x')} \tag{5}$$

where $S_{F_{\alpha\beta}}$ and $\dot{D}_{F_{\mu\nu}}$ are Green's functions for the free (noninteracting) electron and photon fields, respectively.

In Eq. (4) the spinor functions ψ_α and $\bar{\psi}_\beta$ anitcommute with each other.

Ordering operators act on the products of electron and photon field operators taken in the sense of T-products; i.e., in the products under consideration, in every Hamiltonian function, the operators $\bar{\psi}(x)$ always stand to the left of the operators $\psi(x)$.

Let us introduce a coordinate lattice into four dimensional space, of elementary cell volume ω. We shall denote the lattice points (there are N of them) by Latin letters and shall use the following abbreviated notation

$$\begin{gathered} S_{F_{\alpha\beta}} (x_i - x_k) = S_{\alpha\beta} (ik), \\ D_{F_{\mu\nu}} (x_i - x_k) = D_{\mu\nu} (ik), \\ A_\mu (x_i) = A_\mu (i), \\ \psi_\alpha (x_i) = \psi_\alpha (i). \end{gathered} \tag{6}$$

The introduction of the lattice allows one to use sums instead of integrals and partial derivatives instead of functional derivatives. As an illustration of the method, we shall go into detail in what follows by considering the representation of the vacuum expectation value of the S-matrix in the form of a continuous integral. After this, one can write the formulas for Green's functions analogously. Going over from integrals to sums in Eq. (4) we get

$$S_{\text{vac}} = \langle \exp \left\{ \frac{1}{4} S_{\alpha\beta} (ik) \frac{\partial^2}{\partial \psi_\alpha (i)\, \partial \bar{\psi}_\beta (k)} \right\} \times \exp \left\{ \frac{1}{4} D_{\mu\nu} (ik) \frac{\partial^2}{\partial A_\mu (i)\, \partial A_\nu (k)} \right\} \times \exp \left(- \omega \bar{\psi}_\alpha (i) \gamma_\mu^{\alpha\beta} A_\mu (i) \psi_\beta (i) \right) \rangle. \tag{7}$$

This expression can be rewritten in the form of a $3N$-fold integral. For this we make use of the fact that Eq. (7) is the same as the solution of the diffusion-type equations

$$\frac{\partial S_{\text{vac}}}{\partial t_1} = \frac{1}{4} S_{\alpha\beta} (ik) \frac{\partial^2}{\partial \psi_\alpha (i)\, \partial \bar{\psi}_\beta (k)} S_{\text{vac}}; \tag{8}$$

$$\frac{\partial S_{\text{vac}}}{\partial t_2} = \frac{1}{4} D_{\mu\nu} (ik) \frac{\partial^2}{\partial A_\mu (i)\, \partial A_\nu (k)} S_{\text{vac}}, \tag{9}$$

for values of the time-like variables $t_1 = 1$ and $t_2 = 1$ and the vanishing of ψ_α and $A_{\mu\nu}$ (no free electrons or photons), with initial value S_{vac} for $t_1 = t_2 = 0$ given by

$$\exp (- \omega \bar{\psi}_\alpha (i) \gamma_\mu^{\alpha\beta} A_\mu (i) \psi_\beta (i)).$$

Equation (8) contains derivatives with respect to the noncommuting spinor functions ψ_α and $\bar{\psi}_\beta$. This situation makes it more difficult to find solutions to the derived equations. In order to avoid this difficulty, we will remove the operator properties of ψ to the matrix elements $S_{\alpha\beta}(ik)$. The operator Σ (4) will be rewritten in the form

$$\Sigma = \check{S}_{\alpha\beta} (ik) \frac{\delta^2}{\delta \psi_\alpha (i)\, \delta \psi_\beta (k)}, \tag{10}$$

where ψ_α and $\bar{\psi}_\beta$ are now ordinary functions which commute. The matrix elements of $\check{S}(ik)$ are expressed by means of the operator η_{ik} **

$$\check{S} (ik) = S (ik)\, \eta_{ik}. \tag{11}$$

The operators η_{ik} commute with each other***. If in any product of operators an index occurs more than twice, then the product vanishes. The following multiplication rule holds

$$\eta_{ik} \times \eta_{kl} = \eta_{il}. \tag{12}$$

The operators η_{ii} are merely numbers

$$\eta_{ii} = -1. \tag{13}$$

The elements of the inverse matrix $\check{S}^{-1}(ik)$ are determined analogously

$$\check{S}^{-1} (ik) = - S^{-1} (ik)\, \eta_{ik}. \tag{14}$$

From the above properties of the η_{ik} follows the multiplication rule for the matrix elements $\check{S}(ik)$

$$\check{S} (1 i_1) \ldots \check{S} (n i_n) = S (1 i_1) \ldots S (n i_n) (-1)^P. \tag{15}$$

The second indices i_α take on values from 1 to n, and P is the parity of the permutation of the second indices.

We must now determine the value of the integral

$$I = \int \exp\{-\bar{\psi}(i)\,\check{S}^{-1}(ik)\,\psi(k)\}\,\delta\psi\,\delta\bar{\psi}, \tag{16}$$

$$\delta\psi = \Pi d\psi(i).$$

This type of integral will occur below. We evaluate the integral I as the limit of $I(\alpha)$ for $\alpha \to 0$.

$$I(\alpha) = \int \exp\{-\alpha\bar{\psi}(i)\,\psi(i)\} \tag{17}$$

$$\times \exp\{-\bar{\psi}(i)\,\check{S}^{-1}(ik)\,\psi(k)\}\,\delta\psi\,\delta\bar{\psi}.$$

Let us calculate $I(\alpha)$. To do this we expand $\exp(-\psi(i)\,S^{-1}(ik)\,\psi(k))$ in the integral in Eq. (17) into a series. We get

$$I(\alpha) = \int \exp\{-\alpha\bar{\psi}(i)\,\psi(i)\} \tag{18}$$

$$\times \sum \frac{1}{n!}\,(\bar{\psi}(i)\,\check{S}^{-1}(ik)\,\psi(k))^n\,\delta\psi\,\delta\bar{\psi}.$$

Further, after a simple integration, taking into account Eqs. (14) and (15), we get

$$I(\alpha) \tag{19}$$

$$= \frac{\pi^N}{\alpha^N}\sum(-1)^{n+P}\,\frac{1}{\alpha^N}\,S^{-1}(1i_1)\ldots S^{-1}(ni_n)$$

$$= \frac{\pi^N}{\alpha^N}\,\mathrm{Det}\left|\,\delta_{ik} + \frac{S^{-1}(ik)}{\alpha}\,\right|$$

The solution of the system of Eqs. (10) and (11), satisfying initial conditions (12), can be written in the form

$$S_{\mathrm{vac}} = \frac{1}{\pi^{N/2}\sqrt{\mathrm{Det}\,D_{\mu\nu}}} \tag{20}$$

$$\times \int \exp\{-\bar{\psi}(i)\,\check{S}^{-1}(ik)\,\psi(k) - A(i)\,D^{-1}(ik)\,A(k)$$

$$-\,\omega\bar{\psi}(i)\check{A}(ik)\,\psi(k)\}\,\delta\psi\,\delta\bar{\psi}\,\delta A$$

$$\times \left(\int \exp\{-\psi(i)\,S^{-1}(ik)\,\psi(k)\}\,\delta\psi\,\delta\bar{\psi}\right)^{-1},$$

where

$$A_{\alpha\beta}(ik) = \gamma_\mu^{\alpha\beta}\,A_\mu(i)\,\delta_{ik}\,\eta_{\alpha\beta}.$$

Equation (20) is the expression for S_{vac} in quantum electrodynamics in the form of a continuous integral. Equation (20) can also be put in the form

$$S_{\mathrm{vac}} = \frac{\left\{\int \exp\left[i\int L(x,\psi,A)\,dx\right]\delta\psi\,\delta\bar{\psi}\,\delta A\right\}}{\left\{\exp\left[i\int L_0(x,\psi,A)\,dx\right]\delta\psi\,\delta\bar{\psi}\,\delta A\right\}} \tag{21}$$

where L is a Lagrange function depending on spinor field functions with no field interaction term ****.

In Eq. (20) the integration with respect to one of the fields can be carried out. The integration with respect to the electron field functions is carried out as follows:

$$S_{\mathrm{vac}} = \frac{1}{\pi^{N/2}\sqrt{\mathrm{Det}\,D_{\mu\nu}}}\;\frac{\alpha^N}{\mathrm{Det}\left|\,\delta_{ik} + \frac{1}{\alpha}S^{-1}(ik)\right|} \tag{22}$$

$$\times \int \mathrm{Det}\left|\,\delta_{ik} + \frac{1}{\alpha}S^{-1}(ik) + \frac{1}{\alpha}A(ik)\,\omega\right|$$

$$\times \frac{1}{\alpha^N}\exp(-A(i)\,D^{-1}(ik)\,A(k))\,\delta A.$$

From this we finally get[5]

$$S_{\mathrm{vac}} = \frac{1}{\pi^{N/2}\sqrt{\mathrm{Det}\,D_{\mu\nu}}}\exp\{\mathrm{Sp}\,\lg|\,\delta_{ik} \tag{23}$$

$$+\,\omega S(ik)\,\gamma_\mu\,A_\mu(k)\,|\,\}$$

$$\times(-A(i)\,D(ik)\,A(k))\,\delta A.$$

The integration in Eq. (20) can likewise be carried out with respect to the photon field functions. Equations analogous to Eq. (20) can be easily derived for Green's functions in any problem. Thus, for the one electron problem, according to Eq. (1),

$$G(l,m) = \frac{1}{\pi^{N/2}\sqrt{\mathrm{Det}\,D_{\mu\nu}}}\int \bar{\psi}(l)\,\psi(m)\,\eta_{lm} \tag{24}$$

$$\times \exp\{-\bar{\psi}(i)\,\check{S}^{-1}(ik)\,\psi(k) - A(i)\,D^{-1}(ik)\,A(k)$$

$$-\,\psi(i)\,\check{A}(ik)\,\psi(k)\,\omega\}\,\delta\psi\,\delta\bar{\psi}\,\delta A$$

$$\times \left(\int \exp\{-\psi(i)\,S^{-1}(ik)\,\psi(k)\}\,\delta\psi\,\delta\bar{\psi}\right)^{-1} S_{\mathrm{vac}}^{-1}$$

Here S_{vac} is given by Eq. (20). By simple differentiation, one arrives at the following expression

$$G(ik) = S(ik) - \frac{\delta}{\delta S^{-1}(ik)}\,\lg S_{\mathrm{vac}}. \tag{25}$$

In taking the functional derivative with respect to $S^{-1}(ik)$, S_{vac} is considered a functional of $S^{-1}(ik)$. After differentiation, the quantities $S^{-1}(ik)$ take on the given values (see Anderson[4]).

In conclusion, I express my gratitude to Acad. L. D. Landau and B. L. Ioffe for participation in the investigation of this question.

---

* This representation in the case of a Bose field was first derived by Gel'fand and Minlos[2].

** For simplicity, the spinor indices are suppressed and included in the indices i and k.

*** An exception is the case when the corresponding indices in two η_{ik} coincide; such η_{ik} anticommute. As will be shown in the following, however, this situation cannot be ignored, since terms containing combinations of identical operators drop out on integration.

**** An equation of the form (21) was discussed in the literature[2] by analogy with the corresponding formula for a Bose field. In the present case, on account of the anticommutation of the spinors, such an analogy is not valid.

[1] G. Wick, Phys. Rev. **80**, 268 (1950)

[2] I. Gel'fand and R. Minlos, Dokl. Akad. Nauk SSSR **97**, 209 (1954)

[3] S. Hori, Progr. Theor. Phys. **7**, 578 (1952)

[4] J. Anderson, Phys. Rev. **94**, 703 (1954)

[5] M. Neuman, Phys. Rev. **83**, 1258 (1951)

Translated by E. L. Saletan
115

Gas Bubble Chamber -- A Possible Recorder of the Elementary Act of Interaction of Ionizing Radiation with Matter*

G. A. ASKAR'IAN
Moscow

(Submitted to JETP editor October 6, 1954)
J. Exper. Theoret. Phys. USSR **28**, 636 (May, 1955)

THE experimentally sucessful[1,2] attempt to record the tracks of ionizing particles in superheated liquid do not exhaust all possibilities of using the bubbles formed along the track to detect the tracks in the liquid. For example, it is possible to record the tracks of ionizing particles by using a supersaturated solution of gas in the liquid: the instantaneous supersaturation produced by the rapid decrease in gas pressure over the surface of the liquid makes the liquid with the gas dissolved in it internally unstable with respect to the formation of centers for the new phase, namely gas bubbles. The passage of the ionizing particle, causing accumulation of ion centers along the track, local heating of the liquid and break-up of the molecules will contribute to the formation of center volumes inside the liquid and convert them into gas bubbles, which produce the track image (a leading role in the initial stage of formation of the volume is played apparently by the initiating repulsion eruption) of closely located molecular complexes of equal charge, gathered by the ions produced by the ionizing particles. The dead time of the work and the diffusion inertia of the growth of the bubble in the "gas" bubble chamber, associated with the local "impoverishment" of the solution can apparently be reduced considerably by selecting the proper operating conditions and using mixture components having a higher mutual solubility (physical or chemical solution of gas in liquid).

The thermodynamic working conditions of the "gas" bubble chamber are more suitable than the thermodynamic working conditions of the "vapor" bubble chamber: "gas" operating conditions do not require that the liquid be heated to increase its vapor pressure, and the use of these conditions will apparently be advantageous for liquid with low surface tension at those temperatures for which the saturated-vapor pressure of the liquid is insufficient to break away center volumes.

The temperature diffusivity of the "gas" working conditions for the bubble chamber and the possibility of independently varying the components of the working mixture, apparently facilitate the transition to large effective working volumes and to the optimum working mixture.

If the idea of "gas" bubble chamber can be put into practice, it will contribute to the creation of a universal, stable and simple instrument for recording the elementary act of interaction of highly-penetrating radiation with matter.

---

* Author's own summary of a report prepared in 1953 at the Institute for Physical Chemistry of the Academy of Sciences, USSR.

[1] D. Glaser, Phys. Rev. **91**, 762 (1953)

[2] D. Glaser, Nuovo Cim. Suppl. **11**, 2 (1954)

Translated by J. G. Adashko
116

On the Problem of the Negative π-meson Decays

V. I. GOL'DANSKII AND M. I. PODGORETSKII
P. N. Lebedev Institute of Physics,
Academy of Sciences, USSR

(Submitted to JETP editor January 22, 1955)
J. Exper. Theoret. Phys. USSR **28**, 620 (May, 1955)

1. IT is reported[1] that when photographic emulsions were exposed to slow negative π-mesons, 18 π-μ meson decays were observed among 40,000 meson track endings. Convincing arguments are cited to show that it is a question of π-meson decays and not some concomitant background event.

The observed events[1] are characterized by the presence of an appreciable energy distribution spread of μ mesons from $\pi\mu$-decays ($\delta E_\rho \approx 0.5$ Mev), which indicates the motion of π mesons at the instant of their $\pi\mu$ decays. The kinetic energy of the π mesons was estimated to be several tens of Kev[1]. Because of the extremely small stopping time of such π mesons, the author[1] concludes that the observed $\pi\mu$-decay events did not take place "in flight", but after formation of mesonic atoms. If this conclusion is correct, then some very interesting deductions follow from it, to which we wish to draw attention in this note.

2. The energy distribution of μ mesons, produced during the π-meson decays which become part of the mesonic atoms, can be calculated with sufficient accuracy by the method analogous to that used by Podgoretskii and Rosental[2]. This distribution for the K-shells of light nuclei which are a part of the emulsion (C,N,O) agrees within the limits of statistical error with the experimental results. One cannot exclude also the decay of the π meson while it is on the L and M shells of these nuclei. However, while it is on these shells, the π meson must make a transition to the K-shell. The duration of the transition to the K shell does not exceed $\sim 10^{-13}$ sec even for the N-shell of C,N,O. The probability of the π-μ decay during this time is only 5×10^{-6}. If one assumes that the decay of π mesons takes place in the mesonic atoms of the heavy emulsion components (Ag, Br), then the observed energy distribution of μ mesons corresponds to μ meson decays on shells with a principal quantum number $n = 10-15$. Simple calculations show that in this case also the duration of transitions to the K shells does not exceed $\sim 10^{-13}$sec. It is necessary to conclude that the observed[1] π-μ decay of negative π mesons took place in the K-shell of the light mesonic atom of (C,N,O) nuclei, which is clear from the known energy distribution of μ-mesons on the K- shell of mesonic atoms with light nuclei.

3. Such a conclusion strongly contradicts modern conceptions about the properties of π mesons. Since about one half of the π mesons which stop in the emulsion are captured by the coulomb field of light nuclei, then it follows from reference 1 that the probability of a π meson decay is $\sim 10^{-3}$. Beginning with the generally accepted value of the π meson lifetime ($\sim 10^{-8}$ sec), we get a value of $\tau \sim 10^{-11}$ sec for the lifetime in relation to the nuclear capture of a π meson from the K shell of light nuclei. Meanwhile, theoretical estimates of τ, even for hydrogen and deuterium, give $\sim 10^{-15} - 10^{-16}$ sec (see, for example, reference 3), whereas for C,N,O one can expect a decrease in τ by several orders of magnitude[4,5].

Thus, the problem of verifying and refining the observations [1] becomes interesting in order to ascertain whether or not the above mentioned contradiction might not be explained by incorrect experimental data.

Note added in proof: Investigations appeared very recently[6] which reveal the shift of π meson K-levels in light mesonic atoms, indicating an effective repulsion of π mesons by nuclei. The connection between these facts and the results in reference 1 are not excluded.

[1] W. Fry and R. George, Phys. Rev. 93, 1427 (1954)

[2] M. I. Podgoretskii and I. L. Rosental', J. Exper. Theoret. Phys. USSR 27, 129 (1954)

[3] R. F. Marshak, Revs. Mod. Phys. 23, 137 (1951)

[4] K. Aidzu, Y. Fujimoto, H. Fukuda, S. Hayakawa, K. Takayanagi, G. Takeda, Y. Yamaguchi, Progr. Theor. Phys. 5, 931 (1950)

[5] J. Wheeler, Revs. Mod. Phys. 21, 133 (1949)

[6] M. Stearns, et al, Phys. Rev. 96, 804 (1954); 97, 240 (1955)

Translated by H. Kruglak
108

Measurement of the Absorption Coefficient of High Energy Nuclear Interacting Particles

K. P. RYZHKOVA AND L. I. SARYCHEVA
P. N. Lebedev Institute of Physics,
Academy of Sciences, USSR.

(Submitted to JETP editor February 5, 1955)
J. Exper. Theoret. Phys. USSR **28**, 618-619 (May, 1955)

AT the present time the problem of the collision mechanism of high energy nuclear interacting particles is of considerable interest. The data on the elementary act of high energy particle interactions can be obtained by investigating the dependence of the absorption coefficient of such particles on their energy[1]. The pertinent measurements were made by us during fall of 1952 at two elevations: 3860 m (Pamir) and at sea level (Moscow) with identical hodoscopic setups.

In order to obtain a sufficient amount of statistical data for the registration of high energy nuclear interacting particles a detector of large area was used. Its cross section is shown in the Figure. A layer of lead 3×2.5 m^2 in area and 8 cm thick, supported on flooring covered with iron (total thickness ~ 7 gm/cm^2), was placed over a rectangular pit with a 2.5×2 m^2 bottom area and 2.5 m deep. Under this lead layer and at 30 cm from its lower surface another 2 cm lead layer was placed. These lead filters absorbed the electron-photon component of cosmic radiation incident on the apparatus from

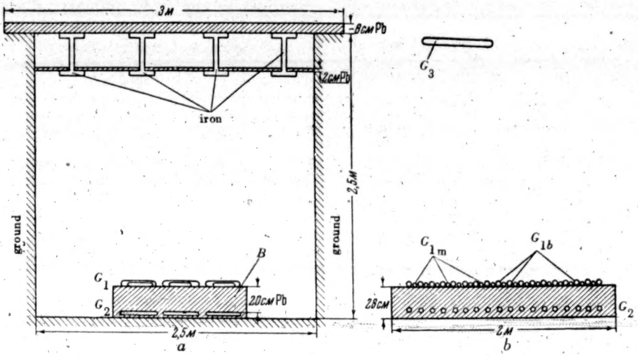

the atmosphere; in them electron-nuclear showers were produced by the nuclear interacting particles. In the center of the pit's bottom a lead block B (see drawing b) with a 2 × 1.2 m^2 base was located, with three layers of counters spaced uniformly over the entire surface; the area of each counter was 100 cm^2 (54 counters labeled G_{1b}) and 24 cm^2 (54 counters labeled G_{1m}). Inside of this lead block there were narrow cylindrical channels into which were placed counters G_2 of 100 cm^2 in area; their arrangement was similar to that of counters G_{1b} . The lead thickness between two adjacent counters was 4 cm, 20 cm above the counters and 4 cm below them. At the ground level at a distance of 1 m from the lead's edge there was placed a box G_3 with 10 counters each 330 cm^2 in area. All the mentioned counters were connected in the hodoscope according to Korablev's scheme[2]

Thus we had essentially three different groups of counters G_1, G_2, G_3 . The counters of group G_1 (G_{1b} and G_{1m}) registered the intensity of the electronic component of the showers, generated by the nuclear interacting particles in the lead above the pit. Counters G_2 registered the penetrating particles in the showers. The counter G_3 gave information about the passage of a wide atmospheric shower. The operation of the hodoscope was effected by the coincidence of not less than three counters of group G_{1b} and two counters of group G_2 . Thus, the registered shower consists of at least three particles, two of which had to be of the penetrating type.

All the recorded showers were subdivided into various energy groups according to the number of strongly penetrating and strongly absorbed particles. The results shown in Table 1 refer to the selection of showers according to the number of penetrating particles. Showers with a greater number of penetrating particles also had the greater intensity of strongly absorbed particles. Consequently, the distribution of showers according to the number of strongly absorbed particles gave the same results as the subdivision in relation to the number of penetrating particles.

If one takes as a value $\gamma = 1.6$ for the index of the energy spectrum of nuclear interacting particles which produce recorded showers, then it follows from the data of Table 1 that the relationship of the number of recorded events pertaining to the extreme energy groups corresponds, to at least a ten-fold difference in the energy of particles producing these showers.

The absolute values of the energies of shower-producing particles were calculated by two independent methods: (1) by extrapolating the number of nuclear interacting particles from 3860 m to the top of the atmosphere and making a comparison with the intensity of the primary component of the cosmic radiation, and (2) according to the number of strongly absorbed particles, apparently electrons, in electron-nuclear showers. Both methods gave the same order of magnitude for the energy of generating particles. Thus, the energies for the nuclear interacting particles producing showers, when referred by us to the extreme energy groups, were $E_{\mathrm{I}} \sim 10^{11}$ eV and $E_{\mathrm{V}} \sim 10^{12}$ eV respectively.

Assuming that the flux of nuclear interacting particles is absorbed with atmospheric depth x according to the law $I_2 = I_1 \exp\{-x/\lambda_{\mathrm{exp}}\}$ we determined from the data of Table 1 the absorption mean free path of these particles $\lambda_{\mathrm{exp}} = x / \ln$

TABLE I

No. of the energy group	No. of coincidence counters in group G_2	At sea level: Time of operation (hours)	At sea level: Total number of events	At sea level: Number of events per hour	3860 m: Time of operation (hours)	3860 m: Total number of events	3860 m: Number of events per hour
I	2; 3	217,8	389	1.79 ± 0.09	156,6	6823	43.57 ± 0.53
II	4; 5		171	0.79 ± 0.06		3169	20.24 ± 0.36
III	6; 7		102	0.26 ± 0.03		1061	6.78 ± 0.21
IV	8; 9	389.6	26	$0,067\pm0.013$		327	2.09 ± 0.12
V	$\geqslant 10$		18	$0,049\pm0.011$		269	1.72 ± 0.11
VI	$\geqslant 10 + \geqq 20 \text{ в } \vec{G}_{1m}$		10	0.026 ± 0.009		153	0.977 ± 0.08

TABLE II

No. of energy groups	I	II	III	IV	V	VI
$\lambda_{\text{exper.}}$	115 ± 2	113 ± 3	113 ± 3	107 ± 6	109 ± 7	100 ± 9
λ_1	131 ± 3	128 ± 4	128 ± 4	120 ± 7	116 ± 9	112 ± 11

where I_1 is the intensity at 3860 m, I_2 that at sea level, and x the air depth in gm/cm^2 between these altitudes. The results are shown in Table 2 .

In the second line of Table 2 are shown the values of the absorption mean free paths of nuclear interacting particles coming in vertically, corrected for the geometry of the apparatus. Our values for the absorption mean free path in air of nuclear interacting particles of 10^{12} eV energy agree well with the data of reference 3, in which for particles of the same energy in the upper half of the atmosphere the obtained value was $\lambda \sim 120$ gm/cm^2.

From our data and the data of other writers it is seen that absorption mean free path of the nuclear interacting flux with an energy interval $10^{10} - 10^{12}$ eV does not vary significantly, exceeding by about a factor of two the value of the interaction path which corresponds to the geometrical nuclear cross section for particles of such energies. Using the relationship of reference 1, $\lambda_0 = \lambda(1 - \Delta)$, where λ_0 is the mean free path of the interaction of nuclear particles and Δ is the effective number of secondary nuclear interacting particles, it is possible to conclude that, in collisions of nucleons with the nuclei of light elements, the energy of the incident nucleon is distributed non-uniformly among the secondary nucleons. Apparently the mechanism of collision is such that more than half of this energy is concentrated in one of these particles.

The writers express their thanks to G. T. Zatsepin who offered to carry out the described measurements, to N. A. Dobrotin who made a number of valuable suggestions, and to S. A. Azinov for his interest in the investigation.

The following students also participated in the investigation: V. Guzhavin, V. Gusynin, P. Karimov, P. Nadyrshin, M. Ovsiankin, and A. Prokoshev.

---

[1] G. T. Zatsepin, J. Exper. Theoret. Phys. USSR **19**, 1104 (1949)

[2] L. N. Korablev, Dokl. Akad. Nauk SSSR **69**, 643 (1949)

[3] M. F. Kaplon, J. Z. Klose, D. M. Ritson and W. D. Walker, Phys. Rev. **91**, 1573 (1953)

Translated by H. Kruglak
107

Possible Application of Pulsed Multiplier Image-Converters for Recording Tracks of Ionizing Particles in Luminescent Media *

G. A. Askar'ian
Moscow

(Submitted to JETP editor December 24, 1954)
J. Exper. Theoret. Phys. USSR 28, 626-627 (May, 1955)

ADVANCES in the use of scintillation counters in experimental nuclear physics indicate the feasibility of developing an electron-optical device for recording elementary interaction-events. For an appraisal of the possibilities and requirements of such a scheme, we shall consider one of the most promising methods by which a detector of this type may be realized.

The basic part of the detector is a magnetically focused, pulsed, image converter of special construction, designed for the intensification of the luminous image of the tracks of particles in a luminescent phosphor, which has a semitransparent photocathode, a series (~ 10) of close-lying dynodes consisting of fine-mesh grids, a supplementary grid for control of the tube, an accelerating anode, and a fluorescent screen located behind the anode. The tube is controlled by a modulator -- a device employing well-known electronic techniques -- which increases the voltage on the control grid to allow the passage of the avalanche associated with the electron image. The modulator is operated by a pulse from a counter which detects the passage of particles through the luminescent phosphor (automatic operation) or is arranged to trigger the tube in synchronism with the bursts of a pulsed beam of particles (semi-automatic operation).

The fluorescent track of an ionizing particle in a luminescent phosphor having a short decay-time (a large luminescent crystal or a layer of luminescent liquid or plastic) is projected on the photocathode of the image converter by an optical system, thus producing an electronic image of the projection of the track because of the photoeffect across the "gap". As this image travels along the length of the tube, it is multiplied in passing through the system of apertured dynodes (grids or perforated foils) having small dimensions ($\leq 10^{-2}$ cm) and passes into the accelerating region due to the action of the control grid, the potential of which has been raised by the operation of the modulator. The electron avalanche then passes through the accelerating anode (made up in the form of a grid or perforated metal layer) and having been accelerated by a voltage of some tens of kilovolts, strikes the fluorescent screen, producing an intense luminous image which is a reproduction of the projection of the track and which can be recorded photographically or observed visually.

The possibility of photo-recording can be seen from the following calculation: the projected charge density of the electronic image of the track after multiplication is $q = \nu \alpha_1 \alpha_2 K (1/\Delta)$ where ν is the number of fluorescent photons per unit length of track excited by a singly-charged relativistic particle in the luminescent phosphor ($\nu = 3 \times 10^4$ in good luminescent phosphors); α_1 is the efficiency of the optical system used to project the fluorescent light on the photocathode (for simplicity we take $\alpha \approx 1\%$, thus obtaining an image scale equal to unity); α_2 is the quantum yield of the semitransparent photocathode (we assume $\alpha_2 \sim 10\%$); K is the multiplication factor associated with the electron avalanche. We may take $K \sim 10^6$, assuming that the magnetic focusing field does not reduce the multiplication efficiency of the mesh dynodes. For focusing fields of the order of hundreds of gauss, this assumption is justified provided that the grids have small dimensions, for example, $\sim 10^{-2}$ cm. (In ordinary mesh multipliers, grids having 40 thousand mesh per cm^2 are used.) The quantity Δ is the width of the trace of the electron image after multiplication. In the case of cascade magnetic focusing, $\Delta \approx 2\, lN (u/U)$, where l and U are the spacing and potential differences between adjacent dynodes, N is the number of dynodes and u is the potential which corresponds to that part of the secondary-emission energy distribution curve which applies to the electrons being considered. For $lN = 3$ cm, $U \approx 150$ v and $u \approx 5$ v, $\Delta \approx 0.2$ cm.

For the assumed values, we get $q \approx 1.5 \times 10^8$ electrons/cm^2 or 24 $\mu\mu$ coulombs/cm^2. This charge density is entirely adequate for contact photography if the accelerating voltage of the electrons striking the screen is of the order of 15 kv (for example, using an Agfa-Isochrome plate and a ZnS-Ag fluorescent screen, the blackening of the plate $S \approx 0.2$ for the values of charge density and accelerating which we have indicated)[1]. There is some possibility of increasing the conversion coefficients so as to allow non-contact photography.

The possibility of automatic control of the tube is determined by the relation between the delay time in the modulator and the emission time, and the time of flight of the electrons from the photocathode to the region in which the control grid is effective. With a favorable arrangement of the tube electrodes, a minimum transit time $\sim 10^{-8}$

sec is possible; the time required for the operation of the modulator is $\sim 3 \times 10^{-8}$ sec.

These figures clearly indicate the advantage of using image converters with localized mesh-dynodes which make possible the combination of fast image-electron accumulation at the anode, easily controlled resolving power at the output, and practically complete freedom from spurious scintillations on the output fluorescent screen for large values of the multiplication factor (down to $K \sim 10^9$). These features permit ultrafast photographic recording (during the accelerating pulse which may last for a time of several milliseconds) of developments in unusual processes under conditions of high noise and radiation backgrounds and they justify certain technical difficulties in the fabrication of fine-mesh dynodes of large dimensions (areas of 300 cm^2). Mesh tubes have the advantages of speed of operation, ease of control and reduction of noise as compared with multiple conversion tubes (for example, the tandem cascade tube due to Holst[2]) in which the intensification of the electronic image is accomplished at the expense of a long overall delay due to the delays (for luminescent phosphors suitable for use in vacuum devices) connected with the emission in the intermediate fluorescent screens.

Some general shortcomings of electron-optical detectors should be noted; the existence of distortions connected with the electron-optical conversions, the variations in the localized conversion parameters, the need for continual localized calibration of the apparatus if it is used for comparative measurements, the difficulty in obtaining stereoptic pictures of the tracks -- all these are substantial obstacles to the reproduction of an accurate picture of the interaction process. However, the inherent positive features of luminescent-electronic detection of elementary events -- the high detection efficiency, the high resolving power, the inertialess operation, the small dead time in detection, the comparative simplicity of transmitting the electronic image of the track and the ease of synchronous operation with a pulsed source of ionizing radiation indicate that this instrument may become a powerful experimental tool in cases where the reconstruction of a qualitative picture of an elementary process is needed in the search for new types of reactions.

Note *added in proof:* in a paper which appeared recently[3] there was reported the sucessful application of the idea of using an image converter for recording tracks of ionizing particles; however, no information was given concerning the image-converter which was used.

* This note is based on a thesis submitted to the physics faculty of Moscow State University by the writer in 1951.

[1] I. S. Stekol'nikov, *The Electron Oscillograph*, State Electronics Press, 1949, p. 112 and 115

[2] Brüche and Recknagel, *Electronic Apparatus*, (translated from German), State Electronics Press, 1949, p. 447 and 458

[3] E. K. Zavoiskii et al, Dokl. Akad. Nauk SSSR **100**, 241 (1955)

Translated by H. Lashinsky
111

High Threshold Scintillation Neutron Detector

P. S. BARANOV AND V. I. GOL'DANSKII
P. N. Lebedev Institute of Physics,
Academy of Sciences, USSR

(Submitted to JETP editor January 25, 1955)
J. Exper. Theoret. Phys. USSR **28**, 621-623(May, 1955)

AT the present time, most existing methods for detecting high energy neutrons (threshold detectors, the observation of the proton recoils) are characterized by a low efficiency-approximately 10^{-4} to 10^{-3} . Only in the last few years have scintillation liquids of large volume been used, permitting the detection of neutrons by proton recoils with an efficiency as high as 10%. However, these counters have a rather high sensitivity for undesirable background (for example, a γ-ray background). The methods using them and in particular the analysis of the results are rather complicated. In connection with these there is presented an interesting possibility of developing a simple and sufficiently efficient detector of high energy neutrons. In principle, the operation of this detector can be expressed by the reaction $C^{12}(n, 2n)C^{11}$, with a threshold at 20.2 Mev. A positron-emitting isotope, C^{11}, is formed, with a half-life of 20.2 min, and with the maximum energy of the β^+- spectrum being about 1 Mev. If ordinary graphite detectors whose activity is detected by means of a Geiger counter are used for observing this reaction, then the sensitive operating thickness of the detector is limited by the range in graphite of the positrons from the decay of C^{11}. This range is approximately equal to 300 microns. If the carbon which is activated by the high energy neutrons is a chemical constituent of an organic phosphor, and if the decay is detected by the subsequent light flashes in the phosphor, then it is possible to increase the sensitive operating thickness of the detector by factors of

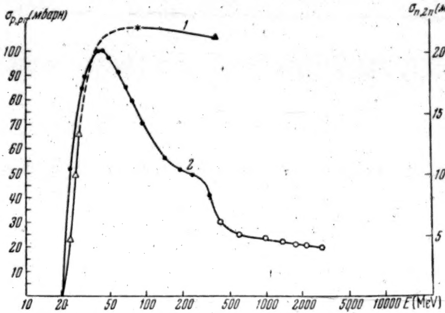

FIG. 1. 1–$C^{12}(n,2n)C^{11}$; 2–$C^{12}(p,pn)C^{11}$ from the data*-ref. 1, ▲-ref 2, Δ-ref. 3, ●-ref. 4, O-ref 5.

ten and one hundred. The reaction $C^{12}(n,2n)C^{11}$ was mainly used as a detector of high energy neutrons because the cross-section of the reaction remains practically constant in the neutron energy interval from 90 Mev (22×10^{-27} cm^2) [1] to 380 Mev (21.4×10^{-27}cm^2) [2]. In Fig. 1 is shown the excitation function for the reaction $C^{12}(n,2n)C^{11}$ (from the data of references 1-5), and for the similar reaction $C^{12}(p,pn)C^{11}$ up to proton energies of 3 Bev (from the data of references 4,5). From Fig. 1 it is obvious that with the aid of a detector, detecting the positrons from the decay of C^{11}, it would be possible to investigate both neutrons and protons with almost identical sensitivity over an extremely wide energy interval.

Use has been reported in the literature[6] of a scintillation detector (anthracene) in which the flashes of light from the decay of C^{11} were detected, but no definite description of the method was given. In the meantime, the usefulness of an organic crystal for observing the decay of C^{11} is in itself obvious; but the main practical difficulty of this method is the inability of obtaining the needed data with a minimum of unwanted background. Since most of the positrons from the decay of C^{11} have energies of about 100 kev, the noise arising from the photomultiplier (PM) was a hinderance. From the two widely used methods of decreasing the noise of a photomultiplier – strongly cooling the photomultiplier or using a coincidence scheme, which only detects those pulses in coincidence – we chose the latter for its simplicity and directness.

A block-diagram of the layout is shown in Fig. 2. A crystal phosphor (stilbene or tolan) in cylindrical form, 35 mm in diameter and 17-20 mm in thickness (weighing 18-24 gm), is placed between two photomultipliers, PM-19, close to their photocathodes. Pulses formed by the photomultiplier ($RC \approx 6 \times 10^{-8}$ sec) were passed through a cathode follower, were shaped by a shorted line, and were fed into a coincidence unit. The resolving time of the coincidence method is $\tau = 1.6 \times 10^{-8}$ sec for the case when the efficiency of the system is 50% for the detection of positrons from the decay of C^{11} in tolan. The absolute efficiency for detecting the decay of C^{11} was determined by comparing the activity of the crystal with the activity of an identically irradiated standard graphite detector. In an independent experiment, the ratio of the operating efficiency and the total mass has been determined. For the case of a high energy neutron field, $n = 20$ neutrons/cm^2 sec, a tolan crystal produces, for a 20 minute irradiation, an activity equal to ~ 0.1 sec^{-1}. The problem concerning the exactness of the measurement in detecting such a small neutron flux is affected by the detector's dependence on the value of the background and is approximately given by the tolerance dose of the neutrons.

Under the conditions of our experiment, the background of chance coincidences of the noise pulses was negligibly small (~ 0.005 sec^{-1}). It was assumed that the largest source of background counts was due to cosmic radiation and radioactive contamination (~ 0.7 sec^{-1}). The background

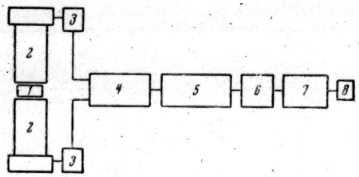

FIG. 2. Block diagram of the circuitry. *1* crystal; *2* PM-19; *3* cathode follower; *4* coincidence unit; *5* amplifier; *6* discriminator; *7* electronic counter; *8* mechanical counter.

coming from cosmic rays can at least partly be removed by placing over the scintillation detector a layer of Geiger tubes connected in anticoincidence. Experiments have shown, however, that the presence of a background from other sources is approximately equal to 0.7 $\sec^{-1}$ when the PM has 1500 volts applied to it. The background sharply increases when the voltage is increased. While the background of cosmic and radioactive origin was removed on removing the crystal, on the other hand, another source of background was increased.

This additional background was completely removed by any thick opaque screen (aluminum foil, black paper), between the photocathodes of the two photomultipliers. In such a manner, the presence of coincidence background due to "optical coupling" was removed. By using the photomultiplier scheme PM-19-P (with "new surface") the effect (of optical coupling) showed up only in a very insignificant degree even with voltage supply of the photomultiplier, insuring an almost 100% efficiency for detecting the positrons from the decay of C^{11}.

In the experimental arrangement cited above, for a neutron flux $\pi = 20$ neutrons /cm^2 sec, the effective quantity in the phosphor was the 10 gm of carbon. Even for a background counting rate of ~ 1.4 $\sec^{-1}$ (i.e., without correcting for cosmic-ray background and "optical coupling" of the PM) the above indicated value of high energy neutron flux can be determined with an accuracy of 45% (for a 20 min exposure of the crystal and with optimum time for observing the decay of C^{11}, equal in this case to $\sim$ 38 min). Yet, even without additional improvement, the above described detector can be used as a dosimeter of high energy neutrons. We used this detector for observing the yield and angular scattering of high energy photoneutrons from various nuclei. In the general case, the accuracy of the measurement of the high energy neutron flux π by means of a crystal, in which N_{eff} carbon nuclei perform efficiently, is determined by the relationship

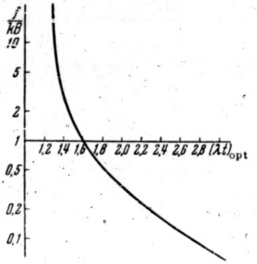

FIG. 3. Curve for determining the optimum length of time for observing the decay of C^{11}

$$\delta = \sqrt{ft + A(1-e^{-\lambda t})} \quad A(1-e^{-\lambda t}), \tag{1}$$

where $f(\sec^{-1})$ is the background counting rate, λ, is the decay constant for C^{11}, t is the length of time for measuring the decay,

$$A = \frac{k}{\lambda} B = \frac{k}{\lambda}(1-e^{-\lambda\tau}), \qquad k = \Pi N_{\text{эфф}}\sigma_{n,2n} e^{-\lambda T} \tag{2}$$

and τ is the length of time of the exposure, and T is the interval of time from the exposure until the beginning of the counting of the decay of C^{11}.

For every given value of f/kB there is an optimum length of time for observing the decay of C^{11}. For determining this quantity see the curve in Fig. 3

A detector for high energy neutrons using the reaction $C^{12}(n,2n)C^{11}$ is sensitive to a γ-ray background only in a relatively narrow range of dipole "resonance" (near 22 Mev) because of the photonuclear reaction $C^{12}(\gamma,n)C^{11}$. The integral cross-section for the whole resonance range (breadth about 10 Mev) consists of about 0.05 Mev-bn[7].

The authors express sincere thanks to A.V. Kutsenko and T. I. Kovalev for valuable aid in preparing the apparatus for our work.

---

[1] E. McMillan and H. York, Phys. Rev. **73**, 262 (1948)

[2] K. O. Oganesian, *Report of the Institute of Technical Nuclear Problem*, Acad. Sci., USSR, 1953

[3] J. Brolley, J. Fowler and L. Schlacks, Phys, Rev. **88**, 618 (1952)

[4] R. Aamodt, V. Peterson and P. Phillips, Phys. Rev. **88**, 739 (1952)

[5] R. Wolfgang and G. Friedlander, Phys. Rev. 96, 190 (1954)

[6] J. Sharpe and G. Stafford, Proc. Phys. Soc. (London) A 64, 211 (1951)

[7] A. Cameron, Phys. Rev. 82, 270 (1951)

Translated by I. B. Berlam
109

Maximum Yield of Photoneutrons and a New Method of Determining the Integral Cross-Section of (γ, n) Reactions for High Energy Photons

V. I. GOL'DANSKII AND V. A. SHKODA-UL'IANOV
P. N. Lebedev Physical Institute

(Submitted to JETP editor January 25, 1955)
J. Exper. Theoret. Phys. USSR 28, 623-626 (May, 1955)

DURING the past year, thanks to the use of the new methods of electron acceleration -- the betatron and the synchrotron -- a wide range of photonuclear reactions, originating under the action of hard bremsstrahlung, was investigated. It was soon established that for a series of photonuclear reactions, the dependence of the cross section on the photon energy was characterized by the presence of a maximum at'the energies in the range 10-25 Mev. The cross section decreased rapidly on both sides of this maximum.

The characteristic resonance character of the excitation function of photonuclear reactions is connected with the excitation in the resonance region of the nuclear dipole oscillations, the theory of which was first given by Migdal[1]. Among the widely investigated photonuclear reactions posessing dipole resonances were reactions producing photoneutrons. In the experiment the following characteristics of the photonuclear reactions were determined: the threshold energy of γ-quanta, E_p, the resonance energy, E_r, as determined by the maximum in the cross section, the half-width of the resonance peak, ΔE, the maximum cross section for the reaction, σ_r, and the integral cross section $\int \sigma(E)\, dE = \sigma_{\text{int}}$. All of these characteristics were determined for independent reactions of the type, (γ, n), (γ, pn), (γ, $2n$). In most of the work these reactions were identified by radioactive isotopes that were produced. By far the smaller amount of work was that in which a neutron detector detected all the neutrons having been emitted by the elements under investigation (for papers or reported work on the production of photoneutrons see references 2, 3). Thus, the yield of photoneutrons in an independent (γ, n) reaction was shown to be similar to the total yield of photoneutrons for the given isotope. From this fact it is possible to conclude that the basic source for the production of photoneutrons, even at high maximum energy of the bremsstrahlung (320 Mev), is the simple (γ, n) reaction.

As a rule, in photonuclear investigations, thin samples have been used as photoneutron sources in which there has been no electro-photon multiplication of the emitted γ-quanta. In our work another goal was set -- the determination of the yield of photoneutrons under the conditions of total development of the electron-photon shower, i.e., the determination of the maximum coefficient for converting photons into neutrons. Thus, the measurements gave, simultaneously, the possibility of determining the integral cross section of the reaction producing the photoneutrons, as well as the possibility of using the equilibrium condition from shower theory[4], i.e., integrating according to the depth of the shower neutron spectrum, produced by the primary γ-quanta with dimensionless energy, ϵ_0 (where $\epsilon_0 = 2.29\, E/\beta$, and β is the critical energy for the given substance):

$$\Gamma_\Gamma(\varepsilon_0, \varepsilon) = (1/\beta\mu(\varepsilon))\,[\chi(\varepsilon_0, \varepsilon)\,\varepsilon_0/\varepsilon + 2{,}29\,\delta(\varepsilon_0 - \varepsilon)].$$

Here

$$\chi(\varepsilon_0, \varepsilon) = \varepsilon e^{\varepsilon} \int_{\varepsilon}^{\varepsilon_0} e^{-x} \frac{dx}{x^2} - \frac{\varepsilon}{\varepsilon_0^2}\,[1 - e^{-(\varepsilon_0 - \varepsilon)}],$$

and the dimensionless cross-section for the absorption of the neutrons is

$$\mu(\varepsilon) = \sigma(E)\, Nt,$$

where N is the density of the substance (in number of nuclei per cm^3), and t is the unit shower length (in cm).

It is obvious that the maximum yield of photoneutrons from an infinite mass of the substance is

$$Q_{\max} = \int_{E_1}^{E_2} \frac{\sigma_{\gamma n}(E)\, dE}{Nt} \int_{\varepsilon_1}^{\varepsilon_m} \Gamma_\Gamma \frac{a\, d\varepsilon_0}{\varepsilon_0},$$

where E_1 and E_2 are the lower and the upper limits of the resonance region, $\sigma_{\gamma n}$ is the photonuclear cross section of the reaction for the formation of photoneutrons, and the emitted spectrum of the bremsstrahlung takes the form $f(\epsilon) = a/\epsilon$ (we note, that for a calculation on the equilibrium spectrum this approximation gives a smaller error than for a direct determination of the cross section in a calculation of this form).

The first integration produces the result

$$Q_{\max} = a \int_{E_1}^{E_2} \frac{\sigma_{\gamma n}(E)\, dE}{\sigma_{\text{absorp}}(E)\, E} \left[1 + \frac{I(\varepsilon)}{2.29}\right],$$

where

$$I(\varepsilon) = \varepsilon_m + \frac{\varepsilon}{\varepsilon_m} - \varepsilon\left(1 + \frac{1}{\varepsilon_m}\right)\exp[-(\varepsilon_m - \varepsilon)]$$

$$+ \varepsilon e^{\varepsilon}(\varepsilon_m + 2)\,[\mathrm{Ei}(-\varepsilon) - \mathrm{Ei}(-\varepsilon_m)].$$

In computing the narrow resonance region, we took out of the integral, the denominator $\overline{\sigma}_{\mathrm{absorp}}(E)\,E_p$, and the multiplier $1 + [I(\epsilon_p)/2.29]$. This is valid for the case when $\epsilon_p \ll \epsilon_m$:

$$I(\varepsilon_p) \approx \varepsilon_m + \varepsilon_p e^{\varepsilon_p}(\varepsilon_m + 2)\,\mathrm{Ei}(-\varepsilon_p).$$

Then

$$Q_{\max} \approx \frac{a}{\sigma_{\mathrm{absorp}} E_p}\left[1 + \frac{I(\varepsilon_p)}{2{,}29}\right]\int_{E_1}^{E_2} \sigma_{\gamma n}(E)\,dE$$

$$= \frac{a\sigma_{\mathrm{int}}}{E_p \sigma_{\mathrm{absorp}}}\left[1 + \frac{I(\varepsilon_p)}{2.29}\right].$$

Experiments for determining the maximum yield of photoneutrons and the integral (γ, n) cross section were performed in June and July of 1951. A beam of bremsstrahlung photons with a maximum energy of 250 Mev passed through a port 10.5 × 10.5 cm into a paraffin block with dimensions of 70 × 70 × 70 cm. In the center of the block were placed photoneutron sources -- cubes of Fe and Cu with dimensions 10 × 10 × 10 cm and samples of Pb and U, 10 × 10 cm^2 in area and of various thicknesses. The flux of γ-rays was determined by means of an integrating chamber. All of the data was obtained with a standard flux equal to $a = 6.5 \times 10^9\ \mathrm{sec}^{-1}$. The yield of photoneutrons was detected by means of an indium detector, wrapped in cadmium. Neutrons near the resonance of the reaction $\mathrm{In}^{115}(n, \gamma)\mathrm{In}^{116}$ with an energy of ~ 1.44 ev were detected. The calibration of the yield of neutrons was made by comparing the area under the slowing-down curve with the result from a standard Ra-Be source ($Q = 1.2 \times 10^7\ \mathrm{sec}^{-1}$) which was placed under the same conditions.

Investigations on the slowing-down curve also permitted the determination of the increase of the photoneutrons moderated to the energy of the indium resonance. This increase was compared to the increase of the moderated Ra-Be neutrons to this same energy. These determinations were made under the following conditions: there was a through port in the paraffin block and there was a lead lining around the Ra-Be source (so that the dimensions and the materials of the neutrons' sources were identical). Knowing the increase of the neutrons, we were able to calculate also the average energy of the photoneutrons, $\overline{E}_n$. Aside from the basic work, measurements of the background were made by means of the activity induced in indium when the blocks -- the source of the photoneutrons -- were removed. Up to a distance of 30-40 cm from the axis of the beam, the background was about 5% of the activity produced by the photoneutrons from lead for $(Q_n)_{\max}$ and did not exceed 20% (of the experiments with Fe). We approximate the precision for determining Q_n as

Neutron Source	Q_n sec^{-1}	τ_n (cm^2)	E_r mev	$\overline{\sigma}_{\mathrm{abs}}$ (bn)	σ_{int} (mev-bn)	$\overline{E}_n$ (Mev)
Ra - Be	1.2×10^7	~ 64				~ 4
Fe	2.4×10^8	~ 40	18.4	3.0	(1.3)	~ 2.1
Cu	4.4×10^8	~ 40	18	3.5	(2.1)	~ 2.1
Pb (1 cm)	2.10^8	~ 35	12.2	18.3		~ 1.9
Pb (2 cm)	3.3×10^8					
Pb (6 cm)	7.3×10^8					
Pb (8 cm)	8.7×10^8					
Pb (10 cm)	10^9					
Pb (19 cm)	$10^9 = Q_{\max}$				5.2	
U* (2 cm)	7.3×10^8	~ 30	11.3	21.4		~ 1.7
U (4 cm)	1.1×10^9					
U (8 cm)	1.5×10^9					
U (12 cm)	$1.6 \times 10^9 = Q_{\max}$				8.2	

* The yield of neutrons from U is corrected for secondary fission photoneutrons.

± 10% (for Pb and U) and ± 20% (for Fe and Cu). The accuracy of determining the integral cross section also depends on the accuracy of the determination of the absolute intensity of the neutron beam, being approximated as ± 10%. For checking this, the yield of neutrons from pure carbon was compared to that from carbon in paraffin. This was done to determine if scattered-unwanted-neutrons would be detected as well as the photoneutrons. The yields were shown to be identical within the limits of error of the measurements, demonstrating the absence of scattered-unwanted-neutrons. In the Table are shown the results of the experiments.

According to the maximum yield of photoneutrons from lead and uranium the determination of the integral cross section for these elements agreed with other data in the literature[2,3].

This agreement is evident from the applicability of the proposed method for determining the integral cross section. The assumption that for uranium $(\sigma_{\gamma n})_{\text{int}} = 92/82\,(\sigma_{\gamma n_{\text{Pb}}})_{\text{int}}$, gives for the photofission of uranium for $\nu_n = 2.5$ the value $(\sigma_{\text{fiss}})_{\text{int}} = (8.2 - 5.8)/2.5 \approx 1$ Mev-bn. The maximum coefficient for converting into photoneutrons of the photons from bremsstrahlung with energies from the threshold of the (γ, n) reaction for lead (6 Mev) to 250 Mev is equal to

$$\alpha_{\gamma n} = Q_{\text{макс}} \Big/ \int\limits_{E_1}^{250\text{MeV}} \frac{a}{E}\, dE \approx 0{,}04.$$

For Fe and Cu the maximum yield of photoneutrons was not determined, because the geometrical conditions of our experiment required the approximation of a point source, and since the dimensions of the blocks were 10 × 10 × 10 cm, only in the case of the heavy nuclei was the electron-photon shower completely developed, and the limiting value of the yield of the neutrons reached. Approximate appraisal of the maximum yield of photoneutrons from Fe and Cu can be made, since certain energy resonances of the (γ, n) reaction, as for Pb and U, do not lie below the critical energy, by assuming that the ratio $Q_n / Q_{\max}$ is identically dependent for all the enumerated elements on the thickness of the block in t-units. Such an approximation gives an integral cross section of 1.3 Mev-bn for iron and 2.1 Mev-bn for copper.

Likewise, measurements of the yield of photoneutrons were made for the light nuclei (C, Al). However, in the cubes of 10 cm thickness in the case of these substances, the electron-photon shower was even less developed. Therefore, there is required the use of the more complicated computation of the shower theory, whose description goes beyond the limits of the present communication.

The method of determining the integral (γ, n)-cross section and the maximum yield of photoneutrons by means of a simple calculation for an equilibrium shower spectrum can certainly be useful, also for the light nuclei. In this case it is necessary to use a block of larger dimensions, determining the number of photoneutrons not by means of a slowing down curve, but by a direct method, i.e., by detecting the photoneutrons being emitted at the various angles by means of a flat boron counter or a fission chamber of U^{235}.

In conclusion, the determination of the maximum yield of photoneutrons by means of developing showers from photons of high energy shows an interesting possibility for calculating the conversion of the electron-photon components of cosmic rays into nucleons.

---

[1] A. B. Migdal, J. Exper. Theoret. Phys. USSR **15**, 81 (1945)

[2] *Problems of Modern Physics* 8, *Photons of large energy and photonuclear reactions,* 1952

[3] *Photonuclear Reactions*, Collection of articles, Moscow, 1953

[4] C. Z. Belen'kii, *The Shower Process in Cosmic Radiation*, State Publishing House, Mos[illegible] 1948

Translated by I. B. Berlam
110

The Fission of Uranium Nuclei Under the Action of Slow Π^- Mesons and High Energy Particles

G. E. BELOVITSKII, T. A. ROMANOVA, L. V. SUKHOV
AND I. M. FRANK
P. N. Lebedev Institute of Physics,
Academy of Sciences, USSR

(Submitted to JETP editor March 9, 1955)
J. Exper. Theoret. Phys. USSR **28**, 729-732 (June, 1955)

IN this work, investigation was made of the fission of uranium nuclei by slow π^- mesons[1,2] by fast neutrons up to 460 mev, and by γ rays up to 250 mev[6]. For the recording of the fission of uranium nuclei, photographic plates were used with an emulsion of 100 μ thick, into which there was introduced uranium acetate[7]. The plates permitted observation of protons up to 30 mev. The irradiation of the plates by slow π^- mesons and fast neutrons was performed in the synchrocyclotron of the Institute for Nuclear Problems, Academy of Sciences, USSR. Irradiation with gamma rays was performed in the synchrotrons of the Institute of Physics, Academy of Sciences, USSR.

Among more than 300 π^- mesons stopped in the emulsion, there were observed 96 π^- mesons which produced fission of uranium nuclei. Out of this total, division into two fragments took place in 81 cases (Fig. 1) and in 15 cases a third fragment was emitted, (Fig. 2). As a rule, the two fragments resulting from the fission fly away in opposite directions. An evaluation of the probability of fission of uranium nuclei under the action of slow π^- mesons results in a value of 0.5, i.e., in approximately 50% of the cases the π^- meson captured by the nucleus causes its fission.

In the plates irradiated with a neutron beam of a uniform energy spectrum up to 460 mev, there were found 309 cases of uranium fission, and among them 69 cases in which the fission was accompanied by the emission of one or more charged particles of long path (Figs. 3 and 4).

Data were also obtained on the fission of uranium by neutrons of maximum energies of 180 mev and also by neutrons of 14 mev. Comparison of the experimental results for the neutrons of the three energy values shows that the number of uranium nuclei fissions which are accompanied by the emission of long path particles increases rapidly with the increase of the energy of the primary neutrons.

On the plates irradiated with γ rays of maximum energy of 250 mev, there were found 2066 cases of fission, and among them 45 cases accompanied by

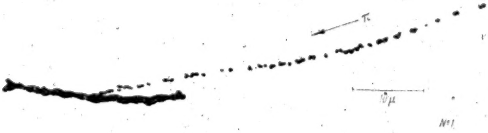

FIG. 1. Fission of a uranium nucleus by a π^- meson into two fragments.

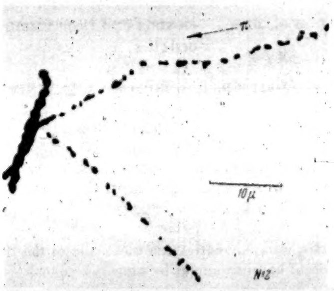

FIG. 2. Fission of a uranium nucleus by a π^- meson accompanied by the emission of a proton of 18 mev energy.

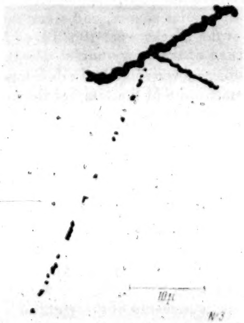

FIG. 3. Fission of a uranium nucleus by a fast neutron accompanied by the emission of a 16 mev proton and an α particle of energy greater than 8 mev.

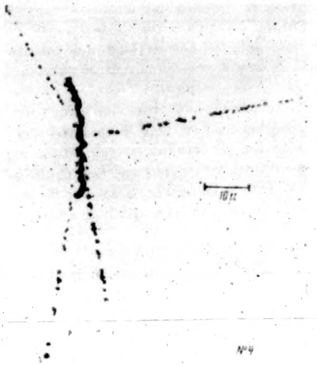

FIG. 4. Fission of a uranium nucleus by a fast neutron accompanied by the emission of 4 protons of 27, 23, 23 and 30 mev.

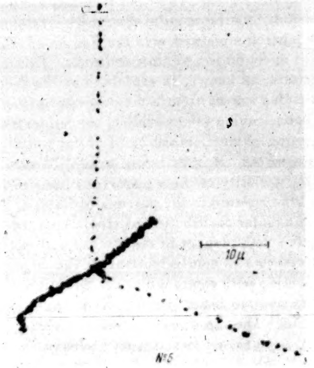

FIG. 5. Fission of a uranium nucleus by a γ quantum up to 250 mev accompanied by the emission of two protons of 11 and 15 mev.

the emission of one or more charged particles of long path (Fig. 5) On the plates irradiated with γ rays of maximum energy of 80 mev, there were found 614 cases of fission and among them three cases accompanied by the emission of a long path particle. Finally, on the plates irradiated with γ rays of energies up to 30 mev, there were found 717 cases of fission, and among them one was accompanied by the emission of an α particle of long path. No emissions of charged particles were observed.

The combined results obtained by us show that fission accompanied by the flight of fast charged particles is actually caused by high energy photons and this permits us to refute the previously prevailing assumption that the effective cross section of fission of uranium nuclei, under the action of γ rays of energy greater than 100 mev, is nearly zero (as is the case for the energy interval 30-100 mev[8]).

This result is confirmed by the data obtained in a recently published work[9], performed with γ rays of energies up to 300 mev.

Multiple paths, i.e., paths of pairs of fragments resulting from uranium nuclei fission under the action of slow π^- mesons, fast neutrons of energies up to 460 mev and γ rays up to 250 mev, fall within the same limits as the paths of the fission fragments under the action of low energy neutrons (several mev), and this agrees with the results of references 10 and 11. It follows that the energy introduced by these agents into the uranium nucleus, as a rule, is not transformed into kinetic energy of the fragments but is spent in other processes.

The comparison of the paths of light and heavy fragments formed in the process of fission by π^- mesons, fast neutrons and gamma rays of high energy** on one hand and slow neutrons on the other, points to the more symmetrical nature of the fission process under the action of high energy particles. Similar results were obtained in recently published works of references 12 and 13.

The majority of the charged particles accompanying the fission of uranium nuclei by the π^- mesons, fast neutrons and high energy γ rays are of a single charge, and are mainly protons (although the possibility is not excluded that a small fraction of these particles are deuterons and tritons), and the remainder, a small number, proved to be α particles. The energy of the protons, evaluated from the measurements of grain density along the trace, lies within the limits 10 to 30 mev. It should be borne in mind that flights of protons of energies greater than 30 mev could not be observed by us because of the limited sensitivity of the plates. The energy of the α particles lies within the limits 14 to 35 mev.

The angular distribution of α particles with respect to the direction of motion of the fragments is anisotropic. Flights at angles close to 90° to the direction of motion of the fragment are predominant. Similar angular distribution is observed for α particles emitted with the fission of uranium nuclei under action of slow neutrons. This characteristic, as known, is explained by the fact that α particles are emitted in the process of fission and upon leaving (the nucleus) are subjected to the action of the Coulomb field of the two departing fragments. It is therefore natural to assume that the majority of the α particles observed by us were also emitted in the process of fission.

The angular distribution of single charged particles with respect to the direction of motion of the fragments is nearly isotropic. The angular distribution with reference to the direction of the primary neutron beam is generally in the forward direction. The direction of emission of the majority of protons forms an angle less than 90° with the direction of the neutron beam.

For fission under the action of high energy photons, the angular distribution of single charged particles with reference to the direction of the incident γ ray beam is characterized by the existence of a maximum angle close to 90°. Such form of angular dependence allows us to make the statement that the majority of the single charged particles accompanying uranium fission are emitted by the uranium nucleus before the process of fission. The absence of isotropic angular distribution of particles of such energy thus indicates that they are basically emitted not in the process of evaporation but are recoil nucleons formed as a result of direct interaction between the primary neutrons, γ quantum or π^- meson with the nucleons in the nucleus, or as a result of a developed cascade process in the nucleus, caused by the primary particle. In this way the emission mechanism of single charged particles accompanying uranium nuclear fission differs substantially from the emission mechanism of the majority of α particles.

We must conclude, on the basis of obtained experimental data, that the special characteristic of the uranium nuclear fission at high excitation energies, is the high probability of emission of fast protons and α particles. These particles carry away only a relatively small portion of the energy received by the uranium nucleus from the primary particle. Since the mean energy of the fragments thereby remains the same as in the case of fission by slow neutrons, it follows that the major part of the energy introduced into the nucleus by π^- mesons, fast neutrons and high energy γ rays, is spent in the emission of neutrons of various energies. A considerable number of these neutrons must be emitted before the fission.

A more detailed communication of results obtained is now in press and will be published in this journal.

In conclusion, we express our thanks to Profs. M. G. Meshcheriakov, G. P. Dzhelepov and E. L. Grigor'ev for the help in carrying out the experiments with the π^- mesons and fast neutrons and to Prof. V. I. Veksler and Iu. S. Ivanov for their cooperation in experiments with high energy γ rays.

---

* The energy spectrum of neutrons from the recharge of 670 mev protons (acting) on beryllium was measured by V. B. Fliagin.

* Fission of uranium by π^- mesons was also investigated independently by Ivanova and Perfilov[3]. References 4 and 5 are also devoted to this problem.

** In cases of fission by fast neutrons and γ rays, the initial point of the flight was taken as the emission point of the fast particle accompanying the fission.

[1] G. E. Belovitskii, L. V. Sukhov, T. A. Romanova and I. M. Frank, Report FIAN (Institute of Physics, Academy of Sciences,USSR), April, 1950

[2] G. E. Belovitskii, L. V. Sukhov, T. A. Romanova and I. M. Frank, Report FIAN (Institute of Physics, Academy of Sciences, USSR), June, 1950; March, 1951

[3] N. A. Perfilov and N. C. Ivanova, J. Exper. Theoret. Phys. USSR **28**, 732 (1955); Soviet Phys. **1**,   (1955)

[4] S. G. Al-Salam, Phys. Rev. **84**, 254 (1951)

[5] W. John and W. Fry., Phys. Rev. **91**, 1234 (1952)

[6] G .E. Belovitskii, L. V. Sukhov and I. M. Frank, Report FIAN (Institute of Physics, Academy of Sciences, USSR), December, 1952

[7] T. A. Romanova and B. E. Belovitskii, Report FIAN (Institute of Physics, Academy of Sciences), June, 1951

[8] G. C. Baldwin and G. S. Kleiber, Phys. Rev. **71**, 3 (1947)

[9] J. Grindler and R. Duffield, Phys. Rev. **94**, 759 (1954)

[10] J. Jungerman and S. Wright, Phys. Rev. **76**, 1112 (1949)

[11] E. Douthett and D. Templeton, Phys. Rev. **94**, 128 (1954)

[12] M. Linder and R. Osborne, Phys. Rev. **94**, 1323 (1954)

[13] R. Schmitt and N. Sugarman, Phys. Rev. **95**, 1260 (1954)

Translated by J. L. Herson
130

Deviations from Mayer's Scheme for Filling Nuclear Shells and the Interaction of Levels

V. A. FILIMONOV
Mariinsko-Posadsk Forestry Technical High School

(Submitted to JETP editor June 26, 1954)
J. Exper. Theoret. Phys. USSR **28**, 753-755 (June, 1955)

THERE are nuclei which do not fit into Mayer's scheme for the filling of shells[1]. These deviations can be explained by making the following assumptions: between similar nucleons which are in neighboring orbital angular momentum quantum number levels and have the same spin orientation with respect to the orbit-namely that for which the total angular momentum j is the largest possible- there exists a strong interaction, leading to the weakening of the coupling between nucleons in the level with the lower angular momentum. The coupling of a pair of nucleons in this level may become weaker than the coupling of a pair of nucleons in higher levels. This phenomenon may be considered as the extraction of a nucleon from the filled level of lower l and the coupling of it to one of the odd nucleons of the higher level.

Consider the first nucleus which deviates from the scheme, ${}_{11}\mathrm{Na}^{23}$. The particles in this nucleus are in the following states: $1s_{1/2}\ 2p_{3/2}\ 2p_{1/2}\ 3d_{5/2}$. The $2p_{3/2}$ and $3d_{5/2}$ levels-satisfy the conditions given above. In the $3d_{5/2}$ level of ${}_{11}\mathrm{Na}^{23}$ there are not less than two particles. They cause a weakening of the coupling between the particles in the $p_{3/2}$ level, resulting in the extraction of a particle from the filled $p_{3/2}$ and the coupling of it to the particles in the $d_{5/2}$ level. The Na nucleus will have the following structure: $1s^{(2)}_{1/2}\ 2p^{(3)}_{3/2}\ 2d^{(2)}_{1/2}\ 3d^{(4)}_{5/2}$. The magnitude of the magnetic moment corroborates the fact that ${}_{11}\mathrm{Na}^{23}$ is in a $p_{3/2}$ state. In shell IV, ${}_{25}\mathrm{Mn}^{55}$ is an exception to the scheme. The following levels enter into the state of the nucleus: $1s_{1/2}\ 2p_{3/2}\ 2p_{1/2}\ 3d_{5/2}\ 3d_{3/2}\ 2s_{1/2}\ 4f_{7/2}$. The $3d_{5/2}$ and $4f_{7/2}$ levels satisfy our conditions. The $4f_{7/2}$ of ${}_{25}\mathrm{Mn}^{55}$ has to be filled by at least two particles; they weaken the coupling between the nucleons in the $3d_{5/2}$ level. As a result, a particle is extracted from the full $3d_{5/2}$ level and is coupled with the particles in the $4f_{7/2}$ level. Thus ${}_{25}\mathrm{Mn}^{55}$ has the following structure:

$$1s^{(2)}_{1/2}2p^{(4)}_{3/2}2p^{(2)}_{1/2}3d^{(5)}_{5/2}3d^{(4)}_{3/2}\ 2s^{(2)}_{1/2}4f^{(6)}_{7/2}.$$

The magnitude of the magnetic moment corroborates the $d_{5/2}$ state of Mn^{55}.

The existence of an unfilled $d_{5/2}$ level together with a filled $d_{3/2}$ level is not inconsistent with spin-orbit coupling, which requires that the $d_{3/2}$ level be filled after the $d_{5/2}$ level is completely full. This requirement is fulfilled when there are no particles in the $4f_{7/2}$ level. With the presence of nucleons in the $4f_{7/2}$ level, however, the energy of a particle in the $d_{5/2}$ level becomes greater than in the $d_{3/2}$ level. These considerations carry over to other appropriate levels also. Especially interesting is the manifestation of this level interaction in shell IV. Here our conditions are satisfied by the $4f_{7/2}$ and $5g_{9/2}$ levels. However, the level interaction does not lead to a nucleus with a ground state spin 7/2, but the excited states have isomers with this spin. The existence of spin 7/2 in the excited states of nuclei with number of particles between 39-49 is difficult to explain in the ordinary shell structure theory. In ${}_{34}\mathrm{Se}^{79}$ the state with spin 7/2 is the ground state. In shell V our conditions are satisfied by the $4g_{9/2}$ and $6h_{11/2}$ levels; as spins of 9/2 do not occur here, we conclude that the extraction of particles from the $g_{9/2}$ level does not occur. The appropriate levels of shell VI are the $6g_{11/2}$ and $7i_{13/2}$ levels. There are few nuclei with unknown spins in this region, and investigating them is difficult.

---

[1] M. I. Korsunskii, Usp. Fiz. Nauk **52**, 1 (1954)

Translated by M. Rosen
141

The Fission of Heavy Nuclei by Slow Mesons

N. A. PERFILOV AND N. S. IVANOVA
Radium Institute of the Academy of Sciences, USSR

(Submitted to JETP editor March 19, 1955)
J. Exper. Theoret. Phys. USSR **28**, 732-734 (June, 1955)

IN this letter, there are briefly described the results of work during 1950-1952 on fission of heavy nuclei as a result of interaction with slow π^- mesons. The results are presented in reports of RIAN (Radium Institute of the Academy of Sciences, USSR)[1-5]. A detailed account of this work will be published in JETP.

Thick layer photographic plates with nuclei of uranium, lead and wolfram introduced into the photo-sensitive layer were irradiated by slow π^- mesons. After development the plates were examined under a microscope. Upon examination of the plates, there were observed shatterings of nuclei by the mesons, with the formation of stars in cases of fission. Events were considered as fission if at the end of the meson trace, there were observed two approximately oppositely directed traces of multiple charge particles of the type of fragments resulting from uranium fission by slow neutrons. Cases of fission were observed resulting from capture of slow π^- mesons by nuclei of uranium, lead and wolfram*.

As it turned out, the probability of fission of wolfram as a result of capture of slow π^- mesons is very small[7]. Basic investigations were made of the interaction between slow π^- mesons and uranium nuclei. There were observed 356 cases of such fission, from the examination of which it was possible to draw certain conclusions concerning the mechanism of interaction between slow mesons and these nuclei.

1. When slow π^- mesons are captured by nuclei of elements located at the end of the periodic system, nuclear fission takes place with a certain probability. The probability of fission is greatest for uranium. The numerical value of the probability of fission for uranium nuclei, computed on the basis of our experimental data, depends on the assumed distribution of the uranium nuclei introduced into the emulsion. In the case of uniform distribution among all the elements entering into the emulsion, the numerical value of the probability is 0.87 ± 0.27. At non-uniform distribution, when the entire quantity of uranium is distributed only in the gelatin of the emulsion and does not enter into the crystals of AgBr**, the value of the probability becomes equal to 0.42 ± 0.15, i.e., about one half of the cases of capture of slow mesons result in fission.

2. For interaction between slow π^- mesons, the distribution according to their track lengths of the single fragments in the resulting fission exhibits a sharp maximum (Fig. 1) which indicates a considerable number of cases of fission into fragments of approximately equal mass.

3. The average combined track of pairs of fragments for fission by slow π^- mesons ($23.7\ \mu$) agrees well, within the experimental error, with the average combined track ($24\ \mu$) of fragments resulting from fission of uranium by slow neutrons. This shows that the energy formed at the expense of the rest mass of the captured π^- meson is not converted into kinetic energy of the fragments.

4. Besides the cases of uranium nuclear fission which appear to be binary, in ten cases out of a hundred the fission is accompanied by the emission of a light charged particle. A special investigation of the nature of these particles showed that they are in most cases protons. Their angular distribution with respect to the line of fission is shown in Fig. 2. These data indicate that the process of fission by capture of slow π^- mesons differs sharply from the process of fission caused by slow neutrons and that the former process corresponds rather to division of nuclei into fast particles.

5. All these presented facts do not contradict the following assumptions concerning the mechanism of the process. A slow π^- meson captured in one of the meson orbits of the uranium atom interacts with a pair of nucleons (np) or (pp)[9] to which it imparts the energy of its rest mass and its charge; as a result, there are obtained two fast particles with energies approximately 70 mev each. Fast particles of such energy in passing through the nucleus may expel from the nucleus, as a result of collisions, one or two nucleons and then emerge (if the energy is sufficient) leaving the nucleus in a highly excited state. The excited nucleus must lose the excitation energy by the evaporation of the nucleons and undergo fission at some stage of the excitation.

The fact that the probability of fission is less than one indicates that in some cases the excitation energy is basically expended only for the evaporation of the nucleons.

6. On the basis of the proposed interaction mechanism, it is possible to explain the binary fission as fission with emission of neutrons (primary or secondary), the fission with emission of charged particles differing from binary fission only in that in this case together with neutrons there are emitted also the primary or the secondary proton. The relatively large number of protons accompanying fission at energies above 20 mev tends to confirm our view that the significant portion of the protons observed in the fission process is related to the knocked out particles and not to evaporation. The observed, nearly isotropic, angular distribution of the emitted protons with respect to the line of flight of the fragments naturally follows from the above.

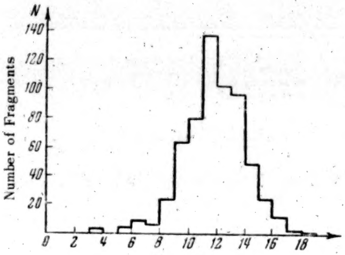

FIG. 1. The distribution of tracks of single fragments in uranium nuclear fission by slow π^- mesons.

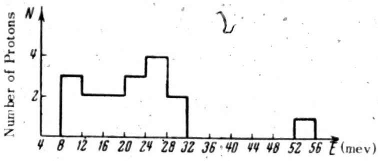

FIG. 2. Distribution by energy of protons emitted in the process of fission of uranium nuclei by slow π^- mesons.

The authors are grateful to Mr. M. G. Meshcheriakov and his laboratory staff for cooperation in carrying out the experimental work related to the study of interaction of slow π^- mesons with nuclei. The authors also remember with deep thanks the late Academician P. I. Lukirskii who showed a steady interest in this work.

---

* The first report was completed in March, 1950. Almost simultaneously and independently of us, fission of uranium with capture of π^- mesons was discovered by Frank and Belovitskii [Report FIAN (Institute of Physics, Academy of Sciences, USSR)]. The first communication concerning fission of uranium by slow π^- mesons appeared in October, 1951, in the work of Al-Salam[6].

** Experimental proof of such unequal distribution is contained in the work of Lozhkin and Shamov[8].

[1] N. A. Perfilov and N. S. Ivanova, Report RIAN, March, 1950

[2] N. A. Perfilov and N. S. Ivanova, Report RIAN, October, 1950

[3] N. S. Ivanova and N. A. Perfilov, Report RIAN, June, 1951

[4] D. V. Viktorov, N. S. Ivanova and N. A. Perfilov, Report RIAN, January, 1952

[5] N. S. Ivanova and N. A. Perfilov, Report RIAN, June, 1952

[6] S. G. Al-Salam, Phys. Rev. **84**, 254 (1951)

[7] N. A. Perfilov, Report RIAN, June, 1953

[8] O. V. Lozhkim and V. Shamov, Report RIAN, January, 1954

[9] S. Tamor, Phys. Rev. 77, 412 (1950)

Translated by J. L. Herson
131

The Probability of Uranium Nuclear Fission by its Absorption of Slow Π⁻ Mesons[1]

O. V. LOZHKIN AND V. P. SHAMOV
Academy of Sciences, USSR

(Submitted to JETP editor March 19, 1955)
J. Exper. Theoret. Phys. USSR **28**, 739-740 (June, 1955)

THE first determinations of the probability of fission of the uranium nucleus by the capture of π^- mesons were carried out in our laboratory in 1951. Perfilov and Ivanova, and Perfilov and the authors[2,3], with the use of thick-layered emulsions, came to the conclusion that apparently practically every capture of a π^- meson by a uranium nucleus leads to fission of the latter. The same conclusion was reached later by Al-Salam[4], using a similar method.

The same method was adopted for the experiments being described. Nuclear plates were soaked in a 4% solution of $UO_2Na(C_2H_3O_2)_3$ and exposed to slow π^- mesons. Under microscopic examination of a given stage of the plate there were counted the number of times that a π^- meson stopped in the photo-layer, the number of cases of fission of uranium nuclei by π^- mesons, and the number of uranium nuclei (by means of the number of α-particle tracks arising from the natural radioactive decay of uranium). For the determination of the total number of cases of capture of π^- mesons by uranium nuclei, it is necessary to know first, how the uranium is distributed throughout the volume of the emulsion, and second, how the probability of capture of slow π^- mesons depends on the Z of the nucleus.

The distribution of uranium in the soaked emulsion was investigated in the following manner. The soaking of the emulsion in uranium salt was carried out and stirred in a special container in a

TABLE

Trial	No. of cases of fission of U per cm^2	No. of cases of stopping of π^- mesons per cm^2	No. of U nuclei per cm^2 × 10^{-17}	No. of cases of capture of π^- mesons by U nuclei per cm^2	Probability of U fission
I	25	7050	6.2 ± 0.6	98 ± 10	0.25 ± 0.05
II	21	5040	5.7 ± 0.2	64 ± 5	0.33 ± 0.08

super-centrifuge (20,000 revolutions per minute). After 20 minutes of centrifuging, the grains of AgBr settled almost completely, covering the walls of the container. The resulting precipitate of grains of AgBr and the leftover gelatin were analyzed for uranium content. The results lead to the conclusion that all the uranium penetrating into the emulsion during the soaking is found in the gelating, and that the adsorption of uranium on the surface of AgBr crystals does not occur. Therefore, in determining the number of π^- mesons interacting with uranium nuclei, it is necessary to count only those mesons which stop in the gelatin (~42% from our data). Assuming further, in agreement with Fermi[5], that the probability of capture of a slow π^- meson in a chemical bond is proportional to the atomic number Z, it is possible to write the following expression for the number of π^- mesons captured by the nuclei of uranium atoms adsorbed by the gelatin, under the condition that the π^- mesons are stopped with uniform distribution throughout the depth of the emulsion:

$$N = 0.42 N_0 \frac{N_U Z_U}{N_U Z_U + \sum_i N_i Z_i}$$

Here N_0 is the number of π^- mesons stopped per square centimeter of the layer of emulsion; Z_i, N_i are the charge and number of nuclei of the elements composing the gelatin per square centimeter of the layer of emulsion.

Two groups of measurements were carried out. The data, reduced to tabular form, are for a layer of emulsion 100 microns thick.

Thus the results of the present work lead to the conclusion that on capture of π^- mesons, uranium nuclei undergo fission in 30% of the cases. However, it should be noted that this conclusion is valid only if the assumption is correct that the probability of capture of π^- mesons by the different nuclei in the mixture is proportional to the atomic number.

The results of the present work were obtained in December, 1953. There are available at the present time in the literature[6] determinations of the probability of fission of the uranium nuclei upon capturing π^- mesons which differ somewhat from our values. In the referenced work the probability of fission is determined to be 0.18 ±0.06.

In conclusion, the authors wish to express their appreciation to Professor N. A. Perfilov for valuable instruction and discussion of the results of the work.

---

[1] O. V. Lozhkin and V. P. Shamov, Report RIAN (Radiation Institute, Academy of Sciences), January, 1954

[2] N. A. Perfilov and N. S. Ivanova, Report RIAN, 1951

[3] N. A. Perfilov, O. V. Lozhkin and V. P. Shamov, Report RIAN, 1952

[4] S. G. Al-Salam, Phys. Rev. **84**, 254 (1951)

[5] E. Fermi and E. Teller, Phys. Rev. **72**, 399 (1947)

[6] W. John and W. Fry, Phys. Rev. **91**, 1234 (1953)

Translated by D. A. Kellogg
134

The Scattering of Fast Neutrons by Non-Spherical Nuclei II

S. I. DROZDOV
Academy of Sciences, USSR

(Submitted to JETP editor March 18, 1955)
J. Exper. Theoret. Phys. USSR **28**, 736-738 (June, 1955)

OUR previous article[1] contains the computation of the effective cross section for scattering of fast neutrons by the black nucleus, which has the form of an ellipsoid of revolution and a spin equal to zero. We shall examine the established results under the assumption that before the scattering interaction the nucleus is found in a particular state.

The differential cross section for an excited rotational state of the nucleus $Y_{lm}(\chi, \phi)$ is determined by the formulas (6), (7) of reference 1:

$$\sigma_{lm}(\theta)=\frac{4}{\pi^2}\frac{(kb)^4}{k^2}I^2_{lm}(\theta), \tag{1}$$

$$I_{lm}(\theta)=\frac{1}{8}\sqrt{(2l+1)\frac{(l-m)!}{(l+m)!}}$$

$$\times\int\limits_{-1}^{1}\int\limits_{0}^{2\pi}dx\,d\varphi\,\xi(x)\,P_l^m(x)\,\frac{J_1(t)}{t}\cos m\varphi;$$

$$t=kb\sqrt{\xi^2(x)\cos^2\varphi+\sin^2\varphi};$$

$$\xi(x)=\sqrt{z^2+(1-z^2)\,x^2}.$$

From this point it is not difficult to obtain the following expression: $\sigma_{lm}(\theta)\neq 0$, provided both l and m are even; $\sigma_{lm}(\theta)=0$ in the remaining cases; in the case of a spherical nucleus, the rotational states are not excited:

$$\sigma_{lm}(\theta)=0,\quad z=1,\quad l\neq 0,\quad m\neq 0.$$

The differential cross section for elastic scattering is obtained from formula (1) with $l=m=0$:

$$\sigma_0(\theta)=\frac{4}{\pi^2}\frac{(kb)^4}{k^2} \tag{2}$$

$$\times\left[\int\limits_{0}^{1}\int\limits_{0}^{\pi/2}dx\,d\varphi\,\xi(x)\frac{J_1\left(kb\theta\sqrt{\xi^2(x)\cos^2\varphi+\sin^2\varphi}\right)}{kb\theta\sqrt{\xi^2(x)\cos^2\varphi+\sin^2\varphi}}\right]^2.$$

In the case of a spherical nucleus ($z=1$) this gives rise to the well-known expression[2]

$$\sigma_0(\theta)=\frac{(kR)^4}{k^2}\left[\frac{J_1(kR\theta)}{kR\theta}\right]^2.$$

In accordance with Eqs. (9) and (11)[1], the summed cross section for scattering into angle θ with distinct excited rotational states, including elastic scattering, is determined by the formula:

$$\sigma_s(\theta)=\frac{2}{\pi}\frac{(kb)^4}{k^2} \tag{3}$$

$$\times\int\limits_{0}^{\pi/2}\int\limits_{0}^{1}d\varphi\,dx\,\xi^2(x)\left[\frac{J_1\left(kb\theta\sqrt{\xi^2(x)\cos^2\varphi+\sin^2\varphi}\right)}{kb\theta\sqrt{\xi^2(x)\cos^2\varphi+\sin^2\varphi}}\right]^2.$$

For a spherical nucleus, $\sigma_s(\theta)=\sigma_0(\theta)$.

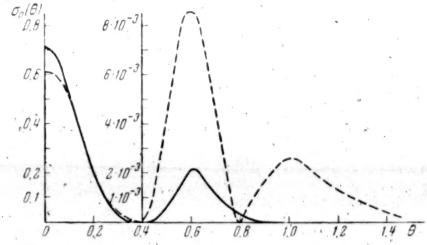

FIG. 1. The function $\sigma_0(\theta)$ for $z=1$ (dotted line) and $z=2$ (solid curve); $kR=10$.

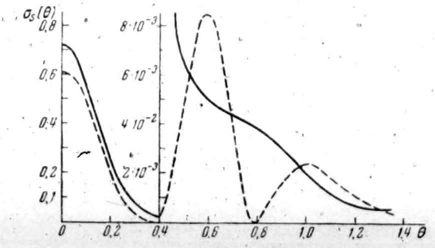

FIG. 2. The function $\sigma_s(\theta)$ for $z=1$ (dotted line) and $z=2$ (solid curve); $kR=10$.

In Fig. 1 is shown the angular distribution of $\sigma_0(\theta)$ for neutrons with energy $kR = 10$ elastically scattered by a non-spherical nucleus ($z = 2$). For comparison there is shown the angular distribution of $\sigma_0(\theta)$ for a spherical nucleus ($z = 1$) of equal volume. From Fig. 1, it can be seen that deformation of the nucleus does not make any radical change in the angular distribution for elastic scattering. As in the case of scattering by a spherical nucleus, the angular distribution of $\sigma_0(\theta)$ has a series of maxima and minima, where, furthermore, the cross section becomes zero at the minima.

Figure 2 shows the summed cross section $\sigma_s(\theta)$ for the non-spherical nucleus ($z = 2$) for energy of the incident neutron $kR = 10$. For comparison there is shown a curve of $\sigma_s(\theta)$ for a spherical nucleus ($z = 1$) of equal volume. From Fig. 2 it can be seen that deformation of the nucleus changes the function $\sigma_s(\theta)$ significantly. In the case of a spherical nucleus, the angular distribution of $\sigma_s(\theta)$ retains the series of maxima and minima, where, furthermore, the cross section $\sigma_s(\theta)$ becomes zero at the minima. But in the presence of observable deformation, the angular distribution of $\sigma_s(\theta)$ no longer has maxima or minima, and does not become zero. In the case of significant deformation, the function $\sigma_s(\theta)$ decreases monotonically with increasing θ.

From the last it follows that the probability of excitation of the lth rotational level of the nucleus decreases rapidly with increasing l. Therefore, the effective energy spread of the neutrons undergoing scattering with excitation of distinct rotational states is found to be of the order $\Delta\epsilon = \hbar^2 l\ (l+1)/2I$, where $l \sim 2$. For heavy nuclei, with $z \approx 2$, $\Delta\epsilon \sim 100$ kev. The angular distribution of $\sigma_s(\theta)$ is convenient for comparison with experimental investigations of angular distribution of elastic scattering, provided that the energy resolution of the experimental detector is of the order of $\Delta\epsilon$.

In accord with formulas (9) - (11) of the previous article[1], the total cross sections σ_t, σ_c, σ_s are found to be independent of the energy, whereupon

$$\sigma_t = 2\sigma_s; \quad \sigma_c = \sigma_s; \quad \sigma_s = \pi R^2 \alpha(z); \tag{4}$$

$$\alpha(z) = \frac{z^{-2/3}}{2}\left(1 + \frac{z^2}{\sqrt{z^2-1}} \arcsin \frac{\sqrt{z^2-1}}{z}\right), \quad z \geqslant 1;$$

$$\alpha(z) = \frac{z^{-2/3}}{2}\left(1 + \frac{z^2}{\sqrt{1-z^2}} \operatorname{Arsh} \frac{\sqrt{1-z^2}}{z}\right), \quad z \leqslant 1,$$

where R is the radius of a spherical nucleus of equal volume.

Given Eq. (2), the total cross section for elastic scattering is determined by the expression:

$$\sigma_0 = \frac{8}{\pi}\frac{(kb)^4}{k^2}\int_0^\infty \theta d\theta \left[\int_0^1\int_0^{\pi/2} dx d\varphi \xi(x) \frac{J_1(kb\theta\sqrt{\xi^2(x)\cos^2\varphi + \sin^2\varphi})}{kb\theta\sqrt{\xi^2(x)\cos^2\varphi + \sin^2\varphi}}\right]^2. \tag{5}$$

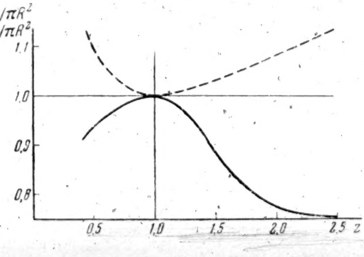

FIG. 3. Total cross section σ_s (dotted line) and σ_0 (solid curve).

The cross section σ_0 is practically independent of energy. Figure 3 shows the total cross section σ_s and σ_0 for different deformations z of the nucleus. The total cross section for excitation of the lth rotational level of the nucleus differs from zero only for even l and diminishes quickly with increasing l. For deformations of the nucleus which are not too great and for $l \geq 2$,

$$\sigma_l \sim 2\pi b^2 \frac{a_l^2}{2^{2l} l},$$

where a_l is the coefficient of resolution

$$\xi(x) = \sum_{l=0}^{\infty} a_l x^l.$$

---

[1] S. Drozdov, J. Exper. Theoret. Phys. USSR **28**, 734-736 (June, 1955); Soviet Phys. 1, (1955)

[2] A. Akhiezer and I. Pomeranchuk, *Several Questions in Nuclear Theory*, Moscow, 1950

Translated by D. A. Kellogg
133

The Scattering of Fast Neutrons by Non-Spherical Nuclei. I

S. I. Drozdov
Academy of Sciences, USSR

(Submitted to JETP editor March 18, 1955)
J. Exper. Theoret. Phys. USSR 28, 734-735 (June, 1955)

ONE examines the scattering of fast neutrons by the black nucleus, which has the form of a body of revolution and spin equal to zero. The solution of the problem of scattering in the adiabatic approximation[1] may be obtained in the following manner. The ψ-function of the system satisfies the Schroedinger equation:

$$(H_0 + T)\psi = E\psi. \tag{1}$$

where H_0 is the Hamiltonian operator of the system consisting of the neutron and the fixed target nucleus; T is the operator for the rotational energy of the nucleus. It is assumed that the energy of the incident neutron is significantly greater than the rotational energy of the nucleus. For this reason, it is possible, in the zero approximation in Eq. (1), to drop the operator T and set up the ψ-function in the form:

$$\psi \approx u_{\mathbf{k}}(\mathbf{r}, \omega)\, \varphi_{n_0}(\omega), \tag{2}$$

where $H_0 u_{\mathbf{k}} = E_k u_{\mathbf{k}}$; $T\phi_n = \epsilon_n \phi_n$; E_k is the energy of the incident neutron; ϵ_n represents the rotational energy levels of the nucleus. The operator H_0 operates only on the radial coordinate $\mathbf{r}$ of the nucleus, and does not operate on the angular coordinate ω, which determines the orientation of the nucleus. By this means one examines, in the adiabatic approximation, neutron scattering on the fixed target nucleus, which was in the rotational state $\phi_{n_0}(\omega)$ with energy ϵ_{n_0} prior to the scattering interaction.

The operator for the rotational energy of the nucleus has the form[2]

$$T = -(\hbar^2/2I)\,\Delta_\omega,$$

where $\Delta\omega$ is the Laplace operator on the unit sphere, I is the moment of inertia of the nucleus with respect to the principal axis, parpendicular to the axis of symmetry. The eigenfunctions $\phi_n(\omega)$, describing the rotation of the nucleus, appear as the spherical functions $Y_{lm}(\omega)$; the rotational levels of the nucleus are determined by the formula:

$$\varepsilon_l = \frac{\hbar^2 l(l+1)}{2I}; \tag{3}$$

When r approaches ∞, the ψ-function (2) has the form:

$$\psi \sim \left[e^{ikr} + \frac{e^{ikr}}{r} f(\omega, \Omega)\right] \varphi_{n_0}(\omega), \tag{4}$$

where $f(\omega, \Omega)$ is the scattering amplitude on the fixed target nucleus in the direction Ω, dependent on the orientation ω of the nucleus. Resolving the quantity $f(\omega, \Omega)\phi_{n_0}(\omega)$ into a series by functions $\phi_n(\omega)$ we obtain:

$$\psi \sim e^{ikr}\varphi_{n_0}(\omega) + \frac{e^{ikr}}{r}\sum_n F_{nn_0}(\Omega)\,\varphi_n(\omega), \tag{5}$$

where

$$F_{nn_0}(\Omega) = \int d\omega\, \varphi_n^*(\omega)\, f(\omega, \Omega)\, \varphi_{n_0}(\omega). \tag{6}$$

The ψ-function (5) describes the system before the scattering interaction as well as the scattering processes, as a result of which the nucleus is left in distinct rotational states $\phi_n(\omega)$. Energy is not conserved in the approximation being used, because the particles, scattered with distinct excited rotational states, all have the identical wave vector $\mathbf{k}$.

With the aid of the expression (5) for the ψ-functions, it is possible to determine the effective cross sections. The differential cross section for scattering in the direction Ω with the nth excited rotational state summed over all orientations of the nucleus, is

$$\sigma_n(\Omega) = |F_{nn_0}(\Omega)|^2. \qquad (7)$$

In particular, the elastic scattering cross section is determined by the diagonal element $F_{n_0 n_0}(\Omega)$. Since $\sigma_n(\Omega) \equiv \sigma_{lm}(\Omega)$, the cross section for excitation of the lth rotational level of the nucleus has the form:

$$\sigma_l(\Omega) = \sum_{m=-l}^{l} \sigma_{lm}(\Omega). \qquad (8)$$

The summed cross section for scattering in the direction Ω with distinct excited rotational states is determined by the formula:

$$\sigma_s = \sum_n \sigma_n(\Omega),$$

or

$$\sigma_s = \int d\omega\, |f(\omega, \Omega)\, \varphi_{n_0}(\omega)|^2. \qquad (9)$$

The corresponding total cross sections are obtained by integrating the differential cross sections over all directions Ω. The expression for the total cross section for all the scattering processes including absorption, is found by the well-known[3] formula:

$$\sigma_t = \frac{4\pi}{k} \operatorname{Im} \int d\omega\, |\varphi_{n_0}(\omega|^2 f(\omega, \Omega)|_{\theta=0}, \qquad (10)$$

where θ is the angle of scattering. The absorption cross section is the difference between the total cross section and the cross section found by integrating the summed cross section σ_s over the angles Ω: $\sigma_c = \sigma_t - \sigma_s$.

The scattering amplitude $f(\omega, \Omega)$ is computed quasi-classically under the assumption that the wave length of the neutron is much smaller than the size of the nucleus R ($kR \gg 1$). It is likewise assumed that the black nucleus has the shape of an ellipsoid of revolution, either oblate or prolate. A physical (optical) analogy is used for the computation of $f(\omega, \Omega)$: the diffraction of light by a black ellipsoid. Using the principle of supplementary screening[4] we obtain

$$f(\omega, \Omega) = \frac{(kb)^2}{ik} \xi(x) \frac{J_1(t)}{t}; \qquad (11)$$

$$t = kb\theta \sqrt{\xi^2(x) \cos^2(\varphi - \Phi) + \sin^2(\varphi - \Phi)},$$

where $\xi(\chi) = \sqrt{z^2 + (1 - z^2)\chi^2}$; $z = a/b$, b is the radius of maximum circular cross section of the ellipsoid, a is half of its axis of symmetry; $\chi = \cos\theta$. The angles θ, ϕ determine the direction of the axis of symmetry ω of the ellipsoid; the angles θ, ϕ determine the direction of scattering Ω. The deformation parameter z assumes values from zero to infinity. For a spherical nucleus, $z = 1$.

To obtain the conditions of applicability of the formulas given for the effective cross section, one computes the corrections of the next approximation to the ψ-functions (2) and by their aid one finds the corrections to the cross sections.

The conditions of applicability follow from the requirement of smallness of these corrections. The condition of applicability of the adiabatic approximation for the computation of the cross section σ_l for the excited rotational level of the nucleus has the form $\varepsilon_l/E_k \ll 1$, $l \neq 0$.

In accord with Eq. (3), this condition is violated when l is large and when there is little deformation of the nucleus ($z \to 1$), since for a spherical nucleus the moment of inertia I becomes zero.

The condition of applicability of the adiabatic approximation for the computation of the elastic cross section has the form

$$\frac{\Delta\varepsilon}{E_k} \int_0^1 P_2(x)\, \xi(x)\, dx \ll 1,$$

where $\Delta\epsilon$ is the effective unmonochromatic condition (effective energy spread) of the neutrons scattered with distinct excited rotational states:

$$\Delta\varepsilon = \frac{\hbar^2 l(l+1)}{2I}, \quad l \sim 2.$$

The author wishes to express his deep appreciation to B. T. Gelikman, who conceived the present computation and also to A. B. Migdal, V. G. Nosov and V. M. Galiskii for valuable discussions.

---

[1] W. Pauli, *General Principles of Wave Mechanics*

[2] L. Landau and E. Lifshitz, *Quantum Mechanics*, Moscow, 1948

[3] L. I. Schiff, Progr. Theor. Phys. 11, 288 (1954)

[4] L. Landau and E. Lifshitz, *Field Theory*, Moscow, 1948

Translated by D. A. Kellogg
132

The Possible β Decay of Hyperions and *K* Mesons

M. MARKOV AND V. STAKHANOV
The P. N. Lebedev Institute of Physics, Academy of Sciences, USSR

(Submitted to JETP editor February 9, 1955)
J. Exper. Theoret. Phys. USSR **28**. 740 (June, 1955)

AT the present time it is apparently possible to consider it established that the Λ^0 particle can enter into the composition of complex nuclei on a par with the nucleons. It is not known to what degree the properties of hyperions and nucleons are related*. In every case there are certain bases for considering a Λ^0 particle as a nucleon which exists in a certain excited state, with all the resultant consequences[1]. For example, such a nucleon could be beta active:

$$\Lambda^0 \rightarrow P + e^- + \nu. \qquad (1)$$

The aim of the present writing is to turn attention on the fact that due to the high upper limit for the disintegration energy, one should expect a short τ_β compared to the observed lifetime of Λ^0 particles, as in the case of $\tau_\pi(\Lambda^0 \rightarrow \pi^- + P)$.

Indeed, the lifetime of the free neutron is about 10 minutes, while the beta spectrum endpoint in this case is $E_0 \sim m_e c^2$. In the case of beta decay of Λ^0 particles, the beta spectrum endpoint is about 350 $m_e c^2$, and the probability of beta decay is approximately proportional to E_0^5. Thus, in deriving the probability of deta decay of Λ^0 particles, there appears a factor of the order of magnitude 10^{10}, which leads to a relatively short lifetime for the Λ^0 particle with respect to beta decay.

The detailed computation[1] shows that in the case of vector** variation (under the assumption that the Λ^0 particle is like the neutron, with $G \sim 10^{-44}$ erg cm^3), τ_β turns out to be $\sim 10^{-9}$ seconds. The Λ^0 particle, as is known, decays into a π^- meson and a proton, with a lifetime of about 10^{-10} seconds. At present, there are known many instances of the decay of a Λ^0 particle into a π^- meson and a proton, and, apparently, unrecorded cases of beta decay. This is evidence that either the Λ^0 particle does not appear as a particle in this case, according to its characteristics when near a nucleon, or else it possesses a higher spin which causes beta decay to be a forbidden transition. Some well-established correlating data point to a high spin for the Λ^0 particle.

The considerations indicated above may also be applied in the case of *K* mesons[2], if, for example, the spin of the latter is equal to zero and their decay can occur with the emission of Fermi particles. Here, the lifetime with respect to such decay will compete with the decay of *K* mesons to π mesons. At the same time the decay of *K* mesons with the emission of weakly interacting Fermi particles (μ mesons and electrons) would indicate the use of a low spin (0 or 1) by the *K* particles.

Data available in the literature appear to indicate the possibility of the decay of *K* mesons with the emission of Fermi particles[3].

---

* The possibility is not excluded that the analogy between a Λ^0 particle and a nucleon is still a weak one, since the Λ^0 particle, for example, interacts weakly with a π field, but interacts strongly with nucleons through other fields (θ field, etc.).

** Pseudoscalar variant gives $\tau_\beta \sim 10^{-7}$ seconds.

[1] V. Stakhanov, Thesis, Moscow State University, 1954

[2] M. A. Markov, Dokl. Akad. Nauk SSSR **101**, 449 (1955)

[3] W. Fry and M. Swami, Phys. Rev. **96**, 235 (1954)

Translated by D. A. Kellogg
135

Multiple Meson Production at Energies of 1-2.2 Bev

S. Z. BELEN'KII AND A. I. NIKISHOV
P. N. Lebedev Institute of Physics Academy of Sciences, USSR

(Submitted to JETP editor March 27, 1955)
J. Exper. Theoret. Phys. USSR **28**, 744-746 (June, 1955)

IN a recent work[1] a study was made of the interaction of protons with neutrons of high energies obtained by means of a Cosmotron. The interaction was studied in a Wilson chamber filled with hydrogen. The authors investigated 154 three-prong stars. Not a single five-prong star was registered. Analysis of the results obtained showed conclusively that, during collisions of high energy nucleons, multiple production of mesons, namely the production of double mesons, takes place in a considerable number of cases. The authors give the following data for the ratio of the number of cases of the production of a single negative π meson (–) and the number of cases of the production of a double π meson: one positive (+) and one negative (−) or one negative (−) and one neutral (0):

$$(pp-):(pn+-):(pp-0)=0.8:3.2:1. \tag{1}$$

Since not a single case of the production of five-prong stars was observed which could be interpreted as the origination of triple mesons ($pp--+$), the authors[1] concluded that the number of three-prong stars, resulting from the formation of triple mesons, is negligibly small.

In the same work a comparison is given of the results obtained with Fermi's statistical theory of the multiple production of particles[2].

Special calculations by the Fermi theory for the corresponding energies (1.7 bev = average energy of the neutron beam and 2.2 bev = the maximum energy of the beam) were carried out by Yang and Christian (cited in reference 1). These calculations led to the following result:

for the energy of 2.2 bev

$$(pp-):(pn+-):(pp-0)=12.2:3.1:1, \tag{2}$$

for the energy of 1.7 bev

$$(pp-):(pn+-):(pp-0)=20.5:3.3:1. \tag{3}$$

From a comparison of Eqs. (1) and (3) it is evident that the experimental ratio of the number of cases of double meson production to the number of cases of single meson production is approximately 20 times as great as the value predicted by Fermi's statistical theory. It should be noted that into the Fermi theory enters a quantity, determined from theory only by the order of magnitude --- namely, the volume Ω in which the energy of the colliding nucleons is concentrated and the formation of particles takes place. It is possible to choose a value for this volume such as to obtain an experimental value for the ratio of the cases of the production of double and single mesons. However, a simple calculation will show that at the same time we will obtain a very large value for the number of five-prong stars. In fact, when in the selection of the volume Ω, proposed by Fermi, the ratio of the number of five-prong stars to the number of three-prong stars is equal to 1/300, which does not contradict the experiment[1], then a change in the volume Ω, giving rise to an inevitable increase in the probability of the production of two mesons simultaneously, will at the same time lead to an increase in the ratio of the number of five-prong stars to the number of three-prong stars. This ratio becomes 3/10, which sharply contradicts the investigation[1] in which not even one five-prong star was observed out of 154 cases of three-prong stars.

From the above it is evident that the statistical Fermi theory in its general form does not agree with experiment. The authors of reference 1 point out that certain properties of the multiple production of mesons during the collisions of nucleons can be qualitatively explained by the presence of excited states of nucleons. Studies on the scattering of π mesons on nucleons indicate the existence of intermediate states of nucleons with an angular momentum of 3/2 and an isotopic spin of 3/2. In the investigations of Tamm and his co-workers[3] intermediate (isobaric) states of nucleons were used for the construction of the phenomenological theory of the interaction of nucleons and mesons. Previously, ideas were also put forward that the formation of mesons partly or even entirely proceeds through the intermediate states of nucleons[4].

In the present investigation an attempt was made to include the isobaric states into the statistical theory of the multiple formation of particles. We have assumed that during the collision of nucleons particles can be produced with a mass of 1.32 M_0, where M_0 is the mass of the nucleon (this value gives the best agreement with the experiments on the scattering meson-nucleon[3]), an isotopic spin of 3/2 and an ordinary spin of 3/2. We have also assumed that the probability of the formation of such particles is determined by the statistical weight. The life-duration of the "isobaric particle" is very small (of the order of the time of nuclear collisions), and it breaks up very rapidly into a nucleon and a meson.

We will designate by N the nucleon, by N' the isobaric state of the nucleon and π- meson. We will consider the following states originating during the collision of nucleons: NN (elastic scattering), $N'N$, $NN\pi$ (formation of a single π meson), $NN'\pi$, $N'N'$, $NN\pi\pi$ (formation of double π mesons), $N'N'\pi$, $N'N\pi\pi$, $NN\pi\pi\pi$ (formation of triple mesons). When computing the statistical weight of the different states, we start with a general formula of the following type (see reference 1):

$$S(n) = \left[\frac{\Omega}{(2\pi\hbar)^3}\right]^{n-1} \frac{dQ(E)}{dE}. \tag{4}$$

here $\Omega = \Omega_0 (2M_0c^2/E)$, Ω_0 is the volume, equal to $4/3\,\pi(\hbar/\mu c)^3$ (μ is the mass of the meson), E is the total energy of two colliding nucleons in a center-of-mass system, $Q(E)$ is the volume in the momentum space corresponding to the total energy E, n is the number of all the particles in a given state. In the calculations the conservation of energy and momentum is taken into account, but the conservation of the moment of the quantity of motion is neglected. The identity of the particles is also taken into account.

If as a result of the collision two heavy particles are produced (the states NN, $N'N$, $N'N'$), then Eq. (4) can be reduced to the following:

$$S_{NN'} = g_N g_{N'} \frac{\Omega}{(2\pi\hbar)^3} \frac{\pi}{c^3} (M_0c^2)^2 \tag{5}$$

$$\times \left\{ \frac{(E^2 + M_2^2 - M_1^2)^2}{4E^2} - M_2^2 \right\}^{1/2} E.$$

g_N and $g_{N'}$ are the numbers of the states for N and N' dependent on the ordinary spin. M_1 and M_2 are the masses of the heavy particles, the quantities E, M_1 and M_2 are measured in the units M_0c^2.

If during the collision three particles are formed (the states $NN\pi$, $NN'\pi$, $N'N\pi$) then with the aid of reference 5 it is not difficult to obtain the following formula:

$$S_{NN'\pi} = g_N g_{N'} \frac{\Omega^2 (M_0c^2)^5}{96\pi^4\hbar^6c^6} \tag{6}$$

$$\times \int_0^{p_{\max}} \frac{B^{1/2}}{(A^2 - p^2)^2} \left[\left(1 - \frac{4A^2}{A^2 - p^2}\right) B + {}^3/_2\, A \frac{dB}{dA} \right] p^2 dp,$$

where

$$A = E - E_1; \quad E_1^2 = p^2 + \mu^2;$$

$$B = (A^2 - p^2 - M_1^2 - M_2^2)^2 - 4M_1^2M_2^2.$$

$$p_{\max}^2 = E_{1\,\max}^2 - M_1^2.$$

$$E_{1\,\max} = \frac{E^2 + \mu^2 - (M_1 + M_2)^2}{2E}.$$

The weight of the state $NN\pi\pi$ can be obtained from the calculation of Yang and Christian cited in reference 1. The states $N'N\pi\pi$ and $NN\pi\pi\pi$ are very unlikely, and their phase weight is evaluated only approximately. For energies of 1.75 bev and lower, the role of these states is negligibly small.

In the calculation of the statistical weights it is also necessary to take into account the conservation of charge and of isotopic spin. Since the colliding particles are a neutron and a proton, therefore the initial state represents a mixture of states with isotopic spins $T = 1$ and $T = 0$; moreover, the contribution of both these states is equal. When making computations it is necessary to calculate the number of states corresponding to the given

End States		Statistical Weight in %			
		1.75 bev		1.46 bev	
$pp-$	$NN\pi$	8.4	10.4	8.4	11.4
	NN'	2		3	
$pn+-$	$N'N\pi$	11	28.5	6.5	20
	$N'N'$	16.5		13.5	
	$NN\pi\pi$	1			
$pp-0$	$N'N\pi$	2.5	5	1.5	3.2
	$N'N'$	2		1.7	
	$NN\pi\pi$	0.5			

values of the isotopic spin and the total charge (see reference 2). However, for comparison with experiment, the distribution of particles according to charge is essential. Such a distribution can often be found on the basis of the conservation of isotopic spin in utilizing the methods of group theory[6].

By carrying out the respective calculations, it is possible to find the statistical weights for the end states with different distributions of charge between the particles. The data for the end states $(pp-)$, $(pn+-)$, $(pn-0)$, which are of interest to us, are compiled in the Table.

From the above Table it follows that the ratios $(pp-)$: $(pn+-)$: $(pp-0)$ at an energy of 1.75 bev are equal to 2.1 : 5.7 : 1 and at an energy of 1.46 bev these are 3.5 : 6.3 : 1. As is shown by the calculation , at 2.2 bev these ratios are 1.4 : 5 : 1. The experimental value of these ratios, as has already been pointed out, is 1 : 3.2 : 1. However, the authors[1] themselves stress that even the ratios 2.4 : 7.6 : 1 do not contradict experiment. In our calculation the probability of the production of five-prong stars was found to be negligibly small.

Thus, the calculation of the multiple production of mesons at energies of the order of 2 bev by the statistical theory, but taking into account the isobaric states gives an entirely satisfactory agreement with experiment. We are postponing the discussion of the angular and energy distributions until the subsequent communication.

---

[1] W. B. Fowler, R. P. Shutt, A. M. Thorndike and W. L. Whittemore, Phys. Rev. **95**, 1026 (1954)

[2] E. Fermi, Progr. Theor. Phys. **5**, 570 (1951); Phys. Rev. **92**, 452 (1953); **93**, 1434 (1954)

[3] I. E. Tamm, Iu. A. Gel'fand and V. Ia. Fainberg, J. Exper. Theoret. Phys. USSR **26**, 649 (1954); V. I. Ritus, J. Exper. Theoret. Phys. USSR **27**, 660 (1954)

[4] F. J. Belinfante, Phys. Rev. **92**, 145 (1953); D. C. Peaslee, Phys. Rev. **94**, 1085 (1954); R. Gatto, Nuovo Cim. 1, 159 (1955)

[5] M. I. Podgoretskii and I. I. Rosental', J. Exper. Theoret. Phys. USSR **27**, 129 (1954)

[6] L. D. Landau and E. M. Lifshitz, *Quantum Mechanics*, Section 97, United Scientific and Technical Publishers, 1948

Translated by E. Rabkin
137

A Study of the Energy Levels of the Lithium Nucleus by the Method of Magnetic Analysis

L. M. KHROMCHENKO AND V. A. BLINOV
Radio Institute of the Academy of Sciences, USSR

(Submitted to JETP editor January 24, 1955)
J. Exper. Theoret. Phys. USSR **28**, 741-743 (June, 1955)

IN this work the energy spectrum of the lithium nucleus was investigated by the method of magnetic analysis of the products of nuclear reactions, which has been described previously[1]. The method used gave the possibility of obtaining lines visible to the eye on a photoplate, at the position of the localization of discrete groups of particles. Such a spectrogram was then studied with the aid of a microphotometer. The length of the whole photoplate and half of its width was covered with a filter of aluminum foil, whose thickness could be varied. Its thickness was calculated to be such that protons would pass through, but that particles having a shorter path would be completely filtered out. When the type of particles, the value of the magnetic field and the geometry of the instrument are known, it is possible to determine definitely the energy of the particles of the group under investigation from the position of the line on the photoplate.

In our experiments a layer of lithium oxide, (obtained by burning metallic lithium in air) was deposited on a copper foil having a thickness of approximately 0.5 μ. The target was bombarded with a monoenergetic beam of deuterons with an energy up to 4.7 mev. The experiments were carried out at three energies of the bombarding deuterons, from 3.7 to 4.7 mev. As in the previous experiments[1,2] carried out by this method, the total spectrum of the element studied was obtained at the same time on one and the same photoplate. The energy of the primary deuterons was determined by the elastic recoil from the nuclei present in the target.

The reproductions of the photoplates obtained during the irradiation of the lithium oxide with deuterons are given in Fig. 1. The microphotograms of these plates are shown in Figs. 2 and 3. In Fig. 2 the upper curve was obtained on the half of the plate without the filter, and the lower curve on the filtered half. As is evident from the Figures, in addition to the deuterons elastically recoiled from Cu^{64}, O^{16}, C^{12}, and Li^7, we have

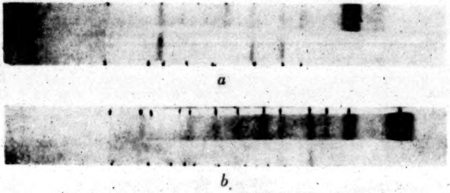

FIG. 1. The energy spectrum of lithium.
a. $E_d = 3.76$ mev; b. $E_d = 4.69$ mev.

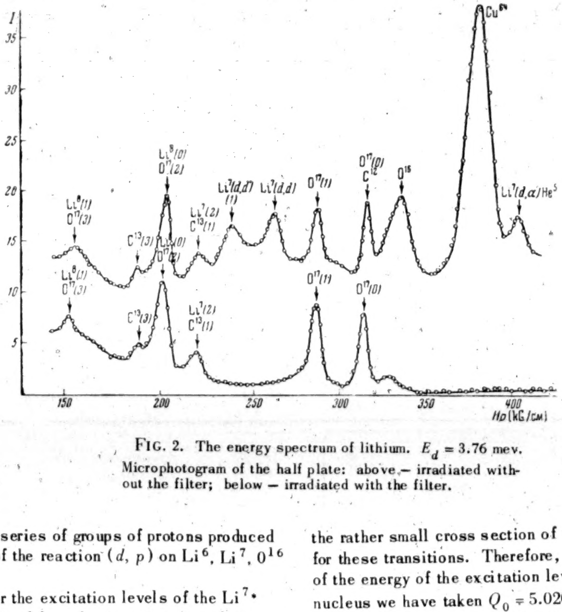

FIG. 2. The energy spectrum of lithium. $E_d = 3.76$ mev. Microphotogram of the half plate: above – irradiated without the filter; below – irradiated with the filter.

registered a series of groups of protons produced as a result of the reaction (d, p) on Li^6, Li^7, O^{16} and C^{12}.

Our data for the excitation levels of the Li^{7*} nucleus obtained from the investigation of six plates containing the lithium spectrum are compiled in Table I. These are compared with the data of a number of authors who obtained the above levels from the reaction Li^6 (d, p), as well as from other nuclear reactions.

No groups of protons corresponding to the transition of the Li^{7*} nucleus to the ground-state and to the first excitation level were observed in our experiments. This can be explained by the low propagation of the Li^6 isotope and, apparently, by the rather small cross section of the reaction (d,p) for these transitions. Therefore, for the calculation of the energy of the excitation levels of the Li^{7*} nucleus we have taken $Q_0 = 5.020$ mev, measured for this reaction by Strait, Van Patter et al[3].

In addition to the proton groups and the elastically recoiled deuterons, we have observed on all the plates a group of deuterons corresponding to the inelastic recoils from the main Li^7 isotope (propagation 92.48%). This group corresponded to the first excitation level of Li^{7*} with the $E^* = 0.476$ mev. The intensity of this group is large; it is comparable with the elastic recoil of deuterons from lithium. The level of Li^{7*} (3) with an excitation energy of 6.53 mev was previously obtained only

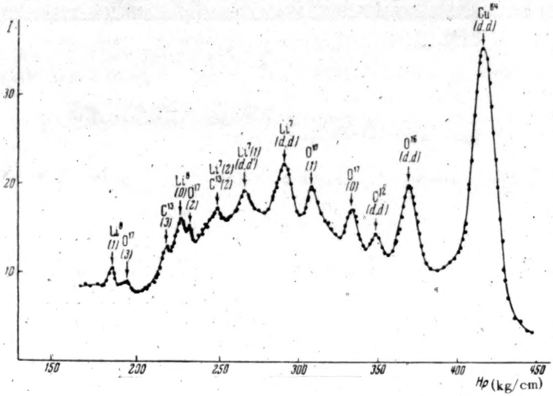

FIG. 3. The energy spectrum of lithium. $E_d = 4.69$ mev. Microphotogram of the half plate irradiated without the filter.

TABLE I. Excitation Levels of the Li^{7*} Nucleus

No. of Group	This Work		Data of Other Authors		
	Q, mev	E^*, mev	E^*, mev	Reactions	Authors
1	—	0.476 (from d,d')	0.483 0.477 0.478	(d, p) γ-rays (p,p') & (d,d')	Beuchner et al. Thomas and Lauritzen Williams et al.
2	(0.566)	(4 454) from (d,p)	4.56 4.61	(p, p') (d, p)	Frenzen and Likely Gelinas and Hanna
3	—1.510	6.530 from (d,p)	6.56	(p, p')	Frenzen and Likely

during the inelastic scattering of protons[4], but in the reaction (d, p) it was observed by us for the first time.

Table II describes the excitation levels of the Li^8 nucleus produced as a result of the reaction $Li^7(d, p)Li^8$. In our experiments the group of protons corresponding to the transition of the Li^8 nucleus into the ground-state is intense and fairly well defined. The value of $Q_0 = -0.183$ mev which we have obtained for this reaction is in very good agreement with the data obtained by a number of authors using very different methods.

In the review of Ajzenberg and Lauritsen[5], the first excitation level of Li^8 was considered doubtful, its energy was given only approximately (of the order of 1 mev). In our experiments the presence of such a level is confirmed quite definitely, the corresponding group of protons being fairly intense and clearly defined.

On all the plates containing the lithium spectrum obtained at $E_d \sim 3.7$ mev (Fig. 2), to the right of the peak of the deuterons which underwent

TABLE II. Excitation Levels of the Li^8 Nucleus

No. of Group	This Work		Data of Other Authors			
	Q, mev	E^*, mev	Q, mev	E^*, mev	Method	Author
0	—0.183	0	—0.187	0	Angular Threshold	Paul
			—0.188	0	Magnetic Spectrograph	Strait et al.
			—0.192	0	Electrostatic Analyzer	Williams et al.
1	—1.160	0.977	—	(1.0)	—	Gove and Harvey

an elastic recoil from the copper backing of the target there can be observed a fairly intense group of particles which did not go through the filter. Spectral analysis of the target substance established the absence of elements heavier than copper. Thus, this group could not be deuterons elastically recoiled from an element heavier than copper. There remained possible three reactions on the main lithium isotope: $Li^7(d,\alpha)He^5$, $Li^7(d, He^3)He^6$ and $Li^7(d, He^3)Li^6$. Special control experiments on thick-layer photoplates made it possible to measure the length of the tracks of the particles of the group under investigation and to establish that these were α-particles, and hence of all the possible reactions, the first takes place. The fact that the reaction (d, α) occurs precisely on the Li^7 isotope indicates a calculation of another variant: $Li^6(d, \alpha)He^4$. This gives a Q_0 value for the latter reaction which is incompatible with the known masses of the reacting particles.

From a study of five plates of the lithium spectrum at $E_d \sim 3.7$ mev we have determined the energy of the reaction to be $Q_0 = 13.719$ mev for the process $Li^7(d, \alpha)He^5$. The values for this quantity published up until now[6-8] vary within the range 13.43 - 14.43 mev. Since these values were measured by methods (ionization chamber, measuring the lengths of tracks, etc.) less accurate than the method of magnetic analysis (which we have used), the value of Q_0 obtained in our experiments may be considered as being more reliable and one which permits a more precise determination of the mass of the He^5 nucleus.

Taking for the mass of the particles participating in reaction, the values: $M_{H^2} = 2.0147411$, $M_{He^4} = 4.0038773$, $M_{Li^7} = 7.018225$[9], we obtain for the mass of He^5 the value $M_{He^5} = 5.014353$ A.M.U. For the values of the excitation energy determined from the well-defined peaks, the average error of measurements is of the order of 20 kev. The less clearly defined peaks give a larger error.

With a sense of deep gratitude and acknowledgement the authors note the constant interest in this work of the late Academician P. I. Lukirskii. The authors also express their thanks to Professor Iu. A. Nemilov for his attention to this work and for a number of suggestions.

---

[1] L. M. Khromchenko, Dokl. Akad. Nauk SSSR **93**, 451 (1953)

[2] L. M. Khromchenko, Dokl. Akad. Nauk SSSR **94**, 1037 (1954)

[3] E. N. Strait, D. M. Van Patter et al, Phys. Rev. **81**, 747 (1951)

[4] W. Frenzen and J. G. Likely, Phys. Rev. **87**, 667 (1952)

[5] F. F. Ajzenberg and T. Lauritsen, Rev. Mod. Phys. **24**, 325 (1952)

[6] J. H. Williams, W. G. Shepherd and R. O. Haxby, Phys Rev. **52**, 390 (1937)

[7] C. M. G. Lattes, P. H. Fowler and P. Cüer, Proc. Phys. Soc. (London) **A59**, 883 (1947)

[8] A. P. French and P. B. Treacy, Proc. Phys. Soc. (London) **A64**, 452 (1951)

[9] B. S. Dzhelepov and L. N. Zyrianova, Uspekhi Fiz. Nauk **47**, 512 (1952)

Translated by E. Rabkin
136

The Formation of Charged Π-Mesons by Nucleons

V. M. SIDOROV
Academy of Sciences of the USSR

(Submitted to JETP editor February 7, 1955)
J. Exper. Theoret. Phys. USSR **28**, 727-729 (June, 1955)

CHARGED π-mesons may be formed with free nucleons as a result of the following reactions:

$$p + p \rightarrow n + p + \pi^+ \text{ or } p + p \rightarrow d + \pi^+; \tag{1}$$

$$p + n \rightarrow n + n + \pi^+; \tag{2}$$

$$p + n \rightarrow p + p + \pi^-; \tag{3}$$

$$n + n \rightarrow n + p + \pi^- \text{ or } n + n \rightarrow d + \pi^-. \tag{4}$$

At the present time, the most complete experimental data exist from the study of the reaction (1). Some information concerning the interactions $(p - n)$ and $(n - n)$ can be obtained from the experimental study of collisions between nucleons and nuclei. Since even at 500 mev the wavelength of the bombarding particle is small compared with the distance between the nucleons, it can be assumed that at energies large compared with 500 mev, mesons are formed in complex nuclei mostly in individual collisions of nucleons.

On the basis of the hypothesis of charge independence of nuclear forces and symmetry of the properties of positive and negative mesons, it can be assumed that the cross sections of the processes of formation of π^+ and π^- mesons in $(p - n)$ collisions are equal.

If we assume also that charged mesons are formed in $(p - p)$ and $(p - n)$ collisions with equal probabilities, there more positive mesons should be formed than negative when complex nuclei are bombarded with protons, namely: $\sigma(\pi^+)/\sigma(\pi^-) = (A + Z)/A - Z)$. Thus when deuterium, carbon, and in general, nuclei having equal numbers of protons and neutrons are bombarded by protons, we can expect the ratio $\sigma(\pi^+)/\sigma(\pi^-)$ to be equal to 3. The ratio $\sigma(\pi^-)/\sigma(\pi^+)$ should be the same for the bombardment of complex nuclei with neutrons. Results of experimental work[1-3] indicate that when complex nuclei are radiated with protons of 340 to 380 mev, the ratio of the cross sections $\sigma(\pi^+)/\sigma(\pi^-)$ is considerably greater than $A + Z/A - Z$. Measurements of ouptuts of charged mesons at 90° to the beam resulting from bombardment of carbon with neutrons of 270 mev[4] showed that the output of π^- mesons in this case exceeds the output of π^+ mesons by a factor of approximately 15. It should be noted that these experiments were made using bombarding particles of energies close to the threshold of meson formation. If this case, in view of Pauli's principle, the ratio of cross sections $\sigma(\pi^+)/\sigma(\pi^-)$ can increase significantly when nuclei are bombarded with protons, and decrease in the case of bombardment with neutrons as noted by Chew and Steinberger[5].

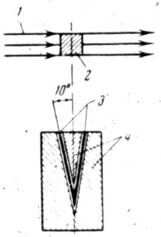

Fig. 1. Experimental arrangement
1. Proton beam. *2*. Target.
3. Photographic plate. *4*. Brass block.

The formation of charged mesons by the action of protons and neutrons on carbon and hydrogen was studied by us in experiments using the synchrocyclotron of the Institute for Nuclear Problems, Academy of Sciences, USSR.

1. *Formation of π^+ and π^- mesons by the action of protons on carbon and hydrogen.* A target of carbon or paraffin was placed in a narrowly collimated beam of protons of 657 ± 8.0 mev[6]. The charged mesons emitted from the target at an angle of 90° were recorded by means of nuclear emulsions. The experimental arrangement is shown in Fig. 1. The photographic plates were placed in the brass block at an angle of 10° to the direction of the incident mesons. The meson stopped within the emulsion was considered positive if it gave rise to a μ-meson trace and negative if it produced a "star".

The differential cross section of formation of mesons was determined according to the following formula:

$$\frac{d^2\sigma}{d\omega dE} = \frac{N}{nN_p t\,[dE/dR]_E}\,\frac{r^2}{S},$$

where N_p is the number of protons that passed through the target; n the number of nuclei on 1 square cm of the target measured in the direction of the incident beam; N the number of mesons found on the emulsion area S; r the distance from the target to the surface of the emulsion; t the thickness of the emulsion; $[dE/dR]_E$ the loss of energy in the emulsion by mesons of energy E.

The number of protons N_p was measured by means of a calibrated ionization chamber. In determining the loss of energy by the mesons, the formula $[dE/dR]_E = 0.067\,R\,\pi^{0.419}$ derived from the path-energy relation for protons[7] was used.

The number of π^- mesons was taken equal to the number of observed "stars" multiplied by the coefficient 1.37. There was also introduced a correction for the mesons leaving the beam as a result of nuclear interaction. The length of the free path of mesons in brass was thereby taken equal to 104.4 gm/cm^2.

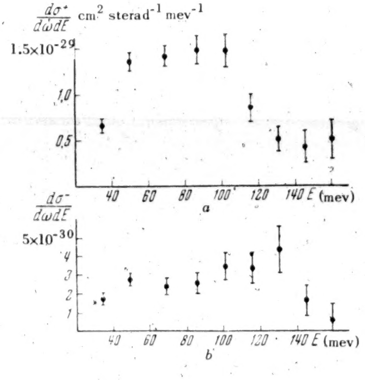

Fig. 2. The spectrum of mesons formed by protons of 657 mev in carbon nuclei and emitted at an angle of 90°. *a*. spectrum of π^+ mesons; *b*. spectrum of π^- mesons.

As a result of examination of the photographic plates irradiated in experiments with a carbon target, there were recorded 629 disintegrations. In the same area of the emulsion, there were found 91 "stars" formed by π^- mesons. The ratio $\sigma(\pi^+)/\sigma(\pi^-)$ was in this case equal to 5.0 ± 0.7. The energy spectra of the π^+ and π^- mesons are shown in Fig. 2. Integration of the spectra gives for the formation cross sections at an angle of 90° $(1.9 \pm 0.4) \times 10^{-27}$ cm^2 sterad^{-1} for positive mesons and $(3.7 \pm 1.3) \times 10^{-28}$ cm^2 sterad^{-1} for negative mesons.

The cross section of formation of π^+ mesons by protons on hydrogen leaving at an angle of 90° was obtained from experiments with paraffin and carbon by subtraction and found to be $d\sigma(\pi^+)/d\omega \approx 0.35 \times 10^{-27}$ cm^2 sterad^{-1} with an accuracy down to a factor of 2.

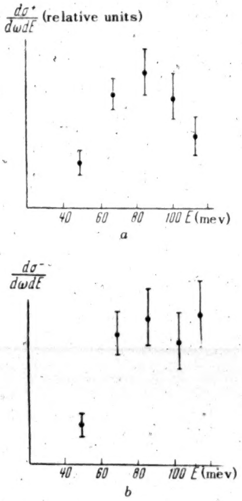

Fig. 3. The spectrum of mesons formed by neutrons in hydrogen and emitted at an angle of 90°. *a*. spectrum of π^+ mesons; *b*. spectrum of π^- mesons.

Comparison of the results of the present experiments with the results of reference 1 shows that the cross section of formation of π^+ mesons in carbon at an angle of 90° increases approximately four times when the energy of the bombarding protons is increased from 381 to 657 mev, while the cross section of formation of π^- mesons increases approximately nine times.

2. *Formation of π^+ and π^- mesons by neutrons on carbon.* Measurements were made of the relative yield of π^+ and π^- mesons at an angle of 90° to the beam for the bombardment of carbon with neutrons. The neutrons were formed as a result of the action of 670 mev protons on the nuclei of beryllium[1]. The method of observing the mesons was similar to that described above. The ratio of the outputs was calculated on the bases of 26 $\pi^+ \to \mu^+$ disintegrations and 102 "stars", formed by the π^- mesons, and found to be equal to $\sigma(\pi^-)/\sigma(\pi^+) = 5.4 \pm 1.1$. This value, within the experimental error, corresponds to the ratio $\sigma(\pi^+)/\sigma(\pi^-)$ determined by bombarding carbon with protons which constitutes a confirmation of the principle of symmetry of charges.

It can be seen, as a result of measurements of the relative outputs of charged mesons formed by protons and neutrons, that in carbon nuclei π^+ and π^- mesons in $(p - n)$ collisions are formed and emitted at an angle of 90° with half the probability of formation of π^+ mesons in $(p - p)$ or π^- mesons in $(n\text{-}n)$ collisions. This indicates that there is a difference in the nature of the process of formation of charged mesons in the $(n - p)$ and $(p - p)$ systems.

3. *Formation of π^+ and π^- mesons in $(n - p)$ collisions.* A vessel containing liquid hydrogen was placed in the path of a neutron beam[8]. Charged mesons formed by the neutrons in hydrogen and leaving the target at an angle of 90° to the direction of the beam were registered by the method described above. As a result of the examination of the emulsion, there were recorded 131 $\pi^+ \to \mu^+$ disintegrations. In the same volume of the emulsion, there were observed 112 "stars" formed by π^- mesons. Thus, the ratio of the number of positive to negative mesons, after applying the correction for stars without rays, was equal to 0.9 ± 0.2. Fig. 3 shows the energy spectra of π^+ and π^- mesons formed by neutrons in hydrogen.

---

[1] M. M. Block, S. Passman and W. W. Havens, Phys. Rev. **88**, 1239 (1952)

[2] S. L. Leonard, Phys. Rev. **93**, 1380 (1954)

[3] Walter F. Dudziak, Phys. Rev. **86**, 602 (1952)

[4] H. Bradner, D. J. O'Connel and B. Rankin, Phys. Rev. **79**, 720 (1950)

[5] G. F. Chew and J. L. Steinberger, Phys. Rev. **78**, 497 (1950)

[6] V. P. Zrelov, Report of the Institute of Nuclear Problems, Academy of Sciences, USSR, 1954

[7] H. Bradner, F. M. Smith, W. H. Barkas and A. S. Bishop, Phys. Rev. **77**, 462 (1950)

[8] V. M. Sidorov, N. I. Frolov, I. Ch. Nozdrin and N. M. Kovaleva, Report of the Institute of Nuclear Problems, Academy of Sciences, USSR

Translated by J. L. Herson
129

"Acoustic Excitations" in Superconductors

IU. L. KLIMONTOVICH
Moscow Aviation Technological Institute

(Submitted to JETP editor November 15, 1954)
J. Exper. Theoret. Phys. USSR **28**, 754-756 (June, 1955)

1. WE investigated the spectrum of elementary energy excitations in superconductors in the framework of the new phenomenological theory of superconductivity of Ginzburg and Landau. In their work [1,2], they made use of the system of equations for the "effective" wave function and the vector potential A:

$$ih\frac{\partial\Psi}{\partial t} = \frac{1}{2m}\left(-ih\nabla - \frac{e}{c}\mathbf{A}\right)^2\Psi + \frac{\partial F_{s0}}{\partial\Psi^*}, \qquad (1)$$

$$\Delta\mathbf{A} = \frac{2\pi ih}{mc^2}(\Psi^*\nabla\Psi - \Psi\nabla\Psi^*) + \frac{4\pi e^2}{mc^2}\mathbf{A}\,|\Psi|^2, \qquad (2)$$

where $F_{s0} = F_{n0} + \alpha|\Psi|^2 + (\beta/2)|\Psi|^4$ is the free energy in the superconducting state, α and β are parameters, $|\Psi|^2$ is the concentration of superconducting electrons. At equilibrium,

$$|\Psi|^2 = n_{s0} = -(\alpha/\beta); \alpha = H^2_{\text{KM}}/4\pi n_{s0},$$

where H_{km} is the critical magnetic field for the mass particles. The term $ih(\partial\Psi/\partial t)$ is essential in the investigation of the excitation spectrum, since it is of the same order as the other terms in the equation. The term $1/c^2(\partial^2\mathbf{A}/\partial t^2)$ has been omitted, since $\omega \ll ck$ for the excitations under consideration here.

In the investigation of the excitation spectrum, it is appropriate to employ the equation for the quantum distribution function in addition to the equation for Ψ:

$$f(\mathbf{q},\mathbf{p})$$

$$= \frac{1}{(2\pi)^3}\int \Psi^*(\mathbf{q} - {}^1\!/_2 h\vec{\tau})\,\Psi(\mathbf{q} + {}^1\!/_2 h\vec{\tau})\,e^{-i\vec{\tau}\mathbf{p}}\,d\vec{\tau},$$

$$\frac{\partial f}{\partial t} = \frac{i}{h}\int\frac{1}{2m}\left(\vec{\eta} - \frac{e}{c}\mathbf{A}(\mathbf{r})\right)^2\left[f\left(\mathbf{r} + {}^1\!/_2 h\vec{\tau},\ \vec{\eta} - {}^1\!/_2 h\vec{\theta}\right)\right.$$

$$-f\left(\mathbf{r}-{}^1\!/_2h\vec{\tau},\ \vec{\eta}+{}^1\!/_2h\vec{\theta}\right)\Big]\exp\left[i\vec{\tau}\left(\vec{\eta}-\mathbf{p}\right)\right. \tag{3}$$

$$\left.+\,i\vec{\theta}\,(\mathbf{r}-\mathbf{q})\right]d\vec{\tau}d\vec{\eta}d\mathbf{r}d\vec{\theta}$$

$$-\frac{i}{h}\int U\left(\mathbf{q}-{}^1\!/_2h\vec{\tau}\right)-U\left(\mathbf{q}+{}^1\!/_2h\vec{\tau}\right)\Big]$$

$$\times\ f\left(\mathbf{q},\vec{\eta}\right)\exp\left[i\vec{\tau}\left(\vec{\eta}-\mathbf{p}\right)\right]d\vec{\tau}d\vec{\eta},$$

where $U=\alpha\,[(\rho/n_{s0})-1],\ \ \rho=\int f\,(\mathbf{q},\,\mathbf{p})\,d\mathbf{p},$

$$\Delta\mathbf{A}=-\frac{4\pi e}{mc}\int\left(\mathbf{p}-\frac{e}{c}\,\mathbf{A}\right)f\,(\mathbf{q},\,\mathbf{p})\,d\mathbf{p},\ \ \mathrm{div}\,\mathbf{A}=0. \tag{4}$$

We have considered only a transverse field. The system of nonlinear equations (3) and (4) has a solution $f_0(\mathrm{p})$ which corresponds to a homogeneous distribution of superconducting electrons:

$$\int f_0\,(\mathbf{p})\,d\mathbf{p}=n_{s0},\quad \mathbf{A}=0.$$

We investigated a solution slightly shifted from the homogeneous one:

$$f=f_0\,(\mathbf{p})+\varphi\,(\mathbf{q},\,\mathbf{p},\,t),$$

$$\varphi\ll f_0,\qquad \rho=n_{s0}+\rho_1\,(\mathbf{q},\,t). \tag{5}$$

Substituting Eq. (5) in Eqs. (3) and (4), and neglecting quadratic terms in ϕ and **A**, we obtained the system of linear equations for the determination of ϕ and **A**:

$$\frac{\partial\varphi}{\partial t}+\frac{\mathbf{p}}{m}\frac{\partial\varphi}{\partial q}=-\frac{i}{h} \tag{6}$$

$$\times\int\frac{e}{mc}\,(\mathbf{A}\,(\mathbf{r},\,t)\,\mathbf{p})\left[f_0\left(\mathbf{p}-{}^1\!/_2h\vec{\theta}\right)-f_0\left(\mathbf{p}+{}^1\!/_2h\vec{\theta}\right)\right]$$

$$\times\,\exp\left[i\vec{\theta}\,(\mathbf{r}-\mathbf{q})\right]d\vec{\theta}d\mathbf{r}-\frac{i\alpha}{hn_{s0}}\int\Big[\rho_1\left(\mathbf{q}-{}^1\!/_2h\vec{\tau}\right)$$

$$-\,\rho_1\left(\mathbf{q}+{}^1\!/_2h\vec{\tau},t\right)\Big]\ \times\,\exp\left[i\vec{\tau}\left(\vec{\eta}-\mathbf{p}\right)\right]f_0\left(\vec{\eta}\right)d\vec{\tau}d\vec{\eta},$$

$$\Delta\mathbf{A}=\frac{\mathbf{A}}{\delta^2}-\frac{4\pi e}{mc}\int\mathbf{p}\varphi\,(\mathbf{q},\,\mathbf{p})\,d\mathbf{p},\quad \mathrm{div}\,\mathbf{A}=0. \tag{7}$$

In the fundamental state $|\Psi|^2=n_{s0}$, whence $f_0=n_{s0}\delta(p)$ which corresponds to the state of total degeneracy in the Bose statistics. The expression for the excitation spectrum which is obtained from the requirements of the solvability of the system of equations (6) and (7), has the following form:

$$1=\frac{\alpha}{n_{s0}}\int\frac{[f_0\,(\mathbf{p}-{}^1\!/_2\mathbf{P})-f_0\,(\mathbf{p}+{}^1\!/_2\mathbf{P})]}{E-(\mathbf{P}\mathbf{p}/m)}\,d\mathbf{p}, \tag{8}$$

where, $E=h\omega$ is the energy of excitation, and $P=hk$ is the momentum of excitation. In obtaining Eq. (8), use was made of the transverse condition, and also of the fact that $f_0=n_{s0}\delta(\mathrm{p})$. After integration over p, we obtain

$$E^2=\frac{H^2_{\text{к.м}}}{4\pi mn_{s0}}\,\mathbf{P}^2+\frac{\mathbf{P}^4}{4m^2}; \tag{9}$$

we found that $\alpha=H^2_{\mathrm{km}}/4\pi n_{s0}$.

For small momenta,

$$E=(H_{\text{к.м}}/\sqrt{4\pi mn_{s0}})\,\mathbf{P}. \tag{10}$$

Thus we obtain an excitation of the acoustic type, the velocity of propagation of which is $v=H_{\mathrm{km}}/\sqrt{4\pi mn_{s0}}\approx10^5\,\mathrm{cm/sec}$.

The equation for the Fourier component of the vector potential $\mathbf{A}_\omega=\int\mathbf{A}e^{-i\omega t}dt$ has the following form:

$$\Delta\mathbf{A}_\omega=\frac{\mathbf{A}_\omega}{\delta^2}$$

$$-\frac{4\pi e\alpha}{mcn_{s0}}\int\frac{\mathbf{k}\omega}{\omega^2-(h^2k^4/4m^2)}\,\rho_{\mathbf{k}}e^{i\mathbf{kq}}d\mathbf{k}. \tag{11}$$

It follows from Eq. (11) that the current

$$\mathbf{j}=\frac{e\alpha}{mn_{s0}}\int\frac{\mathbf{k}\omega}{\omega^2-(h^2\mathbf{k}^4/4m^2)}\,\rho_{\mathbf{k}}e^{i\mathbf{kq}}d\mathbf{k}, \tag{12}$$

which is associated with the excitations under consideration, is screened at a distance of $\delta\approx10^{-5}\,\mathrm{cm}$. The mean value of the current is zero The spectrum which is obtained satisfies the criterion of superconductivity $v_c=[E/P]_{\min}>0$. In this case, the critical velocity v_c, beginning at which the energy of the current can be transformed into the energy of excitation, is given by $v_c\approx H_{\mathrm{km}}/\sqrt{4\pi mn_{s0}}\approx10^5\,\mathrm{cm/sec}$.

2. In the normally conducting state, the electronic heat capacity increases linearly with temperature, i.e., $C_n=\gamma T$. In the superconducting state, the linear term is missing from the expression for the electronic heat capacity. Available experimental data show that in a number of cases the heat capacity of the electrons in the superconducting state is proportional to the cube of the temperature, i.e., $C_s\sim T^3$.

At small values of the momenta, the spectrum under examination has an acoustical character (phonons). The thermodynamic functions for an excitation of the phonon type are well known[3] and have the form

$$F=-\frac{\pi^2\varkappa^4}{90h^3v^3}\,T^4; \tag{13}$$

$$S = \frac{2\pi^2\varkappa^4}{45h^3v^3}T^3; \quad C = \frac{2\pi^2\varkappa^4}{15h^3v^3}T^3.$$

Here F is the free energy, S the entropy, C the heat capacity excited in the superconducting state. We thus obtain the correct temperature dependence for C. If the value of the velocity of the excitation, $v = H_{\mathrm{km}}/\sqrt{4\pi m n_{s0}} \approx 10^5$ cm/sec is substituted in the expression for the heat capacity, then the correct order of magnitude is obtained. The correct value for the electronic heat capacity is obtained without the introduction of the concept of a large dielectric permeability.

If the particles described by the "effective" wave function obeyed Fermi statistics, then the velocity of the phonon type would have been 10^8 cm/sec. Consequently the calculated values of the thermodynamic functions are significantly less than those observed in the superconducting state. Moreover, for very small values of the parameter $\varkappa$ (for low concentration of superconducting electrons), excitations of the Fermi type would arise. Such excitations lead to the appearance of a linear term in T in the expression for the heat capacity.

In the calculation of the interaction, the linear parameter δ enters characteristically. We assume that destruction of the superconducting state by the thermal vibrations of the lattice takes place when $\lambda_{\mathrm{max}} \approx \delta$, where λ_{max} is the wavelength which corresponds to the maximum number of phonons for a given temperature. Following the work of De Launay[4], we assume that

$$\lambda_{\mathrm{max}} T \approx hs/\kappa,$$

where s is the velocity of sound in the lattice. We then get for the critical temperature the expression

$$\kappa T_k \approx hs/\delta \approx (H_{\mathrm{K,M}}/\sqrt{4\pi m n_{s0}})\, s,$$

from which it follows that $T_k \approx 1°$ and $TM^{1/2} = \mathrm{const}$.

---

[1] V. L. Ginzburg and L. D. Landau, J. Exper. Theoret. Phys. USSR **20**, 1064 (1950)

[2] V. L. Ginzburg, J. Exper. Theoret. Phys. USSR **21**, 979 (1951)

[3] E. M. Lifshitz, Supplement to the Russian translation of *Helium*, by V. Keesom.

[4] J. De Launay, Phys. Rev. **79**, 398 (1950)

Translated by R. T. Beyer

The Asymptote of Green's Function in Quantum Electrodynamics

E. S. FRADKIN

P. N. Lebedev Institute of Physics,
Academy of Sciences, USSR

(Submitted to JETP editor March 27, 1955)
J. Exper. Theoret. Phys. USSR **28**, 750-752
(June, 1955)

1. FROM the system of integral equations for Green's function in the presence of external sources of a photon field, one can show the relation*

$$G^{-1}(p, p' + s) - G^{-1}(p - s, p') = s_\mu \Gamma_\mu (p, p', s). \tag{1}$$

Equation (1) is a generalization of Ward's theorem, and, insofar as it follows from the exact equations, we shall in the future make much use of it. The system of renormalized equations for the Green's function in quantum electrodynamics may be written, to order e^2, as follows (we retain the notation of paper[1]):

$$\begin{aligned}\Gamma_\sigma (p, p - l, l) &= \gamma_\sigma + \frac{e^2}{\pi i} \\ \times \int \Big\{ &\Gamma_\mu (f, p - k, k)\, G(p - k)\, \Gamma_\sigma (p - k,\ p - k - l, l) \\ &\times G(p - k - l)\, \Gamma_\nu (p - k - l,\ p - l, - k) \\ &- \Gamma_\mu (p^0, p^0 - k, k)\, G(p^0 - k) \\ &\times \Gamma_\sigma (p^0 - k,\ p^0 - k, 0)\, G(p^0 - k) \\ &\times \Gamma_\nu (p^0 - k,\ p^0, - k)\Big\}\, D_{\mu\nu}(k)\, d^4k,\end{aligned} \tag{2}$$

$$\frac{\partial G^{-1}(p)}{\partial p_\mu} = \Gamma_\mu (p, p) \quad \text{or} \quad G^{-1}(p) - G^{-1}(p - k) = k_\mu \Gamma_\mu (p, p - k, k), \tag{3}$$

$$\begin{aligned}\frac{\partial D^{-1}(k^2)}{\partial k^2} &= 1 + e^2 P = 1 + \frac{e^2}{6\pi}\,\mathrm{Sp} \\ \times \int \Big\{ &\frac{\partial}{\partial k_\nu}\left[\Gamma_\mu (p, p - k, k)\, \frac{\partial G(p - k)}{\partial k_\nu}\, \Gamma_\mu (p - k, p, - k)\right] \\ &- \frac{\partial}{\partial k_\nu^0}\left[\Gamma_\mu (p, p - k^0, k^0)\, \frac{\partial G(p - k^0)}{\partial k_\nu^0} \right. \\ &\left. \times \Gamma_\mu (p - k^0, p_1 - k^0)\right]\Big\}\, G(p)\, d^4p,\end{aligned} \tag{4}$$

where $D_{\mu\nu} = \left(\delta_{\mu\nu} - \frac{k_\mu k_\nu}{k^2}\right) D(k^2) + \frac{k_\mu k_\nu}{k^4}\, d_l (k^2)$,

$$k^{0^2} = 0, \quad p^{0^2} = m^2.$$

The boundary values for D and G are:

$$(p^0 - m)\,G(p^0) = 1, \qquad k^0 D(k_0^2) = 1. \tag{5}$$

These equations for D and G differ somewhat from those in reference 1, and are revised so as to satisfy exactly Ward's relation. This allows a significant simplification in further calculations, such that we need not seek the so-called "small" corrections.(See reference 1). Let us look for the asymptote of G and D, at large momenta, in the form:

$$G^{-1}(p) = \alpha(p^2)\,\hat{p}, \quad D^{-1}(k^2) = \frac{k^2}{d(k^2)}, \tag{6}$$

From Eq. (3) it follows that

$$\Gamma_\mu = \alpha(f)\,\gamma_\mu, \tag{7}$$

where f is the largest of the momenta.

As a consequence of Eq. (3), Eq. (2) becomes a linear integral equation in α. After a simple calculation, we obtain from Eq. (2)

$$\frac{\partial\alpha(\xi)}{\partial\xi} = \frac{e^2}{4\pi}\,\alpha(\xi)\,d_l(\xi), \quad \xi = \ln\left(-\frac{p^2}{m^2}\right) \tag{8}$$

with the boundary value

$$\alpha(0) = 1. \tag{9}$$

From Eqs. (8) and (9) we get

$$\alpha(\xi) = \exp\left\{-\frac{e^2}{4\pi}\int_0^\xi d_l(z)\,dz\right\}. \tag{10}$$

To this approximation, as a result of Eq. (3), α completely drops out of the expression for the polarization operator P, which goes into the value given it in perturbation theory, i.e., one uses the free particle values of G and Γ. As the result of a simple calculation, we obtain from Eq. (4)

$$\frac{1}{d} = 1 - \frac{e^2}{3\pi}\ln\left(-\frac{p^2}{m^2}\right). \tag{11}$$

The asymptotes obtained coincide with those previously gotten by Landau, Abrikosov and Khalatnikov [1].

2. We shall show several general properties of renormalized theories.

I. The radiative corrections to the Green's function of Fermi- and Bose- fields, before renormalization, are equal to zero at infinite momenta. Indeed, let us look, as an example, at the Green's function for a photon. According to reference 2,

$$D_F(p) = z_3 D_{FC}(p), \qquad G_{FC} = \frac{1}{p^2} + \int_0^\infty \frac{f(\mu^2, e^2)}{p^2 + \mu^2}\,\frac{d\mu^2}{\mu^2},$$

$$z_3^{-1} = 1 + \int_0^\infty f(\mu^2, e^2)\,\frac{d\mu^2}{\mu^2}. \tag{12}$$

Since the theory is normalized, it follows from Eq. (12) that $D_F(p^2) = 1$ ($p^2 \to \infty$), i.e., the radiative corrections actually vanish.

II. If the derivative of the polarization operator with respect to the square of the external momentum is infinite for small momenta (and this occurs in existent calculations), then the renormalized charge is equal to zero. In the renormalized equations, where the self-action is absent and the charge is considered finite, this difficulty is manifested in the change in sign of the Green's function at large momenta, whereupon a fictitious singularity arises. The reason why the difficulty crops up lies in the fact that, since the self-action is infinite, the law of interaction at small distances ($r = 0$) is really not correct; in the renormalized equations the self-action is not used, but is effectively taken into account by the introduction of renormalized masses and charge. Considering the renormalized quantities as finite and equal to the experimental values, we correct the self-action (or the interaction at $r = 0$); however, the interaction at $r \to 0$ remains indefinitely increasing – leading to a contradiction to the finiteness of the self-action. If we use, instead of the renormalized charge, its theoretical value, then the Green's function does not change sign, but the renormalized charge itself proves to be zero. Actually, (see reference 3), D_{FC} is related to the polarization operator in the following way:

$$D_{FC} = \frac{1}{k^2(1 + e^2[\Pi(k^2) + \Pi(0)])}, \tag{13}$$

$$\Pi(k^2) = \frac{1}{6k^2 z_1}\,\mathrm{Sp} \times \int \gamma_\mu G(p + k)\,\Gamma_\mu(p + k, k)\,G(p)\,d^4p. \tag{14}$$

If $\Pi(0)$ is infinite ** (and since, according to (1), $\Pi(k^2)$ approaches zero as $k^2 \to \infty$), then D_{FC} changes sign, going through a pole at arbitrary finite e^2. According to theory

$$e^2 = \frac{e_0^2}{1 + e_0^2\,\Pi(0)}. \tag{15}$$

With this meaning for e^2, D_{FC} nowhere changes sign, but e^2 is equal to zero for any "bare" charge e_0^2.

In the case of small "bare" charge, the asymptote adduced in section I is exact and the renormalized charge is equal to zero. In the case, however, where the "bare" charge is large (which apparently happens in quantum electrodynamics [2]), all the diagrams of higher order than e^2, not considered in section I, become extremely important and may radically alter the asymptote found. Using Eq. (1) and property I, and neglecting terms of the type $(\gamma_\nu\gamma_\mu - \gamma_\mu\gamma_\nu) f(p^2)$ in the expression for $\left.\frac{\delta\Gamma_\mu}{\delta x_\nu}\right|_{k=0}$, one can show that $\Pi(0)$ remains infinite in the general case‡. Therefore, it seems likely that in quantum electrodynamics the renormalized charge is equal to zero. Since the experimental charge in quantum electrodynamics is small, one could eliminate the difficulty of the zero charge by a correction to the interaction at very large momenta, and a calculation of gravitational effects could make it, generally speaking, not inconsistent with the mathematical theory[5,1]

---

* The proof of this relation will be given separately.

** $\Pi(0)$ is always ≥ 0.

‡ A discussion of the use of the fact that $\Pi(0)$ is infinite is also given in reference 4

[1] L. D. Landau, A. A. Abrikosov and I. M. Khalatnikov, Dokl. Akad. Nauk SSSR 95, 773 (1954); 96, 261 (1954)

[2] M. Gell-Mann and F. E. Low, Phys. Rev 95, 1300 (1954)

[3] E. S. Fradkin, J. Exper. Theoret. Phys. USSR 26, 753 (1954)

[4] G. Kallen, Dansk. Mat. Phys. Med. 27, 12 (1953)

[5] M. A. Markov, J. Exper. Theoret. Phys. USSR 17, 9 (1947)

Translated by M. Rosen
140

The Optimum Length of an Undulator

A. N. MATVEEV
Moscow State University

(Submitted to JETP editor January 24, 1955)
J. Exper. Theoret. Phys. USSR 28, 760 (June, 1955)

As has been shown by Ginsburg [1], only the utilization of coherent radiation in an undulator [2,3], makes it possible to obtain considerable radiated power. At the same time, the power radiated from an undulator is directly proportional to its length (see, for example, reference 2); therefore it is desirable to increase the length of the undulator. However, these two contributions to the power radiated from an undulator are in contradiction with one another. As the electrons pass through the undulator, the conditions for coherent radiation become worse, in view of the spreading of the bunch. The resolution of this contradiction appears to be the imposition of a restriction on the length of the undulator.

Consider the definiteness, a spherical bunch of N electrons, in a coordinate system moving with the center of the bunch. Making use of the integral of motion $\frac{mv_r^2}{2} + \frac{e^2N}{r} = \frac{e^2N}{r_0}$, we find that the increase of the radius of the bunch by a factor p takes place during proper time $\Delta\tau$, according to the relation

$$\Delta\tau = \frac{1}{e}\sqrt{\frac{m}{2N}}\,[\sqrt{p(p-1)} \tag{1}$$

$$+ \ln(\sqrt{p} + \sqrt{p-1})]\, r_0^{3/2},$$

where r_0 is the initial radius of the bunch, with the initial rate of expansion assumed to be zero, and m and e are the rest mass and charge of the electron, respectively.

The condition for coherent radiation is that the dimensions of the electron bunch be small in comparison with the wavelength of the radiated waves. In order to obtain the wavelength λ in the laboratory system of coordinates, it is necessary to generate the wavelength $\lambda/\sqrt{1-\beta^2}$ in the coordinate system (with velocity $v = c\beta$) moving with the center of the oscillating bunch. In view of this, the condition for coherence is well fulfilled when $r_0 \sim \lambda$, and is completely violated when $p \sim E/mc^2$. When, as was assumed in references 1-3, the fields in the undulator are not too large, the velocities of the electrons are small with respect to a coordinate system moving with the center of the oscillating bunch, and therefore, an interval of proper time of the bunch is approximately equal to an interval of time in the coordinate system moving with the center of the oscillating bunch. Therefore, on the basis of Eq. (1), the time for complete loss of coherence in the laboratory system of coordinates is

$$\Delta t \approx \frac{1}{e}\sqrt{\frac{m}{2N}}\left(\frac{E}{mc^2}\right)^2 \lambda^{3/2}. \tag{2}$$

Denoting the length of the spatial period of the field in the undulator by l_0, and taking into account the equality $\lambda \sim l_0\left(\frac{mc^2}{E}\right)^2$, we find that the number q of spatial periods of the field in the undulator must in any case be no greater than

$$q_{\max} = \frac{c}{e}\sqrt{\frac{m}{2N}}\sqrt{\lambda} \approx \frac{10^6}{\sqrt{N}}\sqrt{\lambda} \;\; (\lambda \text{ cm}). \tag{3}$$

For example, with $\lambda \sim 1$mm and $N \sim 10^8$, we get $q_{max} \sim 30$. The existence of an initial velocity spread of the bunch when entering the undulator, and the impossibility of providing equally good injection conditions for each of the electrons of the bunch, shortens considerably the maximum possible length of the undulator. Therefore, an undulator with too great a number of spatial periods of the field is undesirable.

[1] V. L. Ginsburg, Izv. Akad. Nauk SSSR, Ser. Fiz. 11, 165 (1947)

[2] H. Motz, J. Appl. Phys. 22, 527 (1951)

[3] H. Motz, W. Thon and R. N. Whitehurst, J. Appl. Phys. 24, 826 (1953)

Translated by D. Lieberman
145

On the Paper "The Excitation Spectrum of a System of Many Particles"

V. P. SILIN
P. N. Lebedev Institute of Physics,
Academy of Sciences, USSR

(Submitted to JETP editor February 7, 1955)
J. Exper. Theoret. Phys. USSR 28, 749-750
(June, 1955)

In considering the correlation of identical particles, one should distinguish between the correlation of particles which are in the same spin state and the correlation of particles in different spin states. In reference 1 an approximation to the binary distribution was used appropriate for the calculation of the correlation of identical particles in the same spin state. Strictly speaking, this is realized only in the case of particles having no spin. Hence the results of reference 1 are completely valid in the case of spinless Bose particles. However, in the case of electrons, for example, it is necessary, generally speaking, to make several further considerations.

Let $\rho^{(+)}(\mathbf{q}_1', \mathbf{q}_1)$ and $\rho^{(-)}(\mathbf{q}_1', \mathbf{q}_1)$ be the density matrices for electrons with spin projections $+\frac{1}{2}$ and $-\frac{1}{2}$, respectively. For particles in the same spin state, the coordinate part of the wave function is anti-symmetric. Hence the binary density matrix can be approximated as follows:

$$\rho_2^{(+,+)}(\mathbf{q}_1', \mathbf{q}_2'; \mathbf{q}_1, \mathbf{q}_2) = \rho^{(+)}(\mathbf{q}_2', \mathbf{q}_1)\,\rho^{(+)}(\mathbf{q}_2', \mathbf{q}_2) - \rho^{(+)}(\mathbf{q}_1', \mathbf{q}_2)\,\rho^{(+)}(\mathbf{q}_2', \mathbf{q}_1). \tag{1}$$

In the case of particles in different spin states, the coordinate part of the wave function is symmetric; therefore*

$$\rho_2^{(+,-)}(\mathbf{q}_1', \mathbf{q}_2'; (\mathbf{q}_1, \mathbf{q}_2) = \rho^{(+)}(\mathbf{q}_1', \mathbf{q}_1)\,\rho^{(-)}(\mathbf{q}_2', \mathbf{q}_2) + \rho^{(+)}(\mathbf{q}_1', \mathbf{q}_2)\,\rho^{(-)}(\mathbf{q}_2', \mathbf{q}_1). \tag{2}$$

Relations (1) and (2) allow one to obtain the following equation for the quantum distribution function $f^{(+)}(\mathbf{q},\mathbf{p})$ of an electron with a positive spin projection. (The notation used is that adopted in reference 1):

$$\begin{aligned}&\frac{\partial f^{(+)}}{\partial t} + \frac{\mathbf{p}}{m}\frac{\partial f^{(+)}}{\partial \mathbf{q}} + \frac{i}{\hbar}\frac{1}{(2\pi)^3}\\
&\times\int d\mathbf{q}'d\vec{\tau}d\mathbf{p}'d\mathbf{p}''\left[U\left(\left|\mathbf{q}-\mathbf{q}'+\frac{\hbar\vec{\tau}}{2}\right|\right) - U\left(\left|\mathbf{q}-\mathbf{q}'-\frac{\hbar\vec{\tau}}{2}\right|\right)\right.\\
&\times\left\{e^{i\vec{\tau}(\mathbf{p}''-\mathbf{p})} f^{(+)}(\mathbf{q}, \mathbf{p}'')\,[f^{(+)}(\mathbf{q}', \mathbf{p}') + f^{(-)}(\mathbf{q}';\mathbf{p}')]\right.\\
&+ \exp\left[i\vec{\tau}\left(\frac{\mathbf{p}'+\mathbf{p}''}{2} - \mathbf{p}\right)\right.\\
&\left.+\frac{i(\mathbf{q}'-\mathbf{q})(\mathbf{p}'-\mathbf{p}'')}{\hbar}\right] f^{(+)}\left(\frac{\mathbf{q}+\mathbf{q}'}{2} - \frac{\hbar\vec{\tau}}{4}, \mathbf{p}'\right)\\
&\times\left[f^{(-)}\left(\frac{\mathbf{q}+\mathbf{q}'}{2} + \frac{\hbar\vec{\tau}}{4}, \mathbf{p}''\right)\right.\\
&\left.\left.\left. - f^{(-)}\left(\frac{\mathbf{q}+\mathbf{q}'}{2} + \frac{\hbar\vec{\tau}}{4}, \mathbf{p}''\right)\right]\right\}\right. = 0.\end{aligned} \tag{3}$$

The equation for $f^{(-)}$ is obtained from Eq. (3) by making the substitutions (+) → (–), and (–) → (+). Being interested in the fluctuations of the density, let us look at the equation for the function $f = f^{(+)} + f^{(-)}$. This equation is:

$$\begin{aligned}&\frac{\partial f}{\partial t} + \frac{\mathbf{p}}{m}\frac{\partial f}{\partial \mathbf{q}}\\
&+\frac{i}{\hbar}\frac{1}{(2\tau)^3}\int d\mathbf{q}'d\vec{\tau}d\mathbf{p}'d\mathbf{p}''\left[U\left(\left|\mathbf{q}-\mathbf{q}'+\frac{\hbar\vec{\tau}}{2}\right|\right)\right.\\
&\left.-U\left(\left|\mathbf{q}-\mathbf{q}'-\frac{\hbar\vec{\tau}}{2}\right|\right)\right] \times \left\{e^{i\vec{\tau}(\mathbf{p}''-\mathbf{p})} f(\mathbf{q}, \mathbf{p}'')\, f(\mathbf{q}', \mathbf{p}')\right.\\
&- \Phi\left(\frac{\mathbf{q}+\mathbf{q}'}{2} - \frac{\hbar\vec{\tau}}{4}, \mathbf{p}'\right) \times \Phi\left(\frac{\mathbf{q}+\mathbf{q}'}{2} + \frac{\hbar\vec{\tau}}{4}, \mathbf{p}''\right)\\
&\times\exp\left[i\vec{\tau}\left(\frac{\mathbf{p}'+\mathbf{p}''}{2} - \mathbf{p}\right)\right.\\
&\left.\left.+ i(\mathbf{q}'-\mathbf{p})(\mathbf{p}'-\mathbf{p}'')/\hbar\right]\right\} = 0,\end{aligned} \tag{4}$$

Where $\Phi = f^{(+)} = f^{(-)}$. Equation (4) differs from the corresponding equation in the selfconsistent field approximation by the presence of terms containing Φ. If, in the equilibrium state $f^{(+)} = f^{(-)}$, then upon linearization of Eq. (4) the terms containing Φ contribute nothing whatever. Therefore the vibration spectrum in this case coincides with that obtained in the selfconsistent field approximation. In the case where $f^{(-)} = 0$, the results of paper 1 are obtained.

However, in addition to density fluctuations, for particles with spin, new excitations arise, characterized by the function Φ and similar to a spin wave. The equation for the function Φ, which is gotten from Eq. (3), is:

$$\begin{gathered}\frac{\partial\Phi}{\partial t} + \frac{\mathbf{p}}{m}\frac{\partial\Phi}{\partial\mathbf{q}} \\ + \frac{l}{\hbar}\frac{1}{(2\pi)^3}\int d\mathbf{q}'d\vec{\tau}d\mathbf{p}'d\mathbf{p}''\left[U\left(\left|\mathbf{q}-\mathbf{q}'+\frac{\hbar\vec{\tau}}{2}\right|\right)\right. \\ \left.-U\left(\left|\mathbf{q}-\mathbf{q}'-\frac{\hbar\vec{\tau}}{2}\right|\right)\right] \times \left\{e^{i\vec{\tau}(\mathbf{p}'-\mathbf{p})}\Phi(\mathbf{q},\mathbf{p}'')f(\mathbf{q}',\mathbf{p}')\right. \\ -\Phi\left(\frac{\mathbf{q}+\mathbf{q}'}{2}+\frac{\hbar\vec{\tau}}{4},\mathbf{p}''\right)f\left(\frac{\mathbf{q}+\mathbf{q}'}{2}-\frac{\hbar\vec{\tau}}{4},\mathbf{p}'\right) \\ \left.\times\exp\left[i\vec{\tau}\left(\frac{\mathbf{p}'+\mathbf{p}''}{2}-\mathbf{p}\right)-\frac{i(\mathbf{q}'-\mathbf{q})(\mathbf{p}'-\mathbf{p}'')}{\hbar}\right]\right\} = 0.\end{gathered} \tag{5}$$

Note that for particles with spin one, one should write the opposite sign in front of the curly brackets in Eqs. (3), (4) and (5). If $\Phi = 0$ in the equilibrium state, then upon linearizing Eq. (5)

$$f = f_0 + \varphi_{\mathbf{k}}e^{i\mathbf{kq}},\ \Phi = \Phi_{\mathbf{k}}e^{i\mathbf{kq}}$$

we obtain the following equation, describing the spin fluctuation**,

$$\begin{gathered}\frac{\partial\Phi_{\mathbf{k}}}{\partial t} + \frac{i\mathbf{kp}}{m}\Phi_{\mathbf{k}} \pm \frac{i}{\hbar}\Phi_{\mathbf{k}}\int d\mathbf{p}'\nu\left(\left|\frac{\mathbf{p}-\mathbf{p}'}{\hbar}\right|\right)f_0 \\ \times\left(\mathbf{p}'-\frac{\hbar\mathbf{k}}{2}\right) \mp \frac{i}{\hbar}f_0\left(\mathbf{p}-\frac{\hbar\mathbf{k}}{2}\right)\int d\mathbf{p}'\nu \\ \times\left(\left|\frac{\mathbf{p}-\mathbf{p}'}{\hbar}\right|\right)\Phi_{\mathbf{k}}(\mathbf{p}') = 0.\end{gathered} \tag{6}$$

The upper sign goes with spin ½, the lower with spin 1. For the case of spin 1 and the temperature equal to zero, $f_0(p) = n_0\delta(\mathbf{p})$. In this case the solution to Eq. (6) is

$$\Phi_{\mathbf{k}}(\mathbf{p}) = e^{-i\omega t}\delta\left(\mathbf{p}-\frac{\hbar\mathbf{k}}{2}\right)c(\mathbf{k}),$$

where

$$\hbar\omega = \hbar^2k^2/2m.$$

Thus the spin excitation spectrum of a degenerate Bose gas of spin one particles looks like the spectrum of noninteracting particles. Consequently one can say that (insofar as it is possible to consider liquid helium as a weakly ideal gas) the superfluidity of helium is explained, apparently, not only by the Bose statistics, which the He atoms obey, but also by their lack of spin.

In conclusion, I wish to thank Professor V. L. Ginzburg for a discussion of the results.

---

* For spin one particles, one should take the sum in Eq. (1) rather than the difference; and in Eq. (2) the difference rather than the sum.

** Such an equation is gotten for $f^{(-)}$ in the case where $f_0^{(-)} = 0$, which corresponds to the case of a system of particles whose spins in the ground state are oriented in one direction. In contrast to the ordinary theory of spin waves, Eq. (6) permits the calculation of the interaction not only with nearby particles, but also with those distantly situated.

[1] V. P. Silin, J. Exper. Theoret. Phys. USSR **27**, 269 (1954)

Translated by M. Rosen
139

Detection of the Polarization of Beams of Fast Particles by Means of Nuclear Photoemulsions

E. L. Grigor'ev
Institute of Nuclear Research of the Academy of Sciences, USSR

(Submitted to JETP editor February 7, 1955)
J. Exper. Theoret. Phys. USSR **28**, 761 (June, 1955)

THE experiments of scattering of high energy particles point to the presence of non-central forces in the interactions between nucleons. The presence of such forces results in polarization of beams of the scattered particles. The magnitude of this polarization is experimentally determined by means of the measurement of the asymmetry in double scattering. The value of asymmetry is generally determined from the equation:

$$\varepsilon(\theta) = \frac{I(\theta,\ \varphi = 0^\circ) - I(\theta,\ \varphi = 180^\circ)}{I(\theta,\ \varphi = 0^\circ) + I(\theta,\ \varphi = 180^\circ)},$$

where $I(\theta, \phi = 0)$ and $I(\theta, \phi = 180°)$ are the numbers of particles scattered in second scattering at angle θ to the left or right of the direction of motion of the polarized particles.

At the present time a large number of experiments is devoted to the observation of polarization of beams of fast particles[1-4]. In all similar experiments the direction of particles undergoing second scattering was done by means of scintillation counters. In the present work it was attempted to determine the polarization of beams of protons and neutrons by photographic means from the observation of quasi-elastic scattering of protons from the nucleons of the nuclei of elements that make up the emulsion. The proton beam was obtained by scattering, at an angle of 18°, the internal beam of energy 670 mev in the synchrocyclotron. The scatterer-polarizer was Be target of thickness 4 cm. The medium energy of protons in the partly polarized beam was 570 mev[5]. In this beam were placed photographic plates with emulsions 200μ thick, capable of recording relativistic particles. In one of the experiments the plane of the emulsion was the same as the plane of the first scattering, in other experiments the plane of emulsion was perpendicular to the plane of the first scattering. The placing of the plates was thus selected to correspond to the planes of azimuthal angles $0 - 180^\circ$ and $90^\circ - 270^\circ$.

The stars generated by the protons in the emulsion contained gray tracks whose projections were in the interval of scattering angles $0^\circ \leq \theta \leq 50^\circ$ to the right and to the left depending on the direction of motion of the initial proton beam. Only those tracks were counted whose length exceeded $400\ \mu$ and whose density of grains corresponded to proton energies above 200 mev. In plates placed in the $0^\circ - 180^\circ$ plane, there were recorded 735 such tracks to the right while 922 tracks were recorded to the left. The corresponding value of the asymmetry is $\epsilon(\theta) = 0.11 \pm 0.03$. In plates placed in the $90^\circ - 270^\circ$ plane similarly 203 and 215 tracks were found to the right and left respectively. These values give $\epsilon(\theta) = 0.03 \pm 0.05$ which shows the presence of asymmetry in the $90^\circ - 270^\circ$ plane, as should be expected.

Under the same conditions of selection of tracks, measurements of asymmetry were made from gray tracks in stars produced by neutrons. A beam of neutrons with a broad energy spectrum was produced by charge exchange of protons in a Be target. Neutrons that were scattered from the target at angle 20° to the direction of motion of the proton beam in synchrocyclotron were incident on a photographic plate placed in the plane of the first scattering. In this case the following tracks were registered: to the right 667, to the left 747, yielding the asymmetry 0.06 ± 0.03.

The asymmetry of emerging fast particles after quasi-elastic collisions, found in the described experiments, shows that beams of protons and neutrons originating from interactions of protons of energy 670 mev with Be nuclei are partially polarized.

---

[1] L. F. Wouters, Phys. Rev. **84**, 1069 (1951)

[2] C. L. Oxley, W. F. Cartwright, J. Rouvina, Phys. Rev. **93**, 806 (1954)

[3] A. Roberts, J. Tinlot, E. M. Hafner, Phys. Rev. **95**, 663 (1954)

[4] H. G. de Carvalho, E. Heiberg, J. Marshall, L. Marshall, Phys. Rev. **94**, 1796 (1954)

[5] G. D. Stoletov, S. B. Nurushev, Iu. P. Kumekin, Report of the Institute of Nuclear Research of the Academy of Sciences USSR, 1954

Translated by M. Stevenson
146

The Excitation of Ultrasonic Vibrations by Ponderomotive Forces

S. I. Aksenov, B. P. Vikin and
K. V. Vladimirskii
P. N. Lebedev Institute of Physics,
Academy of Sciences, USSR

(Submitted to JETP editor February 12, 1955)
J. Exper. Theoret. Phys. USSR **28**, 762-764 (June, 1955)

DURING the work with apparatus intended for investigation of nuclear magnetic resonance[1], an interfering resonance effect was observed at frequencies of the order of several megacycles. It was found that this effect was produced by excitation of ultrasonic vibrations by ponderomotive forces in the copper conductor of which the spectrometer coil was constructed. With each of the coils used a series of resonance peaks was observed during a change of the working frequency. The amplitudes of the peaks exceeded considerably the noise level of the instrument. The relative width of the peaks was of the order of magnitude 1:100. The amplitude of the peaks increased linearly with the increase in depth of modulation of the field. The instantaneous values of the other losses present in the circuit depend on the field quadratically. In field of 10^4 oersteds with doubled amplitude of the modulation field (15 oersteds) the strongest resonant lines correspond to modulation of autodyne radiofrequency spectrometer of $\Delta U/U \sim 10^{-6}$. Since the spectrometer was used in a region far from the threshold of self-excitation, this is the change in the Q of the coil as well. The full change in the Q of the coil on application of the field of 10^4 oersteds is $\Delta Q/Q \sim 10^{-3}$. This ratio gives the fraction of energy which was dissipated in generation of the ultrasonic waves.

The connection of the phenomenon with the excitation of ultrasonic vibrations was indicated by the strong decrease of the resonance peaks after application of a thick layer of lacquer. Experiments with coils of different geometry showed that the resonant frequencies depend only on the diameter of the conductor. During a change of the diameter of the conductor, the product of the resonant frequency and the diameter of the conductor remains constant. As a result, it is natural to postulate that resonant frequencies correspond to the natural frequencies of vibration in the mass of the cylindrical conductor. The displacements would lie in the plane of the cross section of the conductor and would not be dependent on the coordinate in the direction of the axis of the conductor (this postulate agrees with the nature of the forces that excite the vibrations). One of the three equations for the free vibrations of a circular cylinder then turns out to be an identity. The solution of the problem was obtained from the solution of vibrations of a circular plate in its cross section [2]. The following values were used for the velocity of propagation of the longitudinal and lateral vibrations in copper: $v_l = 4700$ m/sec, $v_t = 2260$ m/sec[3].

The nume ical solution of the equations yielded the following eigenvalues of the product of the wave number ω/v_l and the radius of the conductor:

$$\begin{array}{lll} & \alpha_{21} = 1.12. & \alpha_{11} = 1.38; \\ \alpha_{31} = 1.77; & \alpha_{22} = 2.13; & \alpha_{01} = 2.18; \\ \alpha_{41} = 2.22; & \alpha_{02} = 2.46; & \alpha_{32} = 2.96; \\ \alpha_{12} = 3.18; & \alpha_{13} = 3.72; & \alpha_{42} = 3.74; \\ \alpha_{23} = 3.85; & \alpha_{03} = 4.05; & \alpha_{33} = 4.48; \\ \alpha_{14} = 4.78; & \alpha_{24} = 4.98; & \alpha_{04} = 5.43. \end{array}$$

The first subscript determines the angular dependence of the eigenfunction of the type cos $n\vartheta$. the second subscript (the order of the root) determines the nature of the radial dependence. The eigenvalues α_{01}, and α_{04} correspond to the radial vibrations, the eigenvalues α_{02} and α_{03} to tangential vibrations. The deviation of the calculated constants from the results of the measurements do not exceed 2%:

Experiment I (diameter of conductor 0.51 mm):
$\alpha_{21} = 1.12$; $\alpha_{11} = 1.38$; $\alpha_{01} = 2.17$;

Experiment II (diameter of conductor 1mm):
$\alpha_{01} = 2.18$; $\alpha_{02} = 2.48$; $\alpha_{32} = 2.98$; $\alpha_{12} = 3.20$;
$\alpha_{13} = 3.76$; $\alpha_{03} = 4.08$;

Experiment III (diameter of conductor 1.5 mm):
$\alpha_{12} = 3.19$; $\alpha_{12} = 3.75$; $\alpha_{23} = 3.88$; $\alpha_{03} = 4.08$;
$\alpha_{14} = 4.82$; $\alpha_{24} = 5.05$; $\alpha_{04} = 5.49$.

The lower modes of vibration were dominantly excited. The most strongly excited vibrations were those corresponding to the eigenvalues α_{11}, α_{12}, since the angular dependence of the displacement is the same as that of the ponderomotive forces. The resonance, corresponding to the eigenvalue α_{32}, was observed in the form of a weak line, the resonance corresponding to α_{31} was observed only in the work with aluminum conductors.

The excitation of vibrations whose angular dependence was different from the angular dependence of the ponderomotive forces and the considerably greater width of the resonance lines observed during the experiments, can be explained by the presence of a firm mechanical contact between the turns of the coil and the frame. The damping of ultrasonic vibrations in metals, known from other measurements [3], should bring the relative width to the order of magnitude 10^{-3}. It is interesting to note that at the frequency of 12.5 mc, a narrow resonance line was observed with largest amplitude with a coil made of lead conductor of diameter 1 mm. This points to small damping in lead at those frequencies. Splitting of some resonance lines was observed during the experiments but was not followed up in detail.

Using the experimental values of the widths of the resonance lines, an estimate of the magnitude of the effect may be made. The ponderomotive forces can be considered as applied to the surface of the metal, since the skin depth is in the present experimental conditions considerably smaller than the diameter of the conductor and the wavelength of the ultrasonic waves. The power of the ultrasonic waves, emitted from a unit surface area of the metal into the mass of the conductor is inside the resonance (in the absence of standing waves), within an order of magnitude equal to:

$$P_u \sim f^2 v_t / 2\mu,$$

where f is the surface density of the ponderomotive forces, μ is the shear modulus. The relationship of this power to the total power around the circumference is

$$P_u / P_{tot} \sim H^2 v_t \, \delta\lambda / 2\mu,$$

where δ is the skin-depth and λ is the conductivity. For $H = 10^4$ oersteds and frequency 3×10^6 cps and $\delta \sim 4 \times 10^{-3}$ cm, $P_s / P_{tot} \sim 5 \times 10^{-5}$. Multiplying this number by the factor obtained from the experimental line widths a number is obtained, close to the experimental value $P_s / P_{tot} \sim 10^{-3}$. This result relates to the modes of vibration that are most strongly excited.

---

[1] S. I. Aksenov and K. V. Vladimiskii, Dokl. Akad. Nauk USSR **96**, 37 (1954)

[2] A. Liav, *Mathematical Theory of Elasticity*, ONTI, 1935

[3] L. Bergman, *Der Ultraschall*, Zurich, 1954

Translated by M. Stevenson
148

The Fine Structure of the Spectrum of the Paramagnetic Resonance of the Ion Cr^{3+} in Chromium Corundum

A. A. Manenkov and A. M. Prokhorov
P. N. Lebedev Institute of Physics, Academy of Sciences, SSSR

(Submitted to JETP editor February 26, 1955)
J. Exper. Theoret. Phys. USSR **28**, 762 (June, 1955)

THE paramagnetic resonance of chromium slats has been studied mostly in alums. The crystalline electric field, acting on a chromium ion in these combinations, has trigonal symmetry, and creates the splitting of two Kramers spin doublets (in the absence of an external magnetic field) in the interval from 0.12 to 0.18 cm^{-1}, depending on the type of alum[1].

We have investigated the spectrum of the paramagnetic resonance in a strong solution Al_2O_3- Cr_2O_3 (chromium corundum), at a chromium concentration of 0.05%. Earlier, this combination was investigated by Kashaev[2]; however, the author failed to explain the spectrum observed by him. We investigated the above-named combination at two frequencies, ν_1= 11970 mc/sec and ν_2=8960 mc/sec, at room temperature.

Chromium corundum represents a uniaxial crystal. When the axis of symmetry of the crystal is parallel to the direction of the applied external magnetic field, a fine structure of the spectrum of paramagnetic resonance is observed, consisting of three lines, which correspond to an electronic spin of Cr^{3+} equal to 3/2. At the frequency ν_2 =8960 mc/sec. two of the observed lines are due to the magnetic dipole transitions $M = 3/2 \leftrightarrow 1/2$, and one of the lines is due to the transition $M = 1/2 \leftrightarrow -1/2$. The transition $M = -3/2 \leftrightarrow -1/2$ is not observed at this frequency, since the initial splitting of the levels $M = \pm 1/2$ and $M = \pm 3/2$, created by the internal crystalline electric field, is greater than $h\nu_2$. At the frequency ν_1 = 11970 mc/sec the observed lines of the fine structure are due to the transitions

$$M = 3/2 \leftrightarrow 1/2, \quad M = 1/2 \leftrightarrow -1/2,$$

$$M = -3/2 \leftrightarrow -1/2.$$

When the axis of symmetry is perpendicular to the direction of the external magnetic field, two lines are observed at the frequency ν_2 =8960 mc/sec, and four lines at the frequency ν_1 =11970 mc/sec. Here in agreement with theory, the relative intensity of the lines depend on the angle between the axis of symmetry of the crystal and the direction of the radiofrequency field.

Assuming that the chromium ion is acted on by an electric field with trigonal symmetry, the observed spectrum may be described with the aid of the following Hamiltonian[1].

$$\hat{H} = D[\hat{S}_z^2 - 1/3\, S(S+1)] + g_{\parallel}\beta H_z \hat{S}_z + g_{\perp}\beta(H_x \hat{S}_x + H_y \hat{S}_y),$$

where D is a constant characterizing the splitting of the levels in the crystalline electric field, S is the electron spin, $\hat{S}_x$, $\hat{S}_y$, $\hat{S}_z$ are the components of the spin operator, g_{11} and $g_{\perp}$ are spectroscopic splitting factors corresponding to parallel and perpendicular orientation of the crystal with respect to the external magnetic field, β is the Bohr magneton, and H_x, H_y, H_z are the components of the magnetic field intensity.

The initial splitting of the spin levels in the absence of the magnetic field $|2D|$, was found to be 0.3824 cm^{-1}, which exceeds the splitting in alum by more than a factor of two. The g-factors are, $g_{\parallel} = 1.984 \pm 0.0006$; $g_{\perp} = 1.9867 \pm 0.0006$.

---

[1] B. Bleaney and K. W. H. Stevens, Rep. Progr. Phys., **16**, 108 (1953)

[2] S. Kh. G. Kashaev, Dissertation, Molotov University, 1954

Translated by D. Lieberman
147

The Radiation of CO_2 in the Region of 15μ in an Electric Discharge

N. Ia. Dodonova and V. V. Sobolev
Leningrad State University

(Submitted to JETP editor January 2, 1955)
J. Exper. Theoret. Phys. USSR **28**, 764-766 (June, 1955)

THE investigation of radiation from electric discharge through CO_2 in the region of 15

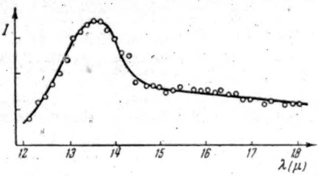

FIG. 1. The emission spectrum of CO_2 in discharge in the region 12-18μ.

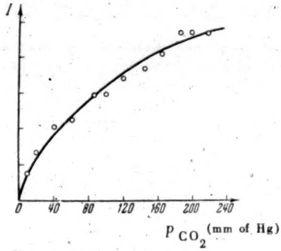

FIG. 2. The dependence of the intensity of the CO_2 emission band at 13.7 μ on the pressure of CO_2 in the discharge tube.

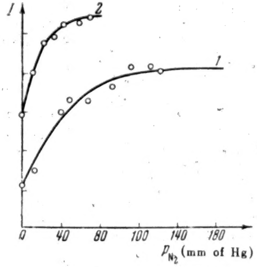

FIG. 3. The dependence of the intensity of the CO_2 emission band at 13.7 μ on the pressure of N_2. Curve 1: $p_{CO_2} = 8$ mm Hg, Curve 2: $p_{CO_2} = 20$ mm Hg;

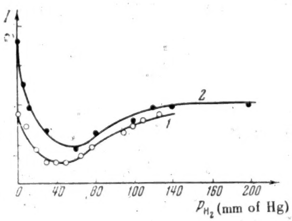

FIG. 4. The dependence of the intensity of the CO_2 emission band at 13.7 μ on the pressure of H_2. Curve 1: $p_{CO_2} = 20$ mm Hg; Curve 2: $p_{CO_2} = 40$ mm Hg.

microns is of interest because it would enlarge our knowledge of excitation, dissipation and transfer of vibration of energy of molecules.

Terenin and Neuimin[1] have discovered in the emission spectrum of CO_2, produced by an electric discharge, bands at 4.65 and 2.8 microns. These bands correspond to the unsymmetric vibration of the molecule and the combination band with simultaneous change of the quantum numbers of unsymmetric and symmetric vibrations. As is well known the absorption band due to deformed vibration of CO_2 is at 14.7μ. The corresponding emission band was found in the emission spectrum of hot gas at 14.1μ and in the Bunsen flame at 13.1μ[2]. In references 3 and 4 the emission spectrum of CO_2 was studied in the region of 15μ, but no emission bands were found. The authors of that work have shown that their apparatus was sensitive to detect bands 50 times weaker than bands at 4.4μ that were observed in the flame spectrum. Silverman, Hornbeck and Herman[5] discovered two bands with maxima at 15 and 13.85μ in the emission spectrum of CO_2 heated to 1400° K and flame spectrum generated by combustion of CO in oxygen. The authors point out that the intensity of these bands is very low.

Both the discharge tube and the source of low frequency voltage used in the present work have been described previously[6]. The measurements were made at pressures between 10 and 200 mm Hg, and with discharge current 280 ma. The discharge current was maintained constant as pressure of the gas changed. The spectrum was observed through a hermetically sealed spectrometer with KCL prism. To absorb moisture and CO_2 found in the air, $CaCl_2$ and KOH were placed inside. The spectrometer was placed closely to a window in the discharge tube made of sodium chloride. The widths of the inlet and outlet slits of the spectrometer were 1mm. As a detector a bolometer was placed directly at the outlet slit of the spectrometer. The sensitive area of the bolometer was 1×8 mm^2 and the sensitivity was 0.57 V/W. The bolometer voltage was amplified using a photo-electrooptical FEOU-15[7], with additional cascade photo-electrooptical amplification. The galvanometer deflection at the output of the FEOU-15 was amplified by a photo-electrooptical amplifier, constructed in our laboratory. The sensitivity of the FEOU-15 was 1.5×10^{-9} V/mm at 2 meters. The application of the additional cascade amplifier increased the sensitivity approximately 90 times.

Emission band was maximum at about 13.7 microns (Fig. 1) was observed in the emission spectrum of CO_2 . The band was about 350 times weaker than the band at 4.65μ. Within the limits of accuracy of the measurements the maximum of the observed band coincides with the maximum of one of the two bands in the flame emission spectrum of $CO + O_2$ and of hot CO_2 [5] at 13.85μ.

It should be noted that while the maximum of the emission band at 4.65 μ corresponding to the unsymmetric vibration of the molecule is displaced in the direction of longer wavelength in comparison with the absorption band at 4.25μ, the maximum of the emission band at 13.7μ corresponding to deformed vibration of the molecule is displaced in the direction of the shorter wavelengths as compared with the absorption band at 14.7μ. The band with maximum at 15μ which is observed in the flame spectrum of $CO + O_2$ and hot CO_2 discharge was not observed by us in the excited emission spectrum of CO_2. The absence of the band in the spectrum may be explained by strong absorption of radiation in that region by CO_2 gas that filled the discharge tube. The emitted radiation passes through a distance 1.5 and 8 cm in the discharge tube, depending on the experimental conditions. It is evident that even with a thickness of the absorbing layer as small as 1.5 cm the absorption is so strong that radiation at 15μ is fully absorbed.

The observed dependence of the emission band at 13.7μ on pressure of CO_2 in the discharge tube is shown if Fig. 2. This curve has the same character as the one for the band at 4.65μ [1]. The addition of nitrogen or hydrogen which have no emission spectra in the infrared region, respectively increase and decrease the intensity of the band at 13.7μ (Fig. 3 and 4). In the case of unsymmetric vibration of the molecule CO_2 (the emission band at 4.65μ) the increase of intensity of the emitted radiation also took place on addition of nitrogen. This increase was explained by Terenin and Neuimin by greater efficiency of molecular transfer of the vibrational quanta between molecules of CO_2 and N_2 . A similar point of view cannot be taken to explain the increase of the intensity of the band at 13.7 μ on addition of nitrogen, since in that case the vibrational quanta of CO ($\nu \sim 700$ cm^{-1}) and nitrogen ($\nu \sim 2000$cm^{-1}) are very different.

The authors wish to express their gratitude to A. N. Terenin under whose guidance the present work was carried out.

---

[1] A. N. Terenin and T. G. Neuimin, Izv. Akad. Nauk SSSR, Ser. Khim. **5**, 2469 (1942)

[2] H. Rubens and E. Aschkinass, Ann.d. Phys. **64**, 584 (1898); Astrophys. J. **8**, 176 (1898)

[3] C. R. Bailey and H. H. Lih, Trans. Farad Soc. **25**, 29 (1929)

[4] W. E. Garner and E. H. Johnson, Phil Mag. **3**, 97 (1927)

[5] S. Silverman, G. A. Hornbeck and R. C. Herman, J. Chem. Phys. **16**, 155 (1948)

[6] H. Ia. Dodonova, Dokl. Akad. Nauk SSSR **98**, 753 (1954)

[7] B. P. Kozyrev, Uspekhi Fiz. Nauk **44**, 173 (1951)

Translated by M. J. Stevenson
149

The Yield and Angular Distribution of Photoneutrons of High Energy

P. S. BARANOV AND V. I. GOL'DANSKII
P. N. Lebedev Institute of Physics,
Academy of Sciences, USSR

(Submitted to JETP editor January 24, 1955)
J. Exper. Theoret. Phys. USSR **28**, 746-748 (June, 1955)

A NUMBER of investigations has been carried out in recent years of photonuclear reactions occurring under the action of γ – quanta with energies of the order of tens and hundreds of mev. However, there still does not exist a satisfactory model describing such reactions at photon energies higher than 50 mev. For the construction of a model, studies are required of the emission by the nuclei of protons, as well as of neutrons, under the action of high energy photons. Although there exists a large number of investigations on the emission of high energy photoprotons, similar investigations for photoneutrons were, until recently, practically non-existent. Moreover, the data on the emission by nuclei of high energy photoneutrons are of great interest, particularly since the most widely held theory of nuclear interaction of high energy protons is based on the so called "double-nucleon" model, according to which the photons interact in the nucleus with the pairs of proton-neutron "quasi-deuterons". Also, it should be noted that there does not yet exist a satisfactory theory describing the function of excitation and the angular distributions at photon energies higher than 50 mev for even the simplest photonuclear reaction, the splitting of deuterium, with which, in accordance with this model, it is necessary to compare the nuclear reactions in complex nuclei.

The absence of data on the yield and the distribution of high energy photoneutrons is associated to a considerable degree with the difficulties of effective registration of these neutrons. In order to obtain such data, we have used a high threshold scintillating detector with an effectiveness of the order of 1-2% based on the reaction $C^{12}(n, 2n)C^{11}$ occurring in the organic luminophors, described in detail in reference 1. With the aid of this detector we have studied the yield and angular distribution of photoneutrons of the nuclei Be, C, Al and Pb produced by retarded radiation having energies up to 250 mev. The diagram of the experiments is shown in Fig. 1. In choosing the dimensions and the form of the sample - sources of neutrons, in addition to fulfilling the requirements for the effective registration of the photoneutron current, we took into account the fact that the thickness of the sample must not exceed 0.4 units, or 0.2 of the path of neutrons with an energy of 30 mev relative to the elastic scattering. Such a thickness of samples (2.7 cm for Be, 4 cm for C, 3 cm for Al and 2mm for Pb) ensured the absence of noticeable distortions in the angular distribution and, moreover, in the yield of photoneutrons of high energy. Crystals of stilbene or tolane with an effective working quantity of carbon up to 10 g were used as detectors of neutrons. The beam of photons was passed through two collimators in lead, total thickness up to 40 cm, lined inside and on the side where the sample neutron sources are located, with an aluminum layer 5 mm thick. In addition, the detectors were screened with a layer of lead 10 cm thick. A special check showed that there was no noticeable activation of the detectors in the experiments without sample-sources of photoneutrons at angles of 45-135° to the direction of the photon beam. Only in the experiments where the yield was studied at angles of 30° and 150° to the direction of the photon beam, the activation due to the background constituted as much as 50% of the activation in the main experiments.

The absolute value of the high energy photon current was determined from the readings of the ionization chamber-integrator. To the readings of this chamber was reduced also the activation of the monitor – fine films of polystyrene, attached to the front wall of the sample – sources of photoneutrons during the irradiation. Comparison of the activities of these films with the activities of graphite detectors of a known effective working mass, made it possible to determine the cross section of the reaction $C^{12}(\gamma, n)C^{11}$ at high energies of photons.

The problem of possible presence in the photon beam of neutrons of high energy, which could be scattered in the direction of the detector, distorting the results of the experiments, was studied in other investigations [2,3]. However it was found that such an impurity, even if it exists, is negligibly small. In order to remove any side activation of the detector (reactions γ, n and p, pn) we have screened it on the side of the source of neutrons with a layer of lead 1.2 cm thick. With this type of protection the activation of the detector is practically independent of the thickness of the screen, that is, it is entirely determined by neutrons.

The form of the excitation function of the reaction $C^{12}(n, 2n)C^{11}$ is given in reference 1. It is found that even with greatly varying assumptions regarding the spectrum of the high energy photoneutrons, for example, for a rectangular spectrum or a spectrum similar to the spectrum of photoprotons of the form $f(E)\,E^{-1.7}$ [4], it is possible, with an error not exceeding 9%, to determine the yield of photoneutrons, taking $\sigma_{n', 2n} \approx 0$ at $E_n \lesssim 30$ mev and $\sigma_{n,2n} = 22 \times 10^{27}$ cm^2 = const at $E_n \gtrsim 30$ mev.

The data obtained for the angular distribution of the photoneutrons emitted by the nuclei Be, Al and Pb at $(h\nu)_{max} = 250$ mev and the nucleus C at $(h\nu)_{max} = 200$ and 250 mev are given in Fig. 2. The differential angular cross section for the angle of 45° for all the nuclei in Fig 2 is taken to be unity. From the point of view of the "double-nucleon model", the angular distribution of the high energy nucleons can be directly determined from the experimental data on the photosplitting of deuterium, taking into account the momentum distribution of "quasi-deuterons" in the nucleus, moreover with very little distortion of the angular distribution of the nucleons. However, the

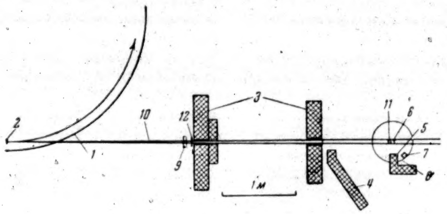

FIG. 1. The diagram of the experiments. 1 – edge of the synchrotron chamber; 2 – the target of the synchrotron; 3 – lead collimators; 4 – auxiliary lead screens; 5 – proton filter; 6 – the sample being bombarded; 7 – neutron detector; 8 – disc supporting the frame; 9 – ionization chamber; 10 – integral chamber-dosimeter; 11 – monitor (graphite or polystyrene).

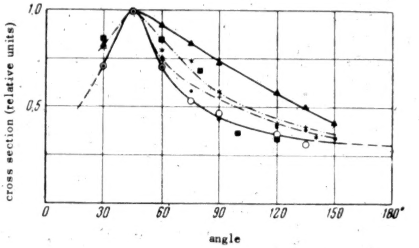

FIG. 2. Angular distribution of photoneutrons with energies higher than 30 mev. ● – C_{250}, + – C_{200}; ▲ – Be_{250}; O – Al_{250}; * – Pb_{250}; ■ – data of work[5].

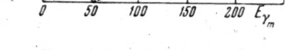

FIG. 3. The dependence of the yield of photoneutrons with energies higher than 30 mev in carbon (in units 10^{-27}cm^2 per eff. quantum) on the maximum energy of retarded radiation.

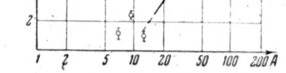

FIG. 4. The dependence of the yield of photoneutrons with energies higher than 30 mev at an angle of 90° (in units 10^{-28}cm^2 per eff. quant steradian on the mass number A).

nucleons produced during the splitting of "quasi-deuterons" may experience new collisions in the same nucleus. Such collisions, in the general case lead to multiple emission of nucleons, registering as photostars in nuclear emulsions. The formation of photostars also results from the processes of the production of mesons with their subsequent absorption in the same nucleus. Thus the angular distribution of the high energy photoneutrons observed in our experiments is, mainly, a result of processes of two types: the pure splitting of "quasi-deuterons" (without the "capture" of nucleons in the nucleus) and the formation of photostars associated mainly with the photoproduction of mesons.

The data given in Fig. 2 for carbon at the maximum photon energies of 200 and 250 mev agree with the results of reference 5, in which the authors measured also for carbon the relative angular distribution of photoneutrons with an energy higher than 50 mev (the yield of such neutrons at an angle of 45° was assumed by them as unity) under the action of retarded radiation with an energy up to 320 mev. We measured the yield of the high energy neutrons from carbon at angle of 45° and at maximum photon energies of 150 and 175 mev. The dependence of the yield on the maximum energy of photons is illustrated in Fig. 3.

Similarly to the angular distribution of the high energy photoneutrons, the excitation function of the yield of such neutrons can be qualitatively interpreted as a result of the superimposition of processes of two types: The formation of photostars and the pure splitting of "quasi-deuterons". The close similarity of the angular distribution of the high energy photoneutrons from the nuclei of carbon, aluminium and lead is analogous to the corresponding results for protons in photostars. For a detailed analysis of the contribution of the various processes in the different nuclei, the study of angular correlation (of the type detected for lithium[6]) between photoprotons and photoneutrons emitted by heavy nuclei becomes significant.

In Fig. 4 the relationship is shown of the yield of photoneutrons with energies higher than 30 mev, at an angle of 90° from the nuclei Li, Be, C, Al, Fe, Cu and Pb at the maximum energy of the retarded radiation of 250 mev. This relationship for the nuclei from C to Pb has approximately the form $\sigma \sim A^{1.4}$; for Li and, particularly, Be the yield of neutrons was found to be higher.

In conclusion it should be noted that our measurements of the cross section of the reaction $C^{12}(\gamma, n)C^{11}$ indicate an increase (in the range of energies of γ – quanta from 50 to 250 mev) in the yield of the direct photoeffect by a value of the order of 10^{-28}cm^2 /eff. quant.

---

[1] P. S. Baranov and V. I. Gol'danskii, J. Exper. Theoret. Phys. USSR **28**, 621 (1955); Soviet Phys **1**, (1955)

[2] A. N. Gorbunov, Report of the Physical Institute, Academy of Sciences, USSR, 1953.

[3] V. I. Gol'danskii and V. A. Shkoda-Ul'ianov, J. Exper. Theoret. Phys. USSR **28**, 623 (1955)

[4] B. Feld, R. Godbole, A. Odian, F. Scherb, P. Stein and A. Wattenberg, Phys. Rev., **94**, 1000 (1954)

[5] D. Kerst, L. Koester, A. Penfold and J. Smith, Phys. Rev. **87**, 197 (1952)

[6] M. Barton and J. Smith, Phys. Rev. **95**, 573 (1954)

Translated by E. Rabkin
138

PARTIAL CONTENTS

DOKLADY AKADEMII NAUK SSSR VOLUME 101, NO. 1 MARCH 1, 1955

HYDROMECHANICS

Condensation of Moving Vapor on a Plane Surface . . . . G. G. Chernyi 39

MATHEMATICAL PHYSICS

Solution of the Linearized Equations of Unsteady Flow of a Viscous Incompressible Fluid in a Bounded Region . . . . A. A. Kiselev 43

PHYSICS

Theory of the Molecular Generator and Molecular Power Amplifier . . . . N. G. Basov and A. M. Prokhorov 47
On the Theory of the Dynamic Deformed Form-factor . . . Assoc. Memb. M. Markov 51
Magnetic Properties of the Exciton . . . . A. G. Samoilovich and M. V. Kononova 55
Improved Equation of the Diffusion of Cosmic Protons in an Interstellar Medium . . . . Ia. P. Terletskii 59

GEOPHYSICS

On the Existence of a Deep Focal Surface on the Boundaries of the Pacific Ocean . . . . S. D. Kogan 63

TECHNICAL PHYSICS

On the Adhesion of Spherical Graphite Impurities in Cast Iron . . . . K. P. Bunin, Iu. N. Taran and T. M. Shpak 65
X-ray Investigation of the Last Stage of the Decomposition of Supersaturated α-solid Solutions of Beryllium in Copper . . . . A. M. Elistratov 69

CRYSTALLOGRAPHY

Theory of Determining the Signs of Structural Amplitude . . . . . A. I. Kitaigorodskii 73

DOKLADY AKADEMII NAUK SSSR VOLUME 101, NO. 2 MARCH 11, 1955

HYDRAULICS

Simplification of the Solution of the Fourier Differential Equation for Problems Related to the Enclosure of a Circular Set of Sources and Sinks . . . . V. N. Shchelkachev 225

ASTRONOMY

Monochromatic Nature of Beams of Solar Radio Radiation . . . . V. V. Vitkevich 229

PHYSICS

'Fine Structure' of the Phenomenon of the Complex Periodic Dependence of the Magnetic Susceptibility of Metals on the Field at Low Temperatures . . . . B. I. Verkin, I. M. Dmitrenko and I. F. Mikhailov 233
Temperature-time Dependence of the Strength of Pure Metals . . . . S. N. Zhurkov and T. P. Sanfirova 237
Ratio of the Quantum Yields of Phosphorescence and Fluorescence in a Number of Phthalimids . . . . V. V. Zelinskii and V. P. Kolobkov 241
On the Nature of Ball Lightning . . . . Acad. P. L. Kapitza 245
Relation between Polarization, Angular Dependence of the Scatter Cross-section and the Magnitude of the Spin-orbital Interaction . . . . I. I. Levintov 249
On the Question of the Lifetime of the Isomeric Nucleus . . . . E. P. Mazets and L. I. Rusinov 253
Computation of Neutron Width through the Model of the Translucent Nucleus . . . . P. E. Nemirovskii 257

DOKLADY AKADEMII NAUK SSSR VOLUME 101, NO. 3 MARCH 21, 1955

ASTRONOMY

Results of Observations on Radiowave Scattering by Electron Inhomogeneities of the Solar Corona . . . . V. V. Vitkevich 429
Age Determination of Rocky Meteorites by the Argon Method . . . . E. K. Gerling and K. G. Rik 433

Diffuse Nebulae and the Interstellar Magnetic Field . . . . Acad. G. A. Shain 437

MATHEMATICAL PHYSICS

On the Two Dimensional Stefan Problem . . . . A. B. Datsev 441

PHYSICS

Spectrum of Fluorescence of Gaseous Nitric Oxide and the Effectc of Foreign Gases on it . . . . A. V. Kleinberg and Acad. A. N. Terenin 445
Hyperons as Excited States of Nucleons. A Possible Mechanism of Multiple Particle Generation . . . . Assoc. Memb. M. A. Markov 449
Broadening of Spectral Lines and the Oscillator Forces of Noble Gases . . . . V. S. Fursov, M. N. Oganov and A. R. Striganov 453
Shifting of the Infra-red Absorption Band of the C = O Group of Acetone in Solutions . . . . V. M. Chulanovskii 457

GEOPHYSICS

On the Determination of the Thickness of the Baroclinic Layer of the Sea . . . . P. S. Lineikin 461

TECHNICAL PHYSICS

On the Propagation of the Fundamental Waves between Parallel Surfaces . . . . E. Burshtein and L. Solov'ev 465
On the Additiveness of the Photographic Action of Spectrally-different Radiation on Multi-layered Color-photographic Material . . . . Iu. N. Gorokhovskii and I. N. Koniushkova 469
X-ray Investigation of the Initial Stage of the Decomposition of Supersaturated δ solid Solution of Ag Al . . . . A. M. Elistratov 473
Investigation of the Kβ Group of X-ray Spectra of Iron and Chromium in the α and σ Phases of Fe Cr Alloy Systems . . . . V. A. Kazantsev 477
Condensation of a Molecular Beam on the Surface of a Metal . . . . N. D. Morgulis, V. M. Gavriliuk and A. E. Kulik 479

DOKLADY AKADEMII NAUK SSSR VOLUME 101, NO. 4 APRIL 1, 1955

MECHANICS

On the Theory of Indirect Regulation Taking Dry Friction in the Sensitive Element into Account . . . . V. V. Petrov and G. M. Ulanov 611

HYDROMECHANICS

On the Effect of Turbulence on the Excitation and Damping of Wind Waves on a Fluid Surface . . . . V. G. Levich 615

ELASTICITY

On the Theory of Small Elastic-plastic Deformations of Anisotropic Media . . . . I. I. Gol'denblatt 619
On the Bending of a Circular Plate Partially Clamped and Partially Supported at the Circumference . . . . D. I. Sherman 623

ASTRONOMY

Brightness of the 5302.8 Å Corona Line in the Solar Chromosphere . . . . M. N. Gnevyshev and R. S. Gnevysheva 627

MATHEMATICAL PHYSICS

On the Three Dimensional Stefan Problem . . . . A. B. Datsev 629
Dielectric Layer with a Spherical Band in a Homogeneous Electrostatic Field . . . . R. N. Kaufman 633

PHYSICS

High-voltage Electrostatic Generator in a Compressed Gas . . . . B. V. Baev P. E. Borotnikov, B. M. Gokhberg, N. I. Sidorov, A. V. Shuf and G. B. Ian'kov 637
On the Theory of Thermal Luminescence . . . . Ch. B. Lushchik 641
Effect of Oxygen, Water Vapor and Organic Compounds on the Photo-electron Process in Zinc Oxide . . . . E. K. Lutseiko and Acad. A. N. Terenin 645
Infra red Absorption Band of the C – O Group of Methyl Alcohol and its Solutions . . . . V. M. Chulanovskii 649

GEOPHYSICS

On Application of Phase Correlation Principles to Distant Earthquakes . . . S. D. Kogan 653
On Phase Fluctuations in a Tube Oscillator . . . . I. S. Gonorovskii 657
X-ray Investigation of Fused Salts of KNO_3 and $NaNO_3$ . . . . Fellow V. I. Danilov[+] and S. Ia. Krasnitskii 661
On the Destruction Mechanism of Cut Specimens under Impact Testing during Bending . . . . B. S. Kasatkin 665
Quantitative Investigation of the Distribution of Elements in Alloys . . . . S. T. Kishkin, S. Z. Bokshtein, L. M. Moroz and T. I. Gudkova 667

CRYSTALLOGRAPHY

New Configuration of Silicon Carbide. System Designation of SiC Type . . E. B. Gasilova 671

DOKLADY AKADEMII NAUK SSSR VOLUME 101, No. 5 APRIL 11, 1955

HYDRAULICS

Formulation and Method of Solution of Hydrodynamic Problems of Controlling Motion of Oil bearing Contour . . . . G. S. Salekhov 809

MATHEMATICAL PHYSICS

On the Two Dimensional Multi-layered Heat Conduction Problem . . . . A. B. Datsev 813
On the Theory of Nonlinear Relativistic Invariant Equations . . . . G. A. Sokolik 817

PHYSICS

On Stable Particles with Mass Larger than the Proton in Cosmic Radiation at 3250m above Sea Level . . . . M. I. Daion 821
On the Natural Width of the Spectral Lines of Electron Yield . . . . Assoc. Memb. B. Dzhelepov 825
Length of the Diffusion Displacement of Excitons in Copper Oxide . . . . Assoc. Memb. V. E. Lashkarev and Iu. I. Karkhanin 829
Energies of Thermal Ionization of Coloring Centers in Alkali-halide Crystal-phosphors . . . . Ch. B. Lushchik 833
Determination of the Effective Cross section of Impacts of the Second Kind from Sensitized Fluorescence . . . . . Assoc. Memb. S. E. Frish and E. K. Kraulinia 837

GEOPHYSICS

High frequency Seismic Prospecting . . . . . . Academ. G. A. Gamburtsev and I. S. Berzon 841
On Brightness of Diurnal Unclouded Sky on a Spherical Earth . . Academ. V. G. Fesenkov 845

BIOPHYSICS

On the Role of Eye Motion in Estimating Distance . . . . L. I. Leushina 849

TECHNICAL PHYSICS

On the Kinetic Isothermal Martensitic Transformation Near Absolute Zero . . . . B. Ia. Libov and Iu. A. Osip'ian 853
Recrystallization Diagram of Titanium Iodide . . . . E. M. Savitskii, A. M. Tylkina and A. N. Turanskaia 857

CRYSTALLOGRAPHY

On Elastic Twinning of Metals . . . . S. I. Startsev and V. M. Kosevich 861

DOKLADY AKADEMII NAUK SSSR VOLUME 101, No. 6 APRIL 21, 1955

HYDROMECHANICS

Solution of the Linearized Axisymmetric Problem of Point Explosions in Media with Variable Density . . . . V. P. Karlikov 1009

HYDRAULICS

Certain Problems of Controlling the Motion of an Oil bearing Contour . . . . G. S. Salehkov and V. D. Chugunov 1013

ASTRONOMY

Certain Results of Uneclipsed Observations of the Solar Corona . . . . M. N. Gnevyshev and R. S. Gnevysheva 1017

[+] Deceased

MATHEMATICAL PHYSICS

On the Three Dimensional Multi-layered Heat Conduction Problem . . . . . A. B. Datsev 1019

PHYSICS

Stabilization of Ion Energies, Accelerated by a High-voltage Electrostatic Generator . . . . V. G. Brovchenko, B. M. Gokherb and V. M. Morozov 1023
Splitting of Heavy Nuclei by High Energy Neutrons . . . . V. I. Gol'danskii, E. Z. Tarumov and V. S. Pen'kina 1027
Scattering of Oscillatory Quanta and Extinction of Fluorescence of NO . . . .
A. V. Kleinberg and Academ. A. N. Tere
. . . . A. V. Kleinberg and Academ. A. N. Terenin 1031
Isotopic Spin and Hypothesis of Neutron Charge . . . . Ia. P. Terletskii 1035
On the Calculation of the Time-correlation Function for a Weak Non ideal Bose Gas . . . . V. V. Tolmachev 1039
Generalization of the Theory of Vector Fields . . . . B. Iu. Urbakh 1043
Internal Breaking Radiation for O – O Nucleus Transition . I. S. Shapiro and Iu. V. Orlov 1047

BIOPHYSICS

On the Use of X-ray Analysis to Study Ice-formation in Grain . . . . G. B. Radzievskii and Ia. L. Shekhtman 1051
Effect of Deep Cooling at Exposure Time on the Disturbance of Syntnesis of Glutatnione and Ascorbic Acid in Wheat Grains During Sprouting . . . . S. D. Chigirev 1055

SOVIET PHYSICS JETP VOLUME 1, NUMBER 3 NOVEMBER, 1955

Author Index to Volume 1

References with (L) are Letters to the Editor

Abaulina, E. I. and N. V. Zavaritskii. The problem of obtaining a metastable modification of thallium – 184 (L)

—— (See **Khaikin, M. S.**) – 189 (L)

Aksenov, S. I., B. P. Vikin and K. V. Vladimirskii. The excitation of ultrasonic vibrations by ponderomotive forces – 609 (L)

Alekseevskii, N. E. and N. B. Brandt. The effect of a uniform compression upon the galvanomagnetic effects in bismuth and its alloys – 384 (L)

—— **G. S. Zhdanov and N. N. Zhuravlev.** The problem of the superconductivity of the compounds Bi_4Rh and Bi_2Rh – 99

Alentsev, M. N., V. V. Antonov-Romanovskii, B. I. Stepanov and M. V. Fok. On the resonance-fluorescence of Atoms – 188 (L)

Al'tshuler, S. A. Resonance absorption of ultrasound in paramagnetic salts – 29

—— On the theory of electronic and nuclear paramagnetic resonance under the action of ultrasound – 37

Andreeshchev, E. and B. M. Isaev. Certain properties of a spark counter for counting α-particles – 212

Andronikashvili, E. L. and I. P. Kaverkin. Rotation of helium II at high speeds – 174 (L)

Ansel'm, A. I. and Iu. A. Firsov. The mean free path of a non-localized exciton in an atomic crystal – 139

Antonov-Romanoviskii, V. V. (see **Alentsev, M. N.**) – 188 (L)

Aronovich, G. V. (see **Neimark, Iu. I.**) – 475

Askar'ian, G. A. Gas bubble chamber -- a possible recorder of the elementary act of interaction of ionizing radiation with matter – 571 (L)

—— Possible application of pulsed multiplier image-converters for recording tracks of ionizing particles in luminescent media – 575 (L)

Baranov, P. S. and V. I. Gol'danskii. High threshold scintillation neutron detector – 576 (L)

—— **and V. I. Gol'danskii.** The yield and angular distribution of photoneutrons of high energy – 613 (L)

Barashenkov, V. S. Some observations on possible formulations of the theory of extended particles – 467

Basov, N. G. and A. M. Prokhorov. Possible methods of obtaining active moleculess for a molecular oscillator – 184 (L)

—— **V. G. Veselago and M. E. Zhabatinskii.** Improvement of the quality of a cavity resonator by means of regeneration – 177 (L)

Bass, F. G. and I. M. Tsidil'kovskii. On the theory of the Hall and Nernst-Ettinghausen effects in semiconductors with mixed conductivities – 267

—— (see **Tsidil'kovskii, I. M.**) – 180 (L)

Belen'kii, S. Z. The theory of multiple production of particles at high energy – 161 (L)

—— **and A. I. Nikishov.** Multiple meson production at energies of 1 - 2.2 bev – 593 (L)

Beliustin, A. V. On the theory of crystal growth – 535

Belovitskii, G. E., T. A. Romanova, L. V. Sukhov and I. M. Frank. The fission of uranium nuclei under the action of slow π-mesons and high energy particles – 581 (L)

Bene, A. A. Calculation of the ultimate thickness of an emulsion layer in the investigation of nuclear processes by means of the photographic method II – 532

Bezuglyi, P. A. (see **Galkin, A. A.**) – 197

Blinov, V. A. (see **Khromchenko, L. M.**) – 596 (L)

Bogoliubov, N. N. and D. N. Zubarev. The wave function of the lowest state of a system of interacting Bose particles – 83

Bonch-Bruevich, V. L. The Fermi distribution at absolute zero, taking into account the interaction of electrons with zero point vibrations of the lattice – 169 (L)

Bondarenko, V. V., I. F. Kvartskhava, A. A. Piutto and A. A. Chernov. Resistance of metals at high current densities – 221

Borgardt, A. A. The gravitational self-energy of particles in the classical field theories – 380 (L)

Borodovskaia, L. N. and S. V. Lebedev. Dependence of the electrical conductivity and electron emission on the energy of a metal in the process of its heating by a current of high density – 71

Brandt, N. B. (see **Alekseevskii, N. E.**) – 384 (L)

Bukke, E. E. The Change in dielectric constant and phosphors under the action of infrared light – 400 (L)

Chavchanidze, V. V. and O. D. Cheitvili. Calculation of the energy distribution function of neutrons by Markov's method – 375 (L)

Cheitvili, O. D. (see **Chavchanidze, V. V.**) – 375 (L)

Cherepanov, V. I. (see **Sokolov, A. V.**) – 231

Cherepnev, A. A. The problem of the position of the copper activator in Zinc-sulfide scintillators – 300

Chernov, A. A. (see **Bondarenko, V. V.**) – 221

Chudakov, A. E. (see **Nesterova, N. M.**) – 388

Chuev, V. I. (see **Vlasov, N. A.**) – 500

Deriagin, B. N. (see **Kirillov-Ugriumov, V. G.**) – 484

Dishkant, G. P. The problem of the invalidity of one statistical treatment of quantum mechanics – 166 (L)

Dodonova, N. Ia. and V. V. Sobolev. The radiation of CO_2 in the region of 15μ in an electrical discharge – 611 (L)

Dontsov, Iu. P. (see **Striganov, A. R.**) – 354

Drokin, A. I. New means of control of compensating the earth's magnetic field in investigations on a vertical astatic magnetometer – 126

Drozdov, S. I. The scattering of fast neutrons by non-spherical nuclei I – 588 (L)

—— The scattering of fast neutrons by non-spherical nuclei II – 591 (L)

Dzhertetov, Kh. A. and G. M. Pateiuk. Investigation of high frequency discharges by the probe method – 326

Eremeev, M. A. In connection with the paper of Arifov, Aiukhanov and Starodubtsev – 390 (L)

Estulin, I. V. and E. M. Moiseeva. Measurement of the coefficients of internal conversion of γ-rays of Sr^{87*}, In^{113*}, In^{115*} and V^{51*} on the electron of the atoms – 463

Fain, V. M. The velocity distribution of electrons in the presence of a varying electric field and a constant magnetic field – 205

Federov, V. M. (see **Kirillov-Ugriumov, V. G.**) – 484

Feinberg, E. L. Collisions of fast nucleons with nuclei – 176

Filimonov, V. A. Deviations from Mayer's scheme for

filling nuclear shells and the interaction of levels – 585 (L)
Firsov, Iu. A. (see **Ansel'm, A. I.**) – 139
Fisher, I. Z. On the stability of a homogeneous phase. I. General theory – 154
—— On the stability of a homogeneous phase II. Determination of the limit of stability – 273
—— The stability of a homogeneous phase III. Theory of the crystallization curve – 280
Flerov, G. N. (see **Podgurskaia, A. V.**) – 392 (L)
Fogel', Ia. M., L. I. Krupnik and **B. G. Safronov.** Capture of electrons and ionization by protons in hydrogen – 419
—— **B. G. Safronov** and **L. I. Krupnik.** Formation of negative hydrogen ions in the passage of protons through thin metal foils – 546
Fok, M. V. (see **Alentsev, M. N.**) – 188 (L)
Fradkin, E. S. The asymptote of Green's function in quantum electrodynamics – 604 (L)
Frank, I. M. (see **Belovitskii, G. E.**) – 581 (L)
Galanin, M. D. The problem of the effect of concentration on the luminescence of solutions – 317
Galkin, A. A. and **P. A. Bezuglyi.** The kinetics of the destruction of superconductivity by a magnetic field – 197
Garif'ianov, N. S. and **M. M. Zaripov.** Hyperfine structure of paramagnetic resonance in copper tutton salts at intermediate fields – 567 (L)
Gasting, N. L. (see **Vergunas, F. I.**) – 284
Gol'danskii, V. I. and **M. I. Podgoretskii.** On the problem of the negative π-meson decays – 571 (L)
—— and **V. A. Shkoda-Ul'ianov.** Maximum yield of photoneutrons and a new method of determining the integral cross section of (γ, n) reactions for high energy photons – 579 (L)
—— (see **Baranov, P. S.**) – 576 (L)
—— (see **Baranov, P. S.**) – 581 (L)
Gol'fand, Iu. A. Construction of a distribution function by the method of quasi-fields – 118
Gol'dman, I. I. and **A. B. Migdal.** The theory of scattering in the semi-classical approximation – 304
Gramenitskii, I. M., E. A. Zamchalova, M. I. Podgoretskii, M. I. Tretiakova and **M. N. Shcherbakova.** Nuclear fissions associated with heavy unstable particles – 562 (L)
Granovskii, V. L. and **G. G. Timofeeva.** The constructior of an arc in rarefied gases at large currents – 381 (L)
Grigor'ev, E. L. Detection of the polarization of beams of fast particles by means of nuclear photoemulsions – 608 (L)
Gubanov, A. I. Zone theory of the three-dimensional model of a liquid – 364
Gubkin, A. N. (see **Skanavi, G. I.**) – 56
Gvozdover, S. D., N. M. Pomerantsov and **A. P. Poliakova.** Determination of the transverse relaxation time of nuclear magnetic moments – 471
Iakovlev, L. G. The velocity of the wave front in nonlinear electrodynamics – 181 (L)
Iappa, Iu. A. On the paper of V. I. Karpman "The problem of the connection between the method of regularization and the theory of particles with arbitrary spin" – 171 (L)
Iashin, N. M. (see **Korostyleva, L. A.**) – 310
Isaev, B. M. (see **Andreeshchev, E.**) – 212
Isaev, P. S. The "equilibrium" energy spectrum of cascades of photons – 379 (L)
Iutsis, A. P. (see **Tsiunaitis, G. K.**) – 358
Ivanenko, D. and **V. N. Tsytovich.** On the theory of energy losses of charged particles traversing a ferromagnetic material – 135
Ivanova, N. S. (see **Perfilov, N. A.**) – 585 (L)
Janossy, L. Statistical problems of an electron multiplier – 520
Kalashnikova, V. I. (see **Podgurskaia, A. V.**) – 392 (L)
Kalinin, S. P. (see **Vlasov, N. A.**) -- 500
Kalitsin, N. S. The relativistic mechanics of a material point of variable mass – 565 (L)
Karanikolov, Khristo. The phenomenological relations of Onsager – 265
Kaverkin, I. P. (see **Andronikashvili, E. L.**) – 174 (L)
Kazantzev, B. I. and **P. V. Meikliar.** The regression of the centers of the latent photographic image – 45
Khaikin, M. S. Investigation of the anisotropy of the surface resistance of tin at low temperatures – 164 (L)
—— (see **Rodionov, S. F.**) – 64
—— and **E. I. Abaulina.** self-neutralizing light meter with adjustable red boundary – 189 (L)
Khalatnikov, I. M. The representation of Green's function in quantum electrodynamics in the form of continual integrals – 568 (L)
Khartman, V. G., I. N. Leont'eva, A. P. Siniavskii and **L. V. Vasil'ev.** A pulse height analyzer with an electron beam tube – 537
Khromchenko, L. M. and **V. A. Blinov.** A study of the energy levels of the lithium nucleus by the method of magnetic analysis – 596 (L)
Khutsishvili, G. R. On the angular distribution of β-radiation. II – 376 (L)
—— The degree of orientation of nuclei – 390 (L)
Kirillov-Ugriumov, V. G., V. M. Federov and **B. N. Deriagin.** Rectangular wilson chamber with bilateral expansion – 484
Kligman, F. I. The statistical theory of heavy nuclei and of nuclear forces – 145
Klimontovich, Iu. L. "Acoustic excitations" in superconductors – 602 (L)
Kocharian, N. M. The proton component of cosmic rays at 3200 meters above sea level – 128
Kolesnikov, N. N. and **S. T. Larin.** The problem of spontaneous fission and beta-stability – 179 (L)
—— (see **Larin, S. T.**) – 178 (L)
Kompaneets, A. S. Multiple scattering in a coulomb field in very thin layers of material – 262
Korostyleva, L. A., A. R. Striganov and **N. M. Iashin.** Hyperfine structure of the spectral lines and nuclear spins of U^{233} and Pu^{229} – 310
—— (see **Striganov, A. R.**) – 354
Krasil'nikov, D. D. Variation of the global intensity of the hard component of cosmic rays during the passage of air mass fronts – 419 (L)
Krivoglaz, M. A. and **Z. A. Matysina.** The theory of the electrical resistivity of ordered alloys – 103
Krupnik, L. I. (see **Fogel', Ia. M.**) – 418
—— (see **Fogel', Ia. M.**) – 546
Kuz'min, A. I. The contribution of meteorological changes in the earth's atmosphere to the diurnal efefect in cosmic rays – 560 (L)
—— and **G. V. Skripin.** The effect of lunar-tidal oscillation of the atmosphere on the intensity of the hard component of cosmic rays – 556 (L)
Kuznetsov, P. I., R. L. Stratonovich and **V. I. Tikhonov.** The effect of electrical fluctuations on a vacuum tube oscillator – 510
Kvartskhava, I. F. (see **Bondarenko, V. V.**) – 221
Larin, S. T. The momentum distribution in the

statistical model of the atom – 394 (L)
—— **and N. N. Kolesnikov.** The neutron subshell in the region of the transuranic elements – 178 (L)
—— **(see Kolesnikov, N. N.)** – 179 (L)
Lebedev, S. V. (see Borodovskaia, L. N.) – 71
Leontiev, N. I. a magnetometer which makes use of the magnetic resonance of protons – 50
Leont'eva, I. N. (see Khartman, V. G.) – 537
Levshin, L. V. The effect of concentration on the optical properties of solutions of 3, 6-diaminoacridine – 244
—— The effect of concentration on the optical properties of solutions of acridine compounds – 235
Lozhkin, O. V. and V. P. Shamov. The probability of uranium nuclear fission by its absorption of slow π^- mesons – 587 (L)
—— **(see Perfilov, N. A.)** – 439
Luchina, A. A. On the longitudinal vibrations of plasma I. – 12
—— **(see Miakishev, G. Ia.)** – 21
Manenkov, A. A. and A. M. Prokhorov. The fine structure of the spectrum of the paramagnetic resonance of the Ion Cr^{3+} in chromium corundum – 611 (L)
Markov, M. and V. Stakhanov. The possible β decay of hyperions and K mesons – 593 (L)
Martynov, A. S. Scattering of mesons by nucleons in the theory of radiation damping – 68
Matveev, A. N. The optimum length of an undulator – 606 (L)
Matysina, Z. A. (see Krivoglaz, M. A.) – 103
Meikliar, P. V. F-centers in silver halide crystals – 187 (L)
—— **(see Kazantsev, B. I.)** – 45
Mel'chenko, V. S. Determination of the absolute concentrations of atoms in a multi-component arc-vapor – 564 (L)
Miakishev, G. Ia. and A. A. Luchina. On longitudinal vibrations of plasma II – 21
Migdal, A. B. The theory of nuclear reactions with production of slow particles – 2
—— Meson production at energies close to threshold – 7
—— **(see Gol'dman, I. I.)** – 304
Moiseeva, E. M. (see Estulin, I. V.) – 463
Neimark, Iu. I. and G. V. Aronovich. The conditions for self-excitation of a singing flame – 475
Neprimerov, W. N. Some notes on the researches of S. G. Salikov – 552
Nesterova, N. M. and A. E. Chudakov. On the observation of Cerenkov radiation accompanying broad atmospheric showers of cosmic rays – 388 (L)

Nikishov, A. I. (see Belen'kii, S. Z.) – 593 (L)
Nikol'skii, S. I. (see Vavilov, Iu. N.) – 399 (L)
Ogloblin, A. A. (see Vlasov, N. A.) – 500
Otpushchennikov, N. F. The absorption of ultrasonic waves in armco iron and plexiglass – 376 (L)
Ovsiannikova, I. A. and M. Ia. Shirobokov. The dynamical theory of electron scattering in crystals – 488
Parchevskii, G. F. and N. P. Penkin. The relation of the oscillator strengths for the components of the resonance doublet of aluminum and copper – 382 (L)
Pateiuk, G. M. (see Dzherpetov, Kh. A.) – 326
Penkin, N. P. (see Parchevskii, G. F.) – 382 (L)
Perfilov, N. A. and N. S. Ivanova. The fission of heavy nuclei by slow mesons – 585 (L)
—— **O. V. Lozhkin and V. P. Shamov.** The yield of fission and star formation processes in the capture of π^- mesons by nuclei of U, Bi and W – 439
Pershitz, Ia. N. The conditions of formation and stability of films at the electrodes in dielectrics – 110
Piutto, A. A. (see Bondarenko, V. V.) – 221
Podgoretskii, M. I. (see Gol'danskii, V. I.) – 571 (L)
—— **(see Gramenitskii, I. M.)** – 562 (L)
Podgurskaia, A. V., V. I. Kalashnikova, G. A. Stoliarov, E. D. Vorob'ev and G. N. Flerov. The spontaneous fission of thorium – 392 (L)
Pokrovskii, V. L. The theory of the dipole lattice of Onsager – 397 (L)
Poliakova, A. P. (see Gvozdover, S. D.) – 471
Pomerantsov, N. M. (see Gvozdover, S. D.) – 471
Popov, Kiril. The mathematical foundations of the theory of irreversible thermodynamical processes – 336
Prohkorov, A. M. (see Vasov, N. G.) – 184 (L)
—— **(see Manenkov, A. A.)** – 611 (L)
Rodionov, S. F., M. S. Khaikin and A. I. Shal'nikov. A self-quenching light meter – 64
Romanova, T. A. (see Belovitskii, G. E.) – 581 (L)
Rozental', I. L. The Fermi theory of multiple particle production in nucleon encounters – 166 (L)
Rozman, I. M. Luminescence of organic scintillators – 185 (L)
Rybakov, B. V. Ranges of protons in medium and heavy elements – 435
Ryzhkova, K. P. and L. I. Sarycheva. Measurement of the absorption coefficient of high energy nuclear interacting particles – 572 (L)
Safronov, B. G. (see Fogel', Ia. M.) – 419
—— **(see Fogel', Ia. M)** – 546
Samoilov, L. N. (see Vlasov, N. A.) – 500
Sarantsev, V. P. (see Vavilov, Iu. N.) – 399 (L)
Sarycheva, L. I. (see Ryzhkova, K. P.) – 572 (L)
Savich, A. V. The absence of stable isotopes of Tc and Pm and other anomalies in the distribution of β-stable nuclei – 291
Shal'nikov, A. I. (see Rodionov, S. F.) – 64
Shamov, V. P. (see Lozhkin, O. V.) – 587 (L)
— **(see Perfilov, N. A.)** – 439
Shcherbakova, M. N. (see Gramenitskii, I. M.) – 562 (L)
Shirobokov, M. Ia. (see Ovsiannikova, I. A.) – 488
Shkoda-Ul'ianov, V. A. (see Gol'danskii V. I.) – 579 (L)
Shteinberg, I. B. (see Sokolov, A. V.) – 231
Sidorov, V. M. The formation of charged π mesons by nucleons – 600 (L)
—— **(see Vlasov, N. A.)** – 500
Silin, V. P. On the paper "The excitation spectrum of a system of many particles" – 607 (L)
Siniavskii, A. P. (see Khartman, V. G.) – 537
Skanavi, G. I. and A. N. Gubkin. The problem of calculating the internal field in polycrystalline dipole dielectrics in the case of relaxation polarization – 56
Skobelkin, V. I. and R. N. Solomko. Magnetostatics with ferromagnetics – 370
Skripin, G. V. (see Kuz'min, A. I.) – 556 (L)
Sobolev, V. V. (see Dodonova, N. Ia.) – 611 (L)
Sokolik, G. A. Remarks on the theory of fusion – 9
Sokolov, A. A. amd I. M. Ternov. The quantum theory of radiating electron, IV – 227
Sokolov, A. V. The absorption and emission of x-rays in ferromagnetic metals – 333
—— **V. I. Cherepanov and I. B. Shteinberg.** Dispersion formulas of the quantum optics of metals in the many-electron theory with consideration of electron damping

– 231
—— **and S. M. Tsipis.** Density of states of conduction electrons in ferromagnetic materials – 218
Solomko, R. N. (**see Skobelkin, V. I.**) – 370
Stakhanov, V. (**see Markov, M.**) – 593 (L)
Stepanov, B. I. Absorption and emission of light by a gray substance – 446
—— (**see Alentsev, M. N.**) – 188 (L)
Stoliarov, G. A. (**see Podgurskaia, A. V.**) – 392 (L)
Stratonovich, R. L. Entropy in quantum statistics – 426
—— The entropy of systems with a random number of particles – 254
—— (**see Kuznetsov, P. I.**) – 510
Striganov, A. R., L. A. Korostyleva and Iu. P. Dontsov. The isotopic shift in the spectrum of plutonium – 354
—— (**see Korostyleva, L. A.**) – 310
Sukhov, L. V. (**see Belovitskii, G. E.**) – 581 (L)
Ternov, I. M. (**see Sokolov, N. A.**) – 227
Tikhonov, V. I. (**see Kuznetsov, P. I.**) – 510
Timofeeva, G. G. (**see Granovskii, V. L.**) – 381 (L)
Tretiakova, M. I. (**see Gramenitskii, I. M.**) – 562 (L)
Tsidil'kovskii, I. M. and F. G. Bass. On the paper of G. M. Avak'iants "The theory of the transfer equation in strong electric fields" – 180 (L)
—— (**see Bass, F. G.**) – 267
Tsipis, S. M. (**see Sokolov, A. V.**) – 218
Tsiunaitis, G. K. and A. P. Iutsis. The double configuration approximation to the two lowest configurations of the boron atom – 358
Tsytovich, V. N. On the causal development of a coupled system in relative time – 377 (L)
—— Relativistic corrections to the two body problem – 163 (L)
—— The spectrum of positronium in external fields – 452
—— (**see Ivanenko, D.**) – 135
Vasil'ev, L. V. (**see Khartman, V. G.**) – 537
Vavilov, Iu. N., S. I. Nikol'skii and V. P. Sarantsev. The spatial distribution of nuclear-active particles in broad atmospheric showers of cosmic rays – 399 (L)
Vergunas, F. I. and N. L. Gasting. The decay laws of the afterglow of zinc sulfide phosphors in the temperature extinction region – 284
Veselago, V. G. (**see Basov, N. G.**) – 177 (L)
Vikin, B. P. (**see Aksenov, S. I.**) – 609 (L)
Vladimirskii, K. V. (**see Aksenov, S. I.**) – 609 (L)
Vlasov, N. A., S. P. Kalinin, A. A. Ogloblin, L. N. Samoilov, V. A. Sidorov and V. I. Chuev. Interaction of protons with tritium and the excited state of He^4 – 500
Vorob'ev, E. D. (**see Podgurskaia, A. V.**) – 392 (L)
Zaitsev, G. A. Description of the electromagnetic field by means of matrices – 411

—— Relativistically invariant equations for the electron which take the place of Dirac's system of equations – 491
Zamchalova, E. A. (**see Gramenitskii, I. M.**) – 562 (L)
Zaripov, M. M. (**see Garif'ianov, N. S.**) – 567 (L)
Zavaritskii, N. V. (**see Abaulina, E. I.**) – 184 (L)
Zhabatinskii, M. E. (**see Basov, N. G.**) – 177 (L)
Zhdanov, G. S. (**see Alekseevskii, N. E.**) – 99
—— (**see Zhuravlev, N. N.**) – 91
Zhuravlev, N. N. and G. S. Zhdanov. The structure of superconductors. VIII. X-ray and metallographic investigations of the system bismuth-rhodium – 91
—— (**see Alekseevskii, N. E.**) – 99
Zinov'eva, K. N. The surface of Liquid He^3 in the temperature range 0.93 - 3.34° K – 173 (L)
Zubarev, D. N. (**see Bogoliubov, N. N.**) – 83

SOVIET PHYSICS JETP VOLUME 1, NUMBER 3 NOVEMBER, 1955

Analytic Subject Index to Volume 1

References with (L) are to Letters to the Editor. Items are listed under the following categories:

- Acoustics
- Atomic Mass and Abundance
- Atomic Structure and Spectra
- Cosmic Radiation
- Crystalline State
- Dielectrics and Dielectric Properties
- Electrical Conductivity and Resistance
- Electrical Discharges
- Electrical Properties
- Electromagnetic Theory and Electrodynamics
- Electrons and Positrons
- Elementary Particle Interactions
- Field Theory
- Films, Properties
- Helium, Liquid
- Ionization
- Ions
- Liquids
- Luminescence
- Magnetic Properties
- Magnetic Resonance
- Mathematical Methods
- Mesons and Hyperons
- Methods and Instruments
- Microwaves
- Noise
- Nuclear Fission
- Nuclear Moments and Spin
- Nuclear Photoeffects
- Nuclear Reactions, General
- Nuclear Reactions Induced by Mesons
- Nuclear Spectra
- Nuclear Structure Theory
- Optical Properties
- Quantum Electrodynamics
- Quantum Mechanics
- Radiation
- Radioactivity
- Range and Energy Loss of Particles
- Relativity and Gravitation
- Scattering, General
- Scattering of Electrons and Positrons
- Scattering of Mesons
- Scattering of neutrons
- Scattering of Protons
- Semiconductors
- Spectra, General
- Statistical Mechanics and Thermodynamics
- Superconductivity

Absorption of Radiation (see **Radiation**)
Acoustics
  "Acoustic excitations" in superconductors, Iu. L. Klimontovich – 602 (L)
  On the theory of electronic and nuclear paramagnetic resonance under the action of ultrasound, S. A. Al'tshuler – 37
  Resonance absorption of ultrasound in paramagnetic salts, S. Al'tshuler – 29
  The absorption of ultrasonic waves in Armco iron and plexiglass, N. F. Otpushchennikov – 376 (L)
  The conditions for self-excitation of a singing flame, Iu. I. Neimark and G. V. Aronovich – 475
  The excitation of ultrasonic vibrations by ponderomotive forces, S. I. Aksenov, B. P. Vikin and K. V. Vladimirskii – 609 (L)
Afterglow (see **Electrical Discharges**)
Alloys (see **Crystalline State**)
Annihilation (see **Electrons and Positrons**)
Antiferroelectric Phenomena (see **Dielectrics and Dielectric Properties**)
Antiferromagnetism (see **Magnetic Properties**)
Arcs (see **Electrical Discharges**)
Atomic Mass and Abundance
  The absence of stable isotopes of Tc and Pm and other anomalies in the distribution of β-stable nuclei, A. V. Savich – 291
Atomic Structure and Spectra
  Hyperfine structure of the spectral lines and nuclear spins of U^{233} and Pu^{239}, L. A. Korostyleva, A. R. Striganov and N. M. Iashin – 310
  The double configuration approximation to the two lowest configurations of the boron atom, G. K. Tsiunaitis and A. P. Iutsis – 358
  The isotopic shift in the spectrum of plutonium, A. R. Striganov, L. A. Korostyleva and Iu. P. Dontsov – 354
  The momentum distribution in the statistical model of the atom, S. I. Larin – 394 (L)
  The relation of the oscillator strengths for the components of the resonance-doublet of aluminum and copper, G. F. Parchevskii and N. P. Penkin – 382 (L)
  The spectrum of positronium in external fields, V. N. Tsytovich – 452
Auger Effect (see **Atomic Structure and Spectra**)

Barkhausen Effect (see **Magnetic Properties**)
Biographical Material
  Albert Einstein – 409
Boson Theory (see **Field Theory**)
Bremsstrahlung (see **Radiation**)
Broadening of Spectral Lines (see **Atomic Structure and Spectra; Spectra, General**)

Capture Cross Sections (see **Electrons and Positrons; Nuclear Reactions; Radiation**)
Cerenkov Effect (see **Radiation**)
Chemiluminescences (see **Luminescence**)
Cold Emission (see **Electrical Properties**)
Campton Effect (see **Radiation**)
Conductivity, Electrical (see **Electrical Conductivity and Resistance**)
Cosmic Radiation (see also **Mesons and Hyperons**)
  On the observation of Cerenkov radiation accompanying broad atmospheric showers of cosmic rays, N. M. Nesterova and A. E. Chudakov – 388 (L)

The contribution of meteorological changes in the earth's atmosphere to the diurnal effect in cosmic rays, A. I. Kuzmin' – 560 (L)
The effect of lunar-tidal oscillation of the atmosphere on the intensity of the hard component of cosmic rays, A. I. Kuz'min and G. V. Skripin – 556 (L)
The "Equilibrium" energy spectrum of cascades of photons, P. S. Isaev – 379 (L)
The proton component of cosmic rays at 3200 meters above sea level, N. M. Kocharian – 128
The spatial distribution of nuclear-active particles in broad atmospheric showers of cosmic rays, Iu. N. Vavilov, S. I. Nikol'skii and V. P. Sarantsev – 399 (L)
Variation of the global intensity of the hard component of cosmic rays during the passage of air mass fronts, D. D. Krasil'nikov -- 557 (L)

Cosmology (see **Relativity and Gravitation**)

Critical Potentials (see **Atomic Structure and Spectra**)

Cross Section (see **Electrons and Positrons; Nuclear Reactions; Radiation; Scattering**)

Crystal Counters (see **Methods and Instruments**)

Crystalline State (see also **Electrical Properties; Magnetic Properties; Semiconductors, etc**)
Density of states of conduction electrons in ferromagnetic materials, A. V. Sokolov and S. M. Tsipis – 218
Dispersion formulas of the quantum optics of metals in the many-electron theory with consideration of electron damping, A. V. Sokolov, V. I. Cherepanov and I. B. Shteinberg – 231
F-centers in silver halide crystals, P. V. Meikliar – 187 (L)
In connection with the paper of Arifov, Aiukhanov and Starodubtsev, M. A. Eremeev – 390 (L)
On the theory of crytsal growth, A. V. Beliustin – 535
The dynamical theory of electron scattering in crystals, I. S. Ovsiannikova and M. Ia. Shirobokov – 488
The effect of a uniform compression upon the galvanomagnetic effects in bismuth and its alloys, N. E. Alekseevskii and N. B. Brandt – 384 (L)
The mean free path of a non-localized exciton in an atomic crystal, A. I. Ansel'm and Iu. A. Firsov – 139
The stability of a homogeneous phase III. Theory of the crystallization curve, I. Z. Fisher – 280
The theory of the dipole lattice of Onsager, V. L. Pokrovskii – 379 (L)

Diamagnetism (see **Magnetic Properties**)

Dielectrics and Dielectric Properties
The change in dielectric constant and phosphors under the action of infrared light, E. E. Bukke – 400 (L)
The conditions of formation and stability of films at the electrodes in dielectrics, Ia. N. Pershits – 110
The mean free path of a non-localized exciton in an atomic crystal, A. I. Ansel'm and Iu. A. Firsov – 139
The problem of calculating the internal field in polycrystalline dipole dielectrics in the case of relaxation polarization, G. I. Skanavi and A. N. Gubkin – 56

Discharge of Electricity in Gases (see **Electrical Discharges**)

Disintegration and Excitation of Nucleus (see **Nuclear Reactions**)

Electrical Breakdown (see **Dielectrics and Dielectric Properties; Electrical Discharges**)

Electrical Conductivity and Resistance (see also **Electrical Properties; Semiconductors; Superconductors**)
Density of states of conduction electrons in ferromagnetic materials, A. V. Sokolov and S. M. Tsipis – 218
Dependence of the electrical conductivity and electron emission on the energy of a metal in the process of its heating by a current of high density, L. N. Borodovskaia and S. V. Lebedev – 71
Investigation of the anisotropy of the surface resistance of tin at low temperatures, M. S. Khaikin – 164 (L)
On the theory of the Hall and Nernst-Ettinghausen effects in semiconductors with mixed conductivities, F. G. Bass and I. M. Tsidil'kovskii – 267
Resistance of metals at high current densities, V. V. Bondarenko, I. F. Kvartskhava, A. A. Piutto and A. A. Chernov – 221

Electrical Discharges
Determination of the absolute concentrations of atoms in a multi-component arc-vapor, V. S. Mel'chenko – 564 (L)
The absorption and emission of x-rays in ferromagnetic metals, A. V. Sokolov – 333
The constriction of an arc in rarefied gases at large currents, V. L. Granovskii and G. G. Timofeeva – 381 (L)
The radiation of CO_2 in the region of 15μ in an electric discharge – 611 (L)

Electrical Properties (see also **Dielectrics and Dielectric Properties; Electrical Conductivity and Resistance; Semiconductors; Superconductors**)
Dependence of the electrical conductivity and electron emission on the energy of a metal in the process of its heating by a current of high density, L. N. Borodovskaia and S. V. Lebedev – 71
The spectrum of positronium in external fields, V. N. Tsytovich – 452
Statistical problems of an electron multiplier, L. Janossy – 520

Electrodynamics (see **Electromagnetic Theory and Electrodynamics**)

Electromagnetic Theory and Electrodynamics (see also **Microwaves**)
Description of the electromagnetic field by means of matrices, G. A. Zaitsev – 411
Dispersion formulas of the quantum optics of metals in the many-electron theory with consideration of electron damping, A. V. Sokolov, V. I. Cherepanov and I. B. Shteinberg – 231
Improvement of the quality of a cavity resonator by means of regeneration, N. G. Basov, V. G. Veselago and M. E. Zhabatinskii – 177 (L)
The velocity distribution of electrons in the presence of a varying electric field and a constant magnetic field, V. M. Fain – 205
The velocity of the Wave Front in nonlinear electrodynamics, L. G. Iakovlev -- 181 (L)

Electron Diffraction (see **Scattering of Electrons and Positrons**)

Electron Optics (see **Electromagnetic Theory and Electrodynamics**)

Electronic Tubes (see **Methods and Instruments**)

Electrons and Positrons (see also **Electromagnetic Theory and Electrodynamics; Elementary Particle**

- **Interactions; Scattering of Electrons and Positrons)**
  - Capture of electrons and ionization by protons in hydrogen, Ia. M. Fogel', L. I. Krupnik and B. G. Safronov – 419
  - Relativistically invariant equations for the electron which take the place of Dirac's system of equations, G. A. Zaitsev – 491
  - The spectrum of positronium in external fields, V. N. Tsytovich – 452
- **Electrons, Scattering of** (see **Scattering of Electrons and Positrons**)
- **Electrons, Secondary** (see **Electrical Properties**)
- **Electro-Optical Effects** (see **Optical Properties**)
- **Electrostriction** (see **Dielectrics and Dielectric Porties**)
- **Elementary Particle Interactions**
  - Calculation of the energy distribution function of neutrons by Markov's method, V. V. Chavchanidze and O. D. Cheitvili – 375 (L)
  - Interaction of protons with Tritium and the Excited State of He^4, N. A. Vlasov, S. P. Kalinin, A. A. Ogloblin, L. N. Samilov, V. A. Sidorov and V. I. Chuev – 500
  - On the causal development of a coupled system in relative time, V. N. Tsytovich -- 377 (L)
- **Elements** (see **Atomic Mass and Abundance**)
- **Energy Loss of Particles** (see **Range and Energy Loss**)
- **Energy States of Atoms** (see **Atomic Structure and Spectra**)
- **Energy States of Nucleus** (see **Nuclear Reactions; Nuclear Spectra; Nuclear Structure Theroy**)
- **Evaporation** (see **Liquids**)
- **Excitation of Atoms** (see **Atomic Structure and Spectra**)
- **Excitation of Nucleus** (see **Nuclear Reactions; Nuclear Spectra; Nuclear Structure Theory**)

- **Faraday Effect** (see **Optical Properties**)
- **Ferroelectric Phenomena** (see **Dielectrics and Dielectric Properties**)
- **Field Emission** (see **Electric Properties**)
- **Field Theory** (see also **Quantum Electrodynamics**)
  - Construction of a Distribution Function by the Method
  - Construction of a distribution function by the method of quasi-fields, Iu. A. Gol'fand – 118
  - Description of the electromagnetic field by means of matrices, G. A. Zaitsev – 411
  - Relativistically invariant equations for the electron which take the place of Dirac's system of equations, G. A. Zaitsev – 491
  - Some observations on possible formulations of the theory of extended particles, V. S. Barashenkov – 467
  - The gravitational self energy of particles in the classical field theories, A. A. Borgardt – 380 (L)
- **Films, Properties**
  - The conditions of formation and stability of films at the electrodes in dielectrics, Ia. N. Pershits – 110
- **Fine Structure** (see **Atomic Structure and Spectra**)
- **Fission of Nucleus** (see **Nuclear Fission**)
- **Fluctuation Phenomena** (see **Noise**)
- **Fluorescence** (see **Luminescence**)
- **Galvanomagnetic Effect** (see **Magnetic Properties**)
- **Gravitation** (see **Relativity and Gravitation**)
- **Gyromagnetization** (see **Magnetic Properties**)
- **Hall Effect** (see **Electrical Conductivity and Resistance; Semiconductors**)
- **Helium, Liquid**
  - Rotation of helium II at high speeds, E. L. Andronikashvili and I. P. Kaverkin – 174 (L)
  - The surface tension of liquid He^3 in the temperature range 0.93-3.34 °K, K. N. Zinov'eva – 173 (L)
  - The wave function of the lowest state of a system of interacting Bose particles, N. N. Bogoliubov and D. N. Zubarev – 83
- **High-Volatge Tubes and Machines** (see **Methods and Instruments**)
- **Hyperfine Structure** (see **Atomic Structure and Spectra; Nuclear Moments and Spin**)
- **Hyperons** (see **Mesons and Hyperons**)

- **Inelastic Scattering** (see **Nuclear Reactions; Scattering**)
- **Instruments** (see **Methods and Instruments**)
- **Internal Conversion** (see **Nuclear Spectra**)
- **Ionization** (see also **Electrical Discharges; Range and Energy Loss of Particles**)
  - Capture of electrons and ionization by protons in hydrogen, Ia. M. Fogel', L. I. Krupnik and B. G. Safronov – 419
- **Ionization Potentials of Atoms** (see **Atomic Structure and Spectra**)
- **Ions** (see also **Electrical Discharges**)
  - Formation of negative hydrogen ions in the passage of protons through thin metal foils, Ia. M. Fogel', B. G. Safronov and L. I. Krupnik -
  - On longitudinal vibrations of plasma. I, A. A. Luchina – 12
  - On longitudinal vibrations of plasma. II, G. Ia. Miakishev and A. A. Luchina – 12
- **Isobars** (see **Atomic Mass and Abundance**)
- **Isomers, Nuclear** (see **Nuclear Spectra**)
- **Isotopes** (see **Atomic Mass and Abundance; Radioactivity**)

- **Kerr Effect** (see **Optical Properties**)

- **Liquid Helium** (see **Helium, Liquid**)
- **Liquids**
  - Zone theory of the three-dimensional model of a liquid, A. I. Gubanov – 364
- **Luminescence**
  - The decay laws of the afterglow of zinc sulfide phosphors in the temperature extinction region, F. I. Vergunas and N. L. Gasting – 284
  - F-centers in silver halide crystals, P. V. Meikliar – 187 (L)
  - On the resonance-fluorescence of atoms, M. N. Alentsev, V. V. Antonov-Romanovskii, V. I. Stepanov and M. V. Fok – 188 (L)
  - The problem of the effect of concentration on the luminescence of solutions, M. D. Galanin – 317
  - The problem of the position of the copper activator in zinc-sulfide scintillators, A. A. Cherepnev – 300

- **Magnetic Fields** (see **Electromagnetic Theory and Electrodynamics**)
- **Magnetic Properties**
  - Magnetostatics with ferromagnetics, V. I. Skobelkin and R. N. Solomko – 370
  - New means of control of compensating the earth's magnetic field in investigations on a vertical astatic magnetometer, A. I. Drokin – 126
  - The effect of a uniform compression upon the galvanomagnetic effects in bismuth and its alloys, N. E. Alekseevskii and N. B. Brandt – 384 (L)
  - The kinetics of the destruction of superconductivity

  by a magnetic field, A. A. Galkin and P. A. Bezuglyi – 197
  The spectrum of positronium in external fields, V. N. Tsytovich – 452
Magnetic Resonance (see also Nuclear Moments and Spin)
  A magnetometer which makes use of the magnetic resonance of protons, N. I. Leontiev – 50
  Hyperfine structure of paramagnetic resonance in copper Tutton salts at intermediate field, N. S. Garif'ianov and M. M. Zaripov – 567 (L)
  On the theory of electronic and nuclear paramagnetic resonance under the action of ultrasound, S. A. Al'tshuler – 37
  Resonance absorption of ultrasound in paramagnetic salts, S. A. Al'tshuler – 29
  The fine structure of the spectrum of the paramagnetic resonance of the ion Cr^{+++} in chromium corundum, A. A. Manenkov and A. M. Prokhorov – (L)
Magneto-Optical Effects (see Optical Properties)
Magnetoresistance (see Electrical Conductivity and Resistance; Semiconductors)
Magnetostriction (see Magnetic Properties)
Mass Defects (see Atomic Mass and Abundance)
Mass Spectroscopy (see Atomic Mass and Abundance; Methods and Instruments)
Mathematical Methods
  The mathematical foundations of the theory of irreversible thermodynamical processes, Kiril Popov – 336
Measurements (see Methods and Instruments)
Mesons and Hyperons (see also Cosmic Radiation; Elementary Particle Interactions; Nuclear Reactions Induced by Mesons; Scattering of Mesons)
  Meson production at energies close to threshold, A. B. Migdal – 7
  Multiple meson production at energies of 1-2 bev, S. Z. Belen'kii and A. I. Nikishov – 593 (L)
  The fission of heavy nuclei by slow mesons, N. A. Perfilov and N. S. Ivanova – 585 (L)
  The fission of uranium nuclei under the action of slow π^- mesons and high energy particles, G. E. Belovitskii, T. A. Romanova, L. V. Sukhov and I. M. Frank – 581 (L)
  The formation of charged π meson by nucleons, V. M. Sidorov – 600 (L)
  The possible β decay of hyperons and K mesons, M. Markov and V. Stakhanov – 593 (L)
  The probability of uranium nuclear fission by its absorption of slow π mesons, O. V. Lozhkin and V. P. Shamov – 597 (L)
Metals (see Crystalline State)
Metastable Atoms (see Atomic Structure and Spectra)
Methods and Instruments
  A magnetometer which makes use of the magnetic resonance of protons, N. I. Leontiev – 50
  A pulse height analyzer with an electron beam tube, V. G. Khartman, I. N. Leont'eva, A. P. Siniavskii and L. V. Vasil'ev – 537
  A self-quenching light meter, S. F. Rodionov, M. S. Khaikin and A. I. Shal'nikov – 64
  Calculation of the ultimate thickness of an emulsion layer in the investigation of nuclear processes by means of the photographic method. II, A. A. Bene – – 532
  Certain properties of the spark counter for counting α-particles, E. Andreeshchev and B. M. Isaev – 212
  Detection of the polarization of beams of fast particles by means of nuclear photoemulsions, E. L. Grigor'ev – 608 (L)
  Gas bubble chamber – a possible recorder of the elementary act of interaction of ionizing radiation with matter, G. A. Askar'ian – 571 (L)
  High threshold scintillation neutron detector, P. A. Baranov and V. I. Gol'danskii – 576 (L)
  Improvement of the quality of a cavity resonator by means of regeneration, N. G. Basov, V. G. Veselago and M. E. Zhabatinskii – 177 (L)
  Investigation of high frequency discharges by the probe method, Kh. A. Dzherpetov and G. M. Pateiuk – 326
  New means of control of compensating the earth's magnetic field in investigations on a vertical astatic magnetometer, A. I. Drokin – 126
  Possible application of pulsed multiplier image-converters for recording tracks of ionizing particles in luminescent media, G. A. Askar'ian – 575 (L)
  Rectangular Wilson chamber with bilateral expansion, V. G. Kirillov-Ugriumov, V. M. Federov and B. N. Deriagin – 484
  Self-neutralizing light meter with adjustable red boundary, M. S. Khaikin and E. I. Abaulina – 189 (L)
Microwaves (see also Atomic Structure and Spectra; Magnetic Resonance; Nuclear Moments and Spin)
  Improvement of the quality of a cavity resonator by means of regeneration, N. G. Basov, V. G. Veselago and M. E. Zhabatanskii – 177 (L)
  The optimum length of an undulator, A. N. Matveev – 606 (L)
  The radiation of CO_2 in the region of 15 μ in an electric discharge, N. Ia. Dodonova and V. V. Sobolev – 611 (L)
  Some notes on the researches of S. G. Salikov, N. N. Neprimerov – 552
Moments, Nuclear (see Nuclear Moments and Spin)
Mechanics, Quantum (see Quantum Mechanics)
Mechanics, Quantum - Atomic Structure and Spectra (see Atomic Structure and Spectra)
Mechanics, Quantum - Nuclear (see Nuclear Structure Theory)
Mechanics, Quantum - of Solid Bodies (see Crystalline State)
Mechanics, Statistical (see Statistical Mechanics and Thermodynamics)
Meson Field Theory (see Field Theory)

Neutrons (see Elementary Particle Interactions)
Noise
  Statistical problems of an electron multiplier, L. Janossy – 520
  The effect of electrical fluctuations on a vacuum tube oscillator, P. I. Kuznetsov, R. L. Stratonovich and V. I. Tikhonov – 510
Nuclear Fission
  Nuclear fissions associated with heavy unstable particles, I. M. Gramenitskii, E. A. Zamchalova, M. I. Podgoretskii, M. I. Tretiakova and M. N. Shcherbakova – 562 (L)
  The fission of heavy nuclei by slow mesons, N. A. Perfilov and N. S. Ivanova – 585 (L)
  The fission of uranium nuclei under the action of slow π mesons and high energy particles, G. E. Belovitskii, T. A. Romanova, L. V. Sukhov and

9

I. M. Frank – 581 (L)
The probability of uranium nuclear fission by its absorption of slow π^- mesons, O. V. Lozhkin and V. P. Shamov – 597 (L)
The spontaneous fission of thorium, A. V. Podgurskaia V. I. Kalashnikova, G. A. Stoliarov, E.D. Vorob'ev G. N. Flerov – 392 (L)
The yield of fission and star formation processes in the capture of π^- mesons by nuclei of U, Bi and W, N. A. Perfilov, O. V. Lozhkin and V. P. Shamov – 439
Nuclear Forces (see Elementary Particle Interactions; Field Theory; Nuclear Structure Theory)
Nuclear Induction (see Magnetic Resonance; Nuclear Moments and Spin)
Nuclear Moments and Spin
Determination of the transverse relaxation time of nuclear magnetic moments, S. D. Gvozdover, N. M. Pomerantsov and A. P. Poliakova – 471
Nuclear Photoeffects
Maximum yield of photoneutrons and a new method of determining the integral cross section of (γ, n) reactions for high energy photons, V. I. Gol'danskii and V. A. Shkoda-Ul'ianov – 579 (L)
The yield of an angular distribution of photoneutrons of high energy, P. S. Baranov and V. I. Gol'danskii – 613 (L)
Nuclear Reactions, General (see also **Elementary Particle Interactions; Scattering**)
Collisons of fast nucleons with nuclei, E. L. Feinberg – 176 (L)
The Fermi theory of multiple particle production in nucleon encounters, I. L. Rozental' – 166 (L)
The theory of multiple production of particles at high energy, S. Z. Belen'kii – 161 (L)
The theory of nuclear reactions with production of slow particles, A. B. Migdal – 2
Nuclear Reactions Induced by Mesons (see also **Elementary Particle Interactions; Mesons; Scattering of Mesons**)
The fission of heavy nuclei by slow mesons, N. A. Perfilov and N. S. Ivanova – (585 (L)
The fission of uranium nuclei under the action of slow π mesons and high energy particles, G. E. Belovitskii, T. A. Romanova, L. V. Sukhov and I. M. Frank – 581 (L)
The probability of uranium nuclear fission by its absorption of slow π mesons, O. V. Lozhkin and V. P. Shamov – 597 (L)
Nuclear Scattering (see Scattering)
Nuclear Spectra (see also **Nuclear Reactions; Radioactivity**)
A study of the energy levels of the lithium nucleus by the method of magnetic analysis, L. M. Khromchenko and V. A. Blinov – 596 (L)
Hyperfine structure of the spectral lines and nuclear spins of U^{233} and Pu^{239}, L. A. Korostyleva, A. R. Striganov and N. M. Iashin – 310
Measurement of the coefficients of internal conversion of γ - rays of Sr^{87*}, In^{113*}, In^{115*} and V^{51*} on the electrons of the atoms, I. V. Estulin and E. M. Moiseeva – 463
Some notes on the researches of S. G. Salikov, N. N. Neprimerov – 552 (L)
Nuclear Structure Theory (see also **Nuclear Reactions; Nuclear Spectra**)
Deviations from Mayer's scheme for filling nuclear shells and the interaction of levels, V. A. Filimonov – 585 (L)
The degree of orientation of nuclei, G. R. Khutsishvili – 390
The neutron subshell in the region of the transuranic elements, S. T. Larin and N. N. Kolesnikov – 178 (L)
The problem of spontaneous fission and beta-stability, N. N. Kolesnikov and S. T. Larin – 179 (L)
The statistical theory of heavy nuclei and of nuclear forces, F. I. Kligman – 145

Optical Instruments (see Methods and Instruments)
Optical Properties (see also **Luminescence**)
A self-quenching light meter, S. F. Rodionov, M. S. Khaikin and A. I. Shal'nikov – 64
Dispersion formulas of the quantum optics of metals in the many-electron theory with consideration of electron damping, A. V. Sokolov, V. I. Cherepanov and I. B. Shteinberg – 231
Self-neutralizing light meter with adjustable red boundary, M. S. Khaikin and E. I. Abaulina – 189 (L)
The effect of concentreation on the optical properties of solutions of acridine compunds, L. V. Levskin – 235
The effect of concentration on the optical properties of 3,6-diaminoacridine, L. V. Levshin – 244
The regression of the centers of the latent photographic image, B. I. Kazantsev and P. V. Meikliear – 45

Pair Production (see **Electrons and Positrons**)
Phosphors and Phosphorescence (see **Luminescence; Semiconductors**)
Photoconductivity (see **Electrical Conductivity and Resistance**)
Photodisintegration (see Nuclear Photoeffects)
Photoelectric Effect (see Electrical Properties)
Photography and Photographic Emulsions (see Methods and Instruments; Optical Properties)
Photometry (see Methods and Instruments; Optical Properties)
Photons (see Radiation)
Photovoltaic Effect (see Electrical Properties; Semiconductors)
Piezoelectric Effect (see Dielectrics and Dielectric Properties)
Polarization, Electrical (see Dielectrics and Dielectric Properties)
Positrons (see Electrons and Positrons)
Probability (see Mathematical Methods)
Protons (see **Elementary Particle Interactions**)

Quantum Electrodynamics (see also **Field Theory**)
Remarks on the theory of fusion, G. I. Sokolik – 9
The asymptote of Green's function in quantum electrodynamics, E. S. Fradkin – 604 (L)
The Fermi theory of multiple particle production in nucleon encounters, I. L. Rozental' – 166 (L)
The quantum theory of the radiating electron. IV, A. A. Sokolov and I. M. Ternov – 227
The representation of Green's function in quantum electrodynamics in the form of continual integrals, I. M. Khalatnikov – 586 (L)
Quantum Mechanics

Construction of a distribution function by the method of quasi-fields, Iu. A. Gol'fand – 118
Dispersion formulas of the quantum optics of metals in the many-electron theory with consideration of electron damping, A. V. Sokolov, V. Cherepanov and I. B. Shteinberg – 231
On the paper of V. I. Karpman, "The problem of the connection between the method of regularization and the theory of particles with arbitrary spin", Iu. A. Iappa – 171 (L)
The wave-function of the lowest state of a system of interacting Bose particles, N. N. Bogoliubov and D. N. Zubarev – 83
Quenching of Radiation (see **Radiation**)

Radar (see **Methods and Instruments; Radiation**)
Radiation (see also **Range and Energy Loss**)
Absorption and emission of light by a gray substance, B. I. Stepanov – 446
On the observation of Cerenkov Radiation accompanying broad atmospheric showers of cosmic rays, N. M. Nesterova and A. E. Chudakov – 388 (L)
On the theory of energy losses of charged particles traversing a ferromagnetic material, D. Ivanenko and V. N. Tytovich – 135
Scattering of mesons by nucleons in the theory of radiation damping, A. S. Martynov – 68
The quantum theory of the radiating electron. IV, A. A. Sokolov and I. M. Ternov – 227
Radio Waves (see **Radiation**)
Radioactivity (see also **Nuclear Spectra**)
The absence of stable isotopes of Tc and Pm and other anomalies in the distribution of β stable nuclei, A. V. Savich – 291
On the angular distribution of β-radiation. II. G. B. Khutsishvili – 376 (L)
The possible β-decay of hyperons and K-mesons, M. Markov and V. Stakhanov – 593 (L)
Range and Energy Loss of Particles
Gass bubble chamber – a possible recorder of the elementary act of interaction of ionizing radiation with matter, G. A. Askar'ian – 571 (L)
On the problem of negative π meson decays, V. I. Gol'danskii and M. I. Podgoretskii – 571
On the theory of energy losses of charged particles traversing a ferromagnetic material, D. Ivanenko and V. N. Tsytovich – 135
The yield of fission and star formation processes in the capture of π^- mesons by nuclei of U, Bi and W, N. W. Perfilov, O. V. Lozhkin and V. P. Shamov – 439
Rectifiers (see **Electrical Conductivity and Resistance; Semiconductors**)
Relativity and Gravitation
On the causal development of a coupled system in relative time, V. N. Tsytovich – 377 (L)
Relativistic corrections to the two body problem, V. N. Tsytovich – 163 (L)
Relativistically invariant equations for the electron which take the place of Dirac's system of equations, G. A. Zaitsev – 491
The gravitational self energy of particles in the classical field theories, A. A. Borgardt – 380 (L)
The relativistic mechanics of a material point of variable mass, N. S. Kalitsin – 565 (L)
Resistance, Electrical (see **Electrical Conductivity and Resistance**)
Resonance Radiation (see **Radiation**)

Scattering, General (see also **Elementary Particle Interactions; Nuclear Reactions; Range and Energy Loss of Particles**)
Gas bubble chamber – a possible recorder of the elementary act of interaction of ionizing radiation with matter, G. A. Askar'ian – 571 (L)
Multiple scattering in a Coulomb field in very thin layers of material, A. S. Kompaneets – 262
The theory of scattering in the semiclassical approximation, I. I. Gold'man and A. B. Migdal – 304
Scattering of Electrons and Positrons (see also **Electrons and Positrons**)
The dynamical theory of electron scattering in crystals, I. A. Ovsiannikova and M. Ia. Shirobokov – 488
Scattering of Mesons (see also **Mesons; Nuclear Reactions Induced by Mesons**)
Scattering of mesons by nucleons in the theory of radiation damping, A. S. Martynov – 68
Scattering of Neutrons (see also **Nuclear Reactions Induced by Neutrons**)
The scattering of fast neutrons by non-spherical nuclei. I. S. I. Drozdov – 588 (L)
The scattering of fast neutrons by non-spherical nuclei, II. S. I. Drozdov – 591 (L)
Scattering of Protons (see also **Nuclear Reactions Induced by Protons**)
Capture of electrons and ionization by protons in hydrogen, Ia. M. Fogel', L. I. Krupnik and B. G. Safronov – 419
Scattering of Radiation (see **Radiation**)
Scintillation Counters (see **Methods and Instruments**)
Secondary Emission (see **Electrical Properties**)
Semiconductors
On the paper of G. M. Avak'iants, "The theory of the transfer equation in strong electric fields," I. M. Tsidil'kovskii and F. G. Bass – 180 (L)
On the theory of the Hall and Nernst-Ettinghausen effects in semiconductors with mixed conductivities F. G. Bass and I. M. Tsidil'kovskii – 267 (L)
Solid State (see **Crystalline State**)
Solutions (see **Liquids**)
Sound (see **Acoustics**)
Spallation (see **Nuclear Reactions**)
Spark Discharge (see **Electrical Discharges**)
Spectra, Atomic (see **Atomic Structure and Spectra**)
Spectra, General
The problem of obtaining a metastable modification of thallium, E. I. Abaulina and N. V. Zavaritskii – 184 (L)
The equilibrium energy spectrum of cascades of photons, P. S. Isaev – 379 (L)
The spectrum of positronium in external fields, V. N. Tsytovich – 452
Spectra, Nuclear (see **Nuclear Spectra**)
Spectroscopy Technique (see **Methods and Instruments**)
Spinor Fields (see **Field Theory**)
Stark Effect (see **Atomic Structure and Spectra**)
Statistical Mechanics and Thermodynamics
Entropy in quantum statistics, R. L. Stratonovich – 426
On the paper "The excitation spectrum of a system of many particles, V. P. Silin – 607 (L)

  On the stability of a homogeneous phase. I. General theory, I. Z. Fisher – 154
  On the stability of a homogeneous phase. II. Determination of the limit of stability, I. Z. Fisher – 273
  On the stability of a homogeneous phase. III. Theory of the crystallization curve, I. Z. Fisher – 280
  The entropy of systems with a random number of particles, R. L. Stratonovich – 254
  The Fermi distribution at absolute zero, taking into account the interaction of electrons with zero point vibrations of the lattice, V. L. Bonch-Bruevich – 169 (L)
  The mathematical foundations of the theory of irreversible thermodynamical processes, Kiril Popov – 336
  The phenomenological relations of Onsager, Khristo Karanikolov – 265

Statistical Methods (see Mathematical Methods)

Superconductivity
  "Acoustic excitations" in superconductors, Iu. L. Klimontovich – (L)
  The kinetics of the destruction of superconductivity by a magnetic field, A. A. Galkin and P. A. Bezuglyi – 197
  The problem of obtaining a metastable modification of thallium, E. I. Abaulina and N. V. Zavaritskii – 184 (L)
  The problem of the superconductivity of the compounds Bi_4Rh and Bi_2Rh, N. E. Alekseevskii, G. S. Zhdanov and N. N. Zhuravlev – 99
  The structure of the superconductors VIII. X-ray and metallographic investigations of the system bismuth-rhodium, N. N. Zhuravlev and G. S. Zhdanov – 91

Thermionic Emission (see Electrical Properties)

Thermodynamics (see Statistical Mechanics and Thermodynamics)

Thermoelectric Effect (see Electrical Properties; Semiconductors)

Thermoluminescence (see Luminescence)

Total Cross Sections (see Electrons and Positrons; Nuclear Reactions)

Transmutation (see Nuclear Reactions)

Uncertainty Principle (see Quantum Mechanics)

Vacuum Tubes (see Methods and Instruments)

Viscosity (see Liquids)

Wave Mechanics (see Quantum Mechanics)

Work Function (see Electrical Properties)

CONTENTS – *continued*

. . . . V. S. Mel'chenko 564

The Relativistic Mechanics of a Material Point of Variable Mass . . . N. S. Kalitsin 565

Hyperfine Structure of Paramagnetic Resonance in Copper Tutton Salts at Intermediate Fields . . . . N. S. Garif'ianov and M. M. Zaripov 567

The Representation of Green's Function in Quantum Electrodynamics in the Form of Continual Integrals . . . . I. M. Khalatnikov 568

Gas Bubble Chamber -- A Possible Recorder of the Elementary Act of Interaction of Ionizing Radiation with Matter . . . . G. A. Askar'ian 571

On the Problem of the Negative π-Meson Decays . . . . V. I. Gol'danskii and M. I. Podgoretskii 571

Measurements of the Absorption Coefficient of High Energy Nuclear Interacting Particles . . . . K. P. Ryzhkova and L. I. Sarycheva 572

Possible Application of Pulsed Multiplier Image-Converters for Recording Tracks of Ionizing Particles in Luminescent Media . . . . G. A. Askar'ian 575

High Threshold Scintillation Neutron Detector . . P. S. Baranov and V. I. Gol'danskii 576

Maximum Yield of Photoneutrons and a New Method of Determining the Integral Cross-Section of (γ, n) Reactions for High Energy Photons . . . . V. I. Gol'danskii and V. A. Shkoda-Ul'ianov 579

The Fission of Uranium Nuclei Under the Action of Slow π^- Mesons and High Energy Particles . . . G. E. Belovitskii, T. A. Romanova, L. V. Sukhov and I. M. Frank 581

Deviations from Mayer's Scheme for Filling Nuclear Shells and the Interaction of Levels . . . . V. A. Filimonov 585

The Fission of Heavy Nuclei by Slow Mesons . . . N. A. Perfilov and N. S. Ivanova 585

The Probability of Uranium Nuclear Fission by Its Absorption of Slow π^- Mesons . . . . O. V. Lozhkin and V. P. Shamov 587

The Scattering of Fast Neutrons by Non-Spherical Nuclei II . . . . . . S. I. Drozdov 588

The Scattering of Fast Neutrons by Non-Spherical Nuclei I . . . . S. I. Drozdov 591

The Possible β Decay of Hyperions and K Mesons . . . M. Markov and V. Stakhanov 593

Multiple Meson Production at Energies of 1 - 2.2 Bev . . . . S. Z. Belen'kii and A. I. Nikishov 593

A Study of the Energy Levels of the Lithium Nucleus by the Method of Magnetic Analysis . . . . L. M. Khromchenko and V. A. Blinov 596

The Formation of Charged π - Mesons by Nucleons . . . . V. M. Sidorov 600

"Acoustic Excitations" in Superconductors . . . . Iu. L. Klimontovich 602

The Asymptote of Green's Function in Quantum Electrodynamics . . . E. S. Fradkin 604

The Optimum Length of an Undulator . . . . A. N. Matveev 606

On the Paper "The Excitation Spectrum of a System of Many Particles" . . V. P. Silin 607

Detection of the Polarization Beams of Fast Particles by Means of Nuclear Photo-Emulsions . . . . E. L. Grigor'ev 608

The Excitation of Ultrasonic Vibrations by Ponderomotive Forces . . . . S. I. Aksenov, B. P. Vikin and K. V. Vladimirskii 609

The Fine Structure of the Spectrum of the Paramagnetic Resonance of the Ion Cr^{3+} in Chromium Corundum . . . . A. A. Manenkov and A. M. Prokhorov 611

The Radiation of CO_2 in the Region of 15μ in an Electric Discharge . . . . N. Ia. Dodonova and V. V. Sobolev 611

The Yield and Angular Distribution of Photoneutrons of High Energy . . . . P. S. Baranov and V. I. Gol'danskii 613

Tables of Contents, Doklady Akademii Nauk SSSR, Volume 101, Nos. 1 - 6 617

Author Index to Volume 1 621

Analytic Index to Volume 1 625

SOVIET PHYSICS JETP VOLUME 1, NUMBER 3 NOVEMBER, 1955

CONTENTS

Albert Einstein 409

Description of the Electromagnetic Field by Means of Matrices . . . . G. A. Zaitsev 411

Capture of Electrons and Ionization by Protons in Hydrogen . . . . Ia. M. Fogel', L. I. Krupnik and B. G. Safronov 415

Entropy in Quantum Statistics . . . . R. L. Stratonovich 426

Ranges of Protons in Medium and Heavy Elements . . . . B. V. Rybakov 435

The Yield of Fission and Star Formation Processes in the Capture of π^--Mesons of U, Bi and W . . . . N. A. Perfilov, O. V. Lozhkin and V. P. Shamov 439

Absorption and Emission of Light by a Gray Substance . . . . B. I. Stepanov 446

The Spectrum of Positronium in External Fields . . . . T. N. Tsytovich 452

Measurement of the Coefficients of Internal Conversion of γ-Rays of Sr^{87*}, In^{113*}, In^{115*} and V^{51*} on the Electrons of the Atoms . . . . . I. V. Estulin and E. M. Moiseeva 463

Some Observations on Possible Formulations of the Theory of Extended Particles . . . . V. S. Barashenkov 467

Determination of the Transverse Relaxation Time of Nuclear Magnetic Moments . . . . S. D. Gvozdover, N. M. Pomerantsov and A. P. Poliakova 471

The Conditions for Self-Excitation of a Singing Flame . . . . Iu. I. Neimark and G. V. Aronovich 475

Rectangular Wilson Chamber with Bilateral Expansion . . . . V. G. Kirillov-Ugriumov, V. M. Federov and B. N. Deriagin 484

The Dynamical Theory of Electron Scattering in Crystals . . . . I. A. Ovsiannikova and M. Ia. Shirobokov 488

Relativistically Invariant Equations for the Electron Which Take the Place of Dirac's System of Equations . . . . G. A. Zaitsev 491

Interaction of Protons with Tritium and the Excited State of He^4 . . . . N. A. Vlasov, S. P. Kalinin, A. A. Ogloblin, L. N. Samoilov, V. A. Sidorov and V. I. Chuev 500

The Effect of Electrical Fluctuations on a Vacuum Tube Oscillator . . . . P. I. Kuznetsov, R. L. Stratonovich and V. I. Tikhonov 510

Statistical Problems of an Electron Multiplier . . . . L. Janossy 520

Calculation of the Ultimate Thickness of an Emulsion Layer in the Investigation of Nuclear Processes by Means of the Photographic Method, II. . . . . A. A. Bene 532

On the Theory of Crystal Growth . . . . A. V. Beliustin 535

A Pulse Height Analyzer with an Electron Beam Tube . . . . V. G. Khartman, I. N. Leont'eva, A. P. Siniavskii and L. V. Vasil'ev 537

Formation of Negative Hydrogen Ions in the Passage of Protons through Thin Metal Foils . . . . Ia. M. Fogel, B. G. Safranav and L. I. Krupnik 546

Some Notes on the Researches of S. G. Salikhov . . . . N. N. Neprimerov 552

Letters to the Editor:

The Effect of Lunar-Tidal Oscillation of the Atmosphere on the Intensity of the Hard Component of Cosmic Rays . . . . A. I. Kuz'min and G. V. Skripin 556

Variation of the Global Intensity of the Hard Component of Cosmic Rays During the Passage of Air Mass Fronts . . . . D. D. Krasil'nikov 557

The Contribution of Meteorological Changes in the Earth's Atmosphere to the Diurnal Effect in Cosmic Rays . . . . A. I. Kuz'min 560

Nuclear Fissions Associated with Heavy Unstable Particles . . . . I. M. Gramenitskii, E. A. Zamchalova, M. I. Podgoretskii, M. I. Tretiakova and M. N. Shcherbakova 562

Determination of the Absolute Concentrations of Atoms in a Multi-Component Arc-Vapor

(Contents continued on inside back cover)